DIRAC FERMIONS
ON ROTATING SPACE-TIMES

VICTOR EUGEN AMBRUŞ

PhD thesis

Supervisor: Prof. Elizabeth Winstanley

School of Mathematics and Statistics

University of Sheffield

December 2014

Abstract

Quantum states of Dirac fermions at zero or finite temperature are investigated using the point-splitting method in Minkowski and anti-de Sitter space-times undergoing rotation about a fixed axis.

In the Minkowski case, analytic expressions presented for the thermal expectation values (t.e.v.s) of the fermion condensate, parity violating neutrino current and stress-energy tensor show that thermal states diverge as the speed of light surface (SOL) is approached. The divergence is cured by enclosing the rotating system inside a cylinder located on or inside the SOL, on which spectral and MIT bag boundary conditions are considered.

For anti-de Sitter space-time, renormalised vacuum expectation values are calculated using the Hadamard and Schwinger-de Witt methods. An analytic expression for the bi-spinor of parallel transport is presented, with which some analytic expressions for the t.e.v.s of the fermion condensate and stress-energy tensor are obtained. Rotating states are investigated and it is found that for small angular velocities Ω of the rotation, there is no SOL and the thermal states are regular everywhere on the space-time. However, if Ω is larger than the inverse radius of curvature of adS, an SOL forms and t.e.v.s diverge as inverse powers of the distance to it.

Contents

List of Figures

List of Tables

Preface

Chapters 1, 2 and 3 are introductory chapters where the notation, key concepts and methods which are relevant to this thesis are introduced. Chapters 4, 5 and 6 are dedicated to the study of rotating quantum states on Minkowski space-time, where, for completeness, the scalar field is also presented, following Refs. [33, 52]. Quantum states on the anti-de Sitter space time with or without rotation are discussed in chapters 7 and 8.

The construction of thermal states for fermions in unbounded Minkowski space extends the discussions in Refs. [47, 72]. The analytic expressions for thermal expectation values calculated in subsection 4.3.2 represent original results which are published in Ref. [10]. For the study of rotating thermal states of fermions inside a boundary, the spectral [43] and MIT bag [23] boundary conditions are considered in sections 5.2 and 5.3, respectively. The analysis of thermal expectation values and of the Casimir effect presented therein represents original research which is due to be published in Ref. [5]. Preliminary results have already been reported in Ref. [8].

Following the preliminary discussion of the construction of two-point functions using a sum of the modes in Ref. [26] and using the geometric approach introduced in Ref. [56], renormalised vacuum expectation values are obtained using the Hadamard renormalisation method. An original result for the analytic expression of the bi-spinor of parallel transport is used in subsection 7.5.1 to obtain thermal expectation values. Preliminary results are avaliable in Ref. [7].

The analysis of fermion quantum states on rotating anti-de Sitter space, presented in chapter 8, draws heavily on the mode solutions and the analytic expression for two-point functions and for the bi-spinor of parallel transport given in chapter 7. This section is completely comprised of original results, which are summarised in Ref. [6].

The author would like to acknowledge the help and support of his supervisor, as well as the financial support of the University of Sheffield through the Graduate Teaching Assistantship.

Natural units ($c = 1$, $\hbar = 1$, $K_B = 1$) are used throughout this work, the metric signature is $(-, +, +, +)$ and the definitions of the Christoffel symbols $\Gamma^\mu_{\ \nu\kappa}$ and of the Riemann tensor $R^\lambda_{\ \kappa\mu\nu}$ follow the convention of Misner, Thorne and Wheeler [55].

Chapter 1. Introduction

Two theories revolutionised the understanding of physics in the twentieth century: the general theory of relativity and quantum field theory, as successors of special relativity and quantum mechanics. To date, both theories have been confirmed experimentally to very high accuracy in their domains of applicability: macroscale for general relativity and accelerator physics for quantum field theory. Alas, these two theories are fundamentally incompatible. Since the theory of relativity is entirely classical, it is expected that it cannot be used for high energy (or small length scale) systems. Similarly, quantum field theory traditionally singles out a particular foliation of space-time by fixing a time coordinate to impose equal-time commutation relations, while at the same time quantum states are defined globally throughout the space-time, thus appearing to violate the locality principle of general relativity. While several attempts at formulating a theory which will include both quantum effects in gravity and interactions between gravity and quantum fields have been made, no general consensus exists as to which approach will emerge as the theory of everything. However, it is possible to investigate the departure from classical theories and the effects of curvature and general covariance requirements on quantum fields through the semi-classical approach of quantum field theory on curved spaces.

Quantum field theory (QFT) on curved space-times (CS) treats the background space-time as a solution of the classical Einstein equations. The requirement of general covariance induces a non-trivial coupling between the propagation of field quanta and the underlying structure of the space-time through the space-time metric. One of the most highly acclaimed predictions of QFT on CS is the evaporation of black holes as an example of particle production, through the Hawking effect [40, 41]. Other areas where quantum phenomena could play important roles are the creation and stabilisation of wormholes or space-travel through Alcubierre's mechanism [2]. Both these phenomena rely on the existence of negative energy density sources, an example of which is the Casimir energy induced through the Casimir effect [46].

While QFT on CS has been studied extensively in the last four decades, most of the work done in this field was focused on the study of scalar fields, due to their mathematical simplicity. However, the quantum behaviour of fermions cannot be inferred directly from that of boson particles, due to the fundamental differences between them. This difference can be seen explicitly in thermal field theory on the rotating Minkowski space-time, where thermal states for scalar particles are impossible to define, while they are regular for fermions up to the speed of light surface (SOL).

Two main topics are studied in this thesis: rigidly rotating thermal states on a Minkowski space-time (with or without a boundary) and fermions on the anti-de Sitter space-time (both rotating and non-rotating).

In 1978, Vilenkin [72] investigated rigidly rotating quantum thermal states for scalars, fermions and photons, concluding that thermal states are impossible to achieve for bosons, unless the space-time is enclosed inside a boundary which cuts out the unphysical space outside the SOL. The mechanism preventing scalar particles from settling into thermal states is rooted in the density of states factor given by Bose-Einstein statistics, which allows infinite occupation numbers for particles with zero local energy. However, energies measured by co-rotating observers are not the same as the Minkowski energies. Hence, particles with vanishing co-rotating energy make infinite contributions to thermal expectation values, rendering thermal states undefinable. On the other hand, the Fermi-Dirac statistics yields finite occupation numbers for any value of the frequency, allowing fermions to form thermal distributions which are regular, but only close to the rotation axis. As the distance from the axis is increased, co-rotating particles rotate increasingly faster, until they reach the speed of light on the speed of light surface (SOL), where the thermal states of fermions break down.

Vilenkin [72] reported spurious temperature-independent terms in the thermal expectation value of the parity-violating neutrino charge current [71] (which he evaluated on the rotation axis only), caused by the possibilty of wave functions extending beyond the SOL. However, Iyer [47] demonstrated that there is a method to quantise fermion fields such that the spurious terms no longer appear in t.e.v.s, by eliminating modes of negative frequency from the set of particle modes.

For both bosons and fermions, there is a consensus in the literature that the space outside the SOL has to be somehow removed for thermal rotating quantum states to be well defined. In the scalar field case, Ref. [33] presents an implementation of Dirichlet boundary conditions which renders thermal states for scalars well-defined and finite as long as the boundary is placed inside or on the SOL. We investigate in this thesis the spectral [43] and MIT bag [23] boundary conditions for fermion fields and compare their predictions for rotating thermal states and for the Casimir divergence.

Before moving on to the investigation of thermal states on anti-de Sitter space-time (adS) using the point-splitting method, the vacuum Feynman propagator must be renormalised. Using the modes obtained in Ref. [26] and the expression for the Feynman propagator obtained in Ref. [56], the Hadamard [59] and Schwinger de-Witt [24] renormalisation methods are used and the results obtained are in excellent agreement with the Zeta-function and Pauli-Villars regularisation methods, respectively. Using an exact form for the bi-spinor of parallel transport, both non-rotating

and rotating thermal states can be analysed, as long as the angular velocity of the rotation does not exceed the inverse radius of curvature of adS.

An introduction to QFT on CS and to the point-splitting method is provided in chapter 2, followed by an analysis of thermal field theory of scalar and fermion particles on non-rotating Minkowski space-time in chapter 3. Rotating quantum states on the unbounded Minkwoski space-time are considered in chapter 4 and bounded states are discussed in chapter 5. Chapter 6 discusses the alternative quasi-Euclidean approach which can be used to investigate bounded rotating thermal states when the boundary is placed outside the SOL.

The renormalisation of the vacuum propagator and the construction of thermal states on adS are introduced in chapter 7, while rotation is introduced in chapter 8. Chapter 9 concludes the thesis.

The numerical results presented in this thesis (chapters 4, 5, 7 and 8 were obtained using Mathematica 8.

Chapter 2. General concepts

In this chapter, a brief introduction to field theory and second quantisation in general relativity for the Klein-Gordon (section 2.1) and Dirac (section 2.2) fields is presented. The aim of this chapter is to introduce the notation and formalism for calculating vacuum expectation values (v.e.v.s) and thermal expectation values (t.e.v.s) using two-point functions (i.e. Hadamard's elementary function, the Feynman propagator or the Euclidean Green's function).

Subsections 2.1.2 and 2.2.3 present the construction of the classical stress-energy tensor (SET) starting from the Lagrangian of the field theory under consideration. Subsections 2.1.3 and 2.2.4 introduce the canonical method for performing second quantisation and the subsequent expressions for the SET and Hamiltonian operators in terms of modes and one-particle creation and annihilation operators. The notion of finite temperature is introduced in subsections 2.1.4 and 2.2.5 and subsections 2.1.5 and 2.2.6 introduce the tools for calculating v.e.v.s and t.e.v.s using the formalism of point splitting and two-point functions.

2.1 The quantised scalar field

2.1.1 Second quantisation

The classical theory of a neutral scalar field $\phi(x)$ of mass μ has as a starting point the Lagrangian density

$$\mathcal{L} = -\frac{1}{2}\sqrt{-g(x)}\left\{g^{\mu\nu}(x)\partial_\mu\phi(x)\partial_\nu\phi(x) + [\mu^2 + \xi R(x)]\phi^2(x)\right\}, \qquad (2.1.1)$$

where $R(x)$ is the Ricci scalar, $g^{\mu\nu}$ is the inverse of the space-time metric $g_{\mu\nu}$ and ξ is a numerical factor giving the coupling between the scalar field and the curvature. All quantities are evaluated at the same point $x = (t, \boldsymbol{x})$ in space-time, where $\boldsymbol{x} = (x^1, x^2, x^3)$ groups the spatial coordinates in a three-vector. The Euler-Lagrange equation following from the Lagrangian density (2.1.1) is the Klein-Gordon equation:

$$[-\Box + \mu^2 + \xi R]\phi = 0, \qquad \Box\phi = \frac{1}{\sqrt{-g}}\partial_\lambda\left[\sqrt{-g}g^{\lambda\nu}\partial_\nu\phi\right], \qquad (2.1.2)$$

which is covariant under general coordinate transformations. For simplicity of notation, the coordinate dependence shall not be given explicitly unless there is a risk

of confusion. In the above, $\sqrt{-g}$ is the square root of the determinant of the matrix formed by the components $g_{\mu\nu}$ of the space-time metric.

Canonical quantisation makes use of the conjugate momentum corresponding to the field $\phi(x)$:

$$\pi = \frac{\partial \mathcal{L}}{\partial(\partial_0 \phi)} = -\sqrt{-g}\, g^{\mu 0} \partial_\mu \phi = -\sqrt{-g}\, \partial^0 \phi. \qquad (2.1.3)$$

The coordinate index of the partial derivative on the right hand side of (2.1.3) has been raised using the familiar rule:

$$A^\lambda = g^{\lambda\nu} A_\nu. \qquad (2.1.4)$$

Before stating the quantisation rule, it is instructive to consider the Hamiltonian density, defined as:

$$\mathcal{H} = \pi \partial_0 \phi - \mathcal{L} = \frac{1}{2}\sqrt{-g}\left\{ -g^{00}[\partial_0\phi]^2 + g^{ij}\partial_i\phi\partial_j\phi + [\mu^2 + \xi R]\phi^2 \right\}. \qquad (2.1.5)$$

The Hamiltonian of the system is the integral of the Hamiltonian density (2.1.5) over the spacelike hypersurface $t = \mathrm{const}$:

$$H = \int d^3x\, \mathcal{H} = \frac{1}{2}\int d^3x\, \pi \overleftrightarrow{\partial_0}\, \phi, \qquad (2.1.6)$$

where the bilateral derivative is defined as:

$$f\overleftrightarrow{\partial_\mu}g = f(\partial_\mu g) - (\partial_\mu f)g. \qquad (2.1.7)$$

Expression (2.1.6) follows from an integration by parts of the space derivatives in (2.1.5), followed by the use of the Klein-Gordon equation (2.1.2).

The quantisation scheme is defined such that the field $\phi(t, \boldsymbol{x})$ obeys Heisenberg's equation of motion:

$$[\phi(t, \boldsymbol{x}), H(t)] = i\partial_0\phi(t, \boldsymbol{x}). \qquad (2.1.8)$$

The standard solution is to impose the following equal time commutation rules:

$$[\phi(t, \boldsymbol{x}), \pi(t, \boldsymbol{x}')] = i\delta^3(\boldsymbol{x} - \boldsymbol{x}'),$$
$$[\phi(t, \boldsymbol{x}), \phi(t, \boldsymbol{x}')] = [\pi(t, \boldsymbol{x}), \pi(t, \boldsymbol{x}')] = 0. \qquad (2.1.9)$$

The evolution equation (2.1.8) can be solved, with the solution for a Hamiltonian with no explicit time dependence being:

$$\phi(t, \boldsymbol{x}) = e^{iH(t-t')}\phi(t', \boldsymbol{x})e^{-iH(t-t')}, \qquad (2.1.10)$$

valid for arbitrary initial time t'.

2.1.2   Stress-energy tensor

In general relativity, the SET plays an active role as the right hand side of Einstein's equations:

$$R_{\alpha\beta} - \frac{1}{2}g_{\alpha\beta}R = 8\pi T_{\alpha\beta}. \tag{2.1.11}$$

Einstein's equations can be derived using Hamilton's principle of least action along the physical trajectory, starting from the Einstein-Hilbert action:

$$S = \int \frac{d^4x}{16\pi}\sqrt{-g}\,R + S_{\text{matter}}, \qquad S_{\text{matter}} = \int d^4x\,\mathcal{L}, \tag{2.1.12}$$

where the second term is the Lagrangian density of any matter fields present. As a consequence, the SET is given by [55]:

$$T_{\alpha\beta} = -\frac{2}{\sqrt{-g}}\frac{\delta S_{\text{matter}}}{\delta g^{\alpha\beta}}, \tag{2.1.13}$$

and assumes the form [16]:

$$
\begin{aligned}
T_{\mu\nu} = {}&(1-2\xi)\nabla_\mu\phi\nabla_\nu\phi + (2\xi - \tfrac{1}{2})g_{\mu\nu}(\nabla\phi)^2 - 2\xi\phi\nabla_\mu\nabla_\nu\phi + \tfrac{2}{\mathfrak{n}}\xi g_{\mu\nu}\phi\Box\phi \\
&- \xi\left[R_{\mu\nu} - \tfrac{1}{2}Rg_{\mu\nu} + \tfrac{2}{\mathfrak{n}}(\mathfrak{n}-1)\xi Rg_{\mu\nu}\right]\phi^2 - 2\left[\tfrac{1}{4} - \left(1 - \tfrac{1}{\mathfrak{n}}\right)\xi\right]\mu^2 g_{\mu\nu}\phi^2,
\end{aligned} \tag{2.1.14}
$$

for the case of a scalar field of mass μ in an $\mathfrak{n}$-dimensional space-time, described by the Lagrangian density (2.1.1). Minimal coupling is achieved by setting $\xi = 0$, while conformal coupling corresponds to $\xi = \frac{1}{4}\frac{\mathfrak{n}-2}{\mathfrak{n}-1}$. In a 4-dimensional Ricci-flat space-time (i.e. $R_{\mu\nu} = 0$) with conformal coupling (i.e. $\xi = \frac{1}{6}$), equation (2.1.14) simplifies to [19]:

$$T_{\mu\nu} = \frac{2}{3}\nabla_\mu\phi\nabla_\nu\phi - \frac{1}{3}\phi\nabla_\mu\nabla_\nu\phi - \frac{1}{6}g_{\mu\nu}[g^{\lambda\kappa}\nabla_\lambda\phi\nabla_\kappa\phi + \mu^2\phi^2]. \tag{2.1.15}$$

In what follows, only conformally coupled scalar fields are considered.

It can be seen from Eq. (2.1.15) that, for any solution $\phi(x)$ of the Klein-Gordon equation (2.1.2), the trace of the SET is proportional to $\phi^2(x)$:

$$T^\mu_{\ \mu} = -\mu^2\phi^2(x), \tag{2.1.16}$$

and vanishes for massless particles. The divergence of the SET automatically vanishes as a consequence of the Klein-Gordon equation (2.1.2):

$$\nabla_\mu T^\mu_{\ \nu} = 0, \tag{2.1.17}$$

and $T_{\mu\nu}$ is symmetric by construction.

The classical SET can be promoted to a quantum operator by replacing any term

quadratic in the field by an anti-commutator:

$$T_{\mu\nu} = \frac{1}{3}\{\nabla_\mu\phi, \nabla_\nu\phi\} - \frac{1}{6}\{\phi, \nabla_\mu\nabla_\nu\phi\} - \frac{1}{12}g_{\mu\nu}[g^{\lambda\kappa}\{\nabla_\lambda\phi, \nabla_\kappa\phi\} + 2\mu^2\phi^2], \quad (2.1.18)$$

where $\phi \equiv \phi(x)$ is now the field operator.

2.1.3 Fock space

Let us consider a complete set of mode solutions $\{f_j, f_j^*\}$ of the Klein-Gordon equation, with $\{j\}$ being a set of discrete or continuous labels distinguishing between independent solutions. The modes are normalised with respect to the inner product:

$$\langle f, g \rangle = -i \int_V d^3x \sqrt{-g}[f^*(t, \boldsymbol{x}) \overleftrightarrow{\partial^0} g(t, \boldsymbol{x})], \quad (2.1.19)$$

such that

$$\langle f_j, f_{j'} \rangle = \delta_{jj'}, \quad \langle f_j^*, f_{j'}^* \rangle = -\delta_{jj'}, \quad \langle f_j^*, f_{j'} \rangle = \langle f_j, f_{j'}^* \rangle = 0. \quad (2.1.20)$$

In Eq. (2.1.19), g is the determinant of the metric tensor $g_{\mu\nu}$, $\overleftrightarrow{\partial^0}$ is the bilateral derivative (2.1.7) and the integration is performed over the three-dimensional hypersurface V of normal dt, where V can be the whole space or some region contained inside a closed boundary. In the above, the modes f_j are identified as solutions of the Klein-Gordon equation with positive norm. Consequently, Eqs. (2.1.2) amd (2.1.19) show that their charge conjugates f_j^* also satisfy the Klein-Gordon equation but they have negative norm.

The inner product (2.1.19) is well-defined if it is time independent:

$$\partial_0 \langle f, h \rangle = (-i) \int_V d^3x \left[\sqrt{-g}(\partial_0 f^*)\partial^0 h + f^*\partial_0(\sqrt{-g}\partial^0 h) - (f \leftrightarrow h)\right] \quad (2.1.21a)$$

$$= (-i) \int_V d^3x \left[\sqrt{-g}(\partial_0 f^*)(\partial^0 h) - f^*\partial_j(\sqrt{-g}\partial^j h) - (f \leftrightarrow h)\right] \quad (2.1.21b)$$

$$= i \int_{\partial V} d\Sigma_j \sqrt{-g}(f^* \overleftrightarrow{\partial^j} h). \quad (2.1.21c)$$

For brevity, only half of the terms have been explicitly written in steps (a) and (b). Expression (2.1.21b) follows from (2.1.21a) after using the Klein-Gordon equation (2.1.2), and the last step involves an integration by parts of the term containing the spatial derivative. The time-invariance of the inner product (2.1.19) requires that the integral (2.1.21c) over the boundary ∂V of the hypersurface V vanishes. Assuming that the inner product is well defined, the corresponding completeness relation can be written as:

$$\sum_j [f_j(t, \boldsymbol{x})\partial^0 f_j^*(t, \boldsymbol{x}') - f_j^*(t, \boldsymbol{x})\partial^0 f_j(t, \boldsymbol{x}')] = -\frac{i}{\sqrt{-g}}\delta^3(\boldsymbol{x} - \boldsymbol{x}'), \quad (2.1.22)$$

The most general solution of the Klein-Gordon equation can be written as a linear combination of the mode solutions f_j and f_j^*:

$$\phi(x) = \sum_j \left[f_j(x)a_j + f_j^*(x)a_j^\dagger \right]. \tag{2.1.23}$$

Second quantisation promotes $\phi(x)$ to an operator, called the field operator, obeying the commutation relation (2.1.9). Consequently, the coefficients a_j and $a_j^\dagger$ obey the following commutation relations:

$$\left[a_j, a_{j'}^\dagger \right] = \delta_{jj'}, \qquad [a_j, a_{j'}] = \left[a_j^\dagger, a_{j'}^\dagger \right] = 0. \tag{2.1.24}$$

The coefficients a_j of the positive norm modes f_j are called annihilation operators and are used to define the vacuum quantum state, which has the physical interpretation of a state containing no particles:

$$a_j \left| 0 \right\rangle = 0, \qquad \text{for all possible } j. \tag{2.1.25}$$

Applying products of creation operators $a_j^\dagger$ to the vacuum state (2.1.25) creates multiparticle states, which form a basis of the Fock space:

$$\left| j_1 j_2 \ldots j_n \right\rangle = (n!)^{-\frac{3}{2}} \sum_{\sigma \in S_n} \prod_{i=1}^n a_{j_{\sigma_i}}^\dagger \left| 0 \right\rangle. \tag{2.1.26}$$

The sum runs over all permutations σ of the first n natural numbers, all terms in the sum being equivalent by virtue of the boson commutation relations (2.1.24). The normalisation factor is chosen such that the vectors obey the normalisation condition:

$$\left\langle j_1' \ldots j_m' | j_1 \ldots j_n \right\rangle = \frac{\delta_{nm}}{n!} \sum_{\sigma \in S_n} \prod_{i=1}^n \delta_{j_i j_{\sigma_i}'}, \tag{2.1.27}$$

where, again, σ is an element of the set S_n of all permutations of the first n natural numbers. For the case $n = m = 2$, equation (2.1.27) reads:

$$\left\langle j_1' j_2' | j_1 j_2 \right\rangle = \frac{1}{2} (\delta_{j_1 j_1'} \delta_{j_2 j_2'} + \delta_{j_1 j_2'} \delta_{j_2 j_1'}). \tag{2.1.28}$$

The identity operator can be written in terms of the basis vectors (2.1.26) as:

$$I = \left| 0 \right\rangle \left\langle 0 \right| + \sum_{n=1}^\infty \sum_{j_1} \cdots \sum_{j_n} \left| j_1 \ldots j_n \right\rangle \left\langle j_1 \ldots j_n \right|, \tag{2.1.29}$$

and satisfies:

$$I^2 = I, \qquad I \left| j_1 \ldots j_n \right\rangle = \left| j_1 \ldots j_n \right\rangle. \tag{2.1.30}$$

In terms of one-particle operators, the SET (2.1.18) for a conformally coupled

scalar field in four space-time dimensions takes the form:

$$T_{\mu\nu} = \sum_{j,j'} \left[a_j a_{j'} \mathcal{T}_{\mu\nu}(f_j, f_{j'}) + a_j^\dagger a_{j'}^\dagger \mathcal{T}_{\mu\nu}(f_j^*, f_{j'}^*) \right.$$

$$\left. + \frac{1}{2} \left\{ a_j, a_{j'}^\dagger \right\} \mathcal{T}_{\mu\nu}(f_j, f_{j'}^*) + \frac{1}{2} \left\{ a_j^\dagger, a_{j'} \right\} \mathcal{T}_{\mu\nu}(f_j^*, f_{j'}) \right], \quad (2.1.31)$$

where $\mathcal{T}_{\mu\nu}(f, h)$ is the bilinear form given by:

$$\mathcal{T}_{\mu\nu}(f, h) = \frac{2}{3} \nabla_\mu f \nabla_\nu h - \frac{1}{3} f \nabla_\mu \nabla_\nu h - \frac{1}{6} g_{\mu\nu} [g^{\lambda\kappa} \nabla_\lambda f \nabla_\kappa h + \mu^2 f h]. \quad (2.1.32)$$

Expression (2.1.31) will prove useful for the computation of the expectation value of the stress tensor in one-particle or thermal states.

Let us specialise further to mode solutions of the Klein-Gordon equation (2.1.2) which satisfy the eigenvalue equations:

$$i\partial_t f_j = \widetilde{\omega}_j f_j, \qquad\qquad i\partial_t f_j^* = -\widetilde{\omega}_j f_j^*,$$
$$-i\partial^t f_j = \omega_j f_j, \qquad\qquad -i\partial^t f_j^* = -\omega_j f_j^*. \quad (2.1.33)$$

An integration of these equations shows that $f_j \sim e^{i\widetilde{\omega}_j t}$. Hence, $\widetilde{\omega}_j$ can be interpreted as the frequency of the mode j. Under the assumptions (2.1.33), the normalisation conditions (2.1.19) and the completeness relation (2.1.22) take the form:

$$(\omega_{j'} + \omega_j) \int d^3x \sqrt{-g} f_j^*(t, \boldsymbol{x}) f_{j'}(t, \boldsymbol{x}) = \delta_{jj'},$$
$$(\omega_{j'} - \omega_j) \int d^3x \sqrt{-g} f_j(t, \boldsymbol{x}) f_{j'}(t, \boldsymbol{x}) = 0,$$
$$\sum_j \omega_j \left[f_j(t, \boldsymbol{x}) f_j^*(t, \boldsymbol{x}') + f_j^*(t, \boldsymbol{x}) f_j(t, \boldsymbol{x}') \right] = \frac{1}{\sqrt{-g}} \delta^3(\boldsymbol{x} - \boldsymbol{x}'), \quad (2.1.34)$$

which requires $\omega_j \geq 0$ (i.e., instead of the eigenvalue $\widetilde{\omega}_j$ of the Hamiltonian). Thus, the norm and frequency of a mode f_j can have opposite signs if $\omega_j \widetilde{\omega}_j < 0$, forcing modes with negative frequency in the set of particle modes.

The conjugate momentum (2.1.3) reads:

$$\pi(t, \boldsymbol{x}) = -i\sqrt{-g} \sum_j \omega_j \left[f_j(t, \boldsymbol{x}) a_j - f_j^*(t, \boldsymbol{x}) a_j^\dagger \right], \quad (2.1.35)$$

hence, the Hamiltonian (2.1.6) assumes the canonical form:

$$H = \frac{1}{2} \sum_j \widetilde{\omega}_j (a_j^\dagger a_j + a_j a_j^\dagger). \quad (2.1.36)$$

The key restriction of having positive norm for the particle modes f_j implies that

each particle makes a contribution of $\widetilde{\omega}_j$ to the total energy of the system:

$$\left[H, a_j^\dagger\right] = \widetilde{\omega}_j a_j^\dagger. \tag{2.1.37}$$

Equation (2.1.37) shows that particles for which $\widetilde{\omega}_j < 0$ make negative contributions to the total Hamiltonian of the system, while particles for which $\widetilde{\omega}_j$ vanishes do not contribute. These simple remarks will have important consequences for constructing rigidly rotating thermal states containing scalar particles, as discussed in subsection 4.2.2.

2.1.4 Finite temperature field theory

The concept of temperature is implemented by considering a quantum state containing a thermal distribution of particle states, with the Hamiltonian operator H playing the role of energy. The expectation value of an operator A in a thermal state at a finite inverse temperature $\beta = T^{-1}$ is defined as:

$$\langle A \rangle_\beta = \frac{1}{Z}\mathrm{tr}(e^{-\beta H}A) = \sum_{n=0}^{\infty}\left\{\sum_{j_1,j_2,\ldots j_n}\langle j_1\ldots j_n|e^{-\beta H}A|j_1\ldots j_n\rangle\right\}, \tag{2.1.38}$$

where Z is the grand partition function:

$$Z = \mathrm{tr}(e^{-\beta H}). \tag{2.1.39}$$

The evaluation of the t.e.v.s of interest in this work requires the t.e.v.s of the following products of two one-particle operators [72]:

$$\langle a_j^\dagger a_{j'}\rangle_\beta = \frac{\delta_{jj'}}{e^{\beta\widetilde{\omega}_j}-1}, \qquad \langle a_j a_{j'}^\dagger\rangle_\beta = \frac{\delta_{jj'}}{1-e^{-\beta\widetilde{\omega}_j}}, \qquad \langle a_j a_{j'}\rangle_\beta = \langle a_j^\dagger a_{j'}^\dagger\rangle_\beta = 0, \tag{2.1.40}$$

where the operators a_j and $a_j^\dagger$ satisfy the commutation relations (2.1.24) and the commutator (2.1.37) of $a_j^\dagger$ and H depends on $\widetilde{\omega}_j$.

The requirement (2.1.19) that particle modes have positive norm allows $\widetilde{\omega}_j$ to be negative, in which case the formulae (2.1.40) are no longer correct, since the expectation value of any operator at $T = 0$ ($\beta \to \infty$) has to be equal to its vacuum expectation value (v.e.v.). Therefore, the t.e.v. of an operator in Wick (normal) order, defined as:

$$: A := A - \langle 0|A|0\rangle, \tag{2.1.41}$$

should vanish. Using (2.1.24) and (2.1.40), it can be seen that:

$$\langle : a_j^\dagger a_{j'} : \rangle_\beta \xrightarrow[\substack{\beta\to\infty \\ \widetilde{\omega}_j<0}]{} -\delta_{jj'}, \tag{2.1.42}$$

Equation (2.1.42) shows that the difference between the thermal and vacuum expectation value of, for example, the SET will receive spurious contributions coming from particle modes with negative frequencies $\widetilde{\omega}_j$, as will be seen in subsection 4.2.2.

The formulae (2.1.40) can be used to compute the t.e.v. of the Hamiltonian (2.1.36):

$$\frac{1}{V} \langle : H : \rangle_\beta = \frac{1}{2} \sum_j \widetilde{\omega}_j \left(\coth \frac{\beta \widetilde{\omega}_j}{2} - 1 \right) = \sum_j \frac{\widetilde{\omega}_j}{e^{\beta \widetilde{\omega}_j} - 1}, \qquad (2.1.43)$$

where V is the volume of space, and of the SET (2.1.31):

$$\langle : T_{\mu\nu} : \rangle_\beta = \sum_j \frac{1}{e^{\beta \widetilde{\omega}_j} - 1} \left[\mathcal{T}_{\mu\nu}(f_j^*, f_{j'}) + \mathcal{T}_{\mu\nu}(f_j, f_{j'}^*) \right]. \qquad (2.1.44)$$

It is remarkable that the t.e.v. (2.1.43) of the Hamiltonian is finite for all j. This is not true for the SET, which receives infinite contributions from modes having $\widetilde{\omega}_j = 0$, as discussed in subsection 4.2.2.

2.1.5 Green's functions

Another approach to computing expectation values uses Green's functions. In quantum field theory, operators like the Hamiltonian or SET can have non-vanishing v.e.v.s. These can be computed using appropriate regularisation and renormalisation methods to isolate and eliminate pathological divergences occuring from the point-like singular behaviour of field commutators (2.1.9), as discussed in chapter 7 for the anti-de Sitter space-time. For the purpose of calculating t.e.v.s, only the difference between thermal states and the (zero temperature) vacuum state are considered in this thesis. To this end, only t.e.v.s of Wick-ordered operators (i.e. of operators with their v.e.v. subtracted) are considered in the remainder of this thesis.

The building blocks for the Green's functions under consideration in this thesis are the Wightman functions $G^\pm(x'x)$, defined with respect to the vacuum as:

$$G^+(x, x') = \langle 0 | \phi(x) \phi(x') | 0 \rangle, \qquad G^-(x, x') = \langle 0 | \phi(x') \phi(x) | 0 \rangle. \qquad (2.1.45)$$

The Wightman functions can be used for the construction of Hadamard's elementary function $G^{(1)}(x, x')$:

$$G^{(1)}(x, x') = \langle 0 | \{ \phi(x), \phi(x') \} | 0 \rangle = G^+(x, x') + G^-(x, x') \qquad (2.1.46)$$

and of the Pauli-Jordan or Schwinger function:

$$iG(x, x') = \langle 0 | [\phi(x), \phi(x')] | 0 \rangle = G^+(x, x') - G^-(x, x'). \qquad (2.1.47)$$

To depart from the vacuum to a thermal state, the Wightman functions (2.1.45) must be defined as t.e.v.s using (2.1.38). The cyclic property of the trace $\operatorname{tr}(ABC) = \operatorname{tr}(CAB)$ and the Heisenberg evolution equation (2.1.10) can be used to show that

$$
\begin{aligned}
G_\beta^-(t, \boldsymbol{x}; t', \boldsymbol{x}') &= Z^{-1}\operatorname{tr}[e^{-\beta H}\phi^\dagger(t', \boldsymbol{x}')\phi(t, \boldsymbol{x})] \\
&= Z^{-1}\operatorname{tr}[\phi^\dagger(t', \boldsymbol{x}')e^{-\beta H}e^{\beta H}\phi(t, \boldsymbol{x})e^{-\beta H}] \\
&= Z^{-1}\operatorname{tr}[\phi^\dagger(t', \boldsymbol{x}')e^{-\beta H}\phi(t - i\beta, \boldsymbol{x})] \\
&= Z^{-1}\operatorname{tr}[e^{-\beta H}\phi(t - i\beta, \boldsymbol{x})\phi^\dagger(t', \boldsymbol{x}')].
\end{aligned}
\tag{2.1.48}
$$

A similar relation can be established for $G_\beta^+(t, \boldsymbol{x}; t', \boldsymbol{x}')$, leading to the following result:

$$
G_\beta^\pm(t, \boldsymbol{x}; t', \boldsymbol{x}') = G_\beta^\mp(t \pm i\beta, \boldsymbol{x}; t', \boldsymbol{x}').
\tag{2.1.49}
$$

By virtue of the commutation relations (2.1.9), the commutator of the field operator with itself is just a number (i.e. it is proportional to the identity operator with respect to the Fock space). Thus, the Schwinger function (2.1.47) is independent of the state in which it is evaluated. To use this property, it is useful to consider its Fourier transform

$$
iG(x, x') = iG_\beta(x, x') = \int_{-\infty}^{\infty} \frac{d\omega}{2\pi} g(\omega; \boldsymbol{x}, \boldsymbol{x}')e^{-i\omega(t-t')},
\tag{2.1.50}
$$

where $g(\omega; \boldsymbol{x}, \boldsymbol{x}') = g_\beta(\omega; \boldsymbol{x}, \boldsymbol{x}')$ is again independent of state. For the Fourier coefficients $g_\beta^\pm(\omega; \boldsymbol{x}, \boldsymbol{x}')$ of the thermal Wightman functions $G_\beta^\pm(x, x')$, defined in a similar fashion, Eq. (2.1.49) implies:

$$
g_\beta^\pm(\omega; \boldsymbol{x}, \boldsymbol{x}') = g_\beta^\mp(\omega; \boldsymbol{x}, \boldsymbol{x}')e^{\pm\omega\beta}.
\tag{2.1.51}
$$

These coefficients are related to $g(\omega; \boldsymbol{x}, \boldsymbol{x}')$ through the definition of the Schwinger function (2.1.47):

$$
g_\beta^\pm(\omega; \boldsymbol{x}, \boldsymbol{x}') = \pm\frac{g(\omega; \boldsymbol{x}, \boldsymbol{x}')}{1 - e^{\mp\omega\beta}}.
\tag{2.1.52}
$$

Substituting back into Eq. (2.1.46), the following Fourier representation can be obtained for the thermal Hadamard function:

$$
G_\beta^{(1)}(x, x') = \int_{-\infty}^{\infty} \frac{d\omega}{2\pi} g(\omega; \boldsymbol{x}, \boldsymbol{x}')e^{-i\omega(t-t')} \coth\frac{\beta\omega}{2}.
\tag{2.1.53}
$$

Since the construction of the thermal Hadamard function only relies on the Fourier transform of the Schwinger function, the thermal state does not depend on the choice of vacuum. However, t.e.v.s do depend on the choice of vacuum, through the Wick ordering process of the operators under consideration.

The t.e.v. of the SET (2.1.18) can be expressed using the thermal Hadamard

function, defined as $\Delta G_\beta^{(1)} = G_\beta^{(1)} - G^{(1)}$:

$$\langle : T_{\mu\nu} : \rangle_\beta = \frac{1}{2} \lim_{x' \to x} \left\{ \frac{2}{3} \nabla_\mu \Delta G_\beta^{(1)}(x, x') \overleftarrow{\nabla}_{\lambda'} g^{\lambda'}{}_\nu - \frac{1}{3} \nabla_\mu \nabla_\nu \Delta G_\beta^{(1)}(x, x') \right.$$
$$\left. - \frac{1}{6} g_{\mu\nu} \left[g^{\lambda\kappa'} \nabla_\lambda \Delta G_\beta^{(1)}(x, x') \overleftarrow{\nabla}_{\kappa'} + \mu^2 \Delta G_\beta^{(1)}(x, x') \right] \right\}, \quad (2.1.54)$$

where $g_{\mu'\nu}$ is the bi-vector of parallel transport introduced to parallel transport tensors from x' to x along the geodesic connecting the two points, as follows:

$$A_\parallel^\mu(x) = g^\mu{}_{\nu'} A^{\nu'}(x'). \quad (2.1.55)$$

Hence, $g_{\mu\nu'}$ satisfies the parallel transport equations:

$$n^{\lambda'} g_{\mu'\nu;\lambda'} = 0, \qquad n^\kappa g_{\mu\nu';\kappa} = 0. \quad (2.1.56)$$

The quadratic field fluctuations (2.1.16) can be calculated as:

$$\langle : \phi^2(x) : \rangle_\beta = \frac{1}{2} \lim_{x' \to x} \Delta G_\beta^{(1)}(x, x'). \quad (2.1.57)$$

To introduce the Euclidean Green's function, useful for the computation of the contribution to the v.e.v. of the SET due to changes in geometry (the Casimir effect), it is useful to first consider the Feynman Green's function, defined as:

$$iG_F(x, x') = \langle 0 | T[\phi(x)\phi^\dagger(x')] | 0 \rangle$$
$$= \theta(t - t') G^+(x, x') + \theta(t' - t) G^-(x, x'), \quad (2.1.58)$$

where T is the time ordering operator, under which operators are in decreasing order of the time parameter and the Heaviside (step) function $\theta(x)$ takes the value 1 when its argument is positive and vanishes otherwise. The Feynman Green's function can be obtained either by using the mode expansion (2.1.23), or by solving the inhomogeneous Klein-Gordon equation directly:

$$(\Box - \mu^2) G_F(x, x') = G_F(x, x')(\overleftarrow{\Box'} - \mu^2) = -\frac{1}{\sqrt{-g}} \delta^4(x - x'). \quad (2.1.59)$$

The v.e.v. of $T_{\mu\nu}$ is given in terms of G_F by (2.1.54) with $\Delta G_\beta^{(1)}$ replaced by $2iG_F$. For the practical purpose of calculating expectation values, it is convenient to change the time coordinate to the imaginary time $\tau = it$. This change to imaginary time can be performed at the level of the manifold, by considering the following Euclidean coordinates [16]:

$$\tau = it, \quad x_E^j = x^j. \quad (2.1.60)$$

If the components of the metric mixing space and time are zero (i.e. if $g_{it} = 0$), the

resulting metric has positive signature and the manifold is Euclidean. Otherwise, the
resulting manifold is quasi-Euclidean [36, 67]. Although it involves a complex-valued
metric, the quasi-Euclidean approach can be useful for the investigation of bounded
rotating states where a speed of light surface forms, as discussed in chapter 6. The
Euclidean equivalent of the Feynman Green's function (2.1.59) is the Euclidean
Green's function, satisfying the inhomogeneous field equation:

$$(\Box_E - \mu^2)G_E(x,x') = G_E(x,x')(\overleftarrow{\Box}'_E - \mu^2) = -\frac{1}{\sqrt{g_E}}\delta(\tau - \tau')\delta^3(\boldsymbol{x} - \boldsymbol{x}'), \quad (2.1.61)$$

together with the requirement of regularity throughout space-time and appropriate
boundary conditions if the space-time includes a boundary. The following formula
can be used to calculate the v.e.v. of ϕ^2:

$$\langle 0|\phi^2|0\rangle = \lim_{x'\to x} G_E(x,x'), \quad (2.1.62)$$

while the SET can be calculated using:

$$\langle 0|T_{\mu\nu}|0\rangle = \lim_{x'\to x}\left\{\frac{2}{3}\nabla_\mu G_E(x,x')\overleftarrow{\nabla}_{\lambda'}g^{\lambda'}{}_\nu - \frac{1}{3}\nabla_\mu\nabla_\nu G_E(x,x')\right.$$
$$\left. -\frac{1}{6}g_{\mu\nu}\left[g^{\lambda\kappa'}\nabla_\lambda G_E(x,x')\overleftarrow{\nabla}_{\kappa'} + \mu^2 G_E(x,x')\right]\right\}, \quad (2.1.63)$$

where all coordinate indices refer to Euclidean coordinates. In this work, Euclid-
ianisation is used solely for the investigation of the Casimir effect on the rotating
Minkowski space in the presence of a boundary. This is discussed for the scalar case
in subsection 5.1.3.

2.2   The quantised Dirac field

2.2.1   Gamma matrices

To construct the Dirac equation, it is necessary to couple its spin part to an or-
thonormal tetrad $e_{\hat{\alpha}} = e_{\hat{\alpha}}^\mu\partial_\mu$. The tetrad is defined such that the metric tensor has
the components of the Minkowski metric $\eta_{\hat{\alpha}\hat{\beta}} = \mathrm{diag}(-1,1,1,1)$ with respect to its
dual co-frame, $\omega^{\hat{\alpha}} = \omega_\mu^{\hat{\alpha}}dx^\mu$:

$$g = g_{\mu\nu}dx^\mu \otimes dx^\nu = \eta_{\hat{\alpha}\hat{\beta}}\omega^{\hat{\alpha}} \otimes \omega^{\hat{\beta}}. \quad (2.2.1)$$

The co-frame is dual to the tetrad in the sense that:

$$\langle \omega^{\hat{\alpha}}, e_{\hat{\beta}}\rangle \equiv \omega_\mu^{\hat{\alpha}}e_{\hat{\beta}}^\mu = \delta^{\hat{\alpha}}{}_{\hat{\beta}}. \quad (2.2.2)$$

In this work, hatted indices refer to components with respect to the orthonormal tetrad.

To construct the Dirac equation, a set of four anti-commuting matrices, called the γ (gamma) matrices, must be introduced. On flat space-time, these matrices satisfy the following anti-commutation relations:

$$\left\{\gamma^{\hat{\alpha}}, \gamma^{\hat{\beta}}\right\} = -2\eta^{\hat{\alpha}\hat{\beta}}, \quad \eta^{\hat{\alpha}\hat{\beta}} = \text{diag}(-1, +1, +1, +1). \tag{2.2.3}$$

and are self-adjoint with respect to the Dirac adjoint:

$$\overline{\gamma}^{\hat{\alpha}} = \gamma^{\hat{0}}\gamma^{\hat{\alpha}\dagger}\gamma^{\hat{0}} = \gamma^{\hat{\alpha}}, \tag{2.2.4}$$

or equivalently, $\gamma^{\hat{0}}$ is hermitian and $\gamma^{\hat{i}}$ are anti-hermitian.

Following the requirement of covariance of the Dirac equation (to be introduced later) under Lorentz transformations, the anti-hermitian generators of Lorentz transformations are given by [46]:

$$\Sigma^{\hat{\alpha}\hat{\beta}} = \frac{1}{4}\left[\gamma^{\hat{\alpha}}, \gamma^{\hat{\beta}}\right]. \tag{2.2.5}$$

The spin operators (generators of rotations) are given by:

$$\Sigma_{\hat{i}} = \frac{1}{2}\varepsilon_{\hat{i}\hat{j}\hat{k}}\Sigma^{\hat{j}\hat{k}}, \tag{2.2.6}$$

where $\varepsilon_{\hat{i}\hat{j}\hat{k}}$ is the Levi-Civitta symbol, taking the value 1 (-1) when $(\hat{i}, \hat{j}, \hat{k})$ is an even (odd) permutation of $(1, 2, 3)$.

In this thesis, the γ matrices are taken to be in the Dirac representation, as follows [46]:

$$\gamma^{\hat{0}} = \begin{pmatrix} 1 & 0 \\ 0 & -1 \end{pmatrix}, \quad \gamma^{\hat{i}} = \begin{pmatrix} 0 & \sigma_i \\ -\sigma_i & 0 \end{pmatrix}, \tag{2.2.7}$$

where the Pauli matrices σ^i are given by:

$$\sigma^1 = \begin{pmatrix} 0 & 1 \\ 1 & 0 \end{pmatrix}, \qquad \sigma^2 = \begin{pmatrix} 0 & -i \\ i & 0 \end{pmatrix}, \qquad \sigma^3 = \begin{pmatrix} 1 & 0 \\ 0 & -1 \end{pmatrix}, \tag{2.2.8}$$

and obey the following relations:

$$\{\sigma_i, \sigma_j\} = 2\delta_{ij}, \quad [\sigma_i, \sigma_j] = 2i\varepsilon_{ijk}\sigma_k. \tag{2.2.9}$$

The anti-hermitian generators of rotations (2.2.6) are:

$$\Sigma_i = -\frac{i}{2}\begin{pmatrix} \sigma_i & 0 \\ 0 & \sigma_i \end{pmatrix}, \tag{2.2.10}$$

and obey the following relations:

$$\{\Sigma_i, \Sigma_j\} = -\frac{1}{2}\delta_{ij}, \quad [\Sigma_i, \Sigma_j] = \varepsilon_{ijk}\Sigma_k. \tag{2.2.11}$$

The chirality operator γ^5 can be defined as:

$$\gamma^5 = i\gamma^0\gamma^1\gamma^2\gamma^3 = \begin{pmatrix} 0 & 1 \\ 1 & 0 \end{pmatrix}. \tag{2.2.12}$$

The anti-commutator of γ^5 with any other gamma matrix vanishes:

$$\{\gamma^5, \gamma^\mu\} = 0. \tag{2.2.13}$$

The chirality operator is especially important for massless Dirac fermions, in which case the Minkowski Dirac equation $i\gamma^\mu\partial_\mu\psi(x) = 0$ can be put in the form [46]:

$$i\gamma^5\partial_t\psi = 2pW_0\psi, \tag{2.2.14}$$

where W_0 is the helicity operator introduced in Eqs. (3.3.1). If ψ is a helicity eigenvector with positive frequency then $\gamma^5 = 2\lambda$ measures the helicity of ψ. If ψ is a negative frequency eigenvector of the helicity operator, $\gamma^5\psi = -2\lambda\psi$, therefore, negative chirality means negative helicity for positive frequency modes and positive helicity for negative frequency modes.

2.2.2   Second quantisation

The Lagrangian density for a spin $\frac{1}{2}$ Dirac field of mass μ has the form [16]:

$$\mathcal{L} = \sqrt{-g}\left[\frac{i}{2}\left(\overline{\psi}\gamma^{\hat{\alpha}}e_{\hat{\alpha}}^\lambda D_\lambda\psi - \overline{D_\lambda\psi}\gamma^{\hat{\alpha}}e_{\hat{\alpha}}^\lambda\psi\right) - \mu\overline{\psi}\psi\right], \tag{2.2.15}$$

where D_μ is the covariant spinor derivative operator:

$$D_\mu = \partial_\mu - \Gamma_\mu, \tag{2.2.16}$$

written using the spin connection coefficients Γ_μ, defined as:

$$\Gamma_\mu = \frac{1}{2}\omega_\mu^{\hat{\alpha}}\Gamma_{\hat{\beta}\hat{\gamma}\hat{\alpha}}\Sigma^{\hat{\beta}\hat{\gamma}}. \tag{2.2.17}$$

The tetrad vectors $\{e_{\hat{\alpha}}\}$ and their dual one-forms $\{\omega^{\hat{\beta}}\}$ are defined (up to a Lorentz transformation) by Eq. (2.2.1). The connection coefficients $\Gamma_{\hat{\beta}\hat{\gamma}\hat{\alpha}}$ are defined as:

$$\Gamma_{\hat{\beta}\hat{\gamma}\hat{\alpha}} = \eta_{\hat{\beta}\hat{\rho}}\left\langle\omega^{\hat{\rho}}, \nabla_{\hat{\alpha}}e_{\hat{\gamma}}\right\rangle, \tag{2.2.18}$$

which can also be written in terms of the Cartan coefficients $c_{\hat{\alpha}\hat{\beta}}{}^{\hat{\gamma}}$:

$$\Gamma_{\hat{\beta}\hat{\gamma}\hat{\alpha}} = \frac{1}{2}(c_{\hat{\beta}\hat{\gamma}\hat{\alpha}} + c_{\hat{\beta}\hat{\alpha}\hat{\gamma}} - c_{\hat{\gamma}\hat{\alpha}\hat{\beta}}), \qquad c_{\hat{\alpha}\hat{\beta}}{}^{\hat{\gamma}} = \langle \omega^{\hat{\gamma}}, \left[e_{\hat{\alpha}}, e_{\hat{\beta}} \right] \rangle. \tag{2.2.19}$$

The resulting Euler-Lagrange equation is the Dirac equation in a covariant form:

$$(i\gamma^{\hat{\alpha}} e_{\hat{\alpha}}^{\lambda} D_{\lambda} - \mu)\psi(x) = 0. \tag{2.2.20}$$

The Hamiltonian following from the Lagrangian (2.2.15) is:

$$\mathcal{H} = \frac{i}{2}\sqrt{-g}\left(\overline{\psi}\gamma^0 \partial_t \psi - \partial_t \overline{\psi}\gamma^0 \psi \right). \tag{2.2.21}$$

Heisenberg's equation of motion,

$$[\psi(t, \boldsymbol{x}), H(t)] = i\partial_0 \psi(t, \boldsymbol{x}), \tag{2.2.22}$$

is satisfied if the following equal time anti-commutation relations hold:

$$\begin{aligned} \left\{ \psi_a(t, \boldsymbol{x}'), \overline{\psi}_b(t, \boldsymbol{x})\gamma^0(t, \boldsymbol{x})_{bc} \right\} &= (-g)^{-1/2}\delta_{ac}\delta^3(\boldsymbol{x} - \boldsymbol{x}'), \\ \left\{ \psi_a(t, \boldsymbol{x}), \psi_b(t, \boldsymbol{x}') \right\} &= 0, \end{aligned} \tag{2.2.23}$$

where the subscripts a, b, c are spinor indices and the summation of repeated indices is implied. The solution to Heisenberg's equation of motion is

$$\psi(t, \boldsymbol{x}) = e^{iH(t-t')}\psi(t', \boldsymbol{x})e^{-iH(t-t')}. \tag{2.2.24}$$

where t' is an arbitrary initial time.

2.2.3 Stress-energy tensor and conserved current

Due to the dependence of the Dirac Lagrangian (2.2.15) on the metric through the tetrad vectors $e_{\hat{\alpha}}$, it is convenient to replace the derivative with respect to $g^{\mu\nu}$ in (2.1.13) using the chain rule:

$$\frac{\delta}{\delta e_{\hat{\alpha}}^{\lambda}} = \eta^{\hat{\alpha}\hat{\beta}}(e_{\hat{\beta}}^{\mu}\delta^{\nu}{}_{\lambda} + e_{\hat{\beta}}^{\nu}\delta^{\mu}{}_{\lambda})\frac{\delta}{\delta g^{\mu\nu}},$$

which gives:

$$T_{\mu\nu} = -\frac{1}{\sqrt{-g}}\frac{\delta\mathcal{L}}{\delta e_{\hat{\alpha}}^{\mu}}\eta_{\hat{\alpha}\hat{\beta}}\omega_{\nu}^{\hat{\beta}}. \tag{2.2.25}$$

The quantum expression for the SET is obtained by substituting the Dirac Lagrangian density (2.2.15) in (2.2.25) and replacing any terms quadratic in the field

by a commutator:

$$T_{\mu\nu} = -\frac{i}{4}\left\{\left[\overline{\psi}, \gamma_{(\nu}D_{\mu)}\psi\right] - \left[\overline{D_{(\nu}\psi}\gamma_{\mu)}, \psi\right]\right\},\tag{2.2.26}$$

where round brackets indicate symmetrisation. The commutators above refer to the order in which the field operators ψ and $\overline{\psi}$ act on quantum states, with the spinor indices left unchanged, as explained in Eq. (2.2.23).

The SET (2.2.26) is conserved by construction if ψ is a solution of the Dirac equation (2.2.20), i.e.:

$$\nabla_\mu T^\mu{}_\nu = 0.\tag{2.2.27}$$

The Dirac equation (2.2.20) can be used to write the trace of the SET in terms of the quantum fermion condensate (FC) operator $\frac{1}{2}\left[\overline{\psi}, \psi\right]$:

$$T^\mu{}_\mu = -\frac{\mu}{2}\left[\overline{\psi}, \psi\right].\tag{2.2.28}$$

The charge current (CC) is:

$$J^\mu(x) = \frac{1}{2}\left[\overline{\psi}, \gamma^\mu\psi\right], \qquad \nabla_\mu J^\mu(x) = 0,\tag{2.2.29}$$

giving rise to the inner product:

$$\langle\psi, \chi\rangle = \int_V d^3x\sqrt{-g}\,\overline{\psi}\gamma^0(x)\chi,\tag{2.2.30}$$

where the integration runs over the spacelike hypersurface V of normal dt. The inner product is time-independent for any combinations of solutions to the Dirac equation (2.2.20) if:

$$\begin{aligned}
\partial_0\langle\psi, \chi\rangle &= \int_V d^3x\left[\sqrt{-g}(\partial_0\overline{\psi})\gamma^0\chi + \sqrt{-g}\,\overline{\psi}\gamma^0(\partial_0\chi) + \overline{\psi}\partial_0(\sqrt{-g}\gamma^0)\chi\right]\\
&= -\int_V d^3x\left\{\sqrt{-g}\left(\partial_i\overline{\psi}\gamma^i\chi + \overline{\psi}\gamma^i\partial_i\chi + \left[\Gamma_\lambda, \gamma^\lambda\right]\chi\right) + \overline{\psi}\partial_i(\gamma^i\sqrt{-g})\chi\right\}\\
&= -\int_{\partial V} d\Sigma_i\sqrt{-g}\,\overline{\psi}\gamma^i\chi,
\end{aligned}\tag{2.2.31}$$

where ∂V is the boundary of the volume of the system. The second line follows from an application of the Dirac equation (2.2.20) and the general covariance $[D_\mu, \gamma^\nu] = 0$ of the γ matrices:

$$\begin{aligned}
\gamma^t\partial_t\chi &= -\gamma^i\partial_i\chi - \gamma^\lambda\Gamma_\lambda\chi - i\mu\chi,\\
\partial_t\overline{\psi}\gamma^t &= -\partial_i\overline{\psi}\gamma^i + \overline{\psi}\Gamma_\lambda\gamma^\lambda + i\mu\psi,\\
\partial_t(\sqrt{-g}\gamma^t) &= -\partial_i(\gamma^i\sqrt{-g}) - \sqrt{-g}\left[\Gamma_\lambda, \gamma^\lambda\right].
\end{aligned}\tag{2.2.32}$$

The result is obtained using integration by parts.

In chapters 3 and 4, where V is the infinite unbounded space, condition (2.2.31) is automatically satisfied, but in sections 5.2 and 5.3 it is used as the starting point for the formulation of boundary conditions for the solutions of the Dirac equation.

2.2.4 Fock space

Let us consider a complete set of mode solutions $\{U_j, V_j\}$ of the Dirac equation (2.2.20), with $\{j\}$ being a set of discrete or continuous labels distinguishing between independent solutions. The modes are normalised with respect to the inner product (2.2.30) as follows:

$$\langle U_j, U_{j'} \rangle = \langle V_j, V_{j'} \rangle = \delta_{jj'}, \qquad \langle U_j, V_{j'} \rangle = 0. \tag{2.2.33}$$

The modes must satisfy the completeness relation compatible with the Dirac inner product:

$$\sum_j [U_j(t, \boldsymbol{x}) \otimes \overline{U}_j(t, \boldsymbol{x}') + V_j(t, \boldsymbol{x}) \otimes \overline{V}_j(t, \boldsymbol{x}')] \gamma^0(t, \boldsymbol{x}') = (-g)^{-1/2} \delta^3(\boldsymbol{x} - \boldsymbol{x}'). \tag{2.2.34}$$

Hence, a general solution $\psi(x)$ of the Dirac equation can be expanded as:

$$\psi(x) = \sum_j \left[U_j(x) b_j + V_j(x) d_j^\dagger \right]. \tag{2.2.35}$$

The upgrade of $\psi(x)$ to a quantum operator requires that it satisfies the anti-commutation relations (2.2.23), implying that the Fourier coefficients b_j and $d_j^\dagger$ introduced above must obey:

$$\left\{ b_j, b_{j'}^\dagger \right\} = \left\{ d_j, d_{j'}^\dagger \right\} = \delta_{jj'}, \tag{2.2.36}$$

with the anti-commutator of any other combination vanishing. Since $\psi(x)$ is a complex-valued spinor, $b_j \neq d_j$ and $b_j^\dagger$ and $d_j^\dagger$ behave as creation operators of particles and anti-particles, respectively. The vacuum quantum state $|0\rangle$ is defined as the state vector which is annihilated by all particle and anti-particle annihilation operators:

$$b_j |0\rangle = d_j |0\rangle = 0, \qquad \text{for all possible } k. \tag{2.2.37}$$

Multiparticle states formed by applying products of creation operators are anti-symmetric with respect to the interchange of any two partices:

$$|j_1 j_2 \dots j_n \widetilde{j}_1 \dots \widetilde{j}_m\rangle = (n!m!)^{-\frac{3}{2}} \sum_{\sigma \in S_n, \widetilde{\sigma} \in S_m} (-1)^\sigma \prod_{i=1}^n b_{j_{\sigma_i}}^\dagger (-1)^{\widetilde{\sigma}} \prod_{k=1}^m d_{j_{\widetilde{\sigma}_k}}^\dagger |0\rangle. \tag{2.2.38}$$

Here $\widetilde{j}_k$ denotes an anti-particle created by the operator $d_{\widetilde{j}_k}^\dagger$ and the factor $(-1)^\sigma$ gives the parity of the permutation σ ($+1$ if σ represents an even number of transpositions, -1 otherwise). The anti-symmetry in the interchange of two particles is a fundamental difference between fermion and boson matter, being the main cause for the difference in finite temperature statistics.

In terms of one-particle operators, the SET (2.2.26) takes the form:

$$T_{\mu\nu} = \sum_{j,j'} \left\{ d_j b_{j'} \mathcal{T}_{\mu\nu}(V_j, U_{j'}) + b_j^\dagger d_{j'}^\dagger \mathcal{T}_{\mu\nu}(U_j, V_{j'}) \right.$$

$$\left. + \frac{1}{2}\left[b_j^\dagger, b_{j'}\right]\mathcal{T}_{\mu\nu}(U_j, U_{j'}) + \frac{1}{2}\left[d_j, d_{j'}^\dagger\right]\mathcal{T}_{\mu\nu}(V_j, V_{j'}) \right\}, \quad (2.2.39)$$

where, $\mathcal{T}_{\mu\nu}(\psi, \chi)$ is the bilinear form:

$$\mathcal{T}_{\mu\nu}(\psi, \chi) = \frac{i}{2}(\overline{\psi}\gamma_{(\mu}D_{\nu)}\chi - \overline{D_{(\mu}\psi}\gamma_{\nu)}\chi). \quad (2.2.40)$$

Expression (2.2.39) can be used to compute the expectation value of the SET in various states.

Let us specialise further to mode solutions which are eigenvectors of the Hamiltonian operator $H = i\partial_t$:

$$i\partial_t U_j = \widetilde{E}_j U_j, \quad i\partial_t V_j = -\widetilde{E}_j V_j, \quad (2.2.41)$$

in which case the Hamiltonian takes the canonical form:

$$H = \sum_j \widetilde{E}_j(b_j^\dagger b_j - d_j d_j^\dagger). \quad (2.2.42)$$

By virtue of the anti-commutation relations (2.2.36), each quanta (either particle or anti-particle) contributes a quantity $\widetilde{E}_j$ to the Hamiltonian:

$$\left[H, b_j^\dagger\right] = \widetilde{E}_j b_j^\dagger, \qquad \left[H, d_j^\dagger\right] = \widetilde{E}_j d_j^\dagger. \quad (2.2.43)$$

It can be seen that a consistent quantum field theory would require particle modes to have $\widetilde{E}_j \geq 0$. Let us recall that in the case of the scalar field, the requirement of having positive norm for the particle modes implied that $\omega_j \geq 0$, allowing both positive and negative values for $\widetilde{\omega}_j$. This is not the case for fermions, since both particle and anti-particle modes have positive norm, as can be seen from (2.2.33), therefore, the second quantisation can be performed such that $\widetilde{E}_j \geq 0$. This discussion is key for the construction of rotating thermal states on the Minkowski space-time in subsection 4.3.1 and on the anti de Sitter space-time (adS), in subsection 8.3.1.

2.2.5 Field theory at finite temperature

The analogue of the formulae (2.1.40) for the expectation values of products of boson one-particle operators takes the following form for fermions [72]:

$$\langle b_j^\dagger b_{j'} \rangle_\beta = \langle d_j^\dagger d_{j'} \rangle_\beta = \frac{\delta_{jj'}}{e^{\beta \widetilde{E}_j} + 1}, \qquad \langle b_j b_{j'}^\dagger \rangle_\beta = \langle d_j d_{j'}^\dagger \rangle_\beta = \frac{\delta_{jj'}}{1 + e^{-\beta \widetilde{E}_j}}, \qquad (2.2.44)$$

where the operators b_j and $d_j^\dagger$ satisfy the anti-commutation relations (2.2.36) and their commutator with H depends on $\widetilde{E}_j$. The t.e.v. of any other combination of two one-particle operators vanishes.

Failure to restrict $\widetilde{E}_j$ to non-negative values introduces temperature-independent terms in thermal expectation values, since the formulae (2.2.44) for $\widetilde{E}_j < 0$ are no longer valid. In a similar fashion to equation (2.1.42) for scalars, the difference between the thermal and vacuum expectation values takes the form:

$$\langle : b_j^\dagger b_{j'} : \rangle_\beta = \langle : d_j^\dagger d_{j'} : \rangle_\beta \xrightarrow[\substack{\beta \to \infty \\ \widetilde{E}_j < 0}]{} -\delta_{jj'}. \qquad (2.2.45)$$

The t.e.v. of the Hamiltonian, divided by the (infinite) volume of space is:

$$\frac{1}{V} \langle : H : \rangle_\beta = \sum_j \widetilde{E}_j \left(1 - \tanh \tfrac{\beta \widetilde{E}_j}{2} \right) = 2 \sum_j \frac{\widetilde{E}_j}{e^{\beta \widetilde{E}_j} + 1}, \qquad (2.2.46)$$

and the t.e.v. of the SET (2.2.39) is:

$$\langle : T_{\mu\nu} : \rangle_\beta = \sum_j \frac{1}{e^{\beta \widetilde{E}_j} + 1} \left[\mathcal{T}_{\mu\nu}(U_j, U_{j'}) + \mathcal{T}_{\mu\nu}(V_j, V_{j'}) \right]. \qquad (2.2.47)$$

The t.e.v.s of both the Hamiltonian and the SET appear to be regular, since the Fermi-Dirac density of states factor $(e^{\beta \widetilde{E}_j} + 1)^{-1}$ is regular for all values of $\widetilde{E}_j$. In subsection 4.3.2 it is shown that in the case of a rotating space-time, t.e.v.s are indeed regular for the Dirac field, but only up to the speed of light surface (SOL).

2.2.6 Green functions

As an analogue for fermions of subsection 2.1.5, the content of this subsection unavoidably repeats some of the structure and ideas presented in the former. As in the scalar case, the building blocks of spinor Green's functions are the Wightman functions, defined as:

$$S^+(x, x') = \langle 0 | \psi(x) \overline{\psi}(x') | 0 \rangle, \qquad S^-(x, x') = \langle 0 | \overline{\psi}(x') \psi(x) | 0 \rangle, \qquad (2.2.48)$$

in terms of which the Schwinger and Hadamard functions can be written as:

$$S(x, x') = S^+(x, x') + S^-(x, x'), \qquad S^{(1)}(x, x') = S^+(x, x') - S^-(x, x'). \quad (2.2.49)$$

As an anti-commutator, $S(x, x')$ is just a number, by virtue of the anti-commutation relations (2.2.23), which makes the Schwinger function independent of the quantum state.

Using the definition of t.e.v.s (2.1.38) and the evolution equation (2.2.24), the following relations can be established for the thermal Wightman functions:

$$S_\beta^\pm(t, \boldsymbol{x}; t', \boldsymbol{x}') = S_\beta^\mp(t \pm i\beta, \boldsymbol{x}; t', \boldsymbol{x}'). \quad (2.2.50)$$

Introducing the Fourier components $s_\beta^\pm(\omega; \boldsymbol{x}, \boldsymbol{x}')$ of the thermal Wightman functions:

$$S_\beta^\pm(t, \boldsymbol{x}; t', \boldsymbol{x}') = \int_{-\infty}^\infty \frac{d\omega}{2\pi} s_\beta^\pm(\omega; \boldsymbol{x}, \boldsymbol{x}') e^{-i\omega(t-t')} \quad (2.2.51)$$

and similarly for the Schwinger function $S(x, x')$, the following equation can be obtained:

$$s_\beta^\pm(\omega; \boldsymbol{x}, \boldsymbol{x}') = \frac{s(\omega; \boldsymbol{x}, \boldsymbol{x}')}{1 + e^{\mp\omega\beta}}.$$

Using a definition analogous to (2.2.49), the thermal Hadamard function can be written in terms of the Fourier coefficients of the Schwinger function:

$$S_\beta^{(1)}(x, x') = \int_{-\infty}^\infty \frac{d\omega}{2\pi} s(\omega; \boldsymbol{x}, \boldsymbol{x}') e^{-i\omega(t-t')} \tanh \frac{\beta\omega}{2}. \quad (2.2.52)$$

By construction, the thermal Hadamard function is independent of the choice of vacuum state. However, in this thesis, t.e.v.s shall be calculated with respect to certain vacuum states, making their value dependent on the quantisation scheme employed.

Alternatively, thermal states can be investigated by considering the thermal analogue of the Feynman propagator, defined as:

$$S_F(x, x') = \theta(t - t')S^+(x, x') + \theta(t' - t)S^-(x, x') \quad (2.2.53a)$$

and satisfying

$$S_F(x, x')[-i\overleftarrow{D}_\nu(x')\gamma^\nu(x') - \mu] = \frac{\delta^4(x - x')}{\sqrt{-g}}. \quad (2.2.53b)$$

In the maximally symmetric vacuum state of Minkowski space-time, the Feynman function for the free Dirac field can be written in terms of the Feynman function for the free Klein-Gordon field [46]:

$$S_F(x, x') = -(i\gamma^\nu D_\nu + \mu)G_F(x, x'). \quad (2.2.53c)$$

At finite temperature, it can be shown that the Feynman propagator is anti-periodic with respect to imaginary time (i.e. with respect to $t \to t + ij\beta$, $j = 0, \pm 1, \pm 2, \dots$). Hence, it can be calculated as [16]:

$$S_F(x, x')^\beta = \sum_{j=-\infty}^{\infty} (-1)^j S_F(t + ij\beta, \boldsymbol{x}; t', \boldsymbol{x}'). \qquad (2.2.54)$$

The t.e.v.s of the FC (2.2.28), CC (2.2.29) and SET (2.2.26) can be calculated using the following formulae:

$$\langle : \overline{\psi}\psi : \rangle_\beta = -\frac{1}{2} \lim_{x' \to x} \text{tr} \left[\Delta S_\beta^{(1)}(x, x') \Lambda(x', x) \right], \qquad (2.2.55a)$$

$$\langle : J^\mu(x) : \rangle_\beta = -\frac{1}{2} \lim_{x' \to x} \text{tr} \left[\gamma^\mu \Delta S_\beta^{(1)}(x, x') \Lambda(x', x) \right], \qquad (2.2.55b)$$

$$\langle : T_{\mu\nu} : \rangle_\beta = \frac{i}{4} \lim_{x' \to x} \text{tr} \Bigg\{$$
$$\left[\gamma_{(\nu} D_{\mu)} \Delta S_\beta^{(1)}(x, x') - \Delta S_\beta^{(1)}(x, x') \overleftarrow{\overline{D}}_{(\lambda'} \gamma_{\kappa'} g^{\lambda'}{}_{(\mu} g^{\kappa'}{}_{\nu)} \right] \Lambda(x', x) \Bigg\},$$
$$(2.2.55c)$$

where the bi-spinor of parallel transport $\Lambda(x, x')$ ensures that the spinors at x' are parallel transported to x along the geodesic connecting the two points, as follows:

$$\psi_{||}(x) = \Lambda(x, x')\psi(x'). \qquad (2.2.56)$$

Hence, $\Lambda(x, x')$ satisfies the parallel transport equations for spinors:

$$n^\mu D_\mu \Lambda(x, x') = 0, \qquad n^{\mu'} D_{\mu'} \Lambda(x, x') = 0, \qquad (2.2.57)$$

where $D_{\mu'} \Lambda(x, x') = \partial_{\mu'} \Lambda(x, x') + \Lambda(x, x') \overline{\Gamma}_{\mu'}(x')$ acts on $\Lambda(x, x')$ from the right. The initial conditions for Eq. (2.2.57) are:

$$\Lambda(x, x) = 1, \qquad \Lambda^{-1}(x, x') = \overline{\Lambda}(x, x') = \Lambda(x', x), \qquad (2.2.58)$$

where the first equation is saying that $\psi(x)$ coincides with its parallel transport at x, while the second ensures that no parallel transport is performed on scalars of the form $\overline{\chi}\psi$.

The Casimir effect can be computed from the Feynman Green's function S_F by using the formula (2.2.55c) with $\Delta S_\beta^{(1)}$ replaced by $2S_F$. As mentioned for scalars in section 2.1.4, it is more convenient to calculate the Casimir effect using the Euclidean Green's function, defined on the (quasi-)Euclidean equivalent of the manifold, obtained through the coordinate change (2.1.60). In addition, the Euclidean analogue

of the gamma matrices are defined as [38]:

$$\gamma_E^{\hat{0}} = \gamma^{\hat{0}}, \quad \gamma_E^{\hat{j}} = -i\gamma^{\hat{j}} \tag{2.2.59}$$

and satisfy the anti-commutation relations:

$$\left\{\gamma_E^{\hat{a}}, \gamma_E^{\hat{b}}\right\} = \delta^{\hat{a}\hat{b}}. \tag{2.2.60}$$

The Euclidean Green's function S_E is a solution to the inhomogeneous field equation:

$$\begin{aligned}(-\gamma^\nu D_\nu - \mu)S_E(x, x') &= S_E(x, x')(\overleftarrow{D_{\nu'}}\gamma^{\nu'} - \mu) \\ &= -\frac{1}{\sqrt{g}}\delta(\tau - \tau')\delta^3(\boldsymbol{x} - \boldsymbol{x}'),\end{aligned} \tag{2.2.61a}$$

where all coordinate indices refer to Euclidean coordinates. In a space-time with full translational symmetry, it can be obtained from the Euclidean Green's function for a scalar field (2.1.61):

$$S_E(x, x') = (-\gamma^\nu \partial_\nu + \mu)G_E(x, x'). \tag{2.2.61b}$$

The fermion SET can be expressed in terms of the Euclidean Green's function by substituting $-2iS_E$ for $S_\beta^{(1)}$ in (2.2.55c):

$$\langle T_{\mu\nu}\rangle = \frac{1}{2}\lim_{x'\to x}\text{tr}\left[\gamma_{(\nu}(x)D_{\mu)}(x)S_E(x, x') - S_E(x, x')\overleftarrow{D}_{(\mu}(x')\gamma_{\nu)}(x')\right]. \tag{2.2.62}$$

2.3   Summary

Aside from introducing notation and general background material used in this thesis, sections 2.1.4 and 2.2.5 touch upon the problem of constructing thermal states in stationary space-times. The key message is that for scalars, the second quantisation split between particle and anti-particle modes is necessarily performed based on the sign of the norm, i.e. positive and negative norm modes are interpreted as particle and anti-particle modes, respectively. Thus, in systems which allow modes to have opposite signs for their norm and frequency, the construction of thermal states of scalar particles is problematic, as negative frequency particle modes will have infinite occupation numbers. On the other hand, fermion modes always have positive norm. Hence, the split between particle and anti-particle modes can be performed such that all particle modes have positive frequencies. Only in this scenario can thermal states be meaningfully defined.

Chapter 3. Minkowski space-time

The present chapter serves as a training ground for the analysis of rotating states in infinite or bounded Minkowski space-time, discussed in chapters 4 and 5, respectively. Section 3.2 refers to scalars and section 3.3 refers to fermions. The field equations, their corresponding mode solutions and the second quantisation procedure are presented in sections 3.2.1 and 3.3.1 and thermal states are constructed in sections 3.2.2 and 3.3.3.

3.1 Space-time characteristics

Minkowski space-time is described by the line element:

$$ds^2 = -dt^2 + dx^2 + dy^2 + dz^2 = -dt^2 + d\rho^2 + \rho^2 d\varphi^2 + dz^2, \qquad (3.1.1)$$

in Cartesian and cylinidrical coordinates ($x = \rho \cos\varphi$, $y = \rho \sin\varphi$) respectively. In cylindrical coordinates, the non-vanishing Christoffel symbols are

$$\Gamma^{\varphi}{}_{\varphi\rho} = \rho^{-1}, \quad \Gamma^{\rho}{}_{\varphi\varphi} = -\rho \qquad (3.1.2)$$

and the Klein-Gordon equation (2.1.2) has the form:

$$(-H^2 - \partial_\rho^2 - \rho^{-1}\partial_\rho + \rho^{-2}L_z^2 + P_z^2 + \mu^2)\phi(x) = 0, \qquad (3.1.3)$$

where $H = i\partial_t$, $P_z = -i\partial_z$ and $L_z = -i\partial_\varphi$ are the Hamiltonian and z components of the momentum and angular momentum operators, respectively.

The Cartesian tetrad is trivially given by:

$$\omega^{\hat{t}} = dt, \qquad \omega^{\hat{x}} = dx, \qquad \omega^{\hat{y}} = dy, \qquad \omega^{\hat{z}} = dz,$$

$$e_{\hat{t}} = \partial_t, \qquad e_{\hat{x}} = \partial_x, \qquad e_{\hat{y}} = \partial_y, \qquad e_{\hat{z}} = \partial_z \qquad (3.1.4)$$

and the Dirac equation in the Cartesian gauge (with respect to the Cartesian tetrad) has the form:

$$(\gamma^{\hat{0}}H - \boldsymbol{\gamma} \cdot \boldsymbol{P} - \mu)\psi(x) = 0, \qquad (3.1.5)$$

where $H = i\partial_t$ and $\boldsymbol{P} = -i\nabla$ are the Hamiltonian and momentum operators, respectively. When the Cartesian tetrad is used, the gamma matrices with respect

to cylindrical coordinates have the following expressions:

$$\gamma^{\hat{\rho}} = \begin{pmatrix} 0 & \sigma^\rho \\ -\sigma^\rho & 0 \end{pmatrix}, \qquad \gamma^{\hat{\varphi}} = \begin{pmatrix} 0 & \sigma^\varphi \\ -\sigma^\varphi & 0 \end{pmatrix}, \tag{3.1.6}$$

where the Pauli matrices σ^φ and σ^ρ are given by:

$$\sigma^\rho = \sigma^1 \cos\varphi + \sigma^2 \sin\varphi = \begin{pmatrix} 0 & e^{-i\varphi} \\ e^{i\varphi} & 0 \end{pmatrix},$$

$$\sigma^\varphi = -\sigma^1 \sin\varphi + \sigma^2 \cos\varphi = -i \begin{pmatrix} 0 & e^{-i\varphi} \\ -e^{i\varphi} & 0 \end{pmatrix}. \tag{3.1.7}$$

The Klein-Gordon equation (3.1.3) and Dirac equation (3.1.5) are the objects of study of sections 3.2 and 3.3, respectively. The alternative formulation of the Dirac theory using a cylindrical tetrad, used in the literature by, e.g., [72], is completely equivalent to the present one.

Before ending this section, let us note that the only non-trivial conservation equation for the SET is the ρ component of (2.1.17):

$$\partial_\rho(\rho T^\rho{}_\rho) = T^\varphi{}_\varphi. \tag{3.1.8}$$

3.2   Scalar field theory in cylindrical coordinates

Starting from Eq. (3.1.3), this section is devoted to the construction of the quantum field theory of the massive Klein-Gordon field using cylindrical coordinates in Minkowski space-time, forming the basis of the analysis of rotating states in section 4.2. The mode solutions and second quantisation are given in subsection 3.2.1, followed by the computation of the t.e.v. of the SET in subsection 3.2.2, where the Stefan-Boltzmann law is recovered.

3.2.1   Modes in cylindrical coordinates

In cylindrical coordinates, it is convenient to work with a complete set of commuting operators (CSCO) which commute with the Klein-Gordon equation (3.1.3). The CSCO is formed by the z components P_z and L_z of the momentum and angular momentum operators $\boldsymbol{P}$ and $\boldsymbol{L}$, respectively, and the Hamiltonian (energy) operator H, having the expressions:

$$H = i\partial_t, \qquad \boldsymbol{P} = -i\nabla, \qquad \boldsymbol{L} = -i\boldsymbol{x} \times \nabla. \tag{3.2.1}$$

The solutions $f_{\omega km}$ of the Klein-Gordon equation (3.1.3) can be chosen to be simultaneous eigenvectors of the above CSCO:

$$H f_{\omega km}(x) = \omega \, f_{\omega km},$$
$$P_z f_{\omega km}(x) = k \, f_{\omega km},$$
$$L_z f_{\omega km}(x) = m \, f_{\omega km}, \tag{3.2.2}$$

where ω and k are real numbers and $m = 0, \pm 1, \pm 2, \ldots$. Since $L_z = -i\partial_\varphi$, the above equations can be satisfied if f_{Ekm} is put in the form:

$$f_{\omega km} = e^{-i\omega t + ikz + im\varphi} R_{\omega km}(\rho), \tag{3.2.3}$$

where $R(\rho)$ only depends on the distance ρ from the z axis. The Klein-Gordon equation (3.1.3) applied to the modes (3.2.3) reduces to Bessel's equation (A.1.1) for $R_{\omega km}(\rho)$:

$$\left[\rho^2 \partial_\rho^2 + \rho \partial_\rho + \rho^2 q^2 - m^2 \right] R_{\omega km}(\rho) = 0,$$

where $q = \sqrt{\omega^2 - p^2}$ is the transverse component of the momentum $p = \sqrt{\omega^2 - \mu^2}$. There are two linearly independent solutions of the above Bessel equation: $J_m(q\rho)$ and $N_m(q\rho)$, however, $N_m(q\rho)$ diverges at $\rho = 0$. Thus,

$$R_{\omega km} = \mathcal{N}_{\omega km} J_m(q\rho), \tag{3.2.4}$$

where $\mathcal{N}_{\omega km}$ is a constant. To impose unit norm on the modes (3.2.3), the inner product (2.1.19) can be used, which can be written in cylindrical coordinates as:

$$\langle \phi, \chi \rangle = \int_{-\infty}^{\infty} dz \int_0^{\infty} \rho \, d\rho \int_0^{2\pi} d\varphi \left[\phi^*(x) i \overleftrightarrow{\partial_t} \phi(x') \right]. \tag{3.2.5}$$

Using the orthogonality relation (A.3.1) for the Bessel functions J_m, it can be shown that the normalised mode solutions of the Klein-Gordon equation have the following expression:

$$f_{\omega km} = \frac{1}{\sqrt{8\pi^2 |\omega|}} e^{-i\omega t + ikz + im\varphi} J_m(q\rho). \tag{3.2.6}$$

The above expression allows for negative values of ω to be considered, however, the norm of $f_{\omega km}$ will retain the sign of ω:

$$\langle f_{\omega km}, f_{\omega' k' m'} \rangle = \frac{\delta(\omega - \omega')}{|\omega|} \delta(k - k') \delta_{mm'}. \tag{3.2.7}$$

Furthermore, the modes (3.2.6) obey the completeness relation

$$\sum_{m=-\infty}^{\infty} \int_{\mu}^{\infty} \omega \, d\omega \int_{-p}^{p} dk \, [f_{\omega km}^*(t, \boldsymbol{x}) i\partial_t f_{\omega km}(t, \boldsymbol{x}') + \text{c.c.}] = \frac{\delta(\rho - \rho')}{\rho} \delta(\varphi - \varphi')\delta(z - z'),$$

(3.2.8)

in agreement with the general formula (2.1.22). In the above, c.c. stands for "complex conjugate" of all previous terms.

Following the discussion in subsection 2.1.3, the split between particle and antiparticle modes must be made on the basis of the sign of their corresponding norm. Thus, the expansion of the quantum field operator $\phi(x)$ can be written as:

$$\phi(x) = \sum_{m=-\infty}^{\infty} \int_{\mu}^{\infty} \omega \, d\omega \int_{-p}^{p} dk \left\{ f_{Ekm}(x) a_{Ekm} + f_{Ekm}^*(x) a_{Ekm}^\dagger \right\},$$

(3.2.9)

where the one-particle operators obey the canonical commutation relations:

$$\left[a_{Ekm}, a_{E'k'm'}^\dagger \right] = \frac{\delta(E - E')}{E} \delta(k - k')\delta_{mm'},$$

(3.2.10)

in agreement with the general theory of chapter 2.

3.2.2   Thermal expectation values

As discussed in subsection 2.1.5, the t.e.v.s can be computed from the thermal Hadamard function (2.1.53). To construct the thermal Hadamard function $\Delta G_\beta^{(1)}(x, x')$, the Schwinger function $G(x, x')$ and the vacuum Hadamard's elementary function $G^{(1)}(x, x')$ are required, which can be constructed using the expansion (3.2.9) of the field operator in Eqs. (2.1.47) and (2.1.46), respectively:

$$G(x, x') = \sum_{m=-\infty}^{\infty} \int_{\mu}^{\infty} \omega \, d\omega \int_{-p}^{p} dk \frac{e^{ik\Delta z + im\Delta\varphi}}{8\pi^2\omega} (e^{-i\omega\Delta t} - e^{i\omega\Delta t}) J_m(q\rho) J_m(q\rho'),$$

(3.2.11a)

$$G^{(1)}(x, x') = \sum_{m=-\infty}^{\infty} \int_{\mu}^{\infty} \omega \, d\omega \int_{-p}^{p} dk \frac{e^{ik\Delta z + im\Delta\varphi}}{8\pi^2\omega} (e^{-i\omega\Delta t} + e^{i\omega\Delta t}) J_m(q\rho) J_m(q\rho').$$

(3.2.11b)

In the above, $\Delta x = x - x'$, where x is t, φ or z.

The Fourier coefficients of the Schwinger function (3.2.11a) are:

$$g(z; \boldsymbol{x}, \boldsymbol{x}') = \sum_{m=-\infty}^{\infty} \int_{\mu}^{\infty} \omega \, d\omega \int_{-p}^{p} dk \frac{e^{ik\Delta z + im\Delta\varphi}}{8\pi^2\omega} [\delta(z - \omega) - \delta(z + \omega)] J_m(q\rho) J_m(q\rho),$$

(3.2.12)

thus, the corresponding thermal Hadamard's function can be written as:

$$\Delta G_\beta^{(1)}(x, x') = \sum_{m=-\infty}^{\infty} \int_\mu^\infty \frac{\omega \, d\omega}{e^{\beta\omega} - 1} \int_{-p}^{p} dk \frac{e^{ik\Delta z + im\Delta\varphi}}{4\pi^2\omega} (e^{-i\omega\Delta t} + e^{i\omega\Delta t}) J_m(q\rho) J_m(q\rho).$$

(3.2.13)

Thermal expectation value of ϕ^2

The formula (2.1.57) can be used to calculate the t.e.v. of ϕ^2:

$$\langle : \phi^2 : \rangle_\beta = \frac{1}{2\pi^2} \sum_{m=-\infty}^{\infty} \int_\mu^\infty d\omega \int_{-p}^{p} \frac{dk}{e^{\beta\omega} - 1} J_m^2(q\rho).$$

(3.2.14)

The sum over m can be performed using Eq. (A.4.2), after which the k integral becomes trivial, leading to the result:

$$\langle : \phi^2 : \rangle_\beta = \frac{1}{2\pi^2} \int_\mu^\infty \frac{p \, d\omega}{e^{\beta\omega} - 1}.$$

(3.2.15)

Using the following integration formula:

$$\int_0^\infty dx \frac{x}{e^{\beta x} - 1} = \frac{\pi^2}{6\beta^2},$$

(3.2.16)

the t.e.v. of ϕ^2 in the massless case can be evaluated to:

$$\langle : \phi^2 : \rangle_\beta = \frac{1}{12\beta^2}.$$

(3.2.17)

An asymptotic analysis can be performed for the massive case, which will be deferred until after the results for the t.e.v. of the SET have been presented.

The t.e.v. of the SET can be computed using the Christoffel symbols (3.1.2) by substituting (3.2.13) in (2.1.54):

$$\langle : T_{\hat\alpha\hat\gamma} : \rangle_\beta = \frac{1}{24\pi^2} \sum_{m=-\infty}^{\infty} \int_\mu^\infty \frac{d\omega}{e^{\beta\omega} - 1} \int_{-p}^{p} dk \, F_{\hat\alpha\hat\gamma},$$

(3.2.18)

where the only non-vanishing components of $F_{\hat\alpha\hat\gamma}$ are:

$$F_{\hat t\hat t} = \left(6\omega^2 + \rho^{-2}m^2 - q^2\right) J_m^2 + q^2 J_m'^2,$$
$$F_{\hat\rho\hat\rho} = \left(-3\rho^{-2}m^2 + 3q^2\right) J_m^2 + 2q\rho^{-1} J_m J_m' + 3q^2 J_m'^2,$$
$$F_{\hat\varphi\hat\varphi} = \left(5\rho^{-2}m^2 + q^2\right) J_m^2 - 2q\rho^{-1} J_m J_m' - q^2 J_m'^2,$$
$$F_{\hat z\hat z} = \left(6k^2 - \rho^{-2}m^2 + q^2\right) J_m^2 - q^2 J_m'^2.$$

(3.2.19)

In the above, the argument of all Bessel functions is $q\rho$ and J_m' represents the derivative of J_m with respect to its argument. The hatted indices indicate that these are

components with respect to the tetrad (3.1.4). It can be checked through straight-forward computation that the trace is proportional to μ^2 and therefore vanishes for a massless field, and that the SET is conserved since it satisfies the conservation equation (3.1.8). Although not immediately obvious, the stress-tensor does not diverge at $\rho = 0$. In fact, it is constant throughout all space, as is shown next.

The sum over m can be performed using the summation formulae in section A.4 of the appendix, after which the k integral can be performed:

$$\langle : T_{\hat{\alpha}\hat{\gamma}} : \rangle_\beta = \frac{1}{2\pi^2} \int_\mu^\infty \frac{p \, d\omega}{e^{\beta\omega} - 1} \, \mathrm{diag}(\omega^2, p^2/3, p^2/3, p^2/3). \tag{3.2.20}$$

While asymptotic methods must be employed in the case of general mass, the ω integral can be performed in the massless case using the Bose-Einstein integral:

$$\int_0^\infty \frac{\omega^3 d\omega}{e^{\beta\omega} - 1} = \frac{\pi^4}{15\beta^4}, \tag{3.2.21}$$

and the SET reduces to:

$$\langle : T_{\hat{\alpha}\hat{\gamma}} : \rangle_\beta = \frac{\pi^2}{30\beta^4} \mathrm{diag}\left(1, \frac{1}{3}, \frac{1}{3}, \frac{1}{3}\right) = \mathrm{diag}(\rho, P, P, P). \tag{3.2.22}$$

The energy density ρ is equal to $\frac{2\sigma}{c} T^4$, where

$$\sigma = \frac{\pi^2 K_B^4}{60\hbar^3 c^2} \tag{3.2.23}$$

is the Stefan-Boltzmann constant, c is the speed of light in vacuum, K_B is Boltzmann's constant and $\hbar = h/2\pi$ is the reduced Planck constant [65]. The equation of state takes the form:

$$\frac{P}{\rho} = \frac{1}{3}, \qquad (\mu = 0). \tag{3.2.24}$$

In the massive case, the pressure P and energy density ρ are given by:

$$P = \frac{1}{6\pi^2} \int_\mu^\infty \frac{p^3 d\omega}{e^{\beta\omega} - 1},$$

$$\rho = \frac{1}{2\pi^2} \int_\mu^\infty \frac{\omega^2 p \, d\omega}{e^{\beta\omega} - 1}. \tag{3.2.25}$$

A change of variable to $t = \frac{\omega}{\mu}$ puts (3.2.25) in the form:

$$P = \frac{\mu^4}{6\pi^2} \int_1^\infty \frac{dt}{e^{\beta\mu t} - 1} (t^2 - 1)^{3/2},$$

$$\rho - 3P = \frac{\mu^4}{2\pi^2} \int_1^\infty \frac{dt}{e^{\beta\mu t} - 1} (t^2 - 1)^{1/2}. \tag{3.2.26}$$

The combination $\rho - 3P$ is equal to minus the trace of the SET and is linked to

the t.e.v. of ϕ^2 through Eq. (2.1.16). The exponential in the denominator can be expanded in a Taylor series:

$$\frac{1}{e^{\beta\mu t} - 1} = \sum_{k=1}^{\infty} e^{-k\beta\mu t}, \tag{3.2.27}$$

which, together with (A.1.17), gives:

$$P = \frac{\mu^2}{2\pi^2\beta^2} \sum_{k=1}^{\infty} \frac{1}{k^2} K_2(k\beta\mu),$$

$$\mu^2 \langle: \phi^2 :\rangle_\beta = \rho - 3P = \frac{\mu^3}{2\pi^2\beta} \sum_{k=1}^{\infty} \frac{1}{k} K_1(k\beta\mu). \tag{3.2.28}$$

Numerical experiments show that terminating the expansion (3.2.28) at $k = 3$ gives an excellent approximation throughout the whole parameter space for μ and β.

If $\beta\mu$ is large, the series (3.2.28) can be terminated at $k = 1$:

$$P \sim \frac{1}{\beta^4} \left(\frac{\beta\mu}{2\pi}\right)^{3/2} e^{-\beta\mu} \left(1 + \frac{15}{8\beta\mu} + \dots\right),$$

$$\mu^2 \langle: \phi^2 :\rangle_\beta = \rho - 3P \sim \frac{\mu}{\beta^3} \left(\frac{\beta\mu}{2\pi}\right)^{3/2} e^{-\beta\mu} \left(1 + \frac{3}{8\beta\mu} + \dots\right),$$

$$\frac{P}{\rho} \sim \frac{1}{\beta\mu} - \frac{3}{2\beta^2\mu^2} + \dots. \tag{3.2.29}$$

Here, the asymptotic forms (A.2.4e) for the modified Bessel functions for large values of the argument have been used. If the argument $\beta\mu$ of the Bessel functions is small, Eq. (3.2.28) can be approximated using (A.2.4b):

$$P = \frac{\pi^2}{90\beta^4} - \frac{\mu^2}{24\beta^2} + O(\mu^2),$$

$$\rho = \frac{\pi^2}{30\beta^4} - \frac{\mu^2}{24\beta^2} + O(\mu^2),$$

$$\frac{P}{\rho} = \frac{1}{3} \left[1 + \frac{5}{2}\pi^2\beta^2\mu^2 + O(\mu^2)\right]^{-1}, \tag{3.2.30}$$

confirming the expression obtained in Eq. (3.2.17) for the t.e.v. of ϕ^2. The validity of these approximations is analysed by comparison with results obtained using the numerical integration of Eqs. (3.2.25). Figure 3.1 shows that massive particles behave as if they were massless when $\beta\mu \lesssim 1$.
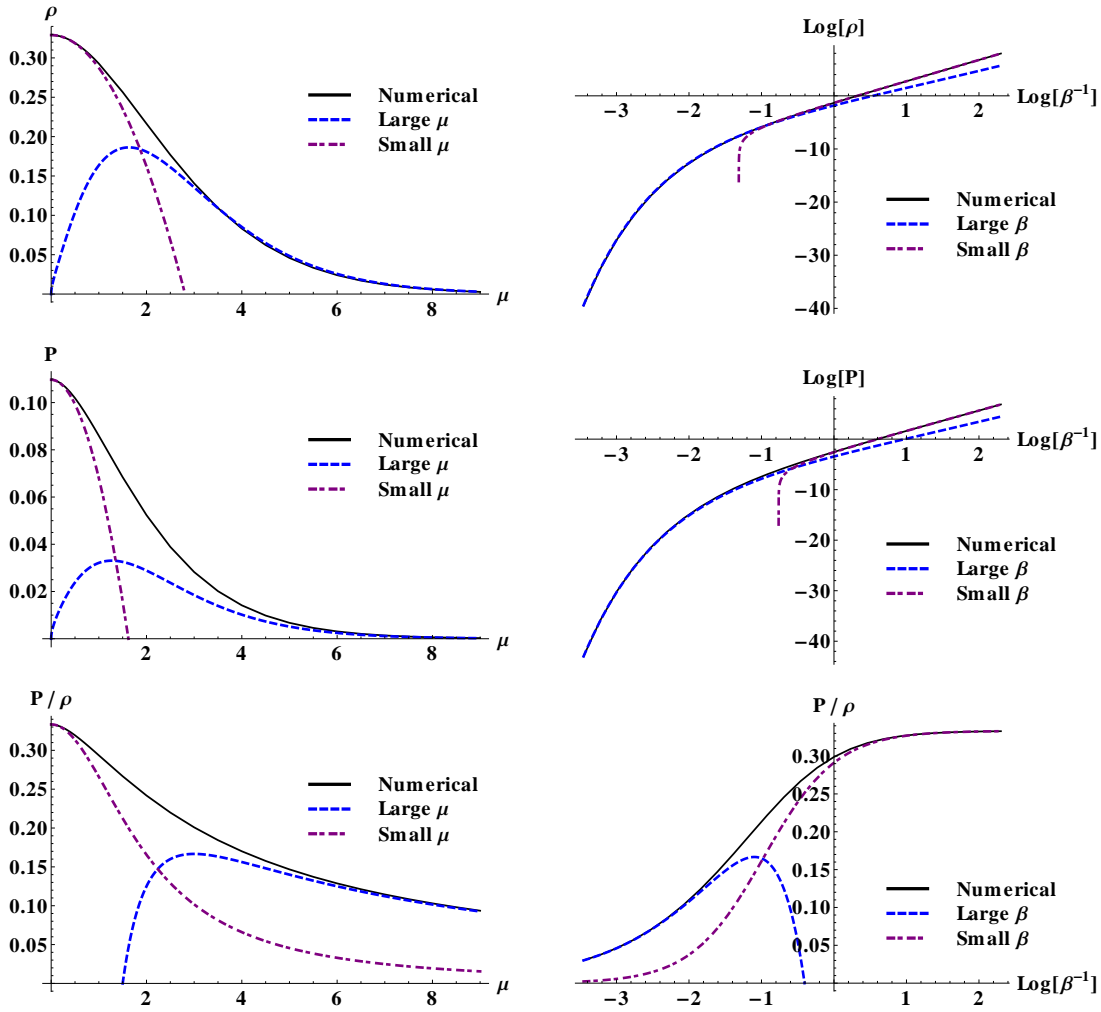
Figure 3.1: The density ρ, pressure P and equation of state $\frac{P}{\rho}$ for a thermal distribution of scalar particles are plotted as functions of the mass μ of the quanta (on the left) and as functions of the logarithm of the temperature $T = \beta^{-1}$, on the right. The solid black curve shows numerical results obtained by integrating (3.2.25) while the dashed blue and purple curves show the asymptotic expressions (3.2.29) and (3.2.30) for large and small values of $\beta\mu$, respectively.

3.3   Polarised Dirac fermions in cylindrical coordinates

This section starts with the construction of the mode solutions of the Dirac equation in cylindrical coordinates, which are then used for the construction of the quantum field operator in subsection 3.3.1. In subsection 3.3.2, a discussion about our choice for the Cartesian gauge and its connection to the cylindrical tetrad not infrequently used in the literature is presented. The modes considered here can be used almost unchanged in section 4.3, where rotation is introduced. Finally, subsection 3.3.3 ends this section with the construction of thermal states.

3.3.1   Modes in cylindrical coordinates

In the construction of the mode solutions of the Klein-Gordon equation in subsection 3.2.1, the Hamiltonian H, momentum P_z and angular momentum L_z operators were sufficient to construct a complete set of modes (i.e. they formed a CSCO). The internal structure of the four-spinor solutions of the Dirac equation leaves room in the CSCO for an extra operator. In Ref. [11], this extra operator is chosen to be the transverse helicity, i.e. the projection of the spin on the transverse part of the momentum. Instead, here we choose the more familiar helicity operator W_0 (i.e. the time component of the Pauli-Lubanski vector [46]), giving the projection of the spin on the direction of motion, using which the modes will have a form similar to that encountered on the Kerr space-time [21]. Bearing in mind that the angular momentum operator $\boldsymbol{J} = \boldsymbol{L} + \boldsymbol{S}$ for the Dirac field comprises of a spin part $\boldsymbol{S}$ as well as an orbital part $\boldsymbol{L}$, the following equations are required to fully define the CSCO:

$$J_z = -i\varphi + \frac{1}{2}\begin{pmatrix} 1 & 0 \\ 0 & -1 \end{pmatrix}, \qquad W_0 = \frac{\boldsymbol{J} \cdot \boldsymbol{P}}{2p} = \begin{pmatrix} h & 0 \\ 0 & h \end{pmatrix}. \tag{3.3.1a}$$

The 2×2 helicity operator h is defined by:

$$2ph = \boldsymbol{\sigma} \cdot \boldsymbol{P} = \begin{pmatrix} P_z & P_- \\ P_+ & -P_z \end{pmatrix}, \tag{3.3.1b}$$

where

$$P_\pm = P^x \pm iP^y = -ie^{\pm i\varphi}\left(\partial_\rho \pm i\rho^{-1}\partial_\varphi\right). \tag{3.3.1c}$$

It can be checked that $(W_0)^2 = \frac{1}{4}$, therefore, its eigenvalues are $\lambda = \pm\frac{1}{2}$.

To solve the eigenvalue equations corresponding to the chosen CSCO, the dependence on t and z of the eigenvectors U_{Ekm}^λ, labelled by their respective eigenvalues, can be put in the form:

$$U_{Ekm}^\lambda(t, \rho, \varphi, z) = \frac{1}{2\pi}e^{-iEt+ikz}u_{Ekm}^\lambda(\rho, \varphi), \tag{3.3.2}$$

where the four-spinor u_{Ekm}^λ only depends on ρ and φ and has the form:

$$u_{Ekm}^\lambda(\rho, \varphi) = \begin{pmatrix} \mathcal{C}_{Ekm}^{\lambda,\mathrm{up}}\phi_{pkm}^\lambda(\rho, \varphi) \\ \mathcal{C}_{Ekm}^{\lambda,\mathrm{down}}\phi_{pkm}^\lambda(\rho, \varphi) \end{pmatrix}, \tag{3.3.3}$$

where the Minkowski momentum p is used to label the two-spinors ϕ_{pkm}^λ. The constants $\mathcal{C}_{Ekm}^{\lambda,\mathrm{up}}$ and $\mathcal{C}_{Ekm}^{\lambda,\mathrm{down}}$ are constrained through the helicity eigenvalue equation, as will be shown in what follows. The angular momentum equation,

$$J_z\phi_{Ekm}^\lambda(\rho, \varphi)\begin{pmatrix} -i\partial_\varphi + \frac{1}{2} & 0 \\ 0 & -i\partial_\varphi - \frac{1}{2} \end{pmatrix}\phi_{Ekm}^\lambda(\rho, \varphi) = m\phi_{Ekm}^\lambda(\rho, \varphi), \tag{3.3.4}$$

can be solved by setting:

$$\phi^\lambda_{Ekm}(\rho, \varphi) = \begin{pmatrix} e^{im\varphi}\phi^{\lambda,-}_{Ekm}(\rho) \\ e^{i(m+1)\varphi}\phi^{\lambda,+}_{Ekm}(\rho) \end{pmatrix}, \tag{3.3.5}$$

where $m = 0, \pm1, \pm2, \ldots$. The helicity equation constrains the two-spinors ϕ^λ_{Ekm} to obey the following equation:

$$\frac{1}{2p}\begin{pmatrix} k & P_- \\ P_+ & -k \end{pmatrix}\phi^\lambda_{Ekm}(\rho, \varphi) = \lambda\phi^\lambda_{Ekm}(\rho, \varphi), \tag{3.3.6}$$

where $\lambda = \pm\frac{1}{2}$. Using the property:

$$P_-P_+ = P_+P_- = -\partial^2_\rho - \rho^{-1}\partial_\rho - \rho^{-2}\partial^2_\varphi, \tag{3.3.7}$$

the functions $\phi^{\lambda,\pm}$ can be shown to obey the Bessel equations:

$$[z^2\partial^2_z + z\partial_z + z^2 - m^2]\phi^{\lambda,-}_{Ekm}(\rho) = 0,$$
$$[z^2\partial^2_z + z\partial_z + z^2 - (m+1)^2]\phi^{\lambda,+}_{Ekm}(\rho) = 0, \tag{3.3.8}$$

where $z = q\rho$ is written in terms of the longitudinal momentum $q = \sqrt{p^2 - k^2}$. The general solution of Eq. (3.3.8) can be written as a linear combinations of Bessel functions of the first and second kind, however, the Bessel functions of the second kind $N_\nu(q\rho)$ are not regular at the origin. Hence, the functions $\phi^{\lambda,\pm}_{Ekm}(\rho)$ take the form:

$$\phi^{\lambda,-}_{Ekm}(\rho) = \mathcal{N}_- J_m(q\rho), \qquad \phi^{\lambda,+}_{Ekm}(\rho) = \mathcal{N}_+ J_{m+1}(q\rho), \tag{3.3.9}$$

where $\mathcal{N}_\pm$ are normalisation constants. It can now be seen that the operators $P_\pm$, defined in Eq. (3.3.1c), act as shifters for the angular momentum quantum number, i.e.:

$$P_\pm e^{im\varphi}J_m(q\rho) = \pm iq e^{i(m\pm1)\varphi}J_{m\pm1}(q\rho). \tag{3.3.10}$$

Hence, the helicity equation (3.3.6) implies that $\mathcal{N}_+ = iq\mathcal{N}_-/(k + 2\lambda p)$, enabling ϕ^λ_{Ekm} to be written as:

$$\phi^\lambda_{Ekm}(\rho, \varphi) = \frac{1}{\sqrt{2}}\begin{pmatrix} \mathfrak{p}_\lambda e^{im\varphi}J_m(q\rho) \\ 2i\lambda\mathfrak{p}_{-\lambda}e^{i(m+1)\varphi}J_{m+1}(q\rho) \end{pmatrix}, \tag{3.3.11}$$

where

$$\mathfrak{p}_\pm \equiv \mathfrak{p}_{\pm\frac{1}{2}} = \sqrt{1 \pm \frac{k}{p}}. \tag{3.3.12}$$

The overall $1/\sqrt{2}$ factor in Eq. (3.3.11) comes from the generalized orthogonality

relation [11]:

$$\sum_{m=-\infty}^{\infty} \phi_{Ekm}^{\lambda\dagger}(\rho, \varphi) \phi_{Ekm}^{\lambda'}(\rho, \varphi) = \delta_{\lambda\lambda'}. \tag{3.3.13}$$

To finalize the construction of the mode solutions (3.3.3), the Dirac equation (3.1.5) must be used to find the constants $\mathcal{C}_{Ekm}^{\lambda,\text{up}}$ and $\mathcal{C}_{Ekm}^{\lambda,\text{down}}$:

$$\begin{pmatrix} E - \mu & -2p\lambda \\ 2p\lambda & -E - \mu \end{pmatrix} \begin{pmatrix} \mathcal{C}_{Ekm}^{\lambda,\text{up}} \\ \mathcal{C}_{Ekm}^{\lambda,\text{down}} \end{pmatrix} = 0, \tag{3.3.14}$$

where the compatibility of the above system links the Minkowski energy E and momentum p through $E^2 = p^2 + \mu^2$. Furthermore, the constraint

$$\mathcal{C}_{Ekm}^{\lambda,\text{up}} = \frac{2p\lambda}{E - \mu} \mathcal{C}_{Ekm}^{\lambda,\text{down}} \tag{3.3.15}$$

enables u_{Ekm}^{λ} to be put in the following form:

$$u_{Ekm}^{\lambda}(\rho, \varphi) = \frac{1}{\sqrt{2}} \begin{pmatrix} \mathfrak{E}_+ \phi_{Ekm}^{\lambda} \\ \frac{2\lambda E}{|E|} \mathfrak{E}_- \phi_{Ekm}^{\lambda} \end{pmatrix}, \tag{3.3.16}$$

where

$$\mathfrak{E}_{\pm} = \sqrt{1 \pm \frac{\mu}{E}} \tag{3.3.17}$$

and the overall factor $1/2\pi$ ensures that the generalised orthogonality relation [11] holds:

$$\sum_{m=-\infty}^{\infty} u_{Ekm}^{\lambda\dagger}(\rho, \varphi) u_{Ekm}^{\lambda'}(\rho, \varphi) = \delta_{\lambda\lambda'}. \tag{3.3.18}$$

Finally, the norm of the modes is given by the inner product (2.2.30), specialised to cylindrical coordinates on Minkowski space-time:

$$\langle \psi, \chi \rangle = \int_{-\infty}^{\infty} dz \int_0^{\infty} \rho \, d\rho \int_0^{2\pi} d\varphi \, \psi^{\dagger} \chi. \tag{3.3.19}$$

It can be checked that the modes (3.3.2) satisfy the following orthogonality relation:

$$\langle U_{Ekm}^{\lambda}, U_{E'k'm'}^{\lambda'} \rangle = \frac{\delta(E - E')}{E} \delta(k - k') \delta_{mm'} \delta_{\lambda\lambda'}, \tag{3.3.20}$$

hence, all modes have positive norm, in agreement with the discussion in subsection 2.2.4.

To conclude the construction of the set of modes, the charge conjugation operation must be used to link the particle modes U_{Ekm}^{λ} to the corresponding anti-particle

modes, as follows:

$$V_{Ekm}^{\lambda} = i\gamma^2 U_{Ekm}^{\lambda*}, \tag{3.3.21}$$

$$i\gamma^2 U_{Ekm}^{\lambda*} = \frac{1}{2\pi} e^{iEt-ikz} i\gamma^2 u_{Ekm}^{\lambda*},$$

$$i\gamma^2 u_{Ekm}^{\lambda*} = \frac{1}{\sqrt{2}} \begin{pmatrix} 0 & i\sigma_2 \\ -i\sigma_2 & 0 \end{pmatrix} \begin{pmatrix} \mathfrak{E}_+ \phi_{pkm}^{\lambda*} \\ \frac{2\lambda E}{|E|} \mathfrak{E}_- \phi_{pkm}^{\lambda*} \end{pmatrix},$$

$$i\sigma_2 \phi_{pkm}^{\lambda*} = \frac{1}{\sqrt{2}} \begin{pmatrix} -2i\lambda \mathfrak{p}_{-\lambda} e^{-i(m+1)\varphi} J_{m+1}(q\rho) \\ -\mathfrak{p}_\lambda e^{-im\varphi} J_m(q\rho) \end{pmatrix}. \tag{3.3.22}$$

Using the property (A.1.4) to change the order of the Bessel functions above, it can be shown that $i\sigma^2 \phi_{pkm}^{\lambda*} = 2i\lambda(-1)^m \phi_{p,-k,-m-1}^{\lambda}$, hence the anti-particle modes are given by:

$$V_{Ekm}^{\lambda}(t,\rho,\varphi,z) = \frac{1}{2\pi} e^{iEt-ikz} v_{Ekm}^{\lambda}(\rho,\varphi), \tag{3.3.23a}$$

$$v_{Ekm}^{\lambda}(\rho,\varphi) = \frac{(-1)^m}{\sqrt{2}} \frac{iE}{|E|} \begin{pmatrix} \mathfrak{E}_- \phi_{p,-k,-m-1}^{\lambda} \\ -\frac{2\lambda E}{|E|} \mathfrak{E}_+ \phi_{p,-k,-m-1}^{\lambda} \end{pmatrix}. \tag{3.3.23b}$$

So far, no assumption has been made on the sign of the Minkowski energy E. According to the Dirac sea interpretation, the vacuum state is defined as the state where all the states for which the eigenvalue of H is negative are filled, while those with positive eigenvalues of H, considered above sea level, are empty. Hence, the natural split between particle and anti-particle modes for an inertial Minkowski observer is done based on the sign of E: particles are described by modes with positive E, while their corresponding charge conjugates describe anti-particles. This choice of vacuum can be made manifest by writing the field operator as:

$$\psi(x) = \sum_j \theta(E_j) \left\{ U_j(x) b_j + V_j(x) d_j^{\dagger} \right\}, \tag{3.3.24}$$

where

$$j = (E_j, k_j, m_j, \lambda_j) \tag{3.3.25}$$

refers to all the labels defining the U and V modes and the sum runs over all their possible combinations:

$$\sum_j = \sum_{\lambda_j=\pm\frac{1}{2}} \sum_{m_j=-\infty}^{\infty} \int_{\substack{-\infty \\ |E_j|>\mu}}^{\infty} |E_j| \, dE_j \int_{-p_j}^{p_j} dk_j. \tag{3.3.26}$$

The step function $\theta(E)$ in Eq. (3.3.24) discards all negative values of the Minkowski energy E. The integration ends for k are $\pm p_j = \sqrt{E_j^2 - \mu^2}$. The operators b_j and $d_j^{\dagger}$ annihilate particles and create anti-particles, respectively, and obey canonical

anti-commutation rules:

$$\left\{b_j, b_{j'}^\dagger\right\} = \left\{d_j, d_{j'}^\dagger\right\} = \delta(j, j'), \tag{3.3.27}$$

where

$$\delta(j, j') = \frac{\delta(E_j - E_{j'})}{E_j}\delta(k_j - k_{j'})\delta_{m_j m_{j'}}\delta_{\lambda_j \lambda_{j'}}. \tag{3.3.28}$$

All other anti-commutators vanish.

Finally, it can be seen that V_{Ekm}^λ is proportional to $U_{-E,-k,-m-1}^\lambda$:

$$V_{Ekm}^\lambda = (-1)^m \frac{iE}{|E|}U_{-E,-k,-m-1}^\lambda, \tag{3.3.29}$$

or, using the notation introduced above,

$$V_j = (-1)^{m_j}\frac{iE_j}{|E_j|}U_{\bar{j}}, \qquad U_j = (-1)^{m_j+1}\frac{iE_j}{|E_j|}V_{\bar{j}}, \tag{3.3.30}$$

where

$$\bar{j} = (-E_j, -k_j, -m_j - 1, \lambda_j). \tag{3.3.31}$$

Massless Dirac particles are traditionally referred to as neutrinos, and are believed to be of negative chirality [46]. Anti-neutrinos also have negative chirality, which means that neutrino and anti-neutrino modes are not related through charge conjugation. The field operator corresponding to neutrinos and anti-neutrinos is obtained by filtering out the positive chirality contributions to Eq. (3.3.24) using the projector $P_L = \frac{1}{2}(1 - \gamma^5)$:

$$\psi_\nu(x) = \lim_{\mu \to 0}\frac{1 - \gamma^5}{2}\psi(x). \tag{3.3.32}$$

3.3.2 Dirac's equation using a cylindrical tetrad

There are quite a few examples in the literature where the Cartesian gauge used in this thesis is not preferred [38, 71, 72, 21]. Instead, a cylindrical (or spherical, depending on the symmetry) gauge is preferred, with respect to which the tetrad is:

$$\omega^{\hat{t}} = dt, \qquad \omega^{\hat{\rho}} = d\rho, \qquad \omega^{\hat{\varphi}} = \rho\, d\varphi, \qquad \omega^{\hat{z}} = dz,$$
$$e_{\hat{t}} = \partial_t, \qquad e_{\hat{\rho}} = \partial_\rho, \qquad e_{\hat{\varphi}} = \rho^{-1}\partial_\varphi, \qquad e_{\hat{z}} = \partial_z, \tag{3.3.33}$$

with the only non-vanishing connection coefficient given by:

$$\Gamma^{\hat{\rho}}{}_{\hat{\varphi}\hat{\varphi}} = -\frac{1}{\rho}. \tag{3.3.34}$$

The Dirac matrices corresponding to the tetrad indices $(\hat{t}, \hat{\varphi}, \hat{\rho}, \hat{z})$ are now chosen to be in the Dirac representation, i.e.:

$$\gamma^{\hat{t}} = \begin{pmatrix} 1 & 0 \\ 0 & -1 \end{pmatrix}, \quad \gamma^{\hat{\rho}} = \begin{pmatrix} 0 & \sigma^1 \\ -\sigma^1 & 0 \end{pmatrix}, \quad \gamma^{\hat{\varphi}} = \begin{pmatrix} 0 & \sigma^2 \\ -\sigma^2 & 0 \end{pmatrix}, \quad \gamma^{\hat{z}} = \begin{pmatrix} 0 & \sigma^3 \\ -\sigma^3 & 0 \end{pmatrix},$$

(3.3.35)

where the Pauli matrices σ^j are defined in Eqs. (2.2.8).

The link between the Dirac theory with respect to the Cartesian and cylindrical tetrads can be understood by finding the transformation which maps the former into the latter. The tetrad in the Cartesian gauge is trivially:

$$e_{\hat{0}} = \partial_t, \quad e_{\hat{1}} = \partial_x, \quad e_{\hat{2}} = \partial_y, \quad e_{\hat{3}} = \partial_z.$$

(3.3.36)

The change to cylindrical coordinates is described by the transformation matrix:

$$\frac{\partial x^{\mu'}}{\partial x^{\nu}} = \begin{pmatrix} 1 & 0 & 0 & 0 \\ 0 & \cos\varphi & \sin\varphi & 0 \\ 0 & -\rho^{-1}\sin\varphi & \rho^{-1}\cos\varphi & 0 \\ 0 & 0 & 0 & 1 \end{pmatrix},$$

(3.3.37)

which also changes the components of the tetrad:

$$\begin{aligned} e_{\hat{0}} &= \partial_t, \\ e_{\hat{1}} &= \cos\varphi\,\partial_\rho - \rho^{-1}\sin\varphi\,\partial_\varphi, \\ e_{\hat{2}} &= \sin\varphi\,\partial_\rho - \rho^{-1}\cos\varphi\,\partial_\varphi, \\ e_{\hat{3}} &= \partial_z. \end{aligned}$$

(3.3.38)

The cylindrical vierbein $e_{\hat{\alpha}}^{\mu'} \sim \delta^{\mu'}_{\hat{\alpha}}$ can be obtained from the above tetrad by applying on the tetrad (hatted) indices the following Lorentz transformation:

$$\Lambda^{\hat{\alpha}}_{\hat{\gamma}} = \begin{pmatrix} 1 & 0 & 0 & 0 \\ 0 & \cos\varphi & \sin\varphi & 0 \\ 0 & -\sin\varphi & \cos\varphi & 0 \\ 0 & 0 & 0 & 1 \end{pmatrix} = e^{i\varphi J_3},$$

(3.3.39)

which is just a rotation of angle φ about the z axis. The Lorentz transformation of the tetrad also transforms the spinor wave-function:

$$\psi^{\Lambda}(\Lambda x) = e^{-\varphi D[\Sigma_3]}\psi(x) = \mathrm{diag}(e^{i\varphi/2}, e^{-i\varphi/2}, e^{i\varphi/2}, e^{-i\varphi/2})\psi(x),$$

(3.3.40)

which transforms the solutions (3.3.2) to:

$$(U^\lambda_{Ekm})^\Lambda(\Lambda x) = \frac{1}{2\pi}e^{-iEt+i(m+\frac{1}{2})\varphi+ikz}\frac{1}{\sqrt{2}}\begin{pmatrix} \mathfrak{E}_+ \\ \frac{2\lambda E}{|E|}\mathfrak{E}_- \end{pmatrix} \otimes \frac{1}{\sqrt{2}}\begin{pmatrix} \mathfrak{p}_\lambda J_m(q\rho) \\ 2i\lambda\mathfrak{p}_{-\lambda}J_{m+1}(q\rho) \end{pmatrix},$$
(3.3.41)

where $\otimes$ denotes the outer (Kronecker) product, which acts as follows. Let A and B be matrices of sizes $m \times n$ and $p \times q$, having elements a_{ij} and b_{kl}, respectively. The outer product $A \otimes B$ creates a matrix of size $np \times mq$ according to the following rule:

$$\begin{pmatrix} a_{11} & \dots & a_{1n} \\ \vdots & \dots & \vdots \\ a_{m1} & \dots & a_{mn} \end{pmatrix} \otimes B = \begin{pmatrix} a_{11}B & \dots & a_{1n}B \\ \vdots & \dots & \vdots \\ a_{m1}B & \dots & a_{mn}B \end{pmatrix}$$
(3.3.42)

The dependence on the angular coordinate φ is now the same for all components of the four-spinor $(U^\lambda_{Ekm})^\Lambda$. Since m was initially an integer, $m+\frac{1}{2}$ is now an odd half-integer, thus guaranteeing the anti-periodicity of spinors under rotations of angle 2π [46, 70].

To prove that m is an integer, let us investigate the behaviour of the wave function under a rotation of angle $\delta\varphi$ about the z axis. The vierbein changes to:

$$\begin{aligned} e^\Lambda_{\hat{t}} &= \partial_t, \\ e^\Lambda_{\hat{x}} &= \cos\delta\varphi\,\partial_x + \sin\delta\varphi\,\partial_y, \\ e^\Lambda_{\hat{y}} &= -\sin\delta\varphi\,\partial_x + \cos\delta\varphi\,\partial_y, \\ e^\Lambda_{\hat{z}} &= \partial_z, \end{aligned}$$
(3.3.43)

which is equivalent to a Lorentz transformation $\Lambda = R_z(-\delta\varphi)$. Consequently, the Cartesian spinor undergoes the transformation:

$$\psi^\Lambda(\varphi) = D[R_z(-\delta\varphi)]\psi(\varphi - \delta\varphi).$$
(3.3.44)

Since $D[R_z(-2\pi)] = -1$, the requirement of anti-periodicity of ψ implies that:

$$\psi(\varphi - 2\pi) = \psi(\varphi),$$
(3.3.45)

hence, the m used in the Cartesian formulation is an integer. It is also clear that m is an integer since $m + \frac{1}{2}$ is the eigenvalue of the third component of the total angular momentum, which is an odd half-integer for fermions.

Under the same transformation (3.3.43), the cylindrical vierbein does not change:

$$e^\Lambda_{\hat{t}} = \partial_t, \quad e^\Lambda_{\hat{\rho}} = \partial_\rho, \quad e^\Lambda_{\hat{\varphi}} = \rho^{-1}\partial_{\hat{\varphi}}, \quad e^\Lambda_{\hat{z}} = \partial_z,$$
(3.3.46)

therefore, the wave function transforms as:

$$\psi^{\Lambda}(\varphi) = \psi(\varphi - 2\pi) = -\psi(\varphi) \tag{3.3.47}$$

which shows that the $m + \frac{1}{2}$ in (3.3.41) must be an odd half-integer.

In this work, the Cartesian tetrad is preferred due to the close analogy of the corresponding Dirac spinors and spin parts of quantum operators to those in flat-space quantum field theory.

3.3.3 Finite temperature expectation values

In this section, the formalism developed in subsection 2.2.6 is used to evaluate the t.e.v. of the SET and the charged current. The first step is to evaluate the vacuum Hadamard and Schwinger functions defined in Eqs. (2.2.49). The latter's Fourier coefficients are required to construct the thermal Hadamard function (2.2.52). The t.e.v.s of the fermion condensate (FC), charge current (CC) and stress-energy tensor (SET) can be computed using Eqs. (2.2.55) by employing the difference between the thermal and vacuum Hadamard functions.

The thermal Hadamard's elementary function

The Schwinger function (2.2.49) can be computed using the expansion (3.3.24) of the field operator:

$$S(x, x') = \sum_j \theta(E_j) \left[U_j(x) \otimes \overline{U}_j(x') + V_j(x) \otimes \overline{V}_j(x') \right], \tag{3.3.48}$$

where the outer product $\otimes$ creates from 4×1 and 1×4 matrices U_j and $\overline{U}_j$ a 4×4 matrix, following the algorithm presented in Eq. (3.3.42).

Using Eqs. (3.3.2) and (3.3.23a), the Fourier coefficients of the Schwinger function can be calculated:

$$s(\omega; \boldsymbol{x}, \boldsymbol{x}') = \sum_j \theta(E_j) e^{ik_j \Delta z} \left[\delta(\omega - E_j) u_j(x) \otimes \overline{u}_j(x') + \delta(\omega + E_j) v_j(x) \otimes \overline{v}_j(x') \right]. \tag{3.3.49}$$

Equation (2.2.52) can be used to compute the thermal Hadamard function:

$$S^{(1)}_{\beta}(x, x') = \sum_j \theta(E_j) \tanh \frac{\beta E}{2} \left[U_j \otimes \overline{U}_j - V_j \otimes \overline{V}_j \right]. \tag{3.3.50}$$

The vacuum Hadamard function can be calculated from Eq. (2.2.49):

$$S^{(1)}(x, x') = \sum_j \theta(E_j) \left[U_j(x) \otimes \overline{U}_j(x') - V_j(x) \otimes \overline{V}_j(x') \right]. \tag{3.3.51}$$

Subtracting Eq. (3.3.51) from Eq. (3.3.50) gives:

$$\Delta S_\beta^{(1)}(x, x') = \sum_j w(E_j) \left[U_j(x) \otimes \overline{U}_j(x') - V_j(x) \otimes \overline{V}_j(x') \right], \qquad (3.3.52)$$

where $w(E_j)$ is the Fermi-Dirac thermal weight, or density of states, factor:

$$w(E_j) = -\frac{2\theta(E_j)}{e^{\beta E_j} + 1}. \qquad (3.3.53)$$

Using Eq. (3.3.30) to replace the anti-particle modes V_j by U_j particle modes, the thermal Hadamard function $\Delta S_\beta^{(1)}$ reduces to:

$$\Delta S_\beta^{(1)}(x, x') = \sum_j [w(E_j) - w(E_{\bar{j}})] e^{-iE_j \Delta t + ik_j \Delta z} M_j, \qquad (3.3.54)$$

where $\bar{j}$ is defined in Eq. (3.3.31) (i.e. $E_{\bar{j}} = -E_j$) and the 4×4 matrix $M_j \equiv M_j(x, x') = u_j(x) \otimes \overline{u}_j(x')$ is given by:

$$M_j = \frac{1}{4\pi^2} \begin{pmatrix} \mathfrak{E}_+^2 & -\frac{2\lambda E}{|E|} \mathfrak{E}_+ \mathfrak{E}_- \\ \frac{2\lambda E}{|E|} \mathfrak{E}_+ \mathfrak{E}_- & -\mathfrak{E}_-^2 \end{pmatrix} \otimes \left[\phi_j(\rho, \varphi) \otimes \phi_j^\dagger(\rho', \varphi') \right], \qquad (3.3.55)$$

where the Kronecker product $\phi_j(\rho, \varphi) \otimes \phi_j^\dagger(\rho', \varphi')$ is copied according to Eq. (3.3.42) into the matrix on its left, thus producing a 4×4 matrix. The result M_{Ekm} of the sum over polarisations $\lambda_j = \pm\frac{1}{2}$ can be written as follows:

$$M_{Ekm} \equiv \sum_{\lambda=\pm 1/2} M_{Ekm}^\lambda = \frac{1}{4\pi^2} \begin{pmatrix} M_{Ekm}^{\text{up}} \circ \mathcal{M}_j & -M_{Ekm}^\times \circ \mathcal{M}_j \\ M_{Ekm}^\times \circ \mathcal{M}_j & -M_{Ekm}^{\text{down}} \circ \mathcal{M}_j \end{pmatrix}, \qquad (3.3.56)$$

where the Hadamard (Schur) product symbol $\circ$ has been used for the element-wise product of two matrices of the same size, defined for two 2×2 matrices A, B as:

$$A \circ B = \begin{pmatrix} a_{11}b_{11} & a_{12}b_{12} \\ a_{21}b_{21} & a_{22}b_{22} \end{pmatrix}. \qquad (3.3.57)$$

The matrix $\mathcal{M}_j$ on the right of the Hadamard product symbol $\circ$ is defined as:

$$\mathcal{M}_j = \begin{pmatrix} e^{im\Delta\varphi} J_m(q\rho) J_m(q\rho') & -ie^{i(m+1)\Delta\varphi - i\varphi} J_m(q\rho) J_{m+1}(q\rho') \\ ie^{im\Delta\varphi + i\varphi} J_{m+1}(q\rho) J_m(q\rho') & e^{i(m+1)\Delta\varphi} J_{m+1}(q\rho) J_{m+1}(q\rho') \end{pmatrix}, \qquad (3.3.58)$$

where $\mathfrak{E}_\pm$ are defined in Eq. (3.3.17). The matrices M_{Ekm}^* in Eq. (3.3.56) can be computed using the explicit expression (3.3.11) for the two-spinors ϕ_{pkm}^λ:

$$M_{Ekm}^{\text{up}} = \mathfrak{E}_+^2 \begin{pmatrix} 1 & 0 \\ 0 & 1 \end{pmatrix}, \quad M_{Ekm}^{\text{down}} = \mathfrak{E}_-^2 \begin{pmatrix} 1 & 0 \\ 0 & 1 \end{pmatrix}, \quad M_{Ekm}^\times = \frac{1}{E} \begin{pmatrix} k & q \\ q & -k \end{pmatrix}.$$

For the purpose of computing t.e.v.s, it is advantageous to express M_{Ekm} as follows:

$$4\pi^2 M_{Ekm} = \frac{1}{2} I_2 \otimes [(M_{Ekm}^{\text{up}} - M_{Ekm}^{\text{down}}) \circ \mathcal{M}_j] + \frac{1}{2}\sigma_3 \otimes [(M_{Ekm}^{\text{up}} + M_{Ekm}^{\text{down}}) \circ \mathcal{M}_j]$$

$$+ \begin{pmatrix} 0 & -1 \\ 1 & 0 \end{pmatrix} \otimes [M_{Ekm}^{\times} \circ \mathcal{M}_j]. \quad (3.3.59)$$

Thus, the following expression is obtained for M_{Ekm}:

$$4\pi^2 M_{Ekm} = \left[\frac{\mu}{E} I_2 + \sigma_3\right] \otimes \left[\begin{pmatrix} 1 & 0 \\ 0 & 1 \end{pmatrix} \circ \mathcal{M}_j\right] + \frac{1}{E}\begin{pmatrix} 0 & -1 \\ 1 & 0 \end{pmatrix} \otimes \left[\begin{pmatrix} k & q \\ q & -k \end{pmatrix} \circ \mathcal{M}_j\right].$$

$$(3.3.60)$$

Thermal expectation value of the fermion condensate

The t.e.v. of the fermion condensate (FC) can be computed from (3.3.50) using (2.2.55a). Since the computation does not involve differentiations, the coincidence limit can be taken first:

$$\lim_{x' \to x} \Delta S_\beta^{(1)}(x, x') = \frac{1}{4\pi^2} \sum_{\substack{m=-\infty \\ |E|>\mu}}^{\infty} \int_{-\infty}^{\infty} dE \int_{-p}^{p} dk \, |E| \, [w(E) - w(-E)]$$

$$\times \left[\left(\frac{\mu}{E} I_2 + \sigma_3\right) \otimes \begin{pmatrix} J_m^2 & 0 \\ 0 & J_{m+1}^2 \end{pmatrix}\right.$$

$$\left. + \frac{1}{E}\begin{pmatrix} 0 & -1 \\ 1 & 0 \end{pmatrix} \otimes \begin{pmatrix} kJ_m^2 & -iqe^{-i\varphi}J_m J_{m+1} \\ iqe^{i\varphi}J_{m+1}J_m & -kJ_{m+1}^2 \end{pmatrix}\right], \quad (3.3.61)$$

where the density of states factor $w(\pm E)$ is defined in Eq. (3.3.53). Due to its anti-symmetry with respect to $E \to -E$, the σ_3 terms drops. Similarly, the diagonal elements in the last term are odd with respect to $k \to -k$ and hence, vanish. Furthermore, the sum over m can be performed using (A.4.2), after which the integral over k is straightforward:

$$\lim_{x' \to x} \Delta S_\beta^{(1)}(x, x') = -\frac{\mu}{\pi^2} \int_\mu^\infty \frac{p \, dE}{e^{\beta E} + 1}. \quad (3.3.62)$$

The fermion condensate is now straightforward to compute:

$$\langle : \overline{\psi}\psi : \rangle_\beta = \frac{2\mu}{\pi^2} \int_\mu^\infty \frac{p \, dE}{e^{\beta E} + 1}. \quad (3.3.63)$$

The integral above can be performed exactly in the massless limit using the Fermi-Dirac integral:

$$\int_0^\infty dx \frac{x}{e^{\beta x} + 1} = \frac{\pi^2}{12\beta^2}, \quad (3.3.64)$$

thus, for small masses, the fermion condensate has the following behaviour:

$$\langle : \overline{\psi}\psi : \rangle_\beta \sim \frac{\mu}{6\beta^2} + O(\mu^2). \tag{3.3.65}$$

A more in-depth analysis of the behaviour of the FC at small and large values of the mass will be performed when the SET is discussed.

Thermal expectation value of the charge current

Since the coincidence limit (3.3.62) of $\Delta S_\beta^{(1)}$ is proportional to the identity matrix, all components of the CC vanish:

$$\langle : J^\mu : \rangle_\beta = -\frac{1}{2}\mathrm{tr}\left\{\Delta S_\beta^{(1)}(x, x' = x)\gamma^\mu\right\} = 0, \tag{3.3.66}$$

since $\mathrm{tr}\,\gamma^\mu = 0$. Moreover, γ^5 and γ^μ anti-commute, hence the t.e.v. of the neutrino current also vanishes:

$$\langle : J_\nu^\mu : \rangle_\beta = -\frac{1}{2}\mathrm{tr}\left\{\frac{1-\gamma^5}{2}\Delta S_\beta^{(1)}(x, x' = x)\gamma^\mu\right\} = 0. \tag{3.3.67}$$

The vanishing of the current everywhere is in agreement with the properties of a thermal state: both particles and antiparticles are in thermal equilibrium at the same temperature but give contributions of opposite sign because of their opposite charge.

Thermal expectation value of the stress-energy tensor

The t.e.v. of the SET can be computed from Eq. (3.3.50) using the formula (2.2.55c), where the coincidence limit can be taken only after the derivatives have been performed. The matrix structure in Eq. (3.3.60) can be used as a guide to see which terms contribute to which component, based on what gamma matrix is multiplying $\Delta S_\beta^{(1)}$ when the trace is taken. For example, when $\gamma^{\hat{t}}$ is multiplying $\Delta S_\beta^{(1)}$, only the σ_3 term contributes. In the case of spatial gamma matrices, only the last term can contribute. The derivatives with respect to $\hat{t}$, φ and z are trivial to perform, while the ρ and ρ' derivatives send products of the form $J_m J_m$ and $J_{m+1}J_{m+1}$ to 0 and turn $J_m J_{m+1}$ into a Wronskian, as follows:

$$\lim_{\rho\to\rho'}[(\partial_\rho - \partial_{\rho'})J_m(q\rho)J_m(q\rho')] = \lim_{\rho\to\rho'}[(\partial_\rho - \partial_{\rho'})J_{m+1}(q\rho)J_{m+1}(q\rho')] = 0,$$

$$\lim_{\rho\to\rho'}[(\partial_\rho - \partial_{\rho'})J_m(q\rho)J_{m+1}(q\rho')] = -qJ_m^+(q\rho) + \rho^{-1}(m+\tfrac{1}{2})J_m^\times(q\rho), \tag{3.3.68}$$

where Eqs. (A.1.11) were used to replace the derivatives of the Bessel functions and the following notation was introduced:

$$J_m^{\pm}(z) = J_m^2(z) \pm J_{m+1}^2(z), \qquad J_m^{\times}(z) = 2J_m(z)J_{m+1}(z). \tag{3.3.69}$$

The components of the SET can now be calculated. All off-diagonal components vanish, while the diagonal ones reduce to:

$$\langle : T_{\hat{\alpha}\hat{\gamma}} : \rangle_{\beta} = \frac{2}{\pi^2} \int_{\mu}^{\infty} \frac{dE}{e^{\beta E} + 1} \mathrm{diag}\left(pE^2, \frac{1}{3}p^3, \frac{1}{3}p^3, \frac{1}{3}p^3\right). \tag{3.3.70}$$

As expected from Eq. (2.2.28), the trace of the SET is proportional to the FC (3.3.63):

$$\langle : T^{\hat{\alpha}}_{\hat{\alpha}} : \rangle_{\beta} = -\mu \langle : \overline{\psi}\psi : \rangle_{\beta} = -\frac{2\mu^2}{\pi^2} \int_{\mu}^{\infty} \frac{p\,dE}{e^{\beta E} + 1}. \tag{3.3.71}$$

In the massless case $E = p$, the formula

$$\int_0^{\infty} \frac{x^3\,dx}{e^{\beta x} + 1} = \frac{7\pi^4}{120\beta^4} \tag{3.3.72}$$

can be used to integrate (3.3.70):

$$\langle : T_{\hat{\alpha}\hat{\gamma}} : \rangle_{\beta} = \frac{7\pi^2}{60\beta^4} \mathrm{diag}\left(1, \frac{1}{3}, \frac{1}{3}, \frac{1}{3}\right). \tag{3.3.73}$$

The value obtained for (charged) fermions differs from that for uncharged scalars (3.2.22) by a factor of $\frac{7}{2}$, which can be explained as follows. A factor of 2 is due to the equal contributions coming from particles and anti-particles, another factor of 2 comes from the two different helicity states $\lambda = \pm\frac{1}{2}$ and finally a factor of $\frac{7}{8}$. The latter factor is related to the difference between Fermi-Dirac and Bose-Einstein statistics. The hallmark of the former is the density of states factor $(e^{\beta E} + 1)^{-1}$ present in the expression for the t.e.v. of the SET (3.3.70), while the SET for a scalar field (3.2.20) is written in terms of $(e^{\beta E} - 1)^{-1}$. As in the scalar case, the equation of state P/ρ (where P is the pressure and ρ is the energy density) is equal to $\frac{1}{3}$ in the massless case.

If $\mu \neq 0$, an asymptotic analysis can be performed, along the lines of that for the massive scalar field in subsection 3.2.2. Changing the variable in Eq. (3.3.73) to $t = E/\mu$ gives:

$$P = \frac{2\mu^4}{3\pi^2} \int_1^{\infty} \frac{dt}{e^{\beta\mu t} + 1}(t^2 - 1)^{3/2},$$
$$\rho - 3P = \frac{2\mu^4}{\pi^2} \int_1^{\infty} \frac{dt}{e^{\beta\mu t} + 1}(t^2 - 1)^{1/2}, \tag{3.3.74a}$$

where $\rho - 3P$ is minus the trace of the SET and is linked to the t.e.v. of the FC through:

$$\rho - 3P = \mu \langle : \overline{\psi}\psi : \rangle_\beta . \tag{3.3.74b}$$

The exponential in the denominators above can be expanded in a Taylor series:

$$\frac{1}{e^{\beta\mu t} + 1} = \sum_{k=1}^{\infty} (-1)^{k+1} e^{-k\beta\mu t}, \tag{3.3.75}$$

which, together with (A.1.17), gives:

$$P = \frac{2\mu^2}{\pi^2\beta^2} \sum_{k=1}^{\infty} \frac{(-1)^{k+1}}{k^2} K_2(k\beta\mu),$$

$$\rho - 3P = \frac{2\mu^3}{\pi^2\beta} \sum_{k=1}^{\infty} \frac{(-1)^{k+1}}{k} K_1(k\beta\mu). \tag{3.3.76}$$

As in the scalar case, terminating the expansion (3.3.76) at $k = 3$ gives an excellent approximation throughout the whole parameter space for μ and β.

The first term in the series (3.3.76) is the same (up to a proportionality factor of 4) as the corresponding one for scalars in Eq. (3.2.29), showing that fermions and scalars have the same large-mass behaviour (when the series can be terminated at $k = 1$). The behaviour of the FC at large masses is:

$$\langle : \overline{\psi}\psi : \rangle_\beta \sim \frac{1}{\beta^3} \left(\frac{\beta\mu}{2\pi} \right)^{3/2} e^{-\beta\mu} \left(1 + \frac{3}{8\beta\mu} + \dots \right). \tag{3.3.77}$$

At small masses (or large temperatures), the argument $\beta\mu$ of the Bessel functions is small and Eq. (3.3.76) can be approximated using (A.2.4b):

$$P = \frac{7\pi^2}{180\beta^4} - \frac{\mu^2}{12\beta^2} + \mathcal{O}(\mu^4),$$

$$\rho = \frac{7\pi^2}{60\beta^4} - \frac{\mu^2}{12\beta^2} + \mathcal{O}(\mu^4),$$

$$\frac{P}{\rho} = \frac{1}{3} \left(1 + \frac{10}{7\pi^2} \beta^2\mu^2 + \mathcal{O}(\mu^4) \right)^{-1}. \tag{3.3.78}$$

Comparing the above results to the small mass expansion (3.3.65) of the t.e.v. of the FC confirms Eq. (3.3.74b). Figure 3.2 shows how the asymptotic expressions for the density, pressure and equation of state for massive fermions at finite temperature for small values of the mass (3.3.78) compare with results obtained using numerical integration. To facilitate the comparison with the results obtained for the scalar field, the plots show the energy density and pressure per degree of freedom, i.e. divided by 4 for fermions (uncharged scalars have only one degree of freedom).
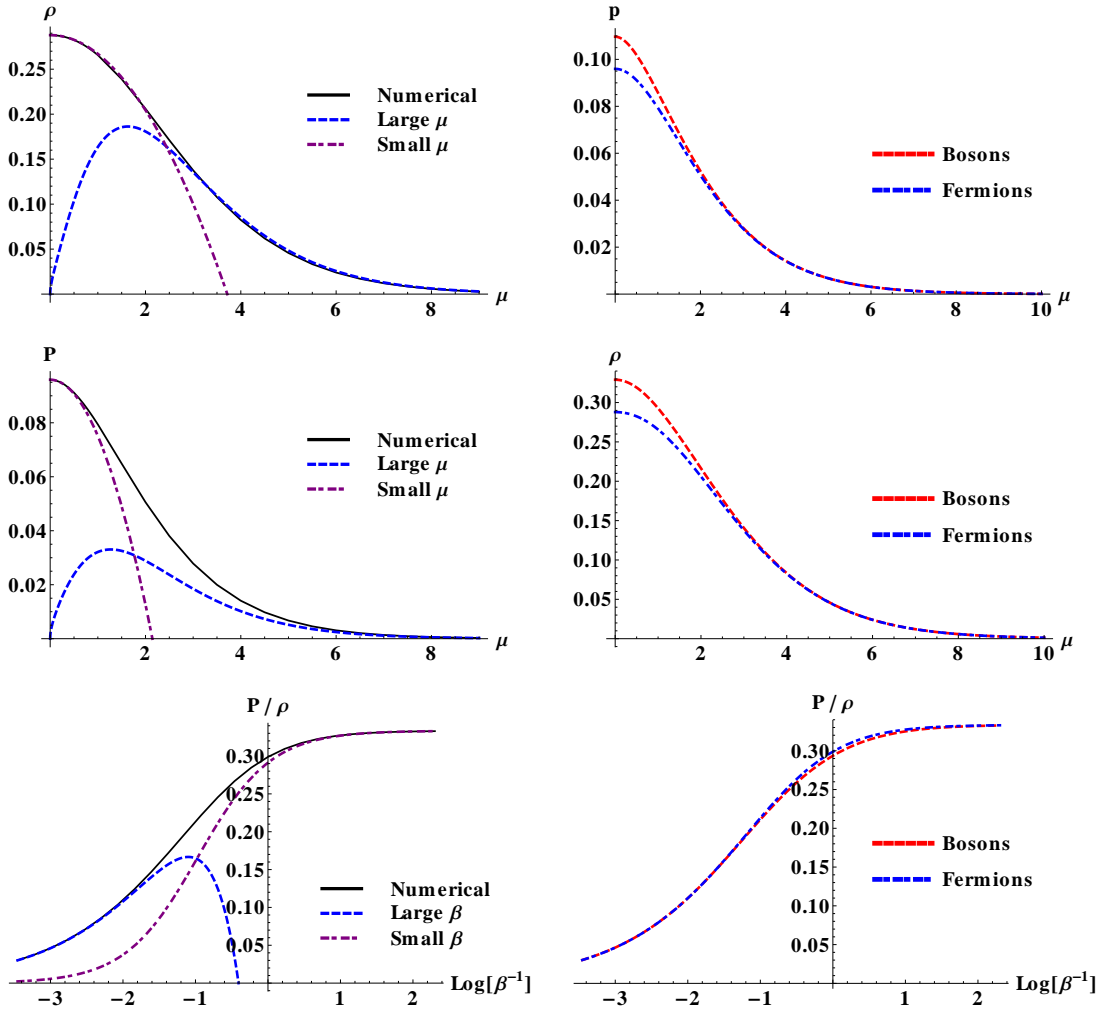
Figure 3.2: On the left hand side, the density ρ, pressure P and equation of state $\frac{P}{\rho}$ per degree of freedom (4 for Dirac fermions) for a thermal distribution of fermions are plotted as functions of the mass μ of the quanta with $\beta = 1$ (first two plots) and as functions of the logarithm of the temperature with $\mu = 1$ (last plot). The solid black curve shows numerical results, the dashed blue curve is the large μ approximation and the dashed purple curve is the small μ approximation. The plots on the right compare numerical results for the density, pressure and equation of state of fermions (blue) and bosons (red). The values for the pressure and density are always higher for bosons, but the equation of state decreases with temperature slower for fermions.

3.4 Summary

As part of the introductory material, this chapter introduces notation and techniques to be used throughout this thesis. The mode solutions of the Klein Gordon and Dirac equations, presented in sections 3.2.1 and 3.3.1, respectively, are used for the construction of quantum states on unbounded and bounded rotating Minkowski space-time, in chapters 4 and 5. The methods used for the construction of the thermal two-point functions and thermal expectation values, presented in sections 3.2.2 and 3.3.3 for the Klein-Gordon and Dirac fields, respectively, are used on the rotating Minkowski space-time in chapters 4 and 5, as well as on non-rotating and rotating anti-de Sitter space-time, in chapters 7 and 8, respectively.

Chapter 4. Rotating Minkowski space-time

Quantum field theory in rotating space-times has been investigated previously. Of relevance to this chapter are especially the paper by Letaw and Pfautsch [52] on the problem of second quantisation of scalar particles, Iyer's paper [47] on the same problem for fermions and Vilenkin's paper [72] on the construction of Green's functions for scalars, fermions and photons. The problem of second quantisation is considered in a co-rotating coordinate system obtained simply by applying a time-dependent rotation $\varphi = \varphi_{\mathrm{M}} - \Omega t_{\mathrm{M}}$ to the Minkowski coordinates $(t_{\mathrm{M}}, \varphi_{\mathrm{M}})$, where the subscript M refers to coordinates with respect to the non-rotating, inertial frame in Minkowski space-time. All these papers report problems not only with the construction of thermal states, but also with second quantisation. The resulting space-time is not physical because the velocity of co-rotating particles increases linearly with the distance from the rotation axis such that at the finite distance $\rho = \Omega^{-1}$ from the rotation axis, co-rotating particles rotate with the speed of light. The surface defined by $\rho = \Omega^{-1}$ is therefore referred to as the speed of light surface (SOL).

There have been attempts at improving this simple description by using a Lorentz transformation instead of the non-relativistic coordinate transformation $\varphi \mapsto \varphi - \Omega t$ [53, 66, 69]. The resulting metric is obtained from the Minkowski metric by performing the coordinate transformation

$$t \mapsto t \cosh \Omega \rho - \rho \varphi \sinh \Omega \rho, \qquad \varphi \mapsto \varphi \cosh \Omega \rho - \tfrac{t}{\rho} \sinh \Omega \rho$$

and suffers from the major drawback of being impractical for exact analytic calculations. For this reason, the discussion in this thesis is restricted to the simple model $\varphi \mapsto \varphi - \Omega t$, where good analytic results can be obtained and understood.

The results of sections 3.2.1 and 3.3.1 are used here for the analysis of the quantum scalar and fermion fields, respectively, on a flat space-time rotating about a fixed axis with constant angular velocity. The space-time metric and other properties are discussed in section 4.1. Scalars are discussed in section 4.2 and fermions in section 4.3. In both cases, novel analytic results are presented, which are also published in Ref. [10].

A main point in our discussion is the fundamental difference between the freedom in the definition of vacuum states for scalars and fermions. While for the latter, the only restriction to how the modes are split to represent particles and anti-particles is the preservation of the charge conjugation symmetry, particle modes

for the former are constrained to having positive norm with respect to the Klein-Gordon inner product [52]. Thus, the set of particle modes can be forced to contain modes with negative frequencies (i.e. negative eigenvalues of the Hamiltonian). In contrast, Iyer [47] shows that for fermions it is possible to choose a vacuum state such that all particle states have positive frequencies with respect to the co-rotating Hamiltonian. The possibility of quantising the field such that no negative frequency modes describe particle states is important for the consistent definition of thermal states. As discussed by Vilenkin [72], particle modes with negative frequency induce spurious temperature-independent terms in thermal expectation values.

The main result of this chapter is the derivation of analytic formulae for co-rotating t.e.v.s of massless fermions, in subsection 4.3.2. These results represent original work which has been published in Ref. [10]. A similar method which allowed the analytic analysis of fermion t.e.v.s is applied to the case of the scalar field, where it is known that co-rotating thermal states are ill-defined, to isolate the divergent contributions from finite terms which can be interpreted physically.

4.1 Space-time characteristics

The space-time rotating with angular speed Ω about the z-axis can be described using a co-rotating coordinate system, by performing the coordinate transformation

$$t = t_M, \qquad \rho = \rho_M, \qquad \varphi = \varphi_M - \Omega t_M, \qquad z = z_M \qquad (4.1.1)$$

on the original Minkowski coordinates $\{t_M, \rho_M, \varphi_M, z_M\}$. Throughout this chapter, coordinate indices refer to the co-rotating coordinate system, with respect to which the line element in cylindrical coordinates has the form:

$$ds^2 = -\varepsilon dt^2 + 2\rho^2\Omega\, dt\, d\varphi + d\rho^2 + \rho^2 d\varphi^2 + dz^2, \qquad (4.1.2)$$

where

$$\varepsilon = 1 - \rho^2\Omega^2 \qquad (4.1.3)$$

decreases to 0 as the SOL is approached. The metric $g_{\mu\nu}$ and its inverse $g^{\mu\nu}$ have the following components:

$$g_{\mu\nu} = \begin{pmatrix} -(1-\rho^2\Omega^2) & 0 & \rho^2\Omega & 0 \\ 0 & 1 & 0 & 0 \\ \rho^2\Omega & 0 & \rho^2 & 0 \\ 0 & 0 & 0 & 1 \end{pmatrix}, \qquad g^{\mu\nu} = \begin{pmatrix} -1 & 0 & \Omega & 0 \\ 0 & 1 & 0 & 0 \\ \Omega & 0 & -\Omega^2 + \rho^{-2} & 0 \\ 0 & 0 & 0 & 1 \end{pmatrix}. \qquad (4.1.4)$$

The non-vanishing Christoffel symbols for the metric (4.1.4) are given by:

$$\Gamma^{\varphi}{}_{t\rho} = \frac{\Omega}{\rho}, \qquad \Gamma^{\varphi}{}_{\varphi\rho} = \frac{1}{\rho}, \qquad \Gamma^{\rho}{}_{tt} = -\rho\Omega^2, \qquad \Gamma^{\rho}{}_{t\varphi} = -\Omega\rho, \qquad \Gamma^{\rho}{}_{\varphi\varphi} = -\rho.$$

(4.1.5)

In the rotating space-time, the complete system of commuting operators (CSCO) contains the same operators as in Minkowski space-time, but this time with respect to the rotating coordinates. Thus, the CSCO for the Klein-Gordon field is comprised of H, P_z and L_z and for the Dirac field, L_z is replaced by J_z and the helicity operator W_0 is added, as explained in subsection 3.3.1. The main difference is that now the Hamiltonian $H = i\partial_t$ contains a derivative with respect to the time in the co-rotating frame and is linked to the Minkowski operators through:

$$H = H_{\mathrm{M}} - \Omega L_{z,\mathrm{M}}.$$

(4.1.6)

The Klein-Gordon equation (2.1.2) can be written as:

$$\left[-(H + \Omega L_z)^2 + \rho^{-2}L_z^2 + P_z^2 - \partial_\rho^2 - \rho^{-1}\partial_\rho + \mu^2 \right] \phi(x) = 0,$$

(4.1.7)

naturally incorporating a coupling between the angular momentum operator $\boldsymbol{L}$ and the angular velocity $\boldsymbol{\Omega}$ of the rotation of the space-time through the term $\boldsymbol{\Omega} \cdot \boldsymbol{L} = \Omega L_z$.

Transforming back to Cartesian coordinates, the line element (4.1.2) takes the form:

$$ds^2 = -[1 - (x^2 + y^2)\Omega^2]dt^2 + 2x\Omega\,dt\,dy - 2y\Omega\,dt\,dx + dx^2 + dy^2 + dz^2, \quad (4.1.8)$$

where $x = \rho\cos\varphi$ and $y = \rho\sin\varphi$. In matrix form, the metric and its inverse have components:

$$g_{\mu\nu} = \begin{pmatrix} -(1 - (x^2 + y^2)\Omega^2) & -y\Omega & x\Omega & 0 \\ -y\Omega & 1 & 0 & 0 \\ x\Omega & 0 & 1 & 0 \\ 0 & 0 & 0 & 1 \end{pmatrix},$$

$$g^{\mu\nu} = \begin{pmatrix} -1 & -y\Omega & x\Omega & 0 \\ -y\Omega & 1 - y^2\Omega^2 & xy\Omega^2 & 0 \\ x\Omega & xy\Omega^2 & 1 - x^2\Omega^2 & 0 \\ 0 & 0 & 0 & 1 \end{pmatrix}.$$

(4.1.9)

A natural choice for the tetrad coframe defined by (2.2.1) is:

$$\omega^{\hat{t}} = dt, \qquad\qquad \omega^{\hat{x}} = -\Omega y\, dt + dx,$$
$$\omega^{\hat{z}} = dz, \qquad\qquad \omega^{\hat{y}} = \Omega x\, dt + dy, \qquad (4.1.10)$$

with the dual frame vectors given by:

$$e_{\hat{t}} = \partial_t - \Omega\partial_\varphi = \partial_t + \Omega y\partial_x - \Omega x\partial_y, \quad e_{\hat{i}} = \partial_i, \qquad (4.1.11)$$

or, in cylindrical coordinates:

$$e_{\hat{t}} = \partial_t - \Omega\partial_\varphi, \quad e_{\hat{\rho}} = \partial_\rho, \quad e_{\hat{\varphi}} = \rho^{-1}\partial_\varphi, \quad e_z = \partial_z. \qquad (4.1.12)$$

The ensuing non-zero Cartan coefficients (2.2.19) are:

$$c_{\hat{t}\hat{x}}{}^{\hat{y}} = c_{\hat{y}\hat{t}}{}^{\hat{x}} = \Omega. \qquad (4.1.13)$$

The Cartan coefficients can be used to compute the only non-vanishing connection coefficient (2.2.18):

$$\Gamma_{\hat{x}\hat{y}\hat{t}} = -\Omega, \qquad (4.1.14)$$

which in turn can be used to calculate the spin connection (2.2.16):

$$D_{\hat{t}} = \partial_t - \Omega\partial_\varphi + \Sigma_z, \quad D_{\hat{i}} = \partial_i. \qquad (4.1.15)$$

Here, $\Sigma_z = \frac{1}{2}\gamma^{\hat{1}}\gamma^{\hat{2}}$ is the anti-hermitian spin part of the generator of rotations about the z-axis. The covariant derivatives (4.1.15) can be expressed with respect to the operators of the CSCO as follows:

$$iD_{\hat{t}} = H_\Omega + \Omega J_z, \qquad -iD_{\hat{i}} = P_i \qquad (4.1.16)$$

and can be substituted into Eq. (2.2.20) to write the Dirac equation as:

$$[\gamma^0(H + \Omega J^z) - \boldsymbol{\gamma}\cdot\boldsymbol{P} - \mu]\psi(x) = 0, \qquad (4.1.17)$$

where $\boldsymbol{\gamma} = (\gamma^{\hat{x}}, \gamma^{\hat{y}}, \gamma^{\hat{z}})$ contains the spatial gamma matrices defined in subsection 2.2.1. The Dirac equation also contains the coupling $\boldsymbol{\Omega}\cdot\boldsymbol{J} = \Omega J_z$ between the angular momentum operator $\boldsymbol{J}$ and the angular velocity $\boldsymbol{\Omega}$ of the space-time.

It is also useful to analyse the connection between the components of vectors and tensors with respect to the Cartesian and cylindrical coordinate bases and with respect to the Cartesian tetrad. The components of the stress tensor in two different

coordinate systems $\{x^\mu\}$ and $\{x'^\lambda\}$ are related through:

$$T'_{\mu\nu} = T_{\kappa\lambda} \frac{\partial x^\kappa}{\partial x'^\mu} \frac{\partial x^\lambda}{\partial x'^\nu}. \tag{4.1.18}$$

Applying the above prescription to the transition from Cartesian coordinates (x, y, z) to cylindrical coordinates (ρ, φ, z) gives:

$$
\begin{aligned}
T_{t\rho} &= T_{0x} \cos \varphi + T_{0y} \sin \varphi, \\
T_{\rho z} &= T_{xz} \cos \varphi + T_{yz} \sin \varphi, \\
\rho^{-1} T_{t\varphi} &= -T_{0x} \sin \varphi + T_{0y} \cos \varphi, \\
\rho^{-1} T_{\varphi z} &= -T_{xz} \sin \varphi + T_{yz} \cos \varphi, \\
T_{\rho\rho} &= T_{xx} \cos^2 \varphi + 2T_{xy} \sin \varphi \cos \varphi + T_{yy} \sin^2 \varphi, \\
\rho^{-2} T_{\varphi\varphi} &= T_{xx} \sin^2 \varphi - 2T_{xy} \sin \varphi \cos \varphi + T_{yy} \cos^2 \varphi, \\
\rho^{-1} T_{\rho\varphi} &= -T_{xx} \sin \varphi \cos \varphi + T_{xy}(\cos^2 \varphi - \sin^2 \varphi) + T_{yy} \sin \varphi \cos \varphi. \tag{4.1.19}
\end{aligned}
$$

The components of the SET with respect to a tetrad can be written as:

$$T_{\hat\alpha\hat\beta} = e^\mu_{\hat\alpha} e^\nu_{\hat\beta} T_{\mu\nu}, \tag{4.1.20}$$

giving rise to the following expressions with respect to the tetrad (4.1.12):

$$
\begin{aligned}
T_{\hat t\hat t} &= T_{tt} - 2\Omega T_{t\varphi} + \Omega^2 T_{\varphi\varphi}, & T_{\hat t\hat\rho} &= T_{t\rho} - \Omega T_{\varphi\rho}, \\
T_{\hat t\hat\varphi} &= \rho^{-1}(T_{t\varphi} - \Omega T_{\varphi\varphi}), & T_{\hat t\hat z} &= T_{tz} - \Omega T_{\varphi z}, \\
T_{\hat\varphi\hat\rho} &= \rho^{-1} T_{\varphi\rho}, & T_{\hat\varphi\hat\varphi} &= \rho^{-2} T_{\varphi\varphi}, \\
T_{\hat\varphi\hat z} &= \rho^{-1} T_{\varphi z}, & & \tag{4.1.21}
\end{aligned}
$$

which can be inverted as follows:

$$
\begin{aligned}
T_{tt} &= T_{\hat t\hat t} + 2\rho\Omega T_{\hat t\hat\varphi} + \rho^2\Omega^2 T_{\hat\varphi\hat\varphi}, & T_{t\rho} &= T_{\hat t\hat\rho} + \rho\Omega T_{\hat\varphi\hat\rho}, \\
T_{t\varphi} &= \rho T_{\hat t\hat\varphi} + \rho^2\Omega T_{\hat\varphi\hat\varphi}, & T_{tz} &= T_{\hat t\hat z} + \rho\Omega T_{\hat\varphi\hat z}, \\
T_{\varphi\rho} &= \rho T_{\hat\varphi\hat\rho}, & T_{\varphi\varphi} &= \rho^2 T_{\hat\varphi\hat\varphi}, \\
T_{\varphi z} &= \rho T_{\hat\varphi\hat z}, & & \tag{4.1.22}
\end{aligned}
$$

Similarly, the components of the current vector with respect to the cylindrical coordinate system can be written as:

$$J^\rho = J^x \cos \varphi + J^y \sin \varphi, \qquad J^\varphi = -\rho^{-1} \sin \varphi J^x + \rho^{-1} \cos \varphi J^y, \tag{4.1.23}$$

and the only tetrad component which differs from the coordinate components is:

$$J^{\hat{\varphi}} = \rho J^{\varphi} + \rho \Omega J^{t}. \tag{4.1.24}$$

Before ending this section, it is worth mentioning that Eqs. (4.1.7) and (4.1.17) can be obtained by applying the following rotation:

$$R[\Omega t] = e^{i\Omega t J_{z}}, \tag{4.1.25}$$

on the Minkowski coordinates in Eqs. (2.1.2) and (2.2.20), with J_{z} replaced by L_{z} for the Klein-Gordon field. The above transformation can be used to obtain the modes and Green's functions from the Minkowski ones calculated in the previous chapter.

4.2 Scalar field theory in a rotating background

Subsection 4.2.1 starts this section by summarising the results presented by Letaw and Pfautsch [52] and Duffy and Ottewill [33] regarding the construction of modes and second quantisation of the Klein-Gordon field in co-rotating coordinates. In subsection 4.2.2, the t.e.v. of the SET is shown to be infinite throughout space-time. Using analytic techniques, the divergences in the t.e.v. of the SET are isolated, facilitating the understanding of their origin, while physical information can be extracted from the finite remainder.

4.2.1 Rigidly rotating modes

To obtain the solutions of the Klein-Gordon equation (4.1.7) in co-rotating coordiantes (4.1.1), it is sufficient to apply the rotation (4.1.25) to the Minkowski modes (3.2.6). Since in the scalar case, $J_{z} = -i\partial_{\varphi}$, the transformation is just a translation of the φ coordinate, i.e.:

$$e^{i\Omega t J_{z}} f(\varphi) = \sum_{n=0}^{\infty} \frac{(\Omega t)^{n}}{n!} \frac{\partial^{n} f(\varphi)}{\partial \varphi^{n}} = f(\varphi + \Omega t). \tag{4.2.1}$$

Thus, the following mode solutions are obtained [33]:

$$f_{\omega k m}(x) = \frac{1}{\sqrt{8\pi^{2} |\omega|}} e^{-i\widetilde{\omega}t + ikz + im\varphi} J_{m}(q\rho), \tag{4.2.2}$$

where $\widetilde{\omega} = \omega - \Omega m$ is the eigenvalue of the Hamiltonian $H = i\partial_{t}$ and the transverse momentum is defined as $q = \sqrt{\omega^{2} - k^{2} - \mu^{2}}$. The Klein-Gordon inner product

(3.2.5) changes according to Eq. (2.1.19) to

$$\langle f, g \rangle = \int_{-\infty}^{\infty} dz \int_{0}^{\infty} \rho \, d\rho \int_{0}^{2\pi} d\varphi \, f \left(i \overleftrightarrow{\partial_t} + i\Omega \overleftrightarrow{\partial_\varphi} \right) g, \tag{4.2.3}$$

therefore, the norm of the modes $f_{\omega km}$ is still given by Eq. (3.2.7). Hence, even though the frequency of the mode $f_{\omega km}$ is $\widetilde{\omega}$, the sign of its norm is still controlled by the Minkowski energy ω, as shown in Eq. (2.1.33).

As discussed by Letaw and Pfautsch [52], in the expansion of the field operator $\phi(x)$, the coefficients of positive norm modes have the interpretation of particle annihilation operators, thus, the field operator must be expanded as:

$$\phi(x) = \sum_{m=-\infty}^{\infty} \int_{\mu}^{\infty} \omega \, d\omega \int_{-p}^{p} dk \left\{ f_{\omega km}(x) a_{\omega km} + f_{\omega km}^*(x) a_{\omega km}^\dagger \right\}, \tag{4.2.4}$$

where

$$p = \sqrt{\omega^2 - \mu^2}. \tag{4.2.5}$$

The vacuum state is defined as the state annihilated by all $a_{\omega km}$ operators:

$$a_{\omega km} |0\rangle = 0. \tag{4.2.6}$$

A comparison at the same point in space-time $\varphi = \varphi_M - \Omega t_M$ of (4.2.4) and the Minkowski expansion (3.2.9) of the field operator shows that the one-particle operators in the rotating space-time are equal to their Minkowski counterparts, hence, the vacuum state seen by the rotating observer is simply the Minkowski vacuum. As discussed in Ref. [52], the norms (rather than the frequencies) of the Klein-Gordon modes restrict the choice of vacuum such that the only natural choice for a rotating vacuum is just the Minkowski vacuum. Consequently, the set of particle modes contains modes with negative frequency, which make the construction of thermal states problematic, as discussed in subsection 2.1.4.

4.2.2   Rigidly rotating thermal states

The vacuum Schwinger (2.1.47) and Hadamard (2.1.46) functions can be obtained either by applying rotations to their Minkowski analogues in Eqs. (3.2.11a) and (3.2.11b), respectively, or by using the mode expansion of the field operator (4.2.4):

$$G(x, x') = \sum_{m=-\infty}^{\infty} \int_{\mu}^{\infty} \frac{d\omega}{8\pi^2} \int_{-p}^{p} dk \, e^{ik\Delta z} (e^{-i\widetilde{\omega}\Delta t + im\Delta\varphi} - e^{i\widetilde{\omega}\Delta t - im\Delta\varphi}) J_m(q\rho) J_m(q\rho'),$$

$$G^{(1)}(x, x') = \sum_{m=-\infty}^{\infty} \int_{\mu}^{\infty} \frac{d\omega}{8\pi^2} \int_{-p}^{p} dk \, e^{ik\Delta z} (e^{-i\widetilde{\omega}\Delta t + im\Delta\varphi} + e^{i\widetilde{\omega}\Delta t - im\Delta\varphi}) J_m(q\rho) J_m(q\rho').$$

$$\tag{4.2.7}$$

The formula (2.1.53) can be used to compute the thermal Hadamard function. The t.e.v. of the SET is the difference between the expectation value of the SET at finite temperature and its v.e.v., which can be calculated using the difference between the thermal and vacuum Hadamard functions:

$$\Delta G_{\beta}^{(1)}(x, x') = \frac{1}{4\pi^2} \sum_{m=-\infty}^{\infty} \int_{\mu}^{\infty} d\omega \int_{-p}^{p} dk \frac{e^{ik\Delta z}}{e^{\beta\widetilde{\omega}} - 1}(e^{-i\widetilde{\omega}\Delta t + im\Delta\varphi} + e^{i\widetilde{\omega}\Delta t - im\Delta\varphi})$$

$$\times J_m(q\rho)J_m(q\rho'). \quad (4.2.8)$$

The density of states factor $(e^{\beta\widetilde{\omega}} - 1)^{-1}$ becomes infinite when the energy $\widetilde{\omega} = \omega - m\Omega$ measured with respect to the co-rotating frame vanishes, making the thermal Hadamard function and any quantities derived from it divergent [33]. However, it is possible to write down expressions for the t.e.v.s and, by applying analytic techniques, to isolate the divergent parts from a remainder which can be interpreted physically by direct analogy to the fermion case, presented in subsection 4.3.2.

Mode sum expressions for t.e.v.s

The mode sum expression for the t.e.v.s can be computed using the formulae (2.1.57) for ϕ^2 and (2.1.54) for the SET. To help simplify notation, it is useful to introduce the following definition:

$$G_{abc} = \frac{1}{\pi^2} \sum_{m=-\infty}^{\infty} \int_{\mu}^{\infty} \frac{d\omega}{e^{\beta\widetilde{\omega}} - 1} \int_{0}^{p} dk \, \omega^a q^b m^c J_m^2(q\rho), \quad (4.2.9)$$

where $G_{abc} \equiv G_{abc}(\rho)$ are functions of the distance ρ from the rotation axis, temperature β, angular momentum of the rotation Ω and the mass μ of the field quanta. The t.e.v. of ϕ^2 is just half the coincidence limit of the thermal Hadamard function (4.2.8):

$$\langle : \phi^2 : \rangle_{\beta} = \frac{1}{2}G_{000}. \quad (4.2.10)$$

To evaluate the t.e.v. of the SET, the coefficient of $g_{\mu\nu}$ in (2.1.54) must be computed:

$$\lim_{x \to x'} \left[g^{\kappa\lambda'} \nabla_{\kappa} \Delta G_{\beta}^{(1)} \overleftarrow{\nabla}_{\lambda'} + \mu^2 \Delta G_{\beta}^{(1)} \right] = \frac{1}{2\pi^2} \sum_{m=-\infty}^{\infty} \int_{\mu}^{\infty} \frac{d\omega}{e^{\beta\widetilde{\omega}} - 1} \int_{-p}^{p} dk$$

$$\times \left[(\rho^{-2}m^2 - q^2)J_m^2(q\rho) + q^2 J_m'^2(q\rho) \right]. \quad (4.2.11)$$

The terms involving derivatives of J_m can be expressed in terms of G_{abc} using the

following relations:

$$2q J_m(q\rho) J'_m(q\rho) = \frac{d}{d\rho} J_m^2(q\rho),$$

$$q^2 J_m'^{\,2}(q\rho) = \frac{1}{2}\left(\frac{d^2}{d\rho^2} + \frac{1}{\rho}\frac{d}{d\rho}\right) J_m^2(q\rho) + \left(q^2 - \frac{m^2}{\rho^2}\right) J_m^2(q\rho), \qquad (4.2.12)$$

allowing Eq. (4.2.11) to be put in the form:

$$\lim_{x\to x'}\left[g^{\kappa\lambda'}\nabla_\kappa \Delta G_\beta^{(1)}\overleftarrow{\nabla_{\lambda'}} + \mu^2 \Delta G_\beta^{(1)}\right] = \frac{1}{2}\left(\frac{d^2}{d\rho^2} + \frac{1}{\rho}\frac{d}{d\rho}\right) G_{000}. \qquad (4.2.13)$$

Equation (4.2.13) can be used in conjunction with the Christoffel symbols (4.1.5) to obtain the covariant components of the SET (2.1.54) with respect to the cylindrical coordinate system:

$$\langle: T_{\mu\nu}:\rangle_\beta = \frac{1}{12\pi^2}\sum_{m=-\infty}^{\infty}\int_\mu^\infty \frac{d\omega}{e^{\beta\widetilde{\omega}}-1}\int_0^p dk\, F_{\mu\nu}, \qquad (4.2.14)$$

with the components $F_{\mu\nu}$ given by:

$$F_{tt} = \left[6\widetilde{\omega}^2 + (\rho^{-2}m^2 - q^2)(1 - \rho^2\Omega^2)\right]J_m^2 - 2\Omega^2 q\rho J_m J'_m + q^2(1-\rho^2\Omega^2)J_m'^{\,2},$$

$$F_{t\varphi} = \left(-6\widetilde{\omega}m - \Omega m^2 + \Omega q^2\rho^2\right)J_m^2 - 2\Omega q\rho J_m J'_m - \Omega q^2\rho^2 J_m'^{\,2},$$

$$F_{\varphi\varphi} = \left(5m^2 + q^2\rho^2\right)J_m^2 - 2q\rho J_m J'_m - q^2\rho^2 J_m'^{\,2},$$

$$F_{\rho\rho} = \left(-3\rho^{-2}m^2 + 3q^2\right)J_m^2 + 2q\rho^{-1}J_m J'_m + 3q^2 J_m'^{\,2},$$

$$F_{zz} = \left(6k^2 - \rho^{-2}m^2 + q^2\right)J_m^2 - q^2 J_m'^{\,2}, \qquad (4.2.15)$$

where the argument of the Bessel functions is $q\rho$. The tetrad components (4.1.21) of the SET have a slightly simplified form:

$$F_{\hat t\hat t} = \left(6\omega^2 + \rho^{-2}m^2 - q^2\right)J_m^2 + q^2 J_m'^{\,2},$$

$$F_{\hat\varphi\hat t} = -6\omega\rho^{-1}m J_m^2,$$

$$F_{\hat\rho\hat\rho} = \left(-3\rho^{-2}m^2 + 3q^2\right)J_m^2 + 2q\rho^{-1}J_m J'_m + 3q^2 J_m'^{\,2},$$

$$F_{\hat\varphi\hat\varphi} = \left(5\rho^{-2}m^2 + q^2\right)J_m^2 - 2q\rho^{-1}J_m J'_m - q^2 J_m'^{\,2},$$

$$F_{\hat z\hat z} = \left(6k^2 - \rho^{-2}m^2 + q^2\right)J_m^2 - q^2 J_m'^{\,2}, \qquad (4.2.16)$$

with the Bessel functions taking the argument $q\rho$. Equations (4.2.12) can be used

to write the tetrad components of Eq. (4.2.14) in terms of the functions G_{abc}:

$$\langle : T_{\hat{t}\hat{t}} :\rangle_\beta = \frac{1}{2}G_{200} + \frac{1}{24}\left(\frac{d^2}{d\rho^2} + \frac{1}{\rho}\frac{d}{d\rho}\right)G_{000}$$

$$\langle : T_{\hat{\varphi}\hat{t}} :\rangle_\beta = -\frac{1}{2\rho}G_{101}$$

$$\langle : T_{\hat{\rho}\hat{\rho}} :\rangle_\beta = \left(\frac{1}{8}\frac{d^2}{d\rho^2} + \frac{5}{24\rho}\frac{d}{d\rho}\right)G_{000} + \frac{1}{2}G_{020} - \frac{1}{2\rho^2}G_{002},$$

$$\langle : T_{\hat{\varphi}\hat{\varphi}} :\rangle_\beta = \left(-\frac{1}{24}\frac{d^2}{d\rho^2} - \frac{1}{8\rho}\frac{d}{d\rho}\right)G_{000} + \frac{1}{2\rho^2}G_{002},$$

$$\langle : T_{\hat{z}\hat{z}} :\rangle_\beta = \frac{1}{2}(G_{200} - G_{020} - \mu^2 G_{000}) - \frac{1}{24}\left(\frac{d^2}{d\rho^2} + \frac{1}{\rho}\frac{d}{d\rho}\right)G_{000}. \qquad (4.2.17)$$

The functions G_{abc} can be written as a sum of a divergent (infinite) quantity and finite terms. The object of the remainder of this subsection is to identify and interpret these finite remainders. The results are given after the following algebraic digresion in Eqs. (4.2.50) and (4.2.51).

Bose-Einstein integrals for massless rotating states

While often the logical order of presenting results in quantum field theory is for the scalar field before the fermion field, the method we employ for the analysis of t.e.v.s is rigorously motivated mathematically for the Dirac field, as described after Eq. (4.3.24). The idea is to expand the density of states factor $(e^{\beta\widetilde{\omega}} - 1)^{-1}$ about $\Omega = 0$, as follows:

$$\frac{1}{e^{\beta(\omega - \Omega m)} - 1} = \sum_{n=0}^{\infty} \frac{(-\Omega)^n}{n!}m^n \frac{d^n}{d\omega^n}\left(\frac{1}{e^{\beta\omega} - 1}\right). \qquad (4.2.18)$$

The above expansion is not well defined when $\omega - \Omega m < 0$, since the expression on the right hand side of Eq. (4.2.18) is positive for all $\omega > 0$, while $(e^{\beta\widetilde{\omega}} - 1)^{-1} < 0$. This discrepancy arises due to the existence of the pole in the Bose-Einstein density of states factor at $\omega = \Omega m$. In spite of its drawbacks when used for the scalar case, the present method can still be used to extract physical information from otherwise infinite t.e.v.s. Thus, substituting the expansion (4.2.18) in Eq. (4.2.9) gives:

$$G_{abc} = \frac{1}{\pi^2}\sum_{n=0}^{\infty}\frac{(-\Omega)^n}{n!}\int_\mu^\infty d\omega\, \omega^a \frac{d^n}{d\omega^n}\left(\frac{1}{e^{\beta\omega} - 1}\right)\int_0^p dk\, q^b \sum_{m=-\infty}^{\infty} m^{n+c}J_m^2(q\rho). \qquad (4.2.19)$$

Sum over m. Due to the symmetry of $J_m^2(q\rho)$ under the transformation $m \to -m$, the sum over m in Eq. (4.2.19) vanishes unless $n + c$ is even, in which case it can be

written as:

$$\sum_{m=-\infty}^{\infty} m^{2n} J_m^2(z) = \sum_{j=0}^{n} \frac{\Gamma(j+\frac{1}{2})}{j!\Gamma(\frac{1}{2})} a_{n,j} z^{2j}, \tag{4.2.20}$$

where the top limit of the sum is n, as will be shown shortly. The coefficients $a_{n,j}$ can be determined by using Eq. (A.1.5) to replace $J_m^2(z)$ with a power series, as follows:

$$J_m^2(z) = \sum_{j=|m|}^{\infty} \frac{\Gamma(j+\frac{1}{2})}{j!\Gamma(\frac{1}{2})} \frac{(-1)^{j-m}}{(j-m)!(j+m)!} z^{2j}. \tag{4.2.21}$$

Hence, $a_{n,j}$ can be written as:

$$a_{n,j} = \sum_{m=-j}^{j} \frac{(-1)^{j-m}}{(j-m)!(j+m)!} m^{2n}. \tag{4.2.22}$$

Writing

$$m^{2n} = \lim_{\alpha \to 0} \frac{d^{2n}}{d\alpha^{2n}} \left(e^{\alpha m} \right), \tag{4.2.23}$$

the coefficients $a_{n,j}$ can be put in the form:

$$a_{n,j} = \frac{1}{(2j)!} \lim_{\alpha \to 0} \frac{d^{2n}}{d\alpha^{2n}} e^{\alpha j} \sum_{m=0}^{2j} \binom{2k}{m} (-e^{-\alpha})^{2k-m}. \tag{4.2.24}$$

Since the over m is just the binomial expansion of $(1 - e^{-\alpha})^{2k}$, the coefficient $a_{n,j}$ simplifies to:

$$a_{n,j} = \frac{1}{(2j)!} \lim_{\alpha \to 0} \frac{d^{2n}}{d\alpha^{2n}} \left(2 \sinh \frac{\alpha}{2} \right)^{2j}. \tag{4.2.25}$$

It is clear that $a_{n,j}$ vanishes if $j > n$, thus proving that the series in Eq. (4.2.20) terminates at $j = n$. Of interest for the computation of the t.e.v. of the SET are the following terms:

$$\begin{aligned} a_{j,j} &= 1, \\ a_{j+1,j} &= \frac{1}{12} j(2j+1)(2j+2), \\ a_{j+2,j} &= \frac{1}{1440} j(2j+1)(2j+2)(2j+3)(2j+4)(5j-1). \end{aligned} \tag{4.2.26}$$

The integral with respect to k.   Following the steps in the previous paragraph, the sum over m in the expression (4.2.19) for G_{abc} is replaced by a sum over j involving powers of q. The integral over k can be computed by changing variables to $k = p \cos \theta$, such that:

$$\int_0^p dk \, q^n = p^{n+1} I_{n+1}, \qquad I_{n+1} = \int_0^{\frac{\pi}{2}} d\theta \, (\cos \theta)^{n+1}. \tag{4.2.27}$$

An integration by parts shows that $I_{n+1} = nI_{n-1}/(n+1)$. Since $I_0 = \frac{\pi}{2}$ and $I_1 = 1$, it can be shown that:

$$I_n = \frac{\Gamma(\frac{n+2}{2})\Gamma(\frac{3}{2})}{\Gamma(\frac{n+3}{2})}, \tag{4.2.28}$$

implying

$$\int_0^p dk\, q^n = \frac{\Gamma(\frac{n+2}{2})\sqrt{\pi}}{2\Gamma(\frac{n+3}{2})} p^{n+1}. \tag{4.2.29}$$

Having found a way to perform the sum over m and the integral over k in Eq. (4.2.19), it remains to tackle the integral over ω, then finally the sum over n.

Analytic expressions in the massless case. While we do not have a method to tackle the integrals over ω in Eq. (4.2.19) for arbitrary masses, we present here an analytic method to compute them in the massless case. To obtain definite expressions, it is necessary to consider the values of a, b and c relevant to the computation of the t.e.v.s of ϕ^2 (4.2.10) and of the SET (4.2.16), i.e. of the functions G_{000}, G_{200}, G_{020}, G_{002} and G_{101}.

Let us start with G_{000}. Performing the sum over m and integral over k in Eq. (4.2.19) yields:

$$G_{000} = \frac{1}{\pi^2} \sum_{n=0}^{\infty} \frac{\Omega^{2n}}{(2n)!} \sum_{j=0}^{n} \frac{\rho^{2j} a_{n,j}}{(2j+1)} \int_{\mu}^{\infty} d\omega\, p^{2j+1} \frac{d^{2n}}{d\omega^{2n}} \left(\frac{1}{e^{\beta\omega}-1} \right). \tag{4.2.30}$$

It is convenient to interchange the sum over j with the sum over n, which in turn can be shifted downwards to $n \to n+j$, such that G_{000} takes the form:

$$G_{000} = \frac{1}{\pi^2} \sum_{j=0}^{\infty} \frac{(\rho\Omega)^{2j}}{2j+1} \sum_{n=0}^{\infty} \frac{\Omega^{2n} a_{n+j,j}}{(2n+2j)!} \int_{\mu}^{\infty} d\omega\, p^{2j+1} \frac{d^{2n+2j}}{d\omega^{2n+2j}} \left(\frac{1}{e^{\beta\omega}-1} \right). \tag{4.2.31}$$

To proceed further, it is necessary to set $\mu = 0$, in which case $p = \omega$. Before giving the result for the integral over ω, it is worth noticing that

$$\frac{1}{e^{\beta\omega}-1} + \frac{1}{e^{-\beta\omega}-1} = -1. \tag{4.2.32}$$

Hence, apart from the term $-\frac{1}{2}$, the series expansion of the Bose-Einstein density of states factor contains only odd powers of ω, as follows:

$$\frac{1}{e^{\beta\omega}-1} = \frac{1}{\beta\omega} - \frac{1}{2} + \frac{\beta\omega}{12} + O(\omega^3). \tag{4.2.33}$$

The first term in the above expansion is divergent as $\omega \to 0$, giving rise to the divergent behaviour of the functions G_{abc}. Using Eq. (3.2.16), the integral over ω in

Eq. (4.2.31) can be performed:

$$\int_0^\infty d\omega\, \omega^{2j+1} \frac{d^{2j+2n}}{d\omega^{2j+2n}} \left(\frac{1}{e^{\beta\omega}-1}\right) = (2j+1)! \times \begin{cases} \dfrac{\pi^2}{6\beta^2} & n=0, \\[2ex] -\dfrac{1}{2} + \dfrac{1}{\beta}\lim_{\omega\to 0}\dfrac{1}{\omega} & n=1, \\[2ex] \dfrac{1}{\beta}(2n-2)!\lim_{\omega\to 0}\dfrac{1}{\omega^{2n-1}} & n>1. \end{cases} \tag{4.2.34}$$

All terms with $n>1$ diverge at the $\omega = 0$ end of the integral and the $n=1$ term has both a temperature-independent finite part and a divergent part. Therefore, G_{000} can be put in the form:

$$G_{000} = \frac{1}{\pi^2}\sum_{j=0}^\infty (\rho\Omega)^{2j}\left[\frac{\pi^2}{6\beta^2} - \frac{j\Omega^2}{24} + \frac{\Omega^2}{\beta}\sum_{n=0}^\infty \frac{\Omega^{2n}(2j)!(2n)!a_{n+j+1,j}}{(2n+2j+2)!}\lim_{\omega\to 0}\frac{1}{\omega^{2n+1}}\right]. \tag{4.2.35}$$

The sum over j can be performed for the finite terms using the following formula, established by induction:

$$\sum_{j=0}^\infty (1-\varepsilon)^j(2j+2)\ldots(2j+2k) = 2^k k!\varepsilon^{-k-1}, \tag{4.2.36}$$

where

$$\varepsilon = 1 - \rho^2\Omega^2. \tag{4.2.37}$$

Denoting by G_{abc}^∞ the infinite terms appearing in G_{abc}, the result for G_{000} can be put in the form:

$$G_{000} = \frac{1}{6\beta^2\varepsilon} - \frac{\rho^2\Omega^4}{24\pi^2\varepsilon^2} + G_{000}^\infty, \tag{4.2.38}$$

where the sum involving j in the second term in Eq. (4.2.35) has been shifted upwards by one unit, giving rise to a $\rho^2\Omega^2$ factor in Eq. (4.2.38). In the above,

$$G_{000}^\infty = \frac{\Omega^2}{\pi^2\beta}\sum_{j=0}^\infty (\rho\Omega)^{2j}\sum_{n=0}^\infty \frac{\Omega^{2n}(2j)!(2n)!a_{n+j+1,j}}{(2n+2j+2)!}\lim_{\omega\to 0}\frac{1}{\omega^{2n+1}}. \tag{4.2.39}$$

Substituting $a = 2$ and $b = c = 0$ in (4.2.19) gives:

$$\begin{aligned} G_{200} &= \sum_{j=0}^\infty (\rho\Omega)^{2j}(2j+2)(2j+3)\left[\frac{\pi^2}{90\beta^4} + \frac{\Omega^2}{72\beta^2}j - \frac{\Omega^4}{2880\pi^2}j(5j-1)\right] + G_{200}^\infty \\ &= \frac{\pi^2}{15\beta^4\varepsilon^3}\left(\frac{4}{3} - \frac{1}{3}\varepsilon\right) + \frac{5\rho^2\Omega^4}{18\beta^2\varepsilon^4}\left(\frac{6}{5} - \frac{\varepsilon}{5}\right) - \frac{\rho^2\Omega^6}{36\pi^2\varepsilon^5}\left(6 - \frac{111}{20}\varepsilon + \frac{11}{20}\varepsilon^2\right) + G_{200}^\infty, \end{aligned} \tag{4.2.40}$$

where the round brackets evaluate to 1 on the rotation axis (i.e. when $\varepsilon = 1$). The

infinite terms are grouped in G_{200}^{∞} as follows:

$$G_{200}^{\infty} = \frac{\Omega^4}{\beta\pi^2} \sum_{j=0}^{\infty} (\rho\Omega)^{2j} \sum_{n=0}^{\infty} \frac{\Omega^{2n}(2j+3)!(2n)!a_{n+j+2,j}}{(2j+1)(2n+2j+4)!} \lim_{\omega\to 0} \frac{1}{\omega^{2n+1}}. \tag{4.2.41}$$

Repeating the same steps for G_{020} yields:

$$G_{020} = \sum_{j=0}^{\infty} (\rho\Omega)^{2j}(2j+2)^2 \left\{ \frac{\pi^2}{90\beta^4} + \frac{\Omega^2}{72\beta^2}j - \frac{\Omega^4}{2880\pi^2}j(5j-1) \right\} + G_{020}^{\infty}$$

$$= \frac{2\pi^2}{45\beta^4\varepsilon^3}(2-\varepsilon) + \frac{2\rho^2\Omega^4}{9\beta^2\varepsilon^4}\left(\tfrac{3}{2} - \tfrac{\varepsilon}{2}\right) - \frac{\rho^2\Omega^6}{45\pi^2\varepsilon^5}\left(\tfrac{15}{2} - \tfrac{63}{8}\varepsilon + \tfrac{11}{8}\varepsilon^2\right) + G_{020}^{\infty}, \tag{4.2.42}$$

with

$$G_{020}^{\infty} = \frac{\Omega^4}{\pi^2\beta} \sum_{j=0}^{\infty} (\rho\Omega)^{2j} \sum_{n=0}^{\infty} \frac{\Omega^{2n}(2j+2)^2(2j)!(2n)!a_{n+j+2,j}}{(2n+2j+4)!} \lim_{\omega\to 0} \frac{1}{\omega^{2n+1}}. \tag{4.2.43}$$

In the computation of G_{002}, the sum over j runs from 0 to $n+1$:

$$G_{002} = \frac{1}{\pi^2} \sum_{n=0}^{\infty} \frac{\Omega^{2n}}{(2n)!} \sum_{j=0}^{n+1} \frac{a_{n+1,j}}{(2j+1)a_{j,j}} \rho^{2j} \int_0^{\infty} d\omega\, \omega^{2j+1} \frac{d^{2n}}{d\omega^{2n}} \left(\frac{1}{e^{\beta\omega} - 1} \right). \tag{4.2.44}$$

By treating the $j = n+1$ case separately (and relabelling the summation index n by j), the following expression can be obtained:

$$\rho^{-2}G_{002} = \sum_{j=0}^{\infty} (\rho\Omega)^{2j}(2j+2) \left[\frac{\pi^2}{90\beta^4}(2j+1) + \frac{\Omega^2}{144\beta^2}(2j+3)(2j+4) \right.$$

$$\left. - \frac{\Omega^4}{2880\pi^2}(2j+5)(2j+6)(5j+4) \right] + \rho^{-2}G_{002}^{\infty}$$

$$= \frac{\pi^2(4-3\varepsilon)}{45\beta^4\varepsilon^3} + \frac{\Omega^2(2-\varepsilon)}{6\beta^2\varepsilon^4} - \frac{\Omega^4}{24\pi^2\varepsilon^5}\left(4 - \tfrac{27}{10}\varepsilon - \tfrac{1}{5}\varepsilon^2 - \tfrac{1}{10}\varepsilon^3\right) + \rho^{-2}G_{002}^{\infty}, \tag{4.2.45}$$

where

$$\rho^{-2}G_{002}^{\infty} = \frac{\Omega^4}{\pi^2\beta} \sum_{j=0}^{\infty} (\rho\Omega)^{2j} \sum_{n=0}^{\infty} \frac{\Omega^{2n}(2j+2)!(2n)!a_{n+j+3,j+1}}{(2n+2j+4)!} \lim_{\omega\to 0} \frac{1}{\omega^{2n+1}}. \tag{4.2.46}$$

For G_{101}, the sum over n runs through odd values:

$$G_{101} = -\frac{\Omega}{\pi^2} \sum_{n=0}^{\infty} \frac{\Omega^{2n}}{(2n+1)!} \sum_{j=0}^{n+1} \frac{a_{n+1,j}}{(2j+1)} \rho^{2j} \int_0^{\infty} d\omega\, \omega^{2j+2} \frac{d^{2n+1}}{d\omega^{2n+1}} \left(\frac{1}{e^{\beta\omega} - 1} \right). \tag{4.2.47}$$

Bearing in mind that this time the number of integrations by parts performed in the integration over ω is odd, consequently changing the minus sign in front of the

sum over n into a plus, the following result can be obtained:

$$
\frac{G_{101}}{\rho^2 \Omega} = \sum_{j=0}^{\infty} (\rho \Omega)^{2j}(j+1)(j+2) \left[\frac{2\pi^2}{45\beta^4} + \frac{\Omega^2(j+2)}{18\beta^2} - \frac{\Omega^4(j+3)(5j+4)}{720\pi^2} \right] + \frac{G_{101}^{\infty}}{\rho^2 \Omega}
$$

$$
= \frac{4\pi^2}{45\beta^4 \varepsilon^3} + \frac{2\Omega^2}{9\beta^2 \varepsilon^4}(\tfrac{3}{2} - \tfrac{1}{2}\varepsilon) - \frac{\Omega^4}{30\pi^2 \varepsilon^5}(5 - 4\varepsilon) + \frac{1}{\rho^2 \Omega}G_{101}^{\infty}, \tag{4.2.48}
$$

where

$$
\frac{1}{\rho^2 \Omega}G_{101}^{\infty} = \frac{\Omega^4}{\pi^2 \beta} \sum_{j=0}^{\infty} (\rho\Omega)^{2j} \sum_{n=0}^{\infty} \frac{\Omega^{2n}(2j+4)!(2n)!a_{n+j+3,j+1}}{(2j+3)(2n+2j+5)!} \lim_{\omega \to 0} \frac{1}{\omega^{2n+1}}. \tag{4.2.49}
$$

Thermal expectation values for massless rotating states

Putting all pieces together, the t.e.v. of ϕ^2 (4.2.10) can be written in the massless case using the result in Eq. (4.2.38) as:

$$
\langle : \phi^2 : \rangle_\beta = \frac{1}{12\beta^2 \varepsilon} - \frac{\rho^2 \Omega^4}{48\pi^2 \varepsilon^2} + \phi_\infty^2. \tag{4.2.50}
$$

Similarly, the t.e.v. of the SET (4.2.16) can be written using Eqs. (4.2.40), (4.2.42), (4.2.45) and (4.2.48) as:

$$
\begin{aligned}
\langle : T_{\hat{t}\hat{t}} : \rangle_\beta =& \frac{\pi^2}{30\beta^4 \varepsilon^3}(\tfrac{4}{3} - \tfrac{1}{3}\varepsilon) + \frac{\Omega^2}{36\beta^2 \varepsilon^4}(6 - 5\varepsilon) \\
& - \frac{\Omega^4}{144\pi^2 \varepsilon^5}(12 - \tfrac{171}{10}\varepsilon + \tfrac{31}{5}\varepsilon^2 - \tfrac{1}{10}\varepsilon^3) + T_{\hat{t}\hat{t}}^{\infty}, \\
\langle : T_{\hat{\varphi}\hat{t}} : \rangle_\beta =& -\rho\Omega \left[\frac{2\pi^2}{45\beta^4 \varepsilon^3} + \frac{\Omega^2}{9\beta^2 \varepsilon^4}(\tfrac{3}{2} - \tfrac{1}{2}\varepsilon) - \frac{\Omega^4}{60\pi^2 \varepsilon^5}(5 - 4\varepsilon) + T_{\hat{\varphi}\hat{t}}^{\infty} \right], \\
\langle : T_{\hat{\rho}\hat{\rho}} : \rangle_\beta =& \frac{\pi^2}{90\beta^4 \varepsilon} + \frac{\Omega^2}{36\beta^2 \varepsilon^3} - \frac{\Omega^4}{144\pi^2 \varepsilon^4}(\tfrac{3}{2} - \tfrac{3}{5}\varepsilon + \tfrac{1}{10}\varepsilon^2) + T_{\hat{\rho}\hat{\rho}}^{\infty}, \\
\langle : T_{\hat{\varphi}\hat{\varphi}} : \rangle_\beta =& \frac{\pi^2}{90\beta^4 \varepsilon^3}(4 - 3\varepsilon) + \frac{\Omega^2}{36\beta^2 \varepsilon^4}(6 - 5\varepsilon) \\
& - \frac{\Omega^4}{144\pi^2 \varepsilon^5}(12 - \tfrac{141}{10}\varepsilon + \tfrac{17}{5}\varepsilon^2 - \tfrac{3}{10}\varepsilon^3) + T_{\hat{\varphi}\hat{\varphi}}^{\infty}, \\
\langle : T_{\hat{z}\hat{z}} : \rangle_\beta =& \frac{\pi^2}{90\beta^4 \varepsilon^2} - \frac{\Omega^2}{36\beta^2 \varepsilon^3} + \frac{\Omega^4}{144\pi^2 \varepsilon^4}(\tfrac{9}{2} - \tfrac{17}{5}\varepsilon - \tfrac{1}{10}\varepsilon^2) + T_{\hat{z}\hat{z}}^{\infty}. \tag{4.2.51}
\end{aligned}
$$

In the above, $\varepsilon = 1 - \rho^2\Omega^2$. Using Eqs. (4.1.22), the t.e.v. of the SET can be expressed with respect to the coordinate basis:

$$\langle : T_{tt} : \rangle_\beta = \frac{\pi^2}{30\beta^4\varepsilon} + \frac{\Omega^2}{36\beta^2\varepsilon^2} - \frac{\Omega^4}{144\pi^2\varepsilon^3}\left(\frac{9}{2} - \frac{19}{5}\varepsilon + \frac{3}{10}\varepsilon^2\right) + T_{tt}^\infty,$$

$$\frac{\langle : T_{\varphi t} : \rangle_\beta}{\rho^2\Omega} = -\frac{\pi^2}{30\beta^4\varepsilon^2} - \frac{\Omega^2}{12\beta^2\varepsilon^3} + \frac{7\Omega^4}{720\pi^2\varepsilon^4}\left(\frac{45}{14} - \frac{17}{7}\varepsilon + \frac{3}{14}\varepsilon^2\right) + \frac{T_{\varphi t}^\infty}{\rho^2\Omega},$$

$$\frac{\langle : T_{\varphi\varphi} : \rangle_\beta}{\rho^2} = \frac{\pi^2(4 - 3\varepsilon)}{90\beta^4\varepsilon^3} + \frac{\Omega^2(6 - 5\varepsilon)}{36\beta^2\varepsilon^4} - \frac{\Omega^4}{144\pi^2\varepsilon^5}\left(12 - \frac{141}{10}\varepsilon + \frac{17}{5}\varepsilon^2 - \frac{3}{10}\varepsilon^3\right) + \frac{T_{\varphi\varphi}^\infty}{\rho^2}.$$

$$(4.2.52)$$

All t.e.v.s presented in this section can be written as a sum of three type of terms, as follows. For a generic operator A, its t.e.v. can be split as:

$$\langle : A : \rangle_\beta = \langle : A : \rangle_\beta^{\text{phys}} + \langle : A : \rangle_\beta^{\text{spurious}} + \langle : A : \rangle_\beta^\infty, \qquad (4.2.53)$$

where $\langle : A : \rangle_\beta^{\text{phys}}$ indicates the physical terms, proportional to β^{-4} or β^{-2} (only to β^{-2} for ϕ^2), $\langle : A : \rangle_\beta^{\text{spurious}}$ contains any temperature-independent contributions and $\langle : A : \rangle_\beta^\infty$ contains the infinite terms.

The terms proportional to β^{-4} or β^{-2} are the terms we were looking for. The application of an analogous (but thoroughly rigorous) analysis to the t.e.v.s of fermions in subsection 4.3.2 reveals terms with similar features when thermal states with respect to the rotating (Iyer) vacuum are considered (i.e. the vacuum state corresponding to a split of modes which does not allow particle modes to have negative frequencies). These terms vanish in the vacuum state (as $\beta \to \infty$) and allow the non-rotating t.e.v.s in subsection 3.2.2 to be recovered when Ω is set to 0. The t.e.v. of the SET receives on the rotation axis, where $\varepsilon = 1$ and the terms in the parentheses reduce to 1, a correction to the non-rotating case proportional to Ω^2, showing that the effects of the rotation can be detected even on its axis. All the physical terms diverge as the speed of light surface (SOL) is approached (i.e. $\varepsilon \to 0$), following an inverse power law with respect to the distance to the latter. The terms proportional to β^{-4} (in the case of the SET) and to β^{-2} (for ϕ^2) agree with the "Planckian forms" given in Ref. [33]. The numerical results presented in subsection 5.1.2 for rotating thermal states inside a bounding cylinder show a very good agreement with the Planckian forms at large enough values of $\beta\Omega$. For completeness,

the physical terms are given below:

$$\langle: \phi^2 :\rangle_\beta^{\text{phys}} = \frac{1}{12\beta^2\varepsilon} - \frac{\rho^2\Omega^4}{48\pi^2\varepsilon^2} + \phi_\infty^2, \tag{4.2.54a}$$

$$\langle: T_{\hat{t}\hat{t}} :\rangle_\beta^{\text{phys}} = \frac{\pi^2}{30\beta^4\varepsilon^3}\left(\tfrac{4}{3} - \tfrac{1}{3}\varepsilon\right) + \frac{\Omega^2}{36\beta^2\varepsilon^4}\left(6 - 5\varepsilon\right), \tag{4.2.54b}$$

$$\langle: T_{\hat{\varphi}\hat{t}} :\rangle_\beta^{\text{phys}} = -\rho\Omega\left[\frac{2\pi^2}{45\beta^4\varepsilon^3} + \frac{\Omega^2}{9\beta^2\varepsilon^4}\left(\tfrac{3}{2} - \tfrac{1}{2}\varepsilon\right)\right], \tag{4.2.54c}$$

$$\langle: T_{\hat{\rho}\hat{\rho}} :\rangle_\beta^{\text{phys}} = \frac{\pi^2}{90\beta^4\varepsilon^2} + \frac{\Omega^2}{36\beta^2\varepsilon^3}, \tag{4.2.54d}$$

$$\langle: T_{\hat{\varphi}\hat{\varphi}} :\rangle_\beta^{\text{phys}} = \frac{\pi^2}{90\beta^4\varepsilon^3}\left(4 - 3\varepsilon\right) + \frac{\Omega^2}{36\beta^2\varepsilon^4}\left(6 - 5\varepsilon\right), \tag{4.2.54e}$$

$$\langle: T_{\hat{z}\hat{z}} :\rangle_\beta^{\text{phys}} = \frac{\pi^2}{90\beta^4\varepsilon^2} - \frac{\Omega^2}{36\beta^2\varepsilon^3}. \tag{4.2.54f}$$

It is remarkable that the above results allow the analytic prediction that $\langle: T_{\hat{z}\hat{z}} :\rangle_\beta^{\text{phys}}$ vanishes on the rotation axis when $\beta\Omega = \pi\sqrt{2/5}$:

$$\left.\langle: T_{\hat{z}\hat{z}} :\rangle_\beta^{\text{phys}}\right|_{\substack{\rho=0 \\ \beta\Omega=\pi\sqrt{\frac{2}{5}}}} = 0. \tag{4.2.55}$$

The temperature-independent terms $\langle: A :\rangle_\beta^{\text{spurious}}$ are induced by the inclusion of modes with $\widetilde{\omega} < 0$ in the set of particle modes, through the mechanism explained in subsection 2.1.4 and are analogous to the temperature-independent terms in t.e.v.s obtained for fermions with respect to the Minkowski (Vilenkin) vacuum state, as discussed in subsection 4.3.2. They are spurious in the sense that t.e.v.s with respect to a thermal state constructed relative to the vacuum state should vanish as the temperature approaches 0. In a similar manner to the terms proportional to β^{-4} or β^{-2}, these terms diverge as inverse powers of the distance to the SOL. However, they vanish identically in the absence of rotation.

The infinite terms $\langle: A :\rangle_\beta^\infty$ appear due to the divergent contributions made by modes with $\widetilde{\omega} = 0$. Their exact expression is given by the corresponding infinite terms G_{abc}^∞ in G_{abc}. All the terms G_{abc}^∞ relevant for the t.e.v.s presented above are proportional to $\Omega^2\beta^{-1}$, thus vanishing when the rotation is absent (i.e. $\Omega = 0$), as would be expected, since the non-rotating t.e.v.s given in subsection 3.2.2 are all finite. Taking the limit $\beta \to \infty$ (vacuum state limit) sends the infinite contributions to 0, showing that they are not spurious in the temperature-independent sense.

In the following section, similar techniques are used to find analytic expressions for expectation values for fermion thermal quantum states. In contrast to the scalar case, the method is completely valid and all the results obtained stay finite inside the SOL. The divergent behaviour as the SOL is approached is retained, together with the presence of spurious temperature-independent terms when the thermal state is constructed with respect to the Minkowski (Vilenkin) vacuum.

4.2.3 Summary

The fundamental requirement that particle modes must have positive norm constrains the rotating vacuum state to be equivalent to the Minkowski vacuum state, forcing modes with negative frequencies with respect to the Hamiltonian of the rotating system into the set of particle modes. Moreover, the Bose-Einstein density of states factor diverges for modes with vanishing rotating frequencies but non-zero Minkowski energies, making thermal states unattainable for scalar particles.

Following the analysis of thermal states for Dirac fermions, presented in subsection 4.3.2, it is possible to isolate the divergences in t.e.v.s and to identify finite terms which can be interpreted physically. Thus, the Planckian forms of Ref. [33] emerge, together with extra correction terms having the same form as those obtained for fermions in subsection 4.3.2.

4.3 Polarised rotating fermions

The quantisation of the Dirac field is less constrained than for scalars, allowing for vacuum states different from the Minkowski vacuum. In subsection 4.3.1, the approaches of Vilenkin [72] and Iyer [47] are introduced. The t.e.v.s of the fermion condensate, neutrino current and SET are calculated in subsection 4.3.2 and the analytic expression for the current for massless fermions is compared with the result obtained by Vilenkin on the rotation axis [72]. It is shown that Vilenkin's quantisation introduces spurious terms in thermal expectation values. Also, the analytic solutions clearly show that all t.e.v.s diverge as inverse powers of the distance to the speed of light surface (SOL).

4.3.1 Construction of modes

By analogy to the scalar case, the mode solutions can be obtained by applying the following rotation to the Minkowski modes:

$$e^{i\Omega t J_z}\psi(\varphi) = I_2 \otimes \begin{pmatrix} e^{\frac{i}{2}\Omega t} & 0 \\ 0 & e^{-\frac{i}{2}\Omega t} \end{pmatrix} \psi(\varphi + \Omega t). \tag{4.3.1}$$

Hence, the modes with respect to the rotating coordinates take the form:

$$U^\lambda_{Ekm}(x) = e^{-i\widetilde{E}t+ikz}u^\lambda_{Ekm}(\rho, \varphi), \tag{4.3.2a}$$

$$V^\lambda_{Ekm}(x) = e^{i\widetilde{E}t-ikz}v^\lambda_{Ekm}(\rho, \varphi), \tag{4.3.2b}$$

where

$$\widetilde{E} = E - \Omega(m + \frac{1}{2}) \tag{4.3.3}$$

and u and v are given by (3.3.16) and (3.3.23b), respectively. The modes are normalised with respect to the Minkowski inner product (3.3.19). Since all modes, regardless of frequency, have positive norm, there are infinitely many possible quantisation schemes, two of which have been used in the literature.

Vilenkin [72] performed the second quantisation for fermions in analogy to the scalar case, splitting the set of modes into particle and anti-particle modes for $E > 0$ and $E < 0$, respectively, allowing particles to be described by modes with negative frequency $\widetilde{E}$:

$$\psi_V(x) = \sum_j \theta(E_j) \left[U_j(x) b_{V;j} + V_j(x) d^\dagger_{V;j} \right]. \tag{4.3.4}$$

Comparing (4.3.4) with the analogue expansion (3.3.24) of the field operator at the same point in space-time $\varphi = \varphi_M - \Omega t$ shows that Vilenkin's one-particle operators are equal to the corresponding Minkowski one-particle operators, hence, the vacuum corresponding to Vilenkin's quantisation scheme coincides with the Minkowski vacuum.

On the other hand, Iyer [47] chose positive frequency modes as particle modes, which sets $\widetilde{E} \geq 0$ and allows for negative E:

$$\psi_I(x) = \sum_j \theta(\widetilde{E}_j) \left\{ U_j(x) b_{I;j} + V_j(x) d^\dagger_{I;j} \right\}. \tag{4.3.5}$$

In the above, E_j can take the values $\pm\sqrt{q_j^2 + k_j^2 + \mu^2}$ but the step function restricts the sum to positive values of $\widetilde{E}_j$. Using the connection (3.3.30) between the U_j and V_j modes, the sum over j in Eq. (4.3.5) can be converted to a sum over positive E_j:

$$\psi_I(x) = \sum_j \theta(E_j) \left\{ U_j[\theta(\widetilde{E}_j) b_{I;j} + i^{2m_j+1}\theta(-\widetilde{E}_j) d^\dagger_{I;\bar{\jmath}}] \right.$$
$$\left. + V_j[\theta(\widetilde{E}_j) d^\dagger_{I;j} + i^{2m_j+3}\theta(-\widetilde{E}_j) b_{I;\bar{\jmath}}] \right\}. \tag{4.3.6}$$

The one-particle operators in Vilenkin's expansion (4.3.4), where $E_j > 0$, can be related to Iyer's directly from Eq. (4.3.6):

$$b_{V;j} = \begin{cases} b_{I;j} & \widetilde{E}_j > 0, \\ i^{2m+1} d^\dagger_{I;\bar{\jmath}} & \widetilde{E}_j < 0, \end{cases} \qquad d^\dagger_{V;j} = \begin{cases} d^\dagger_{I;j} & \widetilde{E}_j > 0, \\ i^{2m+3} b_{I;\bar{\jmath}} & \widetilde{E}_j < 0. \end{cases} \tag{4.3.7}$$

Similarly, Eq. (4.3.4) can be written as:

$$\psi_V(x) = \sum_j \theta(\widetilde{E}_j) \left\{ U_j[\theta(E_j) b_{V;j} + i^{2m+3}\theta(-E_j) d^\dagger_{I;\bar{\jmath}}] \right.$$
$$\left. + V_j[\theta(E_j) d^\dagger_{V;j} + i^{2m+1}\theta(-E_j) b_{V;\bar{\jmath}}] \right\}, \tag{4.3.8}$$

giving the following inverse transformation between the Iyer and Vilenkin one-particle operators:

$$b_{I;j} = \begin{cases} b_{V;j} & E_j > 0, \\ i^{2m+3} d^\dagger_{V;\bar{j}} & E_j < 0, \end{cases} \qquad d^\dagger_{I;j} = \begin{cases} d^\dagger_{V;j} & E_j > 0, \\ i^{2m+1} b_{V;\bar{j}} & E_j < 0, \end{cases} \tag{4.3.9}$$

in agreement with Eqs. (4.3.7). It can be seen that annihilation operators in Vilenkin's quantisation scheme can act as creation operators in Iyer's scheme, therefore, the vacuum state corresponding to Iyer's quantisation differs from the Minkowski vacuum. Both quantisation schemes adopt the canonical quantisation (2.2.36) of the one-particle operators. Figure 4.1 illustrates the difference between the two quantisation schemes [47].
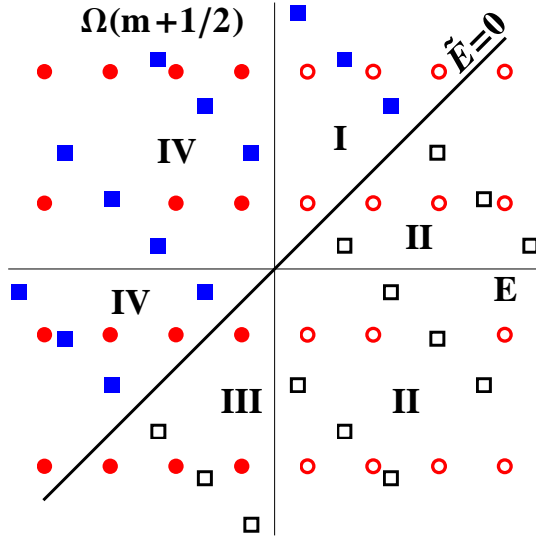
Figure 4.1: The filled shapes represent anti-particle modes while the unfilled shapes represent particle states. The circles represent Vilenkin's quantisation, which defines particle modes as modes with positive energy E. Iyer's quantisation is represented by squares, particle modes having $\widetilde{E} \geq 0$. The two schemes differ in regions I, where Iyer-type antiparticles are Vilenkin-type particles and vice-versa in region III.

4.3.2 Thermal expectation values

As the Schwinger function (2.2.49) is independent of state, it is the same for both Vilenkin's (4.3.4) and Iyer's (4.3.5) quantisations:

$$S(x, x') = \sum_j \theta(E_j) \left[U_j(x) \otimes \overline{U}_j(x') + V_j(x) \otimes \overline{V}_j(x') \right]. \tag{4.3.10}$$

Therefore, the thermal Hadamard function is the same in the two quantisations:

$$S_\beta^{(1)}(x, x') = \sum_j \theta(E_j) \tanh \frac{\beta \widetilde{E}_j}{2} \left[U_j(x) \otimes \overline{U}_j(x') - V_j(x) \otimes \overline{V}_j(x') \right]. \tag{4.3.11}$$

The argument of the hyperbolic tangent has changed from $\beta E/2$ in the Minkowski case (3.3.50) to $\beta\widetilde{E}/2$, since in the rotating case, the thermal weights are calculated using the Hamiltonian of the rotating system, whose eigenvalues are $\widetilde{E}_j$.

The inequivalence of the vacuum states corresponding to the two quantisation schemes gives rise to different vacuum Hadamard functions:

$$S_V^{(1)}(x, x') = \sum_j \theta(E_j) \left[U_j(x) \otimes \overline{U}_j(x') - V_j(x) \otimes \overline{V}_j(x') \right], \qquad (4.3.12a)$$

$$S_I^{(1)}(x, x') = \sum_j \theta(E_j)\mathrm{sgn}(\widetilde{E}) \left[U_j(x) \otimes \overline{U}_j(x') - V_j(x) \otimes \overline{V}_j(x') \right], \qquad (4.3.12b)$$

where in the expression for the Hadamard function $S_I^{(1)}(x, x')$ with respect to the Iyer vacuum, the argument of the step function has been changed from $\widetilde{E}$ to E using the connection formulae (3.3.30). The two-point functions describing thermal states with respect to the above vacua can be written as:

$$\Delta S_\beta^{(1)} = \sum_j e^{-i\widetilde{E}_j\Delta t + ik_j\Delta z}[w(\widetilde{E}_j) - w(\widetilde{E}_{\bar{j}})]M_j, \qquad (4.3.13)$$

where $\bar{j}$ is defined in Eq. (3.3.31), M_j is defined in Eq. (3.3.60) and the thermal weight factors depend on the choice of vacuum, as follows:

$$w_V(\widetilde{E}_j) = -\frac{2\theta(E_j)}{e^{\beta\widetilde{E}_j} + 1}, \qquad w_I(\widetilde{E}_j) = -\frac{2\theta(\widetilde{E}_j)}{e^{\beta\widetilde{E}_j} + 1}. \qquad (4.3.14a)$$

The weight factor $w_I(\widetilde{E}_j)$ can be written in terms of positive Minkowski energies using the properties of the sum in Eq. (4.3.11) as follows:

$$w_I(\widetilde{E}_j) = -\frac{2\mathrm{sgn}(\widetilde{E}_j)\theta(E_j)}{e^{\beta|\widetilde{E}_j|} + 1}. \qquad (4.3.14b)$$

As discussed in subsection 2.2.5, the thermal Hadamard function (4.3.11) does not depend on the choice of vacuum. Hence, the differences in t.e.v.s calculated with respect to different vacuum states will be temperature independent and equal to the difference between the expectation values with respect to the vacuum states under consideration. The differences can be calculated from the following difference of vacuum two-point functions:

$$S_V^{(1)}(x, x') - S_I^{(1)}(x, x') = -\sum_j \theta(-\widetilde{E}_j)M_j. \qquad (4.3.15)$$

As discussed in subsection 2.2.5, t.e.v.s with respect to the Minkowski vacuum (Vilenkin's quantisation) contain spurious temperature-independent terms. To analyse these spurious contributions, the t.e.v.s analysed for the remainder of this section are with respect to the Vilenkin vacuum.

Mode sum expressions for t.e.v.s

As in the scalar case, it is convenient to introduce the notation:

$$S_{abc}^* = \frac{1}{\pi^2} \sum_{m=-\infty}^{\infty} \int_\mu^\infty \frac{dE}{e^{\beta\widetilde{E}} + 1} \int_0^p dk \, E^a q^b (m + \tfrac{1}{2})^c J_m^*(q\rho), \qquad (4.3.16)$$

where $* \in \{+, -, \times\}$ as defined in Eqs. (3.3.69). The above functions appear in t.e.v.s calculated with respect to the Minkowski (Vilenkin) vacuum. At the end of the section the connection to the t.e.v.s with respect to the Iyer vacuum is made, after which the results are discussed.

Thermal expectation value of the fermion condensate. To evaluate the t.e.v.s of the FC and CC, the coincidence limit of the thermal Hadamard function (4.3.13) must be taken:

$$\lim_{x' \to x} \Delta S_\beta^{(1)}(x, x') = \frac{1}{4\pi^2} \sum_{m=-\infty}^{\infty} \int_{\substack{-\infty \\ |E|>\mu}}^{\infty} |E| \, dE \int_{-p}^p dk [w(\widetilde{E}) - w(-\widetilde{E})]$$

$$\times \left[\left(\frac{\mu}{E} I_2 + \sigma_3 \right) \otimes \begin{pmatrix} J_m^2 & 0 \\ 0 & J_{m+1}^2 \end{pmatrix} \right.$$

$$\left. + \frac{1}{E} \begin{pmatrix} 0 & -1 \\ 1 & 0 \end{pmatrix} \otimes \begin{pmatrix} k J_m^2 & -iqe^{-i\varphi} J_m J_{m+1} \\ iqe^{i\varphi} J_{m+1} J_m & -k J_{m+1}^2 \end{pmatrix} \right], \quad (4.3.17)$$

where all Bessel functions take the argument $q\rho$. The difference compared to the Minkowski case (3.3.61) is that the thermal weight factors depend on $\widetilde{E}$ rather than E. The t.e.v. of the FC can be expressed in terms of the functions in Eq. (4.3.16) as follows:

$$\langle : \overline{\psi}\psi : _V \rangle_\beta = \mu S_{000}^+, \qquad (4.3.18)$$

where the V indicates that the Wick ordering has been performed with respect to the Minkowski (Vilenkin) vacuum.

Thermal expectation value of the current. Using Eq. (4.3.17), it can be checked that all components of the charge current vanish:

$$\langle : J^\lambda : _V \rangle_\beta = -\frac{1}{2} \text{tr} \left\{ \Delta S_\beta^{(1)}(x, x' = x) \gamma^\lambda \right\} = 0. \qquad (4.3.19)$$

The t.e.v. of the neutrino current can be computed by multipling (4.3.17) with the projector $\frac{1}{2}(1 - \gamma^5)$. The μ term does not contribute since $\text{tr}(\gamma^\lambda) = \text{tr}(\gamma^5\gamma^\lambda) = 0$, but there is a non-vanishing contribution coming from the last term (containing the

off-diagonal matrix) for the charge current parallel to the rotation axis:

$$\langle : J^z_\nu :_V \rangle_\beta = -\frac{1}{2}S^-_{100}. \tag{4.3.20}$$

Thermal expectation value of the stress-energy tensor   The SET is evaluated using the derivatives $D_{\hat\alpha}$ (4.1.15). Applying the techniques used in subsection 3.3.3, Eq. (3.3.60) can be used to see which terms contribute to any given component of the SET. Keeping in mind that the density of states factor now depends on m, giving rise to a non-zero value for the $T_{\hat\varphi\hat t}$ component of the SET, the following expressions are obtained for the t.e.v. of the SET:

$$\langle : T_{\hat\alpha\hat\sigma}(x) :_V \rangle_\beta = \frac{1}{\pi^2} \sum_{m=-\infty}^{\infty} \int_\mu^\infty \frac{dE}{e^{\beta\tilde E}+1} \int_0^p dk\, F_{\hat\alpha\hat\sigma}, \tag{4.3.21}$$

where

$$F_{\hat t\hat t} = E^2\left(J_m^2 + J_{m+1}^2\right),$$

$$F_{\hat\varphi\hat t} = -qE\left(J_m J_{m+1}\right) - \frac{E}{2\rho}\left[mJ_m^2 + (m+1)J_{m+1}^2\right],$$

$$F_{\hat\rho\hat\rho} = q^2(J_m^2 + J_{m+1}^2) - \frac{q}{\rho}(2m+1)J_m J_{m+1},$$

$$F_{\hat\varphi\hat\varphi} = \frac{q}{\rho}(2m+1)J_m J_{m+1},$$

$$F_{\hat z\hat z} = k^2(J_m^2 + J_{m+1}^2). \tag{4.3.22}$$

The above can be written with respect to the functions S^*_{abc} (4.3.16) as follows:

$$\langle : T_{\hat t\hat t} :_V \rangle_\beta = S^+_{200},$$

$$\langle : T_{\hat\rho\hat\rho} :_V \rangle_\beta = S^+_{020} - \rho^{-1}S^\times_{011},$$

$$\langle : T_{\hat\varphi\hat\varphi} :_V \rangle_\beta = \rho^{-1}S^\times_{011},$$

$$\langle : T_{\hat z\hat z} :_V \rangle_\beta = S^+_{200} - S^+_{020} - \mu^2 S^+_{000},$$

$$\langle : T_{\hat t\hat\varphi} :_V \rangle_\beta = \tfrac{1}{4}\rho^{-1}S^-_{100} - \tfrac{1}{2}\rho^{-1}S^+_{101} - \tfrac{1}{2}S^\times_{110}. \tag{4.3.23}$$

Next, the functions S^*_{abc} are analysed analytically and exact expressions are derived in the massless case. The results are presented after Eq. (4.3.48).

Fermi-Dirac integrals for massless rotating states

To compute the functions S^*_{abc}, defined in Eq. (4.3.16), the Fermi-Dirac density of states factor can be expanded about $\Omega = 0$:

$$\frac{1}{1+e^{\beta[E-\Omega(m+\frac{1}{2})]}} = \sum_{n=0}^{\infty} \frac{(-\Omega)^n}{n!}\left(m+\tfrac{1}{2}\right)^n \frac{d^n}{dE^n}\left(\frac{1}{1+e^{\beta E}}\right), \tag{4.3.24}$$

leading to:

$$S^*_{abc} = \frac{1}{\pi^2} \sum_{n=0}^{\infty} \frac{(-\Omega)^n}{n!} \int_{\mu}^{\infty} dE\, E^a \frac{d^n}{dE^n}\left(\frac{1}{e^{\beta E}+1}\right)$$

$$\times \int_0^p dk\, q^b \sum_{m=-\infty}^{\infty} \left(m+\tfrac{1}{2}\right)^{n+c} J^*_m(q\rho). \quad (4.3.25)$$

Sum over m. The sum over m in Eq. (4.3.25) vanishes unless $n+c$ is even for $* = +$ and odd for $* \in \{-, \times\}$. Equation (A.1.5) can be used to obtain:

$$\sum_{m=-\infty}^{\infty} \left(m+\tfrac{1}{2}\right)^{2n} J^+_m(z) = \sum_{j=0}^{n} \frac{2\Gamma(j+\tfrac{1}{2})}{j!\sqrt{\pi}} s^+_{n,j} z^{2j}, \quad (4.3.26a)$$

$$\sum_{m=-\infty}^{\infty} \left(m+\tfrac{1}{2}\right)^{2n+1} J^-_m(z) = \sum_{j=0}^{n} \frac{2\Gamma(j+\tfrac{1}{2})}{j!\sqrt{\pi}} s^-_{n,j} z^{2j}, \quad (4.3.26b)$$

$$\sum_{m=-\infty}^{\infty} \left(m+\tfrac{1}{2}\right)^{2n+1} J^\times_m(z) = \sum_{j=0}^{n} \frac{2\Gamma(j+\tfrac{1}{2})}{j!\sqrt{\pi}} s^\times_{n,j} z^{2j+1}. \quad (4.3.26c)$$

The above sums over j are finite and terminate at $j = n$, as will be shown shortly. Equation (A.1.5) can be used to express $s^+_{n,j}$ as:

$$s^+_{n,j} = 2 \sum_{m=0}^{j} \frac{(-1)^{j-m}}{(j-m)!(j+m+1)!} \left(m+\tfrac{1}{2}\right)^{2n+1}. \quad (4.3.27)$$

As in Eq. (4.2.25) for the scalar case, the sum over m can be written as the derivative of a binomial expansion:

$$s^+_{n,j} = \frac{1}{(2j+1)!} \lim_{\alpha \to 0} \frac{d^{2n+1}}{d\alpha^{2n+1}} \left\{ \sum_{m=0}^{j} \binom{2j+1}{j-m}(-1)^{j-m}\left[e^{\alpha(m+\frac{1}{2})} - e^{-\alpha(m+\frac{1}{2})}\right] \right\}$$

$$= \frac{1}{(2j+1)!} \lim_{\alpha \to 0} \frac{d^{2n+1}}{d\alpha^{2n+1}} \left\{ e^{\alpha(j+\frac{1}{2})} \sum_{m=0}^{2j+1} \binom{2j+1}{m}(-1)^{2j+1-m}e^{\alpha m} \right\}$$

$$= \frac{1}{(2j+1)!} \lim_{\alpha \to 0} \frac{d^{2n+1}}{d\alpha^{2n+1}} \left(2\sinh\frac{\alpha}{2}\right)^{2j+1}. \quad (4.3.28)$$

Clearly, $s^+_{n,j}$ vanishes when $j > n$. The following values of $s^+_{n,j}$ are important for the calculation of the t.e.v.s in this section:

$$s^+_{j,j} = 1,$$

$$s^+_{j+1,j} = \frac{1}{24}(2j+1)(2j+2)(2j+3),$$

$$s^+_{j+2,j} = \frac{1}{5760}(2j+1)(2j+2)(2j+3)(2j+4)(2j+5)(10j+3). \quad (4.3.29)$$

Using the following properties of J_m^*:

$$\frac{d}{dz}\left(zJ_m^+(z)\right) = (2m+1)J_m^-(z), \qquad \frac{d}{dz}\left(zJ_m^\times(z)\right) = 2zJ_m^-(z), \qquad (4.3.30)$$

it can be shown that $s_{n,j}^-$ and $s_{n,j}^\times$ are related to $s_{n,j}^+$ through:

$$s_{n,j}^- = \left(j + \tfrac{1}{2}\right)s_{n,j}^+, \qquad s_{n,j}^\times = \frac{j + \frac{1}{2}}{j+1}s_{n,j}^+. \qquad (4.3.31)$$

Thus, all $s_{n,j}^*$ vanish for $j > n$, therefore, the sums in Eqs. (4.3.26) terminate at $j = n$.

The integral with respect to k. Following the steps in the previous paragraph, the sum over m involving the Bessel functions in J_m^* is replaced by a sum over j involving powers of q, after which the integral over k can be computed using Eq. (4.2.29).

Analytic expressions in the massless case. The functinos S_{abc}^* required for the computation of the expectation values in Eqs. (4.3.18), (4.3.20) and (4.3.23) are S_{000}^+, S_{200}^+, S_{020}^+, S_{101}^+, S_{100}^-, $S_{110}^\times$ and $S_{011}^\times$.

Let us start with S_{000}^+. Performing the sum over m and integral over k in Eq. (4.3.25) yields:

$$S_{000}^+ = \frac{2}{\pi^2}\sum_{n=0}^\infty \frac{\Omega^{2n}}{(2n)!}\sum_{j=0}^n \frac{\rho^{2j}s_{n,j}^+}{(2j+1)}\int_\mu^\infty dE\, p^{2j+1}\frac{d^{2n}}{dE^{2n}}\left(\frac{1}{e^{\beta E}-1}\right). \qquad (4.3.32)$$

It is convenient to interchange the sum over j with the sum over n, which in turn can be shifted downwards to $n \to n + j$, such that S_{000}^+ takes the form:

$$S_{000}^+ = \frac{2}{\pi^2}\sum_{j=0}^\infty \frac{(\rho\Omega)^{2j}}{2j+1}\sum_{n=0}^\infty \frac{\Omega^{2n}s_{n+j,j}^+}{(2n+2j)!}\int_\mu^\infty dE\, p^{2j+1}\frac{d^{2n+2j}}{dE^{2n+2j}}\left(\frac{1}{e^{\beta E}-1}\right). \qquad (4.3.33)$$

To proceed further, it is necessary to set $\mu = 0$, in which case $p = E$. Before giving the result for the integral over E, it is worth noticing that

$$\frac{1}{e^{\beta\omega}+1} + \frac{1}{e^{-\beta\omega}+1} = 1. \qquad (4.3.34)$$

Hence, apart from the term $\frac{1}{2}$, the series expansion of the Fermi-Dirac density of states factor contains only odd powers of E, as follows:

$$\frac{1}{e^{\beta\omega}+1} = \frac{1}{2} + \frac{\beta E}{4} + O(E^3). \qquad (4.3.35)$$

Using Eq. (3.3.64), the integral over E in Eq. (4.3.33) can be performed:

$$\int_0^\infty dE \, E^{2j+1} \frac{d^{2j+2n}}{dE^{2j+2n}} \left(\frac{1}{e^{\beta E}+1}\right) = (2j+1)! \times \begin{cases} \dfrac{\pi^2}{12\beta^2} & n = 0, \\[2mm] \dfrac{1}{2} & n = 1, \\[2mm] 0 & n > 1. \end{cases} \tag{4.3.36}$$

The $n = 1$ term gives rise to temperature-independent terms in t.e.v.s obtained using Vilenkin's quantisation. Therefore, S^+_{000} can be put in the form:

$$S^+_{000} = \sum_{j=0}^\infty (\rho\Omega)^{2j} \left[\frac{1}{6\beta^2} + \frac{\Omega^2}{24\pi^2}(2j+3)\right]. \tag{4.3.37}$$

The sum over j can be evaluated using the geometric series formula (4.2.36), giving:

$$S^+_{000} = \frac{1}{6\beta^2\varepsilon} + \frac{\Omega^2}{8\pi^2\varepsilon^2}\left(\frac{2}{3} + \frac{\varepsilon}{3}\right), \tag{4.3.38}$$

where the parenthesis evaluates to 1 on the rotation axis, where $\varepsilon = 1 - \rho^2\Omega^2$ is 1.

After substituting $a = 2$ and $b = c = 0$ in Eq. (4.3.25), the expression for S^+_{200} becomes:

$$S^+_{200} = \frac{2}{\pi^2} \sum_{j=0}^\infty \frac{(\rho\Omega)^{2j}}{2j+1} \sum_{n=0}^\infty \frac{\Omega^{2n} s^+_{n+j,j}}{(2n+2j)!} \int_\mu^\infty dE \, E^2 \, p^{2j+1} \frac{d^{2n+2j}}{dE^{2n+2j}}\left(\frac{1}{e^{\beta E}-1}\right). \tag{4.3.39}$$

The integral over E can be performed analytically in the massless case:

$$\begin{aligned}
S^+_{200} &= \sum_{j=0}^\infty (\rho\Omega)^{2j}(2j+2)(2j+3)\left[\frac{7\pi^2}{360\beta^4} + \frac{\Omega^2(2j+3)}{144\beta^2} + \frac{\Omega^4(2j+5)(10j+3)}{5760\pi^2}\right] \\
&= \frac{7\pi^2}{60\beta^4\varepsilon^3}\left(\tfrac{4}{3} - \tfrac{1}{3}\varepsilon\right) + \frac{\Omega^2}{8\beta^2\varepsilon^4}\left(\tfrac{8}{3} - \tfrac{16}{9}\varepsilon + \tfrac{1}{9}\varepsilon^2\right) + \frac{\Omega^4}{64\pi^2\varepsilon^5}\left(\tfrac{64}{3} - \tfrac{376}{15}\varepsilon + \tfrac{196}{45}\varepsilon^2 + \tfrac{17}{45}\varepsilon^3\right),
\end{aligned} \tag{4.3.40}$$

where Eq. (3.3.72) was used to obtain the β^{-4} term. The parentheses above have been normalised to evaluate to 1 on the rotation axis.

In a similar fashion, S^+_{020} can be obtained as follows:

$$S^+_{020} = \frac{2}{\pi^2} \sum_{j=0}^\infty \frac{(\rho\Omega)^{2j}}{2j+1} \sum_{n=0}^\infty \frac{\Omega^{2n} s^+_{n+j,j}}{(2n+2j)!} \frac{2j+2}{2j+3} \int_\mu^\infty dE \, p^{2j+3} \frac{d^{2n+2j}}{dE^{2n+2j}}\left(\frac{1}{e^{\beta E}-1}\right). \tag{4.3.41}$$

Setting $\mu = 0$ gives:

$$S_{020}^+ = \sum_{j=0}^\infty (\rho\Omega)^{2j}(2j+2)^2 \left[\frac{7\pi^2}{360\beta^4} + \frac{\Omega^2}{144\beta^2}(2j+3) + \frac{\Omega^4}{5760\pi^2}(2j+5)(10j+3) \right]$$
$$= \frac{7\pi^2}{90\beta^4\varepsilon^3}(2-\varepsilon) + \frac{\Omega^2}{12\beta^2\varepsilon^4}(4 - \tfrac{10}{3}\varepsilon + \tfrac{1}{3}\varepsilon^2) + \frac{\Omega^4}{96\pi^2\varepsilon^5}(32 - \tfrac{208}{5}\varepsilon + \tfrac{142}{15}\varepsilon^2 + \tfrac{17}{15}\varepsilon^3).$$

$$(4.3.42)$$

The last term in which the integrand is even with respect to the transformation $m \to -m-1$ is:

$$\rho^{-1} S_{011}^\times = \frac{2}{\pi^2} \sum_{j=0}^\infty \frac{(\rho\Omega)^{2j}}{2j+1} \sum_{n=0}^\infty \frac{\Omega^{2n} s_{n+j,j}^+}{(2n+2j)!} \frac{2j+1}{2j+3} \int_\mu^\infty dE\, p^{2j+3} \frac{d^{2n+2j}}{dE^{2n+2j}} \left(\frac{1}{e^{\beta E}-1} \right).$$

$$(4.3.43)$$

The integral over E can be performed in the massless case, yielding:

$$\rho^{-1} S_{011}^\times = \sum_{j=0}^\infty (\rho\Omega)^2(2j+1)(2j+2) \left[\frac{7\pi^2}{360\beta^4} + \frac{\Omega^2(2j+3)}{144\beta^2} + \frac{\Omega^4(2j+5)(10j+3)}{5760\pi^2} \right]$$
$$= \frac{7\pi^2}{180\beta^4\varepsilon^3}(4-3\varepsilon) + \frac{\Omega^2}{24\beta^2\varepsilon^4}(8 - 8\varepsilon + \varepsilon^2)$$
$$+ \frac{\Omega^4}{192\pi^2\varepsilon^5}(64 - \tfrac{456}{5}\varepsilon + \tfrac{124}{5}\varepsilon^2 + \tfrac{17}{5}\varepsilon^3).$$

$$(4.3.44)$$

The simplest term of interest with odd integrand with respect to $m \to -m-1$ is:

$$S_{100}^- = -\frac{\Omega}{\pi^2} \sum_{j=0}^\infty (\rho\Omega)^{2j} \sum_{n=0}^\infty \frac{\Omega^{2n} s_{n+j,j}^+}{(2n+2j+1)!} \int_\mu^\infty dE\, E\, p^{2j+1} \frac{d^{2n+2j+1}}{dE^{2n+2j+1}} \left(\frac{1}{e^{\beta E}-1} \right).$$

$$(4.3.45)$$

An analytic expression can be obtained when $\mu = 0$:

$$S_{100}^- = \Omega \sum_{j=0}^\infty (\rho\Omega)^{2j}(2j+2) \left[\frac{1}{12\beta^2} + \frac{\Omega^2}{48\pi^2}(2j+1) \right]$$
$$= \frac{\Omega}{6\beta^2\varepsilon^2} + \frac{\Omega^3}{24\pi^2\varepsilon^3}(4-3\varepsilon).$$

$$(4.3.46)$$

In the term S_{101}^+, the sum over j runs between 1 and $n+1$. Treating the $j = n+1$

case separately by using the property $s^+_{n+1,n+1} = 1$ and relabelling n by j gives:

$$
\begin{aligned}
S^+_{101} =& \frac{1}{\Omega} \sum_{j=0}^{\infty} (\rho\Omega)^{2j} \left[\frac{7\pi^2\rho^2\Omega^2}{360\beta^4}(2j+2)(2j+4) + \frac{\Omega^2}{144\beta^2}(2j+2)^2(2j+3) \right. \\
& \left. + \frac{\Omega^4}{5760\pi^2}(2j+2)(2j+4)(2j+5)(10j+3) \right] \\
=& \frac{7\pi^2\rho^2\Omega}{45\beta^4\varepsilon^3} + \frac{\Omega}{12\beta^2\varepsilon^4}(4 - \tfrac{10}{3}\varepsilon + \tfrac{1}{3}\varepsilon^2) + \frac{\Omega^3}{48\pi^2\varepsilon^5}(16 - \tfrac{84}{5}\varepsilon + \tfrac{9}{5}\varepsilon^2).
\end{aligned}
\tag{4.3.47}
$$

Finally, $S^\times_{110}$ can be written using Eqs. (A.1.11) as:

$$
\begin{aligned}
S^\times_{110} =& \frac{1}{\rho} S^+_{101} - \frac{1}{2\rho}\frac{d}{d\rho}(\rho S^-_{100}) \\
=& \rho\Omega \left[\frac{7\pi^2}{45\beta^4\varepsilon^3} + \frac{\Omega^2}{18\beta^2\varepsilon^4}(6 - 5\varepsilon) + \frac{\Omega^4}{240\pi^2\varepsilon^5}(80 - 124\varepsilon + 45\varepsilon^2) \right].
\end{aligned}
\tag{4.3.48}
$$

Analytic expressions for t.e.v.s for massless fermions

Substituting Eq. (4.3.38) into Eq. (4.3.18) gives the following result for the FC:

$$
\lim_{\mu \to 0} \frac{1}{\mu} \langle : \overline{\psi}\psi :_V \rangle_\beta = \frac{\pi^2}{6\beta^2}\varepsilon^{-1} + \frac{\Omega^2}{8\varepsilon^2}(\tfrac{2}{3} + \tfrac{1}{3}\varepsilon).
\tag{4.3.49}
$$

where $\varepsilon = 1 - \rho^2\Omega^2$ goes to 0 as the SOL is approached.

The neutrino CC can be obtained by substituting Eq. (4.3.46) into Eq. (4.3.50):

$$
\langle : J^z_\nu :_V \rangle_\beta = -\frac{\Omega}{12\beta^2\varepsilon^2} - \frac{\Omega^3}{48\pi^2\varepsilon^3}(4 - 3\varepsilon).
\tag{4.3.50}
$$

The thermal expectation value of the neutrino current along the rotation axis is non-vanishing. Intuitively, this result can be understood as follows [71]: If $\mathbf{\Omega}$ is pointing along the z axis, the Fermi-Dirac density of states factor $(e^{\beta[E - \Omega(m+\frac{1}{2})]} + 1)^{-1}$ will favour particles which, at the same value of the energy, have a larger value $m + \frac{1}{2}$ of the projection of the spin on the z axis. Neutrinos are particles with negative chirality and therefore have negative helicity, while anti-neutrinos have negative chirality and positive helicity [46]. Since helicity is the projection of the spin on the direction of motion, neutrinos with a negative z component of their velocity will have a positive contribution to their total angular momentum along the z axis coming from their spin and will therefore be favoured by the Fermi-Dirac statistics. Moreover, anti-neutrinos will have a tendency of travelling in the direction of $\mathbf{\Omega}$, so that the total current of neutrinos and anti-neutrinos vanishes. However, the individual contributions to the charge current coming from neutrinos and anti-neutrinos stay finite and have negative and positive signs, respectively.

Finally, the tetrad components of the SET using the Vilenkin vacuum have the form:

$$\langle : T_{\hat{t}\hat{t}} :_V \rangle_\beta = \frac{7\pi^2}{60\beta^4\varepsilon^3}\left(\tfrac{4}{3} - \tfrac{1}{3}\varepsilon\right) + \frac{\Omega^2}{8\beta^2\varepsilon^4}\left(\tfrac{8}{3} - \tfrac{16}{9}\varepsilon + \tfrac{1}{9}\varepsilon^2\right)$$
$$+ \frac{\Omega^4}{64\pi^2\varepsilon^5}\left(\tfrac{64}{3} - \tfrac{376}{15}\varepsilon + \tfrac{196}{45}\varepsilon^2 + \tfrac{17}{45}\varepsilon^3\right),$$

$$\langle : T_{\hat{\varphi}\hat{t}} :_V \rangle_\beta = -\rho\Omega\left[\frac{7\pi^2}{45\beta^4\varepsilon^3} + \frac{2\Omega^2}{9\beta^2\varepsilon^4}\left(\tfrac{3}{2} - \tfrac{1}{2}\varepsilon\right) + \frac{31\Omega^4}{240\pi^2\varepsilon^5}\left(\tfrac{80}{31} - \tfrac{64}{31}\varepsilon + \tfrac{15}{31}\varepsilon^2\right)\right],$$

$$\langle : T_{\hat{\rho}\hat{\rho}} :_V \rangle_\beta = \frac{7\pi^2}{180\beta^4\varepsilon^2} + \frac{\Omega^2}{24\beta^2\varepsilon^3}\left(\tfrac{4}{3} - \tfrac{1}{3}\varepsilon\right) + \frac{\Omega^4}{192\pi^2\varepsilon^4}\left(8 - \tfrac{88}{15}\varepsilon - \tfrac{17}{15}\varepsilon^2\right),$$

$$\langle : T_{\hat{\varphi}\hat{\varphi}} :_V \rangle_\beta = \frac{7\pi^2}{180\beta^4\varepsilon^3}(4 - 3\varepsilon) + \frac{\Omega^2}{24\beta^2\varepsilon^4}\left(8 - 8\varepsilon + \varepsilon^2\right)$$
$$+ \frac{\Omega^4}{192\pi^2\varepsilon^5}\left(64 - \tfrac{456}{5}\varepsilon + \tfrac{124}{5}\varepsilon^2 + \tfrac{17}{5}\varepsilon^3\right), \tag{4.3.51}$$

and $\langle : T_{\hat{z}\hat{z}} :_V \rangle_\beta = \langle : T_{\hat{\rho}\hat{\rho}} :_V \rangle_\beta$. It is remarkable that this latter equality holds in the massive case as well, which can be seen by substituting Eqs. (4.3.38), (4.3.40), (4.3.42) and (4.3.48) into the relevant equations from the set (4.3.23):

$$\langle : T_{\hat{\rho}\hat{\rho}} :_V \rangle_\beta = \langle : T_{\hat{z}\hat{z}} :_V \rangle_\beta = \frac{2}{\pi^2}\sum_{j=0}^{\infty}\frac{(\rho\Omega)^{2j}}{2j+1}\sum_{n=0}^{\infty}\frac{\Omega^{2n}s^+_{n+j,j}}{(2n+2j)!}\frac{1}{2j+3}$$
$$\times \int_\mu^\infty dE\, p^{2j+3}\frac{d^{2n+2j}}{dE^{2n+2j}}\left(\frac{1}{e^{\beta E}-1}\right). \tag{4.3.52}$$

Equations (4.1.22) can be used to express the t.e.v. of the SET (4.3.51) with respect to the coordinate basis:

$$\langle : T_{tt} :_V \rangle_\beta = \frac{7\pi^2}{60\beta^4\varepsilon} + \frac{\Omega^2}{8\beta^2\varepsilon^2}\left(\tfrac{4}{3} - \tfrac{1}{3}\varepsilon\right) + \frac{\Omega^4}{64\pi^2\varepsilon^3}\left(\tfrac{8}{9} + \tfrac{56}{45}\varepsilon - \tfrac{17}{15}\varepsilon^2\right),$$

$$\langle : T_{\varphi t} :_V \rangle_\beta = -\rho^2\Omega\left[\frac{7\pi^2}{60\beta^4\varepsilon^2} + \frac{13\Omega^2}{72\beta^2\varepsilon^3}\left(\tfrac{16}{13} - \tfrac{3}{13}\varepsilon\right) + \frac{119\Omega^4}{960\pi^2\varepsilon^4}\left(\tfrac{200}{119} - \tfrac{64}{119}\varepsilon - \tfrac{1}{7}\varepsilon^2\right)\right],$$

$$\langle : T_{\varphi\varphi} :_V \rangle_\beta = \rho^2\left[\frac{7\pi^2}{180\beta^4\varepsilon^3}(4 - 3\varepsilon) + \frac{\Omega^2}{24\beta^2\varepsilon^4}\left(8 - 8\varepsilon + \varepsilon^2\right)\right.$$
$$\left. + \frac{\Omega^4}{192\pi^2\varepsilon^5}\left(64 - \tfrac{456}{5}\varepsilon + \tfrac{124}{5}\varepsilon^2 + \tfrac{17}{5}\varepsilon^3\right)\right]. \tag{4.3.53}$$

All the t.e.v.s presented so far in this section were calculated with respect to the Minkowski (Vilenkin) vacuum. The results are made up of two types of terms: the physical terms proportional to β^{-4} and β^{-2} (only β^{-2} for the FC and neutrino CC) and the spurious temperature-independent terms.

In Ref. [72], Vilenkin argues that, since the temperature-independent contribution to the neutrino charge current on the rotation axis is due to particle modes with negative frequency with respect to the rotating Hamiltonian, the first type of terms mentioned above can be removed by enclosing the system inside a boundary which

cuts out the space beyond the SOL. This statement is only half-true. As discussed in sections 5.2 and 5.3, putting the system inside a box does indeed eliminate the modes with $E\widetilde{E} < 0$. However, the quantisation proposed by Iyer yields a vacuum state with respect to which thermal states are consistently defined, such that t.e.v.s do not contain spurious temperature-independent terms. The t.e.v.s when the rotating (Iyer) vacuum is considered are exactly equal to those obtained with respect to the Minkowski (Vilenkin) vacuum, but without the temperature-independent terms, as follows:

$$\lim_{\mu \to 0} \frac{1}{\mu} \left\langle : \overline{\psi}\psi :_I \right\rangle_\beta = \frac{\pi^2}{6\beta^2} \varepsilon^{-1}, \tag{4.3.54a}$$

$$\left\langle : J_\nu^z :_I \right\rangle_\beta = -\frac{\Omega}{12\beta^2\varepsilon^2}, \tag{4.3.54b}$$

$$\left\langle : T_{\hat{t}\hat{t}} :_I \right\rangle_\beta = \frac{7\pi^2}{60\beta^4\varepsilon^3}\left(\tfrac{4}{3} - \tfrac{1}{3}\varepsilon\right) + \frac{\Omega^2}{8\beta^2\varepsilon^4}\left(\tfrac{8}{3} - \tfrac{16}{9}\varepsilon + \tfrac{1}{9}\varepsilon^2\right), \tag{4.3.54c}$$

$$\left\langle : T_{\hat{\varphi}\hat{t}} :_I \right\rangle_\beta = -\rho\Omega\left[\frac{7\pi^2}{45\beta^4\varepsilon^3} + \frac{2\Omega^2}{9\beta^2\varepsilon^4}\left(\tfrac{3}{2} - \tfrac{1}{2}\varepsilon\right)\right], \tag{4.3.54d}$$

$$\left\langle : T_{\hat{\rho}\hat{\rho}} :_I \right\rangle_\beta = \frac{7\pi^2}{180\beta^4\varepsilon^2} + \frac{\Omega^2}{24\beta^2\varepsilon^3}\left(\tfrac{4}{3} - \tfrac{1}{3}\varepsilon\right), \tag{4.3.54e}$$

$$\left\langle : T_{\hat{\varphi}\hat{\varphi}} :_I \right\rangle_\beta = \frac{7\pi^2}{180\beta^4\varepsilon^3}(4 - 3\varepsilon) + \frac{\Omega^2}{24\beta^2\varepsilon^4}\left(8 - 8\varepsilon + \varepsilon^2\right) \tag{4.3.54f}$$

and $\left\langle : T_{\hat{z}\hat{z}} :_I \right\rangle_\beta = \left\langle : T_{\hat{\rho}\hat{\rho}} :_I \right\rangle_\beta$. In the above, the subscript I indicates that the Wick ordering is performed with respect to the rotating (Iyer) vacuum. The t.e.v.s (4.3.53) of the SET expressed with respect to the coordinate basis can also be expressed with respect to the Iyer vacuum:

$$\left\langle : T_{tt} :_I \right\rangle_\beta = \frac{7\pi^2}{60\beta^4\varepsilon} + \frac{\Omega^2}{8\beta^2\varepsilon^2}\left(\tfrac{4}{3} - \tfrac{1}{3}\varepsilon\right), , \tag{4.3.55a}$$

$$\left\langle : T_{\varphi t} :_I \right\rangle_\beta = -\rho^2\Omega\left[\frac{7\pi^2}{60\beta^4\varepsilon^2} + \frac{13\Omega^2}{72\beta^2\varepsilon^3}\left(\tfrac{16}{13} - \tfrac{3}{13}\varepsilon\right)\right], \tag{4.3.55b}$$

$$\left\langle : T_{\varphi\varphi} :_I \right\rangle_\beta = \rho^2\left[\frac{7\pi^2}{180\beta^4\varepsilon^3}(4 - 3\varepsilon) + \frac{\Omega^2}{24\beta^2\varepsilon^4}\left(8 - 8\varepsilon + \varepsilon^2\right)\right]. \tag{4.3.55c}$$

Equations (4.3.54) represent the second type of terms mentioned above. As in the scalar case (discussed in subsection 4.2.2), all terms in the t.e.v.s given in this section diverge as inverse powers of the distance to the SOL, showing that the thermal state becomes infinitely energetic close to the SOL. Moreover, the non-rotating Minkowski results in Eqs. (3.3.73) are recovered by setting $\Omega = 0$ in Eqs. (4.3.54). It can be seen that on the rotation axis (obtained when $\varepsilon = 1$ and the parentheses evaluate to 1), the t.e.v. of the SET receives corrections compared to the Minkowski case, which are proportional to Ω^2. In sections section 5.2 and section 5.3, the t.e.v.s obtained using the Iyer quantisation are compared to the t.e.v.s obtained when the system is enclosed inside a boundary.
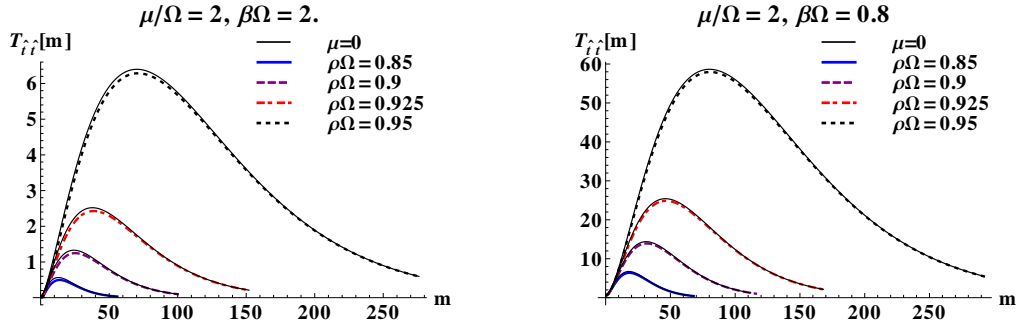
Figure 4.2: The curves show the contributions $T_{\hat{t}\hat{t}}[m]$ made by each value of m (together with $-m-1$) to $\langle: T_{\hat{t}\hat{t}}(x):_I\rangle_\beta$ for a rigidly rotating Dirac field with $\mu = 0$ (thin solid black lines) and $\mu = 2\Omega$ (thick lines) at inverse temperatures (a) $\beta\Omega = 2.0$ and (b) $\beta\Omega = 0.8$, at four distances from the rotation axis. The value of $T_{\hat{t}\hat{t}}[m]$ increases up to a maximum value at m_ρ after which it decreases monotonically to 0. The value m_ρ increases with the distance from the rotation axis, which is why the further the point is, the more values of m must be considered. However, m_ρ does not seem to depend on β or μ. The curves terminate according to the algorithm described in the main text.

The features discussed above remain valid when considering massive fermions. Although we do not have an analytic method for its study, the $\mu > 0$ case can be investigated numerically and the results are represented in the following subsection.

4.3.3 Numerical results

The t.e.v.s with respect to the rotating (Iyer) vacuum of the FC (4.3.18), neutrino CC (4.3.20) SET (4.3.23) can be obtained using the following mode sum equations:

$$\langle: \overline{\psi}\psi :_I\rangle_\beta = \frac{\mu}{\pi^2} \sum_{m=-\infty}^{\infty} \int_\mu^\infty \frac{\text{sgn}\widetilde{E}dE}{e^{\beta|\widetilde{E}|}+1} \int_0^p dk\, J_m^+(q\rho), \tag{4.3.56a}$$

$$\langle: J_\nu^z :_I\rangle_\beta = -\frac{1}{2\pi^2} \sum_{m=-\infty}^{\infty} \int_\mu^\infty \frac{E\text{sgn}\widetilde{E}dE}{e^{\beta|\widetilde{E}|}+1} \int_0^p dk\, J_m^-(q\rho), \tag{4.3.56b}$$

$$\langle: T_{\hat{\alpha}\hat{\gamma}} :_I\rangle_\beta = \frac{1}{\pi^2} \sum_{m=-\infty}^{\infty} \int_\mu^\infty \frac{\text{sgn}\widetilde{E}dE}{e^{\beta|\widetilde{E}|}+1} \int_0^p dk\, F_{\hat{\alpha}\hat{\gamma}}, \tag{4.3.56c}$$

with $F_{\hat{\alpha}\hat{\gamma}}$ given by (4.3.21). To obtain the numerical data necessary to produce the plots in this section, the above t.e.v.s were calculated for each value of m, individually, as follows:

$$\langle: A :_I\rangle_\beta = \sum_{m=0}^{\infty} A[m]. \tag{4.3.57}$$

For the computation of $\langle: T_{\hat{\alpha}\hat{\gamma}} :_I\rangle_\beta$ at a given point ρ, the function $T_{\hat{\alpha}\hat{\gamma}}[m]$ was evaluated for increasing values of m. The thermal weight factor $\text{sgn}(\widetilde{E})(e^{\beta|\widetilde{E}|+1}+1)^{-1}$ supresses the integrand at large values of $\beta|\widetilde{E}|$. Hence, the major contribution to
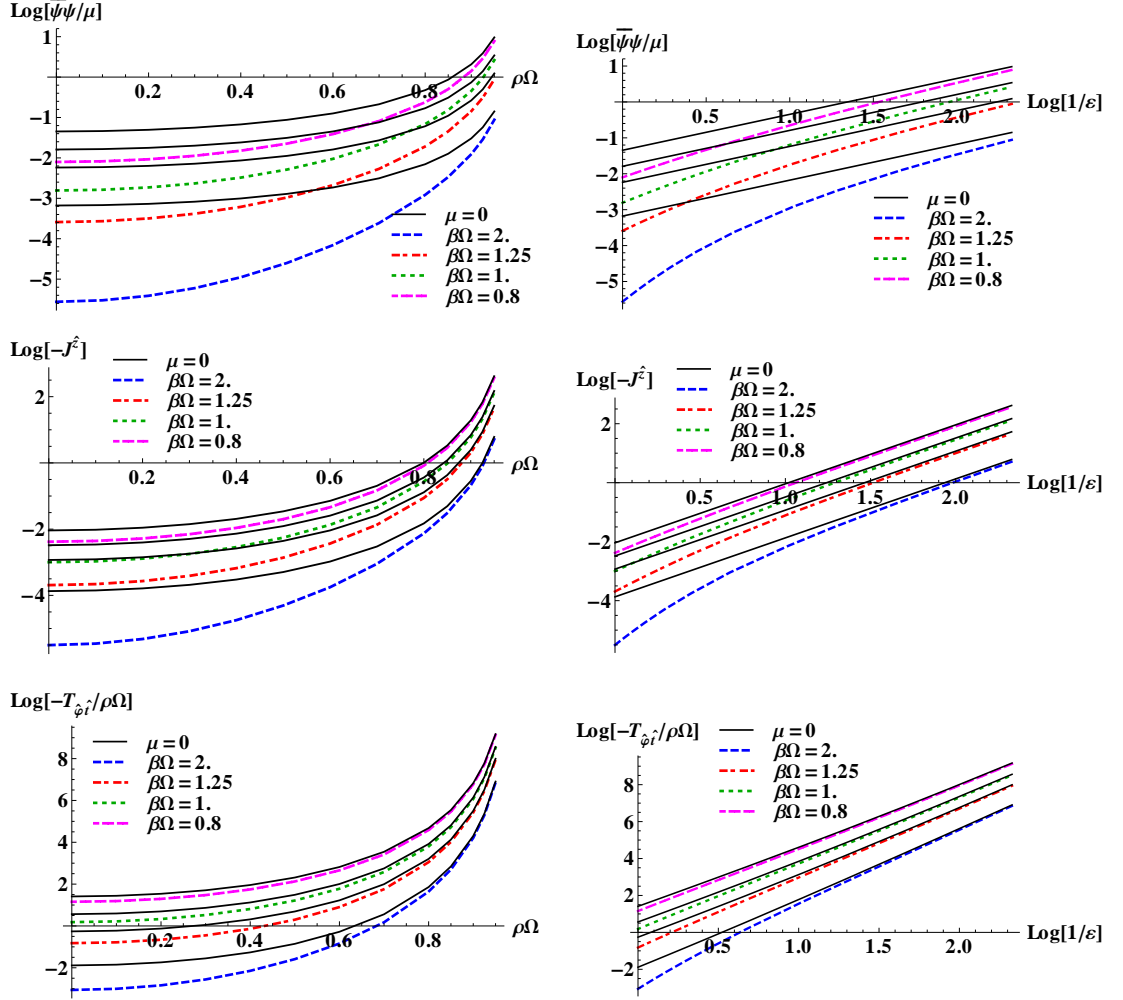
Figure 4.3: The logarithm of the fermion condensate $\langle : \overline{\psi}\psi :_I \rangle_\beta$ (first line), neutrino current $\langle : J_\nu :_I \rangle^{\hat{z}}$ and $-\frac{1}{\rho\Omega} \langle : T_{\hat{\varphi}\hat{t}} :_I \rangle_\beta$ (bottom line) against $\rho\Omega$ on the left and $\ln(1/\varepsilon)$ on the right. The prefactor $-\frac{1}{\rho\Omega}$ has been introduced for to render the argument $-\frac{1}{\rho\Omega} \langle : T_{\hat{\varphi}\hat{t}} :_I \rangle_\beta$ of the logarithm positive and non-zero on the rotation axis. The results for fermions of mass $\mu = 2\Omega$ (coloured dashed lines) are compared to the corresponding expressions in Eqs. (4.3.56), plotted with dark thin lines.
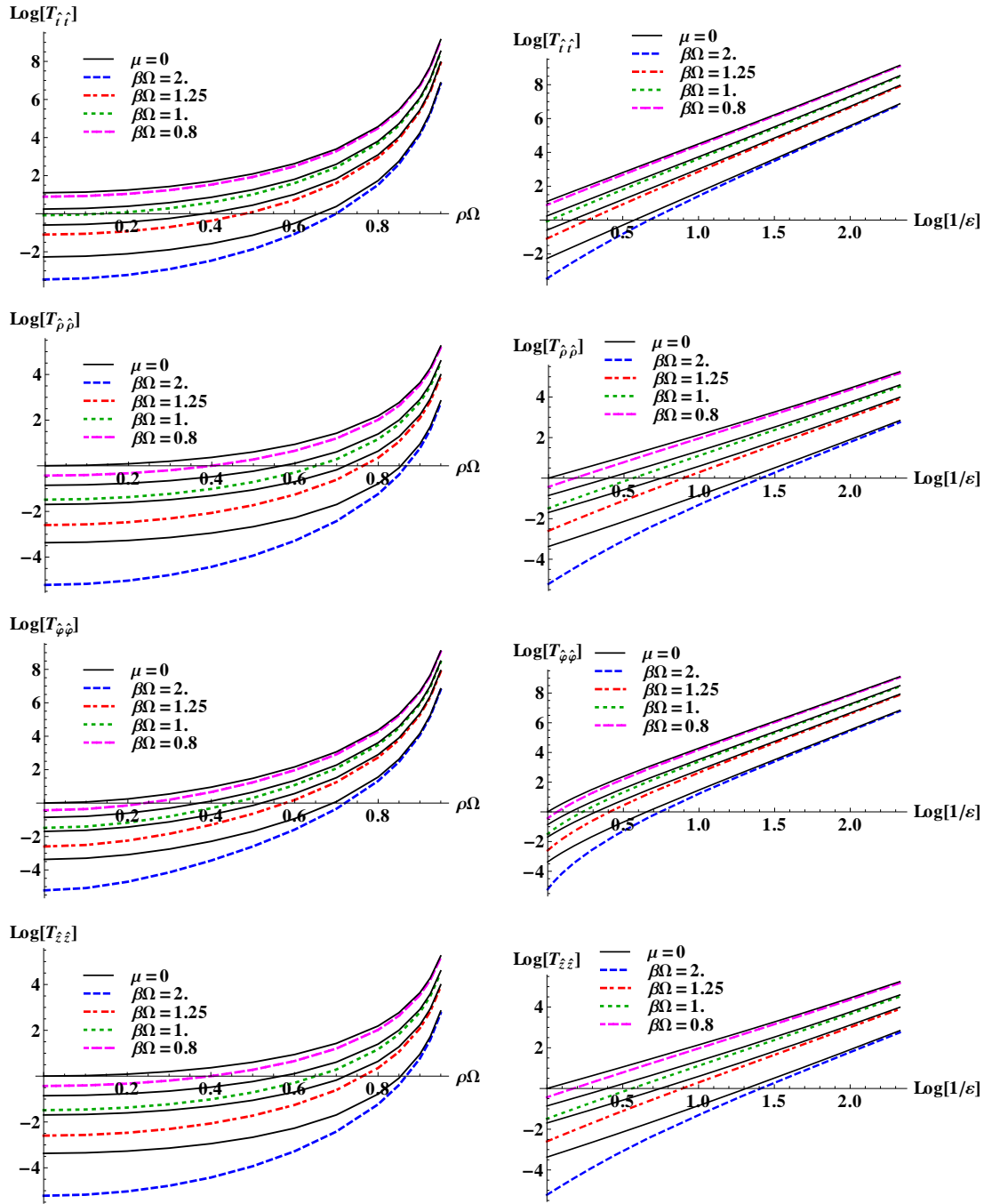
Figure 4.4: The logarithm of the diagonal components of the SET against $\rho\Omega$ (left) and $\ln(1/\varepsilon)$ (right). The results for fermions of mass $\mu = 2\Omega$ (coloured dashed lines) are compared to the corresponding expressions in Eqs. (4.3.56), plotted with dark thin lines.

the integrals in Eqs. (4.3.56) come from the region where $E \sim \Omega(m + \frac{1}{2})$, allowing convergence problems to be avoided by performing the energy integral over the domain $\beta E \in \{\max(\beta\mu, \beta\Omega m - 100), \beta\Omega m + 100\}$. The behaviour of the expectation values is well captured by considering points up to $\rho\Omega = 0.95$, where the t.e.v.s are finite. Knowing that $T_{\hat{\alpha}\hat{\gamma}}[m]$ decreases to 0 at sufficiently large m, the series over m in (4.3.56) was terminated when $T_{\hat{\alpha}\hat{\gamma}}[m]/\max_m(T_{\hat{\alpha}\hat{\gamma}}[m]) < 0.01$. Figure 4.2 illustrates this algorithm applied for the computation of the energy density.

The plots of the t.e.v.s of the fermion condensate, neutrino charge current and SET in Figs. 4.3 and 4.4 present numerical results obtained for fermions of mass $\mu = 2\Omega$ to the analytic expressions (4.3.54), calculated with respect to the rotating (Iyer) vacuum. It can be seen that the profiles of the t.e.v.s for massive fermions set below those for massless fermions. In the aforementioned figures, the plot on the left illustrates the logarithm of the t.e.v. of the operator under consideration with respect to the distance from the rotation axis expressed in units of Ω^{-1}, while the log-log plots on the right show that close to the SOL, the t.e.v.s behave similarly for massless and massive fermions. In particular, the leading order of the divergence as the SOL is approached of the t.e.v.s considered here does not depend on the mass of the field quanta. Since Eq. (4.3.54d) shows that $\langle : T_{\hat{t}\hat{\varphi}} :_I \rangle$ vanishes on the rotation axis due to the factor $\rho\Omega$, the bottom plot in Fig. 4.3 shows instead the ratio $\langle : T_{\hat{t}\hat{\varphi}} :_I \rangle / \rho\Omega$.

4.3.4 Summary

While the quantisation procedure for the scalar case was restricted such that the rotating and non-rotating vacua were forced to coincide, the property that the norm of the particle and anti-particle mode solutions of the Dirac equation are both positive allows different vacuum states for the Dirac field on the rotating space-time, which can differ from the Minkowski vacuum. As discussed by Vilenkin [72], thermalising the Dirac field with respect to the Minkowski vacuum state induces spurious temperature-independent terms in thermal expectation values (t.e.v.s). However, if second quantisation is performed according to Iyer's prescription [47], the resulting vacuum state is different from the Minkowski vacuum and thermal expectation values are well defined and contain no temperature-independent terms. We refer to this latter vacuum state as the rotating vacuum.

Our analytic results, also published in Ref. [10], confirm the presence of the spurious temperature-independent terms reported by Vilenkin [72] in t.e.v.s calculated with respect to the Minkowski vacuum. Vilenkin [72] argues that these terms disappear if the space outside the speed of light surface (SOL) is discarded, by enclosing the system in a boundary. We analyse quantum states for bounded rotating

Minkowski space-times in chapter 5 and indeed find that placing the boundary inside or on the SOL eliminates the spurious temperature-independent terms. We also confirm that when Iyer's quantisation [47] is used for the unbounded space-time, the resulting t.e.v.s contain no temperature independent terms. Hence, we conclude that the spurious terms are induced by the quantisation method employed, more specifically, by allowing modes with $\widetilde{E}E < 0$ in the set of particle modes, as discussed in subsection 2.2.5 and subsection 4.3.1.

The analytic results obtained for the t.e.v.s of the fermion condensate, neutrino charge current and stress-energy tensor for massless fermions show that thermal states become divergent (i.e. yield infinite expectation values) as the SOL is approached, with the t.e.v.s diverging as inverse powers of the distance to the SOL. Furthermore, as explained in Refs. [71, 72] and after Eq. (4.3.50), there is an excess in the flux of neutrinos and anti-neutrinos anti-parallel and parallel to the rotation angular momentum vector, respectively.

Through numerical integration, the t.e.v.s for massless and massive fermions can be compared. The figures in subsection 4.3.3 show that thermal states become less energetic as the mass of the quanta is increased. However, the t.e.v.s of massless and massive fermions diverge at the same rate as the SOL is approached, indicating that the leading order divergences do not depend on the mass of the quanta.

4.4   Chapter summary

The construction of mode solutions and the discussion of vacuum states presented in this chapter also applies to the bounded rotating Minkowski space-time, discussed in chapter 5 and to the construction of quantum states on rotating anti-de Sitter space-time, discussed in chapter 8.

The construction of the rotating vacuum state for the scalar field is restricted by the interpretation that Klein-Gordon modes of positive or negative frequency represent particle or anti-particle modes. In consequence, the vacuum state for rotating scalars is forced to coincide with the Minkowski vacuum. The construction of thermal states is not possible due to the divergent behaviour of the Bose-Einstein density of states factor for modes with vanishing co-rotating frequency. Analytic methods can be used to isolate the divergences of the thermal state, yielding finite terms which can be interpreted physically.

Two fundamental differences between fermions and scalars allow fermion thermal states to be rigorously defined. As opposed to the quantisation of the Klein-Gordon, the norm of Dirac modes is always positive. Hence, the split between particle and anti-particle modes (or equivalently, the choice of vacuum state) can be performed such that $E\widetilde{E} > 0$ for all particle modes. As discussed in subsection 2.2.5, this

property guarantees that thermal states can be consistently defined such that the resulting thermal expectation values contain no temperature-independent terms. While the Bose-Einstein density of states factor renders thermal states for the scalar field infinite due to its divergent behaviour for vanishing co-rotating frequencies, Fermi-Dirac statistics do not allow for infinite occupation numbers. Hence, it is possible to construct thermal states of fermion particles which are well defined and regular up to the speed of light surface.

Chapter 5. Bounded rotating Minkowski space-time

The results of chapter 4 show that scalar particles cannot settle into thermal states as seen by rotating observers, due to the singular behaviour of the Bose-Einstein density of states factor for modes with vanishing frequency with respect to the rotating observer. In contrast, the occupation numbers in Fermi-Dirac statistics are finite for all frequencies, allowing fermions to thermalise with respect to rotating observers. For fermions, it is possible to define thermal expectation values (t.e.v.s) which are finite up to the speed of light surface (SOL), past which they are not defined. As discussed in Refs. [33, 52, 72], the space-time beyond the SOL is not physical. Its exclusion through the confinement of the system inside the SOL can eliminate modes with negative or vanishing frequencies with respect to the rotating observer from the set of particle modes, making the construction of thermal states of scalar particles possible.

The system can be bounded by introducing a cylindrical mirror of radius R parallel to and centred on the rotation axis. Consequently, the transverse momentum is quantised in such a way that Minkowski particle modes have positive frequencies with respect to the rotating observer as well, as long as the mirror is inside or on the SOL. In consequence, there are no modes with infinite density of states factors, making thermal states attainable for scalar particles. An interesting result is that at large enough temperatures the t.e.v. of the SET agrees with the β^{-4} part of the analytic results (4.2.51) and (4.3.51) for the Klein-Gordon and Dirac fields, respectively, in the vicinity of the axis, but deviates from these values as the boundary is approached in such a way that even if the boundary is placed on the SOL, the t.e.v.s stay finite.

The mirror is implemented by imposing Dirichlet boundary conditions for the scalar field [32, 33], while for fermions, spectral [43] and MIT bag [23] boundary conditions are considered. The motivation behind presenting these two types of boundary conditions is their fundamentally different nature: the spectral boundary conditions are non-local, requiring the knowledge of the Fourier transform of wave functions, while the MIT bag boundary conditions are expressed and implemented in a fully local manner. Fundamental differences are noticed in the profiles of thermal expectation values as well as in the investigation of the Casimir effect.

The Casimir effect arises due to the changes induced in the vacuum state by its enclosure inside a bounded system [46]. The thermal states discussed in this chapter are computed with respect to the vacuum state corresponding to the bounded

system. The Casimir effect refers to the difference between vacuum expectation values (v.e.v.s) of operators in the bounded and unbounded vacuum states. In particular, the difference in the energy component of the SET can be interpreted as the amount of energy required to confine the system inside the boundary. Deutsch and Candelas [31] explain that the divergence is due to the unphysical nature of classical perfect conductor boundary conditions and give a general prescription for the computation of the leading order divergences for general boundary conditions, based on the assumption of locality of the SET. While the results obtained for the scalar field and for fermions obeying MIT bag boundary conditions fit perfectly well with the predictions of Ref. [31], the non-local character of the spectral boundary conditions increases the order of the divergence of Casimir v.e.v.s by one unit.

Although the scalar field case has already been analysed in Ref. [33], it is presented in section 5.1 for completeness. Section 5.2 presents the Dirac theory using spectral boundary conditions and the MIT bag model is discussed in section 5.3. The space-time characteristics have already been described in section 4.1. These latter two sections contain original results which are due for publication [5]. A preview of the results is available in Ref. [8].

5.1 Scalars in a cylinder

Subsection 5.1.1 opens the discussion of quantum states of scalar particles inside a cylindrical boundary by presenting the construction of the mode solutions of the Klein-Gordon equation obeying Dirichlet boundary conditions. Furthermore, thermal expectation values (t.e.v.s) are analysed in subsection 5.1.2 and numerical results are presented for the case when the boundary is placed inside or on the speed of light surface (SOL). In subsection 5.1.3 expressions for the Casimir-induced vacuum expectation value (v.e.v.) of ϕ^2 and of the stress-energy tensor (SET) are derived. An asymptotic analysis of the Casimir divergence is performed in subsection 5.1.4.

5.1.1 Modes and field operator

To implement a cylindrical boundary at distance $\rho = R$ from the rotation axis, the modes (4.2.2) must satisfy Dirichlet boundary conditions:

$$f_{\omega k m}(\rho = R) = 0, \tag{5.1.1}$$

which is equivalent to requiring that $J_m(qR) = 0$. Hence, qR must be in the set of roots of J_m. Thus, the following quantisation rule for the transverse momentum arises:

$$q_{m\ell} = \frac{\xi_{m\ell}}{R}, \tag{5.1.2}$$

where $\ell = 1, 2, \ldots$ labels the roots $\xi_{m\ell}$ of J_m, in ascending order, without the trivial solution $\xi_{m\ell} = 0$ which corresponds to a mode function that vanishes at each point in space. The normalised modes satisfying Dirichlet boundary conditions are given by [33]:

$$f_{km\ell}(x) = \frac{e^{-i\widetilde{\omega}t + ikz + im\varphi}}{2\pi R \, |J_{m+1}(\xi_{m\ell})| \, \sqrt{\omega}} J_m(q\rho), \tag{5.1.3}$$

where the indices (m, ℓ) have been omitted on q and quantities derived from it (e.g. ω). The modes in Eq. (5.1.3) are normalised according to the following relation:

$$\langle f_{km\ell}, f_{k'm'\ell'} \rangle = -\int_{-\infty}^{\infty} dz \int_0^R \rho \, d\rho \int_0^{2\pi} d\varphi f_{km\ell}^*(t, \boldsymbol{x}) i \overleftrightarrow{\partial^t} f_{k'm'\ell'}(t, \boldsymbol{x})$$

$$= \delta(k - k')\delta_{ll'}\delta_{mm'}. \tag{5.1.4}$$

The energy spectrum is determined by looking at the form of the Minkowski energy of mode $f_{km\ell}$:

$$\omega^2 = \mu^2 + k^2 + R^{-2}\xi_{m\ell}^2. \tag{5.1.5}$$

According to formula (3) in chapter 15.3 of Ref. [73], the roots of the Bessel functions satisfy:

$$\xi_{m1} > \sqrt{m(m+2)} > m + \frac{1}{2} \quad (m > 0), \tag{5.1.6}$$

and $\xi_{01} = 2.4048255577 > 0.5$ (see Table 9.5 in Ref. [1]), implying the following inequality for the allowed frequencies $\widetilde{\omega}$:

$$\widetilde{\omega} = \omega - \Omega m \geq R^{-1}\xi_{m1} - \Omega m > R^{-1}m(1 - \Omega R). \tag{5.1.7}$$

Hence, $\widetilde{\omega} > 0$ as long as $\Omega R \leq 1$, i.e. as long as the boundary is inside or on the SOL. For the remainder of this section, only this case is considered. The completeness relation compatible with the inner product (5.1.4) satisfied by the modes (5.1.3) is:

$$-\sum_{m=-\infty}^{\infty} \sum_{l=1}^{\infty} \int_{-\infty}^{\infty} dk \left[f_{km\ell}^*(t, \boldsymbol{x}')i\partial^t f_{km\ell}(t, \boldsymbol{x}) - f_{km\ell}(t, \boldsymbol{x}')i\partial^t f_{km\ell}^*(t, \boldsymbol{x}) \right]$$

$$= \delta(\varphi - \varphi')\frac{\delta(\rho - \rho')}{\rho}\delta(z - z'). \tag{5.1.8}$$

Thus, the field operator $\phi(x)$ can be expanded with respect to the complete set of modes (5.1.3):

$$\phi(x) = \sum_{m=-\infty}^{\infty} \sum_{l=1}^{\infty} \int_{-\infty}^{\infty} dk \left[f_{km\ell}(x)a_{km\ell} + f_{km\ell}^*(x)a_{km\ell}^\dagger \right]. \tag{5.1.9}$$

5.1.2 Bounded rigidly rotating thermal states

Using the techniques introduced in section 3.2, the thermal Hadamard function constructed with respect to the bounded vacuum state can be written as:

$$\Delta G^{(1)}_\beta(x, x') = \sum_{m=-\infty}^{\infty} \sum_{l=1}^{\infty} \int_{-\infty}^{\infty} \frac{dk}{2\pi^2 \omega R^2 J^2_{m+1}(\xi_{m\ell})} \frac{e^{ik\Delta z}}{e^{\beta \widetilde{\omega}_{m\ell}} - 1}$$
$$\times (e^{-i\widetilde{\omega}_{m\ell}\Delta t + im\Delta\varphi} + e^{i\widetilde{\omega}_{m\ell}\Delta t - im\Delta\varphi}) J_m(\xi_{m\ell}\overline{\rho}) J_m(\xi_{m\ell}\overline{\rho}'), \quad (5.1.10)$$

where

$$\overline{\rho} = \frac{\rho}{R}. \quad (5.1.11)$$

The t.e.v. of ϕ^2 can be found using Eq. (2.1.57):

$$\langle : \phi^2 : \rangle_\beta = \sum_{m=-\infty}^{\infty} \sum_{l=1}^{\infty} \int_0^{\infty} \frac{dk}{\pi^2 \omega R^2 J^2_{m+1}(\xi_{m\ell})} \frac{1}{e^{\beta\widetilde{\omega}} - 1} J^2_m(\xi_{m\ell}\overline{\rho}). \quad (5.1.12)$$

The calculation of the t.e.v. of the SET from Eq. (2.1.54) can be performed by repeating the steps in subsection 4.2.2, yielding:

$$\langle : T_{\hat{\alpha}\hat{\gamma}} : \rangle_\beta = \sum_{m=-\infty}^{\infty} \sum_{l=1}^{\infty} \int_0^{\infty} \frac{dk}{6\pi^2 \omega R^2 J^2_{m+1}(\xi_{m\ell})} \frac{1}{e^{\beta\widetilde{\omega}} - 1} F_{\hat{\alpha}\hat{\gamma}}, \quad (5.1.13)$$

where $F_{\hat{\alpha}\hat{\gamma}}$ is given by (4.2.16), with q substituted by $R^{-1}\xi_{m\ell}$ in the arguments of Bessel functions and in all derived quantities (e.g. ω).

Since $\widetilde{\omega} > 0$ for all values of k, ℓ and m when $R\Omega \leq 1$, the integrands in Eqs. (5.1.12) and (5.1.13) are well-behaved. Hence, the t.e.v. of ϕ^2 and the SET are finite everywhere inside the bounding surface. Duffy and Ottewill [33] compare the Planckian forms given by the β^{-4} part of (4.2.51) corresponding to a rigidly rotating thermal distribution at a temperature $T = \beta^{-1} = 20\Omega$ for $R\Omega = 0.5$ and find an excellent agreement far from the bounding surface. The behaviour of the SET deviates from the Planckian forms both as the temperature is decreased and as the bounding surface is approached, in such a way that its value on the bounding surface stays finite, even if the boundary is on the SOL. Figure 5.1 compares the Planckian form:

$$\langle : T_{\hat{t}\hat{t}} : \rangle_\beta^{\text{Planck}} = \frac{\pi^2}{30\beta^4 \varepsilon^3} (\tfrac{4}{3} - \tfrac{1}{3}\varepsilon), \quad (5.1.14)$$

plotted as a dark thin curve, to a numerical evaluation of Eq. (5.1.13) (green curve) for two values of the temperature. It can be seen that the two curves overlap around the rotation axis at $\beta\Omega = 0.05$ but differ everywhere at low temperature $\beta\Omega = 2.0$.

Figure 5.2 shows that the value of the energy density on the rotation axis departs from the Planckian value as the inverse temperature is increased and is even further

(a)   (b)
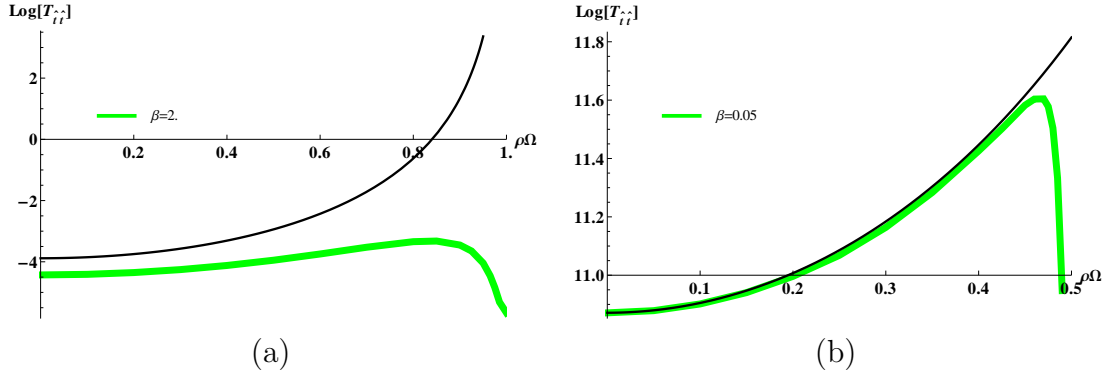
Figure 5.1: The logarithm of $T_{\hat{t}\hat{t}}$ for a rotating system at temperatures (a) $\beta\Omega = 0.05$ and (b) $\beta\Omega = 2$, inside a cylinder located at $R\Omega = 0.5$ (green curve), compared to the Planckian form (5.1.14) (dark thin curve).
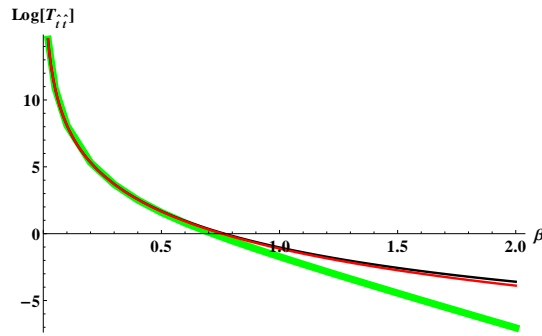
Figure 5.2: The logarithm of $T_{\hat{t}\hat{t}}$ on the rotation axis for a rotating system inside a cylinder located at $R\Omega = 0.5$ as a function of the inverse temperature. The green curve represents numerical results, the red curve is the Planckian form $\langle : T_{\hat{t}\hat{t}} : \rangle_\beta^{\text{Planck}}$ (5.1.14) and the dark curve represents the physical part $\langle : T_{\hat{t}\hat{t}} : \rangle_\beta^{\text{phys}}$ of the t.e.v. of $T_{\hat{t}\hat{t}}$ obtained on the unbounded space-time, given in Eq. (4.2.54b).

away from the physical part $\langle : T_{\hat{t}\hat{t}} : \rangle_\beta^{\text{phys}}$ of the t.e.v. of the SET on the unbounded space, given in Eq. (4.2.54b).

5.1.3   Casimir effect

The presence of the boundary alters the vacuum state. The change in the v.e.v. of the SET due to the confinement of the quantum system inside a boundary is referred to as the Casimir effect [46]. One method of investigating the induced v.e.v.s is to construct the difference between the two Euclidean Green's functions corresponding to the bounded and unbounded systems and then to compute ϕ^2 and the SET using the formulae (2.1.62) and (2.1.63). This subsection mostly reproduces the results of [32, 33] and is included for completeness and to establish notation.

Before making the transition to the Euclidean space-time, it is convenient to switch back to the Minkowski non-rotating coordinates, where the metric has no

components mixing space and time:

$$g^E_{\tau\tau} = g^E_{\rho\rho} = g^E_{zz} = 1, \qquad g^E_{\varphi\varphi} = \rho^2. \tag{5.1.15}$$

In subsection 5.1.2, t.e.v.s are calculated with respect to the Minkowski vacuum, so in this section it is sufficient to calculate expectation values in the bounded vacuum state with respect to the same Minkowski vacuum.

The Euclidean Green's function can be computed as a solution of the Klein-Gordon equation in Euclidean space (2.1.61), which reads:

$$\left(\partial^2_\tau + \partial^2_\rho + \rho^{-1}\partial_\rho + \rho^{-2}\partial^2_\varphi + \partial^2_z - \mu^2\right) G_E(x, x') = -\delta(\tau - \tau')\delta^3(\boldsymbol{x} - \boldsymbol{x}'). \tag{5.1.16}$$

The symmetries of the space-time allow G_E to be Fourier transformed with respect to $\Delta\tau, \Delta z, \Delta\varphi$:

$$G_E(x, x') = \sum_{m=-\infty}^{\infty} \int_{-\infty}^{\infty} d\omega \int_{-\infty}^{\infty} dk \frac{e^{i\omega\Delta\tau + ik\Delta z + im\Delta\varphi}}{8\pi^3} g_E(\omega, m; \rho, \rho'), \tag{5.1.17}$$

The Fourier coefficients g_E are solutions of the inhomogeneous modified Bessel equation (A.1.12):

$$\left[\rho^2\partial^2_\rho + \rho\partial_\rho - (m^2 + \rho^2\alpha^2)\right] g_E = -\rho\delta(\rho - \rho'), \tag{5.1.18}$$

where α is defined as:

$$\alpha^2 = \omega^2 + k^2 + \mu^2. \tag{5.1.19}$$

On the unbounded manifold (i.e. infinite R), the Euclidean Green's function is fixed by requiring regularity at the origin and infinity [19]:

$$G_{E,\infty}(x, x') = \frac{1}{8\pi^3} \sum_{m=-\infty}^{\infty} \int_{-\infty}^{\infty} d\omega \int_{-\infty}^{\infty} dk\, e^{i\omega\Delta\tau + ik\Delta z + im\Delta\varphi} K_m(\alpha\rho_>)I_m(\alpha\rho_<). \tag{5.1.20}$$

Here, $\rho_>$ and $\rho_<$ refer to the larger and smaller of ρ and ρ', respectively, and I_m and K_m are modified Bessel functions, introduced in Appendix A.

In the bounded case, the Euclidean Green's function must satisfy Dirichlet boundary conditions on the bounding cylinder (i.e. when $\rho = R$ or $\rho' = R$). The Euclidean Green's function $G_{E,R}(x, x')$ of the bounded system obeying Dirichlet boundary conditions can be obtained by adding to the unbounded Euclidean function (5.1.20) a solution $\Delta G_{E,R}(x, x') = G_{E,R}(x, x') - G_{E,\infty}(x, x')$ of the homogeneous equivalent of the Klein-Gordon equation (5.1.16) (i.e. with the right hand side set to 0) which is regular inside the boundary, as follows:

$$\Delta G_{E,R}(x, x') = -\frac{1}{8\pi^3} \sum_{m=-\infty}^{\infty} \int_{-\infty}^{\infty} d\omega \int_{-\infty}^{\infty} dk\, e^{i\omega\Delta\tau + ik\Delta z + im\Delta\varphi} \frac{K_m(\alpha R)}{I_m(\alpha R)} I_m(\alpha\rho)I_m(\alpha\rho'). \tag{5.1.21}$$

The v.e.v. of ϕ^2 can be calculated using Eq. (2.1.62):

$$\langle \phi^2 \rangle_{\text{Cas}} = \lim_{x' \to x} \Delta G_E(x, x') = -\frac{1}{8\pi^3} \sum_{m=-\infty}^{\infty} \int_{-\infty}^{\infty} d\omega \int_{-\infty}^{\infty} dk \, \frac{K_m(\alpha R)}{I_m(\alpha R)} I_m^2(\alpha \rho). \quad (5.1.22)$$

The SET can be computed using the formula (2.1.63):

$$T^{\hat{\alpha}}{}_{\hat{\gamma}} = -\frac{1}{48\pi^2} \sum_{m=-\infty}^{\infty} \int_{-\infty}^{\infty} d\omega \int_{-\infty}^{\infty} dk \, \frac{K_m(\alpha R)}{I_m(\alpha R)} E^{\hat{\alpha}}{}_{\hat{\gamma}}, \quad (5.1.23\text{a})$$

where

$$\begin{aligned}
E^{\hat{\tau}}{}_{\hat{\tau}} &= (-\alpha^2 - \rho^{-2}m^2 + 6\omega^2)I_m^2 - \alpha^2 I_m'^{\,2}, \\
E^{\hat{\rho}}{}_{\hat{\rho}} &= (-3\alpha^2 - 3\rho^{-2}m^2)I_m^2 + 2\rho^{-1}\alpha I_m I_m' + 3\alpha^2 I_m'^{\,2}, \\
E^{\hat{\varphi}}{}_{\hat{\varphi}} &= (-\alpha^2 + 5\rho^{-2}m^2)I_m^2 - 2\rho^{-1}\alpha I_m I_m' - \alpha^2 I_m'^{\,2}, \\
E^{\hat{z}}{}_{\hat{z}} &= (-\alpha^2 - \rho^{-2}m^2 + 6k^2)I_m^2 - \alpha^2 I_m'^{\,2}.
\end{aligned} \quad (5.1.23\text{b})$$

The argument of the modified Bessel functions is $\alpha\rho$.

Following [33], the double integral over ω and k in Eqs. (5.1.22) and (5.1.23a) can be viewed as an integral over two-dimensional Euclidean space, admitting a change of variable to polar coordinates (α, θ), as follows:

$$\omega = \sqrt{\alpha^2 - \mu^2} \cos\theta, \quad k = \sqrt{\alpha^2 - \mu^2} \sin\theta. \quad (5.1.24)$$

The Jacobian of the above transformation is $J = \alpha$ and the integration limits for the new variables are $\theta = 0..2\pi$ and $\alpha = \mu..\infty$. The θ integral can be performed analytically and α can be non-dimensionalised to $\mathbf{x} = \alpha R$, yielding:

$$\langle \phi^2 \rangle_{\text{Cas}} = -\frac{1}{4\pi^2 R^2} \sum_{m=-\infty}^{\infty} \int_{\mu R}^{\infty} \mathbf{x} \, d\mathbf{x} \, \frac{K_m(\mathbf{x})}{I_m(\mathbf{x})} I_m^2(\mathbf{x}\bar{\rho}), \quad (5.1.25\text{a})$$

$$\langle T^{\hat{\alpha}}{}_{\hat{\sigma}} \rangle_{\text{Cas}} = -\frac{1}{24\pi^2 R^4} \sum_{m=-\infty}^{\infty} \int_{\mu R}^{\infty} \mathbf{x} \, d\mathbf{x} \frac{K_m(\mathbf{x})}{I_m(\mathbf{x})} \mathcal{E}^{\hat{\alpha}}{}_{\hat{\sigma}},$$

$$\begin{aligned}
\mathcal{E}^{\hat{\tau}}{}_{\hat{\tau}} &= (2\mathbf{x}^2 - 3\mu^2 R^2 - \bar{\rho}^{-2}m^2)I_m^2(\mathbf{x}\bar{\rho}) - \mathbf{x}^2 I_m'^{\,2}(\mathbf{x}\bar{\rho}), \\
\mathcal{E}^{\hat{\rho}}{}_{\hat{\rho}} &= (-3\mathbf{x}^2 - 3\bar{\rho}^{-2}m^2)I_m^2(\mathbf{x}\bar{\rho}) + 2\bar{\rho}^{-1}\mathbf{x} I_m(\mathbf{x}\bar{\rho})I_m'(\mathbf{x}\bar{\rho}) + 3\mathbf{x}^2 I_m'^{\,2}(\mathbf{x}\bar{\rho}), \\
\mathcal{E}^{\hat{\varphi}}{}_{\hat{\varphi}} &= (-\mathbf{x}^2 + 5\bar{\rho}^{-2}m^2)I_m^2(\mathbf{x}\bar{\rho}) - 2\bar{\rho}^{-1}\mathbf{x} I_m(\mathbf{x}\bar{\rho})I_m'(\mathbf{x}\bar{\rho}) - \mathbf{x}^2 I_m'^{\,2}(\mathbf{x}\bar{\rho})
\end{aligned} \quad (5.1.25\text{b})$$

and $\langle T^{\hat{z}}{}_{\hat{z}} \rangle_{\text{Cas}} = \langle T^{\hat{\tau}}{}_{\hat{\tau}} \rangle_{\text{Cas}}$, where $\bar{\rho} = \frac{\rho}{R}$ is defined in Eq. (5.1.11). Introducing the notation:

$$\mathcal{I}_{ln}(\bar{\rho}) = \frac{1}{2\pi^2 R^4} \sum_{m=-\infty}^{\infty} \int_{\mu R}^{\infty} d\mathbf{x} \, \mathbf{x}^l m^n \frac{K_m(\mathbf{x})}{I_m(\mathbf{x})} I_m^2(\mathbf{x}\bar{\rho}) \quad (5.1.26)$$

and using the relations:

$$2\mathbf{x}I_m(\mathbf{x}\overline{\rho})I_m'(\mathbf{x}\overline{\rho}) = \frac{d}{d\overline{\rho}}I_m^2(\mathbf{x}\overline{\rho}),$$

$$\mathbf{x}^2 I_m'{}^2(\mathbf{x}\overline{\rho}) = \left[\frac{1}{2}\frac{d^2}{d\overline{\rho}^2} + \frac{1}{2\overline{\rho}}\frac{d}{d\overline{\rho}} - \mathbf{x}^2 - \overline{\rho}^{-2}m^2\right]I_m^2(\mathbf{x}\overline{\rho}), \qquad (5.1.27)$$

the Eqs. (5.1.25) can be cast in the following form:

$$\langle\phi^2\rangle_{\mathrm{Cas}} = -\frac{R^2}{2}\mathcal{I}_{10}, \qquad (5.1.28a)$$

$$\langle T^{\hat{\tau}}{}_{\hat{\tau}}\rangle_{\mathrm{Cas}} = -\frac{1}{4}\mathcal{I}_{30} + \left(\frac{\mu^2 R^2}{4} + \frac{1}{24}\frac{d^2}{d\overline{\rho}^2} + \frac{1}{24\overline{\rho}}\frac{d}{d\overline{\rho}}\right)\mathcal{I}_{10}, \qquad (5.1.28b)$$

$$\langle T^{\hat{\rho}}{}_{\hat{\rho}}\rangle_{\mathrm{Cas}} = \frac{1}{2}\mathcal{I}_{30} + \frac{1}{2\overline{\rho}^2}\mathcal{I}_{12} - \left(\frac{1}{8}\frac{d^2}{d\overline{\rho}^2} + \frac{5}{24\overline{\rho}}\frac{d}{d\overline{\rho}}\right)\mathcal{I}_{10}, \qquad (5.1.28c)$$

$$\langle T^{\hat{\varphi}}{}_{\hat{\varphi}}\rangle_{\mathrm{Cas}} = -\frac{1}{2\overline{\rho}^2}\mathcal{I}_{12} + \left(\frac{1}{24}\frac{d^2}{d\overline{\rho}^2} + \frac{1}{8\overline{\rho}}\frac{d}{d\overline{\rho}}\right)\mathcal{I}_{10} \qquad (5.1.28d)$$

and $\langle T^{\hat{z}}{}_{\hat{z}}\rangle_{\mathrm{Cas}} = \langle T^{\hat{\tau}}{}_{\hat{\tau}}\rangle_{\mathrm{Cas}}$. As expected by construction, the trace of the stress tensor vanishes if the field is massless:

$$\langle T^{\hat{\alpha}}{}_{\hat{\alpha}}\rangle_{\mathrm{Cas}} = -\mu^2\langle\phi^2\rangle_{\mathrm{Cas}} = \frac{\mu^2 R^2}{2}\mathcal{I}_{10}. \qquad (5.1.29)$$

The asymptotic behaviour (A.2.4) of the modified Bessel functions for large values of their arguments shows that the exponential damping coming from the ratio $K_m(\mathbf{x})/I_m(\mathbf{x})$ disappears on the boundary (when $\overline{\rho} = 1$):

$$\frac{K_m(\mathbf{x})}{I_m(\mathbf{x})}I_m^2(\mathbf{x}) = \frac{1}{2\mathbf{x}}[1 + \mathcal{O}(\mathbf{x}^{-1})], \qquad (5.1.30)$$

hence, the functions $\mathcal{I}_{\ell n}$ in Eq. (5.1.26) cannot converge due to the divergence of the integral over $\mathbf{x}$ at large values of ν and $\mathbf{x}$. The asymptotic behaviour of the functions $\mathcal{I}_{\ell n}$ and of the corresponding expectation values is analysed in the following subsection.

5.1.4 Casimir divergence near the boundary

The expression (5.1.25b) for the SET is obtained from the difference between the Euclidean Green's function (5.1.21) for the space-time bounded by a cylinder of radius R and the one corresponding to the unbounded space-time (5.1.20). Since the former vanishes on the boundary but the latter is known to be singular in the coincidence limit, the SET must diverge as the boundary is approached. Deutsch and Candelas [31] have shown that the divergence can be expressed as a power series in the inverse distance from the surface, which is determined in this section using the methods in Refs. [32, 33].

The conservation equation (3.1.8) is identical when written for tetrad components:

$$\partial_\rho(\rho T^{\hat{\rho}}_{\ \hat{\rho}}) = T^{\hat{\varphi}}_{\ \hat{\varphi}}, \tag{5.1.31}$$

showing that the divergence of $T^{\hat{\rho}}_{\ \hat{\rho}}$ is one order of magnitude less than that of $T^{\hat{\varphi}}_{\ \hat{\varphi}}$. Hence, Eq. (5.1.31) enables the asymptotic behaviour of $T^{\hat{\rho}}_{\ \hat{\rho}}$ to be calculated order by order from that of $T^{\hat{\varphi}}_{\ \hat{\varphi}}$ without looking at the sub-sub-leading terms of its constituent functions $\mathcal{I}_{\ell n}$ in Eq. (5.1.28c).

Equation (5.1.30) shows that the SET diverges due to the behaviour of the integrand in $\mathcal{I}_{ln}$ at large values of α, therefore, the leading orders of the divergence can be safely calculated by considering the field to be massless. The asymptotic analysis of the functions $\mathcal{I}_{ln}$ in Eq. (5.1.26) can be performed after switching the sum over m into an integral:

$$\mathcal{I}_{\ell n} \sim \overline{\mathcal{I}}_{\ell n} = \frac{1}{\pi^2 R^4} \int_0^\infty d\nu \int_0^\infty d\mathbf{x}\, \mathbf{x}^\ell \nu^n \frac{K_\nu(\mathbf{x})}{I_\nu(\mathbf{x})} I_\nu^2(\mathbf{x}\overline{\rho}), \tag{5.1.32}$$

as explained in the following paragraph.

Application of the Abel-Plana sum formula for the conversion of a sum to an integral

With the aid of Cauchy's theorem of residues, a rigorous formula can be obtained for connecting a sum over integer values m into an integral, called the Abel-Plana sum formula [64]:

$$\sum_{m=0}^\infty f(m) = \frac{1}{2}f(0) + \int_0^\infty d\nu\, f(\nu) + i \int_0^\infty dt \frac{f(it) - f(-it)}{e^{2\pi t} - 1}$$
$$+ i\pi \left\{ \sum_k \text{sgn}(\mathfrak{Im}z_{f,k})\text{Res}_{\mathfrak{Re}z>0}[f(z)] - i \sum_k \text{sgn}(\mathfrak{Im}z_{f,k})\text{Res}_{\mathfrak{Re}z_{f,k}>0}[f(z)\cot \pi z] \right\}, \tag{5.1.33}$$

where the sum over k runs over the poles of $f(z)$ located in the upper complex plane (where $\mathfrak{Re}z > 0$) and $\text{Res}_{\mathfrak{Re}z_{f,k}>0}[f(z)]$ represents the residue of the function f at its k'th pole. For the conversion of the sum over m in Eq. (5.1.26) to the integral over ν in Eq. (5.1.32), the functions $f(m)$ of interest are:

$$f_{\ell n}(m, \overline{\rho}) = \int_0^\infty d\mathbf{x}\, \mathbf{x}^\ell m^n \frac{K_m(\mathbf{x})}{I_m(\mathbf{x})} I_m^2(\mathbf{x}\overline{\rho}). \tag{5.1.34}$$

This conversion is worthwhile only if the difference $\delta(\bar{\rho})$ between the sum over m and the integral over ν, defined as:

$$\delta(\bar{\rho}) = \sum_{m=-\infty}^{\infty} f(m) - 2 \int_0^{\infty} d\nu \, f(\nu), \qquad (5.1.35)$$

does not diverge (or if it diverges at a subleading order) as $\bar{\rho} \to 1$.

The residues in Eq. (5.1.33) vanish when $\bar{\rho} = 1$, therefore, they can be ignored in this analysis. Since only even values of n are relevant, $f_{ln}(-m,\bar{\rho}) = f_{ln}(m,\bar{\rho})$. Given that $K_{-i\nu}(z) = K_{i\nu}(z)$ and $I_{-i\nu}(z) = I_{i\nu}^*(z)$ for real z, the difference $\delta(\bar{\rho})$ can be written as:

$$\delta(\bar{\rho}) = -4 \int_0^{\infty} \frac{dt}{e^{2\pi t} - 1} \int_0^{\infty} d\mathbf{x} \, \mathbf{x}^{\ell} (it)^n K_{it}(\mathbf{x}) \mathfrak{Im} \left[\frac{I_{it}^2(\mathbf{x}\bar{\rho})}{I_{it}(\mathbf{x})} \right]. \qquad (5.1.36)$$

The relations (A.1.20) can be used to simplify Eq. (5.1.36) when $\bar{\rho} = 1$ (i.e. on the boundary):

$$\delta(\bar{\rho}) = \frac{4}{\pi} \int_0^{\infty} \frac{dt}{e^{2\pi t} - 1} \int_0^{\infty} d\mathbf{x} \, \mathbf{x}^{\ell} (it)^n K_{it}^2(\mathbf{x}). \qquad (5.1.37)$$

The double integral is now damped in both variables, i.e. by the term $(e^{2\pi t} - 1)^{-1}$ in the t variable and by $K_{it}^2(\mathbf{x})$ in the $\mathbf{x}$ variable. Thus, the approximation $\overline{\mathcal{I}}_{\ell n}$ (5.1.32) exhibits the same divergent behaviour as $\mathcal{I}_{\ell n}$.

Building blocks for the analysis of the Casimir divergence

The analysis of the Casimir divergence for scalars in a cylinder has been performed in Ref. [32]. For completeness, this paragraph presents the details of the calculation. Since the divergence is due to the behaviour of the integrand at large ν and $\mathbf{x}$, the Bessel functions can be replaced by the uniform asymptotic expressions given in Eqs. (A.2.5) and the lower limit of the $\mathbf{x}$ can be approximated to 0. After a change in Eq. (5.1.32) to polar variables $(\nu, \alpha) = (r \cos\theta, r \sin\theta)$, $\overline{\mathcal{I}}_{ln}$ takes the form:

$$\overline{\mathcal{I}}_{\ell n} = \frac{1}{\pi^2 R^4} \int_0^{\frac{\pi}{2}} d\theta \int_0^{\infty} dr \, r^{\ell+n+1} \cos^n\theta \sin^\ell\theta \frac{K_{r\cos\theta}(r\sin\theta)}{I_{r\cos\theta}(r\sin\theta)} I_{r\cos\theta}^2(r\sin\theta\bar{\rho}). \qquad (5.1.38)$$

The asymptotic expansions in Eqs. (A.2.5) can be used to obtain the following expressions:

$$\frac{K_{r\cos\theta}(r\sin\theta)}{I_{r\cos\theta}(r\sin\theta)} = \pi e^{-2r - 2\nu \ln \frac{\sin\theta}{1+\cos\theta}} \left[1 - \frac{3 - 5\cos^2\theta}{12r} + O(r^{-1}) \right], \qquad (5.1.39a)$$

$$I_{r\cos\theta}^2(\bar{\rho}r\sin\theta) = \frac{1}{2\pi\bar{r}} e^{2\bar{r} + 2\nu \ln \frac{\bar{\rho}\sin\theta}{r - 1\bar{r} + \cos\theta}} \left[1 + \frac{3 - 5\frac{r^2}{\bar{r}^2}\cos^2\theta}{12\bar{r}} + O(r^{-1}) \right], \qquad (5.1.39b)$$

where $\bar{r} = \sqrt{\nu^2 + \mathbf{x}^2\bar{\rho}^2}$. Introducting the small quantity

$$\epsilon = 1 - \bar{\rho}, \tag{5.1.40}$$

to obtain the leading and next-to-leading order divergent terms, it is sufficient to ensure the correct capture of the terms of order ϵ and r^{-1}, ignoring any terms of order ϵ^2, ϵr^{-1} and r^{-2}, for reasons which will become apparent shortly.

Using the following intermediate approximations:

$$\frac{\bar{r}}{r} = 1 - \epsilon \sin^2\theta + \tfrac{\epsilon^2}{2}\sin^2\theta\cos^2\theta + O(\epsilon^3), \tag{5.1.41a}$$

$$\frac{r}{\bar{r}} = 1 + \epsilon \sin^2\theta + \tfrac{\epsilon^2}{2}\sin^2\theta(1 + \sin^2\theta) + O(\epsilon^3), \tag{5.1.41b}$$

$$\ln\frac{\bar{\rho}\sin\theta}{\frac{\bar{r}}{r} + \cos\theta} = \ln\frac{\sin\theta}{1 + \cos\theta} - \epsilon\cos\theta - \tfrac{1}{2}\epsilon^2\cos\theta(1 + \sin^2\theta) + O(\epsilon^3), \tag{5.1.41c}$$

the exponent in Eq. (5.1.39b) can be approximated as:

$$2\bar{r} + 2\nu\ln\frac{\bar{\rho}\sin\theta}{r^{-1}\bar{r} + \cos\theta} = 2r + 2\nu\ln\frac{\sin\theta}{1 + \cos\theta} - 2r\epsilon - r\epsilon^2\cos^2\theta + \dots, \tag{5.1.41d}$$

leading to the following asymptotic expansion:

$$\frac{K_\nu(\mathbf{x})}{I_\nu(\mathbf{x})}I_\nu^2(\mathbf{x}\bar{\rho}) = \frac{e^{-2r\epsilon}}{2r}\left[1 + \epsilon\sin^2\theta - \epsilon^2 r\cos^2\theta + \dots\right], \tag{5.1.42}$$

where terms of order r^{-2}, ϵr^{-1} and ϵ^2 have been ignored in the square brackets. The r integral in Eq. (5.1.38) can be written using Gamma functions. It can be seen that each power of r^{-1} in the integrand will contribute a term of order ϵ, hence, the integral (5.1.38) reduces to:

$$\begin{aligned}
\mathcal{I}_{\ell n} &\sim \frac{1}{2\pi^2 R^4}\int_0^{\frac{\pi}{2}}d\theta\int_0^\infty dr\, e^{-2r\epsilon}r^{\ell+n+1}\cos^n\theta\sin^\ell\theta[1 + \epsilon\sin^2\theta - \epsilon^2 r\cos^2\theta + \dots]\\
&= \frac{(l+n)!}{2(2\epsilon)^{l+n+1}\pi^2 R^4}\int_0^{\frac{\pi}{2}}d\theta\cos^n\theta\sin^\ell\theta\left\{1 + [\sin^2\theta - \tfrac{l+n+1}{2}\cos^2\theta]\epsilon + \dots\right\}.
\end{aligned} \tag{5.1.43}$$

Performing the θ integral for the first two terms in the integrand in (5.1.43) gives the leading and next-to-leading terms for the four cases of interest:

$$\begin{aligned}
\bar{\mathcal{I}}_{10} &= \frac{1}{8\pi^2\epsilon^2 R^4}\left[1 + \tfrac{1}{3}\epsilon + O(\epsilon^2)\right],\\
\bar{\mathcal{I}}_{30} &= \frac{1}{8\pi^2\epsilon^4 R^4}\left[1 + \tfrac{2}{5}\epsilon + O(\epsilon^2)\right],\\
\bar{\mathcal{I}}_{12} &= \frac{1}{16\pi^2\epsilon^4 R^4}\left[1 - \tfrac{4}{5}\epsilon + O(\epsilon^2)\right].
\end{aligned} \tag{5.1.44}$$

Result

Having calculated the asymptotic expansions (5.1.44) of $\overline{\mathcal{I}}_{ln}$, Eqs. (5.1.28) can be used to find the asymptotic forms of ϕ^2 and $T^{\hat{\alpha}}_{\hat{\gamma}}$:

$$\langle \phi^2 \rangle_{\text{Cas}} = -\frac{1}{16\pi^2 R^2 \epsilon^2}[1 + \tfrac{1}{3}\epsilon + O(\epsilon^2)], \tag{5.1.45a}$$

$$\langle T^{\hat{\tau}}_{\hat{\tau}} \rangle_{\text{Cas}} = \frac{1}{720\pi^2 R^4 \epsilon^3} + O(\epsilon^{-2}), \tag{5.1.45b}$$

$$\langle T^{\hat{\rho}}_{\hat{\rho}} \rangle_{\text{Cas}} = -\frac{1}{720\pi^2 R^4 \epsilon^2} + O(\epsilon^{-1}), \tag{5.1.45c}$$

$$\langle T^{\hat{\varphi}}_{\hat{\varphi}} \rangle_{\text{Cas}} = -\frac{1}{360\pi^2 R^4 \epsilon^3} + O(\epsilon^{-2}) \tag{5.1.45d}$$

and $\langle T^{\hat{z}}_{\hat{z}} \rangle_{\text{Cas}} = \langle T^{\hat{\tau}}_{\hat{\tau}} \rangle_{\text{Cas}}$. In the above, $\epsilon = 1 - \overline{\rho}$. The asymptotic form of $T^{\hat{\rho}}_{\hat{\rho}}$ was found using Eq. (5.1.31). Equations (5.1.28) and (5.1.44) show that the mass terms make subleading contributions to the SET. Hence, the Casimir divergence of massive scalars near the boundary has the same order of magnitude as that of massless scalars. Equation (5.1.45) is in exact agreement with the results reported in Refs. [31, 32, 33].

5.1.5   Summary

The removal of the space outside the speed of light surface (SOL) by enclosing the system inside a boundary renders t.e.v.s regular at every point inside of it, but only if its location is inside or on the SOL. If the boundary is placed outside the SOL, the old problems of modes with vanishing frequencies but non-vanishing Minkowski energies return. The Planckian forms of Ref. [33] give an excellent approximation of the t.e.v.s of ϕ^2 and the SET around the rotation axis at large enough temperatures. The correction terms calculated in subsection 4.2.2 would become important as $\beta\Omega$ is increased, however, the effect of the boundary becomes highly pronounced as β increases, causing the t.e.v.s to deviate from the analytic expressions obtained in the unbounded case, as shown in Figure 5.2.

An analysis of the expectation values evaluated in the vacuum state of the bounded system with respect to the unbounded vacuum, induced through the Casimir effect, shows that they exhibit the Casimir divergence, diverging as inverse powers of the distance to the boundary. The leading order of the divergences is in complete agreement with the results presented in Refs. [31, 33].

5.2 Dirac fermions obeying spectral boundary conditions

Since the Dirac equation is of first order, its initial (boundary) conditions are also of first order. Hence, the standard Dirichlet or Neumann boundary conditions which can be used with the second-order Klein-Gordon equation cannot be used for fermions. For any choice of boundary conditions, the resulting theory must preserve the self-adjointness of the Dirac Hamiltonian, as discussed at the end of subsection 2.2.3. The problem is equivalent to requiring that the time derivative of the inner product of any two solutions of the Dirac equation, given in Eq. (2.2.31) in terms of a surface integral, vanishes. For the case of a cylindrical boundary, Eq. (2.2.31) reduces to:

$$\partial_t \langle \psi, \chi \rangle = R \int_{-\infty}^{\infty} dz \int_0^{2\pi} d\varphi \, \overline{\psi} \gamma^{\hat{\rho}} \chi + \int_0^{\infty} \rho \, d\rho \int_0^{2\pi} d\varphi \, \overline{\psi} \gamma^{\hat{\rho}} \chi \bigg|_{z=-\infty}^{z=\infty}, \qquad (5.2.1)$$

where ψ and χ are arbitrary solutions of the Dirac equation. The last term above can be written in integral form as $\int dz \, \partial_z \ldots$, which vanishes as the basis modes are eigenvectors of $P^z = -i\partial_z$, implying that the result of the z integral thus introduced is of the form $(k - k')\delta(k - k')$.

In this section, the spectral model [43] is considered. The formulation of the boundary conditions, mode solutions and energy spectrum are discussed in subsection 5.2.1. Thermal states are discussed in subsection 5.2.2 and the Casimir effect is investigated in subsection 5.2.3. The thermal expectation values obtained with the spectral model are compared with those obtained in the MIT model in subsection 5.3.2. Finally, an analysis of the energy density on the rotation axis and on the boundary is provided in subsection 5.4.1, while the case when the SOL is inside the boundary is analysed in sections 5.4.2 and 6.2.

5.2.1 Boundary conditions and mode solutions

As discussed at the beginning of section 5.2, the self-adjointness of the Hamiltonian is guaranteed if the inner product of any two solutions of the Dirac equation is time-independent. For the spectral boundary conditions, this is implemented by ensuring that the inner product of any two modes from the set of mode solutions is time-independent.

Discretisation of transverse momentum

Since the boundary does not change the form of the Dirac equation, the solutions have the same coordinate dependence as the solutions in the unbounded case, given

in Eqs. (3.3.2) and (3.3.23a). Hence, the mode solutions satisfying spectral boundary conditions can be introduced as:

$$U^{\mathrm{sp};\lambda}_{km\ell;E}(x) = \mathcal{C}^{\mathrm{sp};\lambda}_{km\ell;E}U^{\lambda}_{Ekm}(x), \qquad V^{\mathrm{sp};\lambda}_{km\ell;E}(x) = \mathcal{C}^{\mathrm{sp};\lambda\,*}_{km\ell;E}V^{\lambda}_{Ekm}(x), \tag{5.2.2}$$

where $E \equiv E_{m\ell} = \pm\sqrt{\mu^2 + q_{m\ell}^2 + k^2}$ controls the sign of the Minkowski energy (i.e. either plus or minus) and the label ℓ indexes the discrete set of transverse momenta that ensures the time-invariance of the Dirac inner product, as will be discussed shortly. The constants $\mathcal{C}^{\lambda\,*}_{km\ell;E}$ have been introduced to normalise the modes with respect to the inner product (5.2.8) corresponding to the bounded system. Choosing ψ and χ in Eq. (5.2.1) as combinations of the above modes yields:

$$\partial_t \langle U^{\mathrm{sp};\lambda}_{km\ell;E}, U^{\mathrm{sp};\lambda'}_{k'm'\ell';E'} \rangle = \frac{R}{2}\delta(k-k')\delta_{mm'}\mathcal{C}^{\mathrm{sp};\lambda\,*}_{km\ell}\mathcal{C}^{\mathrm{sp};\lambda'}_{km\ell'}e^{i(\widetilde{E}-\widetilde{E}')t}$$
$$\times\left(\frac{2\lambda'E'}{|E'|}\mathfrak{E}_+\mathfrak{E}'_- + \frac{2\lambda E}{|E|}\mathfrak{E}_-\mathfrak{E}'_+\right)$$
$$\times\left[2i\lambda'\mathfrak{p}_\lambda\mathfrak{p}'_{-\lambda'}J_m(q_{m\ell}R)J_{m+1}(q_{m\ell'}R) - 2i\lambda\mathfrak{p}_{-\lambda}\mathfrak{p}'_{\lambda'}J_{m+1}(q_{m\ell}R)J_m(q_{m\ell'}R)\right], \tag{5.2.3a}$$

$$\partial_t \langle U^{\mathrm{sp};\lambda}_{km\ell;E}, V^{\mathrm{sp};\lambda'}_{k'm'\ell';E'} \rangle = \frac{R}{2}(-1)^{m+1}\delta(k+k')\delta_{m,-m'-1}\mathcal{C}^{\mathrm{sp};\lambda\,*}_{km\ell}\mathcal{C}^{\mathrm{sp};\lambda'\,*}_{-k,-m-1,\ell'}e^{i(\widetilde{E}+\widetilde{E}')t}$$
$$\times\left(\mathfrak{E}_+\mathfrak{E}'_+ - \frac{2\lambda E}{|E|}\frac{2\lambda'E'}{|E'|}\mathfrak{E}_-\mathfrak{E}'_-\right)$$
$$\times\left[\mathfrak{p}_\lambda\mathfrak{p}'_{\lambda'}J_m(q_{m\ell}R)J_{m+1}(q_{-m-1,\ell'}R) + 4\lambda\lambda'\mathfrak{p}_{-\lambda}\mathfrak{p}'_{-\lambda'}J_{m+1}(q_{m\ell}R)J_m(q_{-m-1,\ell'}R)\right], \tag{5.2.3b}$$

where $\mathfrak{E}_\pm$ and $\mathfrak{p}_\pm$ are defined in Eqs. (3.3.17) and (3.3.12), respectively and $\widetilde{E} = E - \Omega(m+\frac{1}{2})$ is defined in Eq. (4.3.3). One way to make the above time derivatives vanish is to choose $q_{m\ell}$ such that each term in the square brackets vanishes individually. As discussed in Ref. [43], Eqs. (5.2.3) can be simultaneously set to 0 by making $q_{m\ell}$ a root of J_m for positive values of m and of J_{-m-1} if m is negative, i.e.

$$q_{m\ell}R = \begin{cases} \xi_{m\ell} & m+\frac{1}{2} > 0, \\ \xi_{-m-1,\ell} & m+\frac{1}{2} < 0, \end{cases} \tag{5.2.4}$$

where $\xi_{m\ell}$ is the ℓ'th root of J_m (i.e. $J_m(\xi_{m\ell}) = 0$ for all $\ell = 1,2,\dots$ and $\xi_{m\ell} < \xi_{m,\ell+1}$).

To understand why Eq. (5.2.4) is referred to as spectral boundary conditions by the authors of Ref. [43], consider a solution $\psi(x)$ of the Dirac equation. On the boundary, ψ can be Fourier-transformed with respect to the angular coordinate φ:

$$\psi(x) = \sum_{m=-\infty}^{\infty} e^{im\varphi}\psi_m(t,R,z). \tag{5.2.5}$$

Schematically, the top component of the four-spinor $\psi_m(t, R, z)$ corresponding to the particle modes $U_{km\ell}^{\text{sp};\lambda}$ is proportional to $J_m(q_{m\ell}R)$, while that of the anti-particle modes $V_{km\ell}^{\text{sp};\lambda}$ is proportional to $J_m(q_{-m-1,\ell}R)$. If $m > 0$, $J_m(q_{m\ell}R) = 0$ and also $J_{m\ell}(q_{-m-1,\ell}) = 0$, by virtue of the second branch of Eq. (5.2.4). When m is negative, the top component of $\psi_m(t, R, z)$ no longer vanishes. However, its second component corresponding to particle and anti-particle modes is of the form $J_m(q_{m-1,\ell})$ and $J_m(q_{-m,\ell})$, respectively. Neither of these vanish for positive m, but at negative values of m, both the particle and the anti-particle contributions to this second component vanish. Moreover, when the first component vanishes, so does the third, and similarly for the second and fourth components. Hence, the boundary conditions (5.2.4) ensure that the first and third components of the Fourier components of any solution of the Dirac equation with positive spectral index (positive $m+\frac{1}{2}$) vanish on the boundary, while for negative spectral indices, the second and fourth components vanish. Thus, the scheme earns its name of spectral boundary conditions.

Alternatively, Berry and Mondragon [15] suggested setting to 0 the right-hand side of Eq. (5.2.3) as a whole, keeping individual terms finite, implying:

$$J_{m+1}(qR) = J_m(qR)\text{sgn}(m + \tfrac{1}{2})\frac{2\lambda p + k}{q}. \tag{5.2.6}$$

The signum function is there to preserve the charge conjugation invariance of the theory, ensuring that each V mode is obtained from a U mode through the charge conjugation operation. In this case, the discrete spectrum of the transverse momentum depends on k, m and λ, making its numerical implementation less tractable. We therefore do not consider this possibility further.

Energy spectrum

As in the scalar case, Eq. (5.1.6) can be used to show that

$$\widetilde{E}_{m\ell}R \geq \widetilde{E}_{m1}R > (1 - \Omega R)(m + \tfrac{1}{2}), \tag{5.2.7}$$

for $E > 0$. As discussed in subsection 4.3.1, $E\widetilde{E} > 0$ for all modes as long as the boundary is inside or on the SOL ($\Omega R \leq 1$). Hence, the zones I and III in Figure 4.1 contain no particle states, making the Minkowski (Vilenkin) and rotating (Iyer) vacua equivalent.

Normalisation

The modes (4.3.2a) and their charge conjugates (4.3.2b) must be normalised with respect to the Dirac inner product (2.2.30), which in the case under consideration takes the form:

$$\langle \psi, \chi \rangle = \int_{-\infty}^{\infty} dz \int_0^{2\pi} d\varphi \int_0^R d\rho\, \rho\, \psi^\dagger(x)\chi(x). \tag{5.2.8}$$

For the case of two particle modes $U^\lambda_{km\ell;E}$ and $U^{\lambda'}_{k'm'\ell';E'}$, the above reads:

$$\langle U^{\text{sp};\lambda}_{km\ell;E}, U^{\text{sp};\lambda'}_{k'm'\ell';E'} \rangle = \frac{1}{2} \mathcal{C}^\lambda_{km\ell;E} \mathcal{C}^{\lambda''}_{km\ell';E'} \delta(k-k')\delta_{mm'} e^{i(\widetilde{E}-\widetilde{E}')t}$$
$$\times \left(\mathfrak{E}_+ \mathfrak{E}'_+ + 4\lambda\lambda' \frac{EE'}{|EE'|} \mathfrak{E}_- \mathfrak{E}'_- \right)$$
$$\times \left[\mathfrak{p}_\lambda \mathfrak{p}'_{\lambda'} \int_0^R J_m(q\rho) J_m(q'\rho) \rho \, d\rho + 4\lambda\lambda' \mathfrak{p}_{-\lambda} \mathfrak{p}'_{-\lambda'} \int_0^R J_{m+1}(q\rho) J_{m+1}(q'\rho) \rho \, d\rho \right], \tag{5.2.9}$$

where the m and ℓ indices have been omitted on q, q' and any derived quantities, as there is no risk of confusion. Its value is determined by requiring that the right-hand side of the above reads $\delta(k-k')\delta_{mm'}\delta_{\ell\ell'}\delta_{\lambda\lambda'}\theta(EE')$. Since the boundary conditions preserve the self-adjointness of the Hamiltonian, the time-independence of the inner product requires modes of differing energies $\widetilde{E} - \widetilde{E}' \neq 0$ to be orthogonal. For the evaluation of the integrals of the Bessel functions when $q = q'$, it is convenient to use the following results [37]:

$$\mathfrak{I}^+_m = \int_0^R d\rho \, \rho \, \frac{1}{2}[J_m^2(q\rho) + J_{m+1}^2(q\rho)]$$
$$= \frac{R^2}{2} \left[J_{m+1}^2(qR) - \frac{2m+1}{qR} J_m(qR) J_{m+1}(qR) + J_m^2(qR) \right],$$
$$\mathfrak{I}^-_m = \int_0^R d\rho \, \rho \, \frac{1}{2}[J_m^2(q\rho) - J_{m+1}^2(q\rho)] = \frac{R}{2q} J_m(qR) J_{m+1}(qR), \tag{5.2.10}$$

where the integrals of the Bessel functions have been performed using Eqs. (A.3.6). The spectral boundary conditions ensure that the product $J_m(qR)J_{m+1}(qR)$ vanishes for all m. For positive $m + \frac{1}{2}$, the normalisation constants take the following values:

$$\mathcal{C}^{\text{sp};\lambda}_{km\ell;E} = \mathcal{C}^{\text{sp};\lambda}_{k,-m-1,\ell;E} = \frac{1}{R \, |J_{m+1}(\xi_{m,\ell})|} \qquad (m + \tfrac{1}{2} > 0). \tag{5.2.11}$$

Using Eq. (3.3.29), it can be seen that the particle modes obeying spectral boundary conditions are linked with anti-particle modes via:

$$V^{\text{sp};\lambda}_{km\ell;E}(x) = (-1)^m \frac{iE}{|E|} U^{\text{sp};\lambda}_{-k,-m-1,\ell;-E}(x). \tag{5.2.12}$$

Second quantisation

Having completed the construction of the set of mode solutions of the Dirac equation obeying spectral boundary conditions on the bounding cylinder, the field operator

can be written as:

$$\psi_{\rm sp}(x) = \sum_j \theta(\widetilde{E}_j) \left[U_j^{\rm sp}(x) b_{I;j}^{\rm sp} + V_j^{\rm sp}(x) d_{I;j}^{\rm sp\,\dagger} \right] \tag{5.2.13a}$$

$$= \sum_j \theta(E_j) \left[U_j^{\rm sp}(x) b_{V;j}^{\rm sp} + V_j^{\rm sp}(x) d_{V;j}^{\rm sp\,\dagger} \right], \tag{5.2.13b}$$

with respect to Iyer's and Vilenkin's vacua, respectively, as discussed at the end of Sec. 4.3.1. In the spectral case, $j = (k_j, m_j, \ell_j, \lambda_j)$ and

$$\sum_j \equiv \sum_{m_j=-\infty}^{\infty} \sum_{\ell_j=1}^{\infty} \int_{-\infty}^{\infty} dk_j \sum_{E_j=\pm|E_j|} \sum_{\lambda_j=\pm 1/2}. \tag{5.2.14}$$

5.2.2 Thermal expectation values

In this subsection, the thermal expectation values (t.e.v.s) of the fermion condensate $\overline{\psi}\psi$ (FC), charge current J^μ (CC) and stress-energy tensor $T_{\mu\nu}$ (SET) are calculated following the methods introduced in subsection 4.3.2.

Formally, the thermal Hadamard function has the same expression as in Eq. (3.3.54) for the unbounded rotating space-time, but the Fourier coefficients $M_{km\ell}$, given in (3.3.60), now have different normalisation:

$$4\pi^2 R^2 J_{m+1}^2(\xi_{m\ell}) M_{km\ell} = \left[\frac{\mu}{E} I_2 + \sigma_3 \right] \otimes \left[\begin{pmatrix} 1 & 0 \\ 0 & 1 \end{pmatrix} \circ \mathcal{M}_j \right]$$
$$+ \frac{1}{E} \begin{pmatrix} 0 & -1 \\ 1 & 0 \end{pmatrix} \otimes \left[\begin{pmatrix} k & q \\ q & -k \end{pmatrix} \circ \mathcal{M}_j \right], \tag{5.2.15}$$

where $\mathcal{M}_j$ is given in Eq. (3.3.58). The indices m and ℓ have been omitted on q and derived quantities.

Fermion condensate

As previously, Eq. (2.2.55a) can be used to calculate the t.e.v. of the FC using the expression (3.3.54) for the Hadamard function:

$$\langle : \overline{\psi}\psi : \rangle_\beta^{\rm spec} = -\sum_{m=0}^{\infty} \sum_{\ell=1}^{\infty} \int_0^{\infty} \frac{\mu dk}{E\pi^2 R^2} \frac{w(\widetilde{E}) + w(\overline{E})}{J_{m+1}^2(qR)} J_m^+(q\rho), \tag{5.2.16}$$

where

$$\widetilde{E} = E - \Omega(m + \tfrac{1}{2}), \qquad \overline{E} = E + \Omega(m + \tfrac{1}{2}) \tag{5.2.17}$$

and the thermal factors w depend on the vacuum state as shown in Eqs. (4.3.14) and $J_m^*(q\rho)$ is defined in Eq. (3.3.69). As before, the indices m and ℓ are omitted to simplify notation. Hence, in the spectral model, the t.e.v. of the FC vanishes when massless fermions are considered.

Neutrino charge current

While the t.e.v. of all components of the CC vanish, there is, as in the rotating unbounded case, a non-vanishing neutrino current along the rotation axis:

$$\langle : J_\nu^{\hat{z}} : \rangle_\beta^{\text{spec}} = \sum_{m=0}^\infty \sum_{\ell=1}^\infty \int_0^\infty \frac{dk}{2\pi^2 R^2} \frac{w(\widetilde{E}) - w(\overline{E})}{J_{m+1}^2(qR)} J_m^-(q\rho). \tag{5.2.18}$$

It can be seen that the sign of the charge current changes from negative on the rotation axis to positive on the boundary (the weight factors $w(\widetilde{E})$ and $w(\overline{E})$ are negative):

$$\langle : J_\nu^{\hat{z}} : \rangle_\beta^{\text{spec}} \bigg|_{\rho=0} = \sum_{l=1}^\infty \int_0^\infty \frac{dk [w(\widetilde{E}) - w(\overline{E})]}{2\pi^2 R^2 J_1(qR)}, \tag{5.2.19a}$$

$$\langle : J_\nu^{\hat{z}} : \rangle_\beta^{\text{spec}} \bigg|_{\rho=R} = -\sum_{m=0}^\infty \sum_{l=1}^\infty \int_0^\infty \frac{dk [w(\widetilde{E}) - w(\overline{E})]}{2\pi^2 R^2}. \tag{5.2.19b}$$

Stress-energy tensor

The following results are obtained:

$$\langle : T_{\hat{t}\hat{t}} : \rangle_\beta^{\text{spec}} = -\sum_{m=0}^\infty \sum_{\ell=1}^\infty \int_0^\infty \frac{E dk}{\pi^2 R^2} \frac{w(\widetilde{E}) + w(\overline{E})}{J_{m+1}^2(qR)} J_m^+(q\rho), \tag{5.2.20a}$$

$$\langle : T_{\hat{\rho}\hat{\rho}} : \rangle_\beta^{\text{spec}} = -\sum_{m=0}^\infty \sum_{\ell=1}^\infty \int_0^\infty \frac{q^2 dk}{E\pi^2 R^2} \frac{w(\widetilde{E}) + w(\overline{E})}{J_{m+1}^2(qR)} \left[J_m^+(q\rho) - \frac{m + \frac{1}{2}}{q\rho} J_m^\times(q\rho) \right],$$

$$\langle : T_{\hat{\varphi}\hat{\varphi}} : \rangle_\beta^{\text{spec}} = -\sum_{m=0}^\infty \sum_{\ell=1}^\infty \int_0^\infty \frac{q dk}{\rho E\pi^2 R^2} \frac{w(\widetilde{E}) + w(\overline{E})}{J_{m+1}^2(qR)} (m + \tfrac{1}{2}) J_m^\times(q\rho),$$

$$\langle : T_{\hat{z}\hat{z}} : \rangle_\beta^{\text{spec}} = -\sum_{m=0}^\infty \sum_{\ell=1}^\infty \int_0^\infty \frac{k^2 dk}{E\pi^2 R^2} \frac{w(\widetilde{E}) + w(\overline{E})}{J_{m+1}^2(qR)} J_m^+(q\rho),$$

$$\langle : T_{\hat{t}\hat{\varphi}} : \rangle_\beta^{\text{spec}} = \sum_{m=0}^\infty \sum_{\ell=1}^\infty \int_0^\infty \frac{dk}{\rho\pi^2 R^2} \frac{w(\widetilde{E}) - w(\overline{E})}{J_{m+1}^2(qR)}$$
$$\times \left[(m + \tfrac{1}{2}) J_m^+(q\rho) - \tfrac{1}{2} J_m^-(q\rho) + q\rho J_m^\times(q\rho) \right], \tag{5.2.20b}$$

where the relation

$$J_{m+1}'(z) J_m(z) - J_m'(z) J_{m+1}(z) = J_m^+(z) - z^{-1}(m + \tfrac{1}{2}) J_m^\times(z) \tag{5.2.21}$$

has been used to obtain the expression for $\langle : T_{\hat{\rho}\hat{\rho}} : \rangle_\beta$. Equations (5.2.20) can be used to check the identity:

$$\langle : T^{\hat{\alpha}}_{\ \hat{\alpha}} : \rangle_\beta^{\text{spec}} = -\mu \, \langle : \overline{\psi}\psi : \rangle_\beta^{\text{spec}} . \tag{5.2.22}$$

Numerical results

In this section, the results of the numerical integration of the exact expression for the t.e.v.s of the fermion condensate (5.2.16), charged current (5.2.18) and SET (5.2.20) are shown and compared with the Planckian forms given by the leading terms in inverse powers of β in Eqs. (4.3.50). The Planckian forms for the fermion condensate (FC) and charge current (CC) are given in Eqs. (4.3.54a) and (4.3.54b), respectively. The Planckian forms for the stress-energy tensor (SET) are:

$$\langle : T_{\hat{t}\hat{t}} : \rangle_\beta^{\text{Planck}} = \frac{7\pi^2}{60\beta^4\varepsilon^3} \left(\tfrac{4}{3} - \tfrac{1}{3}\varepsilon \right) , , \tag{5.2.23a}$$

$$\langle : T_{\hat{\varphi}\hat{t}} : \rangle_\beta^{\text{Planck}} = -\rho\Omega \frac{7\pi^2}{45\beta^4\varepsilon^3} , \tag{5.2.23b}$$

$$\langle : T_{\hat{\rho}\hat{\rho}} : \rangle_\beta^{\text{Planck}} = \langle : T_{\hat{z}\hat{z}} : \rangle_\beta^{\text{Planck}} = \frac{7\pi^2}{180\beta^4\varepsilon^2} , \tag{5.2.23c}$$

$$\langle : T_{\hat{\varphi}\hat{\varphi}} : \rangle_\beta^{\text{Planck}} = \frac{7\pi^2}{180\beta^4\varepsilon^3} (4 - 3\varepsilon) \tag{5.2.23d}$$

In Figures 5.3, 5.4 and 5.5, numerical results for massless ($\mu = 0$) and massive ($\mu = 2\Omega$) fermions are represented with thick, dashed coloured lines and thin coloured lines, respectively, at four values of the inverse temperature β. The Planckian forms discussed above are shown for comparison using thin black lines for each value of the inverse temperature β, except when the corresponding profile is off the scale, as explained in the figure captions. It can be seen that increasing the mass of the field quanta sets the profiles of the corresponding t.e.v.s lower than in the case of massless fermions. The plots include results when the boundary is located on (left hand side) or half way (right hand side) between the rotation axis and the speed of light surface (SOL).

Two distinctive features set the spectral model apart from the MIT model, presented in section 5.3: firstly, the parity-violating neutrino charge current changes sign and becomes parallel to the angular velocity of the rotation (as opposed to anti-parallel in the unbounded case); secondly, $\langle : T_{\hat{\varphi}\hat{\varphi}} : \rangle_\beta^{\text{spec}}$ vanishes on the boundary.

According to Figures 5.3 and 5.5, the t.e.v.s $\langle : \overline{\psi}\psi : \rangle_\beta^{\text{spec}}$, $\langle : T_{\hat{t}\hat{t}} : \rangle_\beta^{\text{spec}}$ and $\langle : T_{\hat{z}\hat{z}} : \rangle_\beta^{\text{spec}}$ seem to be lower than the corresponding Planckian form. However, the same figures together with Fig. 5.4 imply that the profiles of the t.e.v.s $\langle : J_\nu^{\hat{z}} : \rangle_\beta^{\text{spec}}$, $\langle : T_{\hat{\varphi}\hat{t}} : \rangle_\beta^{\text{spec}}$, $\langle : T_{\hat{\rho}\hat{\rho}} : \rangle_\beta^{\text{spec}}$ and $\langle : T_{\hat{\varphi}\hat{\varphi}} : \rangle_\beta^{\text{spec}}$ set higher than the profiles of the corresponding Planckian forms.
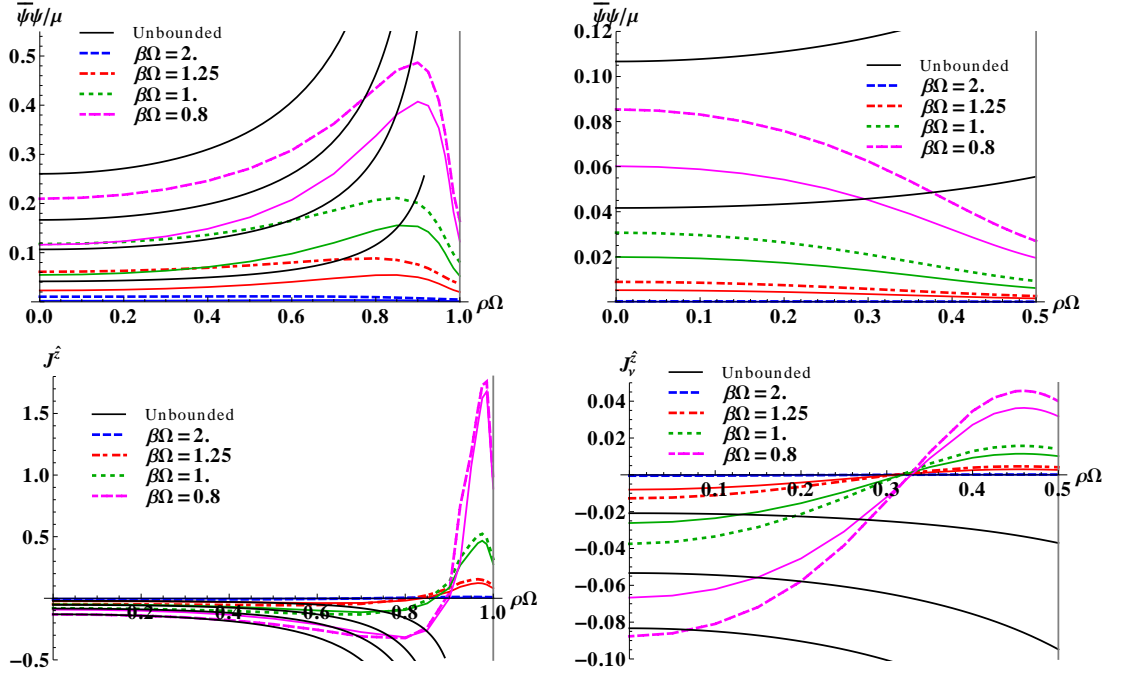
Figure 5.3: Fermion condensate (top) and neutrino charge current (bottom) for the boundary on and half-way to the SOL on the left and right, respectively. The plots compare numerical results for massless (thick dashed coloured lines) and massive (thin coloured lines) fermions with the Planckian forms (4.3.54a) and (4.3.54b) corresponding to the FC and neutrino charge current, respectively. Only the Planckian forms corresponding to $\beta\Omega = 2.0$ and $\beta\Omega = 1.25$ are represented for the FC in the case $R\Omega = 0.5$, the results corresponding to lower values of $\beta\Omega$ being off the scale.

Figure 5.6 (top) indicates that, for $\beta\Omega = 0.05$, the agreement between the analytic results (4.3.54c) and (4.3.54f) for $\langle : T_{\hat{t}\hat{t}} : \rangle_\beta^{\mathrm{spec}}$ and $\langle : T_{\hat{\varphi}\hat{\varphi}} : \rangle_\beta^{\mathrm{spec}}$ and the corresponding numerical results for when the boundary is located at $R\Omega = 0.5$ is very good around the rotation axis. In the plots on the second line of the same figure, the values of $\langle : T_{\hat{t}\hat{t}} : \rangle_\beta^{\mathrm{spec}}$ and $\langle : T_{\hat{\varphi}\hat{\varphi}} : \rangle_\beta^{\mathrm{spec}}$ on the rotation axis are compared to the Planckian forms (5.2.23a) and (5.2.23d) and with the aforementioned analytic results.

5.2.3 Casimir effect

As in the scalar case, it is more convenient to investigate the Casimir effect by considering the Euclidean equivalent of the manifold. As discussed in subsection 5.2.1, if the boundary is located inside or on the SOL, the quantisation (5.2.4) of the transverse momentum guarantees that $E\widetilde{E} > 0$ for all modes, in which case Eqs. (4.3.7) imply that the rotating (Iyer) and Minkowski (Vilenkin) vacua coincide. For the remainder of this section, only the case $\Omega R \leq 1$ (boundary inside or on the SOL) is considered. The case when the rotating and non-rotating vacua do not coincide is not considered here. To simplify the calculations, it is convenient to switch to the inertial non-rotating (Minkowski) coordinates, with respect to which the metric is
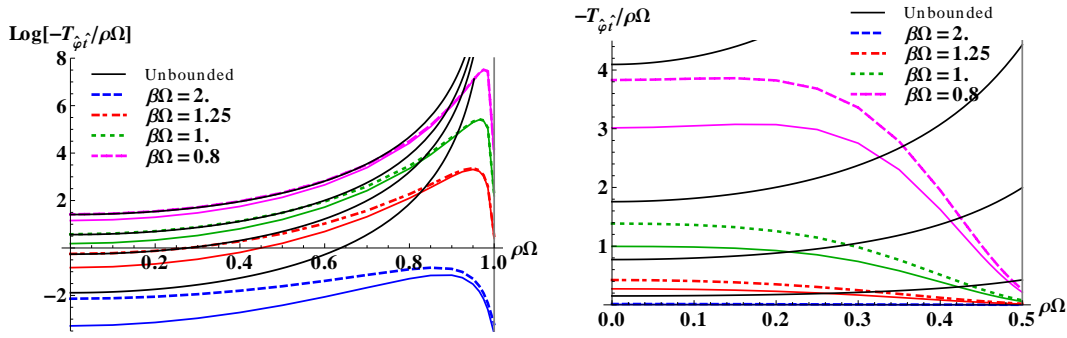
Figure 5.4: The t.e.v. of $-T^{\text{spec}}_{\hat{\varphi}\hat{t}}/\rho\Omega$ for $R\Omega = 0.5$ (right) and of its logarithm for $R\Omega = 1.0$. The factor $-1/\rho\Omega$ is introduced to make the result positive and finite (non-zero) on the rotation axis. Numerical results for massless (thick dashed coloured lines) and massive (thin coloured lines) fermions are compared with the Planckian form (5.2.23b).

given by (5.1.15). The transition to Euclidean coordinates can be made following Eqs. (2.1.60) and (2.2.59).

Euclidean Green's function on the unbounded manifold

The Euclidean Green's function $S_E \equiv S_E(x, x')$ must satisfy the inhomogeneous Dirac equation (2.2.61a). Following the construction of the mode solutions of the Dirac equation in subsection 3.3.1, the Euclidean Green's function can be Fourier-transformed as:

$$S_E(x_E, x'_E) = \int_{-\infty}^{\infty} \frac{d\omega}{8\pi^3} \int_{-\infty}^{\infty} dk \sum_{m=-\infty}^{\infty} e^{i\omega\Delta\tau + ik\Delta z}\chi, \qquad (5.2.24)$$

where the 4×4 matrix χ can be written in terms of four 2×2 matrices χ_{ab}:

$$\chi = \begin{pmatrix} \chi_{11} & \chi_{12} \\ \chi_{21} & \chi_{22} \end{pmatrix}. \qquad (5.2.25)$$

Performing an equivalent Fourier transformation of the delta functions on the right of Eq. (2.2.61a), the inhomogeneous Dirac equation implies:

$$\begin{pmatrix} i\omega + \mu & 2ph \\ -2ph & -i\omega + \mu \end{pmatrix}\begin{pmatrix} \chi_{11} & \chi_{12} \\ \chi_{21} & \chi_{22} \end{pmatrix} = \frac{\delta(\rho - \rho')}{\rho} I_2 \otimes \begin{pmatrix} e^{im\Delta\varphi} & 0 \\ 0 & e^{i(m+1)\Delta\varphi} \end{pmatrix},$$

$$\begin{pmatrix} \chi_{11} & \chi_{12} \\ \chi_{21} & \chi_{22} \end{pmatrix}\begin{pmatrix} i\omega + \mu & 2ph'^{\dagger} \\ -2ph'^{\dagger} & -i\omega + \mu \end{pmatrix} = \frac{\delta(\rho - \rho')}{\rho'} I_2 \otimes \begin{pmatrix} e^{im\Delta\varphi} & 0 \\ 0 & e^{i(m+1)\Delta\varphi} \end{pmatrix}, \quad (5.2.26)$$

where h is the 2×2 component (3.3.1b) of the helicity operator W_0, defined in Eq. (3.3.1a). For the equation in x', the corresponding reducd helicity operator $h'^{\dagger}$ has the form:

$$h'^{\dagger} = \frac{1}{2p}\begin{pmatrix} k & -P'_- \\ -P'_+ & -k \end{pmatrix}. \qquad (5.2.27)$$
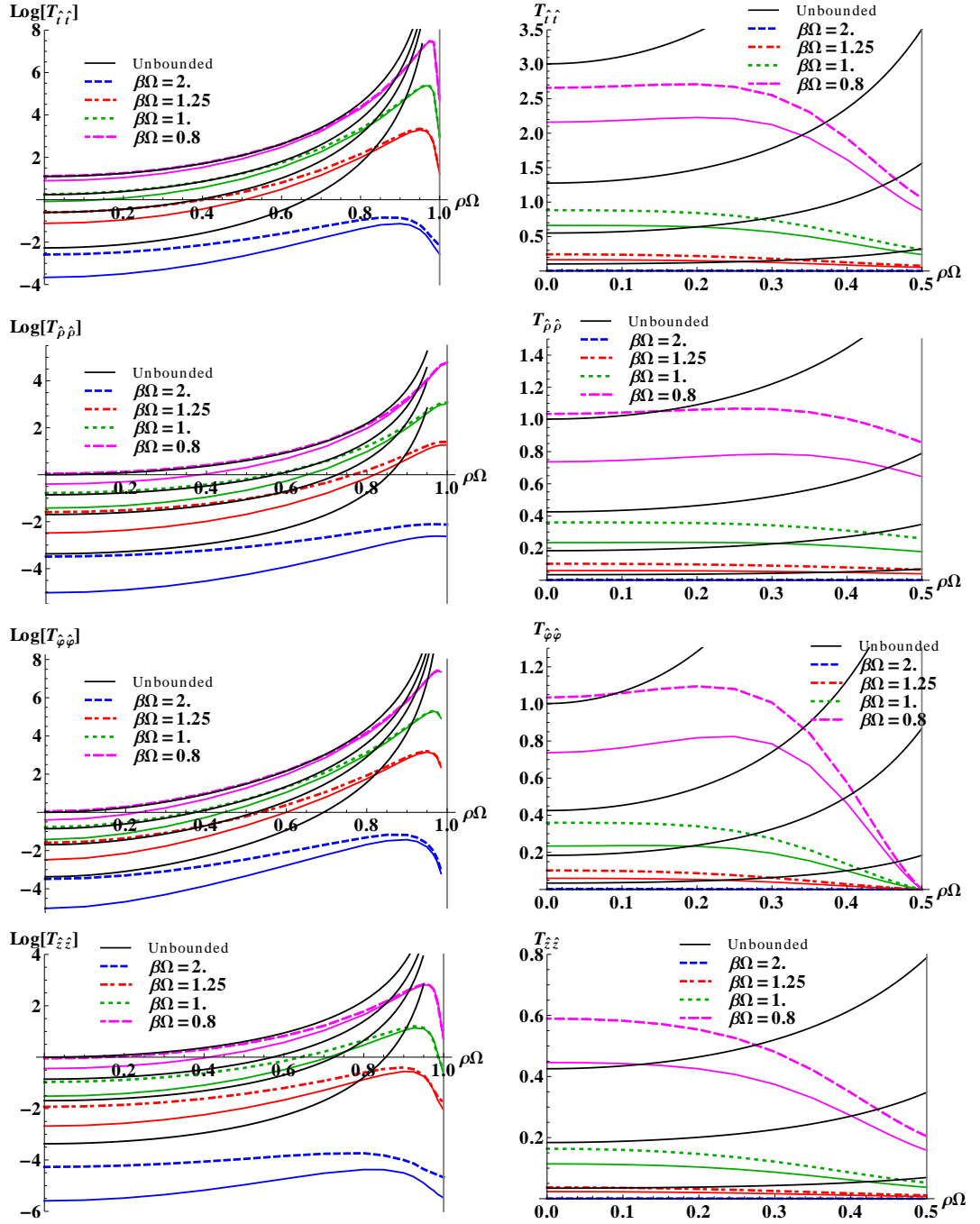
Figure 5.5: The t.e.v. of $T_{\hat{t}\hat{t}}^{\text{spec}}$, $T_{\hat{\rho}\hat{\rho}}^{\text{spec}}$, $T_{\hat{\varphi}\hat{\varphi}}^{\text{spec}}$ and $T_{\hat{z}\hat{z}}^{\text{spec}}$ (from top to bottom) for $R\Omega = 0.5$ (right) and of their logarithms for $R\Omega = 1.0$. Numerical results for massless (thick dashed coloured lines) and massive (thin coloured lines) fermions are compared with the corresponding Planckian forms in Eqs. (5.2.23).
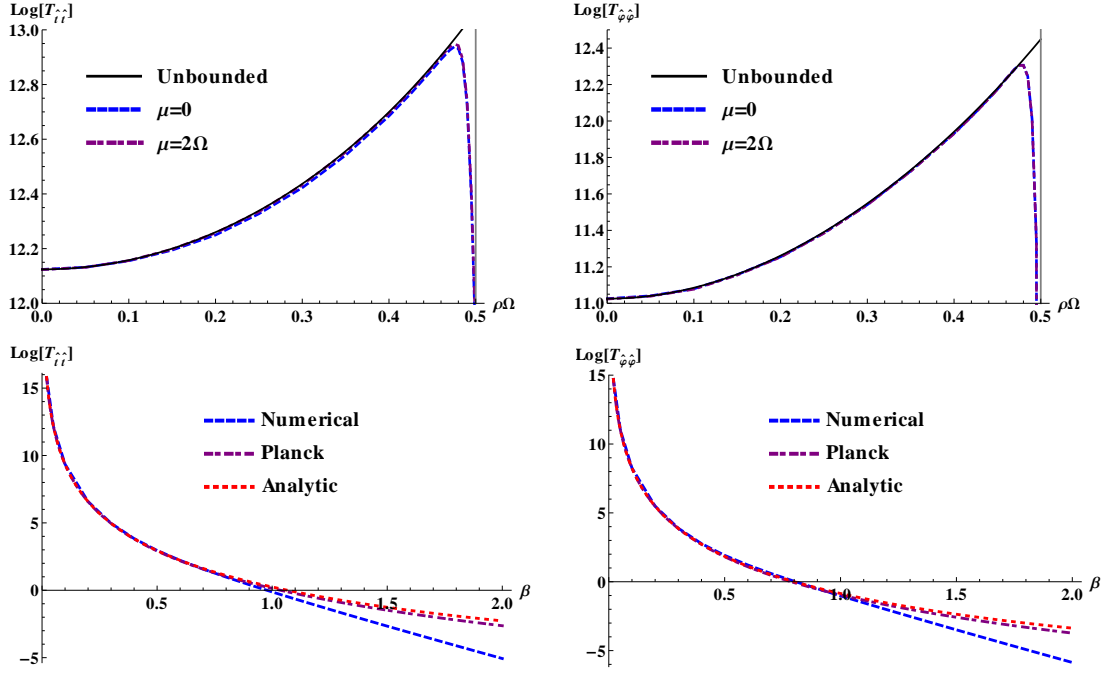
Figure 5.6: (a) The profiles of $\langle : T_{\hat{t}\hat{t}} : \rangle_\beta^{\mathrm{spec}}$ and $\langle : T_{\hat{\varphi}\hat{\varphi}} : \rangle_\beta^{\mathrm{spec}}$ between the rotation axis and the boundary located at $R\Omega = 0.5$ at $\beta\Omega = 0.05$. The profiles for massless and massive fermions overlap each other throughout the whole range of ρ, but depart strongly from the analytic results (4.3.54c) and (4.3.54f). (b) The dependency of the values of $\langle : T_{\hat{t}\hat{t}} : \rangle_\beta^{\mathrm{spec}}$ and $\langle : T_{\hat{\varphi}\hat{\varphi}} : \rangle_\beta^{\mathrm{spec}}$ on the rotation axis on the value of the temperature, compared with the Planckian forms (5.2.23a) and (5.2.23d) and with analytic results.

The primes indicate that the derivatives in the operators $P'_\pm$, defined in Eqs. (3.3.1c) act from the right on ρ' and φ'.

The off-diagonal components of Eqs. (5.2.26) give the following equations:

$$\chi_{21} = -\frac{2ph}{i\omega - \mu}\chi_{11} = \chi_{22}\frac{2ph'^{\,\dagger}}{i\omega + \mu},$$

$$\chi_{12} = -\frac{2ph}{i\omega + \mu}\chi_{22} = \chi_{11}\frac{2ph'^{\,\dagger}}{i\omega - \mu}, \tag{5.2.28}$$

while the diagonal components can be written as modified Bessel equations:

$$[\rho^2\partial_\rho^2 + \rho\partial_\rho + \partial_\varphi^2 - \rho^2\alpha^2]\frac{\chi_{11}}{i\omega - \mu} = \rho\delta(\rho - \rho')\begin{pmatrix} e^{im\Delta\varphi} & 0 \\ 0 & e^{i(m+1)\Delta\varphi} \end{pmatrix},$$

$$[\rho^2\partial_\rho^2 + \rho\partial_\rho + \partial_\varphi^2 - \rho^2\alpha^2]\frac{\chi_{22}}{-i\omega - \mu} = \rho\delta(\rho - \rho')\begin{pmatrix} e^{im\Delta\varphi} & 0 \\ 0 & e^{i(m+1)\Delta\varphi} \end{pmatrix}, \tag{5.2.29}$$

where $\alpha^2 = \omega^2 + k^2 + \mu^2$ (5.1.19). It can be shown that the inhomogeneous Dirac equation in x' also reduces to the above equation (with ρ and φ replaced by ρ' and φ', respectively), hence χ_{11} and χ_{22} can be written as linear combinations of modified Bessel functions. The Euclidean Green's function for the Minkowski space-time must be regular at the origin and at infinity, thus the only non-trivial solution

satisfying these boundary conditions is:

$$-\frac{\chi_{11}}{i\omega - \mu} = \frac{\chi_{22}}{i\omega + \mu}$$

$$= \begin{pmatrix} I_m(\alpha\rho_<)K_m(\alpha\rho_>)e^{im\Delta\varphi} & 0 \\ 0 & I_{m+1}(\alpha\rho_<)K_{m+1}(\alpha\rho_>)e^{i(m+1)\Delta\varphi} \end{pmatrix}, \quad (5.2.30)$$

where $\rho_<$ and $\rho_>$ are the smaller and larger of ρ and ρ', respectively. The notation above is equivalent to the following combination of step functions:

$$f(\alpha\rho_<)g(\alpha\rho_>) = \theta(\rho - \rho')g(\alpha\rho)f(\alpha\rho') + \theta(\rho' - \rho)f(\alpha\rho)g(\alpha\rho'). \quad (5.2.31)$$

The off-diagonal matrices χ_{12} and χ_{21} can be obtained from Eqs. (5.2.28), using the following properties:

$$P_+ I_m(\alpha\rho)e^{im\varphi} = -i\alpha e^{i(m+1)\varphi} I_{m+1}(\alpha\rho),$$
$$P_- I_{m+1}(\alpha\rho)e^{i(m+1)\varphi} = -i\alpha e^{im\varphi} I_m(\alpha\rho),$$
$$P_+ K_m(\alpha\rho)e^{im\varphi} = i\alpha e^{i(m+1)\varphi} K_{m+1}(\alpha\rho),$$
$$P_- K_{m+1}(\alpha\rho)e^{i(m+1)\varphi} = i\alpha e^{im\varphi} K_m(\alpha\rho). \quad (5.2.32)$$

Similar equations hold for $P'_\pm$, which can be applied bearing in mind that $I_{-m}(z) = I_m(z)$ and $K_{-m}(z) = K_m(z)$ for all integer orders m.

Thus, the Euclidean Green's function for the unbounded Minkowski space-time can be written as:

$$S_E(x_E, x'_E) = \int_{-\infty}^{\infty} \frac{d\omega}{8\pi^3} \int_{-\infty}^{\infty} dk \sum_{m=-\infty}^{\infty} e^{i\omega\Delta\tau + ik\Delta z} \chi, \quad (5.2.33a)$$

with χ given by:

$$\chi = [\mu I_2 - i\omega\sigma_3] \otimes \begin{pmatrix} I_m(\alpha\rho_<)K_m(\alpha\rho_>)e^{im\Delta\varphi} & 0 \\ 0 & I_{m+1}(\alpha\rho_<)K_{m+1}(\alpha\rho_>)e^{i(m+1)\Delta\varphi} \end{pmatrix}$$

$$+ k \begin{pmatrix} 0 & -1 \\ 1 & 0 \end{pmatrix} \otimes \begin{pmatrix} I_m(\alpha\rho_<)K_m(\alpha\rho_>)e^{im\Delta\varphi} & 0 \\ 0 & -I_{m+1}(\alpha\rho_<)K_{m+1}(\alpha\rho_>)e^{i(m+1)\Delta\varphi} \end{pmatrix}$$

$$+ \alpha \begin{pmatrix} 0 & -1 \\ 1 & 0 \end{pmatrix} \otimes \begin{pmatrix} 0 & (m, m+1) \\ (m+1, m) & 0 \end{pmatrix}, \quad (5.2.33b)$$

where the Pauli matrix σ_3 is defined in Eq. (2.2.8) and the notation (m, n) is a shorthand for:

$$(m, n) = ie^{i(m\varphi - n\varphi')}[\theta(\rho' - \rho)I_m(\alpha\rho)K_n(\alpha\rho') - \theta(\rho - \rho')K_m(\alpha\rho)I_n(\alpha\rho')]. \quad (5.2.33c)$$

	$m + \frac{1}{2} > 0$	$m + \frac{1}{2} < 0$
$\rho = R$	$\begin{pmatrix} 0 & 0 \\ \times & \times \end{pmatrix}$	$\begin{pmatrix} \times & \times \\ 0 & 0 \end{pmatrix}$
$\rho' = R$	$\begin{pmatrix} 0 & \times \\ 0 & \times \end{pmatrix}$	$\begin{pmatrix} \times & 0 \\ \times & 0 \end{pmatrix}$

Table 5.1: The behaviour of the 2×2 constituent blocks of Lorentzian two-point functions obeying spectral boundary conditions on a cylinder of radius R. Depending on the sign of $m + \frac{1}{2}$ and on which point is on the boundary, certain entries in these 2×2 matrices will vanish, as indicated in the table. Entries marked $\times$ do not necessarily vanish.

The solution (5.2.33) is fixed by requiring regularity at the origin ($\rho = 0$ or $\rho' = 0$) and space-like infinity ($\rho \to \infty$ or $\rho' \to \infty$) and corresponds to the unbounded Minkowski space-time. To obtain the Euclidean Green's function for a system enclosed in a boundary, suitable solutions of the homogeneous Euclidean Dirac equation can be added to the appropriate matrix elements in Eq. (5.2.33).

Euclidean Green's function for the spectral model

To construct a Euclidean Green's function which implements spectral boundary conditions, the behaviour on the boundary of the corresponding vacuum Hadamard function can be considered. Since the dependence on the radial coordinates ρ and ρ' is always that in the 2×2 matrix given in Eq. (3.3.58), it is sufficient to analyze its behaviour on the boundary, as shown in Table 5.1. Furthermore, the Green's functions must stay regular at the origin. Denoting the Euclidean Green's function of the bounded system by $S_E^{\mathrm{sp}}(x, x')$, the difference

$$\Delta S_E^{\mathrm{sp}}(x, x') = S_E^{\mathrm{sp}}(x, x') - S_E(x, x') = \int_{-\infty}^{\infty} \frac{d\omega}{8\pi^3} \int_{-\infty}^{\infty} dk \sum_{m=-\infty}^{\infty} e^{i\omega \Delta\tau + ik\Delta z} \Delta\chi^{\mathrm{sp}},$$
(5.2.34)

with respect to the Euclidean Green's function of the unbounded space is a solution of the homogeneous version of Eq. (5.2.26) (i.e. with the right hand side set to 0).

To implement the boundary conditions shown in Table 5.1, it is sufficient to add the following matrices to χ_{11} and χ_{22} in Eq. (5.2.30):

$$\frac{\Delta\chi_{11}^{\mathrm{sp}}}{-i\omega + \mu} = \frac{\Delta\chi_{22}^{\mathrm{sp}}}{i\omega + \mu} = c_m \begin{pmatrix} 1 & 0 \\ 0 & -1 \end{pmatrix} \circ \mathcal{E}_j, \qquad (5.2.35a)$$

where the Hadamard (Schur) product is taken with the following matrix:

$$\mathcal{E}_j = \begin{pmatrix} I_m(\alpha\rho)I_m(\alpha\rho')e^{im\Delta\varphi} & -iI_m(\alpha\rho)I_{m+1}(\alpha\rho')e^{i(m+1)\Delta\varphi - i\varphi} \\ iI_{m+1}(\alpha\rho)I_m(\alpha\rho')e^{im\Delta\varphi + i\varphi} & I_{m+1}(\alpha\rho)I_{m+1}(\alpha\rho')e^{i(m+1)\Delta\varphi} \end{pmatrix} \qquad (5.2.35b)$$

and c_m is a constant ensuring the structure in Table 5.1, having the value:

$$
c_m = \begin{cases} -\dfrac{K_m(\alpha R)}{I_m(\alpha R)} & m + \frac{1}{2} > 0, \\[2mm] \dfrac{K_{m+1}(\alpha R)}{I_{m+1}(\alpha R)} & m + \frac{1}{2} < 0. \end{cases} \tag{5.2.35c}
$$

Only modified Bessel functions of the first kind (i.e. I_m) have been considered, since their linearly independent partners, K_m, do not satisfy the requirement of regularity at the origin. The structure of the matrices in Eqs. (5.2.35a) is determined by the compatibility conditions (5.2.28), which give the following off-diagonal matrices:

$$
\chi_{21}^{\mathrm{sp}} = -\chi_{12}^{\mathrm{sp}} = c_m \begin{pmatrix} k & -\alpha \\ -\alpha & k \end{pmatrix} \circ \mathcal{E}_j. \tag{5.2.35d}
$$

Thus, the homogeneous solution of the Euclidean Dirac equation inducing spectral boundary conditions is:

$$
\Delta S_E^{\mathrm{sp}}(x, x') = \int_{-\infty}^{\infty} \frac{d\omega}{8\pi^3} \int_{-\infty}^{\infty} dk \sum_{m=-\infty}^{\infty} e^{i\omega\Delta\tau + ik\Delta z} \Delta\chi^{\mathrm{sp}}, \tag{5.2.36a}
$$

where the Fourier components $\Delta\chi^{\mathrm{sp}}$ can be written as:

$$
c_m^{-1}\Delta\chi^{\mathrm{sp}} = (\mu I_2 - i\omega\sigma_3) \otimes \left[\begin{pmatrix} 1 & 0 \\ 0 & -1 \end{pmatrix} \circ \mathcal{E}_j \right] + \begin{pmatrix} 0 & -1 \\ 1 & 0 \end{pmatrix} \otimes \left[\begin{pmatrix} k & -\alpha \\ -\alpha & k \end{pmatrix} \circ \mathcal{E}_j \right]. \tag{5.2.36b}
$$

In the following paragraphs, the Casimir induced expectation values of the fermion condensate and SET are calculated using the difference $\Delta S_E^{\mathrm{sp}}(x, x')$ between the Euclidean Green's functions corresponding to the bounded and unbounded systems.

Casimir expectation values

The Casimir expectation values, induced by the difference between the bounded and unbounded vacua, can be calculated from the difference $\Delta S_E^{\mathrm{sp}}(x, x') = S_E^{\mathrm{sp}}(x, x') - S_E(x, x')$. For the fermion condensate (FC), the following expression is obtained:

$$
\langle \overline{\psi}\psi \rangle_{\mathrm{Cas}}^{\mathrm{sp}} = -\frac{\mu}{2\pi^3} \int_{-\infty}^{\infty} d\omega \int_{-\infty}^{\infty} dk \sum_{m=0}^{\infty} \frac{K_m(\alpha R)}{I_m(\alpha R)} I_m^-(\alpha R), \tag{5.2.37}
$$

where the notation $I_m^-(z)$ is analogous to Eqs. (3.3.69):

$$
I_m^{\pm}(z) = I_m^2(z) \pm I_{m+1}^2(z), \quad I_m^{\times}(z) = 2I_m(z)I_{m+1}(z). \tag{5.2.38}
$$

Switching to polar coordinates (5.1.24), the Casimir FC can be put in the form:

$$\langle \overline{\psi}\psi \rangle^{\text{sp}}_{\text{Cas}} = -\mu R^2 \mathcal{I}^-_{10}, \tag{5.2.39}$$

where

$$\mathcal{I}^*_{\ell n} = \frac{1}{2\pi^2 R^4} \sum_{m=-\infty}^{\infty} \int_{\mu R}^{\infty} d\text{x}\, \text{x}^\ell (m+\tfrac{1}{2})^n c_m\, I^*_m(\text{x}\overline{\rho}), \tag{5.2.40}$$

where $\overline{\rho} = \rho/R$ and c_m is defined in Eq. (5.2.35c).

The calculation of the induced SET can be done using the formula (2.2.62), with $S_E(x, x')$ replaced by $\Delta S^{\text{sp}}_E(x, x')$:

$$\langle T^{\hat{\alpha}}_{\hat{\gamma}} \rangle^{\text{sp}}_{\text{Cas}} = \frac{1}{2\pi^3} \sum_{m=0}^{\infty} \int_{-\infty}^{\infty} dE \int_{-\infty}^{\infty} dk\, \frac{K_m(\alpha R)}{I_m(\alpha R)} \text{diag}\Big\{ -E^2 I^-_m(\alpha\rho),$$

$$\alpha^2 I^-_m(\alpha\rho) - \alpha\rho^{-1}(m+\tfrac{1}{2})I^\times_m(\alpha\rho),\, \alpha\rho^{-1}(m+\tfrac{1}{2})I^\times_m(\alpha\rho),\, k^2 I^-_m(\alpha\rho) \Big\}. \tag{5.2.41}$$

After a change to polar coordinates (5.1.24), the integration over the polar angle θ can be performed:

$$\langle T^{\hat{\tau}}_{\hat{\tau}} \rangle^{\text{sp}}_{\text{Cas}} = \langle T^{\hat{z}}_{\hat{z}} \rangle^{\text{sp}}_{\text{Cas}} = -\mathcal{I}^-_{30} + \mu^2 R^2 \mathcal{I}^-_{10},$$

$$\langle T^{\hat{\rho}}_{\hat{\rho}} \rangle^{\text{sp}}_{\text{Cas}} = 2\mathcal{I}^-_{30} - \frac{2}{\rho}\mathcal{I}^\times_{21},$$

$$\langle T^{\hat{\varphi}}_{\hat{\varphi}} \rangle^{\text{sp}}_{\text{Cas}} = \frac{2}{\rho}\mathcal{I}^\times_{21}. \tag{5.2.42}$$

Equations (A.2.7) can be used to see that the functions $\mathcal{I}_{\ell n}$ diverge at $\overline{\rho} = 1$ due to the large m and x behaviour of their respective integrand:

$$\frac{K_{\nu-\frac{1}{2}}(\text{x})}{I_{\nu-\frac{1}{2}}(\text{x})} I^-_{\nu-\frac{1}{2}}(\text{x}) = \frac{\nu}{\nu + \sqrt{\nu^2 + \text{x}^2}} \left[1 + \frac{1}{2\sqrt{\nu^2 + \text{x}^2}} + O((\nu^2 + \text{x}^2)^{-1}) \right]. \tag{5.2.43}$$

A more detailed analysis of this divergence can be found in the next subsection.

5.2.4   Casimir divergence near the boundary

As in the scalar case, the divergence of the functions $\mathcal{I}^*_{\ell n}$ is best performed by switching the sum over m to an integral. The functions appearing in Eqs. (5.2.39) and (5.2.42) are $\mathcal{I}^-_{10}$, $\mathcal{I}^-_{30}$ and $\mathcal{I}^\times_{21}$. Since in all these terms, the summands in the sum over m are even with respect to the change $m \to -m-1$, the function $\overline{\mathcal{I}}^*_{\ell,n}$ obtained by replacing the sum over m with an integral can be written as follows:

$$\overline{\mathcal{I}}^*_{\ell n} = \frac{1}{\pi^2 R^4} \int_0^{\infty} d\nu \int_{\mu R}^{\infty} d\text{x}\, \text{x}^\ell \nu^n \frac{K_{\nu-\frac{1}{2}}(\text{x})}{I_{\nu-\frac{1}{2}}(\text{x})} I^*_{\nu-\frac{1}{2}}(\text{x}\overline{\rho}). \tag{5.2.44}$$

Since the symmetry of the summands is different from the scalar case (where it was with respect to the transformation $m \to -m$), the Abel-Plana formula used in subsection 5.1.4 must be adapted, as explained in the following paragraph.

Generalised Abel-Plana formula

The Abel-Plana sum formula (5.1.33) can be generalised to sums over odd half-integers, as presented in Ref. [64]:

$$\sum_{m=0}^{\infty} f(m + \tfrac{1}{2}) = \int_0^\infty d\nu\, f(\nu) - i \int_0^\infty dt \frac{f(it) - f(-it)}{e^{2\pi t} + 1}$$
$$+ i\pi \left\{ \sum_k \text{sgn}(\mathfrak{Im}(z_{f,k})) \text{Res}_{\mathfrak{Re}(z_{f,k})>0} f(z) - i \sum_k \text{Res} f(z) \cot \pi z \right\}. \quad (5.2.45)$$

In the above, $z_{f,k}$ represents the k'th pole of the function $f(z)$ and $\text{Res}_{\mathfrak{Re}(z_{f,k})<0} f(z)$ represents the residue of $f(z)$ at $z = z_{f,k}$ in the real half-space of the z-complex plane. As in the scalar case, there are no residues to evaluate in the transition from $\mathcal{I}_{\ell n}^*$ to $\overline{\mathcal{I}}_{\ell n}^*$.

As opposed to the scalar case, the difference $\delta_{\ell n}^*(\overline{\rho})$ between the sum over m in Eq. (5.2.40) and the corresponding integral over ν in Eq. (5.2.44), given by

$$\delta_{\ell n}^*(\overline{\rho}) = i \int_0^\infty dt \frac{f_{\ell n}^*(it) - f_{\ell n}^*(-it)}{e^{2\pi t} + 1}, \quad (5.2.46)$$

diverges as $\epsilon = 1 - \overline{\rho}$ approaches 0 for all three cases ($\mathcal{I}_{10}^-$, $\mathcal{I}_{30}^-$ and $\mathcal{I}_{21}^\times$) considered here. In the above, $f_{\ell n}^*(\nu)$ is

$$f_{\ell n}^*(\nu) = \frac{1}{\pi^2 R^4} \int_{\mu R}^\infty dx\, x^\ell \nu^n \frac{K_{\nu-\frac{1}{2}}(x)}{I_{\nu-\frac{1}{2}}(x)} I_{\nu-\frac{1}{2}}^*(x\overline{\rho}). \quad (5.2.47)$$

Since the $(e^{2\pi t} + 1)^{-1}$ factor in $\delta_{\ell n}^*(\overline{\rho})$ suppresses the integrand in Eq. (5.2.46) at large t, the leading orders of the divergence of $\delta_{\ell n}^*(\overline{\rho})$ can be calculated by considering the large x behaviour of the integrand in Eq. (5.2.47). The following asymptotic behaviours can be obtained, starting from Eqs. (A.2.4d) and (A.2.4e):

$$\frac{K_{\nu-\frac{1}{2}}(x)}{I_{\nu-\frac{1}{2}}(x)} = \pi e^{-2x} \left[1 + \frac{\nu(\nu - 1)}{x} + \frac{\nu^2(\nu - 1)^2}{2x^2} + O(x^{-3}) \right], \quad (5.2.48a)$$

$$I_{\nu-\frac{1}{2}}^2(x) - I_{\nu+\frac{1}{2}}^2(x) = \frac{\nu e^{2x}}{\pi x^2} \left[1 - \frac{(\nu - 1)(\nu + 1)}{2x} - \frac{\nu^2}{x^2} + O(x^{-3}) \right], \quad (5.2.48b)$$

$$2I_{\nu-\frac{1}{2}}(x) I_{\nu+\frac{1}{2}}(x) = \frac{e^{2x}}{\pi x} \left[1 - \frac{\nu^2}{x} + \frac{\nu^4}{x^2} + O(x^{-3}) \right], \quad (5.2.48c)$$

with which the following expressions can be obtained:

$$\frac{K_{\nu-\frac{1}{2}}(\mathbf{x})}{I_{\nu-\frac{1}{2}}(\mathbf{x})}[I_{\nu-\frac{1}{2}}^2(\mathbf{x}\bar{\rho}) - I_{\nu+\frac{1}{2}}^2(\mathbf{x}\bar{\rho})] = \frac{\nu e^{-2\mathbf{x}\epsilon}}{\mathbf{x}^2\bar{\rho}^2}\left[1 - \frac{\nu - \frac{1}{2}}{\mathbf{x}} - \frac{\nu^2 - \frac{1}{2}}{\mathbf{x}}\frac{\epsilon}{\bar{\rho}} + \dots\right], \quad (5.2.49\text{a})$$

$$2\frac{K_{\nu-\frac{1}{2}}(\mathbf{x})}{I_{\nu-\frac{1}{2}}(\mathbf{x})}I_{\nu-\frac{1}{2}}(\mathbf{x}\bar{\rho})I_{\nu+\frac{1}{2}}(\mathbf{x}\bar{\rho}) = \frac{e^{-2\mathbf{x}\epsilon}}{\mathbf{x}\bar{\rho}^2}\left[1 - \frac{\nu^2\epsilon}{\mathbf{x}\bar{\rho}} - \frac{\nu}{\mathbf{x}} + O(\mathbf{x}^{-2})\right], \quad (5.2.49\text{b})$$

where $\epsilon = 1 - \bar{\rho}$ is defined in Eq. (5.1.40). Substituting the above approximations in Eq. (5.2.46) gives:

$$\delta_{10}^-(\bar{\rho}) = -\frac{2}{\pi^2 R^4}\int_0^\infty \frac{dt}{e^{2\pi t}+1}\int_{\mu R}^\infty \frac{d\mathbf{x}}{\mathbf{x}\bar{\rho}^2}e^{-2\mathbf{x}\epsilon}\left[1 + O(\mathbf{x}^{-2})\right],$$

$$\delta_{30}^-(\bar{\rho}) = -\frac{2}{\pi^2 R^4}\int_0^\infty \frac{dt}{e^{2\pi t}+1}\int_{\mu R}^\infty \frac{d\mathbf{x}}{\bar{\rho}^2}\mathbf{x}e^{-2\mathbf{x}\epsilon}\left[1 + \frac{1}{2\mathbf{x}} + \frac{t^2+\frac{1}{2}}{\mathbf{x}\bar{\rho}}\epsilon + O(\mathbf{x}^{-2})\right],$$

$$\delta_{21}^\times(\bar{\rho}) = -\frac{2}{\pi^2 R^4}\int_0^\infty \frac{t, dt}{e^{2\pi t}+1}\int_{\mu R}^\infty \frac{d\mathbf{x}}{\bar{\rho}}\mathbf{x}e^{-2\mathbf{x}\epsilon}\left[1 + \frac{t^2}{\mathbf{x}\bar{\rho}}\epsilon + O(\mathbf{x}^{-2})\right]. \quad (5.2.50)$$

Since the above expressions diverge due to the large $\mathbf{x}$ behaviour of the integrand, the lower limit of the $\mathbf{x}$ integral can be approximated to 0 (i.e. the massless limit can be taken), allowing the integral over $\mathbf{x}$ to be performed in terms of Γ functions:

$$\delta_{10}^- \simeq -\frac{\ln 2}{\pi^3 R^4}[\ln \epsilon^{-1} + O(1)],$$

$$\delta_{30}^- \simeq -\frac{\ln 2}{4\pi^3 R^4\epsilon^2}[1 + 3\epsilon + O(\epsilon^2)],$$

$$\delta_{21}^\times \simeq -\frac{1}{96\pi^2 R^4\epsilon^2}[1 + \epsilon + O(\epsilon^2)]. \quad (5.2.51)$$

As shown in Eq. (5.2.55) for the three cases of interest considered above, the leading order of the divergence of $\delta_{\ell n}^*$ is two orders of magnitude less than that of the corresponding $\mathcal{I}_{\ell n}^*$.

The Casimir divergence near the boundary

Using the polar coorindates (r, θ) introduced in Eq. (5.1.38) and the expansions in Eqs. (5.1.41), the following asymptotic expansions can be made:

$$I^-_{\nu-\frac{1}{2}}(\mathbf{x}) = \frac{\cot\theta\, e^{2r+2\nu\ln\frac{x}{\nu+r}}}{\pi r}\left[1 + \frac{1+5\sin^2\theta}{12r} + \frac{1}{2r^2}\left(1 - \frac{29}{12}\cos^2\theta + \frac{205}{144}\cos^4\theta\right)\right.$$
$$\left. + O(r^{-3})\right], \tag{5.2.52a}$$

$$I^+_{\nu-\frac{1}{2}}(\mathbf{x}) = \frac{e^{2r+2\nu\ln\frac{x}{\nu+r}}}{\pi r\sin\theta}\left[1 + \frac{\cos^2\theta}{12r} + \frac{\cos^2\theta(1+35\sin^2\theta)}{288r^2} + O(r^{-3})\right], \tag{5.2.52b}$$

$$I^\times_{\nu-\frac{1}{2}}(\mathbf{x}) = \frac{e^{2r+2\nu\ln\frac{x}{\nu+r}}}{\pi r}\left[1 - \frac{5\cos^2\theta}{12r} + \frac{\cos^2\theta(61-205\sin^2\theta)}{288r^2} + O(r^{-3})\right], \tag{5.2.52c}$$

$$\frac{K_{\nu-\frac{1}{2}}(\mathbf{x})}{I_{\nu-\frac{1}{2}}(\mathbf{x})} = \frac{\pi\sin\theta\, e^{-2r-2\nu\ln\frac{x}{\nu+r}}}{1+\cos\theta}\left[1 + \frac{5\cos^2\theta}{12r} - \frac{\cos\theta}{2r^2}\left(1 - \frac{5\cos^2\theta}{4} - \frac{25\cos^3\theta}{144}\right)\right.$$
$$\left. + O(r^{-3})\right]. \tag{5.2.52d}$$

The asymptotic expansion for $I^+_{\nu-\frac{1}{2}}(\mathbf{x})$ is included for completeness. Although it is not required for the asymptotic analysis of the Casimir divergence in the spectral model, it will become useful for the same analysis in the MIT bag model, in subsection 5.3.3. In this section, the above functions are evaluated at $\mathbf{x}\bar\rho$. If $\bar\rho = \rho/R$ is close to 1, Eqs. (5.1.41) can be used to derive the following approximations:

$$I^-_{\nu-\frac{1}{2}}(\mathbf{x}\bar\rho) = \frac{e^{2r+2\nu\ln\frac{x}{\nu+r}-2r\epsilon}}{\pi r\tan\theta}\left[1 + \frac{1+5\sin^2\theta}{12r} + \epsilon(1+\sin^2\theta) - r\epsilon^2\cos^2\theta + \dots\right], \tag{5.2.53a}$$

$$I^+_{\nu-\frac{1}{2}}(\mathbf{x}\bar\rho) = \frac{e^{2r+2\nu\ln\frac{x}{\nu+r}-2r\epsilon}}{\pi r\sin\theta}\left[1 + \frac{\cos^2\theta}{12r} + \epsilon - r\epsilon^2\cos^2\theta + \dots\right], \tag{5.2.53b}$$

$$I^\times_{\nu-\frac{1}{2}}(\mathbf{x}\bar\rho) = \frac{e^{2r+2\nu\ln\frac{x}{\nu+r}-2r\epsilon}}{\pi r}\left[1 - \frac{5\cos^2\theta}{12r} + \epsilon\sin^2\theta - r\epsilon^2\cos^2\theta + \dots\right], \tag{5.2.53c}$$

where terms of order r^{-2}, $r^{-1}\epsilon$ and ϵ^2 were ignored. Combining Eq. (5.2.52d) with Eqs. (5.2.53a) and (5.2.53c) gives:

$$\frac{K_{\nu-\frac{1}{2}}(\mathbf{x})}{I_{\nu-\frac{1}{2}}(\mathbf{x})}I^-_{\nu-\frac{1}{2}}(\mathbf{x}\bar\rho) = \frac{e^{-2r\epsilon}\cos\theta}{r(1+\cos\theta)}\left[1 + \frac{1}{2r} + \epsilon(1+\sin^2\theta) - r\epsilon^2\cos^2\theta + \dots\right],$$

$$\frac{K_{\nu-\frac{1}{2}}(\mathbf{x})}{I_{\nu-\frac{1}{2}}(\mathbf{x})}I^\times_{\nu-\frac{1}{2}}(\mathbf{x}\bar\rho) = \frac{e^{-2r\epsilon}\sin\theta}{r(1+\cos\theta)}\left[1 + \epsilon\sin^2\theta - r\epsilon^2\cos^2\theta + \dots\right]. \tag{5.2.54}$$

Hence, the following results are obtained:

$$\overline{\mathcal{I}}_{10}^{-} = \frac{1}{4\pi^2 R^4 \epsilon^2} \left[1 - \ln 2 + \epsilon \left(\tfrac{4}{3} - \ln 2 \right) + O(\epsilon^2) \right],$$

$$\overline{\mathcal{I}}_{30}^{-} = \frac{1}{16\pi^2 R^4 \epsilon^4} \left[1 + \tfrac{43}{30}\epsilon + O(\epsilon^2) \right],$$

$$\overline{\mathcal{I}}_{21}^{\times} = \frac{1}{16\pi^2 R^4 \epsilon^4} \left[1 + \tfrac{1}{10}\epsilon + O(\epsilon^2) \right]. \tag{5.2.55}$$

The divergences of the $\overline{\mathcal{I}}_{\ell n}^{*}$ terms calculated above are two orders of magnitude higher than the corresponding error terms $\delta_{\ell n}^{*}$ calculated in Eqs. (5.2.51). Hence, the leading and subleading order of the divergence of the functions $\mathcal{I}_{\ell n}^{*}$ coincide with the expressions obtained above.

Substituting Eqs. (5.2.55) into Eqs. (5.2.16) and (5.2.20) gives the following asymptotic behaviours:

$$\langle \overline{\psi}\psi \rangle_{\text{Cas}}^{\text{sp}} = -\frac{\mu}{4\pi^2 R^2 \epsilon^2} \left[1 - \ln 2 + \left(\tfrac{4}{3} - \ln 2 \right)\epsilon + \dots \right],$$

$$\langle T^{\hat{\tau}}{}_{\hat{\tau}} \rangle_{\text{Cas}}^{\text{sp}} = \langle T^{\hat{z}}{}_{\hat{z}} \rangle_{\text{Cas}}^{\text{sp}} = -\frac{1}{16\pi^2 R^4 \epsilon^4} \left[1 + \tfrac{43}{30}\epsilon + \dots \right],$$

$$\langle T^{\hat{\rho}}{}_{\hat{\rho}} \rangle_{\text{Cas}}^{\text{sp}} = \frac{1}{24\pi^2 R^4 \epsilon^3} \left(1 + \tfrac{23}{20}\epsilon + \dots \right),$$

$$\langle T^{\hat{\varphi}}{}_{\hat{\varphi}} \rangle_{\text{Cas}}^{\text{sp}} = \frac{1}{8\pi^2 R^4 \epsilon^4} \left[1 + \tfrac{1}{10}\epsilon + \dots \right], \tag{5.2.56}$$

where $\langle T^{\hat{\rho}}{}_{\hat{\rho}} \rangle_{\text{Cas}}^{\text{sp}}$ was obtained from $\langle T^{\hat{\varphi}}{}_{\hat{\varphi}} \rangle_{\text{Cas}}^{\text{sp}}$ using Eq. (5.1.31). The divergence of the Dirac field is one order of magnitude higher compared to the scalar field case (5.1.45). Before attempting to give a physical explanation for this difference, a comment on how this result fits in with Deutsch and Candelas' analysis [31] is worthwhile.

In their paper [31], Deutsch and Candelas assume that the SET can be written as:

$$T_{\mu\nu} = \epsilon^{-n_*} T_{\mu\nu}^{(n_*)} + \epsilon^{-n_*+1} T_{\mu\nu}^{(n_*-1)} + \dots, \tag{5.2.57}$$

with ϵ measuring the geodesic perpendicular distance from the boundary ($\epsilon = R - \rho$ for the cylindrical boundary considered in this chapter) and n_* being the leading order divergence of the SET (actually $T_{\mu\nu}^{(n_*)} = 0$, so $n_* - 1$ is the leading order). Each term $T^{(j)\mu}{}_{\mu}$ is assumed to be traceless. As a consequence, the leading order divergence of the SET in the present case of a cylindrical boundary is given by:

$$T^{\mu}{}_{\nu} = \alpha_* \operatorname{diag}[-\epsilon^{-n_*+1}, \frac{2}{n_* - 2}\epsilon^{-n_*+2}, 2\epsilon^{-n_*+1}, -\epsilon^{-n_*+1}), \tag{5.2.58}$$

where α_* is a constant which depends on the type of the analysed field. A comparison with (5.1.45) and (5.2.56) shows that the values for α_* and n_* are

$$\alpha_G = -\frac{1}{720\pi^2 R^4}, \qquad n_G = 4 \tag{5.2.59}$$

for scalars and

$$\alpha_S^{\rm sp} = -\frac{1}{16\pi^2 R^4}, \qquad n_S^{\rm sp} = 5, \tag{5.2.60}$$

for fermions.

It should be noted that Deutsch and Candelas start their analysis by assuming $n_* = 4$ on dimensional grounds. They regard ϵ as a geodesic distance having the dimension of length, then require that the SET is a tensor built exclusively using local quantities. However, the spectral boundary conditions have an intrinsic global character, directly involving the size of the system (the radius R of the cylinder). The results obtained in Refs. [12, 28, 29] for fermions in a $2 + 1$-dimensional space-time obeying inside a cylindrical boundary obeying MIT bag boundary conditions show that the Casimir divergence of the energy density as the boundary is approached is two orders of magnitude less than that obtained in this section. One order of magnitude can be attributed to the lower dimensionality of the space-time considered, while the second comes from the local nature of the MIT bag boundary conditions. The MIT bag model is considered in section 5.3, with the analysis of the Casimir effect performed in subsection 5.3.3.

Numerical results

The plots in Fig. 5.7 compare the asymptotic results in Eqs. (5.2.56) with numerical evaluations of Eqs. (5.2.42) for $\mu R = 0$ and $\mu R = 2$. The agreement between the asymptotic and numerical results as the boundary is approached is excellent, confirming the predicted order of divergence in Eqs. (5.2.56).

5.3 Dirac fermions obeying MIT bag boundary conditions

In this section, the MIT bag model [23] is considered. The boundary conditions, modes and energy spectrum are discussed in subsection 5.3.1. Thermal states are discussed in subsection 5.3.2, where the results obtained using the MIT and spectral models are compared qualitatively and quantitatively. The Casimir effect is investigated in subsection 5.3.3 and the result is compared with those obtained in the spectral case and with predictions from the literature [31].

5.3.1 Boundary conditions and mode solutions

In this subsection, the MIT bag boundary conditions are introduced, with an emphasis on the quantisation of the transverse momentum q and the corresponding
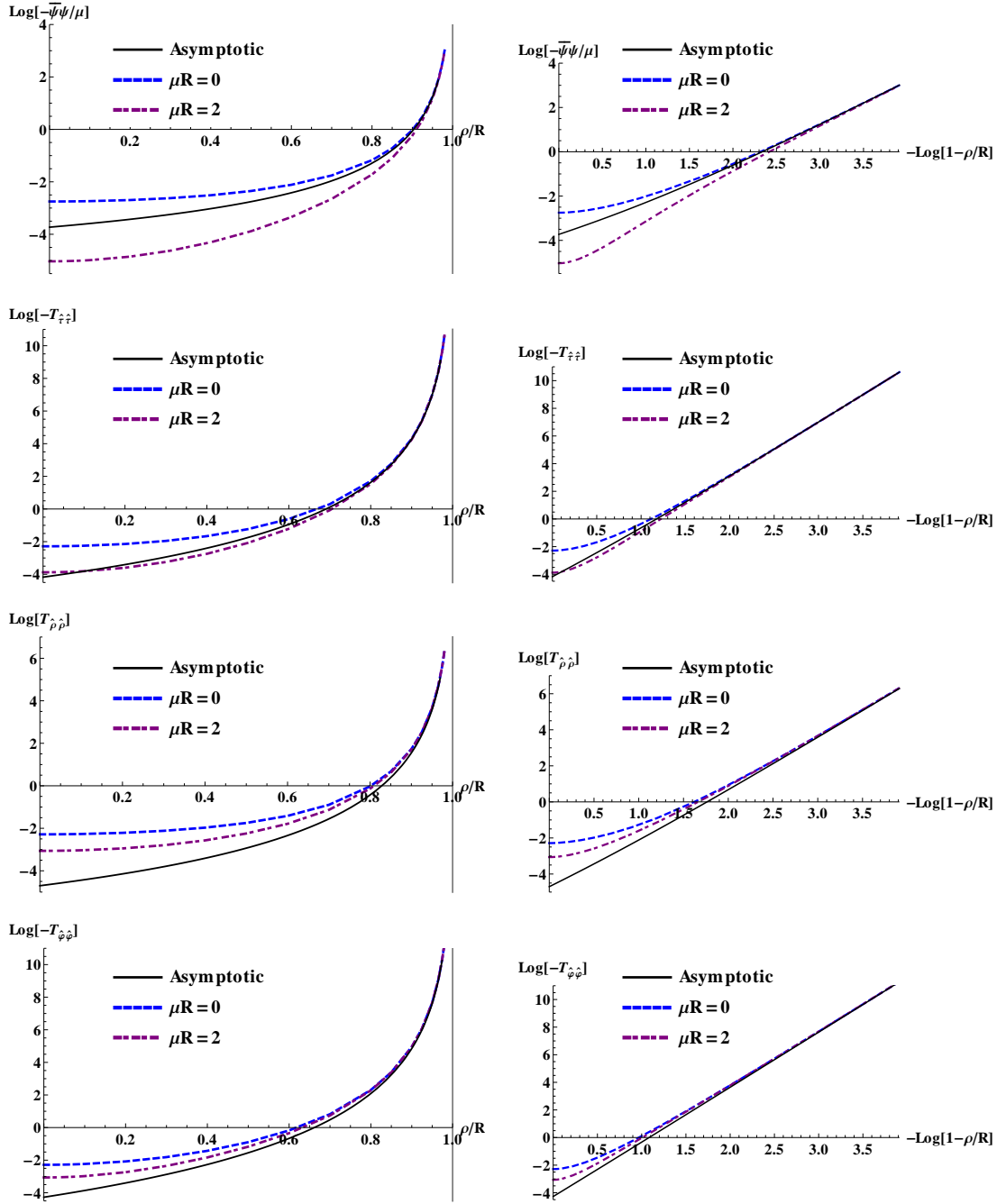
Figure 5.7: Logarithm of the Casimir expectation values of the fermion condensate $\overline{\psi}\psi$ (first line) and stress-energy tensor with respect to the distance from the rotation axis (left) and the logarithm of the inverse distance ϵ^{-1} to the boundary. The plots compare the results for massless (blue dashed curves) and massive (purple dashed curves) fermions to the asymptotic results (dark thin curves) in Eqs. (5.2.56).

energy spectrum. First introduced in Ref. [23], the MIT boundary conditions are designed to satisfy Eq. (2.2.31) in a purely local manner:

$$i\not{n}\psi(x_{\rm b}) = \varsigma\,\psi(x_{\rm b}), \qquad (5.3.1)$$

for any point $x_{\rm b}$ on the boundary, where n_μ represents the four-normal to the boundary and $\varsigma = \pm 1$.

Discretisation of transverse momentum

For a cylindrical boundary, $n = d\rho$, hence, the boundary conditions read as:

$$i\gamma^{\hat{\rho}}\psi(x_{\rm b}) = \varsigma\psi(x_{\rm b}). \qquad (5.3.2)$$

It can be checked that if $\psi(x)$ obeys the above boundary conditions, so does its charge conjugate, $i\gamma^{\hat{2}}\psi^*(x)$. Mode solutions $U^{\rm MIT}_{km\ell;E}$ that satisfy MIT boundary conditions can be constructed starting from the complete set of modes described in subsection 4.3.1. Since H, P_z and M_z commute with $i\gamma^{\hat{\rho}}$, the spinor $U^{\rm MIT}_{km\ell;E}$ can be a simultaneous eigenvector of these operators. However, the helicity operator W_0 does not commute with $i\gamma^{\hat{\rho}}$, therefore, $U^{\rm MIT}_{km\ell;E}$ must be a linear combination of the modes (3.3.2) corresponding to the two possible helicities, $\pm\frac{1}{2}$:

$$U^{\rm MIT}_{km\ell;E}(x) = {\sf b}^+_{km\ell;E}U^+_{Ekm}(x) + {\sf b}^-_{km\ell;E}U^-_{km\ell;E}(x), \qquad (5.3.3)$$

where ${\sf b}^\pm_{km\ell;E}$ are constants and $E \equiv E_{m\ell} = \pm\sqrt{\mu^2 + q^2_{m\ell} + k^2}$ controls the sign of the Minkowski energy (i.e. positive or negative). By analogy to the spectral boundary conditions case, the index ℓ has been introduced anticipating the quantisation of the transverse momentum q. For a given value of m, the allowed values of the transverse momentum are labeled by ℓ in increasing order, such that $q_{m,\ell} < q_{m,\ell+1}$. To avoid cumbersome notation, the indices m and ℓ are omitted from the corresponding momentum $p_{m,\ell}$ or Minkowski energy $E_{m,\ell}$ where there is no risk of confusion. Thus, Eq. (5.3.2) becomes:

$$\varsigma\mathfrak{E}_+({\sf b}^+_{km\ell;E}\phi^+_{km\ell} + {\sf b}^-_{km\ell;E}\phi^-_{km\ell}) = \frac{iE}{|E|}\mathfrak{E}_-({\sf b}^+_{km\ell;E}\sigma^\rho\phi^+_{km\ell} - {\sf b}^-_{km\ell;E}\sigma^\rho\phi^-_{km\ell}), \qquad (5.3.4)$$

where σ^ρ is defined in Eqs. (3.1.7) and $\mathfrak{E}_\pm$ is defined in Eq. (3.3.17). Equation (5.3.4) can be written as a set of linear equations in ${\sf b}^\pm_{km\ell;E}$:

$$\begin{pmatrix} \varsigma\mathfrak{E}_+{\sf p}_+J_m + \frac{E}{|E|}\mathfrak{E}_-{\sf p}_-J_{m+1} & \varsigma\mathfrak{E}_+{\sf p}_-J_m + \frac{E}{|E|}\mathfrak{E}_-{\sf p}_+J_{m+1} \\ \varsigma\mathfrak{E}_-{\sf p}_+J_m - \frac{E}{|E|}\mathfrak{E}_+{\sf p}_-J_{m+1} & -\varsigma\mathfrak{E}_-{\sf p}_-J_m + \frac{E}{|E|}\mathfrak{E}_+{\sf p}_+J_{m+1} \end{pmatrix}\begin{pmatrix} {\sf b}^+_{km\ell;E} \\ {\sf b}^-_{km\ell;E} \end{pmatrix} = 0, \qquad (5.3.5)$$

where $\mathfrak{p}_\pm$ is defined in Eq. (3.3.12). The system (5.3.5) has non-trivial solutions if:

$$\mathfrak{j}_{m\ell}^2 - \frac{2\varsigma\mu}{q_{m\ell}}\mathfrak{j}_{m\ell} - 1 = 0, \tag{5.3.6}$$

where

$$\mathfrak{j}_{m\ell} = J_m(q_{m\ell}R)/J_{m+1}(q_{m\ell}R). \tag{5.3.7}$$

Eq. (5.3.6) can be solved numerically to yield an infinite number of roots. Since Eq. (5.3.6) is invariant under $E \to -E$, the transverse momentum $q_{m,\ell}$ does not depend on the sign of E. Moreover, the relation $J_{-m}(z) = (-1)^m J_m(z)$ given in Eq. (A.1.4) ensures that

$$q_{-m-1,\ell} = q_{m,\ell}. \tag{5.3.8}$$

Equation (5.3.5) fixes $\mathfrak{b} \equiv \mathfrak{b}_{km\ell;E} = \mathfrak{b}_{km\ell;E}^+/\mathfrak{b}_{km\ell;E}^-$ to be

$$\mathfrak{b} = -\frac{\frac{\varsigma E}{|E|}\mathfrak{E}_+\mathfrak{p}_-\mathfrak{j} + \mathfrak{E}_-\mathfrak{p}_+}{\frac{\varsigma E}{|E|}\mathfrak{E}_+\mathfrak{p}_+\mathfrak{j} + \mathfrak{E}_-\mathfrak{p}_-} = \frac{\frac{\varsigma E}{|E|}\mathfrak{E}_-\mathfrak{p}_-\mathfrak{j} - \mathfrak{E}_+\mathfrak{p}_+}{\frac{\varsigma E}{|E|}\mathfrak{E}_-\mathfrak{p}_+\mathfrak{j} - \mathfrak{E}_+\mathfrak{p}_-}, \tag{5.3.9}$$

which is invariant under $(E, k, m) \to (-E, -k, -m-1)$.

There are simpler situations, e.g. the parallel plates system [39], where the MIT bag model method is easily implemented. A downside of the MIT bag boundary conditions is that they cannot be implemented using neutrinos, since negative chirality selects only one helicity state for neutrino particle modes (see [54] for a discussion of the MIT boundary conditions for neutrinos on Kerr). The MIT bag boundary conditions have been implemented succesfully for fermions confined inside a cylindrical boundary in a $2+1$-dimensional non-rotating space-time in Refs. [12, 28, 29]. Their results for the Casimir effect are compared with our original results presented in subsection 5.3.3.

Energy spectrum

To find the energy spectrum of the Dirac theory employing MIT bag boundary conditions, let us start by considering massless particles. In this case, the solutions of Eq. (5.3.6) are $\mathfrak{j}_{m\ell} = \pm 1$, the solutions $q_{m\ell}R$ of which are guaranteed by theorem 3.1 of Ref. [13] to satisfy:

$$\xi'_{m\ell} < q_{m,2\ell-1}R < \xi_{m\ell} < q_{m,2\ell}R < \xi'_{m,\ell+1}, \tag{5.3.10}$$

where

$$J_m(q_{m\ell}R) = (-1)^{\ell+1}J_{m+1}(q_{m\ell}R). \tag{5.3.11}$$

The first zero $\xi'_{m,1}$ of J'_m is bounded from below by [73]:

$$\xi'_{m,1} > \sqrt{m(m+2)}, \tag{5.3.12}$$
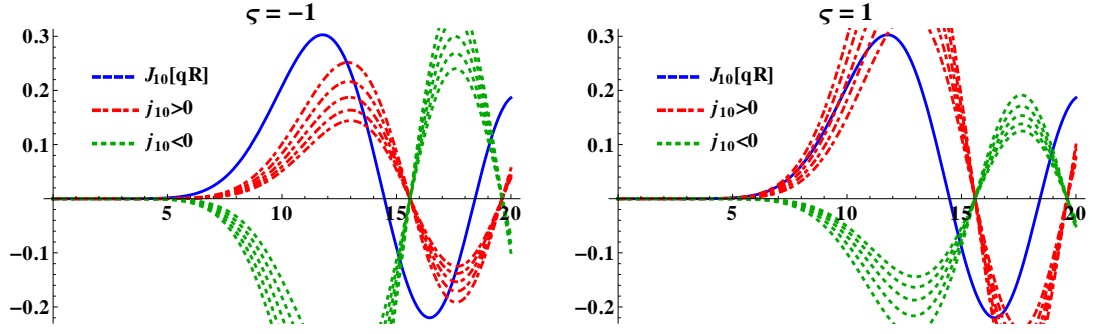
Figure 5.8: The first few values of the longitudinal momentum $q_{m\ell}$ allowed by the MIT bag boundary conditions at $m = 10$. The roots are located at the intersection between the solid line (representing $J_m(qR)$) and the dashed lines (representing $J_{m+1}(qR)$ multiplied by the right-hand side of Eq. (5.3.14)). The dotted curves correspond to $\mu = 0$, 2, 4, 6, 8 and 10. In the plot on the left, $\varsigma = -1$, and in the plot on the right, $\varsigma = 1$.

ensuring that $\xi'_{m,1} > m + \frac{1}{2}$ for $m > 0$, while at $m = 0$, the first root can be obtained numerically: $q_{0,1}R \simeq 1.4347$. Thus, the following inequality can be established:

$$|E_{m\ell}| R \geq q_{m\ell}R > m + \tfrac{1}{2}, \tag{5.3.13}$$

hence, $\widetilde{E}_{m\ell} = E_{m\ell} - \Omega(m + \frac{1}{2}) > 0$ for positive $E_{m\ell}$ and all values of m and ℓ as long as $R\Omega \leq 1$ (i.e. when the boundary is inside or on the SOL).

When the mass is non-zero, j can take the following values:

$$\mathsf{j}_{m\ell} = \frac{\varsigma\mu}{q_{m\ell}} \pm \sqrt{1 + \frac{\mu^2}{q_{m\ell}^2}}. \tag{5.3.14}$$

When $\varsigma = -1$, the positive value taken by j is smaller than 1, meaning that the smallest value $q_{m,1}$ for the longitudinal momentum allowed by the boundary conditions has to be larger than that for the massless case (i.e. when $J_m(q_{m,1}R) < J_{m+1}(q_{m,1}R)$, which occurs as $J_{m,1}$ decreases from its first maximum towards its first zero). Figure 5.8(b) illustrates this behaviour. Hence, it is clear that in this case, the lowest allowed energy obeys $\widetilde{E}R > (1 - \Omega R)(m + \frac{1}{2})$, meaning again that $E\widetilde{E} > 0$ for all $R \leq \Omega^{-1}$.

If $\varsigma = 1$, the quantity j increases as the mass increases and $q_{m,1}R$ approaches the origin. To establish the minimum value allowed for the energy $E(\mu) = \sqrt{\mu^2 + q^2}$, Eq. (5.3.14) can be rearranged as:

$$q\frac{J_m(qR)}{J_{m+1}(qR)} = \mu + E(\mu), \tag{5.3.15}$$

Equation (A.1.2) can be used to obtain

$$\lim_{z \to 0} z \frac{J_m(z)}{J_{m+1}(z)} = 2(m+1), \tag{5.3.16}$$

showing that $q = 0$ is a solution of Eq. (5.3.15) when $\mu R = m + 1$. If the mass increases further, the first root no longer corresponds to $j > 0$ (i.e. the first root disappears). In this case, $ER > m + \frac{1}{2}$ just from the mass contribution. To investigate the behaviour of the smallest allowed energy $E_{m,1}$ between $\mu = 0$ and $\mu = m + 1$, let us consider its derivative with respect to μ:

$$\partial_\mu E_{m,1}(\mu) = \frac{1}{E_{m,1}(\mu)} [\mu + q_{m,1}(\mu)\partial_\mu q_{m,1}], \tag{5.3.17}$$

Since $q_{m,1}(\mu)$ decreases as the mass increases, $\partial_\mu q_{m,1} < 0$ and $\partial_\mu E_{m,1}(\mu = 0) < 0$. The energy reaches a minimum when

$$q_{m,1}\partial_\mu q_{m,1}\big]_{\mu=\mu_0} = -\mu_0. \tag{5.3.18}$$

Using Eqs. (A.1.11) to replace the derivatives of the Bessel functions, the derivative with respect to μ of Eq. (5.3.15) gives:

$$\partial_\mu E = \frac{\mu(2m+1) - 2\mu ER + E}{E(2m+1) - 2E^2 R + \mu}. \tag{5.3.19}$$

It is easy to see from the above equation that $\partial_\mu E(\mu = 0) < 0$. However, the limit $\mu \to m + 1$ is not so easy to evaluate. By virtue of $E(\mu = m + 1) = R^{-1}(m + 1)$, the limit takes the following value:

$$\lim_{\mu \to m+1} \partial_\mu E = (2m + 1)/[2E(\mu)R + 1] = (2m + 1)/(2m + 3). \tag{5.3.20}$$

However,

$$\lim_{q \to 0} \partial_\mu E = 1. \tag{5.3.21}$$

The discrepancy between Eqs. (5.3.20) and (5.3.21) should not come as a surprise, since $m + 1$ is the largest value of μ at which the first root exists. Since the derivative is negative at $\mu = 0$, we either admit that the minimum value of $E_{m,1}$ is $R^{-1}(m+1)$ (i.e. $E_{m,1}$ continually decreases as μ increases to $R^{-1}(m + 1)$, or there is a value $\mu = \mu_0$ where $\partial_\mu E(\mu_0) = 0$. At such a point, Eq. (5.3.19) predicts that the value of the energy would be:

$$E(\mu_0) = \frac{\mu_0(2m+1)}{2\mu_0 R - 1} > R^{-1}(m + \tfrac{1}{2}). \tag{5.3.22}$$

Equation (5.3.22) seems to imply that the energy cannot be at a minimum with respect to the mass if $\mu R \leq \frac{1}{2}$. If a stationary point occurs for any $\mu R > \frac{1}{2}$, the
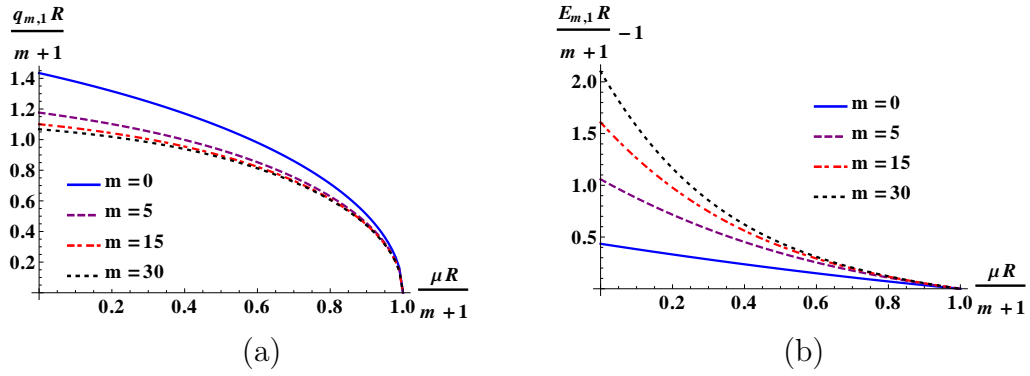
Figure 5.9: The dependence of the smallest allowed longitudinal momentum (a) and energy (b) in the MIT bag model corresponding to $\varsigma = 1$ for $\mu R = 0 \ldots m + 1$ at $m = 0, 5, 15, 30$. The horizontal axis represents the ratio $\mu R/(m + 1)$, normalizing the mass such that for any value of m, the range of the x axis is from 0 to 1. The longitudinal momentum $q_{m,1}$ and energy $E_{m,1}$ are divided by $R^{-1}(m + 1)$ and plot (b) shows the departure of $E_{m,1}R/(m+1)$ from the minimum value $m+1$. It can be seen that as m increases, the behaviour of $q_{m,1}$ tends towards an asymptotic trend. It can be seen that the energy does not present any stationary points throughout the range $\mu = 0 \ldots m + 1$.

corresponding value of the energy will be greater than $R^{-1}(m+\frac{1}{2})$. Since the energy is above $R^{-1}(m + \frac{1}{2})$ at the endpoints $\mu = 0$ and $\mu = m+1$ and since its stationary points are also above the aforementioned value, we can conclude that for all $E > 0$, $\widetilde{E}$ will satisfy:

$$\widetilde{E}_{m\ell}R > (1 - \Omega R)(m + \tfrac{1}{2}). \tag{5.3.23}$$

Hence, the MIT bag boundary conditions restrict the energy spectrum such that $E\widetilde{E} > 0$ for all acceptable modes, as long as the boundary is inside or on the SOL. Our numerical experiments confirm Eq. (5.3.19). Furthermore, the energy seems to be on a continuous decrease towards $m+1$ as μ increases from 0 to $m+1$, as shown in Figure 5.9.

Normalisation

The overall normalisation of the MIT modes is determined by the following orthogonality condition:

$$\langle U^{\mathrm{MIT}}_{km\ell;E}, U^{\mathrm{MIT}}_{k'm'\ell';E'}\rangle = \delta(k - k')\delta_{mm'}\delta_{\ell\ell'}\theta(EE'), \tag{5.3.24}$$

with respect to the Dirac inner product (2.2.30). Although an explicit check that the MIT modes are orthogonal if any of the labels do not match is a good exercise in algebra, it is unnecessary since the time invariance of the Dirac inner product, guaranteed to hold in the MIT bag model, ensures that the result of the inner product of modes with different energies (i.e. non-zero $E - E'$) vanishes. Thus, the

following result is obtained:

$$\langle U^{\mathrm{MIT}}_{km\ell;E}, U^{\mathrm{MIT}}_{k'm'\ell';E'}\rangle = \frac{1}{2}\delta(k-k')\delta_{mm'}\delta_{\ell\ell'}\theta(EE')\left|\mathfrak{b}^{-}_{km\ell;E}\right|^2$$

$$\times\left[(\mathcal{S}^{+}_{+}+\mathcal{S}^{-}_{+})\mathfrak{I}^{+}_{m}+(\mathcal{S}^{+}_{-}+\mathcal{S}^{-}_{-})\mathfrak{I}^{-}_{m}\right], \quad (5.3.25)$$

where the coefficients of the integrals $\mathfrak{I}^{\pm}_{m}$ (5.2.10) are given by:

$$\mathcal{S}^{+}_{\pm} = \mathfrak{E}^{2}_{+}(\mathfrak{b}_{km\ell;E}\mathfrak{p}_{+}+\mathfrak{p}_{-})^2 \pm \mathfrak{E}^{2}_{-}(\mathfrak{b}_{km\ell;E}\mathfrak{p}_{-}+\mathfrak{p}_{+})^2, \qquad (5.3.26a)$$

$$\mathcal{S}^{-}_{\pm} = \mathfrak{E}^{2}_{-}(\mathfrak{b}_{km\ell;E}\mathfrak{p}_{+}-\mathfrak{p}_{-})^2 \pm \mathfrak{E}^{2}_{+}(\mathfrak{b}_{km\ell;E}\mathfrak{p}_{-}-\mathfrak{p}_{+})^2, \qquad (5.3.26b)$$

where $\mathfrak{b}_{km\ell;E}$ is defined in Eq. (5.3.9). The following identities are useful:

$$\mathcal{S}^{+}_{\pm} = \frac{4k^2}{E^2}\frac{1\pm\mathfrak{j}^2}{(\frac{\varsigma E}{|E|}\mathfrak{E}_{+}\mathfrak{p}_{+}\mathfrak{j}+\mathfrak{E}_{-}\mathfrak{p}_{-})^2},$$

$$\mathcal{S}^{-}_{\pm} = \frac{4k^2}{E^2}\frac{1\pm\mathfrak{j}^2}{(\frac{\varsigma E}{|E|}\mathfrak{E}_{-}\mathfrak{p}_{+}x-\mathfrak{E}_{+}\mathfrak{p}_{-})^2},$$

$$\mathcal{S}^{+}_{\pm}+\mathcal{S}^{-}_{\pm} = \frac{8(1\pm\mathfrak{j}^2)}{\mathfrak{p}^{2}_{+}\mathfrak{j}^2+\mathfrak{p}^{2}_{-}},$$

$$\mathcal{S}^{+}_{\pm}-\mathcal{S}^{-}_{\pm} = -\frac{8(1\pm\mathfrak{j}^2)}{(\mathfrak{p}^{2}_{+}\mathfrak{j}^2+\mathfrak{p}^{2}_{-})^2}\left[(\mathfrak{j}^2-1)\frac{\mu^2+q^2}{\mu E}+(\mathfrak{j}^2+1)\frac{\mu k}{pE}\right]. \qquad (5.3.27)$$

Hence, the modes (5.3.3) are normalised according to Eq. (5.3.24) if

$$\mathfrak{b}^{-}_{km\ell;E} = \frac{1}{R\sqrt{2}\,|J_{m+1}(qR)|}\sqrt{\frac{\mathfrak{p}^{2}_{-}+\mathfrak{p}^{2}_{+}\mathfrak{j}^2}{(\mathfrak{j}^2+1)(\mathfrak{j}^2+1-\frac{2m+1}{qR}\mathfrak{j})-(\mathfrak{j}^2-1)\frac{\mathfrak{j}}{qR}}}, \qquad (5.3.28)$$

which is invariant under $(E,k,m)\to(-E,-k,-m-1)$. Recalling that $\mathfrak{b}_{km\ell;E}$ (5.3.9) is also invariant under the same transformation and using the properties (3.3.29) shows that the U and V spinors are equivalent:

$$V^{\mathrm{MIT}}_{km\ell;E} = (-1)^m\frac{iE}{|E|}U^{\mathrm{MIT}}_{-k,-m-1,\ell;-E}, \qquad (5.3.29)$$

or equivalently, in the language of Eq. (3.3.30),

$$V^{\mathrm{MIT}}_{j} = i(-1)^{m_j}U^{\mathrm{MIT}}_{\bar{\jmath}}, \qquad (5.3.30)$$

where $j=(E_j,k_j,\ell_j,m_j)$ and $\bar{\jmath}=(-E_j,-k_j,\ell_j,-m_j-1)$.

Equation (5.3.6) can be used to eliminate from Eq. (5.3.28) powers of $\mathfrak{j}$ higher than 1:

$$\mathfrak{b}^{-}_{km\ell;E} = \frac{1}{2R\,|J_{m+1}(qR)|}\sqrt{\frac{1+\frac{\varsigma\mu\mathfrak{j}}{q}\mathfrak{p}^{2}_{+}}{\left[1-\frac{\varsigma\mu}{q^2R}(m+1)+\frac{\mu^2}{q^2}\right](1+\frac{2\varsigma\mu}{q}\mathfrak{j})-\frac{\mathfrak{j}}{qR}(m+\frac{1}{2})}}. \qquad (5.3.31)$$

It is worth mentioning that in the massless limit, $b_{km\ell;E}^-$ simplifies to:

$$b_{km\ell;E}^-\big]_{\mu=0} = \frac{1}{2R\,|J_{m+1}(qR)|}\left[1 - \frac{j(m+\frac{1}{2})}{qR}\right]^{-\frac{1}{2}}. \tag{5.3.32}$$

Second quantisation

Having finished the construction of the field modes, the field operator can be expanded with respect to the rotating and Minkowski vacua:

$$\psi^{\mathrm{MIT}} = \sum_j \theta(\widetilde{E}_j)\left[U_j^{\mathrm{MIT}}b_{I;j}^{\mathrm{MIT}} + V_j^{\mathrm{MIT}}d_{I;j}^{\mathrm{MIT}\,\dagger}\right] \tag{5.3.33a}$$

$$= \sum_j \theta(E_j)\left[U_j^{\mathrm{MIT}}b_{V;j}^{\mathrm{MIT}} + V_j^{\mathrm{MIT}}d_{V;j}^{\mathrm{MIT}\,\dagger}\right], \tag{5.3.33b}$$

where

$$j = (k, m, \ell, E) \tag{5.3.34}$$

and the sum over j is understood as:

$$\sum_j \equiv \sum_{m_j=-\infty}^{\infty}\sum_{\ell_j=1}^{\infty}\int_{-\infty}^{\infty}dk_j\sum_{E_j=\pm|E_j|}. \tag{5.3.35}$$

5.3.2   Thermal expectation values

In this section, the thermal expectation values (t.e.v.s) of the fermion condensate $\overline{\psi}\psi$ (FC), charge current J^μ (CC) and stress-energy tensor $T_{\mu\nu}$ (SET) are calculated as described in subsection 4.3.2.

Thermal Hadamard function

The thermal Hadamard function for the MIT model is more challenging to calculate than in the spectral case due to the combination of positive and negative helicities in the modes. An expression equivalent to Eq. (3.3.54) can be written for the MIT case, keeping in mind that the sum over j does not include the helicity λ:

$$\Delta S_\beta^{(1)}(x, x') = \sum_j e^{-i\widetilde{E}_j\Delta t + ik_j\Delta z}[w(\widetilde{E}_j) - w(-\widetilde{E}_j)]M_j, \tag{5.3.36}$$

where the density of states factors $w(E)$ are defined in Eqs. (4.3.14) for the Minkowski and Iyer vacua, while M_j is defined in terms of the spinors in Eqs. (3.3.16) and

(3.3.23b) as:

$$M_j = \mathfrak{b}_j^2 u_j^+(x) \otimes \overline{u}_j^+(x') + \mathfrak{b}_j[u_j^+(x) \otimes \overline{u}_j^-(x') + u_j^-(x) \otimes \overline{u}_j^+(x')] + u_j^-(x) \otimes \overline{u}_j^-(x').$$
(5.3.37)

In the above, the superscripts $\pm$ indicate the helicity. The following direct products of u_j spinors are required:

$$\frac{u_j^\pm \otimes \overline{u}_j^\pm}{|b_-|^2} = \begin{pmatrix} \mathfrak{E}_+^2 & \mp\frac{E}{|E|}\mathfrak{E}_-\mathfrak{E}_+ \\ \pm\frac{E}{|E|}\mathfrak{E}_-\mathfrak{E}_+ & -\mathfrak{E}_-^2 \end{pmatrix} \otimes \left[\phi_j^\pm \otimes \phi_j^{\pm\,\dagger}\right],$$

$$\frac{u_j^\pm \otimes \overline{u}_j^\mp}{|b_-|^2} = \begin{pmatrix} \mathfrak{E}_+^2 & \pm\frac{E}{|E|}\mathfrak{E}_-\mathfrak{E}_+ \\ \pm\frac{E}{|E|}\mathfrak{E}_-\mathfrak{E}_+ & \mathfrak{E}_-^2 \end{pmatrix} \otimes \left[\phi_j^\pm \otimes \phi_j^{\mp\,\dagger}\right],$$
(5.3.38)

Using their exact form (3.3.11), the direct products of the ϕ two-spinors can be written as:

$$\phi_j^\pm \otimes \phi_j^{\pm\,\dagger} = \frac{1}{2} \begin{pmatrix} \mathfrak{p}_\pm^2 & \pm p_- p_+ \\ \pm p_- p_+ & p_\mp^2 \end{pmatrix} \circ \mathcal{M}_j,$$

$$\phi_j^\pm \otimes \phi_j^{\mp\,\dagger} = \frac{1}{2} \begin{pmatrix} p_+ p_- & \mp p_\pm^2 \\ \pm p_\mp^2 & -p_+ p_- \end{pmatrix} \circ \mathcal{M}_j,$$
(5.3.39)

where Eq. (3.3.58) gives the matrix $\mathcal{M}_j$ on the right hand side of the Hadamard (Schur) product sign $\circ$. Next, M_j can be written in a manner similar to Eq. (3.3.56):

$$M_j = \frac{|b_-|^2}{4\pi^2} \begin{pmatrix} M_j^{\mathrm{up}} \circ \mathcal{M}_j & -M_j^\times \circ \mathcal{M}_j \\ M_j^{\times\,\dagger} \circ \mathcal{M}_j & -M_j^{\mathrm{down}} \circ \mathcal{M}_j \end{pmatrix},$$
(5.3.40)

where the Hadamard product $\circ$ is taken with the matrix $\mathcal{M}_j$ defined in Eq. (3.3.58) and

$$M_j^{\mathrm{up}} = \frac{\mathfrak{E}_+^2}{2} \begin{pmatrix} (\mathfrak{b}\mathfrak{p}_+ + \mathfrak{p}_-)^2 & (\mathfrak{b}\mathfrak{p}_+ + \mathfrak{p}_-)(\mathfrak{b}\mathfrak{p}_- - \mathfrak{p}_+) \\ (\mathfrak{b}\mathfrak{p}_+ + \mathfrak{p}_-)(\mathfrak{b}\mathfrak{p}_- - \mathfrak{p}_+) & (\mathfrak{b}\mathfrak{p}_- - \mathfrak{p}_+)^2 \end{pmatrix},$$

$$M_j^{\mathrm{down}} = \frac{\mathfrak{E}_-^2}{2} \begin{pmatrix} (\mathfrak{b}\mathfrak{p}_+ - \mathfrak{p}_-)^2 & (\mathfrak{b}\mathfrak{p}_+ - \mathfrak{p}_-)(\mathfrak{b}\mathfrak{p}_- + \mathfrak{p}_+) \\ (\mathfrak{b}\mathfrak{p}_+ - \mathfrak{p}_-)(\mathfrak{b}\mathfrak{p}_- + \mathfrak{p}_+) & (\mathfrak{b}\mathfrak{p}_- + \mathfrak{p}_+)^2 \end{pmatrix},$$

$$M_j^\times = \frac{p}{2E} \begin{pmatrix} (\mathfrak{b}^2\mathfrak{p}_+^2 - \mathfrak{p}_-^2) & (\mathfrak{b}\mathfrak{p}_+ + \mathfrak{p}_-)(\mathfrak{b}\mathfrak{p}_- + \mathfrak{p}_+) \\ (\mathfrak{b}\mathfrak{p}_+ - \mathfrak{p}_-)(\mathfrak{b}\mathfrak{p}_- - \mathfrak{p}_+) & (\mathfrak{b}^2\mathfrak{p}_-^2 - \mathfrak{p}_+^2) \end{pmatrix},$$
(5.3.41)

Using the definition (5.3.9) for $\mathfrak{b}$, the following identities can be established:

$$\mathfrak{b} = \frac{-2\varsigma E}{p}\frac{\mathfrak{j}}{\mathfrak{p}_+^2\mathfrak{j}^2 + \mathfrak{p}_-^2}, \qquad \mathfrak{b}^2 + 1 = \frac{2(\mathfrak{j}^2 + 1)}{\mathfrak{p}_+^2\mathfrak{j}^2 + \mathfrak{p}_-^2}, \qquad \mathfrak{b}^2 - 1 = -\frac{2k}{p}\frac{\mathfrak{j}^2 - 1}{\mathfrak{p}_+^2\mathfrak{j}^2 + \mathfrak{p}_-^2}.$$
(5.3.42)

Thus, the matrices M_j^* given in (5.3.41) can be put in the form:

$$M_j^{\text{up}} = \frac{\mathfrak{E}_+^2}{\mathfrak{p}_+^2 \mathfrak{j}^2 + \mathfrak{p}_-^2} \begin{pmatrix} \mathfrak{j}^2 + 1 - \frac{k^2}{p^2}(\mathfrak{j}^2 - 1) - \frac{2\varsigma qE}{p^2}\mathfrak{j} & -\frac{kq}{p^2}\left(\mathfrak{j}^2 - 1 - \frac{2\varsigma E}{q}\mathfrak{j}\right) \\ -\frac{kq}{p^2}\left(\mathfrak{j}^2 - 1 - \frac{2\varsigma E}{q}\mathfrak{j}\right) & \mathfrak{j}^2 + 1 + \frac{k^2}{p^2}(\mathfrak{j}^2 - 1) + \frac{2\varsigma qE}{p^2}\mathfrak{j} \end{pmatrix},$$

$$M_j^{\text{down}} = \frac{\mathfrak{E}_-^2}{\mathfrak{p}_+^2 \mathfrak{j}^2 + \mathfrak{p}_-^2} \begin{pmatrix} \mathfrak{j}^2 + 1 - \frac{k^2}{p^2}(\mathfrak{j}^2 - 1) + \frac{2\varsigma qE}{p^2}\mathfrak{j} & -\frac{kq}{p^2}\left(\mathfrak{j}^2 - 1 + \frac{2\varsigma E}{q}\mathfrak{j}\right) \\ -\frac{kq}{p^2}\left(\mathfrak{j}^2 - 1 + \frac{2\varsigma E}{q}\mathfrak{j}\right) & \mathfrak{j}^2 + 1 + \frac{k^2}{p^2}(\mathfrak{j}^2 - 1) - \frac{2\varsigma qE}{p^2}\mathfrak{j} \end{pmatrix},$$

$$M_j^{\times} = \frac{1}{\mathfrak{p}_+^2 \mathfrak{j}^2 + \mathfrak{p}_-^2} \begin{pmatrix} \frac{2k}{E} & \frac{q}{E}(\mathfrak{j}^2 + 1) - 2\varsigma\mathfrak{j} \\ \frac{q}{E}(\mathfrak{j}^2 + 1) + 2\varsigma\mathfrak{j} & -\frac{2k\mathfrak{j}^2}{E} \end{pmatrix}. \tag{5.3.43}$$

Employing the symmetrization (3.3.59), M_j can be put in the form:

$$4\pi^2 M_j = \frac{|\mathsf{b}_-|^2}{\mathfrak{p}_+^2 \mathfrak{j}^2 + \mathfrak{p}_-^2} \left\{ 2\sigma_3 \otimes \left[\begin{pmatrix} 1 & 0 \\ 0 & \mathfrak{j}^2 \end{pmatrix} \circ \mathcal{M}_j \right] \right.$$

$$+ I_2 \otimes \left[\begin{pmatrix} \frac{\mu}{E}(\mathfrak{j}^2 + 1) - \frac{2\varsigma\mathfrak{j}}{qE}(\mu^2 + q^2) & 1 \\ 1 & \frac{\mu}{E}(\mathfrak{j}^2 + 1) + \frac{2\varsigma\mathfrak{j}}{qE}(\mu^2 + q^2) \end{pmatrix} \circ \mathcal{M}_j \right]$$

$$\left. + \frac{1}{E} \begin{pmatrix} 0 & -1 \\ 1 & 0 \end{pmatrix} \otimes \left[\begin{pmatrix} 2k & q(\mathfrak{j}^2 + 1) - 2\varsigma E\mathfrak{j} \\ q(\mathfrak{j}^2 + 1) + 2\varsigma E\mathfrak{j} & -2k \end{pmatrix} \circ \mathcal{M}_j \right] \right\}, \tag{5.3.44}$$

where σ_3 is a Pauli matrix, defined in Eqs. (2.2.8).

Fermion condensate

Taking the trace of Eq. (5.3.44) gives the following t.e.v. for the FC:

$$\langle : \overline{\psi}\psi : \rangle_\beta^{\text{MIT}} = -\sum_{m=0}^\infty \sum_{\ell=1}^\infty \int_0^\infty \frac{dk}{2\mathcal{D}_{m\ell}^{\text{MIT}}} [w(\widetilde{E}) + w(\overline{E})]$$

$$\times \left[\frac{\mu}{E}(\mathfrak{j}^2 + 1) J_m^+(q\rho) - \frac{2\varsigma\mathfrak{j}}{qE}(q^2 + \mu^2) J_m^-(q\rho) \right]. \tag{5.3.45}$$

where $J_m^\pm(q\rho)$ are defined in Eqs. (3.3.69) and the denominator $\mathcal{D}_{m\ell}^{\text{MIT}}$ is given by:

$$\mathcal{D}_{m\ell}^{\text{MIT}} = \pi^2 R^2 J_{m+1}^2(qR) \left[(\mathfrak{j}^2 + 1)\left(\mathfrak{j}^2 + 1 - \frac{2m+1}{qR}\mathfrak{j}\right) - \frac{\mathfrak{j}}{qR}(\mathfrak{j}^2 - 1) \right]. \tag{5.3.46}$$

As opposed to the FC in the spectral model, given in Eq. (5.2.16), the massless limit of the FC in the MIT model is finite, giving a first qualitative difference between the models. It is also remarkable that the sign of the massless limit of the FC depends on the sign of ς. It is also worth evaluating the FC on the boundary, where $J_m(qR) = \mathfrak{j}J_{m+1}(qR)$, for the purpose of which the square brackets in Eq. (5.3.45)

can be divided by $J_{m+1}^2(qR)$:

$$\langle : \overline{\psi}\psi :\rangle_\beta^{\mathrm{MIT}}\Big|_{\rho=R} = -\sum_{m=0}^\infty \sum_{\ell=1}^\infty \int_0^\infty dk \frac{\mu\, J_{m+1}^2(qR)}{2E\mathcal{D}_{m\ell}^{\mathrm{MIT}}}[w(\widetilde{E}) + w(\overline{E})]$$

$$\times \left[(\mathsf{j}^2 + 1)^2 - \tfrac{2\varsigma\mathsf{j}}{q\mu}(q^2 + \mu^2)(\mathsf{j}^2 - 1)\right]. \quad (5.3.47)$$

Equation (5.3.6) can now be used to replace $\mathsf{j} = \frac{2\sigma\mu}{q}\mathsf{j} + 1$ to show that the term in the brackets vanishes. Thus, the FC vanishes on the boundary for any mass and regardless of the sign of ς.

Neutrino charge current

As in the spectral case, the t.e.v. of the CC vanishes because the summands corresponding to the t, ρ and φ, and z components are odd with respect to $m \to -m - 1$ and $k \to -k$, respectively. The rules for checking the transformation properties under $m \to -m - 1$ are:

$$\mathsf{j} \to -\frac{1}{\mathsf{j}}, \qquad m + \tfrac{1}{2} \to -m - \tfrac{1}{2}, \qquad J_m^\pm \to \pm J_m^\pm, \qquad J_m^\times \to -J_m^\times,$$

$$w(\widetilde{E}) \pm w(\overline{E}) \to \pm[w(\widetilde{E}) \pm w(\overline{E})]. \qquad (5.3.48)$$

The only non-vanishing component of the neutrino charge current (2.2.55b) is, like in the spectral model case, the z component:

$$\langle : J_\nu^{\hat{z}} :\rangle_\beta^{\mathrm{MIT}} = \sum_{m=0}^\infty \sum_{\ell=1}^\infty \int_0^\infty \frac{dk}{4\mathcal{D}_{m\ell}^{\mathrm{MIT}}}[w(\widetilde{E}) - w(\overline{E})]\left[(\mathsf{j}^2 + 1)J_m^-(q\rho) - (\mathsf{j}^2 - 1)J_m^+(q\rho)\right].$$

$$(5.3.49)$$

While it is not clear from the above expression whether the charge current changes sign as ρ increases from 0 to R, it is remarkable that it vanishes on the boundary:

$$\langle : J_\nu^{\hat{z}} :\rangle_\beta^{\mathrm{MIT}}\Big|_{\rho=0} = \sum_{\ell=1}^\infty \int_0^\infty \frac{dk[w(\widetilde{E}) - w(\overline{E})]}{2\mathcal{D}_{m\ell}^{\mathrm{MIT}}} \qquad (5.3.50\text{a})$$

$$\langle : J_\nu^{\hat{z}} :\rangle_\beta^{\mathrm{MIT}}\Big|_{\rho=R} = 0. \qquad (5.3.50\text{b})$$

The property that the neutrino charge current vanishes on the boundary gives a second qualitative difference between the spectral and MIT bag models (in the former case, it reaches a finite value having the sign opposite to its sign on the rotation axis).

Stress-energy momentum

The non-vanishing components of the t.e.v. of the SET are:

$$\langle: T_{\hat{t}\hat{t}}:\rangle_\beta^{\mathrm{MIT}} = -\sum_{m=0}^\infty \sum_{\ell=1}^\infty \int_0^\infty \frac{E\,dk}{2\mathcal{D}_{m\ell}^{\mathrm{MIT}}}[w(\widetilde{E}) + w(\overline{E})]$$
$$\times \left[(\mathrm{j}^2+1)J_m^+(q\rho) - (\mathrm{j}^2-1)J_m^-(q\rho)\right], \tag{5.3.51a}$$

$$\langle: T_{\hat{\rho}\hat{\rho}}:\rangle_\beta^{\mathrm{MIT}} = -\sum_{m=0}^\infty \sum_{\ell=1}^\infty \int_0^\infty \frac{q^2\,dk}{2E\mathcal{D}_{m\ell}^{\mathrm{MIT}}}[w(\widetilde{E}) + w(\overline{E})]$$
$$\times (\mathrm{j}^2+1)\left[J_m^+(q\rho) - \frac{m+\frac{1}{2}}{q\rho}J_m^\times(q\rho)\right], \tag{5.3.51b}$$

$$\langle: T_{\hat{\varphi}\hat{\varphi}}:\rangle_\beta^{\mathrm{MIT}} = -\sum_{m=0}^\infty \sum_{\ell=1}^\infty \int_0^\infty \frac{q^2\,dk}{2E\mathcal{D}_{m\ell}^{\mathrm{MIT}}}[w(\widetilde{E}) + w(\overline{E})](\mathrm{j}^2+1)\frac{m+\frac{1}{2}}{q\rho}J_m^\times(q\rho),$$
$$\tag{5.3.51c}$$

$$\langle: T_{\hat{z}\hat{z}}:\rangle_\beta^{\mathrm{MIT}} = -\sum_{m=0}^\infty \sum_{\ell=1}^\infty \int_0^\infty \frac{k^2\,dk}{2E\mathcal{D}_{m\ell}^{\mathrm{MIT}}}[w(\widetilde{E}) + w(\overline{E})]$$
$$\times \left[(\mathrm{j}^2+1)J_m^+(q\rho) - (\mathrm{j}^2-1)J_m^-(q\rho)\right], \tag{5.3.51d}$$

$$\langle: T_{\hat{t}\hat{\varphi}}:\rangle_\beta^{\mathrm{MIT}} = \sum_{m=0}^\infty \sum_{\ell=1}^\infty \int_0^\infty \frac{[w(\widetilde{E}) - w(\overline{E})]dk}{4\rho\mathcal{D}_{m\ell}^{\mathrm{MIT}}}\left\{(\mathrm{j}^2-1)\left[\tfrac{1}{2}J_m^+(q\rho) - (m+\tfrac{1}{2})J_m^-(q\rho)\right]\right.$$
$$\left. + (\mathrm{j}^2+1)\left[(m+\tfrac{1}{2})J_m^+(q\rho) - \tfrac{1}{2}J_m^-(q\rho) + q\rho J_m^\times(q\rho)\right] \right\}. \tag{5.3.51e}$$

The above results reveal a third qualitative difference between the MIT and spectral models: $\langle: T_{\hat{\varphi}\hat{\varphi}}:\rangle_\beta$ stays finite on the boundary in the MIT model, while Eqs. (5.2.20) show that it vanishes in the spectral model. As in the spectral case, the relation (2.2.28) between the trace of the SET and the FC can be verified directly.

Numerical results

The plots in this section show the t.e.v.s of the fermion condensate (FC), neutrino charge current (CC) and stress-energy tensor (SET) obtained in the MIT model, using Eqs. (5.3.45), (5.3.49) and (5.3.51).

Figures 5.10 and 5.11 show numerical results for the case when the boundary is located at $\Omega R = 0.5$. Results for massless fermions (shown with thick dashed coloured lines) are compared with results for fermions of mass $\mu R = 2$ with $\varsigma = 1$ (left) and $\varsigma = -1$ (right). The analytic results for the unbounded case obtained with respect to the rotating (Iyer) vacuum, given in Eqs. (4.3.56), are shown in thin black lines. The results for massless fermions are independent of ς, except in the case of the FC, when ς controls its sign. It can be seen from the plots that the profiles for $\varsigma = 1$ are more energetic (i.e. correspond to larger values) than those obtained with ς set to -1. This can be understood by looking at the position of the roots in the
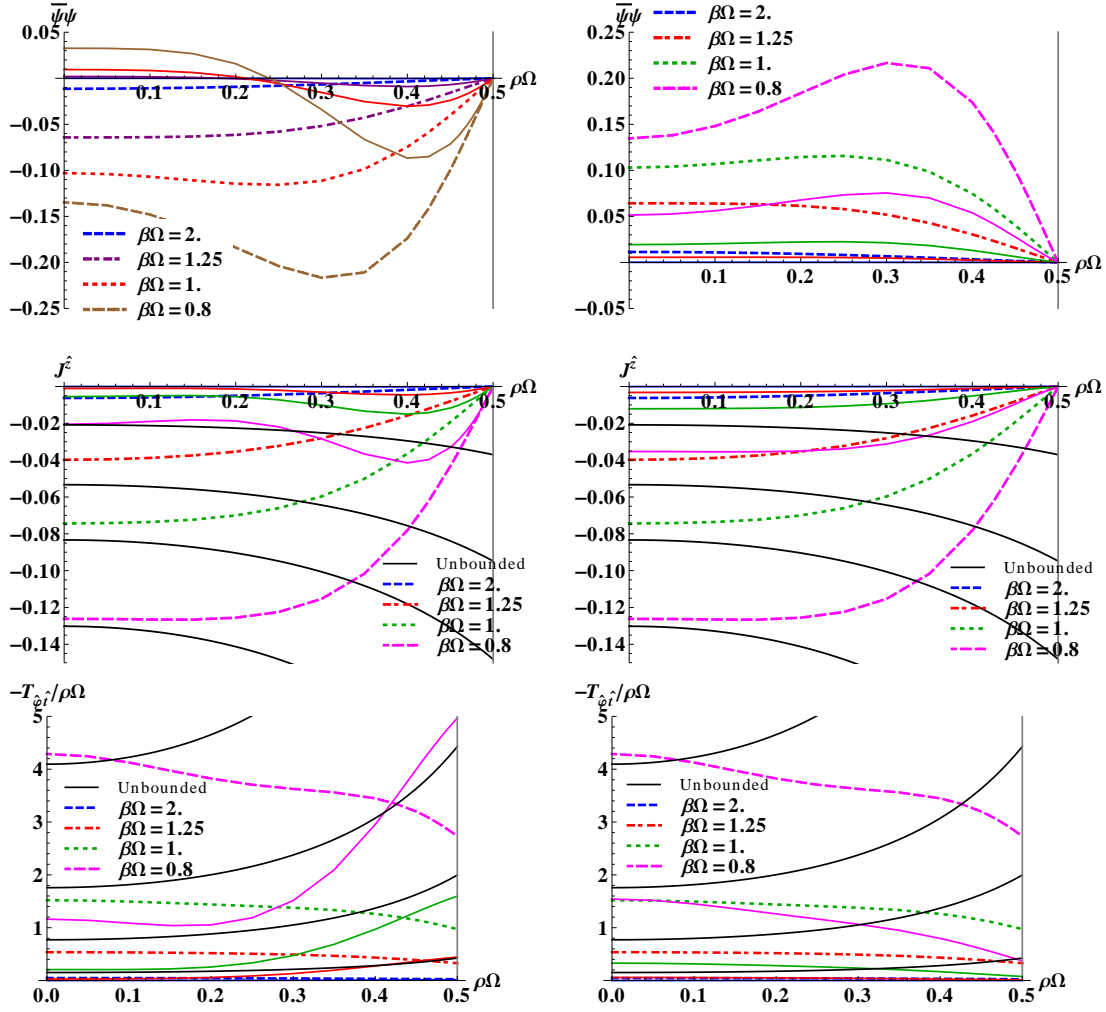
Figure 5.10: Comparison of t.e.v.s corresponding to massless (thick coloured dashed lines) and massive (thin coloured lines, $\mu R = 2$) to the analytic results (4.3.56) obtained in the unbounded case with respect to the rotating (Iyer) vacuum. The value of ς on the left and right columns is -1 and 1. The boundary is placed at $R\Omega = 0.5$. From top to bottom, the plots display: the fermion condensate, the neutrino charge current along the rotation axis and $\langle : T_{\hat{\varphi}\hat{t}} : \rangle_\beta$.

two cases, depicted in Figure 5.8. As the mass increases, the value of the first root for the $\varsigma = 1$ case decreases, while when $\varsigma = -1$, it increases. This behaviour can be extrapolated to subsequent roots. Consequently, the roots from the $\varsigma = 1$ case make contributions to t.e.v.s. which are less suppressed by the Fermi-Dirac density of states factor than in the $\varsigma = -1$ case, resulting in more energetic t.e.v.s. What is unexpected is that the profiles for massive fermions at $\varsigma = 1$ can sit higher than the massless profile, but we explain this behaviour with the same argument presented above. Another peculiar feature is that the sign of the FC changes between the rotation axis and the boundary, for both values of ς. The numerical results confirm the analytic predictions that the FC and the neutrino CC vanish on the boundary, while $\langle : T_{\hat{\varphi}\hat{t}} : \rangle_\beta$ stays finite.

The same comparisons are made (using the same conventions for the line types and colours) for the case when the boundary is placed on the speed of light surface ($\Omega R = 1.0$) in Figures 5.12 and 5.13. All plots show the logarithm of the t.e.v., except for the plot for the FC when $\sigma = 1$, which changes sign between the rotation axis and the boundary. As for the case when $\Omega R = 0.5$, the t.e.v.s corresponding to $\varsigma = 1$ are more energetic (i.e. correspond to larger values) than those obtained with ς set to -1. The FC and neutrino CC vanish on the axis, while the SET stays finite throughout the domain.

Figure 5.14 provides a comparison of the behaviour of the t.e.v.s of the neutrino charge current and SET for the MIT and spectral models. The boundary is on the SOL and the mass is set to 0. Since the FC is 0 in the spectral case for massless fermions, it is not shown in the Figure. However, qualitative differences can be seen between the two models in the plots, as follows. The neutrino CC in the MIT model stays negative throughout the domain but reaches 0 on the boundary, while in the spectral case, it changes sign, reaching a positive value on the boundary; and the component $\langle : T_{\hat{\varphi}\hat{\varphi}} : \rangle_\beta$ reaches a finite value on the boundary in the MIT case, but vanishes on the boundary in the spectral case.

A comparison between the MIT and spectral models and the analytic results (4.3.56) at large temperature ($\beta\Omega = 0.05$) is performed in Figure 5.15, which shows that for $\beta = 0.05$ the agreement between the analytic solution for the unbounded space-time and the numerical results for the space-time inside a boundary at $R\Omega = \frac{1}{2}$ is excellent at sufficiently large distances from the rotation axis and the surface. However, the energy density in the spectral model strongly departs from the analytic profile as the boundary is approached, while the results in the MIT case follow it closely. There are strong deviations in both models in the profile of the neutrino charge current: in the spectral model, $\langle : J_\nu^{\hat{z}} : \rangle_\beta$ changes sign from negative to positive, after which it grows, becoming significantly bigger in absolute value than the analytic prediction; in the MIT bag model, the neutrino charge current sharply drops to 0 as the boundary is approached.
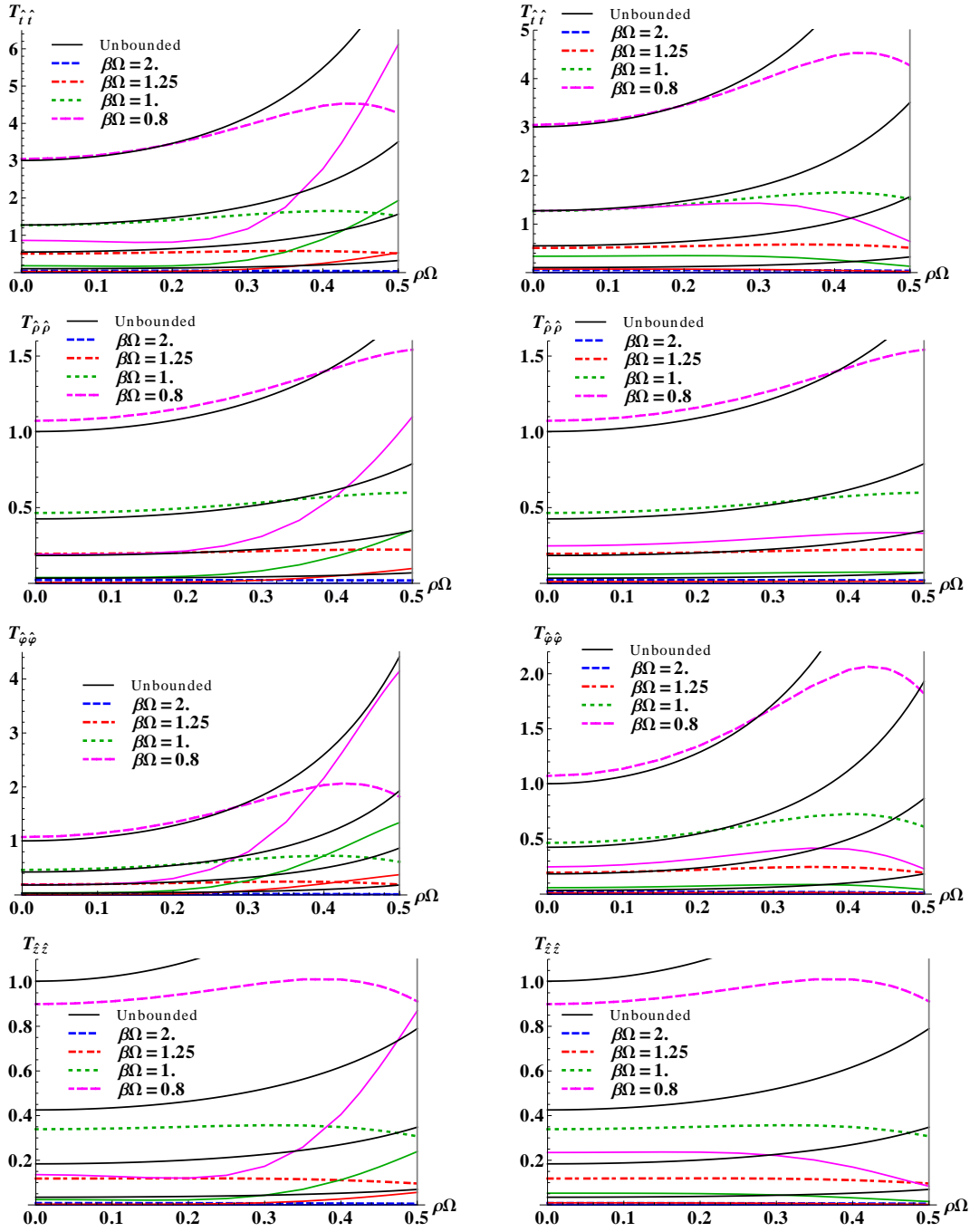
Figure 5.11: Comparison of t.e.v.s corresponding to massless (thick coloured dashed lines) and massive (thin coloured lines, $\mu R = 2$) with the analytic results (4.3.56) obtained in the unbounded case with respect to the rotating (Iyer) vacuum. The boundary is placed at $R\Omega = 0.5$ and ς is 1 and -1 on the left and right columns, respectively. From top to bottom, the plots display: $\langle : T_{\hat{t}\hat{t}} : \rangle_\beta$, $\langle : T_{\hat{\rho}\hat{\rho}} : \rangle_\beta$, $\langle : T_{\hat{\varphi}\hat{\varphi}} : \rangle_\beta$ and $\langle : T_{\hat{z}\hat{z}} : \rangle_\beta$.
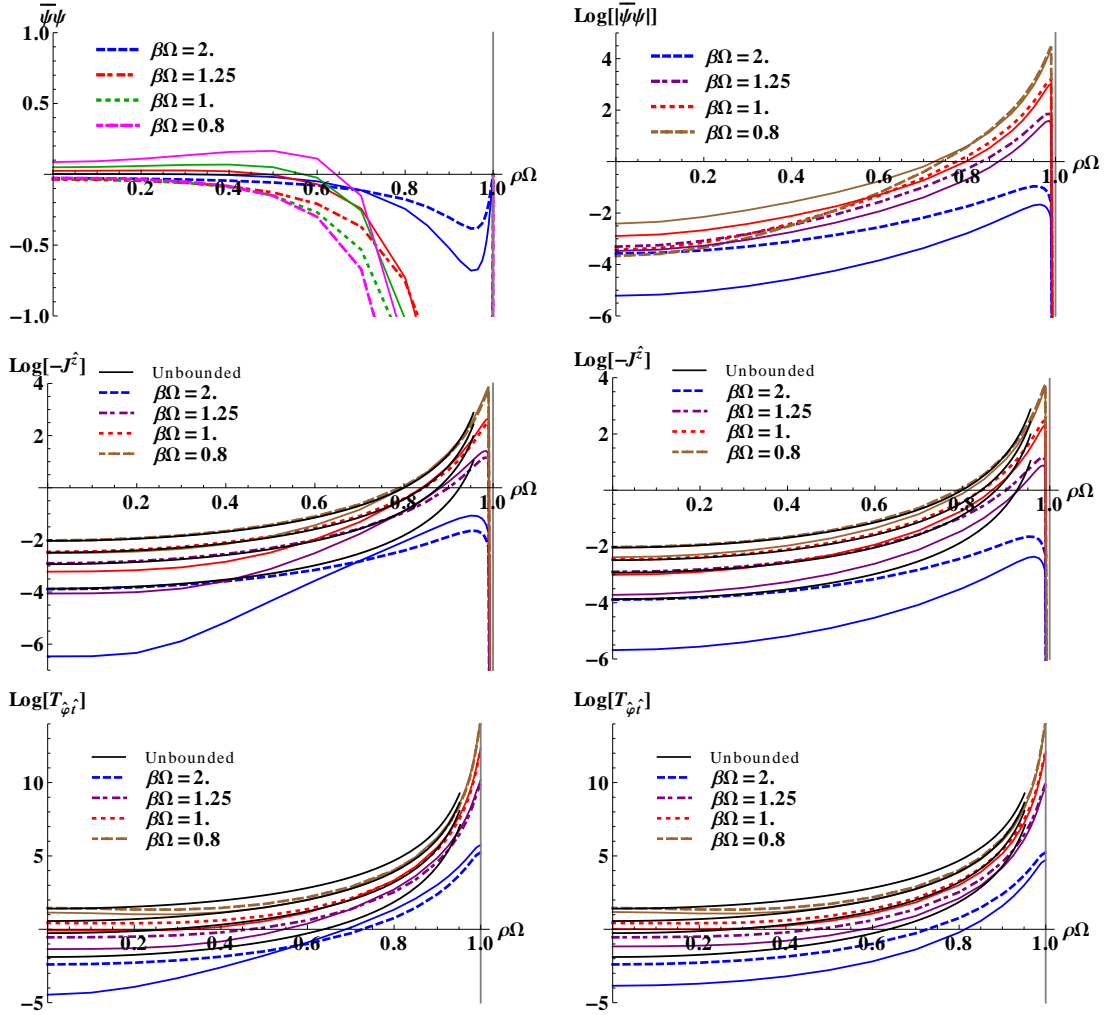
Figure 5.12: Comparison of t.e.v.s corresponding to massless (thick coloured dashed lines) and massive (thin coloured lines, $\mu R = 2$) to the analytic results (4.3.56) obtained in the unbounded case with respect to the rotating (Iyer) vacuum. The value of ς on the left and right columns is -1 and 1. The boundary is placed on the speed of light surface, at $R\Omega = 1.0$. From top to bottom, the plots display: the fermion condensate, the neutrino charge current along the rotation axis and $\langle : T_{\hat{\varphi}\hat{t}} : \rangle_\beta$. Apart from the FC in the case $\varsigma = 1$ (where its t.e.v. changes sign in the massive case).
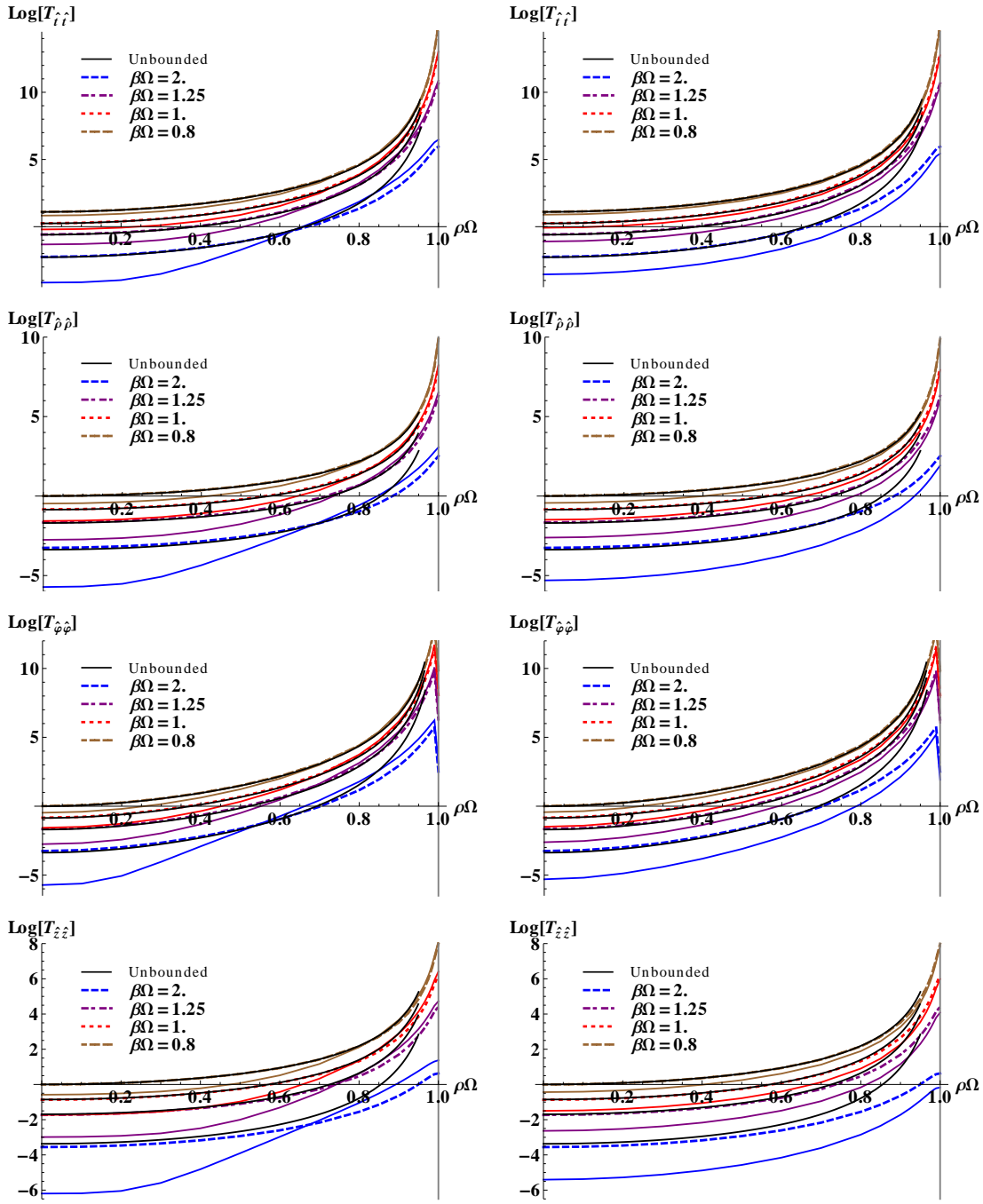
Figure 5.13: Comparison of t.e.v.s corresponding to massless (thick coloured dashed lines) and massive (thin coloured lines, $\mu = 2\Omega$) with the analytic results (4.3.56) obtained in the unbounded case with respect to the rotating (Iyer) vacuum. The boundary is placed at $R\Omega = 1.0$ and ς is 1 and -1 on the left and right columns, respectively. From top to bottom, the plots display: $\langle : T_{\hat{t}\hat{t}} : \rangle_\beta$, $\langle : T_{\hat{\rho}\hat{\rho}} : \rangle_\beta$, $\langle : T_{\hat{\varphi}\hat{\varphi}} : \rangle_\beta$ and $\langle : T_{\hat{z}\hat{z}} : \rangle_\beta$.
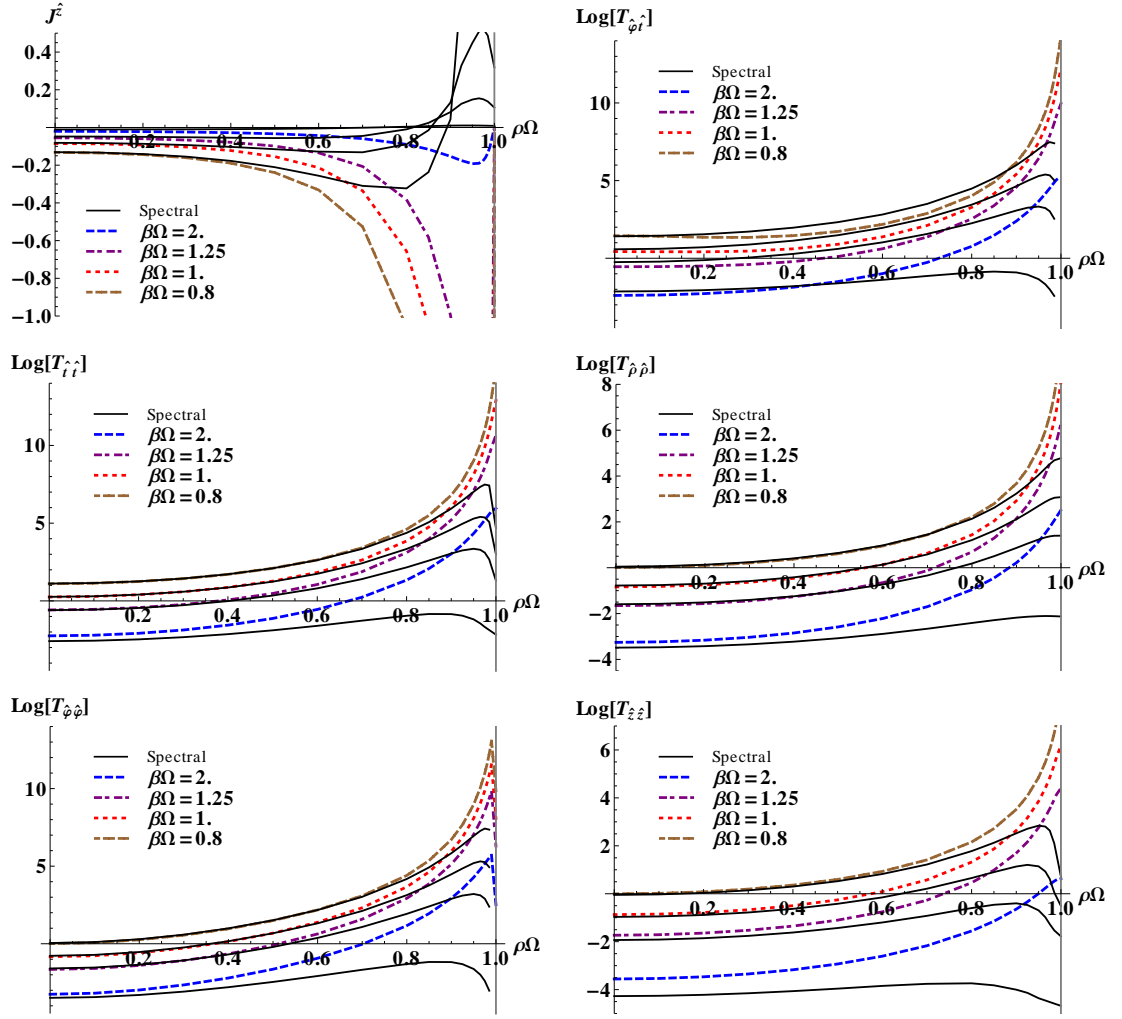
Figure 5.14: Numerical results for t.e.v.s computed in the MIT (thick dashed coloured lines) and spectral (thin black lines) models are presented for comparison. Apart from the neutrino charge current (which changes sign between the rotation axis and the boundary), the plots show the logarithm of t.e.v.s in terms of the distance from the rotation axis. The boundary is located at $R\Omega = 1.0$ and the field is taken to be massless. It can be seen that the neutrino current goes to 0 on the boundary in the MIT case and does not change sign across the channel. It can also be seen that in the spectral case, $\langle : T_{\hat{\varphi}\hat{\varphi}} : \rangle_\beta$ and $\langle : T_{\hat{\varphi}\hat{t}} : \rangle_\beta$ go to 0 on the boundary, while in the MIT, case they stay finite.
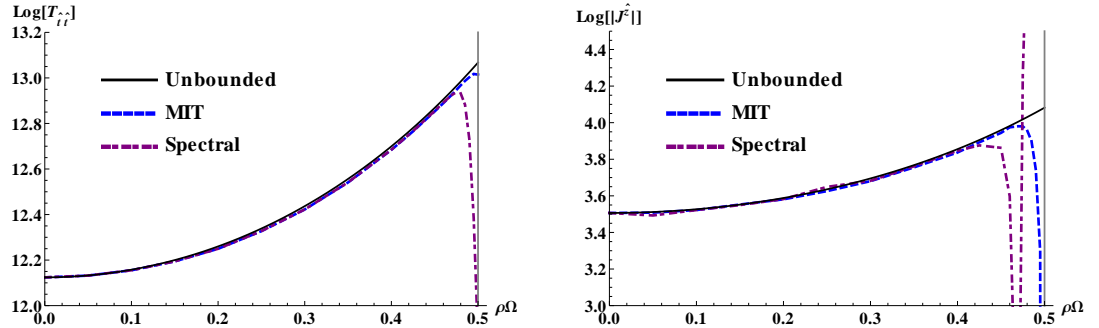
Figure 5.15: Logarithm of energy density (left) and charge current (right) at $\beta\Omega = 0.05$ for a system of massless fermions confined inside a cylinder located at $R\Omega = 0.5$. While both models agree very well with the analytic results in Eqs. (4.3.56) close to the rotation axis, the energy density in the spectral model strongly departs from the analytic profile as the boundary is approached, while the results in the MIT case follow it closely.
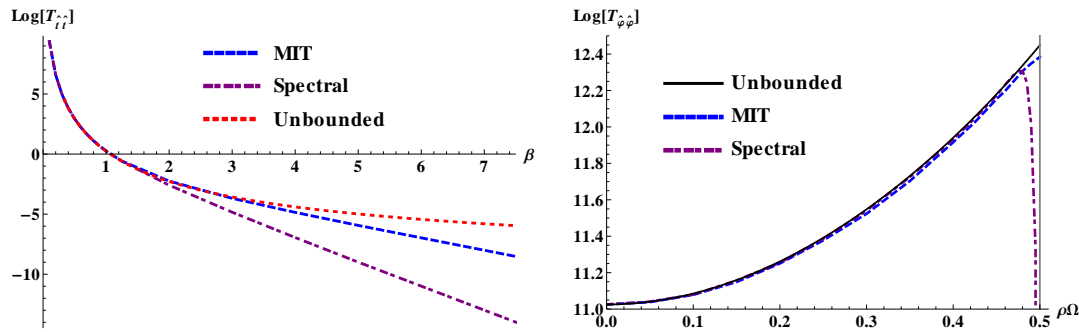
Figure 5.16: The plot on the left compares the logarithm of the energy density on the rotation axis in the MIT bag and spectral models with the analytic results Eqs. (4.3.56) obtained with respect to the rotating (Iyer) vacuum for the rotating unbounded space-time, represented in terms of the inverse temperature β. The plot on the right presents the logarithm of $\langle : T_{\hat{\varphi}\hat{\varphi}} : \rangle_\beta$ for massless fermions at $\beta\Omega = 0.05$, with $R\Omega = 0.5$.

Finally, Figure 5.16 shows the behaviour of the energy density on the rotation axis (μ was set to 0). While at large temperatures (small values of β), the energy density in the MIT and spectral models is superposed to that corresponding to the unbounded case, as the temperature decreases, the energy density in both the MIT and spectral cases decreases exponentially with β, however, the slope in the two cases differs (in the unbouded case, the energy density falls off as β^{-2}). The exponential decrease with β in the bounded case is explained through an asymptotc analysis in subsection 5.4.1. The difference in the slope is coming from a term of the form $e^{-\beta q_{0,1}}$, where $q_{0,1}$ is the smallest value of the transverse momentum corresponding to $m = 0$. In the spectral case, $q_{0,1}$ is the first root $\xi_{0,1}$ of $J_0(qR)$, while in the MIT case, $q_{0,1}R < \xi_{0,1}$, as implied by Eq. (5.3.10).

5.3.3 Casimir effect

Euclidean Green's function for the MIT bag model

Owing to its formal equivalence to the Lorentzian Feynman propagator, the boundary conditions of the MIT bag model that the Euclidean Green's function for the bounded space-time must satisfy are analogous to Eqs. (5.3.2):

$$(i\gamma^{\hat{\rho}} - \varsigma)S_E^{\mathrm{MIT}}(x, x')\rfloor_{\rho=R} = 0,$$
$$S_E^{\mathrm{MIT}}(x, x')(-i\gamma^{\hat{\rho}'} - \varsigma)\rfloor_{\rho'=R} = 0. \tag{5.3.52}$$

To form the Euclidean Green's function $S_E^{\mathrm{MIT}}(x, x')$ for the bounded system, a solution $\Delta S_E^{\mathrm{MIT}}(x, x')$ of the homogeneous correspondent of Eq. (2.2.61a) (i.e. with the right hand side set to zero) must be added to the Euclidean Green's function (5.2.33) for the unbounded space. A Fourier transform can be performed on $\Delta S_E^{\mathrm{MIT}}(x, x')$,

as described in Eq. (5.2.24):

$$\Delta S_E^{\text{MIT}}(x,x') = \int_{-\infty}^{\infty} \frac{d\omega}{8\pi^3} \int_{-\infty}^{\infty} dk \sum_{m=-\infty}^{\infty} e^{i\omega\Delta\tau + ik\Delta z} \begin{pmatrix} \Delta\chi_{11}^{\text{MIT}} & \Delta\chi_{12}^{\text{MIT}} \\ \Delta\chi_{21}^{\text{MIT}} & \Delta\chi_{22}^{\text{MIT}} \end{pmatrix}, \quad (5.3.53)$$

where the 2×2 matrices $\Delta\chi_{ik}^{\text{MIT}}$ can be written as:

$$\Delta\chi_{11}^{\text{MIT}} = (i\omega - \mu)\begin{pmatrix} a_{11} & b_{11} \\ c_{11} & d_{11} \end{pmatrix} \otimes \mathcal{E}_j, \qquad \Delta\chi_{12}^{\text{MIT}} = \begin{pmatrix} a_{12} & b_{12} \\ c_{12} & d_{12} \end{pmatrix} \otimes \mathcal{E}_j,$$

$$\Delta\chi_{22}^{\text{MIT}} = (i\omega + \mu)\begin{pmatrix} a_{22} & b_{22} \\ c_{22} & d_{22} \end{pmatrix} \otimes \mathcal{E}_j, \qquad \Delta\chi_{21}^{\text{MIT}} = \begin{pmatrix} a_{21} & b_{21} \\ c_{21} & d_{21} \end{pmatrix} \otimes \mathcal{E}_j, \quad (5.3.54)$$

where a_{ik}, b_{ik}, c_{ik} and d_{ik} are constants, the matrix $\mathcal{E}_j$ on the right of the Hadamard (Schur) product is defined in Eq. (5.2.35b) and j is a generic label for the parameters $m \equiv m_j$, $\omega \equiv \omega_j$ and $k \equiv k_j$.

The matrix elements of the off-diagonal blocks $\Delta\chi_{12}^{\text{MIT}}$ and $\Delta\chi_{21}^{\text{MIT}}$ can be found using Eqs. (5.2.28), as follows:

$$\begin{pmatrix} a_{12} & b_{12} \\ c_{12} & d_{12} \end{pmatrix} = \begin{pmatrix} -ka_{22} - \alpha c_{22} & -kb_{22} - \alpha d_{22} \\ \alpha a_{22} + kc_{22} & \alpha b_{22} + kd_{22} \end{pmatrix} = \begin{pmatrix} ka_{11} + \alpha b_{11} & -\alpha a_{11} - kb_{11} \\ kc_{11} + \alpha d_{11} & -\alpha c_{11} - kd_{11} \end{pmatrix},$$
$$(5.3.55a)$$

$$\begin{pmatrix} a_{21} & b_{21} \\ c_{21} & d_{21} \end{pmatrix} = \begin{pmatrix} -ka_{11} - \alpha c_{11} & -kb_{11} - \alpha d_{11} \\ \alpha a_1 + kc_{11} & \alpha b_{11} + kd_{11} \end{pmatrix} = \begin{pmatrix} ka_{22} + \alpha b_{22} & -\alpha a_{22} - kb_{22} \\ kc_{22} + \alpha d_{22} & -\alpha c_{22} - kd_{22} \end{pmatrix}.$$
$$(5.3.55b)$$

These equations can be effectively used to express all matrix elements of $\Delta\chi^{\text{MIT}}$ in terms of the matrix elements of $\Delta\chi_{11}^{\text{MIT}}$. Although not required in this calcualtion, the matrix elements of $\Delta\chi_{22}^{\text{MIT}}$ are given below with respect to thos of $\Delta\chi_{11}^{\text{MIT}}$, for completeness:

$$\begin{pmatrix} a_{22} \\ b_{22} \\ c_{22} \\ d_{22} \end{pmatrix} = \frac{1}{\alpha^2 - k^2} \begin{pmatrix} k^2 & \alpha k & \alpha k & \alpha^2 \\ -\alpha k & -k^2 & \alpha^2 & -\alpha k \\ -\alpha k & \alpha^2 & -k^2 & -\alpha k \\ \alpha^2 & \alpha k & \alpha k & k^2 \end{pmatrix} \begin{pmatrix} a_{11} \\ b_{11} \\ c_{11} \\ d_{11} \end{pmatrix}. \quad (5.3.56)$$

To begin the construction of $\Delta S_E^{\text{MIT}}(x,x')$, the form of the Fourier transform χ of the Euclidean function $S_E(x,x')$ for the unbounded space on the boundary is

required. It can be inferred from Eq. (5.2.33):

$$\chi\rfloor_{\rho=R} = \begin{pmatrix} (\mu - i\omega)\frac{K_m}{I_m} & 0 & -k\frac{K_m}{I_m} & \alpha\frac{K_m}{I_m} \\ 0 & (\mu - i\omega)\frac{K_{m+1}}{I_{m+1}} & -\alpha\frac{K_{m+1}}{I_{m+1}} & k\frac{K_{m+1}}{I_{m+1}} \\ k\frac{K_m}{I_m} & -\alpha\frac{K_m}{I_m} & (\mu + i\omega)\frac{K_m}{I_m} & 0 \\ \alpha\frac{K_{m+1}}{I_{m+1}} & -k\frac{K_{m+1}}{I_{m+1}} & 0 & (\mu + i\omega)\frac{K_{m+1}}{I_{m+1}} \end{pmatrix} \circ \begin{pmatrix} \mathcal{E}_j & \mathcal{E}_j \\ \mathcal{E}_j & \mathcal{E}_j \end{pmatrix},$$

$$\chi\rfloor_{\rho'=R} = \begin{pmatrix} (\mu - i\omega)\frac{K_m}{I_m} & 0 & -k\frac{K_m}{I_m} & -\alpha\frac{K_m}{I_m} \\ 0 & (\mu - i\omega)\frac{K_{m+1}}{I_{m+1}} & \alpha\frac{K_{m+1}}{I_{m+1}} & k\frac{K_{m+1}}{I_{m+1}} \\ k\frac{K_m}{I_m} & \alpha\frac{K_m}{I_m} & (\mu + i\omega)\frac{K_m}{I_m} & 0 \\ -\alpha\frac{K_{m+1}}{I_{m+1}} & -k\frac{K_{m+1}}{I_{m+1}} & 0 & (\mu + i\omega)\frac{K_{m+1}}{I_{m+1}} \end{pmatrix} \circ \begin{pmatrix} \mathcal{E}_j & \mathcal{E}_j \\ \mathcal{E}_j & \mathcal{E}_j \end{pmatrix},$$

$$(5.3.57)$$

where the modified Bessel functions explicitly displayed in the ratios K_m/I_m and K_{m+1}/I_{m+1} take the argument αR, with the coordinate dependence fully contained in the matrices $\mathcal{E}_j$. The boundary conditions (5.3.52) give a number of 32 equations for the matrix elements of $\Delta\chi^{\mathrm{MIT}}$. However, only a small number of equations are required to fully determine these elements. The $(1,1)$ components of Eqs. (5.3.52) (i.e. the top left components of the equations for both $\rho = R$ and $\rho' = R$),

$$-\alpha K_{m+1} - \varsigma(\mu - i\omega)K_m + \varsigma(\mu - i\omega)I_m a_{11} - I_{m+1}c_{21} = 0,$$
$$-\alpha K_{m+1} - \varsigma(\mu - i\omega)K_m + \varsigma(\mu - i\omega)I_m a_{11} + I_{m+1}b_{12} = 0, \quad (5.3.58)$$

show that

$$c_{21} = -b_{12}. \quad (5.3.59)$$

A similar inspection of the $(2,2)$ components of Eqs. (5.3.52) shows that:

$$-\alpha K_m - \varsigma(\mu - i\omega)K_{m+1} + \varsigma(\mu - i\omega)I_{m+1}d_{11} + I_m b_{21} = 0,$$
$$-\alpha K_m - \varsigma(\mu - i\omega)K_{m+1} + \varsigma(\mu - i\omega)I_{m+1}d_{11} - I_m c_{12} = 0, \quad (5.3.60)$$

leading to:

$$b_{21} = -c_{12}. \quad (5.3.61)$$

Comparing the expressions for b_{12} and c_{21} in Eqs. (5.3.55) shows that:

$$c_{11} = b_{11}, \quad (5.3.62)$$

which can be used together with the expressions for d_{12}, d_{21}, a_{12} and a_{21} in the same equations to show that:

$$a_{21} = -a_{12}, \qquad d_{21} = -d_{12}. \quad (5.3.63)$$

Using $d_{21} = \alpha b_{11} + k d_{11}$ into the $(1,2)$ component of Eq. (5.3.52) for $\rho = R$ gives:

$$b_{11} = \frac{k(I_{m+1} d_{11} - K_{m+1})}{\varsigma(\mu - i\omega) I_m - \alpha I_{m+1}}, \tag{5.3.64}$$

where the argument of the modified Bessel functions is, as before, αR. Substituting the above into $b_{21} = -k b_{11} - \alpha d_{11}$ gives:

$$b_{21} = \frac{K_{m+1} k^2 + (\mu - i\omega) d_{11} [I_{m+1} (i\omega + \mu) - \alpha \varsigma I_m]}{\varsigma(\mu - i\omega) I_m - \alpha I_{m+1}}. \tag{5.3.65}$$

Substituting b_{21} into the second equation in (5.3.60) gives:

$$d_{11} = \frac{K_{m+1}}{I_{m+1}} - \frac{1}{\mathfrak{U}} \frac{I_m}{I_{m+1}} + \frac{1}{\mathfrak{U}} \frac{\varsigma \alpha}{\mu - i\omega}, \tag{5.3.66}$$

where $\mathfrak{U} \equiv \mathfrak{U}_m(\alpha R)$ is defined as [12, 28, 29]:

$$\mathfrak{U}_m(\alpha R) = \alpha R [I_m^2(\alpha R) + I_{m+1}^2(\alpha R)] - 2\varsigma \mu R\, I_m(\alpha R) I_{m+1}(\alpha R). \tag{5.3.67}$$

Substituting d_{11} back into Eq. (5.3.64) gives:

$$b_{11} = -\frac{\varsigma k}{\mathfrak{U}(\mu - i\omega)}. \tag{5.3.68}$$

The constant a_{11} can be found by substituting $a_{21} = -k a_{11} - \alpha c_{11}$ into the $(2,1)$ component of Eq. (5.3.52) for $\rho = R$:

$$a_{11} = \frac{K_m}{I_m} - \frac{1}{\mathfrak{U}} \frac{I_{m+1}}{I_m} + \frac{1}{\mathfrak{U}} \frac{\varsigma \alpha}{\mu - i\omega}. \tag{5.3.69}$$

The results in Eqs. (5.3.69), (5.3.68) and (5.3.66) can be summarised as:

$$\Delta S_E^{\mathrm{MIT}}(x, x') = \int_{-\infty}^{\infty} \frac{d\omega}{8\pi^3} \int_{-\infty}^{\infty} dk \sum_{m=-\infty}^{\infty} e^{i\omega\Delta\tau + ik\Delta z} \begin{pmatrix} \Delta\chi_{11}^{\mathrm{MIT}} & \Delta\chi_{12}^{\mathrm{MIT}} \\ \Delta\chi_{21}^{\mathrm{MIT}} & \Delta\chi_{22}^{\mathrm{MIT}} \end{pmatrix}, \tag{5.3.70a}$$

where the 2×2 matrix element $\Delta\chi_{11}^{\mathrm{MIT}}$ is given by:

$$\Delta\chi_{11}^{\mathrm{MIT}} = -(\mu - i\omega) \begin{pmatrix} \frac{K_m}{I_m} - \frac{1}{\mathfrak{U}} \frac{I_{m+1}}{I_m} + \frac{1}{\mathfrak{U}} \frac{\varsigma \alpha}{\mu - i\omega} & -\frac{1}{\mathfrak{U}} \frac{\varsigma k}{\mu - i\omega} \\ -\frac{1}{\mathfrak{U}} \frac{\varsigma k}{\mu - i\omega} & \frac{K_{m+1}}{I_{m+1}} - \frac{1}{\mathfrak{U}} \frac{I_m}{I_{m+1}} + \frac{1}{\mathfrak{U}} \frac{\varsigma \alpha}{\mu - i\omega} \end{pmatrix} \circ \mathcal{E}_j. \tag{5.3.70b}$$

The 2×2 matrix $\Delta\chi_{12}^{\mathrm{MIT}}$ can be found from Eq. (5.3.55a):

$$\Delta\chi_{12}^{\mathrm{MIT}} = \begin{pmatrix} k\left(\frac{K_m}{I_m} - \frac{1}{\mathfrak{U}} \frac{I_{m+1}}{I_m}\right) & -\alpha\left(\frac{K_m}{I_m} - \frac{1}{\mathfrak{U}} \frac{I_{m+1}}{I_m}\right) - \frac{\varsigma(\mu + i\omega)}{\mathfrak{U}} \\ \alpha\left(\frac{K_{m+1}}{I_{m+1}} - \frac{1}{\mathfrak{U}} \frac{I_m}{I_{m+1}}\right) + \frac{\varsigma(\mu + i\omega)}{\mathfrak{U}} & -k\left(\frac{K_{m+1}}{I_{m+1}} - \frac{1}{\mathfrak{U}} \frac{I_m}{I_{m+1}}\right) \end{pmatrix} \circ \mathcal{E}_j. \tag{5.3.70c}$$

The matrix elements of $\Delta\chi_{21}^{\mathrm{MIT}}$ can be found from Eq. (5.3.70c) using Eqs. (5.3.61),

(5.3.59) and (5.3.63):

$$\Delta\chi_{21}^{\text{MIT}} = \begin{pmatrix} -k\left(\frac{K_m}{I_m} - \frac{1}{\mathfrak{U}}\frac{I_{m+1}}{I_m}\right) & -\alpha\left(\frac{K_{m+1}}{I_{m+1}} - \frac{1}{\mathfrak{U}}\frac{I_m}{I_{m+1}}\right) - \frac{\varsigma(\mu+i\omega)}{\mathfrak{U}} \\ \alpha\left(\frac{K_m}{I_m} - \frac{1}{\mathfrak{U}}\frac{I_{m+1}}{I_m}\right) + \frac{\varsigma(\mu+i\omega)}{\mathfrak{U}} & k\left(\frac{K_{m+1}}{I_{m+1}} - \frac{1}{\mathfrak{U}}\frac{I_m}{I_{m+1}}\right) \end{pmatrix} \circ \mathcal{E}_j.$$

$$(5.3.70\text{d})$$

Finally, the components of $\Delta\chi_{22}^{\text{MIT}}$ can be found by inverting Eq. (5.3.55a):

$$\Delta\chi_{22}^{\text{MIT}} = (\mu+i\omega)\begin{pmatrix} -\frac{K_m}{I_m} + \frac{1}{\mathfrak{U}}\frac{I_{m+1}}{I_m} - \frac{1}{\mathfrak{U}}\frac{\varsigma\alpha}{\mu+i\omega} & \frac{1}{\mathfrak{U}}\frac{\varsigma k}{\mu+i\omega} \\ \frac{1}{\mathfrak{U}}\frac{\varsigma k}{\mu+i\omega} & -\frac{K_{m+1}}{I_{m+1}} + \frac{1}{\mathfrak{U}}\frac{I_m}{I_{m+1}} - \frac{1}{\mathfrak{U}}\frac{\varsigma\alpha}{\mu+i\omega} \end{pmatrix} \circ \mathcal{E}_j.$$

$$(5.3.70\text{e})$$

Casimir expectation values

The Casimir-induced fermion condensate can be calculated by taking the trace of Eq. (5.3.53):

$$\langle\overline{\psi}\psi\rangle_{\text{Cas}}^{\text{MIT}} = -\frac{1}{8\pi^3}\sum_{m=-\infty}^{\infty}\int_{-\infty}^{\infty}d\omega\int_{-\infty}^{\infty}dk\Bigg\{\frac{\alpha\varsigma}{\mathfrak{U}}\left[I_m^2(\alpha\rho) + I_{m+1}^2(\alpha\rho)\right]$$

$$- \mu\left[\left(-\frac{K_m}{I_m} + \frac{1}{\mathfrak{U}}\frac{I_{m+1}}{I_m}\right)I_m^2(\alpha\rho) + \left(-\frac{K_{m+1}}{I_{m+1}} + \frac{1}{\mathfrak{U}}\frac{I_m}{I_{m+1}}\right)I_{m+1}^2(\alpha\rho)\right]\Bigg\}, \quad (5.3.71)$$

where the argument of the modified Bessel functions is αR unless explicitly stated otherwise. The above expression can be simplified by performing the θ integral after a change to the polar coordinates defined in Eq. (5.1.24). Afterwards, the terms involving $I_m^2(\alpha\rho)$ and $I_{m+1}^2(\alpha\rho)$ can be symmetrised to only contain the combinations $I_m^+(\alpha\rho)$ and $I_m^-(\alpha\rho)$, defined in Eq. (5.2.38), as follows:

$$\langle\overline{\psi}\psi\rangle_{\text{Cas}}^{\text{MIT}} = -\frac{1}{2\pi^2 R^3}\sum_{m=-\infty}^{\infty}\int_{\mu R}^{\infty}\frac{d\mathbf{x}}{\mathfrak{U}_m(\mathbf{x})}\left[\mathbf{x}\mu R\mathfrak{W}_m(\mathbf{x})\,I_m^-(\mathbf{x}\overline{\rho}) + \varsigma(x^2 - \mu^2 R^2)\,I_m^+(\mathbf{x}\overline{\rho})\right],$$

$$(5.3.72)$$

where $\mathbf{x} = \alpha R$ and $\mathfrak{W}_m(\mathbf{x})$ is defined as [12, 28, 29]:

$$\mathfrak{W}_m(\mathbf{x}) = \mathbf{x}\left[K_m(\mathbf{x})I_m(\mathbf{x}) - K_{m+1}(\mathbf{x})I_{m+1}(\mathbf{x})\right]$$

$$- \varsigma\mu R\left[K_m(\mathbf{x})I_{m+1}(\mathbf{x}) - K_{m+1}(\mathbf{x})I_m(\mathbf{x})\right]. \quad (5.3.73)$$

The Casimir induced expectation value of the SET can be calculated using

Eq. (2.2.62), grouping terms as for the fermion condensate:

$$\langle T^{\hat{\tau}}_{\hat{\tau}}\rangle = -\frac{1}{2\pi^2 R^4}\sum_{m=0}^{\infty}\int_{\mu R}^{\infty}\frac{d\mathbf{x}}{\mathfrak{U}_m(\mathbf{x})}(\mathbf{x}^2 - \mu^2 R^2)\left[-\varsigma\mu R\, I_m^+(\mathbf{x}\overline{\rho}) + \mathbf{x}\mathfrak{W}_m(\mathbf{x})\, I_m^-(\mathbf{x}\overline{\rho})\right]$$

$$\langle T^{\hat{\rho}}_{\hat{\rho}}\rangle = \frac{1}{\pi^2 R^4}\sum_{m=0}^{\infty}\int_{\mu R}^{\infty}\frac{\mathbf{x}^3\, d\mathbf{x}}{\mathfrak{U}_m(\mathbf{x})}\left[I_m^-(\mathbf{x}\overline{\rho}) - \frac{m+\frac{1}{2}}{\mathbf{x}\overline{\rho}}I_m^\times(\mathbf{x}\overline{\rho})\right]\mathfrak{W}_m(\mathbf{x})$$

$$\langle T^{\hat{\varphi}}_{\hat{\varphi}}\rangle = \frac{1}{\pi^2 R^4}\sum_{m=0}^{\infty}\int_{\mu R}^{\infty}\frac{\mathbf{x}^3\, d\mathbf{x}}{\mathfrak{U}_m(\mathbf{x})}\frac{m+\frac{1}{2}}{\mathbf{x}\overline{\rho}}I_m^\times(\mathbf{x}\overline{\rho})\mathfrak{W}_m(\mathbf{x}), \tag{5.3.74}$$

and $\langle T^{\hat{z}}_{\hat{z}}\rangle = \langle T^{\hat{\tau}}_{\hat{\tau}}\rangle$.

By analogy to Eqs. (5.2.55) for the spectral case, it is convenient to introduce the following notation:

$$\mathcal{I}^{\mathrm{M},+}_{\ell n} = \frac{1}{2\pi^2 R^4}\sum_{m=-\infty}^{\infty}\int_{\mu R}^{\infty}\frac{d\mathbf{x}}{\mathfrak{U}_m(\mathbf{x})}\mathbf{x}^\ell(m+\tfrac{1}{2})^n I_m^+(\mathbf{x}\overline{\rho}),$$

$$\mathcal{I}^{\mathrm{M},-}_{\ell n} = \frac{1}{2\pi^2 R^4}\sum_{m=-\infty}^{\infty}\int_{\mu R}^{\infty}\frac{d\mathbf{x}}{\mathfrak{U}_m(\mathbf{x})}\mathbf{x}^\ell(m+\tfrac{1}{2})^n \mathfrak{W}_m(\mathbf{x})I_m^-(\mathbf{x}\overline{\rho}),$$

$$\mathcal{I}^{\mathrm{M},\times}_{\ell n} = \frac{1}{2\pi^2 R^4}\sum_{m=-\infty}^{\infty}\int_{\mu R}^{\infty}\frac{d\mathbf{x}}{\mathfrak{U}_m(\mathbf{x})}\mathbf{x}^\ell(m+\tfrac{1}{2})^n \mathfrak{W}_m(\mathbf{x})I_m^\times(\mathbf{x}\overline{\rho}), \tag{5.3.75}$$

where the notation $I_m^*(z)$ was introduced in Eqs. (5.2.38). The Casimir expectation values of the FC and SET can be written with respect to the above functions as follows:

$$\langle\overline{\psi}\psi\rangle^{\mathrm{MIT}}_{\mathrm{Cas}} = -\mu R^2\mathcal{I}^{\mathrm{M},-}_{10} - \varsigma R(\mathcal{I}^{\mathrm{M},+}_{20} - \mu^2 R^2\mathcal{I}^{\mathrm{M},+}_{00}), \tag{5.3.76a}$$

$$\langle T^{\hat{\tau}}_{\hat{\tau}}\rangle^{\mathrm{MIT}}_{\mathrm{Cas}} = \frac{1}{2}\varsigma\mu R(\mathcal{I}^{\mathrm{M},+}_{20} - \mu^2 R^2\mathcal{I}^{\mathrm{M},+}_{00}) - \frac{1}{2}(\mathcal{I}^{\mathrm{M},-}_{30} - \mu^2 R^2\mathcal{I}^{\mathrm{M},-}_{10}), \tag{5.3.76b}$$

$$\langle T^{\hat{\rho}}_{\hat{\rho}}\rangle^{\mathrm{MIT}}_{\mathrm{Cas}} = \mathcal{I}^{\mathrm{M},-}_{30} - \overline{\rho}^{-1}\mathcal{I}^{\mathrm{M},\times}_{21}, \tag{5.3.76c}$$

$$\langle T^{\hat{\varphi}}_{\hat{\varphi}}\rangle^{\mathrm{MIT}}_{\mathrm{Cas}} = \overline{\rho}^{-1}\mathcal{I}^{\mathrm{M},\times}_{21} \tag{5.3.76d}$$

and $\langle T^{\hat{z}}_{\hat{z}}\rangle^{\mathrm{MIT}}_{\mathrm{Cas}} = \langle T^{\hat{\tau}}_{\hat{\tau}}\rangle^{\mathrm{MIT}}_{\mathrm{Cas}}$. As discussed in subsection 5.2.3 for the case of spectral boundary conditions, the Casimir-induced expectation values diverge as the boundary is approached. To perform an analysis of this divergence, the sums over m in Eqs. (5.3.75) are replaced with integrals through the application of the generalised Abel-Plana formula (5.2.45).

5.3.4   Casimir divergence near the boundary

The generalised Abel-Plana formula (5.2.45) can be used to convert the sums over m in Eqs. (5.3.75) to integrals over ν, as follows:

$$
\begin{aligned}
\overline{\mathcal{I}}_{\ell n}^{\mathrm{M},+} &= \frac{1}{\pi^2 R^4} \int_0^\infty d\nu \int_{\mu R}^\infty \frac{d\mathrm{x}}{\mathfrak{U}_{\nu-\frac{1}{2}}(\mathrm{x})} \mathrm{x}^\ell \nu^n I_{\nu-\frac{1}{2}}^+(\mathrm{x}\overline{\rho}), \\
\overline{\mathcal{I}}_{\ell n}^{\mathrm{M},-} &= \frac{1}{\pi^2 R^4} \int_0^\infty d\nu \int_{\mu R}^\infty \frac{d\mathrm{x}}{\mathfrak{U}_{\nu-\frac{1}{2}}(\mathrm{x})} \mathrm{x}^\ell \nu^n \mathfrak{W}_{\nu-\frac{1}{2}}(\mathrm{x}) I_{\nu-\frac{1}{2}}^-(\mathrm{x}\overline{\rho}), \\
\overline{\mathcal{I}}_{\ell n}^{\mathrm{M},\times} &= \frac{1}{\pi^2 R^4} \int_0^\infty d\nu \int_{\mu R}^\infty \frac{d\mathrm{x}}{\mathfrak{U}_{\nu-\frac{1}{2}}(\mathrm{x})} \mathrm{x}^\ell \nu^n \mathfrak{W}_{\nu-\frac{1}{2}}(\mathrm{x}) I_{\nu-\frac{1}{2}}^\times(\mathrm{x}\overline{\rho}). \quad (5.3.77)
\end{aligned}
$$

The above expressions are more convenient to work with for the purpose of analysing the asymptotic behaviour of Eqs. (5.3.75) near the boundary (as $\overline{\rho} \to 1$). The following paragraph is dedicated to analysing the asymptotic behaviour of the errors introduced by approximating the sum over m with the integral over ν.

Generalised Abel-Plana formula remainder

To analyse the asymptotic behaviour of the difference between the functions $\overline{\mathcal{I}}_{\ell n}^{\mathrm{M},*}$ introduced in Eqs. (5.3.77) and the functions $\mathcal{I}_{\ell n}^{\mathrm{M},*}$ defined in Eqs. (5.3.75), it is convenient to introduce the following notation:

$$
\begin{aligned}
\mathcal{I}_{\ell n}^{\mathrm{M},*} &= \sum_{m=0}^\infty f_{\ell n}^{\mathrm{M},*}(m + \tfrac{1}{2}), \\
\delta_{\ell n}^{\mathrm{M},*}(\overline{\rho}) &= \overline{\mathcal{I}}_{\ell n}^{\mathrm{M},*} - \mathcal{I}_{\ell n}^{\mathrm{M},*}. \quad (5.3.78)
\end{aligned}
$$

Since $f_{\ell n}^{\mathrm{M},*}(\nu)$ does not have residues in the region $\mathfrak{Re}(\nu) > 0$, Eq. (5.2.45) can be used to put $\delta_{\ell n}^{\mathrm{M},*}$ in the following form:

$$
\delta_{\ell n}^{\mathrm{M},*}(\overline{\rho}) = 2 \int_0^\infty \frac{dt}{e^{2\pi t} + 1} \mathfrak{Im}[f_{\ell n}^{\mathrm{M},*}(it)]. \quad (5.3.79)
$$

To investigate the asymptotic behaviour of $\delta_{\ell n}^{\mathrm{M},*}(\overline{\rho})$ as $\overline{\rho} \to 1$, the asymptotic behaviour of the integrand in the integrals with respect to x in Eqs. (5.3.75) must be investigated. Since the $(e^{2\pi t} + 1)^{-1}$ factor ensures the suppression of $\mathfrak{Im}[f_{\ell n}^{\mathrm{M},*}(it)]$ at large t, the formulae (A.2.4d) and (A.2.4e) for the asymptotic expansion of the modified Bessel functions for large arguments can be used.

The factor $\mathfrak{U}_{\nu-\frac{1}{2}}(\mathrm{x})$ in the denominators of $f_{\ell n}^{\mathrm{M},*}(\nu)$, defined in Eq. (5.3.67), and

its inverse $[\mathfrak{U}_{\nu-\frac{1}{2}}(\mathbf{x})]^{-1}$, have the following asymptotic behaviours:

$$\mathfrak{U}_{\nu-\frac{1}{2}}(\mathbf{x}) = \frac{1}{\pi}e^{2\mathbf{x}}\left[1 - \frac{\nu^2 + \varsigma\mu R}{\mathbf{x}} + \frac{\nu^2(\nu^2 + 2\mu R)}{2\mathbf{x}^2} + O(\mathbf{x}^{-3})\right], \qquad (5.3.80a)$$

$$\mathfrak{U}_{\nu-\frac{1}{2}}(\mathbf{x}) = \pi e^{-2\mathbf{x}}\left[1 + \frac{\nu^2 + \varsigma\mu R}{\mathbf{x}} + \frac{\nu^4 + 2\varsigma\mu R\nu^2 + 2\mu^2 R^2}{2\mathbf{x}^2} + O(\mathbf{x}^{-3})\right], \qquad (5.3.80b)$$

where Eq. (5.2.48c) was used for $I^{\times}_{\nu-\frac{1}{2}}(\mathbf{x})$ and $I^{+}_{\nu-\frac{1}{2}}(\mathbf{x})$ can be shown to have the following asymptotic behaviour:

$$I^{+}_{\nu-\frac{1}{2}}(\mathbf{x}) = \frac{e^{2\mathbf{x}}}{\pi\mathbf{x}}\left[1 - \frac{\nu^2}{\mathbf{x}} + \frac{\nu^4}{2\mathbf{x}^2} + O(\mathbf{x}^{-3})\right]. \qquad (5.3.81)$$

Hence, the asymptotic expansion of the integrand in the integral with respect to $\mathbf{x}$ in $f^{\mathrm{M},+}_{\ell n}(\nu)$ is:

$$\frac{1}{\mathfrak{U}_{\nu-\frac{1}{2}}(\mathbf{x})}\mathbf{x}^{\ell}\nu^{n}\, I^{+}_{\nu-\frac{1}{2}}(\mathbf{x}\overline{\rho}) = \frac{1}{\overline{\rho}}x^{\ell-1}\nu^{n}e^{-2\mathbf{x}\epsilon}$$

$$\times \left[1 - \frac{\nu^2(1-\overline{\rho})}{\mathbf{x}\overline{\rho}} + \frac{\varsigma\mu R}{\mathbf{x}} + \frac{\nu^4\epsilon^2}{2\overline{\rho}\mathbf{x}^2} - \frac{\nu^2\varsigma\mu R(1-\overline{\rho})}{\overline{\rho}\mathbf{x}^2} + \frac{\mu^2 R^2}{\mathbf{x}^2} + O(\mathbf{x}^{-3})\right]. \qquad (5.3.82)$$

For the analysis of the Casimir divergence for the FC and SET, only the cases $(\ell, n) \in \{(0,0), (2,0)\}$ are required. It can be seen that the terms in the bracket contain only even powers of ν, which stay real under the transition $\nu \to it$. Hence, the following asymptotic behaviour can be obtained:

$$\mathfrak{Im}\left[\frac{1}{\mathfrak{U}_{it-\frac{1}{2}}(\mathbf{x})}\mathbf{x}^{\ell}\, I^{+}_{it-\frac{1}{2}}(\mathbf{x}\overline{\rho})\right] = \frac{1}{\overline{\rho}}e^{-2\mathbf{x}\epsilon}O(\mathbf{x}^{\ell-3}). \qquad (5.3.83)$$

Since ℓ is either 0 or 2, it can be seen that $\delta^{\mathrm{M},+}_{00}(\overline{\rho})$ and $\delta^{\mathrm{M},+}_{20}(\overline{\rho})$ do not diverge as $\overline{\rho} \to 1$.

To analyse $\delta^{\mathrm{M},-}_{\ell n}(\overline{\rho})$ and $\delta^{\mathrm{M},\times}_{\ell n}(\overline{\rho})$, the asymptotic behaviour of $\mathfrak{W}_{\nu-\frac{1}{2}}(\mathbf{x})$, defined in Eq. (5.3.73), is required. Using the intermediate expansions:

$$K_{\nu-\frac{1}{2}}(\mathbf{x})I_{\nu-\frac{1}{2}}(\mathbf{x}) - K_{\nu+\frac{1}{2}}(\mathbf{x})I_{\nu+\frac{1}{2}}(\mathbf{x}) = \frac{\nu}{2\mathbf{x}^3}\left[1 + \frac{\nu^2(\nu^2-1)(\nu^2-13)}{24\mathbf{x}^2} + O(\mathbf{x}^{-4})\right],$$

$$K_{\nu-\frac{1}{2}}(\mathbf{x})I_{\nu+\frac{1}{2}}(\mathbf{x}) - K_{\nu+\frac{1}{2}}(\mathbf{x})I_{\nu-\frac{1}{2}}(\mathbf{x}) = -\frac{\nu}{\mathbf{x}^2}\left[1 - \frac{\nu^2-1}{2\mathbf{x}^2} + O(\mathbf{x}^{-4})\right], \qquad (5.3.84)$$

the following expression can be written for $\mathfrak{W}_{\nu-\frac{1}{2}}(\mathbf{x})$:

$$\mathfrak{W}_{\nu-\frac{1}{2}}(\mathbf{x}) = \frac{\nu}{2\mathbf{x}^2}\left[1 + 2\varsigma\mu R + \frac{(\nu^2-1)(\nu^4 - 13\nu^2 - 24\varsigma\mu R)}{24\mathbf{x}^2} + O(\mathbf{x}^{-4})\right]. \qquad (5.3.85)$$

Hence, the ratio $\mathfrak{W}_{\nu-\frac{1}{2}}(\mathbf{x})/\mathfrak{U}_{\nu-\frac{1}{2}}(\mathbf{x})$ can be written as:

$$
\begin{aligned}
\frac{\mathfrak{W}_{\nu-\frac{1}{2}}(\mathbf{x})}{\mathfrak{U}_{\nu-\frac{1}{2}}(\mathbf{x})} = {}& \frac{\pi\nu}{2\mathbf{x}^2}e^{-2\mathbf{x}}\left\{1 + 2\varsigma\mu R + \frac{(\nu^2 + \varsigma\mu R)(1 + 2\varsigma\mu R)}{\mathbf{x}}\right. \\
& \left. + \frac{1}{\mathbf{x}^2}\left[\frac{\nu^2(\nu^4 - 2\nu^2 + 13)}{24} + (\nu^4 + 1)\varsigma\mu R + (2\nu^2 + 1)\mu^2 R^2 + 2\varsigma\mu^3 R^3\right] + O(\mathbf{x}^{-3})\right\}.
\end{aligned}
$$
$$(5.3.86)$$

Since the asymptotic expansions (5.2.48b) (5.2.48c) for $I_{\nu-\frac{1}{2}}^{-}(\mathbf{x})$ and $I_{\nu-\frac{1}{2}}^{\times}(\mathbf{x})$ contain only odd and even powers of ν, respectively, the following asymptotic behaviours can be established:

$$
\begin{aligned}
\mathfrak{Im}\left[\frac{\mathfrak{W}_{it-\frac{1}{2}}(\mathbf{x})}{\mathfrak{U}_{it-\frac{1}{2}}(\mathbf{x})}\mathbf{x}^{\ell} I_{it-\frac{1}{2}}^{-}(\mathbf{x})\right] &= -\frac{t^2}{2\overline{\rho}^2}e^{-2\mathbf{x}\epsilon}O(\mathbf{x}^{\ell-7}), \\
\mathfrak{Im}\left[\frac{\mathfrak{W}_{it-\frac{1}{2}}(\mathbf{x})}{\mathfrak{U}_{it-\frac{1}{2}}(\mathbf{x})}\mathbf{x}^2(it) I_{it-\frac{1}{2}}^{\times}(\mathbf{x})\right] &= -\frac{t^2}{2\overline{\rho}}e^{-2\mathbf{x}\epsilon}O(\mathbf{x}^{-4}).
\end{aligned}
$$
$$(5.3.87)$$

Thus, the functions $\delta_{\ell n}^{\mathrm{M},*}(\overline{\rho})$ are regular as $\overline{\rho}$ for all the combinations of ℓ, n and $* \in \{+,-,\times\}$ of interest. Hence, the asymptotic behaviour of the functions $\overline{\mathcal{I}}_{\ell n}^{\mathrm{M},*}$, defined in Eq. (5.3.77) coincides with that of $\mathcal{I}_{\ell n}^{\mathrm{M},*}$, defined in Eq. (5.3.75).

The Casimir divergence near the boundary

The Casimir divergence occurs due to the divergence of the functions $\mathcal{I}_{\ell n}^{\mathrm{M},*}$, defined in Eqs. (5.3.75), as $\overline{\rho} \to 1$. The asymptotic behaviour of these functions can be analysed by considering the high ν and $\mathbf{x}$ expansion of the integrand in the functions $\overline{\mathcal{I}}_{\ell n}^{\mathrm{M},*}$, defined with respect to $\mathcal{I}_{\ell n}^{\mathrm{M},*}$ in Eq. (5.3.77). Equations (5.2.52b) and (5.2.52c) can be used to obtain the following asymptotic expansions for $\mathfrak{U}_{\nu-\frac{1}{2}}(\mathbf{x})$, defined in Eq. (5.3.67), and its inverse:

$$
\begin{aligned}
\mathfrak{U}_{\nu-\frac{1}{2}}(\mathbf{x}) ={}& \frac{1}{\pi}e^{2r+2\nu\ln\frac{x}{\nu+r}}\left[1 + \frac{\cos^2\theta - 12\varsigma\mu R}{12r}\right. \\
& \left. + \frac{\cos^2\theta}{288r^2}\left(1 + 35\sin^2\theta + 120\varsigma\mu R\cos^2\theta\right) + O(r^{-3})\right], \\
\frac{1}{\mathfrak{U}_{\nu-\frac{1}{2}}(\mathbf{x})} ={}& \pi e^{-2r-2\nu\ln\frac{x}{\nu+r}}\left[1 - \frac{\cos^2\theta - 12\varsigma\mu R}{12r}\right. \\
& \left. + \frac{1}{r^2}\left(\mu^2 R^2 + \frac{\varsigma\mu R}{4}\cos^2\theta + \frac{1}{8}\cos^2\theta - \frac{11}{96}\cos^4\theta\right) + O(r^{-3})\right].
\end{aligned}
$$
$$(5.3.88)$$

Using the following asymptotic expansions:

$$
K_{\nu-\frac{1}{2}}(\mathbf{x})I_{\nu-\frac{1}{2}}(\mathbf{x}) - K_{\nu+\frac{1}{2}}(\mathbf{x})I_{\nu+\frac{1}{2}}(\mathbf{x}) = \frac{\cos}{2r^2}\left[1 + \frac{12 - 45\cos^2\theta + 35\cos^4\theta}{8r^2} + O(r^{-4})\right],
$$

$$
K_{\nu+\frac{1}{2}}(\mathbf{x})I_{\nu-\frac{1}{2}}(\mathbf{x}) - K_{\nu-\frac{1}{2}}(\mathbf{x})I_{\nu+\frac{1}{2}}(\mathbf{x}) = \frac{\cot\theta}{r}\left[1 - \frac{\sin^2\theta(1 - 5\sin^2\theta)}{8r^2} + O(r^{-4})\right],
$$

$$\tag{5.3.89}$$

the asymptotic expansion of $\mathfrak{W}_{\nu-\frac{1}{2}}(\mathbf{x})$, defined in Eq. (5.3.73), and of the ratio $\mathfrak{W}_{\nu-\frac{1}{2}}(\mathbf{x})/\mathfrak{U}_{\nu-\frac{1}{2}}(\mathbf{x})$ can be found:

$$
\mathfrak{W}_{\nu-\frac{1}{2}}(\mathbf{x}) = \frac{\cot\theta}{2r}\Bigg\{ \sin^2\theta + 2\varsigma\mu R +
$$
$$
\frac{\sin^2\theta}{8r^2}\left[12 - 2\varsigma\mu R(1 - 5\sin^2\theta) - 45\cos^2\theta + 35\cos^4\theta\right] + O(r^{-4})\Bigg\},
$$
$$
\frac{\mathfrak{W}_{\nu-\frac{1}{2}}(\mathbf{x})}{\mathfrak{U}_{\nu-\frac{1}{2}}(\mathbf{x})} = \frac{\pi\cot\theta}{2r}e^{-2r-2\nu\ln\frac{\mathbf{x}}{\nu+r}}(\sin^2\theta + 2\varsigma\mu R)\left[1 + \frac{12\varsigma\mu R - \cos^2\theta}{12r} + O(r^{-2})\right].
$$

$$\tag{5.3.90}$$

Equations (5.2.53) can be used to obtain the following expansions:

$$
\frac{1}{\mathfrak{U}_{\nu-\frac{1}{2}}(\mathbf{x})}I^{+}_{\nu-\frac{1}{2}}(\mathbf{x}\overline{\rho}) = \frac{e^{-2r\epsilon}}{\mathbf{x}}\left[1 + \frac{\varsigma\mu R}{r} + \epsilon - r\epsilon^2\cos^2\theta + \dots\right], \tag{5.3.91a}
$$

$$
\frac{\mathfrak{W}_{\nu-\frac{1}{2}}(\mathbf{x})}{\mathfrak{U}_{\nu-\frac{1}{2}}(\mathbf{x})}I^{-}_{\nu-\frac{1}{2}}(\mathbf{x}\overline{\rho}) = \frac{\cot^2\theta}{2r^2}e^{-2r\epsilon}(\sin^2\theta + 2\varsigma\mu R)\left[1 + \frac{\sin^2\theta + 2\varsigma\mu R}{2r}\right. \tag{5.3.91b}
$$

$$\tag{5.3.91c}$$

$$
\left. + \epsilon(1 + \sin^2\theta) - r\epsilon^2\cos^2\theta + \dots\right],
$$

$$
\frac{\mathfrak{W}_{\nu-\frac{1}{2}}(\mathbf{x})}{\mathfrak{U}_{\nu-\frac{1}{2}}(\mathbf{x})}I^{\times}_{\nu-\frac{1}{2}}(\mathbf{x}\overline{\rho}) = \frac{\cot\theta}{2r^2}e^{-2r\epsilon}(\sin^2\theta + 2\varsigma\mu R)\left[1 + \frac{2\varsigma\mu R - \cos^2\theta}{2r}\right.
$$

$$
\left. + \epsilon\sin^2\theta - r\epsilon^2\cos^2\theta + \dots\right]. \tag{5.3.91d}
$$

The presence of powers of $\sin\theta$ in the denominators of Eqs. (5.3.91a) and (5.3.91b) makes $\overline{\mathcal{I}}^{\mathrm{M},+}_{00}$ and $\overline{\mathcal{I}}^{\mathrm{M},-}_{10}$ divergent at the lower limit of the integral with respect to θ. However, this divergence is introduced due to the replacement of the integrand with its expansion for large arguments and orders, thus being unphysical. It can be seen by looking at the power of r that both $\overline{\mathcal{I}}^{\mathrm{M},+}_{00}$ and $\overline{\mathcal{I}}^{\mathrm{M},-}_{10}$ diverge as ϵ^{-1} and thus, contribute subleadingly to the asymptotic behaviour of the expectation values in Eqs. (5.3.76). The other relevant $\overline{\mathcal{I}}^{\mathrm{M},*}_{\ell n}$ can be analysed using the same techniques

as in subsections 5.1.4 and 5.2.3:

$$
\begin{aligned}
\overline{\mathcal{I}}_{20}^{\mathrm{M},+} &= \frac{1}{4\pi^2 R^4 \epsilon^3} \left[1 + \tfrac{1}{2}(1 + 2\varsigma\mu R)\epsilon + O(\epsilon^2) \right], \\
\overline{\mathcal{I}}_{30}^{\mathrm{M},-} &= \frac{1}{60\pi^2 R^4 \epsilon^3} \left[1 + 5\varsigma\mu R + \left(\tfrac{17}{14} + \tfrac{9}{2}\varsigma\mu R + 5\mu^2 R^2 \right)\epsilon + O(\epsilon^{-2}) \right], \\
\overline{\mathcal{I}}_{21}^{\mathrm{M},\times} &= \frac{1}{60\pi^2 R^4 \epsilon^3} \left[1 + 5\varsigma\mu R - \left(\tfrac{2}{7} + 3\varsigma\mu R - 5\mu^2 R^2 \right)\epsilon + O(\epsilon^{-2}) \right].
\end{aligned}
\tag{5.3.92}
$$

The Casimir divergence can now be computed by substituting the above results in Eqs. (5.3.76):

$$
\begin{aligned}
\langle \overline{\psi}\psi \rangle_{\mathrm{Cas}}^{\mathrm{MIT}} &\sim - \frac{\varsigma}{4\pi^2 R^3 \epsilon^3} \left[1 + \tfrac{\epsilon}{2}(1 + 2\varsigma\mu R) \right], \\
\langle T^{\hat{\tau}}_{\hat{\tau}} \rangle_{\mathrm{Cas}}^{\mathrm{MIT}} &\sim - \frac{1}{120\pi^2 R^4 \epsilon^3} \left[1 - 10\varsigma\mu R + \epsilon \left(\tfrac{17}{14} - 3\varsigma\mu R - 10\mu^2 R^2 \right) \right], \\
\langle T^{\hat{\rho}}_{\hat{\rho}} \rangle_{\mathrm{Cas}}^{\mathrm{MIT}} &\sim \frac{1}{120\pi^2 R^4 \epsilon^2} \left[1 + 5\varsigma\mu R + \epsilon \left(\tfrac{17}{7} + 9\varsigma\mu R + 10\mu^2 R^2 \right) \right] \\
\langle T^{\hat{\varphi}}_{\hat{\varphi}} \rangle_{\mathrm{Cas}}^{\mathrm{MIT}} &\sim \frac{1}{60\pi^2 R^4 \epsilon^3} \left[1 + 5\varsigma\mu R + \epsilon \left(\tfrac{5}{7} + 2\varsigma\mu R + 5\mu^2 R^2 \right) \right]
\end{aligned}
\tag{5.3.93}
$$

and $\langle T^{\hat{z}}_{\hat{z}} \rangle_{\mathrm{Cas}}^{\mathrm{MIT}} = \langle T^{\hat{\tau}}_{\hat{\tau}} \rangle_{\mathrm{Cas}}^{\mathrm{MIT}}$. It can be checked that Eqs. (5.3.93) satisfy Eq. (2.2.28). The above expressions are accurate to first and second orders in terms of the distance to the boundary (i.e. terms of order $O(\epsilon^2)$ have been neglected in the brackets). In contrast to (5.2.56), Eqs. (5.3.93) show that the Casimir divergence of a SET in the MIT bag model is one order less than in the spectral model, agreeing with the predictions of Deutsch and Candelas [31]. A possible explanation for this behaviour is that the MIT boundary conditions can be formulated in a completely local fashion, while the spectral boundary conditions require knowledge of the spectral components obtain through a Fourier transform of the wave function, making the definition of the SET non-local. It is also remarkable that, the divergence of the Casimir expectation value (5.2.56) of the FC in the spectral model vanishes when $\mu = 0$ (in the MIT case, the leading order divergence is independent of mass) and its leading order divergence when $\mu > 0$ is one order of magnitude less than in the MIT case.

Numerical results

Figure 5.17 compares the asymptotic analysis (5.3.93) of the Casimir divergence with numerical results for a cylindrical boundary for $\mu R = 0$ and $\mu R = 2$. In the massless case, ς only influences the sign of the fermion condensate (FC), hence, the plots do not show separate curves for $\varsigma = 1$ and -1 in this case. However, there are significant differences between the cases corresponding to the two values of ς, which deserve separate curves.

The numerical results confirm the asymptotic results presented in Eqs. (5.3.93), showing that in the MIT case, the Casimir divergence of the SET is one order of

magnitude smaller than in the spectral case, presented in Eqs. (5.2.56), while the Casimir divergence of the FC is one order of magnitude higher. Also, the mass of the quanta affects the leading order of the divergence, while the sign of ς (i.e. either $+1$ or -1) in Eq. (5.3.1), where the MIT boundary conditions are defined, affects the sign of the Casimir expectation value of the FC even in the massless case.

The plots in the left column show the logarithm of the Casimir expectation values as functions of the distance from the rotation axis, while the log-log plots on the right show their logarithms as functions of the logarithm of the inverse distance $\epsilon = 1 - \overline{\rho}$ from the boundary.

5.4 Estimates of the energy density

The key to estimating t.e.v.s for bounded systems is tackling the integral with respect to k. After an analysis in subsection 5.4.1 of the value of the energy density on the rotation axis and the boundary, the case when the boundary is outside the SOL is discussed in subsection 5.4.2. The purpose of the latter section is to give some evidence that if the SOL is inside the boundary, t.e.v.s become divergent as the SOL is approached.

It is important to note that when the SOL is inside the boundary, both scalar and fermion modes with $E\widetilde{E} < 0$ start appearing, as discussed in subsections 5.1.1 (for scalars), 5.2.1 (for fermions obeying spectral boundary conditions) and 5.3.1 (for the MIT bag model). Since thermal states cannot be constructed for scalars if the system allows such modes, only fermions are discussed in this section. Although occasionally calculations will be presented for a general mass, the results of this section are given only for massless fermions.

5.4.1 Boundary inside the speed of light surface

The t.e.v. of the energy density with respect to the rotating (Iyer) vacuum, given in Eqs. (5.2.20a) and (5.3.51a) for the spectral and the MIT bag model, respectively, is written in terms of the integral:

$$\mathcal{F}_{\pm} = \int_0^{\infty} dk \frac{E \operatorname{sgn}(E \pm E_0)}{e^{\beta|E\pm E_0|} + 1}, \tag{5.4.1}$$

where E and E_0 are given by:

$$E_0 = \Omega(m + \tfrac{1}{2}), \qquad E = \sqrt{E_q^2 + k^2}, \qquad E_q = \sqrt{q^2 + \mu^2}. \tag{5.4.2}$$

As discussed throughout this chapter, $E_q > E_0$ for any value of m when $R\Omega \leq 1$. In what follows, an approximation for Eq. (5.4.1) is derived, after which it is used to
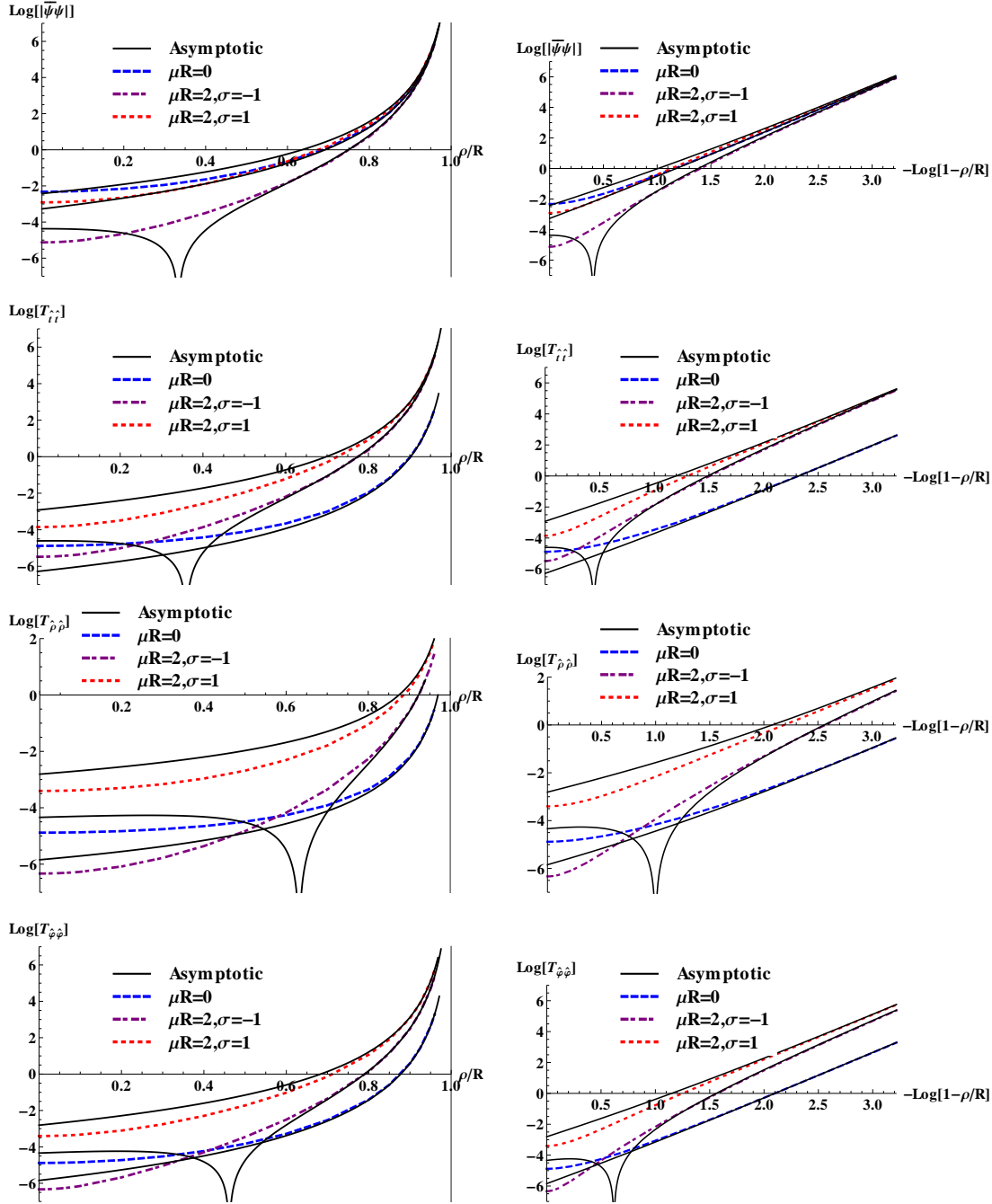
Figure 5.17: Casimir divergence in the MIT model for a cylindrical boundary. The plots show numerical results (thick dashed coloured curves) for $\mu = 0$ and $\mu = 2$, for both $\varsigma = 1$ and $\varsigma = -1$. The plots show the logarithm of the FC (top line) and SET (following three lines) with respect to the distance to the rotation axis (left) and the logarithm of the inverse of the distance $\epsilon = 1 - \overline{\rho}$ to the boundary (right). The asymptotic behaviour of the Casimir divergence is matched against Eqs. (5.3.93), represented using thin dark lines. The asymptotic forms have zeroes in the domain due to the second order corrections.

estimate the energy density on the rotation axis and on the boundary. The results are validated numerically.

Fermi-Dirac integral for boundary inside SOL

It is convenient to change the integration variable in Eq. (5.4.1) from k to $t = (E/E_q) - 1$:

$$\mathcal{F}_{\pm} = E_q^2 \int_0^{\infty} dt \, \frac{(t+1)^2}{\sqrt{t(t+2)}} \frac{\text{sgn}(t+1 \pm \frac{E_0}{E_q})}{e^{\beta E_q \left| t+1 \pm \frac{E_0}{E_q} \right|} + 1}. \tag{5.4.3}$$

Since $E_q > E_0$ when the boundary is inside the SOL, the signum function evaluates to 1 and the modulus disappears in the Fermi-Dirac factor, which can be expanded in a power series, as follows:

$$\mathcal{F}_{\pm} = E_q^2 \sum_{j=1}^{\infty} (-1)^{j+1} e^{-j\beta(E_q \pm E_0)} \int_0^{\infty} \frac{dt(t+1)^2}{\sqrt{t(t+2)}} e^{-j\beta E_q t}. \tag{5.4.4}$$

The integral above can be expressed in terms of modified Bessel functions of the second kind, starting from:

$$K_0(j\beta E_q) = \int_0^{\infty} dz \, e^{-j\beta E_q \cosh z} = \int_0^{\infty} \frac{dt}{\sqrt{t(t+2)}} e^{-j\beta E_q(t+1)}. \tag{5.4.5}$$

Differentiating the above twice and using the recurrence relations (A.1.21), Eq. (5.4.4) can be written as:

$$\mathcal{F}_{\pm} = \frac{E_q^2}{2} \sum_{j=1}^{\infty} (-1)^{j+1} e^{\mp j\beta E_0} [K_0(j\beta E_q) + K_2(j\beta E_q)]. \tag{5.4.6}$$

The energy density in the spectral and MIT models can be written using Eqs. (5.2.20a) and (5.3.51a), respectively:

$$\langle : T_{\hat{t}\hat{t}} :_I \rangle_{\beta}^{\text{spec}} = \frac{2}{\pi^2 R^2} \sum_{m=0}^{\infty} \sum_{\ell=1}^{\infty} \frac{J_m^+(q\rho)}{J_{m+1}^2(qR)} (\mathcal{F}_- + \mathcal{F}_+),$$

$$\langle : T_{\hat{t}\hat{t}} :_I \rangle_{\beta}^{\text{MIT}} = \frac{1}{2\pi^2 R^2} \sum_{m=0}^{\infty} \sum_{\ell=1}^{\infty} \frac{J_m^+(q\rho)}{J_{m+1}^2(qR)(1 + \frac{m+\frac{1}{2}}{qR}(-1)^{\ell})} (\mathcal{F}_- + \mathcal{F}_+). \tag{5.4.7}$$

For simplicity, the mass μ was set to 0, such that $\mathtt{j} \equiv \mathtt{j}_{m\ell} = J_m(q_{m\ell})/J_{m+1}(q_{m\ell}) = (-1)^{l+1}$.

On the rotation axis

Setting $\rho = 0$ selects only the $m = 0$ terms in Eqs. (5.4.7):

$$\langle : T_{\hat{t}\hat{t}} :_I \rangle^{\text{spec}}_\beta \Big|_{\rho=0} = \frac{2}{\pi^2 R^4} \sum_{\ell=1}^\infty \frac{(qR)^2}{J_1^2(qR)} \sum_{j=1}^\infty (-1)^{j+1} \cosh\left(\frac{j\beta\Omega}{2}\right) [K_0(j\beta q) + K_2(j\beta q)],$$

$$\langle : T_{\hat{t}\hat{t}} :_I \rangle^{\text{MIT}}_\beta \Big|_{\rho=0} = \frac{1}{2\pi^2 R^4} \sum_{\ell=1}^\infty \frac{(qR)^2}{J_{m+1}^2(qR)[1 + \frac{(-1)^\ell}{2qR}]} \sum_{j=1}^\infty (-1)^{j+1} \cosh\left(\frac{j\beta\Omega}{2}\right)$$
$$\times [K_0(j\beta q) + K_2(j\beta q)]. \tag{5.4.8}$$

The exponentially decreasing behaviour (A.2.4e) of the MacDonald functions for large arguments indicates that the sum over j can be safely truncated after the first term. At sufficiently small temperatures (large β), the $\ell = 1$ represents the dominant contribution to the sum over ℓ, for the same reason. Also, the modified Bessel functions can be replaced with the asymptotic expansions (A.2.4e):

$$K_0(z) + K_2(z) \sim e^{-z}\sqrt{\frac{2\pi}{z}}\left(1 + \frac{7}{8z} + \frac{57}{128z^2} - \frac{195}{1024z^3} + \cdots\right) \tag{5.4.9}$$

On the rotation axis the terms with $m > 0$ vanish and Eqs. (5.4.7) reduce to:

$$\langle : T_{\hat{t}\hat{t}} :_I \rangle^{\text{spec}}_\beta \Big|_{\rho=0} = \frac{2}{\pi^2 R^2} \frac{E_q^2}{J_1^2(qR)} \cosh\frac{\beta\Omega}{2} e^{-\beta E_q}\sqrt{\frac{2\pi}{\beta E_q}},$$

$$\langle : T_{\hat{t}\hat{t}} :_I \rangle^{\text{MIT}}_\beta \Big|_{\rho=0} = \frac{1}{2\pi^2 R^2} \frac{E_q^2}{J_1^2(qR)(1 - \frac{1}{2qR})} \cosh\frac{\beta\Omega}{2} e^{-\beta E_q}\sqrt{\frac{2\pi}{\beta E_q}}, \tag{5.4.10}$$

where only the leading order term in Eq. (5.4.9) was kept. Thus, for both the spectral and MIT models, the t.e.v. of the energy density decreases exponentially as β increases:

$$\langle : T_{\hat{t}\hat{t}} :_I \rangle_\beta \Big|_{\rho=0} \sim \frac{1}{\sqrt{\beta}} e^{-\frac{\beta}{R}(E_q R - \Omega R/2)}. \tag{5.4.11}$$

The exponent is negative since $E_q R > \frac{1}{2}$ (guaranteed by the discussion in the Energy spectrum paragraph of subsection 5.3.1), while $\Omega R \leq 1$. This exponentially decreasing behaviour is also confirmed in Figure 5.6. Figure 5.18 compares the approximations in Eqs. (5.4.21) and (5.4.10) with numerical results.

For small values of β, terms with higher l make significant contributions. The dependence of the roots for the spectral model at $m = 0$ (which are related to the zeros of the Bessel function J_0) on the index ℓ is given in Ref. [1, 60]:

$$q^{\text{spec}}_{0,\ell} = \pi\ell - \frac{\pi}{4} + O(\ell^{-1}). \tag{5.4.12}$$

The roots in the MIT case are located between roots of the Bessel functions and for each root of the Bessel function, there are two roots in the MIT model, as described

in Figure 5.8. Thus, it is expected that at large enough ℓ, the MIT roots will obey
the law:

$$q_{0,\ell}^{\text{MIT}} = \frac{\pi\ell}{2} + O(\ell^{-1}). \tag{5.4.13}$$

We have confirmed the absence of the constant term numerically through linear
regression by considering the first 500 roots of Eq. (5.3.11).

It is now convenient to replace the function $J_1(q_{0\ell}R)$ in the denominators of
Eqs. (5.4.8) using the approximation (A.2.3a) for the Bessel functions at large values
of their argument:

$$J_1(q_{0\ell}R) \sim \sqrt{\frac{2}{\pi q_{0\ell}R}} \cos\left(q_{0\ell}R - \frac{3\pi}{4}\right) \to \begin{cases} \sqrt{\frac{2}{\pi^2(\ell-\frac{1}{4})}} & \text{(spectral)}, \\ \sqrt{\frac{2}{\pi^2\ell}} & \text{(MIT)}. \end{cases} \tag{5.4.14}$$

Using just the leading order term in Eq. (5.4.12) and approximating $[1+(-1)^\ell/\pi\ell]^{-1}$
by 1 for $\langle: T_{\hat{t}\hat{t}} :_I\rangle_\beta^{\text{MIT}}$ in Eq. (5.4.8) gives:

$$\langle: T_{\hat{t}\hat{t}} :_I\rangle_\beta^{\text{spec}}\bigg|_{\rho=0} = \frac{\pi^2}{R^4}\sum_{j=1}^\infty (-1)^{j+1}\cosh\frac{j\beta\Omega}{2}\sum_{\ell=1}^\infty \ell^3\left[K_0\left(\frac{j\beta\pi}{R}\ell\right) + K_2\left(\frac{j\beta\pi}{R}\ell\right)\right],$$

$$\langle: T_{\hat{t}\hat{t}} :_I\rangle_\beta^{\text{MIT}}\bigg|_{\rho=0} = \frac{\pi^2}{16R^4}\sum_{j=1}^\infty (-1)^{j+1}\cosh\frac{j\beta\Omega}{2}\sum_{\ell=1}^\infty \ell^3\left[K_0\left(\frac{j\beta\pi}{2R}\ell\right) + K_2\left(\frac{j\beta\pi}{2R}\ell\right)\right].$$

$$\tag{5.4.15}$$

The sum over ℓ can be approximated by an integral, yielding:

$$\langle: T_{\hat{t}\hat{t}} :_I\rangle_\beta\bigg|_{\rho=0} = \frac{1}{\pi^2\beta^4}\sum_{j=1}^\infty \frac{(-1)^{j+1}}{j^4}\cosh\frac{j\beta\Omega}{2}\int_0^\infty dz\, z^3[K_0(z) + K_2(z)]. \tag{5.4.16}$$

It is remarkable that the above expression is obtained in both the spectral and the
MIT model. As expected, the above expression does not depend on R. The integral
over z can be performed analytically using the following property [60]:

$$\int_0^\infty dz\, z^{\mu-1}K_\nu(z) = 2^{\mu-2}\Gamma\left(\frac{\mu-\nu}{2}\right)\Gamma\left(\frac{\mu+\nu}{2}\right), \tag{5.4.17}$$

after which Eq. (5.4.16) reduces to:

$$\langle: T_{\hat{t}\hat{t}} :_I\rangle_\beta\bigg|_{\rho=0} = \frac{12}{\pi^2\beta^4}\sum_{j=1}^\infty \frac{(-1)^{j+1}}{j^4}\cosh\frac{j\beta\Omega}{2}. \tag{5.4.18}$$

Expanding the hyperbolic function:

$$\cosh\frac{j\beta\Omega}{2} = 1 + \frac{1}{2}\left(\frac{j\beta\Omega}{2}\right)^2 + \dots, \tag{5.4.19}$$

the sum over j can be performed using the following identities [37]:

$$\sum_{j=1}^{\infty} \frac{(-1)^{j+1}}{j^4} = \frac{7\pi^4}{720}, \tag{5.4.20a}$$

$$\sum_{j=1}^{\infty} \frac{(-1)^{j+1}}{j^2} = \frac{\pi^2}{12}, \tag{5.4.20b}$$

leading to:

$$\langle : T_{\hat{t}\hat{t}} :_I \rangle_\beta \Big|_{\rho=0} \sim \frac{7\pi^2}{60\beta^4} + \frac{\Omega^2}{8\beta^2}. \tag{5.4.21}$$

which matches perfectly the expression (4.3.54c) obtained in the unbounded case.

On the boundary

On the bounding surface, Eqs. (5.4.7) reduce to:

$$\langle : T_{\hat{t}\hat{t}} :_I \rangle_\beta^{\text{spec}} \Big|_{\rho=R} = \frac{2}{\pi^2 R^2} \sum_{m=0}^{\infty} \sum_{\ell=1}^{\infty} (\mathcal{F}_- + \mathcal{F}_+),$$

$$\langle : T_{\hat{t}\hat{t}} :_I \rangle_\beta^{\text{MIT}} \Big|_{\rho=R} = \frac{1}{\pi^2 R^2} \sum_{m=0}^{\infty} \sum_{\ell=1}^{\infty} \frac{1}{1 + \frac{m+\frac{1}{2}}{qR}(-1)^\ell} (\mathcal{F}_- + \mathcal{F}_+). \tag{5.4.22}$$

For large values of β, the dominant contribution to the energy density comes from the $m = 0$ and $\ell = 1$ term, in which case Eqs. (5.4.22) reduce to:

$$\langle : T_{\hat{t}\hat{t}} :_I \rangle_\beta^{\text{spec}} \Big|_{\rho=R} = \frac{q_{0,1}^2}{\pi^2 R^2} \sqrt{\frac{2\pi}{\beta q_{0,1}}} e^{-\beta(q_{0,1} - \frac{\Omega}{2})},$$

$$\langle : T_{\hat{t}\hat{t}} :_I \rangle_\beta^{\text{MIT}} \Big|_{\rho=R} = \frac{q_{0,1}^2}{2\pi^2 R^2 (1 - \frac{1}{2q_{0,1}R})} \sqrt{\frac{2\pi}{\beta q_{0,1}}} e^{-\beta(q_{0,1} - \frac{\Omega}{2})}. \tag{5.4.23}$$

The sum over m can be approximated by an integral and as a first approximation, the sum over l can be truncated to the first contribution. The roots in the spectral and MIT cases can be written as:

$$q_{\nu,1} R \sim \nu + a\nu^{1/3}, \tag{5.4.24a}$$

where the coefficient a can be found in Refs. [1, 60] for the spectral case and it can be determined numerically through regression for the MIT case:

$$a_{\text{spec}} \simeq 1.856, \qquad a_{\text{MIT}} \simeq 0.804. \tag{5.4.24b}$$

Hence, the energy density can be approximated as:

$$\langle : T_{\hat{t}\hat{t}} :_I \rangle_\beta^{\text{spec}} \bigg|_{\rho=R} = \frac{1}{\pi^2 R^4} \sqrt{\frac{2\pi R}{\beta}} \int_0^\infty d\nu\, \nu^{\frac{3}{2}} e^{-\frac{\beta\nu}{R}(1-\Omega R) - \frac{\beta a}{R}\nu^{\frac{1}{3}}},$$

$$\langle : T_{\hat{t}\hat{t}} :_I \rangle_\beta^{\text{MIT}} \bigg|_{\rho=R} = \frac{1}{2a\pi^2 R^4} \sqrt{\frac{2\pi R}{\beta}} \int_0^\infty d\nu\, \nu^{\frac{13}{6}} e^{-\frac{\beta\nu}{R}(1-\Omega R) - \frac{\beta a}{R}\nu^{\frac{1}{3}}}. \tag{5.4.25}$$

If the boundary is on the SOL, the integrals with respect to ν can be written in terms of the Gamma function:

$$\langle : T_{\hat{t}\hat{t}} :_I \rangle_\beta^{\text{spec}} \bigg|_{\rho=R} = \frac{27\sqrt{2\pi a}\,\Gamma(\frac{13}{2})}{\pi^2 R^4} \left(\frac{R}{a\beta}\right)^8,$$

$$\langle : T_{\hat{t}\hat{t}} :_I \rangle_\beta^{\text{MIT}} \bigg|_{\rho=R} = \frac{27\Gamma(\frac{17}{2})}{\pi R^4 \sqrt{2\pi a}} \left(\frac{R}{a\beta}\right)^{10}. \tag{5.4.26}$$

If the boundary is not on the SOL, the $\nu^{1/3}$ term in the exponent can be neglected. Using the relation [60]:

$$\int_0^\infty dz\, \cosh(az) K_0(z) = \frac{\pi}{2(1-a^2)^{\frac{1}{2}}}, \tag{5.4.27}$$

the following expression can be derived:

$$\int_0^\infty dz\, z^2 \cosh(\Omega R z)[K_0(z) + K_2(z)] = \frac{\pi(2 + \Omega^2 R^2)}{(1 - \Omega^2 R^2)^{\frac{5}{2}}}, \tag{5.4.28}$$

with which the spectral case can be evaluated analytically:

$$\langle : T_{\hat{t}\hat{t}} :_I \rangle_\beta^{\text{spec}} \bigg|_{\rho=R} = \frac{2}{\pi^2 R\beta^3} \sum_{j=1}^\infty \frac{(-1)^{j+1}}{j^3} \int_0^\infty dz\, z^2 \cosh(z\Omega R)[K_0(z) + K_2(z)]$$

$$= \frac{3\zeta(3)}{2\pi R\beta^3} \frac{2 + \Omega^2 R^2}{(1 - \Omega^2 R^2)^{\frac{5}{2}}}, \tag{5.4.29}$$

where the zeta function is defined as:

$$\zeta(z) = \sum_{s=1}^\infty \frac{1}{s^z}, \tag{5.4.30}$$

and it evaluates at $z = 3$ to $\zeta(3) \simeq 1.20206$. For the MIT case, the $\nu^{\frac{1}{3}}$ term in the exponent in Eq. (5.4.25) can be neglected, giving:

$$\langle : T_{\hat{t}\hat{t}} :_I \rangle_\beta^{\text{MIT}} \bigg|_{\rho=R} = \frac{\Gamma(\frac{19}{6})\sqrt{2\pi}}{2a\pi^3 R^4} \left(\frac{R}{\beta}\right)^{\frac{11}{3}} \frac{1}{(1 - \Omega R)^{\frac{19}{6}}}. \tag{5.4.31}$$

In all the cases considered above, the t.e.v. of the energy density is inversely proportional to a power of β. The approximations for the energy density on the rotation
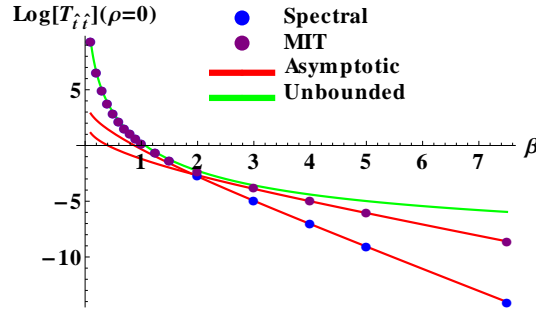
Figure 5.18: Comparison of numerical results for the energy density on the rotation axis in the spectral and MIT bag models, using blue and purple coloured dots, respectively. For low values of β, it can be seen that the numerical results are superposed with the value of the energy density in the unbounded case (represented using green lines). The numerical results for large β validate the approximations given in Eqs. (5.4.10).
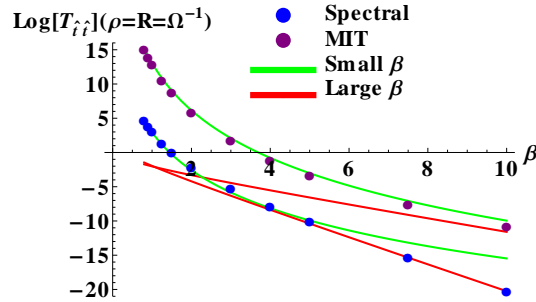
Figure 5.19: Comparison of numerical results for the energy density on the boundary in the spectral and MIT bag models, using blue and purple coloured dots, respectively. The boundary is placed at $R\Omega = 0.5$. While the analytic approximations (5.4.29) and (5.4.31) for small β (green lines) seem to agree only qualitatively with the numerical results, the large β regime is well captured by Eqs.(5.4.23), as shown by the red lines.

axis at small (5.4.21) and large (5.4.10) values of β are validated numerically in Figure 5.18. The expressions in Eqs. (5.4.26) for the energy density on the boundary when the boundary is on the SOL are compared to numerical results in Figure 5.19, while Figure 5.20 validates Eqs. (5.4.29) and (5.4.31), giving the energy density on the boundary when the boundary is inside the SOL.

5.4.2   Boundary outside the speed of light surface

The challenging part of this subsection is estimating the integral over k, defined in Eq. (5.4.3). The next paragraph is dedicated to obtaining an approximation for this integral.
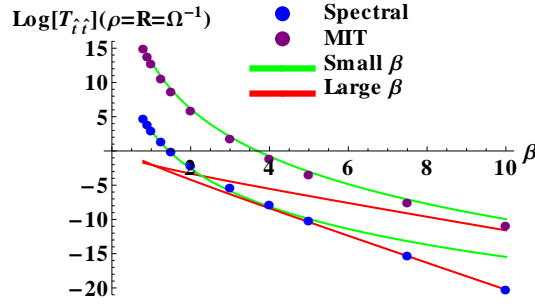
Figure 5.20: Comparison of numerical results for the energy density on the boundary when the boundary is on the speed of light surface ($\Omega R = 1$) in the spectral and MIT bag models, using blue and purple coloured dots, respectively. The analytic formulae (5.4.26), shown using green lines, are in excellent agreement with numerical results at small values of β (in the MIT case, the agreement stays good up to $\beta\Omega \sim 5$). It can be seen that the approximations (5.4.23), plotted in red, capture the large β behaviour of the energy density.

Fermi-Dirac integral for boundary inside SOL

When $q < E_0$, the integral $\mathcal{F}_+$ defined in Eq. (5.4.3) can be tackled using the method described in subsection 5.4.1:

$$\mathcal{F}_+ = \frac{E_q^2}{2} \sum_{j=1}^{\infty} (-1)^{j+1} e^{-j\beta E_0} [K_0(j\beta E_q) + K_2(j\beta E_q)]. \tag{5.4.32}$$

For the $\mathcal{F}_-$ term, it is convenient to split the integral over k into two parts:

$$\mathcal{F}_- = \mathcal{F}_-^{\infty} + \mathcal{F}_-^0, \tag{5.4.33a}$$

where

$$\mathcal{F}_-^{\infty} = \int_0^{\infty} \frac{dE}{1 + e^{\beta E}} \frac{(E + E_0)^2}{\sqrt{(E + E_0)^2 - E_q^2}}, \tag{5.4.33b}$$

$$\mathcal{F}_-^0 = -\int_0^{E_0 - E_q} \frac{dE}{1 + e^{\beta(E_0 - E_q - E)}} \frac{(E + E_q)^2}{\sqrt{E(E + 2E_q)}}. \tag{5.4.33c}$$

An approximation for $\mathcal{F}_-^{\infty}$ above can be derived by considering its values at the extreme cases $E_q = 0$ and $E_q = E_0$. For the case $E_q = 0$, Eq. (5.4.33b) reduces to:

$$\mathcal{F}_-^{\infty}(q = 0) = \int_0^{\infty} \frac{dE}{1 + e^{\beta E}}(E + E_0) = \frac{\pi^2}{12\beta^2} + \frac{E_0}{\beta} \ln 2. \tag{5.4.34}$$

When $E_q = E_0$, a closed form cannot be obtained, but the method outlined in

subsection 5.4.2 can be used:

$$\mathcal{F}_-^\infty(E_q = E_0) = \int_0^\infty \frac{dE}{1 + e^{\beta E}} \frac{(E + E_0)^2}{\sqrt{E(E + 2E_0)}}$$

$$= \frac{E_0^2}{2} \sum_{j=1}^\infty (-1)^{j+1} e^{j\beta E_0} [K_2(j\beta E_0) + K_0(j\beta E_0)]. \qquad (5.4.35)$$

After replacing the Bessel functions by the asymptotic series (5.4.9), the sum over j can be performed:

$$\mathcal{F}_-^\infty(q = E_0) = E_0^2 \sqrt{\frac{\pi}{2\beta E_0}} \left[\widetilde{\zeta}\left(\tfrac{1}{2}\right) + \frac{7}{8\beta E_0} \widetilde{\zeta}(\tfrac{3}{2}) + \frac{57}{128(\beta E_0)^2} \widetilde{\zeta}(\tfrac{5}{2}) + \dots \right], \qquad (5.4.36)$$

where $\widetilde{\zeta}(z)$ is defined as

$$\widetilde{\zeta}(z) \equiv \sum_{j=1}^\infty \frac{(-1)^{j+1}}{j^z} = \begin{cases} \ln 2 & z = 1, \\ (1 - 2^{1-z})\,\zeta(z) & \text{otherwise.} \end{cases} \qquad (5.4.37)$$

in terms of the ζ function:

$$\zeta(z) = \sum_{n=1}^\infty n^{-z}. \qquad (5.4.38)$$

The values of $\widetilde{\zeta}(z)$ in the first few terms in the series (5.4.36) are:

$$\widetilde{\zeta}(\tfrac{1}{2}) = 0.604899, \qquad \widetilde{\zeta}(\tfrac{3}{2}) = 0.765147, \qquad \widetilde{\zeta}(\tfrac{5}{2}) = 0.8672, \qquad (5.4.39)$$

while the rest of the terms are between 0.9 and 1.

The derivative of $\mathcal{F}_-^\infty$ with respect to E_q,

$$\partial_{E_q} \mathcal{F}_-^\infty(E_q) = E_q \int_0^\infty \frac{dE}{1 + e^{\beta E}} \frac{(E + E_0)^2}{[(E + E_0)^2 - E_q^2]^{\frac{3}{2}}}, \qquad (5.4.40)$$

is positive for all E_q between 0 and E_0, showing that its value increases monotonically in this domain. To get an idea on what the behaviour of the integral is between the points $E_q = 0$ and $E_q = E_0$, the Fermi-Dirac factor $(e^{\beta E} + 1)^{-1}$ can be expanded as:

$$\mathcal{F}_-^\infty \sim \sum_{j=1}^\infty \frac{(-1)^{j+1}}{(j\beta)^2} \int_0^\infty dx\, e^{-x} \frac{(x + j\beta E_0)^2}{\sqrt{(x + j\beta E_0)^2 - (j\beta E_q)^2}}. \qquad (5.4.41)$$

The square root in the denominator can be expanded in powers of x, after which the integral over x can be performed, giving:

$$\mathcal{F}_-^\infty \sim \frac{E_0^2}{\beta k_0} \ln 2 + \frac{\pi^2}{12\beta^2} \left[2\frac{E_0}{k_0} - \left(\frac{E_0}{k_0}\right)^3 \right] + \frac{3\zeta(3)}{4\beta^3 k_0} \left[2 - 5\left(\frac{E_0}{k_0}\right)^2 + 3\left(\frac{E_0}{k_0}\right)^4 \right] + \dots,$$

$$(5.4.42)$$
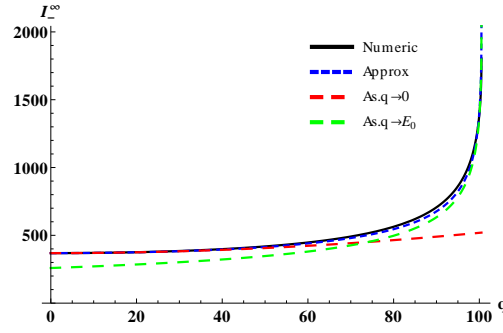
Figure 5.21: The numerical result for the $\mathcal{F}_-^\infty$ integral (solid dark line) is compared with the approximation (5.4.44) and with the asymptotic limits of the latter in the cases $E_{\to 0}$ and $E_{\to E_0}$ (the high E_0 expansion).

where

$$k_0 = \sqrt{E_0^2 - E_q^2}. \tag{5.4.43}$$

The coefficients of powers of β lower than -2 should vanish when $q = 0$, as is the case for the coefficient of β^{-3} above. The expansion (5.4.42) is not valid when E_q approaches E_0 (and $k_0 \to 0$).

Numerical plots indicate that $\mathcal{F}_-^\infty(E_q)$ can be written as follows:

$$\mathcal{F}_-^\infty(E_q) = \frac{\mathcal{F}_-^\infty(0)\mathcal{F}_-^\infty(E_0)}{\mathcal{F}_-^\infty(0) + \frac{k_0}{E_0}[\mathcal{F}_-^\infty(E_0) - \mathcal{F}_-^\infty(0)]}, \tag{5.4.44}$$

where $\mathcal{F}_-^\infty(0)$ and $\mathcal{F}_-^\infty(E_0)$ are given in Eqs. (5.4.34) and (5.4.36), respectively.

The expression (5.4.44) for $\mathcal{F}_-^\infty(q)$ has the following asymptotic limits:

$$\mathcal{F}_-^\infty(E_q) \sim \mathcal{F}_-^\infty(0) \left\{ 1 + \frac{E_q^2}{2E_0^2} \left(1 - \frac{\mathcal{F}_-^\infty(0)}{\mathcal{F}_-^\infty(E_0)} \right) + O(q^4) \right\}, \tag{5.4.45a}$$

$$\mathcal{F}_-^\infty(E_q) \sim \mathcal{F}_-^\infty(E_0) \left\{ 1 + \frac{k_0}{E_0} \left(1 - \frac{\mathcal{F}_-^\infty(E_0)}{\mathcal{F}_-^\infty(0)} \right) + O(k_0^2) \right\}. \tag{5.4.45b}$$

Figure 5.21 shows the validity of the above approximations.

As for $\mathcal{F}_-^0$ in (5.4.33), the value when $E_q = E_0$ is trivially equal to 0. An expression valid for small E_q can be obtained by expanding $[E(E + 2E_q)]^{-\frac{1}{2}}$ about $E_q = 0$. The problem with this expansion is that higher order terms come with increasing inverse powers of E, which diverge at the lower end of the integral, limiting the number of terms that can be produced by this method:

$$\mathcal{F}_-^0 = -\int_0^{E_0 - E_q} \frac{dE}{1 + e^{\beta(E_0 - E_q - E)}} (E + E_q + \dots). \tag{5.4.46}$$

As before, the Fermi-Dirac factor can be expanded in a power series. The following

identities shall be used:

$$\sum_{j=1}^{\infty} \frac{(-1)^{j+1}}{j} e^{-j\beta(E_0-E_q)} = \ln(1 + e^{-\beta(E_0-E_q)}), \tag{5.4.47}$$

$$\sum_{j=1}^{\infty} \frac{(-1)^{j+1}}{j^2} e^{-j\beta(E_0-E_q)} = -\text{Li}_2(-e^{-\beta(E_0-E_q)}), \tag{5.4.48}$$

where $\text{Li}_2(z)$ is the dilogarithm [60], a particular case of the polylogarithm function, which is defined as:

$$\text{Li}_s(z) = \sum_{k=1}^{\infty} \frac{z^k}{k^s}. \tag{5.4.49}$$

The best expansion around $E_q = 0$ obtainable using the method outlined above is:

$$\mathcal{F}_-^0 \sim -\left[\frac{E_0}{\beta}\ln 2 - \frac{E_q}{\beta}\ln(1 + e^{-\beta(E_0-E_q)})\right] + \frac{1}{\beta^2}\left[\frac{\pi^2}{12} + \text{Li}_2(-e^{-\beta(E_0-E_q)})\right] + \dots, \tag{5.4.50}$$

which reduces when $E_q = 0$ to:

$$\mathcal{F}_-^0(E_q = 0) = -\frac{E_0}{\beta}\ln 2 + \frac{\pi^2}{12\beta^2} + \frac{1}{\beta^2}\text{Li}_2(-e^{-\beta E_0}). \tag{5.4.51}$$

Another way to obtain an approximation for $\mathcal{F}_-^0$ is to expand the Fermi-Dirac factor in a power series about $x \equiv \frac{E}{E_0} = 0$:

$$\mathcal{F}_-^0 = -E_0^2 \sum_{n=0}^{\infty} \frac{(-\beta E_0)^n}{n!}\left[\mathcal{I}_{n+2} + \frac{2E_q}{E_0}\mathcal{I}_{n+1} + \left(\frac{E_q}{E_0}\right)^2 \mathcal{I}_n\right] \times \frac{d^n}{dz^n}\frac{1}{1+e^z}\bigg|_{z=\beta(E_0-E_q)}, \tag{5.4.52}$$

where $\mathcal{I}_n$ is defined as follows:

$$\mathcal{I}_n = \int_0^{1-\frac{E_q}{E_0}} \frac{x^n dx}{\sqrt{x(x + \frac{2E_q}{E_0})}}. \tag{5.4.53}$$

The integrals $\mathcal{I}_n$ can be solved exactly by starting from the recurrence relation:

$$\mathcal{I}_{n+1} = \frac{1}{n+1}\frac{k_0}{E_0}\left(1 - \frac{E_q}{E_0}\right)^n - \frac{2n+1}{n+1}\frac{E_q}{E_0}\mathcal{I}_n, \tag{5.4.54}$$

which follows by noting that:

$$\frac{x}{\sqrt{x\left(x + \frac{2E_q}{E_0}\right)}} = \frac{d}{dx}\sqrt{x(x + \frac{2E_q}{E_0})} - \frac{E_q}{E_0}\frac{1}{\sqrt{x(x + \frac{2E_q}{E_0})}}, \tag{5.4.55}$$

To start the recurrence, $\mathcal{I}_0$ can be computed using:

$$2\frac{d}{dx}\ln\left(\sqrt{x}+\sqrt{x+\frac{2E_q}{E_0}}\right)=\frac{1}{\sqrt{x\left(x+\frac{2E_q}{E_0}\right)}}. \tag{5.4.56}$$

The result is:

$$\mathcal{I}_0=\ln\frac{E_0+k_0}{E_q}. \tag{5.4.57}$$

Solving Eq. (5.4.54) gives the following expression for $\mathcal{I}_n$:

$$\mathcal{I}_n=\frac{\Gamma(n+\frac{1}{2})}{\Gamma(\frac{1}{2})n!}\left\{\ln\frac{E_0+k_0}{E_q}+\frac{k_0}{E_0}\sum_{k=0}^{n-1}\frac{k!\Gamma(\frac{1}{2})}{\Gamma(k+\frac{3}{2})}\left(1-\frac{E_q}{E_0}\right)^k\left(-\frac{2E_q}{E_0}\right)^{n-k-1}\right\}. \tag{5.4.58}$$

Using Eq. (5.4.54), the combination in Eq. (5.4.52) can be written as:

$$\mathcal{I}_{n+2}+\frac{2E_q}{E_0}\mathcal{I}_{n+1}+\left(\frac{E_q}{E_0}\right)^2\mathcal{I}_n=\frac{k_0}{E_0}\frac{\left(1-\frac{E_q}{E_0}\right)^n\left[1+n\left(1-\frac{E_q}{E_0}\right)\right]}{(n+1)(n+2)}$$
$$+\frac{n^2+n+1}{(n+1)(n+2)}\left(\frac{E_q}{E_0}\right)^2\mathcal{I}_n. \tag{5.4.59}$$

Thus, $\mathcal{F}_-^0$ reduces to:

$$\mathcal{F}_-^0=-E_0^2\sum_{n=0}^{\infty}\frac{(-\beta E_0)^n}{(n+2)!}\frac{d^n}{dz^n}\frac{1}{1+e^z}\bigg|_{z=\beta(E_0-E_q)}$$
$$\times\left\{\frac{k_0}{E_0}\left(1-\frac{E_q}{E_0}\right)^n\left[1+n\left(1-\frac{E_q}{E_0}\right)\right]+\frac{\Gamma(n+\frac{1}{2})(n^2+n+1)}{n!\Gamma(\frac{1}{2})}\left(\frac{E_q}{E_0}\right)^2\right.$$
$$\times\left[\left(-\frac{2E_q}{E_0}\right)^n\ln\frac{E_0+k_0}{E_q}+\frac{k_0}{E_0}\sum_{k=0}^{n-1}\frac{k!\Gamma(\frac{1}{2})}{\Gamma(k+\frac{3}{2})}\left(1-\frac{E_q}{E_0}\right)^k\left(-\frac{2E_q}{E_0}\right)^{n-k-1}\right]\bigg\}. \tag{5.4.60}$$

The sum over n can be performed for the first term in Eq. (5.4.60) by expanding the Fermi-Dirac factor in a power series:

$$-k_0E_0\sum_{n=0}^{\infty}\frac{[-\beta(E_0-E_q)]^n}{(n+2)!}\left[1+n\left(1-\frac{E_q}{E_0}\right)\right]\frac{d^n}{dz^n}\frac{1}{1+e^z}\bigg|_{z=\beta(E_0-E_q)}$$
$$=-k_0E_0\sum_{j=1}^{\infty}(-1)^{j+1}e^{-j\beta(E_0-E_q)}\sum_{n=0}^{\infty}\frac{[j\beta(E_0-E_q)]^n}{(n+2)!}\left[1+n\left(1-\frac{E_q}{E_0}\right)\right]. \tag{5.4.61}$$

The sum over n now looks like the Taylor series expansion of $e^{j\beta(E_0-E_q)}$:

$$\sum_{n=0}^{\infty} \frac{[j\beta(E_0-E_q)]^n}{(n+2)!}\left[1+n\left(1-\frac{E_q}{E_0}\right)\right]=$$

$$\frac{\frac{2E_q}{E_0}-1}{[j\beta(E_0-E_q)]^2}\left[e^{j\beta(E_0-E_q)}-1\right]+\frac{1}{j\beta E_0}\left[e^{j\beta(E_0-E_q)}-\frac{E_q}{E_0-E_q}\right]. \quad (5.4.62)$$

Using the definition of the dilogarithm function (5.4.49), the sum over j yields:

$$-k_0 E_0 \sum_{n=0}^{\infty} \frac{[-\beta(E_0-E_q)]^n}{(n+2)!}\left[1+n\left(1-\frac{E_q}{E_0}\right)\right]\frac{d^n}{dz^n}\frac{1}{1+e^z}\bigg|_{z=\beta(E_0-E_q)}$$

$$=-\frac{k_0(2E_q-E_0)}{\beta^2(E_0-E_q)^2}\left[\frac{\pi^2}{12}+\mathrm{Li}_2(-e^{-\beta(E_0-E_q)})\right]-\frac{k_0}{\beta}\left\{\ln 2-\frac{E_q}{E_0-E_q}\ln[1+e^{-\beta(E_0-E_q)}]\right\}. \quad (5.4.63)$$

The limit $E_q = 0$ agrees with Eq. (5.4.51).

The best approximation that we could find can be obtained by combining the result (5.4.63) with the first three terms in the sum over n in Eq. (5.4.60):

$$\mathcal{F}_-^0 = -\frac{k_0(2q-E_0)}{\beta^2(E_0-q)^2}\left[\frac{\pi^2}{12}+\mathrm{Li}_2(-e^{-\beta(E_0-q)})\right]$$

$$-\frac{k_0}{\beta}\left\{\ln 2-\frac{q}{E_0-q}\ln[1+e^{-\beta(E_0-q)}]\right\}$$

$$-\frac{q^2}{2(1+e^{\beta(E_0-q)})}\left\{\ln\frac{(E_0+k_0)}{q}-\frac{\beta q}{1+e^{-\beta(E_0-q)}}\left(\ln\frac{E_0+k_0}{q}-\frac{k_0}{q}\right)\right\}$$

$$+\frac{7(\beta q)^2}{16}\frac{\tanh\frac{\beta(E_0-q)}{2}}{1+e^{-\beta(E_0-q)}}\left[\ln\frac{E_0+k_0}{q}-\frac{k_0}{q}\left(1-\frac{E_0-q}{3q}\right)\right]+\ldots\bigg\}. \quad (5.4.64)$$

As can be seen in Figure 5.22, this approximation captures the essential features of the integral both at small q and at small $\varepsilon \equiv E_0 - q$, and has the following asymptotic limits:

$$\mathcal{F}_-^0(q) \sim \frac{\pi^2}{12\beta^2}-\frac{E_0\ln 2}{\beta}-\frac{\pi^2 q^2}{8\beta^2 E_0^2}-\frac{q^2\ln 2}{2\beta E_0}+O(q^4), \quad (5.4.65a)$$

$$\mathcal{F}_-^0(q) \sim \sqrt{2E_0^3\varepsilon}\left\{\frac{1}{\beta^2\varepsilon^2}\left[\frac{\pi^2}{12}-\beta\varepsilon\ln(1+e^{-\beta\varepsilon})+\mathrm{Li}_2(-e^{-\beta\varepsilon})\right]\right.$$

$$+\frac{1+e^{\beta\varepsilon}\left[1+\frac{1}{3}\beta\varepsilon+\frac{7}{120}\beta^2\varepsilon^2\tanh\frac{\beta\varepsilon}{2}\right]}{2(1+e^{\beta\varepsilon})^2}$$

$$+\frac{1}{16\beta^2 E_0\varepsilon}\left[-3\pi^2+16\beta\varepsilon\ln 2+20\beta\varepsilon\ln(1+e^{-\beta\varepsilon})-36\mathrm{Li}_2(-e^{-\beta\varepsilon})\right]$$

$$\left.-\frac{\frac{\varepsilon}{E_0}}{960(1+e^{\beta\varepsilon})}\left[760+e^{\beta\varepsilon}(760+264\beta\varepsilon+47\beta^2\varepsilon^2\tanh\frac{\beta\varepsilon}{2})\right]+O(E_0^{-2})\right\} \quad (5.4.65b)$$
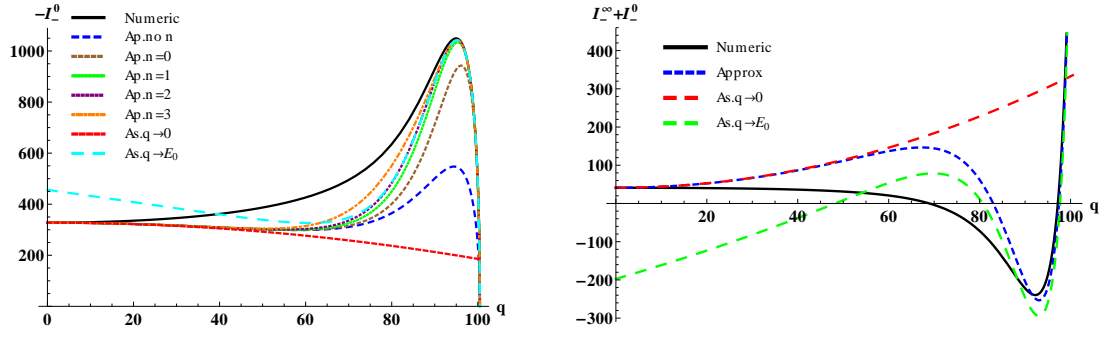
Figure 5.22: (a) The numerical result for $-\mathcal{F}_-^0$ (solid dark line, taken with a negative sign such that the plot is over positive values) is compared against the following orders of the approximation (5.4.60): the *no n* curve represents the k_0 term given by Eq. (5.4.63), the $n = 0, 1, 2, 3$ represent the k_0 term with terms from the sum over n added up to the inscribed n and finally, the low q and low $E_0 - q$ asymptotic limits of the approximation (5.4.64). (b) The numerical result for $\mathcal{F}_- = \mathcal{F}_-^\infty + \mathcal{F}_-^0$ compared to the approximation and asymptotic forms at small q and large E_0.

A number of distinctive features can be read from Figure 5.22. The graph of $\mathcal{F}_-$ can be roughly divided into three parts. In the first part, where $\frac{E_q}{E_0}$ is small, $\mathcal{F}_-$ has a roughly constant value, which we can estimate by combining the asymptotic expressions for small E_q from Eqs. (5.4.45) and (5.4.65):

$$\mathcal{F}_- \sim \frac{\pi^2}{6\beta^2} + \frac{q^2}{\beta E_0}\ln 2 + \ldots \qquad (5.4.66)$$

The value of $\mathcal{F}_-$ for $q \ll E_0$ can be written as a constant temperature-dependent term plus corrections in inverse powers of E_0.

The middle region corresponds to $\mathcal{F}_- < 0$. Even though the approximations obtained in this chapter do not capture the width of this region properly, they can still be used to estimate the value of $\mathcal{F}_-$ at the peak and its location. For this purpose, let us introduce the new variable $x = \beta(E_0 - q)$. We can then construct the function $f(x)$ as follows:

$$\mathcal{F}_- \sim E_0^2 \sqrt{\frac{2}{\beta E_0}} f(x), \qquad (5.4.67\text{a})$$

where

$$f(x) = \frac{\ln 2\,\widetilde{\zeta}(\frac{1}{2})\sqrt{\pi}}{2(\ln 2 + \widetilde{\zeta}(\frac{1}{2})\sqrt{\pi x})} - \frac{\pi^2 x^{-\frac{3}{2}}}{12} + x^{-\frac{1}{2}}\ln(1 + e^{-x}) - x^{-\frac{3}{2}}\mathrm{Li}_2(-e^{-x})$$
$$- \frac{x^{\frac{1}{2}}}{2(1 + e^x)} - \frac{x^{\frac{3}{2}}(1 + \frac{7}{40}x\tanh\frac{x}{2})}{6(1 + e^x)(1 + e^{-x})}. \qquad (5.4.67\text{b})$$

The expression for $f(x)$ follows from the first order terms in the expansions in inverse powers of E_0 of $\mathcal{F}_-^\infty$ (5.4.45) and $\mathcal{F}_-^0$ (5.4.65). The interval we are interested in is
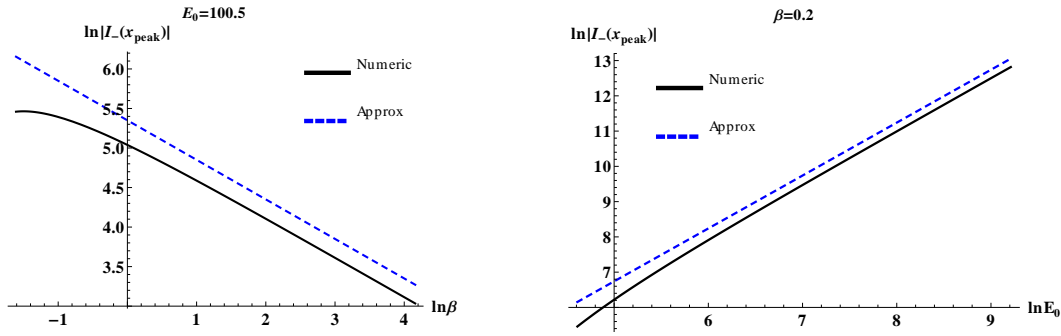
Figure 5.23: Log-log plot of the numeric result for the $\mathcal{F}_-$ integral (solid dark line) evaluated at the point where the asymptotic analysis indicates the minimum value would be compared with (5.4.71) as functions of (a) β (with $E_0 = 100.5$ fixed); β ranges from 0.2 to 64; and of (b) E_0 (with $\beta = 0.2$ fixed), ranging from $E_0 = 100.5$ to $E_0 = 10000.5$.

between the zeros of $f(x)$, which we can compute numerically:

$$x_{\text{left}} = 4.4365, \qquad x_{\text{right}} = 0.3545. \tag{5.4.68}$$

The peak is located inside this interval, where the derivative of $f(x)$ with respect to x vanishes. The derivative of $f(x)$ is given by:

$$f'(x) = -\frac{\ln 2}{4x^{\frac{1}{2}}}\left[\frac{\widetilde{\zeta}(\frac{1}{2})\sqrt{\pi}}{\ln 2 + \widetilde{\zeta}(\frac{1}{2})\sqrt{\pi x}}\right]^2 + \frac{\pi^2 x^{-\frac{5}{2}}}{8} - \frac{3x^{-\frac{3}{2}}}{2}\ln(1 + e^{-x}) + \frac{3x^{-\frac{5}{2}}}{2}\text{Li}(-e^{-x})$$

$$- \frac{5x^{-\frac{1}{2}}}{4(1 + e^x)} + \frac{x^{\frac{1}{2}}}{16\cosh^2\frac{x}{2}}\left(1 + \frac{3}{8}x\tanh\frac{x}{2} - \frac{7x^2}{120}\frac{1 - 2\sinh^2\frac{x}{2}}{\cosh^2\frac{x}{2}}\right). \tag{5.4.69}$$

It is remarkable that, in the first order approximation, the position of the extremum and of the margins of the interval do not depend on any of the parameters E_0 and β only through x. The zero of $f'(x)$ can be solved using numerical methods:

$$x_{\text{peak}} \simeq 1.46338, \qquad f(x_{\text{peak}}) \simeq -0.14783. \tag{5.4.70}$$

Thus, the value of $\mathcal{F}_-$ at its minimum is:

$$\mathcal{F}_-(x_{\text{peak}}) \simeq -0.14783 E_0^2 \sqrt{\frac{2}{\beta E_0}}. \tag{5.4.71}$$

Although the above approximation is about 15% off (mainly due to the inaccuracy of the approximations obtained for $\mathcal{F}_-^\infty$ and $\mathcal{F}_-^0$), the order of magnitude and the dependence on E_0 and β seem to be correctly captured, as illustrated in Figure 5.23.

Finally, there is a narrow strip in the domain $0 \leq x < x_{\text{right}} = 0.3545$, where $\mathcal{F}_-^\infty$ dominates over $\mathcal{F}_-^0$. Here, $\mathcal{F}_-^0$ goes to 0 as $x^{\frac{1}{2}}$, while $\mathcal{F}_-^\infty$ increases as $(1 + \alpha x^{\frac{1}{2}})^{-1}$,

where α is a constant. The value of $\mathcal{F}_-$ at $x = 0$ is:

$$\mathcal{F}_-(x = 0) \simeq 0.53608 E_0^2 \sqrt{\frac{2}{\beta E_0}}. \tag{5.4.72}$$

A quantitative measure of the overall significance of the middle part relative to the third would be a numerical integration of $f(x)$ multiplied by powers of x. Defining

$$I_n = I_n^{\text{left}} + I_n^{\text{right}}, \tag{5.4.73}$$

where

$$I_n^{\text{left}} = \int_{x_{\text{right}}}^{x_{\text{left}}} dx \, f(x) \, x^n, \qquad I_n^{\text{right}} = \int_0^{x_{\text{right}}} dx \, f(x) \, x^n, \tag{5.4.74}$$

the following values can be obtained through numerical integration:

$$
\begin{aligned}
I_0^{\text{left}} &= -0.344726, & I_1^{\text{left}} &= -0.675283, & I_2^{\text{left}} &= -1.58059, \\
I_0^{\text{right}} &= 0.0550712, & I_1^{\text{right}} &= 0.00596215, & I_2^{\text{right}} &= 0.00106664, \\
I_0 &= -0.289655, & I_1 &= -0.669321, & I_2 &= -1.57952.
\end{aligned}
\tag{5.4.75}
$$

The results of the numerical integrations are clearly smaller in absolute value for the third region than for the second, giving a bigger weight factor to the terms in the sum over ℓ in Eqs. (5.2.20a) and (5.3.51a) for which the corresponding discrete momentum $q_{m\ell}$ is located inside the second region.

On the boundary

According to Eqs. (5.4.24), $q_{m\ell} > q_{m1} = \frac{1}{R}(m + am^{\frac{1}{3}} + \dots)$, which implies that at large enough m, there are a number of values for ℓ such that $E_q - E_0 < 0$, where

$$E_q = \sqrt{\mu^2 + q^2}, \qquad E_0 = \Omega(m + \tfrac{1}{2}). \tag{5.4.76}$$

For simplicity, the discussion in this paragraph will be restricted to massless fermions, such that $E_q = q$.

Since excluding the terms for which $q < E_0 = \Omega(m + \frac{1}{2})$ reduces the discussion to the case when the SOL is inside the boundary, when the energy density is finite everywhere inside the boundary, it follows that any divergent behaviour would be introduced by modes for which $q < \Omega(m + \frac{1}{2})$. In this regime, $\mathcal{F}_-$ dominates especially when $x = \beta(E_0 - q)$ is between $x = x_{\text{left}} = 4.4365$ and $x = 0$ [see Figure 5.23 and Eq. (5.4.68)].

According to Figure 4.2, increasingly higher values of m make significant contributions to the energy density as $\rho\Omega \to 1$. Hence, the asymptotic behaviour of the energy density in the spectral (5.2.20a) and MIT bag (5.3.51a) models can be investigated by considering $m \to \infty$.

Let us first look at the energy density on the boundary, given in Eqs. (5.4.22). As implied by Eq. (5.4.6), $\mathcal{F}_+ \sim e^{-(E_0+q)}$ and stays finite for all values of $R\Omega$. The sum over ℓ can be approximated by an integral running over x between 0 and x_{left}, where $\mathcal{F}_-$ is dominant. In this domain, $\mathcal{F}_-$ can be replaced using Eq. (5.4.67) and Eq. (5.4.75) can be used for the integral over x, yielding:

$$\langle : T_{\hat{t}\hat{t}} :_I \rangle_\beta \Big|_{\rho=R} \sim \Omega^{\frac{3}{2}} I_0 \sum_{m=0}^{\infty} (m + \tfrac{1}{2})^{\frac{3}{2}}, \tag{5.4.77}$$

for both the spectral and the MIT bag models. The sum over m diverges as $m^{\frac{3}{2}}$, therefore, the energy density is infinite on the boundary if the boundary is outside the SOL.

On the SOL

For a point inside, but close to the SOL, q can be approximated such that:

$$q = \Omega(m + \tfrac{1}{2}). \tag{5.4.78}$$

In this case, the integral $\mathcal{F}_-^\infty$ is given by Eq. (5.4.36), while $\mathcal{F}_-^0 = 0$. Let the small parameter be $\varepsilon = 1 - \rho^2\Omega^2$, as defined in Eq. (4.1.3). In this case, $q\rho < m + \tfrac{1}{2}$, but because the boundary is outside the SOL, $qR > m + \tfrac{1}{2}$.

If the boundary is sufficiently far from the SOL, the term $(m + \tfrac{1}{2})/qR$ in the expression for $\langle : T_{\hat{t}\hat{t}} :\rangle_\beta^{\text{MIT}}$ in Eq. (5.4.7) can be neglected, in which case the spectral and MIT models stand on the same footing. Using Eqs. (A.2.8) to approximate the Bessel functions in Eqs. (5.4.7) gives:

$$\frac{J_m^2(q\rho) + J_{m+1}^2(q\rho)}{J_m^2(qR)} \sim \sqrt{\frac{\Omega^2 R^2 - 1}{4\varepsilon}} \exp\left[2(m + \tfrac{1}{2})\left(\sqrt{\varepsilon} + \ln\frac{\sqrt{1-\varepsilon}}{1+\sqrt{\varepsilon}}\right)\right]. \tag{5.4.79}$$

Hence, $\langle : T_{\hat{t}\hat{t}} :\rangle_\beta^{\text{MIT}}$ can be approximated close to the SOL as:

$$\langle : T_{\hat{t}\hat{t}} :\rangle_\beta = \frac{\Omega^{\frac{3}{2}}}{4\pi^2 R^2} \sqrt{\frac{2(R^2\Omega^2 - 1)}{\beta\varepsilon}} \widetilde{\zeta}(\tfrac{1}{2}) \int_0^\infty d\nu\, \nu^{\frac{3}{2}} \exp\left[-\nu\left(\ln\frac{1+\sqrt{\varepsilon}}{1-\sqrt{\varepsilon}} - 2\sqrt{\varepsilon}\right)\right], \tag{5.4.80}$$

where the sum over m was approximated by an integral, which can be solved in terms of Gamma functions:

$$\langle : T_{\hat{t}\hat{t}} :\rangle_\beta = \frac{\Omega^{\frac{3}{2}}}{4\pi^2 R^2} \sqrt{\frac{2(R^2\Omega^2 - 1)}{\beta\varepsilon}} \frac{\widetilde{\zeta}(\tfrac{1}{2})\Gamma(\tfrac{5}{2})}{\left[\ln\frac{1+\sqrt{\varepsilon}}{1-\sqrt{\varepsilon}} - 2\sqrt{\varepsilon}\right]^{\frac{5}{2}}}. \tag{5.4.81}$$

Thus, $\langle : T_{\hat{t}\hat{t}} : \rangle_\beta$ appears to diverge as the SOL is approached as $\varepsilon^{-\frac{17}{4}}$:

$$\langle : T_{\hat{t}\hat{t}} : \rangle_\beta = \frac{9\Omega^2 \widetilde{\zeta}(\frac{1}{2})\Gamma(\frac{5}{2})}{16\pi^2 R^2 \varepsilon^{\frac{17}{4}}} \sqrt{\frac{3(\Omega^2 R^2) - 1}{\beta\Omega}}. \tag{5.4.82}$$

Although the plethora of approximations performed in this analysis are more than likely to have influenced the result, it is nevertheless compelling evidence confirming that if the bounding surface is outside the SOL, the t.e.v. of the energy density no longer converges on the SOL. The order $\frac{17}{4}$ of the divergence is very close to 4, which is the leading order of the divergence found for the t.e.v. (4.3.54c) of the energy density with respect to the rotating vacuum in the unbounded case.

5.4.3 Summary

Enclosing the rotating system inside a boundary placed inside or on the speed of light surface (SOL) induces regular and well defined thermal states with respect to which thermal expectation values (t.e.v.s) stay finite throughout the space enclosed inside the boundary, for both scalars and fermions. The mechanism which allows the construction of regular thermal states of scalar particles and through which the divergences near the SOL of the t.e.v.s corresponding to fermion operators are removed is the quantisation of the transverse momentum q imposed by the boundary conditions. If the boundary is not outside the SOL, the quantisation of q ensures that there are no modes for which $\widetilde{\omega}\omega < 0$ ($\widetilde{E}E < 0$ for fermions). A consequence of this restriction is the absence of spurious temperature independent terms in t.e.v.s, or, in other words, the equivalence of the rotating and non-rotating vacua.

Two models for implementing fermion boundary conditions were considered in this chapter. The spectral model, discussed in section 5.2, imposes boundary conditions on the Fourier transform of wave-functions, thus having a non-local character. In the MIT bag model, discussed in section 5.3, the boundary conditions are formulated locally. The graphical comparison in Figure 5.14 between the two models shows that the t.e.v.s in the MIT model follow the profiles of the corresponding t.e.v.s in the unbounded case more closely than those corresponding to the spectral model. Three fundamental differences were found between the two models: the fermion condensate (FC) for massless fermions does not vanish in the MIT model, but it does in the spectral model; the neutrino charge current (CC) along the rotation axis changes sign between the rotation axis and the boundary, where it attains a finite (non-zero) value, whereas in the MIT model, its sign does not change while it's value on the boundary is 0; finally, $\langle : T_{\hat{\varphi}\hat{\varphi}} : \rangle_\beta$ vanishes on the boundary in the spectral model, but not in the MIT model.

In the analysis of the changes induced in the vacuum state by the presence of the boundary, the Casimir divergence close to the boundary of the t.e.v. of the

stress-energy tensor (SET) was one order of magnitude higher in the spectral model than in the MIT bag model. Also, previous work [31] on the Casimir divergence for arbitrary boundaries and fields showed that a fully local SET would diverge at most as in the MIT bag model. The MIT model indeed confirms the results of Ref. [31] due to the purely local formulation of the boundary conditions, while in the spectral model, the boundary conditions are formulated in a non-local manner, contradicting the assumption of locality in Ref. [31]. It is interesting that the Casimir divergence of the FC has a higher order of magnitude in the MIT bag model than in the spectral model.

Finally, an attempt at approximating the Fermi-Dirac integral corresponding to a bounded system brought evidence in subsection 5.4.2 that the t.e.v. of the energy density in a bounded systems where the SOL is inside the boundary diverge as the SOL is approached. While the analysis performed in subsection 5.4.2 is not sufficiently rigorous to show beyond doubt that thermal states suffer from the same divergent behaviour as in the unbounded case, the quasi-Euclidean approach of section 6.2 supports this finding.

Chapter 6. Quasi-Euclidean formulation of QFT on a rotating space-time

The analysis of the Casimir effect performed in chapter 5 showed that in the Euclidean approach the expression for observables has the form of a continuous integral over the equivalent of the longitudinal momentum q. We would like to retain this feature in the analysis of thermal states inside a bounding surface, where we previously had to compute sums over roots of some non-trivial equation involving Bessel functions. To this end, a quasi-Euclidean approach is considered in this chapter.

The first problem we are faced with is that the metric (4.1.4) of the space-time has non-diagonal terms which mix space and time coordinates. Changing to a purely imaginary time coordinate would make these components of the metric imaginary, therefore rendering the manifold non-Riemannian. Even though it looks as if the space-time does not lend itself to Euclideanisation, such approaches have given positive results in, e.g. the analysis of the Kerr space-time [36, 67].

In this chapter, the quasi-Euclidean approach is used to obtain an Euclidean version of the Lorentzian Feynman propagator, by changing coordinates from real to imaginary time. After such a propagator is obtained, the method outlined by Groves, Anderson and Carlsen [38] is used to compute the thermal Euclidean function, from which thermal expectation values can be computed.

In sections 6.1.1, 6.1.2 and 6.1.3 a consistency check on the Euclidean approach is performed by comparing the results obtained for the renormalised thermal expectation values (t.e.v.s) in the Minkowski non-rotating, rotating and bounded rotating space-times, respectively with those already obtained in previous chapters through the Lorentzian formulation. The highlight of this chapter is section 6.2, where the behaviour of the t.e.v. of the energy density close to the speed of light surface (SOL) is investigated for the case when the SOL is inside the boundary.

The aim is to prove that the renormalised expectation value of the energy density for a system of fermions enclosed in a boundary located outside the SOL surface diverges as the SOL is approached. The approach, for reasons which shall become apparent in the appropriate section, is to take the difference between the unrenormalised (i.e. without performing Wick ordering) expectation values with respect the thermal state on the bounded and unbounded spaces. If the bounded thermal state is regular in the vicinity of the SOL, this difference must diverge exactly as the unbounded thermal state, i.e. as described in subsection 4.3.2.

6.1   Equivalence between the quasi-Euclidean and Lorentzian formulations

6.1.1   Quasi-Euclidean formulation of non-rotating thermal distributions

Starting with the Euclidean Green's function for the unbounded Minkowski space-time, given in Eq. (5.2.33), it is possible to construct the corresponding thermal Euclidean function starting from the Fourier components $s_E(\omega)$ of the Euclidean Green's function $S_E(x, x')$:

$$S_E(x, x') = \int_{-\infty}^{\infty} d\omega \, e^{i\omega\Delta\tau} s_E(\omega). \qquad (6.1.1)$$

The thermal Euclidean Green's function can be obtained by replacing the above integral with a sum [38]:

$$S_E^{\beta}(x, x') = \frac{2\pi}{\beta} \sum_{j=-\infty}^{\infty} e^{i\omega_j\Delta\tau} s_E(\omega_j), \qquad (6.1.2)$$

where j is an integer and

$$\omega_j = \frac{2\pi}{\beta}(j + \tfrac{1}{2}). \qquad (6.1.3)$$

Thermal expectation values with respect to the vacuum state can be calculated by subtracting $S_E(x, x')$ from $S_E^{\beta}(x, x')$, using the generalised Abel-Plana sum formula, given in Eq. (5.2.45).

The t.e.v. of the energy density can be calculated using Eq. (2.2.62):

$$\langle : T_{\hat{t}\hat{t}} : \rangle_{\beta} = \frac{1}{8\pi^3} \int_{-\infty}^{\infty} dk \sum_{m=-\infty}^{\infty} \left[\int_{-\infty}^{\infty} d\omega \, f(\omega) - \frac{2\pi}{\beta} \sum_{j=-\infty}^{\infty} f(\omega_j) \right], \qquad (6.1.4)$$

where

$$f(\omega) = \omega^2[I_m(\alpha\rho)K_m(\alpha\rho) + I_{m+1}(\alpha\rho)K_{m+1}(\alpha\rho)] \qquad (6.1.5)$$

and $\alpha = \sqrt{\omega_k^2 + \omega^2}$ (5.1.19) is written in terms of

$$\omega_k = \sqrt{k^2 + \mu^2}. \qquad (6.1.6)$$

Since $f(\omega)$ has no residues in the complex plane, the generalised Abel-Plana formula (5.2.45) can be applied to yield:

$$\langle : T_{\hat{t}\hat{t}} : \rangle_{\beta} = \frac{-i}{2\pi^3} \int_{-\infty}^{\infty} dk \sum_{m=-\infty}^{\infty} \int_0^{\infty} \frac{d\omega}{e^{\beta\omega} + 1}[f(i\omega) - f(-i\omega)]. \qquad (6.1.7)$$

The difference $f(i\omega) - f(-i\omega)$ can be performed using the following identities [1, 60]:

$$I_m(e^{\pm i\pi/2} z) = e^{\pm \frac{1}{2} im\pi} J_m(z) \qquad (-\pi \leq \pm arg\, z \leq \frac{\pi}{2}),$$

$$K_m(e^{i\pi/2} z) = -\frac{i\pi}{2} e^{-\frac{1}{2} im\pi} H_m^{(2)}(z) \qquad (-\pi \leq arg\, z \leq \frac{\pi}{2}),$$

$$K_m(e^{-i\pi/2} z) = \frac{i\pi}{2} e^{\frac{1}{2} im\pi} H_m^{(1)}(z) \qquad (-\frac{\pi}{2} \leq arg\, z \leq \pi), \qquad (6.1.8)$$

which are valid for the ranges of the argument of z ($arg\, z$) given in the corresponding parentheses. where the inequalities in the parentheses give the validity domain of The phase of α after the transition $\omega \to \pm i\omega$ is essential for the correct recovery of the form of $f(\pm i\omega)$. Writing

$$\omega = \omega_{\Re e} + i\omega_{\Im m}, \qquad (6.1.9)$$

the change in the phase of α can be understood by looking at its square:

$$\alpha^2 = \left[(\omega_k^2 + \omega_{\Re e}^2 - \omega_{\Im m}^2) + 4\omega_{\Re e}^2 \omega_{\Im m}^2 \right]^{\frac{1}{2}} e^{i\varphi}, \qquad (6.1.10)$$

where

$$\varphi = \arctan \frac{2\omega_{\Re e}\omega_{\Im m}}{\omega_k^2 + \omega_{\Re e}^2 - \omega_{\Im m}^2}. \qquad (6.1.11)$$

Before the transformation, $\omega_{\Im m} = 0$ and the phase is 0. After the transformation, $\omega_{\Re e} = 0$, but the phase can be 0 or $\pm\varphi$. If $\omega_k > \omega$, the denominator in the arctan never vanishes, so the phase becomes positive or negative (following the sign of $\omega_{\Re e}\omega_{\Im m}$) and returns to 0 as $\omega_{\Re e} \to 0$. However, if $\omega_k < \omega$, the argument of the arctan becomes $\pm\infty$ (again, following the sign of $\omega_{\Re e}\omega_{\Im m}$), at which point $\varphi = \pm\frac{\pi}{2}$. As $\omega_{\Re e} \to 0$, φ continues departing from 0 to $\pm\pi$, as follows:

$$\alpha \xrightarrow[x \to \pm it]{} \begin{cases} \sqrt{\omega_k^2 - \omega^2} & \omega_k > \omega, \\ e^{\pm \frac{i\pi}{2}} q & \omega_k < \omega, \end{cases} \qquad (6.1.12)$$

where q is the familiar transverse momentum:

$$q = \sqrt{\omega^2 - \omega_k^2}. \qquad (6.1.13)$$

Equations (6.1.12) imply the following transformation properties:

$$I_m(\alpha\rho) K_m(\alpha\rho) \xrightarrow[x \to \pm it]{} \begin{cases} I_m(\rho\sqrt{\omega_k^2 - \omega^2}) K_m(\rho\sqrt{\omega_k^2 - \omega^2}) & \omega_k > \omega, \\ \mp\frac{i\pi}{2} J_m(q\rho)[J_m(q\rho) \pm iY_m(q\rho)] & \omega_k < \omega, \end{cases} \qquad (6.1.14)$$

where the definition (A.1.9) was used to replace the Hankel functions in Eqs. (6.1.8). If $\omega_k > \omega$, the product $I_m(\alpha\rho) K_m(\alpha\rho)$ stays real and its contribution to the t.e.v. of the energy density is null. Thus, the integrand in the integral over ω in Eq. (6.1.4)

is proportional to $\theta(\omega - \omega_k)$:

$$\langle : T_{\hat{\tau}\hat{\tau}} : \rangle_\beta = -\frac{1}{\pi^2} \int_{-\infty}^{\infty} dk \sum_{m=-\infty}^{\infty} \int_0^\infty \frac{\omega^2 \, d\omega}{e^{\beta\omega} + 1} \theta \left(\omega - \omega_k \right) J_m^+(q\rho), \qquad (6.1.15)$$

where $J_m^+(q\rho) = J_m^2(q\rho) + J_{m+1}^2(q\rho)$, as defined in Eq. (3.3.69). Changing the integration order reduces Eq. (6.1.15) to:

$$\langle : T_{\hat{\tau}\hat{\tau}} : \rangle_\beta = -\frac{1}{\pi^2} \sum_{m=-\infty}^{\infty} \int_\mu^\infty \frac{\omega^2 \, d\omega}{e^{\beta\omega} + 1} \int_0^p dk \, J_m^+(q\rho). \qquad (6.1.16)$$

Performing the sum over m using Eq. (A.4.2) reduces Eq. (6.1.16) to the familiar expression in Eq. (3.3.70), taking into account that $\langle : T_{\tau\hat{\tau}} : \rangle_\beta = - \langle : T_{\hat{t}\hat{t}} : \rangle_\beta$.

6.1.2   Quasi-Euclidean formulation of unbounded rotating thermal distributions

The coordinate transformation $\phi = \phi_{\text{Mink}} - \Omega t_{\text{Mink}}$ changes the phase in Eq. (6.1.1) from ω to $\omega + i\Omega(m + \frac{1}{2})$. To construct a co-rotating thermal state, the variable in the ω integral in Eq. (6.1.1) has to be changed such that the coefficient of $s_E(x, x')$ becomes $e^{i\omega\Delta t}$:

$$_\Omega S_E(x, x') = \int_{-\infty}^{\infty} d\omega \, e^{i\omega\Delta\tau} \chi_\Omega. \qquad (6.1.17)$$

The subscript Ω indicates that ω is replaced in all explicit and implicit ω dependent quantities by ω_Ω, defined as:

$$\omega_\Omega = \omega - i\Omega(m + \tfrac{1}{2}). \qquad (6.1.18)$$

The t.e.v. of the energy density can be obtained following the same steps as in subsection 6.1.1:

$$\langle : T_{\hat{\tau}\hat{\tau}} : \rangle_\beta = \frac{i}{\pi^3} \int_{-\infty}^{\infty} dk \sum_{m=-\infty}^{\infty} \int_0^\infty \frac{d\omega}{e^{2\pi\omega} + 1} [f_\Omega(i\omega) - f_\Omega(-i\omega)], \qquad (6.1.19)$$

where $f_\Omega(\omega)$ is defined as in Eq. (6.1.5) the subscript Ω indicates that ω has been replaced by ω_Ω:

$$f_\Omega(\omega) = \omega_\Omega^2 [I_m(\alpha_\Omega\rho)K_m(\alpha_\Omega\rho) + I_{m+1}(\alpha_\Omega\rho)K_{m+1}(\alpha_\Omega\rho)]. \qquad (6.1.20)$$

Applying the same reasoning as in obtaining Eq. (6.1.12), the following transformation properties for α_Ω can be deduced:

$$\alpha_\Omega(i\omega) = \begin{cases} \sqrt{\omega_k^2 - \widetilde{\omega}^2} & \omega_k > |\widetilde{\omega}|, \\ e^{\frac{i\pi}{2}}\sqrt{\widetilde{\omega}^2 - \omega_k^2} & \widetilde{\omega} > \omega_k, \\ e^{-\frac{i\pi}{2}}\sqrt{\widetilde{\omega}^2 - \omega_k^2} & \widetilde{\omega} < -\omega_k, \end{cases}$$

$$\alpha_\Omega(-i\omega) = \begin{cases} \sqrt{\omega_k^2 - \overline{\omega}^2} & \omega_k > |\overline{\omega}|, \\ e^{-\frac{i\pi}{2}}\sqrt{\overline{\omega}^2 - \omega_k^2} & \overline{\omega} > \omega_k, \\ e^{\frac{i\pi}{2}}\sqrt{\overline{\omega}^2 - \omega_k^2} & \overline{\omega} < -\omega_k, \end{cases} \quad , \qquad (6.1.21)$$

where

$$\widetilde{\omega} = \omega - \Omega(m + \tfrac{1}{2}), \qquad \overline{\omega} = \omega + \Omega(m + \tfrac{1}{2}). \qquad (6.1.22)$$

Using the transformation properties (6.1.8) together with Eqs. (6.1.21) gives:

$$\langle : T_{\hat\tau\hat\tau} : \rangle_\beta = -\frac{1}{\pi^2} \sum_{m=-\infty}^{\infty} \int_0^p dk \int_0^\infty \frac{\widetilde{\omega}^2\, d\omega}{e^{\beta\omega} + 1} J_m^+(\rho\sqrt{\widetilde{\omega}^2 - \omega_k^2})$$
$$\times [\theta(\widetilde{\omega} - \omega_k) - \theta(-\widetilde{\omega} - \omega_k)], \quad (6.1.23)$$

where the transformation $m \to -m - 1$ has been performed for the terms involving $\overline{\omega}$, changing $\overline{\omega}$ to $\widetilde{\omega}$. Changing variable from ω to $E = \omega - \Omega(m + \tfrac{1}{2})$ and converting the sum over m so it runs only over positive values yields:

$$\langle : T_{\hat\tau\hat\tau} : \rangle_\beta = -\frac{1}{\pi^2} \sum_{m=-\infty}^{\infty} \int_\mu^\infty dE\, E^2 \left(\frac{1}{e^{\beta\overline{\omega}} + 1} + \frac{\operatorname{sgn}\widetilde{E}}{e^{\beta|\widetilde{E}|} + 1} \right) \int_0^p dk\, J_m^+(q\rho). \quad (6.1.24)$$

A comparison with Eq. (4.3.56c) shows that the t.e.v. of the energy density thus obtained is expressed with respect to the rotating vacuum. It is remarkable that the quasi-Euclidean procedure correctly selects the rotating vacuum in detriment of the Minkowski vacuum.

6.1.3 Quasi-Euclidean formulation of bounded rotating thermal distributions

When a boundary is present, a homogeneous solution of the Dirac equation must be added to the Euclidean Green's function Eq. (6.1.17) for the rotating space-time. Equations (5.2.36) and (5.3.70) give these extra solutions for the spectral and MIT bag models, respectively, but with respect to Minkowski coordinates. As in subsection 6.1.2, these functions can be expressed in the rotating system by changing ω to ω_Ω (6.1.18) in all quantities, except for the phase. For simplicity, only the spectral case is discussed in this subsection.

The t.e.v. of the energy density can be written for the spectral case as:

$$\langle : T_{\hat{\tau}\hat{\tau}} : \rangle_\beta = \frac{2i}{\pi^3} \int_{-\infty}^{\infty} dk \sum_{m=0}^{\infty} \int_0^{\infty} \frac{d\omega}{e^{2\pi\omega} + 1} [f_{\Omega,R}(i\omega) - f_{\Omega,R}(-i\omega)], \qquad (6.1.25)$$

where

$$f_{\Omega,R}(\omega) = \omega_\Omega^2 [I_m(\alpha_\Omega \rho) K_m(\alpha_\Omega \rho) + I_{m+1}(\alpha_\Omega \rho) K_{m+1}(\alpha_\Omega \rho) + f_{\Omega,R}^{\text{spec}}(\omega)]. \qquad (6.1.26)$$

The boundary term $f_{\Omega,R}^{\text{spec}}(\omega)$ is given by:

$$f_{\Omega,R}^{\text{spec}}(\omega) = \frac{K_m(\alpha_\Omega R)}{I_m(\alpha_\Omega R)} I_m^-(\alpha_\Omega \rho). \qquad (6.1.27)$$

After applying the generalised Abel-Plana sum formula (5.2.45), ω is sent to $\pm i\omega$. Let us consider for definiteness the case $\omega \to i\omega$. Three cases emerge: α_Ω stays real or it becomes $e^{\pm \frac{i\pi}{2}} \sqrt{\tilde{\omega}^2 - \omega_k^2}$ ($\tilde{\omega}^2$ is replaced by $\overline{\omega}^2$ if $\omega \to -i\omega$). The terms where α stays real cancel through the subtraction $f(i\omega) - f(-i\omega)$, hence they do not need to be discussed further. In the other two cases, the following transformation occur:

$$\frac{K_m(\alpha R)}{I_m(\alpha R)} I_m^-(\alpha \rho) \to \begin{cases} -\frac{1}{2}\pi i \frac{H_m^{(2)}(q_\sim R)}{J_m(q_\sim R)} J_m^+(q_\sim \rho) & \alpha \to e^{\frac{i\pi}{2}}\alpha, \\ \frac{1}{2}\pi i \frac{H_m^{(1)}(q_\sim R)}{J_m(q_\sim R)} J_m^+(q_\sim \rho) & \alpha \to e^{-\frac{i\pi}{2}}\alpha, \end{cases} \qquad (6.1.28)$$

where

$$q_\sim = \sqrt{\tilde{\omega}^2 - \omega_k^2}. \qquad (6.1.29)$$

In the Abel-Plana summation formula, the two pieces in Eq. (6.1.28) are subtracted. Using the definition (A.1.9) of the Hankel functions, the following result is obtained:

$$\frac{K_m(e^{\frac{i\pi}{2}} q_\sim R)}{I_m(e^{\frac{i\pi}{2}} q_\sim R)} I_m^-(e^{\frac{i\pi}{2}} q_\sim \rho) - \frac{K_m(e^{-\frac{i\pi}{2}} q_\sim R)}{I_m(e^{-\frac{i\pi}{2}} q_\sim R)} I_m^-(e^{-\frac{i\pi}{2}} q_\sim \rho) = -i\pi J_m^+(q_\sim \rho). \qquad (6.1.30)$$

This expression is equal in magnitude but opposite in sign to the equivalent expressions coming from the unbounded terms, thus cancelling their contributions.

However, since the boundary-induced terms have poles on the imaginary axes, the residue terms in the Abel-Plana formula must also be computed, starting from:

$$\text{Res}\left[\frac{1}{I_m(z)}\right]_{z \to i\xi} = \lim_{z \to i\xi} \frac{z - i\xi}{I_m(i\xi + z - i\xi)} = \lim_{\varepsilon \to 0} \frac{i\varepsilon}{I_m[e^{\frac{i\pi}{2}}(\xi + \varepsilon)]} = \frac{ie^{-\frac{i}{2}m\pi}}{J_m'(\xi)} = \frac{-ie^{-\frac{i}{2}m\pi}}{J_{m+1}(\xi)},$$

$$\text{Res}\left[\frac{1}{I_m(z)}\right]_{z \to -i\xi} = \lim_{z \to -i\xi} \frac{z + i\xi}{I_m(-i\xi + z + i\xi)} = \lim_{\varepsilon \to 0} \frac{-i\varepsilon}{I_m[e^{-\frac{i\pi}{2}}(\xi + \varepsilon)]} = \frac{-ie^{\frac{i}{2}m\pi}}{J_{m+1}(\xi)}, \qquad (6.1.31)$$

where $\xi \equiv \xi_{m\ell}$ is the ℓ'th root of $J_m(z)$. Thus, the residues of the boundary term

can be calculated as follows:

$$\text{Res}\left\{\frac{K_m(\alpha R)}{I_m(\alpha R)}I_m^-(\alpha\rho)\right\}_{\alpha R=i\xi_{m,l}} = -\frac{\pi}{2}\frac{H_m^{(2)}(\xi_{m\ell})}{J_{m+1}(\xi_{m\ell})}J_m^+(\xi_{m\ell}\bar{\rho}),$$

$$\text{Res}\left\{\frac{K_m(\alpha R)}{I_m(\alpha R)}I_m^-(\alpha\rho)\right\}_{\alpha R=-i\xi_{m,l}} = -\frac{\pi}{2}\frac{H_m^{(1)}(\xi_{m\ell})}{J_{m+1}(\xi_{m\ell})}J_m^+(\xi_{m\ell}\bar{\rho}), \tag{6.1.32}$$

where $\bar{\rho} = \frac{\rho}{R}$. It should be noted there are no contributions coming from the case when α stays real. The Hankel functions in Eqs. (6.1.32) can be written in terms of $J_{m+1}(\xi_{m\ell})$ using the Wronskian relation (A.1.3):

$$H_m^{(1)}(\xi_{m\ell}) = -H_m^{(2)}(\xi_{m\ell}) = iY_m(\xi_{m\ell}) = \frac{2i}{\pi\xi_{m\ell}J_{m+1}(\xi_{m\ell})}, \tag{6.1.33}$$

Since the residues need to be computed with respect to the variable $x = \frac{\beta\omega}{2\pi} \geq 0$, the results in Eqs. (6.1.32) need to be multiplied by the factor:

$$\frac{\partial x}{\partial(\alpha R)} = \frac{\beta}{2\pi R^2\omega}\alpha R. \tag{6.1.34}$$

The value of ω corresponding to a given root $\xi_{m\ell}$ depends on the relative sign of ω and $m+\frac{1}{2}$ after the rotation of ω to $\pm i\omega$. for positive or negative signs, ω is replaced by $\widetilde{\omega}_{m\ell}$ or $\omega = \bar{\omega}_{m\ell}$, subject to the constraints $\widetilde{\omega}_{m\ell} > 0$ or $\bar{\omega}_{m\ell} > 0$, respectively. Here, $\omega_{m\ell}$ has the usual meaning introduced in chapter 5:

$$\omega_{m\ell} = \sqrt{\mu^2 + k^2 + q_{m\ell}^2}, \qquad q_{m\ell} = \frac{\xi_{m\ell}}{R}. \tag{6.1.35}$$

Explicitly, the residues of the generalised Abel-Plana formula (5.2.45) have the following form:

$$\text{Res}_{\text{Im}\omega>0}f_{\Omega,R}^{\text{spec}}(\omega)(1 - i\tan\tfrac{\omega}{2}) = -\frac{i\beta}{\pi\omega_{m\ell}R^2}\frac{J_m^+(q\rho)}{J_{m+1}^2(\xi_{m\ell})}\left[\frac{\theta(\widetilde{\omega}_{m\ell})}{1+e^{\beta\widetilde{\omega}_{m\ell}}} - \frac{\theta(-\widetilde{\omega}_{m\ell})}{1+e^{-\beta\widetilde{\omega}_{m\ell}}}\right], \tag{6.1.36a}$$

$$\text{Res}_{\text{Im}\omega<0}f_{\Omega,R}^{\text{spec}}(\omega)(-1 - i\tan\tfrac{\omega}{2}) = -\frac{i\beta}{\pi\omega_{m\ell}R^2}\frac{J_m^+(q\rho)}{J_{m+1}^2(\xi_{m\ell})}\left[\frac{\theta(\bar{\omega}_{m\ell})}{1+e^{\beta\bar{\omega}_{m\ell}}} - \frac{\theta(-\bar{\omega}_{m\ell})}{1+e^{-\beta\bar{\omega}_{m\ell}}}\right]. \tag{6.1.36b}$$

Adding up all the residues gives the final expression for the energy density:

$$\langle : T_{\hat{\tau}\hat{\tau}} : \rangle_\beta = -\frac{2}{\pi^2 R^2}\sum_{m=0}^{\infty}\sum_{\ell=1}^{\infty}\frac{J_m^+(q_{m\ell}\rho)}{J_{m+1}^2(\xi_{m\ell})}\int_0^{\infty}dk\,\omega_{m\ell}\left[\frac{1}{e^{\beta\bar{\omega}}+1} + \frac{\text{sgn}\widetilde{\omega}_{m\ell}}{e^{\beta|\widetilde{\omega}|}+1}\right]. \tag{6.1.37}$$

The quasi-Euclidean approach has again naturally selected the Iyer vacuum, as can be seen by comparing to Eq. (5.2.20a), obtained using a mode sum.

6.2   Analysis of bounded thermal states near the speed of light surface

The preceding section was used to establish that the quasi-Euclidean approach produces correct results in the systems studied so far. Next, an analysis is performed of the behaviour of the t.e.v. of the energy density for a bounded rotating system with the boundary outside the speed of light surface (SOL) as the latter is approached, using the advantage of having t.e.v.'s expressed as sums over an integer variable n rather than over roots of some equation involving Bessel functions. To preserve this aspect of the Euclidean approach, it is clear the vacuum contribution cannot be subtracted from the corresponding thermal expectation value, as this will reduce any expression to the corresponding one obtained using mode sums. Therefore, we anticipate that the singularity structure of the vacuum for the bounded system is the same as that for its unbounded counterpart and construct the difference between the t.e.v.s in the rotating bounded and unbounded systems:

$$(\Delta T_{\hat{\tau}\hat{\tau}})_\beta = \langle T_{\hat{\tau}\hat{\tau}} \rangle_{\beta,R,\Omega} - \langle T_{\hat{\tau}\hat{\tau}} \rangle_{\beta,\infty,\Omega} = \frac{2}{\beta\pi^2} \sum_{m=0}^{\infty} \sum_{n=0}^{\infty} \int_0^{\infty} dk\, f_{\Omega,R}^{\mathrm{spec}}(\omega_n). \qquad (6.2.1)$$

Since the divergent behaviour is induced by large values of m, n and k, the field quanta can be approximated as massless. Also, for simplicity, only the spectral case is considered in this section, in which case Eq. (6.2.1) takes the form:

$$(\Delta T_{\hat{\tau}\hat{\tau}})_\beta = -\frac{2}{\beta\pi^2} \sum_{m=0}^{\infty} \sum_{n=0}^{\infty} \mathrm{Re}[\omega_{n,\Omega}^2 \mathcal{K}_{mn}], \qquad (6.2.2)$$

where

$$\mathcal{K}_{mn} = \int_0^{\infty} dk \frac{K_m(\alpha_\Omega R)}{I_m(\alpha_\Omega R)} I_m^-(\alpha_\Omega \rho), \qquad (6.2.3)$$

where $\omega_n = \frac{2\pi}{\beta}(n+\frac{1}{2})$. To analyse the behaviour of $\mathcal{K}_{mn}$, the approximations (A.2.5) for the ratio K_m/I_m and (5.2.52d) for $I_m^-(\alpha_\Omega \rho)$ are used.

First, the integral over k can be approximated using the method of steepest descent [51], by introducing the following notation:

$$\mathcal{K}_{mn} \sim \int_0^{\infty} dk\, e^{-\eta(k)} f(k), \qquad (6.2.4a)$$

where

$$f(k) = \frac{R}{\nu\rho[1 + z(R)]z(\rho)}, \qquad (6.2.4b)$$

$$\eta(k) = 2\nu \left[z(R) - z(\rho) + \ln\frac{R}{\rho} - \ln\frac{1 + z(R)}{1 + z(\rho)} \right], \qquad (6.2.4c)$$

and

$$z(\rho) = \sqrt{1 + \left(\frac{\alpha\rho}{\nu}\right)^2}, \qquad \nu = m + \tfrac{1}{2}. \tag{6.2.4d}$$

The first two derivatives of $\eta(k)$ with respect to k can be computed:

$$\eta'(k) = \frac{2k}{m}\left[\frac{R^2}{1+z(R)} - \frac{\rho^2}{1+z(\rho)}\right], \tag{6.2.5}$$

$$\eta''(k) = \frac{2}{m}\left\{\frac{R^2}{1+z(R)} - \frac{\rho^2}{1+z(\rho)} - \frac{k^2}{m^2}\left[\frac{R^4}{z(R)(1+z(R))^2} - \frac{\rho^4}{z(\rho)(1+z(\rho))^2}\right]\right\}. \tag{6.2.6}$$

Given that the first derivative $\eta'(k)$ vanishes when $k = 0$, the integral $\mathcal{K}_{mn}$ can be approximated as [51]:

$$\mathcal{K}_{mn} \sim e^{-\eta(0)} \int_0^\infty dk\, e^{-\frac{1}{2}\eta''(0)k^2}[f(0) + \tfrac{1}{2}f''(0)k^2 + \dots]$$

$$\sim e^{-\eta(0)}\sqrt{\frac{\pi}{2\eta''(0)}}\left[f(0) + \frac{1}{2\eta''(0)}f''(0) + \dots\right]. \tag{6.2.7}$$

As can be seen in Figure 6.1, this first order approximation captures reasonably well the essential features of $\mathcal{K}_{mn}$, therefore, the higher order terms can be omitted from the asymptotic result.
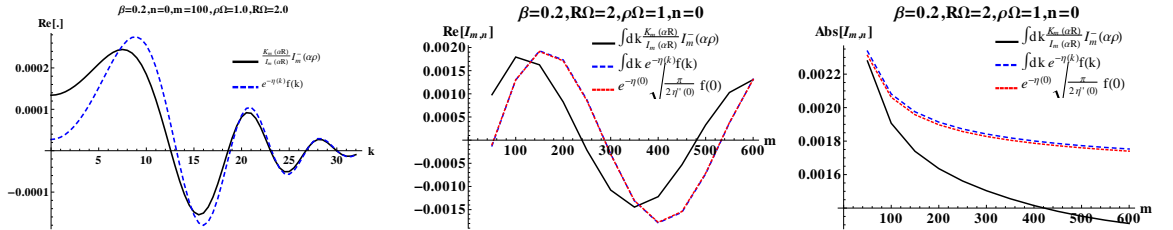
Figure 6.1: The plot on the left compares the real part of the integrand in $\mathcal{K}_{mn}$ in Eq. (6.2.4) to the exact integrand in (6.2.3). On the plot in the middle (right), the real part (absolute value) of the numerical value of $\mathcal{K}_{mn}$ is compared (as a function of m) to the numerical value of the asymptotic form of $\mathcal{K}_{mn}$ represented in the plot on the left (sparser dashed curve) and the asymptotic result (6.2.7) (denser dashed curve).

Next, we anticipate that the contributions made by high values of m will become increasingly important as the SOL is approached, as can be seen in Figure 4.2. The

pieces needed for an expansion of $\eta(0)$ in inverse powers of ν are:

$$
z(\rho) = \left[\delta^2 - \frac{2i\omega}{\nu\Omega}(1 - \delta^2) + \frac{\omega^2}{\nu^2\Omega^2}(1 - \delta^2)\right]^{\frac{1}{2}}
$$
$$
= \delta - \frac{i\omega}{\nu\Omega}\frac{1-\delta^2}{\delta} + \dots , \tag{6.2.8a}
$$

$$
z(R) = \left[-\Delta^2 - \frac{2i\omega}{\nu\Omega}(\Delta^2 + 1) + \frac{\omega^2}{\nu^2\Omega^2}(\Delta^2 + 1)\right]^{\frac{1}{2}}
$$
$$
= i\Delta - \frac{\omega}{\nu\Delta}\frac{\Delta^2 + 1}{\Delta} + \dots , \tag{6.2.8b}
$$

$$
\ln[1 + z(\rho)] = \ln(1 + \delta) - i\frac{\omega}{\nu\Omega}\frac{1-\delta}{\delta} + \dots , \tag{6.2.8c}
$$

$$
\ln[1 + z(R)] = \ln(1 + i\Delta) - \frac{\omega}{\nu\Omega}\frac{1 - i\Delta}{\Delta} + \dots , \tag{6.2.8d}
$$

$$
\eta(k = 0) = 2\nu\left[\operatorname{arctanh}\delta - \delta + i(\Delta - \arctan\Delta)\right] - \frac{2\omega}{\Omega}(\Delta - i\delta) + \dots , \tag{6.2.8e}
$$

where δ, and Δ are defined as:

$$
\delta = \sqrt{1 - \rho^2\Omega^2}, \qquad \Delta = \sqrt{R^2\Omega^2 - 1}, \qquad \hat{\omega} = \frac{\omega}{\Omega} + \frac{i}{2}. \tag{6.2.9}
$$

To illustrate the divergent behaviour of the t.e.v. of the energy density as the SOL is approached, δ is regarded as tending to 0. To approximate the term $z(\rho)$ in the denominator of $f(0)$, it is convenient write it as:

$$
z(\rho) = \sqrt{\delta^2 - \left(\frac{2i\omega}{\nu\Omega} - \frac{\omega^2}{\nu^2\Omega^2}\right)(1 - \delta^2)}
$$
$$
\sim \frac{2\omega}{\nu\Omega}e^{-\frac{i\pi}{4}} + \dots . \tag{6.2.10}
$$

Hence, the factor multiplying the exponential in Eq. (6.2.7) can be approximated using:

$$
\sqrt{\frac{\pi}{2\eta''(0)}} \sim \frac{\sqrt{\nu\pi\Omega^2}}{2(\delta^2 + \Delta^2)^{\frac{1}{4}}}e^{\frac{i\pi}{4} - \frac{i}{2}\arctan\frac{\delta}{\Delta}}(1 + \dots),
$$
$$
f(0) \sim \frac{R\Omega}{1 + i\Delta}\sqrt{\frac{\Omega}{2\omega\nu}}e^{\frac{i\pi}{4}},
$$
$$
f(0)\sqrt{\frac{\pi}{2\eta''(0)}} \sim \frac{i + \Delta}{2R}\sqrt{\pi\Omega}2\omega\Delta + \dots . \tag{6.2.11a}
$$

Putting everything together gives:

$$
(\Delta T_{\hat{\tau}\hat{\tau}})_\beta = -\frac{2}{\beta\pi^2}\sum_{m=0}^{\infty}\sum_{n=0}^{\infty}\operatorname{Re}\left\{\omega_{n,\Omega}^2\frac{i + \Delta}{2R}\sqrt{\frac{\pi\Omega}{2\omega_n\Delta}}\right.
$$
$$
\left.\times e^{-2\nu[\operatorname{arctanh}\delta - \delta + i(\Delta - \arctan\Delta)]}e^{-\frac{2\omega_n}{\Omega}(\Delta - i\delta)}\right\}. \tag{6.2.12}
$$

The sums over n and m can be approximated with integrals by applying the generalised Abel-Plana sum formla (5.2.45). Each power of ν pulls down a factor of

$$\frac{1}{2[(\operatorname{arctanh}\delta - \delta) + i(\Delta - \arctan\Delta)]} = \frac{e^{-\frac{i\pi}{2}+i\arctan\frac{\operatorname{arctanh}\delta-\delta}{\Delta-\arctan\Delta}}}{2[(\operatorname{arctanh}\delta - \delta)^2 + (\Delta - \arctan\Delta)^2]^{\frac{1}{2}}},$$

(6.2.13)

while each power of ω_n brings out the following factor:

$$\frac{\Omega}{2(\Delta - i\delta)} = \frac{\Omega e^{i\arctan\frac{\delta}{\Delta}}}{2(\Delta^2 + \delta^2)^{\frac{1}{2}}}.$$

(6.2.14)

Neither of these factors diverges when $\delta \to 0$ if $\Delta > 0$, indicating that the difference in energy density in the bounded and unbounded cases is finite even on the SOL, when the boundary is outside the SOL. In other words, the t.e.v. of the energy density diverges in the bounded case just like in the unbounded case.

However, if the bounding surface approaches the SOL ($\Delta \to 0$), it seems that $(\Delta T_{\hat{\tau}\hat{\tau}})_\beta$ diverges as $\delta \to 0$. The order of divergence is difficult to estimate from the above results, but a power count indicates that it is predicted to be higher than in the analytic expression (4.3.54c). It is possible to conduct similar analyses by setting $\delta = 0$ and taking $\Delta \to 0$, or $\Delta = 0$ and taking $\delta \to 0$. The conclusion is the same: the difference between the t.e.v. of the SET on the SOL in the bounded and unbounded spaces diverges when the bounding surface is on the SOL.

6.3 Summary

The quasi-Euclidean approach was introduced in this chapter. In section 6.1 it is shown that the quasi-Euclidean formulation leads to the same expressions as the Lorentzian formulation for thermal expectation values in Minkowski space, in rotating Minkowski space and in rotating Minkowski space inside a boundary. The true strength of the quasi-Euclidean approach is in investigating the difference between thermal expectation values in the bounded and unbounded spaces. Our analysis shows that if the boundary is placed outside the speed of light surface (SOL), the difference between the energy densities in the bounded and unbounded systems is finite on the SOL, implying that the energy density diverges in the bounded case as the SOL is approached just like in the unbounded case. Setting the boundary on the SOL shows that the same difference now diverges as an inverse power of the distance to the SOL. Although the analysis in its current form is not accurate enough to predict the exact order of the divergence, we expect that a further refinement of the approximations employed would be sufficient to obtain a more accurate result.

Chapter 7. Anti-de Sitter space-time

Anti-de Sitter space-time (adS) is maximally symmetric, allowing for elegant analytic investigations to be performed. It is remarkable that renormalisation can be performed analytically and that simple expressions can be obtained for the thermal expectation values (t.e.v.s) of the fermion condensate (FC), charge current (CC) and stress-energy tensor (SET).

Section 7.1 introduces the features of adS and the tools of geodesic theory necessary for the discussion of the quantum field theory of fermions. The mode solutions of the Dirac equation are presented in section 7.2 and two-point functions are obtained in section 7.3. Renormalisation is performed in section 7.4 and section 7.5 concludes this chapter with a discussion of thermal states.

7.1 Geometric structure

In this section, the intrinsic geometry of adS is discussed. In subsection 7.1.1, the metric, connection coefficients and Riemann tensor are presented. The geodesics of adS are discussed in subsection 7.1.2, where geodesic theory techniques are applied to introduce the bi-vector and bi-spinor of parallel transport, for which analytic expressions are given in subsections 7.1.3 and 7.1.4, respectively. Finally, subsection 7.1.6 is dedicated to the construction of the quantum operators corresponding to the isometries of adS.

7.1.1 Metric, tetrad and connection

The adS manifold can be considered as a 4-surface embeded in a 5-dimensional flat space with metric $\eta_{ab} = \mathrm{diag}(-1, 1, 1, 1, -1)$ ($a, b, c, \cdots \in \{0, 1, 2, 3, 5\}$ are coordinate indices in the embedding space). The equation of the adS 4-surface is then:

$$\eta_{ab} z^a z^b = -\frac{1}{\omega^2}, \tag{7.1.1}$$

where $\omega = R^{-1}$ is the inverse radius of curvature of adS. Equation (7.1.1) can be satisfied automatically by introducing the adS coordinates $\{t, x^i\}$ such that:

$$z^0 = \frac{1}{\omega} \frac{\cos \omega t}{\cos \omega r}, \qquad z^5 = \frac{1}{\omega} \frac{\sin \omega t}{\cos \omega r}, \qquad z^i = \frac{\tan \omega r}{\omega r} x^i, \tag{7.1.2}$$
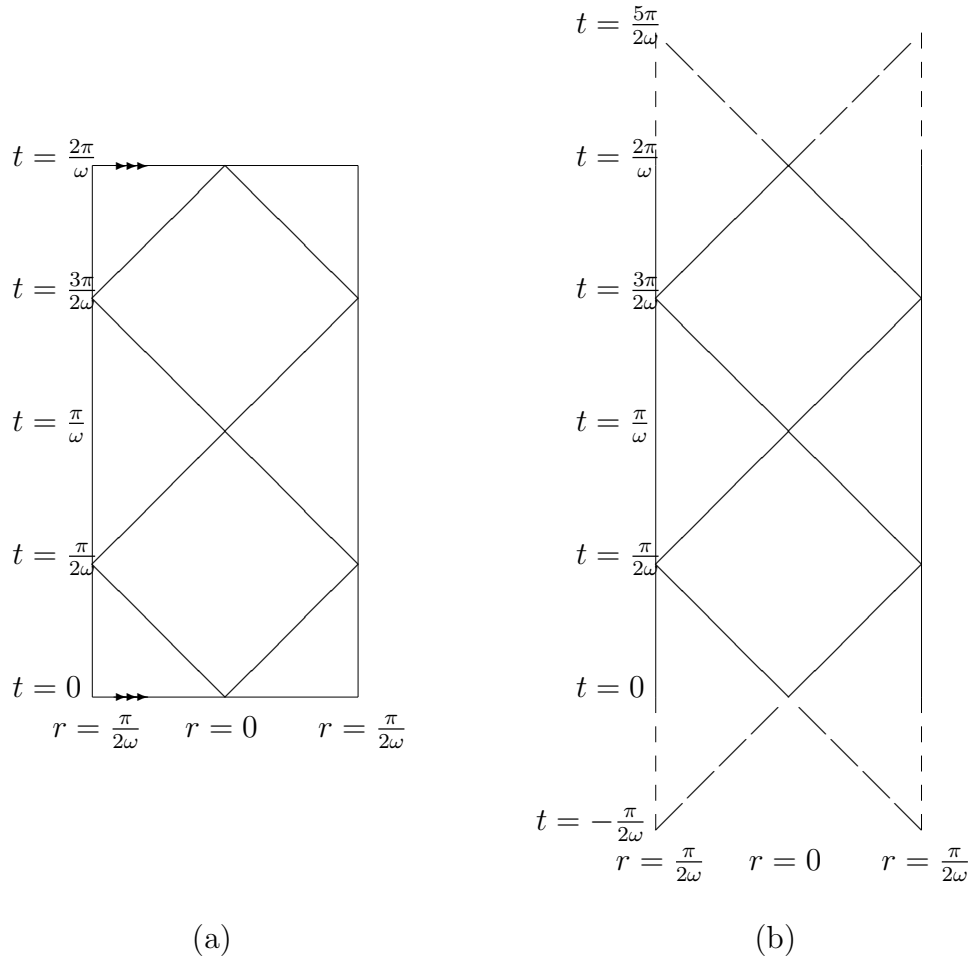
Figure 7.1: Penrose diagram of (a) anti-de Sitter space (adS) and (b) the universal covering group of adS (CadS). On adS, the horizontal lines corresponding to $t = 0$ and $t = \frac{2\pi}{\omega}$ are identified, thereby giving a periodicity in the time coordinate, while in CadS, no such identifications are made. The angular coordinates are suppressed. Null trajectories passing through the origin $r = 0$ at $t = 0$ reach spatial infinity $(r = \frac{\pi}{2\omega})$ at $t = \frac{\pi}{2\omega}$, from where the origin can be reached at $t = \frac{\pi}{\omega}$. As can be seen from the diagram, the coordinate system in Eq. (7.1.4) covers CadS entirely.

where $i \in \{1, 2, 3\}$ is the spatial index and $x^i = \{x, y, z\}$ and $\{r, \theta, \varphi\}$ are related through the standard definition of spherical coordinates:

$$x = r \sin\theta \cos\varphi, \quad y = r \sin\theta \sin\varphi, \quad z = r \cos\theta. \tag{7.1.3}$$

The radial coordinate r varies between 0 at the (arbitrary) origin and $\frac{\pi}{2\omega}$ on the boundary. The metric $ds^2 = \eta_{ab} dz^a dz^b$ on adS is:

$$ds^2 = \frac{1}{\cos^2\omega r}\left[-dt^2 + dr^2 + \frac{\sin^2\omega r}{\omega^2}(d\theta^2 + \sin^2\theta \, d\varphi^2)\right]. \tag{7.1.4}$$

In what follows, the domain of t is extended from $[0, \frac{2\pi}{\omega})$ to $(-\infty, \infty)$, in which case the space-time is referred to as the covering space of adS. The Lagrangian method [55] can be applied to the Lagrangian function $L = \frac{1}{2}g_{\mu\nu}\dot{x}^\mu \dot{x}^\nu$ corresponding to the metric (7.1.4) to determine the following non-zero Christoffel symbols:

$$\Gamma^t{}_{tr} = \Gamma^r{}_{tt} = \Gamma^r{}_{rr} = \omega \tan\omega r,$$

$$\Gamma^r{}_{\theta\theta} = -\frac{1}{\omega}\tan\omega r, \qquad \Gamma^r{}_{\varphi\varphi} = -\frac{1}{\omega}\tan\omega r \sin^2\theta,$$

$$\Gamma^\theta{}_{r\theta} = \frac{\omega}{\sin\omega r \cos\omega r}, \qquad \Gamma^\theta{}_{\varphi\varphi} = -\sin\theta \cos\theta,$$

$$\Gamma^\varphi{}_{r\varphi} = \frac{\omega}{\sin\omega r \cos\omega r}, \qquad \Gamma^\varphi{}_{\theta\varphi} = \cot\theta. \tag{7.1.5}$$

Alternatively, the adS metric (7.1.4) can be expressed with respect to the Cartesian coordinates (7.1.3):

$$g_{tt} = -\frac{1}{\cos^2\omega r}, \quad g_{ti} = 0, \quad g_{ij} = \frac{1}{\cos^2\omega r}\left[\frac{\sin^2\omega r}{\omega^2 r^2}\left(\delta_{ij} - \frac{x^i x^j}{r^2}\right) + \frac{x^i x^j}{r^2}\right], \tag{7.1.6a}$$

$$g^{tt} = -\cos^2\omega r, \quad g^{ti} = 0, \quad g^{ij} = \cos^2\omega r\left[\frac{\omega^2 r^2}{\sin^2\omega r}\left(\delta_{ij} - \frac{x^i x^j}{r^2}\right) + \frac{x^i x^j}{r^2}\right]. \tag{7.1.6b}$$

The corresponding Cartesian gauge tetrad [26] is given by:

$$e_{\hat{t}} = \cos\omega r \, \partial_t, \qquad e_{\hat{i}} = \cos\omega r\left[\frac{\omega r}{\sin\omega r}\left(\delta_{ij} - \frac{x^i x^j}{r^2}\right) + \frac{x^i x^j}{r^2}\right]\partial_j, \tag{7.1.7a}$$

$$\omega^{\hat{t}} = \frac{dt}{\cos\omega r}, \qquad \omega^{\hat{i}} = \frac{1}{\cos\omega r}\left[\frac{\sin\omega r}{\omega r}\left(\delta_{ij} - \frac{x^i x^j}{r^2}\right) + \frac{x^i x^j}{r^2}\right]dx^j. \tag{7.1.7b}$$

The connection coefficients with respect to this tetrad can be computed using the Cartan method [55], by looking at the exterior derivative of the dual basis $\omega^{\hat{\alpha}}$:

$$d\omega^{\hat{t}} = \omega \sin\omega r \frac{x^i}{r}\omega^{\hat{i}} \wedge \omega^{\hat{t}}, \qquad d\omega^{\hat{i}} = \frac{\omega(1 - \cos\omega r)}{\sin\omega r}\frac{x^k}{r}\omega^{\hat{k}} \wedge \omega^{\hat{i}}. \tag{7.1.8}$$

The following equation:

$$d\omega^{\hat{\alpha}} + \omega^{\hat{\alpha}}{}_{\hat{\beta}} \wedge \omega^{\hat{\beta}} = 0 \tag{7.1.9}$$

can be used to evaluate the connection 1-forms $\omega^{\hat{\alpha}}{}_{\hat{\beta}} = \Gamma^{\hat{\alpha}}{}_{\hat{\beta}\hat{\gamma}}\omega^{\hat{\gamma}}$:

$$\omega^{\hat{t}}{}_{\hat{i}} = \omega \sin \omega r \frac{x^i}{r}\omega^{\hat{t}}, \qquad \omega^{\hat{i}}{}_{\hat{j}} = \frac{\omega(1 - \cos \omega r)}{r \sin \omega r}\left(x^j\omega^{\hat{i}} - x^i\omega^{\hat{j}}\right). \qquad (7.1.10)$$

The connection coefficients can be read from the definition of the connection 1-forms:

$$\Gamma^{\hat{t}}{}_{\hat{i}\hat{t}} = \omega \sin \omega r \frac{x^i}{r}, \qquad \Gamma^{\hat{i}}{}_{\hat{j}\hat{k}} = \frac{\omega(1 - \cos \omega r)}{r \sin \omega r}\left(x^j\delta_{ik} - x^i\delta_{jk}\right). \qquad (7.1.11)$$

For completeness, the Cartan coefficients (2.2.19) are given below:

$$c_{\hat{t}\hat{i}}{}^{\hat{t}} = \omega \sin \omega r \frac{x^i}{r}, \qquad c_{\hat{i}\hat{j}}{}^{\hat{k}} = \frac{\omega(1 - \cos \omega r)}{r \sin \omega r}\left(x^j\delta_{ki} - x^i\delta_{kj}\right), \qquad (7.1.12)$$

which are consistent with the connection coefficients listed in Eq. (7.1.11). The spin connection coefficients can be calculated using Eqs. (7.1.11) in Eq. (2.2.17):

$$\Gamma_{\hat{t}} = \frac{\omega \sin \omega r}{2r}\gamma^{\hat{t}}\left(\boldsymbol{x} \cdot \boldsymbol{\gamma}\right), \qquad \Gamma_{\hat{k}} = -\frac{\omega(1 - \cos \omega r)}{2r \sin \omega r}\left[x^k + \gamma^k\left(\boldsymbol{x} \cdot \boldsymbol{\gamma}\right)\right],$$

$$\not{\Gamma} = \frac{\omega}{r \sin \omega r}\left(1 - \cos \omega r + \frac{\sin^2 \omega r}{2}\right)\left(\boldsymbol{x} \cdot \boldsymbol{\gamma}\right). \qquad (7.1.13)$$

We end this section with a calculation of the curvature two-forms and Riemann tensor, using:

$$\mathcal{R}^{\hat{\alpha}}{}_{\hat{\beta}} = d\omega^{\hat{\alpha}}{}_{\hat{\beta}} + \omega^{\hat{\alpha}}{}_{\hat{\gamma}}\omega^{\hat{\gamma}}{}_{\hat{\beta}}, \qquad \mathcal{R}^{\hat{\alpha}}{}_{\hat{\beta}} = \frac{1}{2}R^{\hat{\alpha}}{}_{\hat{\beta}\hat{\gamma}\hat{\delta}}\omega^{\hat{\gamma}} \wedge \omega^{\hat{\delta}}. \qquad (7.1.14)$$

The exterior derivatives of the connection 1-forms can be expressed as:

$$d\omega^{\hat{t}}{}_{\hat{i}} = \omega^2\left[\cos \omega r \delta_{ik} + (1 - \cos \omega r)\frac{x^i x^k}{r^2}\right]\omega^{\hat{k}} \wedge \omega^{\hat{t}}, \qquad (7.1.15a)$$

$$d\omega^{\hat{i}}{}_{\hat{j}} = \frac{\omega^2(1 - \cos \omega r)}{\sin^2 \omega r}\left[-2\cos \omega r \delta_{ik}\delta_{jl} + (1 - \cos \omega r)\frac{x^k}{r^2}(x^j\delta_{il} - x^i\delta_{jl})\right]\omega^{\hat{k}} \wedge \omega^{\hat{l}}, \qquad (7.1.15b)$$

from which the components of the curvature two-forms, Riemann tensor, Ricci tensor, Ricci scalar and Einstein tensor can be calculated:

$$\mathcal{R}^{\hat{\alpha}\hat{\beta}} = -\omega^2\omega^{\hat{\alpha}} \wedge \omega^{\hat{\beta}}, \qquad (7.1.16a)$$

$$R_{\hat{\alpha}\hat{\beta}\hat{\gamma}\hat{\delta}} = -\omega^2(\eta_{\hat{\alpha}\hat{\gamma}}\eta_{\hat{\beta}\hat{\delta}} - \eta_{\hat{\alpha}\hat{\delta}}\eta_{\hat{\beta}\hat{\gamma}}), \qquad (7.1.16b)$$

$$R_{\hat{\alpha}\hat{\beta}} = -3\omega^2\eta_{\hat{\alpha}\hat{\beta}}, \qquad R = -12\omega^2, \qquad G_{\hat{\alpha}\hat{\beta}} = 3\omega^2\eta_{\hat{\alpha}\hat{\beta}}. \qquad (7.1.16c)$$

The Riemann tensor (7.1.16b) assumes the standard form for a maximally symmetric space-time [3].

For completeness, the tetrad 1-forms and connection coefficients for the adS

metric written in spherical coordinates are listed below:

$$\omega^{\hat{t}} = \frac{dt}{\cos \omega r}, \quad \omega^{\hat{r}} = \frac{dr}{\cos \omega r}, \quad \omega^{\hat{\theta}} = \frac{1}{\omega} \tan \omega r d\theta, \quad \omega^{\hat{\varphi}} = \frac{1}{\omega} \tan \omega r \sin \theta d\varphi,$$

$$\Gamma^{\hat{t}}{}_{\hat{r}\hat{t}} = \omega \sin \omega r, \qquad \Gamma^{\hat{\theta}}{}_{\hat{r}\hat{\theta}} = \Gamma^{\hat{\varphi}}{}_{\hat{r}\hat{\varphi}} = \frac{\omega}{\sin \omega r}, \qquad \Gamma^{\hat{\varphi}}{}_{\hat{\theta}\hat{\varphi}} = \omega \cot \omega r \cot \omega \theta. \quad (7.1.17)$$

7.1.2   Geodesic structure

Using the method introduced in Ref. [14], the geodesics of adS can be computed as curves of minimum length in the embedding space satisfying Eq. (7.1.1). Using the connection between Hamilton's least-action principle and the Euler-Lagrange formulation, such curves can be derived from the Lagrangian:

$$L = \frac{1}{2}\eta_{ab}\dot{z}^a \dot{z}^b + \frac{\Lambda}{2}\left(\eta_{ab}z^a z^b + \frac{1}{\omega^2}\right), \qquad (7.1.18)$$

where the dot denotes differentiation with respect to the geodesic parameter λ and Λ is a Lagrange multiplier guaranteeing that the curves lie in adS. The ensuing Euler-Lagrange equations are:

$$\ddot{z}^a - \Lambda z^a = 0. \qquad (7.1.19)$$

The tensor

$$K_{ab} = z_a \dot{z}_b - z_b \dot{z}_a \qquad (7.1.20)$$

is constant along geodesics, since $\dot{K}_{ab} = 0$. Using Eq. (7.1.1), it can be seen that $z \cdot \dot{z} = 0$, hence:

$$K_{ab}K^{ab} = -\frac{2}{\omega^2}\dot{z}^2, \qquad K_{ab}z^b = \frac{1}{\omega^2}\dot{z}_a, \qquad K_{ab}\dot{z}^b = \dot{z}^2 z_a. \qquad (7.1.21)$$

Thus, $\Lambda = \omega^2 \dot{z}^2$. Therefore, the geodesics of adS can be written in terms of two constant vectors, m and n:

$$z^a = m^a \cos(\omega\sqrt{-\dot{z}^2}\lambda) + n^a \sin(\omega\sqrt{-\dot{z}^2}\lambda), \qquad (7.1.22)$$

where $m^2 = n^2 = -\omega^{-2}$ and $m \cdot n = 0$.

The distance along a geodesic between two points with coordinates x and x' in the adS chart, having geodesic parameters λ_1 and λ_2, respectively, can be calcuated as:

$$s(x, x') = \int_{\lambda_1}^{\lambda_2} d\lambda \sqrt{-\dot{z}^2} = (\lambda_2 - \lambda_1)\sqrt{-\dot{z}^2}. \qquad (7.1.23)$$

By virtue of Eq. (7.1.22), $s(x, x')$ simplifies to:

$$s(x, x') = \frac{1}{\omega} \arccos\left(-\omega^2 z \cdot z'\right), \qquad (7.1.24)$$

which can be written in terms of the adS coordinates as:

$$\cos \omega s = \frac{\cos \omega \Delta t}{\cos \omega r \cos \omega r'} - \cos \gamma \tan \omega r \tan \omega r'. \tag{7.1.25}$$

In the above, γ is the angle between $\boldsymbol{x}$ and $\boldsymbol{x}'$ and

$$\cos \gamma = \cos \theta \cos \theta' + \sin \theta \sin \theta' \cos \Delta \varphi \tag{7.1.26}$$

Two tangents to the geodesic are of particular interest:

$$n_\mu \equiv n_\mu(x, x') = \nabla_\mu s(x, x'), \qquad n_{\mu'} \equiv n_{\mu'}(x, x') = \nabla_{\mu'} s(x, x'), \tag{7.1.27}$$

where the primed index indicates a derivative with respect to x'. Their components can be calculated from Eq. (7.1.25):

$$
\begin{aligned}
n_t &= \frac{1}{\sin \omega s} \frac{\sin \omega \Delta t}{\cos \omega r \cos \omega r'}, \\
n_r &= -\frac{1}{\sin \omega s} \left(\cos \omega s \tan \omega r - \cos \gamma \tan \omega r' \right), \\
n_{r'} &= -\frac{1}{\sin \omega s} \left(\cos \omega s \tan \omega r' - \cos \gamma \tan \omega r \right), \\
n_\theta &= -\frac{1}{\omega \sin \omega s} \tan \omega r \tan \omega r' \left(\sin \theta \cos \theta' - \cos \theta \sin \theta' \cos \Delta \varphi \right), \\
n_{\theta'} &= -\frac{1}{\omega \sin \omega s} \tan \omega r \tan \omega r' \left(\sin \theta' \cos \theta - \cos \theta' \sin \theta \cos \Delta \varphi \right), \\
n_\varphi &= -\frac{1}{\omega \sin \omega s} \tan \omega r \tan \omega r' \sin \theta \sin \theta' \sin \Delta \varphi, \tag{7.1.28}
\end{aligned}
$$

together with $n_{t'} = -n_t$ and $n_{\varphi'} = -n_\varphi$. It can be checked that $n^2 = -1$. The tangents can also be expressed with respect to the Cartesian basis:

$$
\begin{aligned}
n_t &= \frac{1}{\sin \omega s} \frac{\sin \omega \Delta t}{\cos \omega r \cos \omega r'}, \\
n_i &= -\frac{1}{\sin \omega s} \left\{ \left[\cos \omega s \tan \omega r + \cos \gamma \tan \omega r' \left(\frac{\tan \omega r}{\omega r} - 1 \right) \right] \frac{x^i}{r} \right. \\
&\qquad \left. - \frac{\tan \omega r \tan \omega r'}{\omega r} \frac{x^{i'}}{r'} \right\}, \\
n_{i'} &= -\frac{1}{\sin \omega s} \left\{ \left[\cos \omega s \tan \omega r' + \cos \gamma \tan \omega r \left(\frac{\tan \omega r'}{\omega r'} - 1 \right) \right] \frac{x^{i'}}{r'} \right. \\
&\qquad \left. - \frac{\tan \omega r \tan \omega r'}{\omega r'} \frac{x^i}{r} \right\}, \tag{7.1.29}
\end{aligned}
$$

with $n_{t'} = -n_t$. These tangent vectors are also normalised with respect to the metric in Eq. (7.1.6). The corresponding components with respect to the tetrad in

Eq. (7.1.7) are:

$$
\begin{aligned}
n_{\hat{t}} &= \frac{1}{\sin \omega s} \frac{\sin \omega \Delta t}{\cos \omega r'}, \\
n_{\hat{t}'} &= -\frac{1}{\sin \omega s} \frac{\sin \omega \Delta t}{\cos \omega r}, \\
n_{\hat{i}} &= -\frac{1}{\sin \omega s} \left\{ [\cos \omega s \sin \omega r + \cos \gamma \tan \omega r'(1 - \cos \omega r)] \frac{x^i}{r} - \tan \omega r' \frac{x^{i'}}{r'} \right\}, \\
n_{\hat{i}'} &= -\frac{1}{\sin \omega s} \left\{ [\cos \omega s \sin \omega r' + \cos \gamma \tan \omega r(1 - \cos \omega r')] \frac{x^{i'}}{r'} - \tan \omega r \frac{x^i}{r} \right\}.
\end{aligned}
$$

$$(7.1.30)$$

Again, these tangent vectors are normalised according to $\eta^{\hat{\alpha}\hat{\beta}} n_{\hat{\alpha}} n_{\hat{\beta}} = \eta^{\hat{\alpha}\hat{\beta}} n_{\hat{\alpha}'} n_{\hat{\beta}'} = -1$. Finally, the contraction of the tangent vector with the gamma matrices is:

$$
\begin{aligned}
\not{n} \sin \omega s &= \frac{\sin \omega \Delta t}{\cos \omega r'} \gamma^{\hat{t}} - [\cos \omega s \sin \omega r + \cos \gamma \tan \omega r'(1 - \cos \omega r)] \frac{\boldsymbol{x} \cdot \boldsymbol{\gamma}}{r} \\
&\quad + \tan \omega r' \frac{\boldsymbol{x}' \cdot \boldsymbol{\gamma}}{r'}.
\end{aligned}
$$

$$(7.1.31)$$

According to Allen and Jacobson [3], the following relations hold on maximally symmetric space-times:

$$n_{\mu;\nu} = -A(g_{\mu\nu} + n_\mu n_\nu), \tag{7.1.32a}$$

$$n_{\mu;\nu'} = -C(g_{\mu\nu'} - n_\mu n_{\nu'}), \tag{7.1.32b}$$

where A and C are functions of s only, with C related to A through:

$$\frac{dC}{ds} = -AC. \tag{7.1.33}$$

Analytic expressions and a small distance expansion for the bi-vector of parallel transport $g_{\mu\nu'}$, essential in the point-splitting method for the computation of expectation values (see subsection 2.1.5 and subsection 2.2.6) are presented in subsections 7.1.3 and 7.1.5. Having found explicit expressions for n_μ and $n_{\mu'}$, the coefficients A and C can be computed explicitly. Since the covariant derivative of n_t with respect to t is

$$\nabla_t n_t = -\omega \cot \omega s \left(-\frac{1}{\cos^2 \omega r} + n_t^2 \right), \tag{7.1.34}$$

it follows that the functions A and C must be given by:

$$A = \omega \cot \omega s, \qquad C = -\frac{\omega}{\sin \omega s}, \tag{7.1.35}$$

in agreement with the expressions in Ref. [56].

The Van Vleck-Morette determinant $\Delta(x, x')$ is now straightforward to compute,

starting from the definition of the Van Vleck-Morette matrix [63]:

$$\Delta^{\alpha'}{}_{\beta'}(x, x') = -g^{\alpha'}{}_{\alpha} g^{\alpha\gamma} \sigma_{\gamma\beta'}, \qquad \Delta \equiv \det(\Delta^{\alpha'}{}_{\beta'}) = \frac{\det(-\sigma_{\mu\nu'})}{\sqrt{-g(x)}\sqrt{-g(x')}}, \qquad (7.1.36)$$

where $\sigma = -\frac{1}{2}s^2$ and the indices on sigma denote covariant diferentiation, e.g. $\sigma_{\mu\nu'} = \nabla_{\nu'}\nabla_{\mu}\sigma$. It can be shown that the Van Vleck-Morette determinant obeys the following equation [30, 63]:

$$\sigma^{\mu}\nabla_{\mu}\ln\Delta = 4 - \sigma^{\mu}{}_{\mu}. \qquad (7.1.37)$$

On adS, $\sigma^{\mu}{}_{\mu} = 3\omega s \cot \omega s + 1$, by virtue of Eqs. (7.1.32a) and (7.1.35). If we make the ansatz that, in a space-time with maximal symmetry, Δ is a function of s only, the above equation reduces to:

$$s\frac{d}{ds}\ln\Delta = 3(1 - \omega s \cot \omega s), \qquad (7.1.38)$$

with the solution that satisfies the boundary condition $\Delta(s = 0) = 1$ given by:

$$\Delta = \left(\frac{\omega s}{\sin \omega s}\right)^3. \qquad (7.1.39)$$

The above expression is in agreement with the result given in Ref. [50] for the n-dimensional adS space-time.

7.1.3   Bi-vector of parallel transport

The bi-vector of parallel transport can be obtained explicitly from Eq. (7.1.32b):

$$g_{\mu\nu'} = n_{\mu}n_{\nu'}(1 - \cos\omega s) + \frac{1}{\cos\omega r \cos\omega r'}\widetilde{g}_{\mu\nu'}, \qquad (7.1.40)$$

$$\widetilde{g}_{\mu\nu'} = \begin{pmatrix} -c_{\omega\Delta t} & s_{\omega\Delta t}t_{\omega r'} & 0 & 0 \\ -s_{\omega\Delta t}t_{\omega r} & \frac{\cos\gamma - c_{\omega\Delta t}s_{\omega r}s_{\omega r'}}{c_{\omega r}c_{\omega r'}} & \frac{s_{\omega r'}(-c_{\theta}s_{\theta'}+s_{\theta}c_{\theta'}c_{\Delta\varphi})}{\omega c_{\omega r}} & \frac{s_{\omega r'}s_{\theta}s_{\theta'}s_{\Delta\varphi}}{\omega c_{\omega r}} \\ 0 & -\frac{s_{\omega r}(s_{\theta}c_{\theta'}-s_{\theta'}c_{\theta}c_{\Delta\varphi})}{\omega c_{\omega r'}} & \frac{s_{\omega r}s_{\omega r'}(s_{\theta}s_{\theta'}+c_{\theta}c_{\theta'}c_{\Delta\varphi})}{\omega^2} & \frac{s_{\omega r}s_{\omega r'}c_{\theta}s_{\theta'}s_{\Delta\varphi}}{\omega^2} \\ 0 & -\frac{s_{\omega r}s_{\theta}s_{\theta'}s_{\Delta\varphi}}{\omega c_{\omega r'}} & -\frac{s_{\omega r}s_{\omega r'}s_{\theta}c_{\theta'}s_{\Delta\varphi}}{\omega^2} & \frac{s_{\omega r}s_{\omega r'}s_{\theta}s_{\theta'}c_{\Delta\varphi}}{\omega^2} \end{pmatrix},$$

where the standard trigonometric functions have been abbreviated by their initial, with their argument written as a subscript, e.g. $s_{\Delta\varphi} = \sin\Delta\varphi$. It can be checked that the equations $g_{\mu\nu'}n^{\nu'} = -n_{\mu}$ and $n^{\mu}g_{\mu\nu'} = -n_{\nu'}$ are satisfied. The bi-vector of

parallel transport can also be written with respect to Cartesian coordinates:

$$\widetilde{g}_{tt'} = -\cos\omega\Delta t, \tag{7.1.41a}$$

$$\widetilde{g}_{it'} = -\sin\omega\Delta t \tan\omega r \frac{x^i}{r}, \tag{7.1.41b}$$

$$\widetilde{g}_{ti'} = \sin\omega\Delta t \tan\omega r' \frac{x^{i'}}{r'}, \tag{7.1.41c}$$

$$\widetilde{g}_{ij'} = \frac{\sin\omega r}{\omega r}\frac{\sin\omega r'}{\omega r'}\left(\delta_{ij} - \frac{x^i x^j}{r^2} - \frac{x^{i'}x^{j'}}{r'^2}\right) + \frac{\sin\omega r'}{\omega r'}\frac{1}{\cos\omega r}\frac{x^i x^j}{r^2} + \frac{\sin\omega r}{\omega r}\frac{1}{\cos\omega r'}\frac{x^{i'}x^{j'}}{r'^2}$$

$$+ \left(-\cos\omega\Delta t \tan\omega r \tan\omega r' + \cos\gamma \frac{\omega r' - \sin\omega r'}{\omega r' \cos\omega r'}\frac{\omega r - \sin\omega r}{\omega r \cos\omega r}\right)\frac{x^i x^{j'}}{r r'}. \tag{7.1.41d}$$

For completeness, subsection 7.1.5 gives a coincidence limit expansion of $g_{\mu\nu'}$ in powers of σ^α.

7.1.4   Bi-spinor of parallel transport

The bi-spinor of parallel transport satisfies the parallel transport equation (2.2.57) for spinors, which on adS takes the form [4, 56]:

$$D_\mu\Lambda(x,x') = -\frac{\omega^2}{2}\frac{\tan\frac{\omega s}{2}}{\frac{\omega s}{2}}\Sigma_{\mu\nu}\sigma^\nu\Lambda(x,x'), \tag{7.1.42}$$

where $\Sigma_{\mu\nu} = -\frac{i}{4}[\gamma_\mu, \gamma_\nu]$ are the anti-Hermitian generators (2.2.8) of Lorentz transformations. Furthermore, it satisfies the conditions in Eqs. (2.2.58):

$$\Lambda(x,x) = 1, \qquad \Lambda^{-1}(x,x') = \overline{\Lambda}(x,x') = \Lambda(x',x). \tag{7.1.43}$$

The covariant γ matrices obey the following parallel transport equation:

$$\Lambda(x,x')\gamma^{\mu'} = g^{\mu'}{}_\nu\gamma^\nu\Lambda(x,x'). \tag{7.1.44}$$

To gain some insight on the form of the solution of Eq. (7.1.42), it is instructive to first consider the case when $r' = 0$, where n takes the form:

$$n_{\hat{t}}\big]_{r'=0} = \frac{\sin\omega\Delta t}{\sin\omega s}, \qquad n_{\hat{k}}\big]_{r'=0} = -\frac{\cos\omega\Delta t \tan\omega r}{\sin\omega s}\frac{x^k}{r}, \tag{7.1.45}$$

$$\not{n}\big]_{r'=0} = \frac{\cos\omega\Delta t}{\sin\omega s}\begin{pmatrix} \tan\omega\Delta t & -\frac{\boldsymbol{x}\cdot\boldsymbol{\sigma}}{r}\tan\omega r \\ \frac{\boldsymbol{x}\cdot\boldsymbol{\sigma}}{r}\tan\omega r & -\tan\omega\Delta t \end{pmatrix}. \tag{7.1.46}$$

Using Eq. (7.1.11) for the spin connection matrices, the following equations follow:

$$\partial_t \Lambda \big]_{r'=0} = -\frac{\omega}{2} \frac{\sin \omega r}{\cos \omega \Delta t + \cos \omega r} \begin{pmatrix} 0 & \frac{\boldsymbol{x} \cdot \boldsymbol{\sigma}}{r} \\ \frac{\boldsymbol{x} \cdot \boldsymbol{\sigma}}{r} & 0 \end{pmatrix} \Lambda, \tag{7.1.47a}$$

$$\boldsymbol{\nabla} \Lambda \big]_{r'=0} = -\frac{\omega}{2} \frac{\sin \omega \Delta t}{\cos \omega \Delta t + \cos \omega r} \left\{ \frac{\sin \omega r}{\omega r} \tan \frac{\omega r}{2} \tan \frac{\omega \Delta t}{2} \begin{pmatrix} \frac{i}{r} \boldsymbol{x} \times \boldsymbol{\sigma} & 0 \\ 0 & \frac{i}{r} \boldsymbol{x} \times \boldsymbol{\sigma} \end{pmatrix} \right.$$
$$\left. + \begin{pmatrix} 0 & 1 \\ 1 & 0 \end{pmatrix} \otimes \left[\frac{\sin \omega r}{\omega r} \boldsymbol{\sigma} + \frac{\boldsymbol{x}}{r} \left(\frac{\boldsymbol{x} \cdot \boldsymbol{\sigma}}{r} \right) \left(1 - \frac{\sin \omega r}{\omega r} \right) \right] \right\} \Lambda. \tag{7.1.47b}$$

The second equation can be simplified by multiplying both sides by x^j/r:

$$\partial_r \Lambda \big]_{r'=0} = -\frac{\omega}{2} \frac{\sin \omega \Delta t}{\cos \omega \Delta t + \cos \omega r} \begin{pmatrix} 0 & \frac{\boldsymbol{x} \cdot \boldsymbol{\sigma}}{r} \\ \frac{\boldsymbol{x} \cdot \boldsymbol{\sigma}}{r} & 0 \end{pmatrix} \Lambda. \tag{7.1.47c}$$

Eqs. (7.1.47a) and (7.1.47c) can be solved for the 2×2 components Λ_{ij} $(i, j \in \{1, 2\})$ of Λ. Both Λ_{11} and Λ_{22} satisfy the same equations:

$$\left(\frac{\cos \omega \Delta t + \cos \omega r}{\sin \omega r} \frac{\partial}{\partial(\omega t)^2} - \frac{\sin \omega \Delta t}{\sin \omega r} \frac{\partial}{\partial(\omega t)} - \frac{1}{4} \frac{\sin \omega r}{\cos \omega \Delta t + \cos \omega r} \right) \Lambda_{ii} = 0,$$
$$\left(\frac{\cos \omega \Delta t + \cos \omega r}{\sin \omega \Delta t} \frac{\partial}{\partial(\omega r)^2} - \frac{\sin \omega r}{\sin \omega \Delta t} \frac{\partial}{\partial(\omega r)} - \frac{1}{4} \frac{\sin \omega \Delta t}{\cos \omega \Delta t + \cos \omega r} \right) \Lambda_{ii} = 0. \tag{7.1.48}$$

The solution of the above equations is:

$$\Lambda_{ii} = \frac{\mathcal{C}_{ii}(r, \gamma) \cos \frac{\omega \Delta t}{2} + \mathcal{S}_{ii}(r, \gamma) \sin \frac{\omega \Delta t}{2}}{\sqrt{\cos \omega r + \cos \omega \Delta t}}, \tag{7.1.49}$$

where the 2×2 matrices $\mathcal{C}_{ii}$ and $\mathcal{S}_{ii}$ are harmonic functions of $\frac{r\omega}{2}$:

$$\mathcal{C}_{ii} = A_{ii}(\gamma) \cos \frac{\omega r}{2} + B_{ii}(\gamma) \sin \frac{\omega r}{2}, \qquad \mathcal{S}_{ii} = C_{ii}(\gamma) \cos \frac{\omega r}{2} + D_{ii}(\gamma) \sin \frac{\omega r}{2}. \tag{7.1.50}$$

The other two components of Λ can be found using:

$$\Lambda_{21} = -\frac{2}{\omega} \frac{\cos \omega \Delta t + \cos \omega r}{\sin \omega r} \frac{\boldsymbol{x} \cdot \boldsymbol{\sigma}}{r} \partial_t \Lambda_{11},$$
$$\Lambda_{12} = -\frac{2}{\omega} \frac{\cos \omega \Delta t + \cos \omega r}{\sin \omega r} \frac{\boldsymbol{x} \cdot \boldsymbol{\sigma}}{r} \partial_t \Lambda_{22}. \tag{7.1.51}$$

If $\mathcal{C}_{ii}$ and $\mathcal{S}_{ii}$ do not depend on the angular variables, their values can be found from the initial conditions:

$$\Lambda_{11} \big]_{x=x'} = \Lambda_{22} \big]_{x=x'} = 1, \qquad \Lambda_{12} \big]_{x=x'} = \Lambda_{21} \big]_{x=x'} = 0, \tag{7.1.52}$$

which show that $A_{ii} = D_{ii} = 1$ and $B_{ii} = C_{ii} = 0$. The final solution is:

$$\Lambda\big|_{r'=0} = \sqrt{\frac{2}{\cos\omega\Delta t + \cos\omega r}}\begin{pmatrix} \cos\dfrac{\omega r}{2}\cos\dfrac{\omega\Delta t}{2} & -\dfrac{\boldsymbol{x}\cdot\boldsymbol{\sigma}}{r}\sin\dfrac{\omega r}{2}\sin\dfrac{\omega\Delta t}{2} \\ -\dfrac{\boldsymbol{x}\cdot\boldsymbol{\sigma}}{r}\sin\dfrac{\omega r}{2}\sin\dfrac{\omega\Delta t}{2} & \cos\dfrac{\omega r}{2}\cos\dfrac{\omega\Delta t}{2} \end{pmatrix},$$

$$(7.1.53)$$

and it can be checked that it satisfies Eq. (7.1.47b). The following quantity is also useful to compute:

$$\slashed{n}\Lambda\big|_{r'=0} = \frac{\sqrt{\cos\omega\Delta t + \cos\omega r}}{\sin\omega s\,\cos\omega r/\sqrt{2}}\begin{pmatrix} \cos\dfrac{\omega r}{2}\sin\dfrac{\omega\Delta t}{2} & -\dfrac{\boldsymbol{x}\cdot\boldsymbol{\sigma}}{r}\sin\dfrac{\omega r}{2}\cos\dfrac{\omega\Delta t}{2} \\ \dfrac{\boldsymbol{x}\cdot\boldsymbol{\sigma}}{r}\sin\dfrac{\omega r}{2}\cos\dfrac{\omega\Delta t}{2} & -\cos\dfrac{\omega r}{2}\sin\dfrac{\omega\Delta t}{2} \end{pmatrix}.$$

$$(7.1.54)$$

Let us now find Λ for general point separations. The connection coefficients for the covariant derivatives of spinors are given in Eqs. (7.1.11) and the tetrad components of the tangent vector to the geodesic connecting the points x and x' are given in Eqs. (7.1.30). The form of Λ when $r' = 0$, given in Eq. (7.1.53), suggests the following ansatz:

$$\Lambda(x, x') = \sqrt{\frac{2}{\cos\omega r\,\cos\omega r'(1 + \cos\omega s)}}\lambda(x, x').$$

$$(7.1.55)$$

It is now necessary to consider the equations involving the derivatives with respect to both x^μ and x'^μ. It is simpler to solve the equations involving derivatives with respect to the time or radial coordinate if they are set out in the following format:

$$\begin{pmatrix} A & B \\ B & A \end{pmatrix}\lambda = 0, \qquad \lambda\begin{pmatrix} A' & B' \\ B' & A' \end{pmatrix} = 0,$$

$$(7.1.56a)$$

where the first and second equations correspond to equations involving derivatives with respect to t or r, and t' or r', respectively, and the relations $[A, B] = [A', B'] = 0$ must be satisfied. The above systems of equations can be easily diagonalised using the property:

$$\begin{pmatrix} A & -B \\ -B & A \end{pmatrix}\begin{pmatrix} A & B \\ B & A \end{pmatrix} = \begin{pmatrix} A^2 - B^2 & [A, B] \\ [A, B] & A^2 - B^2 \end{pmatrix}.$$

$$(7.1.56b)$$

After some algebra, the following expressions are found for the matrices A and

B required for the equations in t and t':

$$A_t = 2\cos\omega r\cos\omega r'(1+\cos\omega s)\partial_{\omega t} + \sin\omega\Delta t, \tag{7.1.57a}$$

$$B_t = [\sin\omega r\cos\omega r' - \cos\gamma\sin\omega r'(1-\cos\omega r)]\frac{\boldsymbol{x}\cdot\boldsymbol{\sigma}}{r} + \sin\omega r'\frac{\boldsymbol{x}'\cdot\boldsymbol{\sigma}}{r'}, \tag{7.1.57b}$$

$$A'_t = \overleftarrow{\partial}_{\omega t'} \times 2\cos\omega r\cos\omega r'(1+\cos\omega s) - \sin\omega\Delta t, \tag{7.1.57c}$$

$$B'_t = -\left[\sin\omega r'\cos\omega r - \cos\gamma\sin\omega r(1-\cos\omega r')\right]\frac{\boldsymbol{x}'\cdot\boldsymbol{\sigma}}{r'} - \sin\omega r\frac{\boldsymbol{x}\cdot\boldsymbol{\sigma}}{r}, \tag{7.1.57d}$$

The matrices A and B for the equations in r and r' are:

$$A_r = \frac{\boldsymbol{x}\cdot\boldsymbol{\sigma}}{r}\cos\omega r\cos\omega r'$$
$$\times\left[2(1+\cos\omega s)\partial_{\omega r} + \tan\omega r + \cos\gamma\tan\omega r' + i\frac{\tan\omega r'}{\cos\omega r}\frac{(\boldsymbol{x}\times\boldsymbol{x}')\cdot\boldsymbol{\sigma}}{rr'}\right], \tag{7.1.57e}$$

$$B_r = \sin\omega\Delta t, \tag{7.1.57f}$$

$$A'_r = \left[\overleftarrow{\partial}_{\omega r'}\times 2(1+\cos\omega r) + \tan\omega r' + \cos\gamma\tan\omega r + i\frac{\tan\omega r}{\cos\omega r'}\frac{(\boldsymbol{x}\times\boldsymbol{x}')\cdot\boldsymbol{\sigma}}{rr'}\right]$$
$$\times\cos\omega r\cos\omega r'\frac{\boldsymbol{x}'\cdot\boldsymbol{\sigma}}{r'}, \tag{7.1.57g}$$

$$B'_r = \sin\omega\Delta t, \tag{7.1.57h}$$

Finally, the squares A^2 and B^2 of the above matrices are given by:

$$A_t^2 = 1 + \cos^2\omega r\cos^2\omega r'$$
$$\times\left[4(1+\cos\omega s)^2\partial_{\omega t}^2 + (1+\cos\omega s)^2 - (1-\cos\gamma\tan\omega r\tan\omega r')^2\right], \tag{7.1.58a}$$

$$B_t^2 = 1 - \cos^2\omega r\cos^2\omega r'(1-\cos\gamma\tan\omega r\tan\omega r')^2, \tag{7.1.58b}$$

$$A_t'^2 = 1 + \left[\overleftarrow{\partial}_{\omega t'}^2\times 4(1+\cos\omega s)^2 + (1+\cos\omega s)^2 - (1-\cos\gamma\tan\omega r\tan\omega r')^2\right]$$
$$\times\cos^2\omega r\cos^2\omega r', \tag{7.1.58c}$$

$$B_t'^2 = 1 - \cos^2\omega r\cos^2\omega r'(1-\cos\gamma\tan\omega r\tan\omega r')^2, \tag{7.1.58d}$$

$$A_r^2 = \sin^2\omega\Delta t + \cos^2\omega r\cos^2\omega r'(1+\cos\omega s)^2\left[\partial_{\omega r}^2 + \frac{1}{4}\right], \tag{7.1.58e}$$

$$B_r^2 = \sin^2\omega\Delta t, \tag{7.1.58f}$$

$$A_{r'}^2 = \sin^2\omega\Delta t + \left[\overleftarrow{\partial}_{\omega r'}^2 + \frac{1}{4}\right]\cos^2\omega r\cos^2\omega r'(1+\cos\omega s)^2, \tag{7.1.58g}$$

$$B_r'^2 = \sin^2\omega\Delta t, \tag{7.1.58h}$$

Hence, λ is a solution of the following equations:

$$\left(\partial^2_{\omega t} + \frac{1}{4}\right)\lambda = 0, \quad \left(\partial^2_{\omega t'} + \frac{1}{4}\right)\lambda = 0, \quad \left(\partial^2_{\omega r} + \frac{1}{4}\right)\lambda = 0, \quad \left(\partial^2_{\omega r'} + \frac{1}{4}\right)\lambda = 0.$$

$$(7.1.59)$$

Due to the translational symmetry with respect to the time coordinate, λ_{ii} can be written without loss of generality as:

$$\lambda_{ii} = \mathcal{C}_{ii}(r, r', \gamma) \cos \frac{\omega \Delta t}{2} + \mathcal{S}_{ii}(r, r', \gamma) \sin \frac{\omega \Delta t}{2}, \qquad (7.1.60)$$

where $\mathcal{C}_{ii}$ and $\mathcal{S}_{ii}$ are harmonic functions of both $\frac{\omega r}{2}$ and $\frac{\omega r'}{2}$. Their exact forms can be determined using Eqs. (7.1.57) and the initial conditions in Eq. (7.1.52). Let us find λ_{21} by acting with $B_t^{-1} A_t$ on λ_{11}. The A_t operator changes the cos into sin and vice-versa, in the following way:

$$A_t \lambda_{11} = \mathcal{C}_{11} \sin \frac{\omega \Delta t}{2} (1 - C_\gamma) + \mathcal{S}_{11} \cos \frac{\omega \Delta t}{2} (1 + C_\gamma), \qquad (7.1.61)$$

where C_γ is given by:

$$C_\gamma = \cos \omega r \cos \omega r' (1 - \cos \gamma \tan \omega r \tan \omega r'). \qquad (7.1.62)$$

Hence, the following expression for λ_{21} is obtained:

$$\lambda_{21} = -\left[(\sin \omega r \cos \omega r' + \cos \gamma \sin \omega r' \cos \omega r)\frac{\boldsymbol{x} \cdot \boldsymbol{\sigma}}{r}\right.$$
$$\left. + \sin \omega r' \left(-\cos \gamma \frac{\boldsymbol{x} \cdot \boldsymbol{\sigma}}{r} + \frac{\boldsymbol{x}' \cdot \boldsymbol{\sigma}}{r'}\right)\right] \times \left(\frac{\mathcal{C}_{11} \sin \frac{\omega \Delta t}{2}}{1 + C_\gamma} + \frac{\mathcal{S}_{11} \cos \frac{\omega \Delta t}{2}}{1 - C_\gamma}\right). \quad (7.1.63)$$

This expression can be further rearranged into:

$$\lambda_{21} = -\frac{\boldsymbol{x} \cdot \boldsymbol{\sigma}}{r} \left\{\left[\frac{1 + \cos \gamma}{2} \sin \omega (r + r') + \frac{1 - \cos \gamma}{2} \sin \omega (r - r')\right]\right.$$
$$\left. + i\frac{\boldsymbol{x} \times \boldsymbol{x}'}{rr'} \cdot \boldsymbol{\sigma} \sin \omega r'\right\} \left[\frac{\mathcal{C}_{11} \sin \frac{\omega \Delta t}{2}}{(1 + \cos \gamma) \cos^2 \frac{\omega (r+r')}{2} + (1 - \cos \gamma) \cos^2 \frac{\omega (r-r')}{2}}\right.$$
$$\left. + \frac{\mathcal{S}_{11} \cos \frac{\omega \Delta t}{2}}{(1 + \cos \gamma) \sin^2 \frac{\omega (r+r')}{2} + (1 - \cos \gamma) \sin^2 \frac{\omega (r-r')}{2}}\right]. \quad (7.1.64)$$

Two simple cases can be analysed next:

$$\lambda_{21}\big|_{\gamma=0} = \tan \frac{\omega (r + r')}{2} \sin \frac{\omega \Delta t}{2} \frac{\boldsymbol{x} \cdot \boldsymbol{\sigma}}{r} \mathcal{C}_{11} + \cot \frac{\omega (r + r')}{2} \cos \frac{\omega \Delta t}{2} \frac{\boldsymbol{x} \cdot \boldsymbol{\sigma}}{r} \mathcal{S}_{11},$$
$$\lambda_{21}\big|_{\gamma=\pi} = \tan \frac{\omega (r - r')}{2} \sin \frac{\omega \Delta t}{2} \frac{\boldsymbol{x} \cdot \boldsymbol{\sigma}}{r} \mathcal{C}_{11} + \cot \frac{\omega (r - r')}{2} \cos \frac{\omega \Delta t}{2} \frac{\boldsymbol{x} \cdot \boldsymbol{\sigma}}{r} \mathcal{S}_{11}.$$

$$(7.1.65)$$

According to Eqs. (7.1.59), λ_{21} is a harmonic function of $\frac{\omega r}{2}$ and $\frac{\omega r'}{2}$. Thus, $\mathcal{C}_{11}$ must be proportional to $\cos\frac{\omega(r+r')}{2}$ at $\gamma = 0$ and to $\cos\frac{\omega(r-r')}{2}$ at $\gamma = \pi$ and similarly for $\mathcal{S}_{11}$ (with cos replaced by sin). Since Eq. (7.1.53) implies that λ_{11} must reduce to $\cos\frac{\omega\Delta t}{2}\cos\frac{\omega r}{2}$ when $r' = 0$, the following ansatz can be made:

$$
\begin{aligned}
\mathcal{S}_{11} =&\, 0, \\
\mathcal{C}_{11} =&\, \frac{1+\cos\gamma}{2}\cos\frac{\omega(r+r')}{2} + \frac{1-\cos\gamma}{2}\cos\frac{\omega(r-r')}{2} \\
&+ ia\frac{\boldsymbol{x}\times\boldsymbol{x'}}{rr'}\cdot\boldsymbol{\sigma}\sin\frac{\omega r}{2}\sin\frac{\omega r'}{2} \\
=&\, \cos\frac{\omega r}{2}\cos\frac{\omega r'}{2} + \left[a\frac{\boldsymbol{x}\cdot\boldsymbol{\sigma}\,\boldsymbol{x'}\cdot\boldsymbol{\sigma}}{r\ r'} - (a+1)\cos\gamma\right]\sin\frac{\omega r}{2}\sin\frac{\omega r'}{2} \\
=&\, cos\frac{\omega r}{2}\cos\frac{\omega r'}{2} - \left[a\frac{\boldsymbol{x'}\cdot\boldsymbol{\sigma}\,\boldsymbol{x}\cdot\boldsymbol{\sigma}}{r'\ r} - (a-1)\cos\gamma\right]\sin\frac{\omega r}{2}\sin\frac{\omega r'}{2}, \qquad (7.1.66)
\end{aligned}
$$

where a can only depend on γ. The property that λ_{21} is a harmonic function of $\frac{\omega r}{2}$ and $\frac{\omega r'}{2}$ transfers individually to the coefficients of $\frac{\boldsymbol{x}\cdot\boldsymbol{\sigma}}{r}$ and $\frac{\boldsymbol{x'}\cdot\boldsymbol{\sigma}}{r'}$ resulting from substituting Eq. (7.1.66) in Eq. (7.1.64):

$$
\begin{aligned}
\lambda_{21} =&- \sin\frac{\omega\Delta t}{2}\Bigg\{\sin\frac{\omega r}{2}\cos\frac{\omega r'}{2}\frac{\boldsymbol{x}\cdot\boldsymbol{\sigma}}{r} + \sin\frac{\omega r'}{2}\cos\frac{\omega r}{2}\frac{\boldsymbol{x'}\cdot\boldsymbol{\sigma}}{r'} + \frac{a+1}{1+C_\gamma}\sin\frac{\omega r}{2}\sin\frac{\omega r'}{2} \\
&\times\left[-\frac{\boldsymbol{x}\cdot\boldsymbol{\sigma}}{r}\left(\sin\omega r' + \cos\gamma\sin\omega r\cos\omega r' - 2\cos^2\gamma\sin\omega r'\sin^2\frac{\omega r}{2}\right)\right. \\
&\left.+\frac{\boldsymbol{x'}\cdot\boldsymbol{\sigma}}{r'}\left(\sin\omega r\cos\omega r' + \cos\gamma\sin\omega r'\left(\sin\frac{\omega r'}{2} - 2\sin^2\frac{\omega r}{2}\right)\right)\right]\Bigg\}. \qquad (7.1.67)
\end{aligned}
$$

The solution is to set $a = -1$, putting λ_{21} in the following form:

$$
\lambda_{21} = -\sin\frac{\omega\Delta t}{2}\left(\sin\frac{\omega r}{2}\cos\frac{\omega r'}{2}\frac{\boldsymbol{x}\cdot\boldsymbol{\sigma}}{r} + \sin\frac{\omega r'}{2}\cos\frac{\omega r}{2}\frac{\boldsymbol{x'}\cdot\boldsymbol{\sigma}}{r'}\right). \qquad (7.1.68)
$$

The final result for $\Lambda(x,x')$ can be summarised as:

$$
\begin{aligned}
\Lambda =&\, \frac{\left(\cos\frac{\omega s}{2}\right)^{-1}}{\sqrt{\cos\omega r\cos\omega r'}}\left[\cos\frac{\omega\Delta t}{2}\left(\cos\frac{\omega r}{2}\cos\frac{\omega r'}{2} + \sin\frac{\omega r}{2}\sin\frac{\omega r'}{2}\frac{\boldsymbol{x}\cdot\boldsymbol{\gamma}\,\boldsymbol{x'}\cdot\boldsymbol{\gamma}}{r\ r'}\right)\right. \\
&\left.+ \sin\frac{\omega\Delta t}{2}\left(\sin\frac{\omega r}{2}\cos\frac{\omega r'}{2}\frac{\boldsymbol{x}\cdot\boldsymbol{\gamma}}{r}\gamma^{\hat{t}} + \sin\frac{\omega r'}{2}\cos\frac{\omega r}{2}\frac{\boldsymbol{x'}\cdot\boldsymbol{\gamma}}{r'}\gamma^{\hat{t}}\right)\right], \qquad (7.1.69a)
\end{aligned}
$$

with $\displaystyle{\not{p}\Lambda(x,x')}$ given by:

$$
\begin{aligned}
\not{p}\Lambda =&\, \frac{\left(\sin\frac{\omega s}{2}\right)^{-1}}{\sqrt{\cos\omega r\cos\omega r'}}\left[\sin\frac{\omega\Delta t}{2}\left(\cos\frac{\omega r}{2}\cos\frac{\omega r'}{2}\gamma^{\hat{t}} - \sin\frac{\omega r}{2}\sin\frac{\omega r'}{2}\frac{\boldsymbol{x}\cdot\boldsymbol{\gamma}\,\boldsymbol{x'}\cdot\boldsymbol{\gamma}}{r\ r'}\gamma^{\hat{t}}\right)\right. \\
&\left.- \cos\frac{\omega\Delta t}{2}\left(\sin\frac{\omega r}{2}\cos\frac{\omega r'}{2}\frac{\boldsymbol{x}\cdot\boldsymbol{\gamma}}{r} - \sin\frac{\omega r'}{2}\cos\frac{\omega r}{2}\frac{\boldsymbol{x'}\cdot\boldsymbol{\gamma}}{r'}\right)\right], \qquad (7.1.69b)
\end{aligned}
$$

Since Λ only contains products of even numbers of γ matrices, all traces involving

Λ and an odd number of γ matrices vanish:

$$\text{tr}[\gamma^\mu \Lambda(x, x')] = 0, \qquad \text{tr}[\gamma^\mu \gamma^\nu \gamma^\lambda \Lambda(x, x')] = 0, \ldots \qquad (7.1.70)$$

A bit of algebra shows that Eqs. (7.1.69) satisfy Eqs. (7.1.56a), and it can be shown that the remaining defining equations, (7.1.43) and (7.1.44), are also satisfied. For completeness, subsection 7.1.5 gives the coincidence limit expansion of $\Lambda(x, x')$.

7.1.5 Coincidence limit expansions

Although in this case, the bi-vector and bi-spinor of parallel transport are known explicitly, it is still instructive to consider their coincidence limit expansions. The method of finding these expansions is by employing the differential equations (7.1.73) and (7.1.42) for the bi-vector and bi-spinor of parallel transport, respectively. We mention that these equations are exact, representing the anti-de Sitter version of the coincidence limit expansions of the derivatives of the bi-vector and bi-spinor of parallel transport reported in the Appendix of Ref. [24].

Expansion of the bi-vector of parallel transport

To derive a coincidence limit expansion of $g_{\mu\nu'}(x, x')$ in a power series in $\sigma_\mu \equiv -sn_\mu$, the following ansatz can be made:

$$g_{\mu\nu'} = g_{\mu\nu} + g_{\mu\nu\alpha}\sigma^\alpha + \frac{1}{2!}g_{\mu\nu\alpha\beta}\sigma^\alpha\sigma^\beta + \frac{1}{3!}g_{\mu\nu\alpha\beta\gamma}\sigma^\alpha\sigma^\beta\sigma^\gamma + \frac{1}{4!}g_{\mu\nu\alpha\beta\gamma\delta}\sigma^\alpha\sigma^\beta\sigma^\gamma\sigma^\delta + \ldots,$$
$$(7.1.71)$$

where the coefficients $g_{\mu\nu\alpha\ldots}$ are functions of x only and the coincidence limit ($\sigma^\alpha = 0$) of $g_{\mu\nu'}$ is the metric at x. These coefficients can be found iteratively starting from the differential equation [56]:

$$\nabla_\lambda g_{\mu\nu'} = -(A + C)(g_{\lambda\mu}n_{\nu'} + g_{\lambda\nu'}n_\mu), \qquad (7.1.72)$$

which can be written on adS in the following way:

$$\nabla_\lambda g_{\mu\nu'} = \frac{\omega^2}{2}\frac{\tan\frac{\omega s}{2}}{\frac{\omega s}{2}}(g_{\mu\lambda}g_{\nu'\alpha} - g_{\mu\alpha}g_{\nu'\lambda})\sigma^\alpha. \qquad (7.1.73)$$

The prefactor in the RHS of Eq. (7.1.73) can be written as a power series in σ^α by using $2\sigma = -s^2 = \sigma_\alpha\sigma^\alpha$:

$$\frac{\tan\frac{\omega s}{2}}{\frac{\omega s}{2}} = 1 - \frac{\omega^2}{12}g_{\alpha\beta}\sigma^\alpha\sigma^\beta + \frac{\omega^4}{120}g_{\alpha\beta}g_{\gamma\delta}\sigma^\alpha\sigma^\beta\sigma^\gamma\sigma^\delta + \ldots \qquad (7.1.74)$$

Thus, the expansion of the RHS of Eq. (7.1.73) in powers of σ^α reads:

$$\nabla_\lambda g_{\mu\nu'} = \frac{\omega^2}{2} \left\{ g_{\mu\lambda} \left[g_{\nu\alpha}\sigma^\alpha + g_{\nu\alpha\beta}\sigma^\alpha\sigma^\beta + \left(\frac{1}{2!}g_{\nu\alpha\beta\gamma} - \frac{\omega^2}{12}g_{\nu\alpha}g_{\beta\gamma} \right) \sigma^\alpha\sigma^\beta\sigma^\gamma + \dots \right] \right.$$
$$\left. - (\nu \leftrightarrow \alpha) \right\}. \quad (7.1.75)$$

Next, Eq. (7.1.32a) can be used to expand the covariant derivative of σ:

$$\nabla_\lambda \sigma^\mu = n^\mu n_\lambda (As - 1) + As\delta^\mu{}_\lambda$$
$$= \delta^\mu{}_\lambda + (n^\mu n_\lambda + \delta^\mu{}_\lambda) \left(\frac{\omega^2}{3}g_{\alpha\beta}\sigma^\alpha\sigma^\beta - \frac{\omega^4}{45}g_{\alpha\beta}g_{\gamma\delta} + \dots \right). \quad (7.1.76)$$

Keeping in mind that $g_{\mu'\nu}$ is a vector at x, the series expansion of the LHS of Eq. (7.1.73) is given by:

$$\nabla_\lambda g_{\mu\nu'} = g_{\mu\nu\lambda} + g_{\mu\nu;\lambda} + \Gamma_{\mu\nu\lambda} + (g_{\mu\nu\lambda\alpha} + g_{\mu\nu\alpha;\lambda} + g_{\mu\kappa\alpha}\Gamma^\kappa{}_{\nu\lambda})\sigma^\alpha$$
$$+ \frac{1}{2!} \left[g_{\mu\nu\lambda\alpha\beta} + g_{\mu\nu\alpha\beta;\lambda} + g_{\mu\kappa\alpha\beta}\Gamma^\kappa{}_{\nu\lambda} + \frac{2\omega^2}{3}g_{\alpha\beta}g_{\mu\nu\kappa}\left(n^\kappa n_\lambda + \delta^\kappa{}_\lambda \right) \right] \sigma^\alpha\sigma^\beta$$
$$+ \frac{1}{3!} \left[g_{\mu\nu\lambda\alpha\beta\gamma} + g_{\mu\nu\alpha\beta\gamma;\lambda} + g_{\mu\kappa\alpha\beta\gamma}\Gamma^\kappa{}_{\nu\lambda} + \omega^2 g_{\alpha\beta}g_{\mu\nu\kappa\gamma}\left(n^\kappa n_\lambda + \delta^\kappa{}_\lambda \right) \right] \sigma^\alpha\sigma^\beta\sigma^\gamma + \dots$$
$$(7.1.77)$$

When applied to the non-tensor coefficients $g_{\mu\nu\alpha\dots\beta}$, the semicolon notation above is interpreted as standard covariant differentiation with respect to all coordinate indices (i.e. not just λ and μ), such that $g_{\mu\nu;\lambda} = 0$. It should be stressed that, as in Eq. (21.20) in Ref. [55], the use of the semicolon does not imply that the object to which it is applied transforms covariantly under general coordinate transformations.

The expressions for the coefficients $g_{\mu\nu\alpha\dots\beta}$ in Eq. (7.1.71) are obtained by taking the totally symmetric part (denoted using parenthesis) of Eqs. (7.1.75) and (7.1.77) with respect to the indices λ and α, β, etc.:

$$g_{\mu\nu\alpha} = -\Gamma_{\mu\nu\alpha}, \quad (7.1.78a)$$
$$g_{\mu\nu\alpha\beta} = -g_{\mu\nu(\alpha;\beta)} - g_{\mu\kappa(\alpha}\Gamma^\kappa{}_{\beta)\nu}, \quad (7.1.78b)$$
$$g_{\mu\nu\alpha\beta\gamma} = -g_{\mu\nu(\alpha\beta;\gamma)} + g_{\mu\kappa(\alpha\beta}\Gamma^\kappa{}_{\gamma)\nu} - \frac{2\omega^2}{3}g_{\mu\nu\pi}g_{(\alpha\beta}[n_{\gamma)}n^\pi + \delta^\pi{}_{\gamma)}], \quad (7.1.78c)$$
$$g_{\mu\nu\alpha\beta\gamma\pi} = -g_{\mu\nu(\alpha\beta\gamma;\pi)} - g_{\mu\kappa(\alpha\beta\gamma}\Gamma^\kappa{}_{\pi)\nu} - \omega^2 g_{\mu\nu\kappa(\alpha}g_{\beta\gamma}[n_{\pi)}n^\kappa + \delta^\kappa{}_{\pi)}]. \quad (7.1.78d)$$

Substituting Eqs. (7.1.78) in Eqs. (7.1.75) and (7.1.77) gives a series of identities which are automatically satisfied on adS. For example, the equation corresponding to the first order in σ^α is:

$$g_{\mu\nu\lambda\alpha} - \Gamma_{\mu\nu\alpha,\lambda} + \Gamma^\kappa{}_{\mu\lambda}\Gamma_{\kappa\nu\alpha} = \frac{\omega^2}{2}(g_{\mu\lambda}g_{\nu\alpha} - g_{\mu\alpha}g_{\nu\lambda}). \quad (7.1.79)$$

The identity corresponding to the above equation is:

$$\Gamma_{\mu\nu[\alpha,\beta]} + \Gamma_{\kappa\mu[\alpha}\Gamma^{\kappa}{}_{\beta]\nu} = -\omega^2 g_{\mu[\beta}g_{\alpha]\nu}. \tag{7.1.80}$$

The LHS is just the definition of $\frac{1}{2}R_{\mu\nu\beta\alpha}$, while the RHS is the Riemann tensor in adS, given in Eq. (7.1.16), divided by 2. Similar identities follow from the second and third order equations, but they are omitted since they are of little relevance to the current work.

Expansion of the metric tensor

To find the expansion of the metric tensor $g_{\mu'\nu'}$ at x' in terms of the metric tensor $g_{\mu\nu}$ at x, the following simple equation can be used:

$$\nabla_{\lambda'}g_{\mu'\nu'} = 0. \tag{7.1.81}$$

The following ansatz can be made:

$$g_{\mu'\nu'} = g_{\mu\nu} + g'_{\mu\nu\alpha}\sigma^{\alpha} + \frac{1}{2!}g'_{\mu\nu\alpha\beta}\sigma^{\alpha}\sigma^{\beta} + \frac{1}{3!}g'_{\mu\nu\alpha\beta\gamma}\sigma^{\alpha}\sigma^{\beta}\sigma^{\gamma} + \frac{1}{4!}g'_{\mu\nu\alpha\beta\gamma\delta}\sigma^{\alpha}\sigma^{\beta}\sigma^{\gamma}\sigma^{\delta} + \dots, \tag{7.1.82}$$

after which Eq. (7.1.81) takes the form:

$$g'_{\mu\nu\lambda} + 2\Gamma_{(\mu\nu)\lambda} + \left(\nabla_{\lambda}g'_{\mu\nu\alpha} + 2\Gamma^{\kappa}{}_{\lambda(\mu}g'_{\nu)\kappa\alpha} + g'_{\mu\nu\lambda\alpha}\right)\sigma^{\alpha}$$
$$+ \frac{1}{2!}\left[\nabla_{\lambda}g'_{\mu\nu\alpha\beta} + 2\Gamma^{\kappa}{}_{\lambda(\mu}g'_{\nu)\kappa\alpha\beta} + g'_{\mu\nu\lambda\alpha\beta} + \frac{2\omega^2}{3}g_{\mu\nu\kappa}g_{\alpha\beta}\left(n^{\kappa}n_{\lambda} + \delta^{\kappa}{}_{\lambda}\right)\right]\sigma^{\alpha}\sigma^{\beta}$$
$$+ \frac{1}{3!}\left[\nabla_{\lambda}g'_{\mu\nu\alpha\beta\gamma} + 2\Gamma^{\kappa}{}_{\lambda(\mu}g'_{\nu)\kappa\alpha\beta\gamma} + g'_{\mu\nu\lambda\alpha\beta\gamma} + \omega^2 g_{\mu\nu\kappa\alpha}g_{\beta\gamma}\left(n^{\kappa}n_{\lambda} + \delta^{\kappa}{}_{\lambda}\right)\right]\sigma^{\alpha}\sigma^{\beta}\sigma^{\gamma}$$
$$+ \dots = 0, \tag{7.1.83}$$

where the covariant derivatives act on all the coordinate indices. The coefficients up to order 4 are:

$$g'_{\mu\nu\alpha} = -\Gamma_{\mu\nu\alpha} - \Gamma_{\nu\mu\alpha}, \tag{7.1.84a}$$

$$g'_{\mu\nu\alpha\beta} = -g'_{\mu\nu(\alpha;\beta)} - g'_{\mu\kappa(\alpha}\Gamma^{\kappa}{}_{\beta)\nu} - g'_{\nu\kappa(\alpha}\Gamma^{\kappa}{}_{\beta)\mu}, \tag{7.1.84b}$$

$$g'_{\mu\nu\alpha\beta\gamma} = -g'_{\mu\nu(\alpha\beta;\gamma)} - g'_{\mu\kappa(\alpha\beta}\Gamma^{\kappa}{}_{\gamma)\nu} - g'_{\nu\kappa(\alpha\beta}\Gamma^{\kappa}{}_{\gamma)\mu} - \frac{2\omega^2}{3}g'_{\mu\nu\kappa}g_{(\alpha\beta}(n^{\kappa}n_{\gamma)} + \delta^{\kappa}{}_{\gamma)}), \tag{7.1.84c}$$

$$g'_{\mu\nu\alpha\beta\gamma\delta} = -g'_{\mu\nu(\alpha\beta\gamma;\delta)} - g'_{\mu\kappa(\alpha\beta\gamma}\Gamma^{\kappa}{}_{\delta)\nu} - g'_{\nu\kappa(\alpha\beta\gamma}\Gamma^{\kappa}{}_{\delta)\mu} - \omega^2 g'_{\mu\nu\kappa(\alpha}g_{\beta\gamma}(n^{\kappa}n_{\delta)} + \delta^{\kappa}{}_{\delta)}). \tag{7.1.84d}$$

Expansion of the bi-spinor of parallel transport

As for the bi-vector of parallel transport, it is possible to express $\Lambda(x, x')$ in terms of functions defined at x multiplied by powers of σ^μ, using the following ansatz:

$$\Lambda(x, x') = 1 + \Lambda_\alpha \sigma^\alpha + \frac{1}{2!} \Lambda_{\alpha\beta} \sigma^\alpha \sigma^\beta + \frac{1}{3!} \Lambda_{\alpha\beta\gamma} \sigma^\alpha \sigma^\beta \sigma^\gamma + \frac{1}{4!} \Lambda_{\alpha\beta\gamma\delta} \sigma^\alpha \sigma^\beta \sigma^\gamma \sigma^\delta + \dots. \quad (7.1.85)$$

The coefficients Λ_α, $\Lambda_{\alpha\beta}$, etc, can be found using Eq. (7.1.42), in which the LHS can be expanded as:

$$D_\mu \Lambda(x, x') = \Gamma_\mu + \Lambda_\mu + (D_\mu \Lambda_\alpha + \Lambda_\alpha \Gamma_\mu + \Lambda_{\mu\alpha}) \sigma^\alpha$$
$$+ \frac{1}{2!} \left[D_\mu \Lambda_{\alpha\beta} + \Lambda_{\alpha\beta} \Gamma_\mu + \Lambda_{\mu\alpha\beta} + \frac{2\omega^2}{3} g_{\alpha\beta} \Lambda_\kappa (n^\kappa n_\mu + \delta^\kappa{}_\mu) \right] \sigma^\alpha \sigma^\beta$$
$$+ \frac{1}{3!} \left[D_\mu \Lambda_{\alpha\beta\gamma} + \Lambda_{\alpha\beta\gamma} \Gamma_\mu + \Lambda_{\mu\alpha\beta\gamma} + \omega^2 g_{\alpha\beta} \Lambda_{\gamma\kappa} (n^\kappa n_\mu + \delta^\kappa{}_\mu) \right] \sigma^\alpha \sigma^\beta \sigma^\gamma + O(s^4).$$
$$(7.1.86a)$$

The RHS of the same equation takes the form:

$$-\frac{\omega^2}{2} \frac{\tan \frac{\omega s}{2}}{\frac{\omega s}{2}} \Sigma_{\mu\nu} \sigma^\nu \Lambda = \frac{\omega^2}{2} \Sigma_{\mu\alpha} \sigma^\alpha \left[1 + \Lambda_\beta \sigma^\beta + \left(\frac{1}{2!} \Lambda_{\beta\gamma} - \frac{\omega^2}{12} g_{\beta\gamma} \right) \sigma^\beta \sigma^\gamma + \dots \right].$$
$$(7.1.86b)$$

Equating the coefficients of each power of σ individually in Eqs. (7.1.86a) and (7.1.86b) gives:

$$\Lambda_\alpha = -\Gamma_\alpha, \quad (7.1.87a)$$

$$\Lambda_{\alpha\beta} = -D_{(\alpha} \Lambda_{\beta)} - \Lambda_{(\alpha} \Gamma_{\beta)}, \quad (7.1.87b)$$

$$\Lambda_{\alpha\beta\gamma} = -D_{(\alpha} \Lambda_{\beta\gamma)} - \Lambda_{(\alpha\beta} \Gamma_{\gamma)} - \frac{2\omega^2}{3} g_{(\alpha\beta} \left(n^\kappa n_{\gamma)} + \delta^\kappa{}_{\gamma)} \right) \Lambda_\kappa, \quad (7.1.87c)$$

$$\Lambda_{\alpha\beta\gamma\delta} = -D_{(\alpha} \Lambda_{\beta\gamma\delta)} - \Lambda_{(\alpha\beta\gamma} \Gamma_{\delta)} - \omega^2 g_{(\alpha\beta} \left(n^\kappa n_\gamma + \delta^\kappa{}_\gamma \right) \Lambda_{\delta)\kappa}, \quad (7.1.87d)$$

where the coefficients $\Lambda_{\alpha\dots\beta}$ are considered to be matrices for the purpose of covariant differentiation, e.g. $D_\alpha \Lambda_\beta = \partial_\alpha \Lambda_\beta + [\Gamma_\alpha, \Lambda_\beta] - \Gamma^\kappa{}_{\beta\alpha} \Lambda_\kappa$.

As was the case for the bi-vector of parallel transport, substituting the results in Eqs. (7.1.87) back into Eq. (7.1.42) gives a series of identities satisfied automatically for the adS space-time. The first such identity is obtained from the coefficient of σ^α:

$$\nabla_\alpha \Gamma_\mu - \nabla_\mu \Gamma_\alpha - [\Gamma_\mu, \Gamma_\alpha] = \omega^2 \Sigma_{\mu\alpha}, \quad (7.1.88)$$

where ∇ is the covariant derivative with respect to coordinate indices. Writing

$$\Gamma_\mu = -\frac{1}{2} \omega_\mu^{\hat\alpha} \eta_{\hat\beta\hat\rho} \omega_\kappa^{\hat\rho} \nabla_{\hat\alpha} e_{\hat\gamma}^\kappa \Sigma^{\hat\beta\hat\gamma}, \quad (7.1.89)$$

the following identity can be established:

$$\nabla_\nu \Gamma_\mu - \nabla_\mu \Gamma_\nu = \omega_\nu^{\hat{\alpha}} \omega_\mu^{\hat{\delta}} \Gamma^{\hat{\kappa}}{}_{\hat{\beta}\hat{\delta}} \Gamma_{\hat{\kappa}\hat{\gamma}\hat{\alpha}} \Sigma^{\hat{\beta}\hat{\gamma}} + \frac{1}{2} R^\lambda{}_{\pi\mu\nu} e_{\hat{\gamma}}^\pi \omega_\lambda^{\hat{\beta}} \Sigma_{\hat{\beta}}{}^{\hat{\gamma}}. \tag{7.1.90}$$

Using the commutation relations of the generators of the Lorentz group [70], it can be shown that the first term above is equal to the commutator $[\Gamma_\mu, \Gamma_\alpha]$. The use of the Riemann tensor (7.1.16) on adS establishes the identity (7.1.88). The identities supplied by the second and third orders of Eq. (7.1.42) are not discussed here.

To investigate the traces of the bi-spinor of parallel transport $\Lambda(x, x')$, it is convenient to introduce the following notation:

$$\text{tr}(\gamma^{\mu_1} \gamma^{\mu_2} \dots \gamma^{\mu_s}) = -4 \Xi^{\mu_1 \mu_2 \dots \mu_s}. \tag{7.1.91}$$

Using the anti-commutation relation (2.2.3), the following recurrence can be established:

$$\Xi^{\mu_1 \mu_2 \dots \mu_s} = g^{\mu_1 \mu_2} \Xi^{\mu_3 \dots \mu_s} - g^{\mu_1 \mu_3} \Xi^{\mu_2 \mu_4 \dots \mu_s} \dots + (-1)^s g^{\mu_1 \mu_s} \Xi^{\mu_2 \dots \mu_{s-1}}, \tag{7.1.92}$$

which links Ξ with s indices with Ξ with $s - 2$ indices. The sequence generated by the above recursion can be started with the following values:

$$\Xi^{\mu\nu} = g^{\mu\nu}, \qquad \Xi^\mu = 0. \tag{7.1.93}$$

Explicitly, $\text{tr}(\gamma^\mu \gamma^\nu \gamma^\lambda \gamma^\kappa) = -4(g^{\mu\nu} g^{\lambda\kappa} - g^{\mu\lambda} g^{\nu\kappa} + g^{\mu\kappa} g^{\nu\lambda})$, etc., while Ξ with any odd number of indices vanishes. Since the exact solution (7.1.69a) shows that $\Lambda(x, x')$ contains only products of even numbers of γ matrices, it follows that the trace of $\Lambda(x, x')$ multiplied by any odd number of γ matrices vanishes, i.e.:

$$\text{tr}(\gamma^\mu \Lambda) = 0, \tag{7.1.94}$$

while the opposite holds for $\not{p}\Lambda(x, x')$, since $\not{p}$ changes the parity of the products of γ matrices from odd to even and vice-versa.

The same conclusion can be reached by considering the coincidence limit expansion of Λ. Equations (7.1.86) show that the coefficient $\Lambda_{\alpha_1 \alpha_2 \dots \alpha_s}$ with s indices can be written in terms of the coefficients with a number of $s - 1$ or less indices, multiplied by even numbers of γ matrices coming from $\Sigma_{\alpha\beta} = \frac{1}{4}[\gamma_\alpha, \gamma_\beta]$, either on its own in Eq. (7.1.86b) or through the spin connection Γ_α, defined in Eq. (2.2.17). The spinor covariant derivative $D_\mu = \partial_\mu + \Gamma_\mu$ also contributes a product of an even number of γ matrices. Since the first order term in the expansion of $\Lambda(x, x')$ is the identity, which contains zero γ matrices, it can be concluded that all higher order terms $\Gamma_{\alpha\beta\dots\gamma}$ will only contain products of an even number of γ matrices. Hence, Eq. (7.1.94) is established.

For completeness, the traces of Λ_α and $\Lambda_{\alpha\beta}$ are given in what follows. For Λ_α, Eq. (7.1.87a) can be used to obtain the following results:

$$\text{tr}(\Lambda_\xi) = 0, \tag{7.1.95a}$$

$$\text{tr}(\gamma_\mu\gamma_\nu\Lambda_\xi) = -2\Gamma_{\hat\beta\hat\gamma\hat\rho}\omega_\xi^{\hat\rho}\omega_\mu^{\hat\beta}\omega_\nu^{\hat\gamma}, \tag{7.1.95b}$$

$$\text{tr}(\gamma_\mu\gamma_\nu\gamma_\lambda\gamma_\kappa\Lambda_\xi) = \omega_\xi^{\hat\alpha}\Gamma^{\hat\beta}{}_{\hat\pi\hat\alpha}\eta^{\hat\pi\hat\gamma}\omega_\mu^{\hat\delta}\omega_\nu^{\hat\rho}\omega_\lambda^{\hat\sigma}\omega_\kappa^{\hat\xi}\Delta_{\hat\delta\hat\rho\hat\sigma\hat\xi\hat\beta\hat\gamma}. \tag{7.1.95c}$$

Higher order traces have been included to facilitate the calculation of the traces of higher order coefficients (e.g. $\Lambda_{\alpha\beta}$). Hence, the traces of $\Lambda_{\alpha\beta}$ are:

$$\text{tr}(\Lambda_{\xi\zeta}) = -\frac{1}{2}\omega_\xi^{\hat\alpha}\omega_\zeta^{\hat\beta}\Gamma^{\hat\rho}{}_{\hat\gamma\hat\alpha}\Gamma^{\hat\gamma}{}_{\hat\rho\hat\beta}, \tag{7.1.96a}$$

$$\text{tr}(\gamma_\mu\gamma_\nu\Lambda_{\xi\zeta}) = -\frac{1}{2}\omega_\xi^{\hat\alpha}\omega_\zeta^{\hat\beta}\left(\omega_\mu^{\hat\gamma}\omega_\nu^{\hat\delta}\Gamma_{\hat\gamma\hat\delta\hat\rho}\Gamma^{\hat\rho}{}_{\hat\alpha\hat\beta} + \omega_{[\mu}^{\hat\rho}g_{\nu]\kappa}\nabla_{\hat\alpha}\nabla_{\hat\beta}e_{\hat\rho}^\kappa + 2g_{\mu\nu}\Gamma^{\hat\rho}{}_{\hat\gamma\hat\alpha}\Gamma^{\hat\gamma}{}_{\hat\rho\hat\beta}\right)$$

$$= -\frac{1}{2}\omega_\xi^{\hat\alpha}\omega_\zeta^{\hat\beta}\left(\omega_\mu^{\hat\gamma}\omega_\nu^{\hat\delta}\Gamma_{\hat\gamma\hat\delta\hat\alpha,\hat\beta} + 2g_{\mu\nu}\Gamma^{\hat\rho}{}_{\hat\gamma\hat\alpha}\Gamma^{\hat\gamma}{}_{\hat\rho\hat\beta}\right). \tag{7.1.96b}$$

7.1.6 Generators of isometries and conserved operators

The generators of isometries corresponding to the symmetries of adS can be determined using the formalism introduced in Ref. [25]. Starting from the five-dimensional embedding space, the symmetry group of Eq. (7.1.1) defining the adS four-surface is $SO(3,2)$. Using latin letters $a, b, c, \ldots$ to denote indices in the embedding spacetime, the 10 Killing vectors $k_{ab} \equiv k_{[ab]}$ of the adS manifold can be parametrised as follows:

$$(k_{ab})_c = (\eta_{ad}\eta_{bc} - \eta_{ac}\eta_{bd})z^d, \tag{7.1.97}$$

where $(k_{ab})_c$ represent the covariant components of the Killing vector k_{ab}. Differentiating Eqs. (7.1.2), k_{ab} can be written with respect to the adS coordinates:

$$(k_{ij})_c dz^c = \left(\frac{\tan\omega r}{\omega r}\right)^2 \left(x^i\delta_{jk} - x^j\delta_{ik}\right)dx^k,$$

$$(k_{0i})_c dz^c = -\frac{\tan\omega r}{\omega r}\frac{\sin\omega t}{\cos\omega r}x^i dt - \frac{\cos\omega t}{\omega\cos\omega r}\left[\frac{\tan\omega r}{\omega r}\left(\delta_{ij} - \frac{x^i x^j}{r^2}\right) + \frac{x^i x^j}{r^2}\right]dx^j,$$

$$(k_{i5})_c dz^c = -\frac{\tan\omega r}{\omega r}\frac{\cos\omega t}{\cos\omega r}x^i dt + \frac{\sin\omega t}{\omega\cos\omega r}\left[\frac{\tan\omega r}{\omega r}\left(\delta_{ij} - \frac{x^i x^j}{r^2}\right) + \frac{x^i x^j}{r^2}\right]dx^j,$$

$$(k_{05})_c dz^c = \frac{dt}{\omega\cos^2\omega r}. \tag{7.1.98}$$

The contravariant components of the Killing vectors, obtained from the above covariant components using the inverse metric (7.1.6b), can be used to form the orbital part $L_{ab} = -i(k_{ab})^\mu\partial_\mu$ of the generator of the associated symmetry transformations

$(i^2 = -1$ when i is not an index$)$:

$$L_{jk} = -i(x^j \partial_k - x^k \partial_j),$$

$$L_{0j} = -i \sin \omega t \frac{\sin \omega r}{\omega r} x^j \partial_t + \frac{i}{\omega} \cos \omega t \left[\frac{\omega r}{\sin \omega r} \left(\delta_{jk} - \frac{x^j x^k}{r^2} \right) + \cos \omega r \frac{x^j x^k}{r^2} \right] \partial_k,$$

$$L_{j5} = -i \cos \omega t \frac{\sin \omega r}{\omega r} x^j \partial_t - \frac{i}{\omega} \sin \omega t \left[\frac{\omega r}{\sin \omega r} \left(\delta_{jk} - \frac{x^j x^k}{r^2} \right) + \cos \omega r \frac{x^j x^k}{r^2} \right] \partial_k,$$

$$L_{05} = \frac{i}{\omega} \partial_t. \tag{7.1.99}$$

The rotation generators L_{ij} have the familiar $SO(3)$ form and L_{05} generates time translations. The generators of space-like translations have a more cumbersome expression:

$$\left[\frac{\sin \omega r}{\omega r} \left(\delta_{ij} - \frac{x^i x^j}{r^2} \right) + \frac{1}{\cos \omega r} \frac{x^i x^j}{r^2} \right] (\cos \omega t \, L_{0j} - \sin \omega t \, L_{j5}) = \frac{i}{\omega} \partial_i. \tag{7.1.100}$$

The spin part of the isometries generators can be calculated using the formula [25]:

$$S_{ab}(x) = \frac{i}{2} \Omega_{ab}^{\hat{\alpha}\hat{\beta}}(x) \Sigma_{\hat{\alpha}\hat{\beta}}, \tag{7.1.101}$$

where $\Sigma_{\hat{\alpha}\hat{\beta}} = -\frac{i}{4} \left[\gamma_{\hat{\alpha}}, \hat{\beta} \right]$ and

$$\Omega_{ab}^{\hat{\alpha}\hat{\beta}}(x) = - \left\langle \omega^{\hat{\alpha}}, \left[e_{\hat{\beta}}, k_{ab} \right] \right\rangle. \tag{7.1.102}$$

Before embarking on the calculation of the commutators between the Killing vector fields and the tetrad vectors, it is useful to write the former in terms of the latter:

$$k_{ij} = \frac{\tan \omega r}{\omega r} (x^i \delta_{jk} - x^j \delta_{ik}) e_{\hat{k}},$$

$$k_{0i} = \sin \omega t \frac{\tan \omega r}{\omega r} x^i e_{\hat{t}} - \frac{1}{\omega} \cos \omega t \left[\frac{1}{\cos \omega r} \left(\delta_{ij} - \frac{x^i x^j}{r^2} \right) + \frac{x^i x^j}{r^2} \right] e_{\hat{j}},$$

$$k_{i5} = \cos \omega t \frac{\tan \omega r}{\omega r} x^i e_{\hat{t}} + \frac{1}{\omega} \sin \omega t \left[\frac{1}{\cos \omega r} \left(\delta_{ij} - \frac{x^i x^j}{r^2} \right) + \frac{x^i x^j}{r^2} \right] e_{\hat{j}},$$

$$k_{05} = \frac{i}{\omega \cos \omega r} e_{\hat{t}}. \tag{7.1.103}$$

Thus, the spin part of the generators of isometries are given by:

$$S_{jk}(x) = i \Sigma_{\hat{j}\hat{k}},$$

$$S_{0j}(x) = \sin \omega t \left(\delta_{jk} - \frac{x^j x^k}{r^2} + \cos \omega r \frac{x^j x^k}{r^2} \right) i \Sigma_{\hat{t}\hat{k}} + \cos \omega t \frac{1 - \cos \omega r}{\sin \omega r} \frac{x^k}{r} i \Sigma_{\hat{j}\hat{k}},$$

$$S_{j5}(x) = \cos \omega t \left(\delta_{jk} - \frac{x^j x^k}{r^2} + \cos \omega r \frac{x^j x^k}{r^2} \right) i \Sigma_{\hat{t}\hat{k}} - \sin \omega t \frac{1 - \cos \omega r}{\sin \omega r} \frac{x^k}{r} i \Sigma_{\hat{j}\hat{k}},$$

$$S_{05}(x) = 0. \tag{7.1.104}$$

In particular, the generators of rotations, which become angular momentum operators in quantum field theory, have the following form:

$$J_k = \frac{1}{2}\varepsilon_{kij}(L_{ij} + S_{ij}) = -i(\boldsymbol{x} \times \nabla)_k + i\Sigma_k. \tag{7.1.105}$$

The spin part of the translation operator with orbital part given in Eq. (7.1.100) follows from Eq. (7.1.104):

$$\left[\frac{\sin \omega r}{\omega r}\left(\delta_{jk} - \frac{x^j x^k}{r^2}\right) + \frac{1}{\cos \omega r}\frac{x^j x^k}{r^2}\right][S_{0k}(x)\cos \omega t - S_{k5}(x)\sin \omega t]$$
$$= \frac{1 - \cos \omega r}{\omega r}\frac{x^k}{r}iD[\Sigma_{\hat{j}\hat{k}}]. \tag{7.1.106}$$

Contracting both sides with x^j shows that the spin part of the generator of radial translations, having the orbital part given by Eq. (7.1.100), vanishes:

$$x^j[S_{0j}(x)\cos \omega t - S_{j5}(x)\sin \omega t] = 0. \tag{7.1.107}$$

7.2 Mode solutions of the Dirac equation

The Dirac equation with respect to the Cartesian tetrad (7.1.7) for fermions of mass μ can be written as

$$(E_D - \mu)\psi = 0, \tag{7.2.1}$$

where $E_D = i\gamma^\mu D_\mu$ can be written as:

$$E_D = i\gamma^{\hat{\alpha}}e_{\hat{\alpha}}^\lambda \partial_\lambda + \frac{i}{2}\frac{1}{\sqrt{-g}}\partial_\lambda(\sqrt{-g}e_{\hat{\alpha}}^\lambda)\gamma^{\hat{\alpha}}. \tag{7.2.2}$$

The square root $\sqrt{-g}$ of the determinant of the adS metric (7.1.6) with respect to Cartesian coordinates is given by:

$$\sqrt{-g} = \frac{1}{\cos^3 \omega r}\frac{\sin^2 \omega r}{\omega^2 r^2} \tag{7.2.3}$$

The mode solutions of the Dirac equation (7.2.1) are already known [26]. For completeness and to introduce the notation used in the following sections, their construction is rederived here.

A complete set of commuting operators (CSCO) is given by $\{H_D, J_3, \boldsymbol{J}^2, K\}$, where $\boldsymbol{J}$ is the total angular momentum operator (7.1.105), $H_D = i\partial_t$ is the Dirac Hamiltonian and the spin-orbit operator K is given by [68]:

$$K = \gamma^{\hat{t}}(2i\boldsymbol{\Sigma} \cdot \boldsymbol{L} + 1). \tag{7.2.4}$$

These operators are conserved, since they commute with H_D and with E_D, hence, they admit a set of simultaneous igenvectors $U_{E,j,m,\kappa}$ satisfying the following eigenvalue equations:

$$H_D U_{E,j,m,\kappa} = U_{E,j,m,\kappa} E, \tag{7.2.5a}$$

$$\boldsymbol{J}^2 U_{E,j,m,\kappa} = U_{E,j,m,\kappa} j(j+1), \tag{7.2.5b}$$

$$J_3 U_{E,j,m,\kappa} = U_{E,j,m,\kappa} m, \tag{7.2.5c}$$

$$K U_{E,j,m,\kappa} = U_{E,j,m,\kappa}(-\kappa), \tag{7.2.5d}$$

where

$$\kappa = \pm(j + \frac{1}{2}) \tag{7.2.6}$$

is the eigenvalue of K. The solutions of these equations can be written as:

$$U_{E,j,\kappa,m}(x) = \omega r \frac{(\cos \omega r)^{\frac{3}{2}}}{\sin \omega r} \widetilde{U}_{E,j,\kappa,m}(x), \tag{7.2.7a}$$

where the reduced mode $\widetilde{U}_{E,j,\kappa,m}$, introduced to simplify the Dirac equation, can be put in the form:

$$\widetilde{U}_{E,j,\kappa,m}(x) = \frac{1}{r} \left[f_{E,\kappa}^+(r)\Phi_{m,\kappa}^+(\theta,\varphi) + f_{E,\kappa}^-(r)\Phi_{m,\kappa}^-(\theta,\varphi) \right] e^{-iEt}, \tag{7.2.7b}$$

The four-spinors $\Phi_{m,\kappa}^{\pm}$ are solutions of the angular eigenvalue equations (7.2.5b), (7.2.5c) and (7.2.5d) and are given by [68]:

$$\Phi_{\kappa,m}^+ = \begin{pmatrix} i\psi_{j+\frac{1}{2}\mathrm{sgn}\kappa}^m \\ 0 \end{pmatrix}, \qquad \Phi_{\kappa,m}^- = \begin{pmatrix} 0 \\ \psi_{j-\frac{1}{2}\mathrm{sgn}\kappa}^m \end{pmatrix}, \tag{7.2.8a}$$

where the two-spinors $\psi_{j\pm\frac{1}{2}\mathrm{sgn}\kappa}^m$ have the following expressions:

$$\psi_{j\pm\frac{1}{2}}^m = \frac{1}{\sqrt{2j+1\pm 1}} \begin{pmatrix} \sqrt{j+\frac{1}{2}\mp(m-\frac{1}{2})} Y_{j\pm\frac{1}{2}}^{m-\frac{1}{2}} \\ \mp\sqrt{j+\frac{1}{2}\pm(m+\frac{1}{2})} Y_{j\pm\frac{1}{2}}^{m+\frac{1}{2}} \end{pmatrix}. \tag{7.2.8b}$$

The spherical harmonics $Y_\ell^{m\pm\frac{1}{2}}$, as well as properties of the two-spinors ψ_ℓ^m, are discussed in Appendix C.

The radial functions $f_{E,\kappa}^{\pm}$ can be found by solving the reduced Dirac equation [26]:

$$\widetilde{H}_D \widetilde{U}_{E,j,\kappa,m} = \widetilde{U}_{E,j,\kappa,m} E, \tag{7.2.9a}$$

where the Hamiltonian $\widetilde{H}_D$ corresponding to the reduced Dirac equation can be written in terms of spatial derivatives only as:

$$\widetilde{H}_D = \frac{-i}{r^2}\gamma^{\hat{t}}(\boldsymbol{\gamma}\cdot\boldsymbol{x})(1+\boldsymbol{x}\cdot\nabla) - \frac{i\omega}{r\sin\omega r}(\boldsymbol{\gamma}\cdot\boldsymbol{x})K + \frac{\mu}{\cos\omega r}\gamma^{\hat{t}}. \tag{7.2.9b}$$

The following identities:

$$\frac{\boldsymbol{x} \cdot \boldsymbol{\gamma}}{r} \Phi_{\kappa,m}^{\pm} = -i\Phi_{\kappa,m}^{\mp},$$

$$\gamma^{\hat{t}} \Phi_{\kappa,m}^{\pm} = \mp\Phi_{\kappa,m}^{\pm},$$

$$(1 + \boldsymbol{x} \cdot \nabla)\frac{1}{r} f_{E,\kappa}^{(\pm)}(r) = \frac{d}{dr} f_{E,\kappa}^{(\pm)}(r), \tag{7.2.10}$$

can be used to convert Eq. (7.2.9a) into a system of equations for the radial functions:

$$H_r \mathcal{F}_{E,\kappa} = \frac{E}{\omega} \mathcal{F}_{E,\kappa}, \tag{7.2.11a}$$

where the radial Hamiltonian H_r is a 2×2 matrix operator having the expression:

$$H_r = \begin{pmatrix} \frac{k}{\cos \omega r} & -\frac{d}{d(\omega r)} + \frac{\kappa_j}{\sin \omega r} \\ \frac{d}{d(\omega r)} + \frac{\kappa_j}{\sin \omega r} & -\frac{k}{\cos \omega r} \end{pmatrix}, \tag{7.2.11b}$$

and the radial functions have been grouped in a two-vector as follows:

$$\mathcal{F}_{E,\kappa} = \begin{pmatrix} f_{E,\kappa}^{+} \\ f_{E,\kappa}^{-} \end{pmatrix}. \tag{7.2.11c}$$

In the above, the ratio between the mass μ and the inverse curvature ω has been abbreviated using

$$k = \frac{\mu}{\omega}. \tag{7.2.12}$$

To solve the system of equations (7.2.11a), it is convenient to put the radial Hamiltonian H_r in superpotential form [26]:

$$\hat{H}_r = R H_r R^T - \tfrac{1}{2} = \begin{pmatrix} k - \kappa & -\frac{d}{d(\omega r)} + \kappa \cot \omega r + k \tan \omega r \\ \frac{d}{d(\omega r)} + \kappa \cot \omega r + k \tan \omega r & -k + \kappa \end{pmatrix}, \tag{7.2.13}$$

where R is a rotation matrix having the form

$$R = \begin{pmatrix} \cos \frac{\omega r}{2} & -\sin \frac{\omega r}{2} \\ \sin \frac{\omega r}{2} & \cos \frac{\omega r}{2} \end{pmatrix}. \tag{7.2.14}$$

Applying the same rotation to the radial functions gives:

$$\hat{\mathcal{F}} = \begin{pmatrix} \hat{f}_{E,\kappa}^{+} \\ \hat{f}_{E,\kappa}^{-} \end{pmatrix} = R\mathcal{F} \tag{7.2.15}$$

and Eq. (7.2.11a) become:

$$\hat{H}_r \hat{\mathcal{F}} = \varepsilon \hat{\mathcal{F}}, \tag{7.2.16}$$

where

$$\varepsilon = \frac{E}{\omega} - \frac{1}{2}. \tag{7.2.17}$$

Equations (7.2.16) can be used to construct a second order differential equation for $f_{E,\kappa}^{\pm}$:

$$\left[-\frac{d^2}{d(\omega r)^2} + \frac{\kappa(\kappa \pm 1)}{\sin^2 \omega r} + \frac{k(k \mp 1)}{\cos^2 \omega r} - \varepsilon^2 \right] \hat{f}_{E,\kappa}^{\pm} = 0. \tag{7.2.18}$$

Changing variable to $z = \sin^2 \omega r$ and letting $\hat{f}_{E,\kappa}^{\pm} = (\sin \omega r)^{2s_\pm} (\cos \omega r)^{2p_\pm} g_{E,\kappa}^{\pm}$ puts the above equation in the hypergeometric equation (D.1) form:

$$\left\{ z(1-z)\frac{d^2}{dz^2} + [2s_\pm + \tfrac{1}{2} - z(2s_\pm + 2p_\pm + 1)]\frac{d}{dz} - (s_\pm + p_\pm)^2 + \frac{\varepsilon^2}{4} \right\} g_{E,\kappa}^{\pm} = 0, \tag{7.2.19}$$

where $s_\pm$ and $p_\pm$ must obey:

$$2s_\pm(2s_\pm - 1) = \kappa(\kappa \pm 1), \qquad 2p_\pm(2p_\pm - 1) = k(k \mp 1). \tag{7.2.20}$$

Thus the radial functions take the form:

$$\hat{f}_{E,\kappa}^{(\pm)} = \mathcal{N}_\pm (\sin \omega r)^{2s_\pm} (\cos \omega r)^{2p_\pm} \, {}_2F_1(s_\pm + p_\pm - \tfrac{\varepsilon}{2}, s_\pm + p_\pm + \tfrac{\varepsilon}{2}; 2s_\pm + \tfrac{1}{2}; \sin^2 \omega r), \tag{7.2.21}$$

with $\mathcal{N}_\pm$ being arbitrary constants. The above solutions are acceptable only if the corresponding modes can be normalised. For eigenmodes of the eigenvalue equations (7.2.5a), the Dirac inner product reduces to:

$$\begin{aligned}
\langle U_{E,j,m,\kappa}, U_{E',j',m',\kappa'} \rangle &= \delta_{mm'}\delta_{jj'}\delta_{\kappa\kappa'} \langle \mathcal{F}_{E,\kappa}, \mathcal{F}_{E',\kappa'} \rangle \\
&= \delta_{mm'}\delta_{jj'}\delta_{\kappa\kappa'} \langle \hat{\mathcal{F}}_{E,\kappa}, \hat{\mathcal{F}}_{E',\kappa'} \rangle \\
&= \delta_{mm'}\delta_{jj'}\delta_{\kappa\kappa'} \int_0^{\frac{\pi}{2\omega}} dr [\hat{f}_{E,\kappa}^{(+)}(r)\hat{f}_{E',\kappa'}^{(+)}(r) + \hat{f}_{E,\kappa}^{(-)}(r)\hat{f}_{E',\kappa'}^{(-)}(r)] \\
&= \delta_{mm'}\delta_{jj'}\delta_{\kappa\kappa'} \delta(E, E').
\end{aligned} \tag{7.2.22}$$

The condition that the modes (7.2.7) have unit norm restricts the values of the parameters $2p_\pm$, $2s_\pm$ and ε. Firstly, for the hypergeometric functions in $f^{(\pm)}$ to be regular at $r = \frac{\omega}{2\pi}$, one of its first two arguments must be a negative integer $-n_\pm$, leading to a quantisation of the energy:

$$\varepsilon = 2n_+ + 2s_+ + 2p_+ = 2n_- + 2s_- + 2p_-. \tag{7.2.23}$$

Secondly, the powers of the sines and cosines under the integration sign must be strictly greater than -1. This restriction, together with Eqs. (7.2.20), give the

	$(2p_+, 2p_-)$	$2s_\pm$	n_-	restrictions
1	$(k, k+1)$	$j + 1 \pm \frac{1}{2}\mathrm{sgn}\kappa$	$n_+ - \frac{1}{2} + \frac{1}{2}\mathrm{sgn}\kappa$	$-\frac{1}{2} < k$
2	$(1-k, -k)$	$j + 1 \pm \frac{1}{2}\mathrm{sgn}\kappa$	$n_+ + \frac{1}{2} + \frac{1}{2}\mathrm{sgn}\kappa$	$|k| < \frac{1}{2}$
3	$(k, -k)$	$1 \pm \mathrm{sgn}\kappa$	$n_+ + \mathrm{sgn}\kappa$	$k = 0, j = \frac{1}{2}$
4	$(1-k, k+1)$	$1 \pm \mathrm{sgn}\kappa$	$n_+ - k + \mathrm{sgn}\kappa$	$k = \pm 1, j = \frac{1}{2}$
5	$(1-k, k+1)$	$j + 1 \pm \mathrm{sgn}\kappa$	$n_+ - k - \frac{1}{2}\mathrm{sgn}\kappa$	$k = \pm\frac{1}{2}$

Table 7.1: Permissible values for $s_\pm$ and $p_\pm$

following permissible combinations:

$$(2p_+, 2p_-) = \begin{cases} (k, k+1) & k > -\frac{1}{2} \\ (k, -k) & |k| < \frac{1}{2} \\ (1-k, k+1) & |k| < \frac{3}{2} \\ (1-k, -k) & k < \frac{1}{2} \end{cases}, \quad (2s_+, 2s_-) = \begin{cases} (j + \frac{3}{2}, j + \frac{1}{2}) & \kappa > 0 \\ (j + \frac{3}{2}, \frac{1}{2} - j) & \kappa = 1 \\ (j + \frac{1}{2}, j + \frac{3}{2}) & \kappa < 0 \\ (\frac{1}{2} - j, j + \frac{3}{2}) & \kappa = -1 \end{cases}.$$
$$(7.2.24)$$

Since both n_+ and $n_- = n_+ + (s_+ - s_-) + (p_+ - p_-)$ must be integers, some of the combinations in Eq. (7.2.24) are not compatible. Table 7.1 gives the values of n_- corresponding to each permissible combination. The first and second lines correspond to the regular and irregular modes in Ref. [26], respectively. Even though the irregular modes are divergence at spatial infinity, they are integrable and thus are part of the vector space of integrable mode solutions. When $k = \frac{1}{2}$ or $-\frac{1}{2}$, the fifth line coincides with the first or second line, respectively, hence, it can be interpreted as an extension of the latter to $k = \pm\frac{1}{2}$. The third and fourth lines do not represent solutions of the Dirac equation, as will be shown shortly. If $|k| \leq \frac{1}{2}$, both the first and the second line should be considered when constructing a full set of modes. In Ref. [26], a detailed discussion of irregular modes is avoided by only considering $k \geq \frac{1}{2}$. For completeness, both regular and irregular modes are considered in this chapter.

Using the relation (B.2), the hypergeometric function in the expression of the radial functions (7.2.21) can be replaced by Jacobi polynomials, introduced in Appendix B:

$$\hat{f}_{E,\kappa}^{(\pm)} = N_\pm \left(\frac{1-z}{2}\right)^{s_\pm} \left(\frac{1+z}{2}\right)^{p_\pm} P_{n_\pm}^{(2s_\pm - \frac{1}{2}, 2p_\pm - \frac{1}{2})}(z), \qquad (7.2.25)$$

where $z = \cos 2\omega r$ and the constants in Eq. (B.2) have been absorbed in the new normalisation constant $N_\pm$. The unit norm condition (7.2.22) places the following constraint on the absolute value of the normalisation constants $N_\pm$:

$$|N_+|^2 \frac{\Gamma(n_+ + 2s_+ + \frac{1}{2})\Gamma(n_+ + 2p_+ + \frac{1}{2})}{n_+!\Gamma(n_+ + 2s_+ + 2p_+)} + |N_-|^2 \frac{\Gamma(n_- + 2s_- + \frac{1}{2})\Gamma(n_- + 2p_- + \frac{1}{2})}{n_-!\Gamma(n_- + 2s_- + 2p_-)}$$
$$= 2\omega\varepsilon. \quad (7.2.26)$$

The normalisation constants N_+ and N_- are related through the Dirac equation (7.2.16), which reduces to the following system:

$$N_+ \left[(1-z)(k - 2p_+) + (1+z)(\kappa + 2s_+) - 2(1-z)(1+z)\frac{d}{dz} \right] P_{n_+}^{(2s_+ - \frac{1}{2}, 2p_+ - \frac{1}{2})}(z)$$

$$= 2N_-(\varepsilon + k - \kappa) \left(\frac{1-z}{2} \right)^{s_- - s_+ + \frac{1}{2}} \left(\frac{1+z}{2} \right)^{p_- - p_+ + \frac{1}{2}} P_{n_-}^{(2s_- - \frac{1}{2}, 2p_- - \frac{1}{2})}(z), \quad (7.2.27\text{a})$$

$$N_- \left[(1-z)(-k - 2p_-) + (1+z)(-\kappa + 2s_-) - 2(1-z)(1+z)\frac{d}{dz} \right]$$

$$\times P_{n_-}^{(2s_- - \frac{1}{2}, 2p_- - \frac{1}{2})}(z)$$

$$= 2N_+(-\varepsilon + k - \kappa) \left(\frac{1-z}{2} \right)^{s_+ - s_- + \frac{1}{2}} \left(\frac{1+z}{2} \right)^{p_+ - p_- + \frac{1}{2}} P_{n_+}^{(2s_+ - \frac{1}{2}, 2p_+ - \frac{1}{2})}(z).$$

$$(7.2.27\text{b})$$

The above equations can be used together with Eqs. (B.9) and Eq. (7.2.26) to find $N_\pm$ up to an arbitrary phase for any of the permissible combinations of $p_\pm$ and $s_\pm$ listed in Table 7.1. In the following, the normalisation constants $N_\pm$ introduced in Eq. (7.2.25) are calculated for each entry in Table 7.1.

Line 1, $\kappa > 0$: $(2p_+, 2p_-, 2s_+, 2s_-, n_-) = (k, k+1, j+\frac{3}{2}, j+\frac{1}{2}, n_+)$.

Since in this case, $-\kappa + 2s_- = 0$, it is convenient to use Eq. (7.2.27b) to obtain the following relation between N_- and N_+:

$$N_- = N_+ \frac{n_+ + j + 1}{n_+ + k + \frac{1}{2}}. \tag{7.2.28}$$

Substituting N_- into Eq. (7.2.26) gives:

$$N_\pm = \eta\sqrt{2\omega} \sqrt{\frac{n_+! \Gamma(n_+ + k + j + \frac{3}{2})}{\Gamma(n_+ + j + 1)\Gamma(n_+ + k + \frac{1}{2})}} \left(\frac{n_+ + k + \frac{1}{2}}{n_+ + j + 1} \right)^{\pm \frac{1}{2}}, \tag{7.2.29}$$

where η is an arbitrary phase.

Line 1, $\kappa < 0$: $(2p_+, 2p_-, 2s_+, 2s_-, n_-) = (k, k+1, j+\frac{1}{2}, j+\frac{3}{2}, n_+ - 1)$.

Since $\kappa + 2s_+ = 0$, Eq. (7.2.27a) can be used to show that $N_- = -N_+$, thus Eq. (7.2.26) gives:

$$N_\pm = \pm\eta\sqrt{2\omega} \sqrt{\frac{n_+! \Gamma(n_+ + k + j + \frac{3}{2})}{\Gamma(n_+ + j + 1)\Gamma(n_+ + k + \frac{1}{2})}}. \tag{7.2.30}$$

Line 2, $\kappa > 0$: $(2p_+, 2p_-, 2s_+, 2s_-, n_-) = (1 - k, -k, j + \frac{3}{2}, j + \frac{1}{2}, n_+ + 1)$.

Equation (7.2.27b) shows that $N_+ = N_-$. The normalisation constants can be found using Eq. (7.2.26):

$$N_\pm = \eta\sqrt{2\omega}\sqrt{\frac{(n_+ + 1)!\Gamma(n_+ - k + j + \frac{5}{2})}{\Gamma(n_+ + j + 2)\Gamma(n_+ - k + \frac{3}{2})}}. \tag{7.2.31}$$

Line 2, $\kappa < 0$: $(2p_+, 2p_-, 2s_+, 2s_-, n_-) = (1 - k, -k, j + \frac{1}{2}, j + \frac{3}{2}, n_+)$.

The relation between N_+ and N_- is in this case:

$$N_- = -N_+ \frac{n_+ - k + \frac{1}{2}}{n_+ + j + 1}, \tag{7.2.32}$$

thus the normalisation constants are given by:

$$N_\pm = \pm\eta\sqrt{2\omega}\sqrt{\frac{n_+!\Gamma(n_+ - k + j + \frac{3}{2})}{\Gamma(n_+ + j + 1)\Gamma(n_+ - k + \frac{1}{2})}} \left(\frac{n_+ + j + 1}{n_+ - k + \frac{1}{2}}\right)^{\pm\frac{1}{2}}. \tag{7.2.33}$$

Line 3, $\kappa > 0$: $(2p_+, 2p_-, 2s_+, 2s_-, n_-) = (0, 0, 2, 0, n_+ + 1)$.

Choosing $z = 1$ in Eq. (7.2.27b) shows that:

$$- 2N_- P_{n_+ + 1}^{(-\frac{1}{2}, -\frac{1}{2})}(1) = 0, \tag{7.2.34}$$

implying that:

$$N_+ \left[3 - 2(1 - z)\frac{d}{dz}\right] P_{n_+}^{(\frac{3}{2}, -\frac{1}{2})} = 0 \tag{7.2.35}$$

for all values of z. Hence, $N_\pm = 0$, showing that the combination considered here does not represent a valid solution of the Dirac equation.

Line 3, $\kappa < 0$: $(2p_+, 2p_-, 2s_+, 2s_-, n_-) = (0, 0, 0, 2, n_+ - 1)$.

Choosing $z = 1$ in Eq. (7.2.27a) shows that:

$$- N_+ P_{n_+}^{(-\frac{1}{2}, -\frac{1}{2})}(1) = 0, \tag{7.2.36}$$

implying again that $N_\pm = 0$.

Line 4, $\kappa > 0$: $(2p_+, 2p_-, 2s_+, 2s_-, n_-) = (1 - k, 1 + k, 2, 0, n_+ + 1 - k)$.

Setting $z = 1$ in Eq. (7.2.27b) gives

$$- 2N_- P_{n_+ + 1 - k}^{(-\frac{1}{2}, \frac{1}{2} + k)}(1) = 0. \tag{7.2.37}$$

Hence, $N_- = 0$.

Line 4, $\kappa < 0$: $(2p_+, 2p_-, 2s_+, 2s_-, n_-) = (1 - k, 1 + k, 0, 2, n_+ - 1 - k)$.

Substituting $z = 1$ in Eq. (7.2.27a) shows that

$$- 2N_+ P_{n_+}^{(-\frac{1}{2}, \frac{1}{2} - k)}(z) = 0. \tag{7.2.38}$$

Line 5:   As discussed previously, line 5 is just an extension of lines 1 and 2 to $k = \pm\frac{1}{2}$.

Having found the normalisation constants above, the mode solutions are fully determined. The negative energy spinors $V_{E,j,m,\kappa} = i\hat{\gamma}^2(U_{E,j,m,\kappa})^*$ can be obtained from Eq. (7.2.7) through charge conjugation (3.3.21):

$$V_{E,j,m,\kappa} = \omega r \frac{(\cos \omega r)^{\frac{3}{2}}}{\sin \omega r} \widetilde{V}_{E,j,m,\kappa},$$

$$\widetilde{V}_{E,j,m,\kappa} = i \operatorname{sgn}\kappa (-1)^{m - \frac{1}{2}} e^{iEt} \frac{1}{r} \left[f_{E,\kappa}^{(+)*} \Phi_{-\kappa,-m}^- + f_{E,\kappa}^{(-)*} \Phi_{-\kappa,-m}^+ \right]. \tag{7.2.39}$$

The following property was used:

$$i\gamma^2 \left(\Phi_{\kappa,m}^{\pm} \right)^* = i \operatorname{sgn}\kappa (-1)^{m_j - \frac{1}{2}} \Phi_{-\kappa,-m}^{\mp}. \tag{7.2.40}$$

Thus, the field operator for the Dirac field can be written as follows:

$$\psi(x) = \sum_{n_+=0}^{\infty} \sum_{j=-\infty}^{\infty} \sum_{m=-j}^{j} \sum_{\kappa=\pm(j+\frac{1}{2})} \left[U_{E,j,\kappa,m}(x) b_{E,j,\kappa,m} + V_{E,j,\kappa,m}(x) d_{E,j,\kappa,m}^{\dagger} \right], \tag{7.2.41}$$

where the sum over j goes over all odd half-integers $\pm\frac{1}{2}$, $\pm\frac{3}{2}$, ... Second quantisation is performed by promoting the constants $b_{E,j,\kappa,m}$ and $d_{E,j,\kappa,m}^{\dagger}$ to particle annihilation and anti-particle creation operators obeying canonical anti-commutation relations:

$$\left\{ b_{E,j,\kappa,m}, b_{E',j',\kappa',m'}^{\dagger} \right\} = \left\{ d_{E,j,\kappa,m}, d_{E',j',\kappa',m'}^{\dagger} \right\} = \delta_{E,E'} \delta_{j,j'} \delta_{\kappa,\kappa'} \delta_{m,m'}. \tag{7.2.42}$$

All other anti-commutators vanish.

7.3   Two-point functions

The maximal symmetry of adS greatly simplifies the form of two-point functions. As argued in Ref. [56], the Feynman propagator can be written in the form:

$$S_F(x, x') = (\alpha_F + \beta_F \slashed{n}) \Lambda(x, x'), \tag{7.3.1}$$

where α_F and β_F are functions of the geodetic interval s (7.1.25) only, $\slashed{n}$ is the contraction of the tangent $n = ds$ to the geodesic connecting x and x' with the

γ matrices, and $\Lambda(x, x')$ is the bi-spinor of parallel transport (2.2.56), given by Eq. (7.1.69a) on adS. For consistency, two methods of constructing the Feynman propagator are presented: a mode sum approach in subsection 7.3.1 and solving the inhomogeneous Dirac equation directly in subsection 7.3.3 [56]. The mode sum approach has the advantage of being easily applicable to thermal (subsection 7.5.2) or rotating thermal (subsection 8.3.1) states. The geometric approach can provide simpler and more easily interpretable algebraic expressions, but unfortunately we have not been able to apply it to the case of rotating thermal states when the rotation of the space-time is large enough to pull the speed of light surface (SOL) at $r\omega \leq \frac{\pi}{2}$.

7.3.1 Using mode sums

As presented in subsection 2.2.6, the Hadamard, Schwinger and Feynman two-point functions can be constructed using the Wightman functions $S^{\pm}(x, x')$ (2.2.48). Using the anti-commutation relations (7.2.42), the Wightman functions can be written as mode sums over direct products of four-spinors:

$$S^{\pm} = \frac{\omega^2(\cos\omega r \cos\omega r')^{\frac{3}{2}}}{\sin\omega r \sin\omega r'} \sum_{n_+=0}^{\infty} \sum_{j,\kappa,m} e^{\mp iE\Delta t} \begin{pmatrix} f^{\pm}f^{\pm}\psi_{\pm}\otimes\psi_{\pm}^{\dagger} & -if^{\pm}f^{\mp}\psi_{\pm}\otimes\psi_{\mp}^{\dagger} \\ -if^{\mp}f^{\pm}\psi_{\mp}\otimes\psi_{\pm}^{\dagger} & -f^{\mp}f^{\mp}\psi_{\mp}\otimes\psi_{\mp}^{\dagger} \end{pmatrix},$$

$$(7.3.2)$$

where the following conventions have been used: $f^{\pm} \equiv f_{E,\kappa}^{\pm}$ are the radial functions introduced in Eq. (7.2.7b) and $\psi_{\pm} \equiv \psi_{j\pm\frac{1}{2}\mathrm{sgn}\kappa}^{m}$ are the two spinors introduced in Eq. (7.2.8b). In products of two functions, the first one depends on x and the second, on x', e.g. $f^{-}f^{+} \equiv f_{E,\kappa}^{-}(r)f_{E,\kappa}^{+}(r')$ and $\psi_{+}\otimes\psi_{-}^{\dagger} \equiv \psi_{j+\frac{1}{2}\mathrm{sgn}\kappa}^{m}(\theta, \varphi) \otimes \psi_{j-\frac{1}{2}\mathrm{sgn}\kappa}^{m\dagger}(\theta', \varphi')$.

The next step is to write out explicitly the terms in the sum over κ, then perform the summation over m using the formulae (C.4.2):

$$S^{\pm}(x, x') = \frac{\omega^2}{4\pi} \frac{(\cos\omega r \cos\omega r')^{\frac{3}{2}}}{\sin\omega r \sin\omega r'} \sum_{n_+,j} s^{\pm}(x, x'), \qquad (7.3.3\mathrm{a})$$

where $s^{\pm}$ is given by:

$$s^{\pm}(x, x') = \begin{pmatrix} e^{\mp iE_{\pm}\Delta t}f_{\pm}^{\pm}f_{\pm}^{\pm} & -ie^{\mp iE_{\mp}\Delta t}f_{\mp}^{\pm}f_{\mp}^{\mp}\frac{\boldsymbol{x}\cdot\boldsymbol{\sigma}}{r} \\ -ie^{\mp iE_{\pm}\Delta t}f_{\pm}^{\mp}f_{\pm}^{\pm}\frac{\boldsymbol{x}\cdot\boldsymbol{\sigma}}{r} & -e^{\mp iE_{\mp}\Delta t}f_{\mp}^{\mp}f_{\mp}^{\mp} \end{pmatrix} \otimes (j+\tfrac{1}{2}-\boldsymbol{\sigma}\cdot\boldsymbol{L})P_{j+\frac{1}{2}}(\cos\gamma)$$

$$+ \begin{pmatrix} e^{\mp iE_{\mp}\Delta t}f_{\mp}^{\pm}f_{\mp}^{\mp} & -ie^{\mp iE_{\pm}\Delta t}f_{\pm}^{\pm}f_{\pm}^{\mp}\frac{\boldsymbol{x}\cdot\boldsymbol{\sigma}}{r} \\ -ie^{\mp iE_{\mp}\Delta t}f_{\mp}^{\mp}f_{\mp}^{\pm}\frac{\boldsymbol{x}\cdot\boldsymbol{\sigma}}{r} & -e^{\mp iE_{\pm}\Delta t}f_{\pm}^{\mp}f_{\pm}^{\pm} \end{pmatrix} \otimes (j+\tfrac{1}{2}+\boldsymbol{\sigma}\cdot\boldsymbol{L})P_{j-\frac{1}{2}}(\cos\gamma),$$

$$(7.3.3\mathrm{b})$$

where $P_{j\pm\frac{1}{2}}(\cos\gamma)$ are Legendre polynomials (discussed in section C.1 of the appendix) and γ is the angle between $\boldsymbol{x}$ and $\boldsymbol{x}'$, introduced in Eq. (7.1.25). The

subscripts on f and E refer to the sign of κ, e.g. $f_-^+ \equiv f_{E_-,-j-\frac{1}{2}}^+$ and $E_\pm =$ represent the energies corresponding to $\kappa = \pm(j+\frac{1}{2})$, through Eqs. (7.2.17) and (7.2.23). The arguments of the radial functions follow the same convention used in Eq. (7.3.2).

According to the ansatz (7.3.1) the Feynman propagator depends on r or r' only through s, $\not{n}$ and Λ. Its form for general coordinates x and x' can thus be inferred from its expression when $r' = 0$, in which case Eq. (7.3.3a) simplifies considerably. In what follows, the Feynman propagator is calculated separately for regular and irregular modes.

Regular modes

The construction of the Feynman propagator for arbitrary point separations is considerably simpler by first one of the points at the origin. In the limit of vanishing r, the hatted radial functions introduced in Eq. (7.2.16) of the regular modes corresponding to the first line of Table 7.1 have the following form:

$$\hat{f}_+^+ \sim (\sin\omega r)^{j+\frac{3}{2}} \frac{\eta\sqrt{2\omega}}{\Gamma(j+2)}(n_+ + k + \tfrac{1}{2})\sqrt{\frac{\Gamma(n_+ + j + 2)\Gamma(n_+ + j + k + \frac{3}{2})}{n_+!\,\Gamma(n_+ + k + \frac{3}{2})}},$$

$$\hat{f}_-^+ \sim (\sin\omega r)^{j+\frac{1}{2}} \frac{\eta\sqrt{2\omega}}{\Gamma(j+1)}\sqrt{\frac{\Gamma(n_+ + j + 1)\Gamma(n_+ + j + k + \frac{3}{2})}{n_+!\,\Gamma(n_+ + k + \frac{1}{2})}},$$

$$\hat{f}_+^- \sim (\sin\omega r)^{j+\frac{1}{2}} \frac{\eta\sqrt{2\omega}}{\Gamma(j+1)}\sqrt{\frac{\Gamma(n_+ + j + 2)\Gamma(n_+ + j + k + \frac{3}{2})}{n_+!\,\Gamma(n_+ + k + \frac{3}{2})}},$$

$$\hat{f}_-^- \sim (\sin\omega r)^{j+\frac{3}{2}} \frac{\eta\sqrt{2\omega}}{\Gamma(j+2)}n_+\sqrt{\frac{\Gamma(n_+ + j + 1)\Gamma(n_+ + j + k + \frac{3}{2})}{n_+!\,\Gamma(n_+ + k + \frac{1}{2})}}. \tag{7.3.4}$$

Using Eq. (7.2.16) to express $f^\pm$ in terms of $\hat{f}^\pm$, at $r = 0$ the former take the form:

$$\frac{1}{\sin\omega r}f_+^+ \xrightarrow{r\to 0} 0,$$

$$\frac{1}{\sin\omega r}f_-^+ \xrightarrow{r\to 0} 2\eta\sqrt{\frac{2\omega}{\pi}}\sqrt{\frac{\Gamma(n_+ + \frac{3}{2})\Gamma(n_+ + k + 2)}{n_+!\,\Gamma(n_+ + k + \frac{1}{2})}}\,\delta_{j,\frac{1}{2}},$$

$$\frac{1}{\sin\omega r}f_+^- \xrightarrow{r\to 0} 2\eta\sqrt{\frac{2\omega}{\pi}}\sqrt{\frac{\Gamma(n_+ + \frac{5}{2})\Gamma(n_+ + k + 2)}{n_+!\,\Gamma(n_+ + k + \frac{3}{2})}}\,\delta_{j,\frac{1}{2}},$$

$$\frac{1}{\sin\omega r}f_-^- \xrightarrow{r\to 0} 0. \tag{7.3.5}$$

Given that all the terms of the form $f_\pm^\pm$ vanish when $r' = 0$, the terms multiplying $P_{j+\frac{1}{2}}(\cos\gamma)$ in Eq. (7.3.3b) do not contribute. In what follows, the non-vanishing contributions to the Feynman propagator are evaluated term by term, starting from

the following building blocks:

$$\sum_{n_+=0}^{\infty} e^{\mp iE_+\Delta t}\frac{\hat{f}_+^+ f_+^{-*}}{\sin\omega r'} \xrightarrow[r'\to 0]{} e^{\mp\frac{i}{2}\omega\Delta t}\tan^2\omega r\,\chi^{\frac{3}{2}}\frac{d}{d\chi}\mathcal{H}_+,$$

$$\sum_{n_+=0}^{\infty} e^{\mp iE_+\Delta t}\frac{\hat{f}_+^- f_+^{-*}}{\sin\omega r'} \xrightarrow[r'\to 0]{} \tan\omega r\left[\frac{e^{\pm\frac{i}{2}\omega\Delta t}}{\cos\omega r}\left(-\frac{1+k}{2}+\chi\frac{d}{d\chi}\right)-e^{\mp\frac{i}{2}\omega\Delta t}\chi^{\frac{3}{2}}\frac{d}{d\chi}\right]\mathcal{H}_+,$$

$$\sum_{n_+=0}^{\infty} e^{\mp iE_-\Delta t}\frac{\hat{f}_-^+ f_-^{+*}}{\sin\omega r'} \xrightarrow[r'\to 0]{} e^{\mp\frac{i}{2}\omega\Delta t}\tan\omega r\left[\frac{1+k}{2}\pm i\tan\omega(\Delta t)\chi\frac{d}{d\chi}\right]\mathcal{H}_+,$$

$$\sum_{n_+=0}^{\infty} e^{\mp iE_-\Delta t}\frac{\hat{f}_-^- f_-^{+*}}{\sin\omega r'} \xrightarrow[r'\to 0]{} -e^{\mp\frac{i}{2}\omega\Delta t}\tan^2\omega r\left(-\frac{1+k}{2}+\chi\frac{d}{d\chi}\right)\mathcal{H}_+, \tag{7.3.6}$$

where the arguments of the radial functions on the left hand side above follow the convention introduced in Eq. (7.3.2) and $\mathcal{H}_+$ is given by:

$$\mathcal{H}_\pm = \frac{4\omega}{\sqrt{\pi}}\frac{\Gamma(1\pm k)}{2^{1\pm k}\Gamma(\frac{1}{2}\pm k)}\chi^{\frac{1\pm k}{2}}{}_2F_1\left(\frac{1\pm k}{2},\frac{2\pm k}{2};\frac{1}{2}\pm k;\chi\right), \tag{7.3.7}$$

where $\mathcal{H}_-$ has been introduced in anticipation for the construction of the Feynman propagator using irregular modes. Finally, χ is defined as:

$$\chi = \left(\frac{\cos\omega r}{\cos\omega\Delta t}\right)^2 \tag{7.3.8}$$

and is related to the geodetic interval s, defined in Eq. (7.1.25), through:

$$\chi = \left.\frac{1}{\cos^2\omega s}\right|_{r'=0}. \tag{7.3.9}$$

Irregular modes

In the case when $k < \frac{1}{2}$, the contributions coming from irregular modes corresponding to the second line in Table 7.1 must be considered. Repeating the analysis for

the regular modes, the leading behaviour of $\hat{f}^{\pm}$ as r goes to 0 is:

$$\hat{f}_+^+ \sim (\sin \omega r)^{j+\frac{3}{2}} \frac{\eta\sqrt{2\omega}}{\Gamma(j+2)} (n_+ + 1) \sqrt{\frac{\Gamma(n_+ + j + 2)\Gamma(n_+ + j - k + \frac{5}{2})}{n_+!\Gamma(n_+ - k + \frac{3}{2})}},$$

$$\hat{f}_-^+ \sim (\sin \omega r)^{j+\frac{1}{2}} \frac{\eta\sqrt{2\omega}}{\Gamma(j+1)} \sqrt{\frac{\Gamma(n_+ + j + 2)\Gamma(n_+ + j - k + \frac{3}{2})}{n_+!\Gamma(n_+ - k + \frac{3}{2})}},$$

$$\hat{f}_+^- \sim (\sin \omega r)^{j+\frac{1}{2}} \frac{\eta\sqrt{2\omega}}{\Gamma(j+1)} \sqrt{\frac{\Gamma(n_+ + j + 2)\Gamma(n_+ + j - k + \frac{5}{2})}{(n_+ + 1)!\Gamma(n_+ - k + \frac{3}{2})}},$$

$$\hat{f}_-^- \sim - (\sin \omega r)^{j+\frac{3}{2}} \frac{\eta\sqrt{2\omega}}{\Gamma(j+2)} (n_+ - k + \tfrac{1}{2}) \sqrt{\frac{\Gamma(n_+ + j + 2)\Gamma(n_+ + j - k + \frac{3}{2})}{n_+!\Gamma(n_+ - k + \frac{3}{2})}},$$

$$(7.3.10)$$

giving the following leading order behaviour for $f^{\pm}$:

$$\frac{1}{\sin \omega r} f_+^+ \xrightarrow[r' \to 0]{} 0,$$

$$\frac{1}{\sin \omega r} f_-^+ \xrightarrow[r' \to 0]{} 2\eta\sqrt{\frac{2\omega}{\pi}} \sqrt{\frac{\Gamma(n_+ + \frac{5}{2})\Gamma(n_+ - k + 2)}{n_+!\Gamma(n_+ - k + \frac{3}{2})}} \delta_{j,\frac{1}{2}},$$

$$\frac{1}{\sin \omega r} f_+^- \xrightarrow[r' \to 0]{} 2\eta\sqrt{\frac{2\omega}{\pi}} \sqrt{\frac{\Gamma(n_+ + \frac{5}{2})\Gamma(n_+ - k + 3)}{(n_+ + 1)!\Gamma(n_+ - k + \frac{3}{2})}} \delta_{j,\frac{1}{2}},$$

$$\frac{1}{\sin \omega r} f_-^- \xrightarrow[r' \to 0]{} 0. \qquad (7.3.11)$$

Now the analogues of Eqs. (7.3.6) can be computed:

$$\sum_{n_+=0}^{\infty} e^{\mp iE_+\Delta t} \frac{\hat{f}_+^+ f_+^{-*}}{\sin \omega r'} \xrightarrow[r' \to 0]{} e^{\mp \frac{i}{2}\omega\Delta t} \tan^2 \omega r \left(-\frac{1-k}{2} + \chi \frac{d}{d\chi} \right) \mathcal{H}_-,$$

$$\sum_{n_+=0}^{\infty} e^{\mp iE_+\Delta t} \frac{\hat{f}_+^- f_+^{-*}}{\sin \omega r'} \xrightarrow[r' \to 0]{} e^{\mp \frac{i}{2}\omega\Delta t} \tan \omega r \left(\frac{1-k}{2} \pm i \tan \omega\Delta t \chi \frac{d}{d\chi} \right) \mathcal{H}_-,$$

$$\sum_{n_+=0}^{\infty} e^{\mp iE_-\Delta t} \frac{\hat{f}_+^+ f_-^{+*}}{\sin \omega r'} \xrightarrow[r' \to 0]{} \tan \omega r \left[\frac{e^{\pm \frac{i}{2}\omega\Delta t}}{\cos \omega r} \left(-\frac{1-k}{2} + \chi \frac{d}{d\chi} \right) - e^{\mp \frac{i}{2}\omega\Delta t} \chi^{\frac{3}{2}} \frac{d}{d\chi} \right] \mathcal{H}_-,$$

$$\sum_{n_+=0}^{\infty} e^{\mp iE_-\Delta t} \frac{\hat{f}_-^{-*} f_-^+}{\sin \omega r'} \xrightarrow[r' \to 0]{} - e^{\mp \frac{i}{2}\omega\Delta t} \tan^2 \omega r \, \chi^{\frac{3}{2}} \frac{d}{d\chi} \mathcal{H}_-, \qquad (7.3.12)$$

where $\mathcal{H}_-$ was introduced in Eq. (7.3.7). The similarity to Eqs. (7.3.6) is remarkable.

Result

Combining Eqs. (7.3.6) and (7.3.12) for regular modes and irregular modes, respectively, and applying Eq. (7.2.16) to switch from $\hat{f}$ to f gives:

$$\sum_{n_+=0}^{\infty} e^{-iE_-\Delta t} \frac{f_-^+ f_-^{+*}}{\sin \omega r'} \xrightarrow[r'\to 0]{} \frac{\cos \frac{\omega r}{2}}{\cos \omega r} \tan \omega r \left[e^{-\frac{i}{2}\omega\Delta t} \left(\frac{1\pm k}{2} - \chi \frac{d}{d\chi} \right) + e^{\frac{i}{2}\omega\Delta t} \chi^{\frac{3}{2}} \frac{d}{d\chi} \right] \mathcal{H}_\pm,$$

$$\sum_{n_+=0}^{\infty} e^{-iE_+\Delta t} \frac{f_+^- f_+^{-*}}{\sin \omega r'} \xrightarrow[r'\to 0]{} -\frac{\cos \frac{\omega r}{2}}{\cos \omega r} \tan \omega r \left[e^{\frac{i}{2}\omega\Delta t} \left(\frac{1\pm k}{2} - \chi \frac{d}{d\chi} \right) + e^{-\frac{i}{2}\omega\Delta t} \chi^{\frac{3}{2}} \frac{d}{d\chi} \right] \mathcal{H}_\pm,$$

$$\sum_{n_+=0}^{\infty} e^{-iE_+\Delta t} \frac{f_+^+ f_+^{-*}}{\sin \omega r'} \xrightarrow[r'\to 0]{} -\frac{\sin \frac{\omega r}{2}}{\cos \omega r} \tan \omega r \left[e^{\frac{i}{2}\omega\Delta t} \left(\frac{1\pm k}{2} - \chi \frac{d}{d\chi} \right) - e^{-\frac{i}{2}\omega\Delta t} \chi^{\frac{3}{2}} \frac{d}{d\chi} \right] \mathcal{H}_\pm,$$

$$\sum_{n_+=0}^{\infty} e^{-iE_-\Delta t} \frac{f_-^- f_-^{+*}}{\sin \omega r'} \xrightarrow[r'\to 0]{} \frac{\sin \frac{\omega r}{2}}{\cos \omega r} \tan \omega r \left[e^{-\frac{i}{2}\omega\Delta t} \left(\frac{1\pm k}{2} - \chi \frac{d}{d\chi} \right) - e^{\frac{i}{2}\omega\Delta t} \chi^{\frac{3}{2}} \frac{d}{d\chi} \right] \mathcal{H}_\pm.$$

$$(7.3.13)$$

In the above, the $+$ and $-$ signs correspond to contributions from regular and irregular modes, respectively. The sums involving $e^{iE_\kappa \Delta t}$ can be found by applying complex conjugation of the above relations, keeping in mind that the only non-real terms are the exponentials involving it. It can be checked that, at least when $r' = 0$, the Wightman functions satisfy $S^+ = -S^-$. Thus, ignoring $i\varepsilon$ terms traditionally used to control the position of the poles in two-point functions, $S^+ = S_F = \frac{1}{2}S^{(1)}$. The Wightman functions can be obtained by substituting Eqs. (7.3.13) in Eq. (7.3.3a). Keeping in mind that the $i\varepsilon$ terms are neglected, the 2×2 matrix elements (i,j) of the Feynman function can be found from the Wightman functions using Eq. (2.2.53a):

$$S_F(x, x') = \begin{pmatrix} (1,1) & (1,2) \\ (2,1) & (2,2) \end{pmatrix}, \qquad (7.3.14a)$$

where

$$(1,1) = \frac{\omega^2}{4\pi} \frac{\cos \frac{\omega r}{2}}{\cos^{\frac{1}{2}} \omega r} \left[e^{-\frac{i}{2}\omega\Delta t} \left(\frac{1\pm k}{2} - \chi \frac{d}{d\chi} \right) + e^{\frac{i}{2}\omega\Delta t} \chi^{\frac{3}{2}} \frac{d}{d\chi} \right] \mathcal{H}_\pm,$$

$$(2,2) = \frac{\omega^2}{4\pi} \frac{\cos \frac{\omega r}{2}}{\cos^{\frac{1}{2}} \omega r} \left[e^{\frac{i}{2}\omega\Delta t} \left(\frac{1\pm k}{2} - \chi \frac{d}{d\chi} \right) + e^{-\frac{i}{2}\omega\Delta t} \chi^{\frac{3}{2}} \frac{d}{d\chi} \right] \mathcal{H}_\pm,$$

$$(1,2) = i\frac{\boldsymbol{x}\cdot\boldsymbol{\sigma}}{r} \frac{\omega^2}{4\pi} \frac{\sin \frac{\omega r}{2}}{\cos^{\frac{1}{2}} \omega r} \left[e^{\frac{i}{2}\omega\Delta t} \left(\frac{1\pm k}{2} - \chi \frac{d}{d\chi} \right) - e^{-\frac{i}{2}\omega\Delta t} \chi^{\frac{3}{2}} \frac{d}{d\chi} \right] \mathcal{H}_\pm,$$

$$(2,1) = -i\frac{\boldsymbol{x}\cdot\boldsymbol{\sigma}}{r} \frac{\omega^2}{4\pi} \frac{\sin \frac{\omega r}{2}}{\cos^{\frac{1}{2}} \omega r} \left[e^{-\frac{i}{2}\omega\Delta t} \left(\frac{1\pm k}{2} - \chi \frac{d}{d\chi} \right) - e^{\frac{i}{2}\omega\Delta t} \chi^{\frac{3}{2}} \frac{d}{d\chi} \right] \mathcal{H}_\pm.$$

$$(7.3.14b)$$

Hence, the contributions $S_F^\pm(x, x')$ to the Feynman propagator coming from the regular $(+)$ and irregular $(-)$ modes can be written as:

$$S_F^\pm(x, x') = 2\omega \left[S_\pm \left(\frac{1 \pm k}{2} - \chi \frac{d}{d\chi} \right) + S_\mp \chi^{\frac{3}{2}} \frac{d}{d\chi} \right] [-iG_F^\pm(x, x')], \qquad (7.3.15\text{a})$$

where

$$S_\pm = \frac{1}{\sqrt{\cos \omega r}} \begin{pmatrix} \cos \frac{\omega r}{2} e^{\mp \frac{i}{2}\omega\Delta t} & \pm i \sin \frac{\omega r}{2} e^{\pm \frac{i}{2}\omega\Delta t} \frac{\boldsymbol{x} \cdot \boldsymbol{\sigma}}{r} \\ \mp i \sin \frac{\omega r}{2} e^{\mp \frac{i}{2}\omega\Delta t} \frac{\boldsymbol{x} \cdot \boldsymbol{\sigma}}{r} & \cos \frac{\omega r}{2} e^{\pm \frac{i}{2}\omega\Delta t} \end{pmatrix}, \qquad (7.3.15\text{b})$$

where $G_F^\pm$ are the Feynman propagators of the scalar field [49, 50] corresponding to the mass parameters $\mathfrak{k} \equiv \mathfrak{k}_\pm = 1 \pm k$ (using the notation therein), which can be related to the functions $\mathcal{H}_\pm$ in Eq. (7.3.7) through:

$$\mathcal{H}_\pm = \frac{8\pi}{\omega}(-iG_F^\pm). \qquad (7.3.16)$$

The functions $S_\pm$, defined in Eq. (7.3.15b), can be written in terms of the bi-spinor of parallel transport Λ discussed in subsection 7.1.4, using Eqs. (7.1.53) and (7.1.54):

$$S_\pm(x, x') = \left(\cos \frac{\omega s}{2} \mp i \sin \frac{\omega s}{2} \slashed{n} \right) \Lambda(x, x'), \qquad (7.3.17)$$

where the relation $\cos \frac{\omega s}{2} = [(1 + \cos \omega\Delta t / \cos \omega r)/2]^{\frac{1}{2}}$ has been used. As discussed in the introduction of this section, the Feynman propagator on maximally symmetric space-times can be written as in Eq. (7.3.1), thus depending on the coordinates x and x' only through s, $\slashed{n}$ and Λ. Hence, substituting Eq. (7.3.17) in Eq. (7.3.15a) allows the Feynman propagator to be written as follows:

$$S_F^\pm(x, x') = (\alpha_F^\pm + \beta_F^\pm \slashed{n})\Lambda(x, x'), \qquad (7.3.18)$$

where $\alpha_F^\pm$ and $\beta_F^\pm$ are functions of the geodetic interval s given by:

$$\alpha_F^\pm = \pm \frac{\omega^3 \cos \frac{\omega s}{2}}{\pi^{\frac{3}{2}} 2^{1 \pm k}} \frac{\Gamma(1 \pm k)}{\Gamma(\frac{1}{2} \pm k)} \left[\frac{1 \pm k}{2} + \chi(\sqrt{\chi} - 1)\frac{d}{d\chi} \right] \chi^{\frac{1 \pm k}{2}} {}_2F_1 \left(\tfrac{1 \pm k}{2}, \tfrac{2 \pm k}{2}; \tfrac{1}{2} \pm k; \chi \right),$$

$$\beta_F^\pm = \frac{i\omega^3 \sin \frac{\omega s}{2}}{\pi^{\frac{3}{2}} 2^{1 \pm k}} \frac{\Gamma(1 \pm k)}{\Gamma(\frac{1}{2} \pm k)} \left[-\frac{1 \pm k}{2} + \chi(\sqrt{\chi} + 1)\frac{d}{d\chi} \right] \chi^{\frac{1 \pm k}{2}} {}_2F_1 \left(\tfrac{1 \pm k}{2}, \tfrac{2 \pm k}{2}; \tfrac{1}{2} \pm k; \chi \right).$$

$$(7.3.19)$$

It can be seen that the contributions made by irregular modes $(-)$ can be related to those coming from regular modes $(+)$ by changing the sign of the mass term $k = \frac{\mu}{\omega}$, as follows:

$$\alpha_F^-(k) = -\alpha_F^+(-k), \qquad \beta_F^-(k) = \beta_F^+(-k). \qquad (7.3.20)$$

7.3.2 Small distance behaviour of two-point functions

To compute renormalised expectation values, the coincidence limit of the Feynman propagator (7.3.18) and its derivatives are required. It is convenient to extract the small distance behaviour of $\alpha_F^{\pm}$ and $\beta_F^{\pm}$ by changing the variable in the hypergeometric functions in Eqs. (7.3.19) from $\chi = (\cos \omega s)^{-2}$ to $q = \sin^2 \frac{\omega s}{2}$. This change of variable can be achieved using standard formulae [1, 60] in three stages, as follows.

Using Eq. (D.4a), the functions $\alpha_F^{\pm}$ and $\beta_F^{\pm}$ can be written as:

$$\alpha_F^{\pm} = \pm \frac{\omega^3 N_{\pm k}}{16\pi^2} \left(\cos \frac{\omega s}{2} \right)^{-3 \mp 2k} {}_2F_1 \left(\pm k, 2 \pm k; 1 \pm 2k; \frac{1}{\cos^2 \frac{\omega s}{2}} \right), \qquad (7.3.21a)$$

$$\beta_F^{\pm} = i \frac{\omega^3 N_{\pm k}}{16\pi^2} \sin \frac{\omega s}{2} \left(\cos \frac{\omega s}{2} \right)^{-4 \mp 2k} {}_2F_1 \left(1 \pm k, 2 \pm k; 1 \pm 2k; \frac{1}{\cos^2 \frac{\omega s}{2}} \right), \quad (7.3.21b)$$

with

$$N_{\pm k} = \frac{\Gamma(2 \pm k) \sqrt{\pi}}{4^{\pm k} \Gamma(\frac{1}{2} \pm k)}, \qquad (7.3.21c)$$

where Eqs. (D.3e) and (D.3d) have been used for α and β, respectively. Next, Eq. (D.4b) can be used to change the argument of the hypergeometric functions to $(\sin \frac{\omega s}{2})^{-2}$:

$$\alpha_F^{\pm} = \pm \frac{\omega^3 N_{\pm k}}{16\pi^2} \cos \frac{\omega s}{2} \left(-\sin^2 \frac{\omega s}{2} \right)^{-2 \mp k} {}_2F_1 \left(1 \pm k, 2 \pm k; 1 \pm 2k; \frac{1}{\sin^2 \frac{\omega s}{2}} \right),$$
$$(7.3.22a)$$

$$\beta_F^{\pm} = i \frac{\omega^3 N_{\pm k}}{16\pi^2} \sin \frac{\omega s}{2} \left(-\sin^2 \frac{\omega s}{2} \right)^{-2 \mp k} {}_2F_1 \left(\pm k, 2 \pm k; 1 \pm 2k; \frac{1}{\sin^2 \frac{\omega s}{2}} \right). \quad (7.3.22b)$$

Finally, Eq. (D.4c) can be used to change the argument of the hypergeometric functions to $\sin^2 \frac{\omega s}{2}$:

$$\begin{aligned} \alpha_F^{\pm} = {} & \frac{\omega^3 k(k^2 - 1)}{16\pi^2} \cos \frac{\omega s}{2} \left\{ -\frac{1}{(k^2 - 1) \sin^2 \frac{\omega s}{2}} \right. \\ & + \left[\mp \pi \cot \pi k + \ln \left(-\sin^2 \frac{\omega s}{2} \right) \right] {}_2F_1 \left(2 + k, 2 - k; 2; \sin^2 \frac{\omega s}{2} \right) \\ & + \left. \sum_{n=0}^{\infty} \frac{(2 + k)_n (2 - k)_n}{(2)_n n!} \left(\sin^2 \frac{\omega s}{2} \right)^n \Psi_n^{(-1)} \right\}, \\ \beta_F^{\pm} = {} & -\frac{i\omega^3 k^2 (k^2 - 1)}{16\pi^2} \sin \frac{\omega s}{2} \left\{ -\frac{1}{k^2 (k^2 - 1) \sin^4 \frac{\omega s}{2}} \left(1 + k^2 \sin^2 \frac{\omega s}{2} \right) \right. \\ & + \frac{1}{2} \left[\mp \pi \cot \pi k + \ln \left(-\sin^2 \frac{\omega s}{2} \right) \right] {}_2F_1 \left(2 + k, 2 - k; 3; \sin^2 \frac{\omega s}{2} \right) \\ & + \left. \frac{1}{2} \sum_{n=0}^{\infty} \frac{(2 + k)_n (2 - k)_n}{(3)_n n!} \left(\sin^2 \frac{\omega s}{2} \right)^n \left[\Psi_n^{(-1)} - \frac{1}{2 + n} \right] \right\}, \qquad (7.3.23a) \end{aligned}$$

where $(z)_n = z(z + 1) \dots (z + n)$ is the Pochhammer symbol [1, 60] and $\Psi_n^{(-1)}$ is

defined in terms of the polygamma function $\psi(z)$ [1, 60] as:

$$\Psi_n^{(-1)} = \psi(2 + k + n) + \psi(2 - k + n) - \psi(2 + n) - \psi(1 + n). \qquad (7.3.23b)$$

It should be noted that in Eqs. (7.3.23), the geodetic interval s is taken along time-like geodesics. For space-like geodesics, s would be imaginary and the arguments of the logarithms above would be positive. It can be seen that the difference between the contributions of the regular and irregular modes is regular in the coincidence limit. Alternatively, the polygamma functions in Eq. (7.3.23b) can be expressed in terms of $\pm k$, as follows:

$$
\begin{aligned}
\alpha_F^\pm =& \frac{\omega^3 k(k^2 - 1)}{16\pi^2} \cos\frac{\omega s}{2} \left\{ -\frac{1}{(k^2 - 1)\sin^2\frac{\omega s}{2}} \right. \\
& + \ln\left(-\sin^2\frac{\omega s}{2}\right) {}_2F_1\left(2 + k, 2 - k; 2; \sin^2\frac{\omega s}{2}\right) \\
& \left. + \sum_{n=0}^\infty \frac{(2 + k)_n(2 - k)_n}{(2)_n n!}\left(\sin^2\frac{\omega s}{2}\right)^n \Psi_n^\pm \right\}, \\
\beta_F^\pm =& -\frac{i\omega^3 k^2(k^2 - 1)}{16\pi^2}\sin\frac{\omega s}{2}\left\{ -\frac{1}{k^2(k^2 - 1)\sin^4\frac{\omega s}{2}}\left(1 + k^2\sin^2\frac{\omega s}{2}\right) \right. \\
& + \frac{1}{2}\ln\left(-\sin^2\frac{\omega s}{2}\right) {}_2F_1\left(2 + k, 2 - k; 3; \sin^2\frac{\omega s}{2}\right) \\
& \left. + \sum_{n=0}^\infty \frac{(2 + k)_n(2 - k)_n}{2(3)_n n!}\left(\sin^2\frac{\omega s}{2}\right)^n\left[\Psi_n^\pm - \frac{1}{2 + n}\right] \right\}, \qquad (7.3.24)
\end{aligned}
$$

where

$$\Psi_n^\pm = \psi(2 \pm k + n) + \psi(-1 \pm k - n) - \psi(2 + n) - \psi(1 + n). \qquad (7.3.25)$$

For the purpose of calculating the v.e.v. of the SET, the following expansions around $s = 0$ are needed:

$$
\begin{aligned}
\alpha_F^\pm \xrightarrow{s\to0}\ & -\frac{k\omega}{4\pi^2 s^2} \mp \frac{\omega^3}{16\pi^2}\left(1 \pm \frac{5k}{6} - k^2 \pm k^3\right) \\
& + \frac{k\omega^3}{8\pi^2}(k^2 - 1)\left\{\frac{1}{2}\ln\left[-\left(\frac{\omega s}{2}\right)^2\right] + \psi(\pm k) + \gamma\right\}, \\
\beta_F^\pm \xrightarrow{s\to0}\ & \frac{i}{2\pi^2 s^3} + \frac{i\omega^2(1 + 2k^2)}{16\pi^2 s}, \\
4i\left(\frac{\omega}{2}\cot\frac{\omega s}{2}\right)\beta_F^\pm \xrightarrow{s\to0}\ & -\frac{1}{2\pi^2 s^4} - \frac{\omega^2(1 + 6k^2)}{12\pi^2 s^2} + \frac{\omega^4}{8\pi^2}\left(\frac{17}{360} \mp \frac{k}{2} - \frac{k^2}{12} \pm \frac{k^3}{2} - \frac{3k^4}{4}\right) \\
& + \frac{\omega^4 k^2(k^2 - 1)}{8\pi^2}\left\{\frac{1}{2}\ln\left[-\left(\frac{\omega s}{2}\right)^2\right] + \gamma + \psi(\pm k) - \frac{1}{2}\ln(-4)\right\}, \\
-4i\left(\frac{\partial}{\partial s} - \frac{\omega}{2}\cot\frac{\omega s}{2}\right)\beta_F^\pm \xrightarrow{s\to0}\ & -\frac{8}{\pi^2 s^4} - \frac{\omega^2(1 + 3k^2)}{3\pi^2 s^2} + \frac{\omega^4}{2\pi^2}\left(\frac{17}{360} + \frac{k^2}{3} - \frac{k^4}{4}\right).
\end{aligned}
$$
$$\qquad (7.3.26)$$

In the massless limit, $\alpha_F^{\pm}$ and $\beta_F^{\pm}$ take the following values:

$$\alpha_F^{\pm}\big|_{k=0} = \frac{\omega^3}{16\pi^2 \cos^3 \frac{\omega s}{2}}, \qquad \beta_F^{\pm}\big|_{k=0} = \frac{i\omega^3}{16\pi^2 \sin^3 \frac{\omega s}{2}}. \tag{7.3.27}$$

It is remarkable that the above expressions are the same for regular and irregular modes.

7.3.3 Using the spinor parallel propagator

In subsection 7.3.1, an expression for the Feynman propagator at arbitrary point separation was obtained by extrapolating the result obtained for one point at the origin, based on the ansatz (7.3.1). Following Ref. [56], the inhomogeneous Dirac equation is solved directly by substituting the aforementioned ansatz into Eq. (2.2.53b), leading to the following equation:

$$\left\{ \slashed{n} \left[i\alpha_F' + i\alpha_F \frac{3}{2}(A+C) - \mu\beta_F \right] + i\beta_F' + i\beta_F \frac{3}{2}(A-C) - \mu\alpha_F \right\} \Lambda = \frac{1}{\sqrt{-g}} \delta(x-x'), \tag{7.3.28}$$

valid for any maximally symmetric space-time. On adS, A and C are given by Eqs. (7.1.35). As discussed in subsections 7.1.4 and 7.1.5, Λ only depends on products of even number of γ functions, hence, $\operatorname{tr}(\slashed{n}\Lambda) = 0$. Taking the trace of the above equation multiplied by $\slashed{n}$ shows that the coefficient of $\slashed{n}$ above has to vanish identically, leading to the following equations:

$$i\alpha_F' - \frac{3i\omega}{2} \tan \frac{\omega s}{2} \alpha_F - \mu\beta_F = 0, \tag{7.3.29a}$$

$$i\beta_F' + \frac{3i\omega}{2} \cot \frac{\omega s}{2} \beta_F - \mu\alpha_F = \frac{1}{\sqrt{-g}} \delta(x, x'). \tag{7.3.29b}$$

These two equations can be combined to form a second order differential equation for α_F:

$$\alpha_F'' + 3\omega\alpha_F' \cot \omega s + \left[\mu^2 + \frac{3\omega^2}{2} \left(\frac{\cos \omega s - 1}{\sin^2 \omega s} - \frac{3}{2} \right) \right] \alpha_F = -\mu \frac{\delta(x-x')}{\sqrt{-g}}. \tag{7.3.30}$$

Changing variable to $z = \cos^2 \frac{\omega s}{2}$ and writing $\alpha_F = z^{\frac{1}{2}} \widetilde{\alpha}_F$ puts Eq. (7.3.30) in the hypergeometric equation form (D.1):

$$\left[z(1-z) \frac{d^2}{dz^2} + (3-5z) \frac{d}{dz} + (k-2)(k+2) \right] \widetilde{\alpha}_F = -\frac{k}{\omega z^{\frac{1}{2}}} \frac{\delta(x-x')}{\sqrt{-g}}, \tag{7.3.31}$$

which agrees with the expression in Ref. [56]. Changing variable to $q = 1 - z$ puts Eq. (7.3.31) in the following form:

$$\left[q(1-q)\frac{d^2}{dq^2} + (2-5q)\frac{d}{dq} - (2-k)(2+k)\right]\widetilde{\alpha}_F = -\frac{k}{\omega(1-q)^{\frac{1}{2}}}\frac{\delta(x-x')}{\sqrt{-g}}.$$
(7.3.32)

The parameters of the hypergeometric differential equation are now $a = 2 - k$, $b = 2 + k$ and $c = 2$, and the two linearly independent solutions are [60]:

$$\alpha_F = \lambda\cos\frac{\omega s}{2}\left\{-\frac{1}{(k^2-1)q} + {}_2F_1(2-k,2+k;2;q)(\lambda' + \ln q)\right.$$
$$\left. + \sum_{n=0}^{\infty}\frac{(2+k)_n(2-k)_n}{(2)_n n!}q^n[\psi(2+k+n) + \psi(2-k+n) - \psi(2+n) - \psi(1+n)]\right\}.$$
(7.3.33)

The constants λ and λ' can be found by matching the small distance behaviour of α_F with that of the Minkowski propagator α_{Mink} [56]:

$$\alpha_{\text{Mink}} = -\left(\frac{\mu}{2\pi}\right)^2\frac{1}{s}K_1(\mu s) \xrightarrow[s\to 0]{} -\frac{\omega k}{4\pi^2 s^2}.$$
(7.3.34)

Thus, λ is given by:

$$\lambda = \frac{k\omega^3}{16\pi^2}(k^2-1).$$
(7.3.35)

Furthermore, a comparison with the expression (7.3.24) is enough to fix both constants:

$$\lambda_{\pm} = \frac{k\omega^3}{16\pi^2}(k^2-1), \qquad \lambda'_{\pm} = \mp\pi\cot\pi k,$$
(7.3.36)

where the upper and lower signs correspond to regular and irregular modes, respectively.

7.4   Renormalised vacuum expectation values

The vacuum expectation values (v.e.v.s) of the fermion condensate (FC), charge current (CC) and stress-energy tensor (SET) can be calculated using the Feynman propagator by replacing the thermal Hadamard function $\Delta S_\beta^{(1)}(x, x')$ by $2S_F(x, x')$ in Eqs. (2.2.55), as follows:

$$\langle\overline{\psi}\psi\rangle = -\lim_{x'\to x}\text{tr}\left[S_F(x,x')\Lambda(x',x)\right],$$
(7.4.1a)

$$\langle J^\mu\rangle = -\lim_{x'\to x}\text{tr}\left[\gamma^\mu S_F(x,x')\Lambda(x',x)\right],$$
(7.4.1b)

$$\langle T_{\mu\nu}\rangle = \frac{i}{2}\lim_{x'\to x}\text{tr}\left\{\left[\gamma_{(\nu}D_{\mu)}S_F(x,x') - S_F(x,x')\overleftarrow{D}_{\lambda'}\gamma_{\kappa'}g^{\lambda'}{}_{(\mu}g^{\kappa'}{}_{\nu)}\right]\Lambda(x',x)\right\}.$$
(7.4.1c)

If the ansatz (7.3.1) is made for the form of $S_F(x, x')$, the formula (7.1.42) for the derivative of Λ, together with the formulae (7.1.32a) for the differentiation of the tangent vector can be used to write the above v.e.v.s using the functions α_F and β_F:

$$\langle \overline{\psi}\psi \rangle = 4 \lim_{x' \to x} \alpha_F(s), \tag{7.4.2a}$$

$$\langle J^\mu \rangle = 4 \lim_{x' \to x} n^\mu \beta_F(s), \tag{7.4.2b}$$

$$\langle T_{\mu\nu} \rangle = 4i \lim_{x' \to x} \left[-n_\mu n_\nu \left(\frac{\partial}{\partial s} - \frac{\omega}{2} \cot \frac{\omega s}{2} \right) \beta_F + g_{\mu\nu} \frac{\omega}{2} \beta_F \cot \frac{\omega s}{2} \right]. \tag{7.4.2c}$$

The tangents to the geodesic n_μ depend on the direction along which the points are split. For consistency, their coefficients should vanish identically in the coincidence limit, since the final expressions for the v.e.v.s above must be independent of the mathematical technique employed. Thus, the v.e.v. of the CC should vanish. Furthermore, the adS symmetries imply that the FC must be a constant scalar, while the SET should be a constant multiplying the metric tensor $g_{\mu\nu}$. The above expressions are infinite due to the divergence in the coincidence limit of α_F and β_F, demonstrated in Eqs. (7.3.26). In subsections 7.4.1 and 7.4.2, the Schwinger-de Witt and Hadamard methods are applied for the renormalisation of the above expressions.

7.4.1 Schwinger-de Witt method

In the Schwinger-de Witt method, v.e.v.s are renormalised by subtracting from $S_F(x, x')$ in Eqs. (7.4.1) counter terms which are determined separately. In Ref. [24], Christensen uses covariant point splitting to calculate the divergent contributions $\mathcal{T}_{\mu\nu}^{\text{div}} \equiv \mathcal{T}_{\mu\nu}(x, x')$ to the SET as point-split tensors, using Eq. (7.4.1c). Renormalisation is performed by subtracting $\mathcal{T}_{\mu\nu}^{\text{div}}$ from the function inside the limit in Eq. (7.4.2c), after which the limit can be safely taken.

Specialising to adS reduces Christensen's expressions [24] to the following:

$$\mathcal{T}_{\mu\nu}^{\text{div}} = \mathcal{T}_{\mu\nu}^{\text{div,quartic}} + \mathcal{T}_{\mu\nu}^{\text{div,quadratic}} + \mathcal{T}_{\mu\nu}^{\text{div,ln}} + \mathcal{T}_{\mu\nu}^{\text{div,finite}}, \tag{7.4.3a}$$

where

$$\mathcal{T}_{\mu\nu}^{\text{div,quartic}} = \frac{-1}{\pi^2 s^4}(g_{\mu\nu} + 4n_\mu n_\nu),$$

$$\mathcal{T}_{\mu\nu}^{\text{div,quadratic}} = \frac{-\omega^2}{4\pi^2 s^2} \left[g_{\mu\nu} \left(\frac{1}{6} + k^2 \right) + 2n_\mu n_\nu \left(\frac{1}{3} + k^2 \right) \right],$$

$$\mathcal{T}_{\mu\nu}^{\text{div,ln}} = \frac{\omega^4}{16\pi^2} k^2(k^2 - 1)(\gamma + \ln |\mu s|)g_{\mu\nu},$$

$$\mathcal{T}_{\mu\nu}^{\text{div,fin}} = \frac{\omega^4}{4\pi^2} \left[g_{\mu\nu} \left(\frac{5}{144} - \frac{k^2}{24} - \frac{3k^4}{16} \right) + n_\mu n_\nu \left(\frac{17}{360} + \frac{k^2}{3} - \frac{k^4}{4} \right) \right], \tag{7.4.3b}$$

where γ is Euler's constant and μ is the mass of the field.

The following identities were used:

$$R^{\lambda\xi\kappa\varepsilon}R_{\lambda\xi\kappa\varepsilon} = 24\omega^4,$$
$$R^{(\mu}{}_\lambda R_{\xi\kappa}n^{\nu)}n^\lambda n^\xi n^\kappa = -9\omega^4 n^\mu n^\nu,$$
$$R^{(\mu|\alpha}{}_\lambda{}^\beta R_{\xi\alpha\kappa\beta}n^{|\nu)}n^\lambda n^\xi n^\kappa = -3\omega^4 n^\mu n^\nu,$$
$$R^\alpha{}_\lambda R^\mu{}_{\xi\alpha\kappa}n^\nu n^\lambda n^\xi n^\kappa = 0,$$
$$R_{\lambda\xi}R^\mu{}_\kappa{}^\nu{}_\varepsilon n^\lambda n^\xi n^\kappa n^\varepsilon = 3\omega^4(g^{\mu\nu}+n^\mu n^\nu),$$
$$R^\mu{}_\lambda{}^\alpha{}_\xi R^\nu{}_{\kappa\alpha\varepsilon}n^\lambda n^\xi n^\kappa n^\varepsilon = \omega^4(g^{\mu\nu}+n^\mu n^\nu),$$
$$R^\alpha{}_\lambda{}^\beta{}_\xi R_{\alpha\kappa\beta\varepsilon}n^\lambda n^\xi n^\kappa n^\varepsilon = 3\omega^4,$$
$$R^{\alpha\beta}R_\alpha{}^\mu{}_{\beta\lambda}n^\nu n^\lambda = 9\omega^4 n^\mu n^\nu,$$
$$R^{\alpha\beta\gamma\mu}R_{\alpha\beta\gamma\lambda} = 6\omega^4\delta^\mu{}_\lambda,$$
$$R^{\mu\alpha\nu\beta}R_{\alpha\lambda\beta\xi}n^\lambda n^\xi = \omega^2(-2g^{\mu\nu}+n^\mu n^\nu),$$
$$R_{\lambda\alpha}R^{\alpha(\mu\nu)}{}_\xi n^\lambda n^\xi = 3\omega^4(g^{\mu\nu}+n^\mu n^\nu),$$
$$R^{\mu\alpha\beta}{}_\lambda R^\nu{}_{\beta\alpha\xi}n^\lambda n^\xi = 3\omega^4 n^\mu n^\nu,$$
$$R^{\mu\alpha\beta}{}_\lambda R^\nu{}_{\alpha\beta\xi}n^\lambda n^\xi = \omega^4(-g^{\mu\nu}+2n^\mu n^\nu). \tag{7.4.4}$$

The renormalised v.e.v. of the SET can be calculated separately for regular $(+)$ and irregular $(-)$ modes by subtracting $\mathcal{T}_{\mu\nu}^{\text{div}}$ from the coincidence limit expansions (7.3.26) of the terms appearing in Eq. (7.4.2c). The coefficient of $n_\mu n_\nu$ vanishes identically, which is in agreement with the geometrical argument that $T_{\mu\nu}$ should be proportional to $g_{\mu\nu}$ in a maximally symmetric space-time. Therefore, the renormalised expectation value of the SET can be written in terms of its trace T as:

$$\langle T_{\mu\nu}\rangle_{\text{SdW}}^\pm = \frac{1}{4}g_{\mu\nu}\langle T\rangle_{\text{SdW}}^\pm, \tag{7.4.5}$$

where

$$\langle T\rangle_{\text{SdW}}^\pm = -\frac{\omega^4}{4\pi^2}\left\{\frac{11}{60}\pm k - \frac{k^2}{6}\mp k^3 + 2k^2(k^2-1)\left[\ln\frac{2\mu}{\omega}-\psi(\pm k)\right]\right\}. \tag{7.4.6}$$

The result (7.4.6) can be compared with the trace $T_{\text{P-V}}$ of the renormalised expectation value $\langle T_{\mu\nu}\rangle_{\text{P-V}}$ of the SET obtained using the Pauli-Villars regularisation method in Ref. [18]:

$$T_{\text{P-V}} = -\frac{\omega^4}{4\pi^2}\left\{\frac{11}{60}+k-\frac{k^2}{6}-k^3+2k^2(k^2-1)\left[\ln\frac{\nu}{\omega}-\psi(k)\right]\right\}, \tag{7.4.7}$$

where ν is an arbitrary renormalisation mass scale. The agreement with Eq. (7.4.6) is excellent if only regular modes are considered.

7.4.2 Hadamard renormalisation

A series of theorems by Hadamard [3, 58] for the scalar field allow the unambiguous isolation of the singular part of the scalar field propagator in a state-independent fashion. This approach, extended to fermions in Refs. [42, 59], can be used to isolate the singular part of the Feynman propagator $S_F(x, x')$ into the Hadamard form $S_H(x, x')$. Thus, a regularised propagator $S_{\text{reg}}(x, x')$ can be obtained as the remainder of $S_F(x, x')$ after the subtraction of its singular elements:

$$S_{\text{reg}}(x, x') = S_F(x, x') - S_H(x, x'). \tag{7.4.8}$$

Hadamard renormalisation is performed by replacing S_F by S_{reg} in Eqs. (7.4.1).

The first step towards using the powerful Hadamard theorems is to introduce an auxiliary bi-spinor function $\mathcal{G}_F$ [24, 59], by analogy with the flat space-time, such that:

$$S_F(x, x') = (i\gamma^\mu D_\mu + \mu)\mathcal{G}_F(x, x'). \tag{7.4.9}$$

By acting with the Dirac operator $i\slashed{D} - \mu$ on S_F, the following equation is obtained:

$$\left(\Box - \frac{1}{2}[\gamma^\mu, \gamma^\nu] D_{[\mu} D_{\nu]} - \mu^2\right)\mathcal{G}_F = (-g)^{-\frac{1}{2}}\delta^{\mathfrak{n}}(x, x'), \tag{7.4.10}$$

where $\mathfrak{n}$ is the number of space-time dimensions and the spinor box operator $\Box$ is defined by analogy with the scalar case as:

$$\Box \equiv g^{\mu\nu} D_\mu D_\nu. \tag{7.4.11}$$

Analogously to the commutator of ordinary (tensor) covariant derivatives, the commutator $[D_\mu, D_\nu]$ can be written for any number of space-time dimensions using the Riemann tensor [24]:

$$[D_\mu, D_\nu]\mathcal{G}_F(x, x') = -\frac{1}{2}R_{\rho\lambda\mu\nu}\Sigma^{\rho\lambda}\mathcal{G}_F(x, x'), \tag{7.4.12}$$

where $\Sigma^{\rho\lambda} = \frac{1}{4}[\gamma^\rho, \gamma^\lambda]$ are the anti-Hermitian spin part of the generators of Lorentz transformations. Due to the symmetry $R_{\rho\lambda\mu\nu} = R_{\mu\nu\rho\lambda}$, the commutator term in Eq. (7.4.10) can be written as:

$$\frac{1}{2}[\gamma^\mu, \gamma^\nu] D_{[\mu} D_{\nu]} = -\frac{1}{8}R_{\rho\lambda\mu\nu}\left\{\Sigma^{\rho\lambda}, \Sigma^{\mu\nu}\right\}, \tag{7.4.13}$$

where the anticommutator of the Σ matrices can be written as:

$$\left\{\Sigma^{\rho\lambda}, \Sigma^{\mu\nu}\right\} = -\frac{1}{2}(g^{\rho\mu}g^{\lambda\nu} - g^{\rho\nu}g^{\lambda\mu}) + \frac{i}{2}\varepsilon^{\rho\lambda\mu\nu}\gamma^{\hat{5}}, \tag{7.4.14}$$

where

$$\varepsilon^{\rho\lambda\mu\nu} = e^{\rho}_{\hat{\alpha}} e^{\lambda}_{\hat{\beta}} e^{\mu}_{\hat{\gamma}} e^{\nu}_{\hat{\rho}} \varepsilon^{\hat{\alpha}\hat{\beta}\hat{\gamma}\hat{\rho}} \tag{7.4.15}$$

is written in terms of the Levi-Civita symbol $\varepsilon^{\hat{\alpha}\hat{\beta}\hat{\gamma}\hat{\rho}}$, with the convention $\varepsilon_{\hat{0}\hat{1}\hat{2}\hat{3}} = 1$. Finally, the Bianchi identity $R_{\rho[\lambda\mu\nu]} = 0$ can be used to show that $\mathcal{G}_F$ satisfies the following equation [59], irrespective of the number $\mathfrak{n}$ of space-time dimensions:

$$\left(\Box - \tfrac{1}{4}R - \mu^2\right)\mathcal{G}_F(x, x') = (-g)^{-\frac{1}{2}}\delta^{\mathfrak{n}}(x, x'). \tag{7.4.16}$$

It can be shown by using Eq. (7.1.42) that, if $S_F = (\alpha_F + \beta_F \not{\!s})\Lambda$, then:

$$\mathcal{G}_F(x, x') = \frac{\alpha_F(s)}{\omega k}\Lambda(x, x'). \tag{7.4.17}$$

Equation (7.4.16) can be written as a set of 16 scalar second order differential equations involving the matrix elements of the auxiliary propagator $\mathcal{G}_F(x, x')$. As discussed in Ref. [59], extrapolating Hadamard's theorem to the spinor case allows the singularity structure of $\mathcal{G}_F$ to be isolated as follows:

$$\mathcal{G}_F(x, x') = \frac{1}{8\pi^2}\left(\frac{u}{\sigma} + v\ln(\nu^2 |\sigma|) + w\right), \tag{7.4.18}$$

where ν is an arbitrary renormalisation mass scale introduced to make the argument of the logarithm dimensionless and u, v and w are bi-spinor functions of x and x' which are regular in the coincidence limit. However, in the case of a maximally symmetric space-time, Eq. (7.4.17) shows that they reduce to functions of the geodetic interval s multiplied by the bi-spinor of parallel transport Λ. According to the Hadamard theorem, the functions u and v are independent of the quantum state of the system, being fully determined by the space-time geometry. Hadamard renormalisation amounts to the subtraction of the Hadamard form $\mathcal{G}_H$, defined as the divergent part of $\mathcal{G}_F$:

$$\begin{aligned} \mathcal{G}_H(x, x') &= \frac{1}{8\pi^2}\left[\frac{u}{\sigma} + v\ln(\nu^2 |\sigma|)\right] \\ &= \frac{\alpha_H(s)}{\mu}\Lambda(x, x), \end{aligned} \tag{7.4.19}$$

where it is understood that $\mathcal{G}_H$ does not necessarily satisfy the Dirac equation, hence, α_H is not necessarily a solution of Eq. (7.3.30).

The bi-spinor functions u and v can be found by solving Eq. (7.4.16). The first derivative of $\mathcal{G}_F$ in Eq. (7.4.18) is:

$$8\pi^2 D_\mu \mathcal{G}_F = -\frac{u\sigma_\mu}{\sigma^2} + \frac{u_{;\mu} + v\sigma_\mu}{\sigma} + v_{;\mu}\ln(\nu^2 |\sigma|) + w_{;\mu}, \tag{7.4.20}$$

and the Dirac equation (7.4.16) reads:

$$8\pi^2(\Box - \tfrac{1}{4}R - \mu^2)\mathcal{G}_F(x, x') = -\frac{2}{\sigma^2}\left[\sigma^\lambda u_{;\lambda} + \tfrac{1}{2}(\Box\sigma - 4)u\right]$$

$$+ \frac{2}{\sigma}\left[\sigma^\lambda v_{;\lambda} + \tfrac{1}{2}(\Box\sigma - 2)v + \tfrac{1}{2}(\Box - \tfrac{1}{4}R - \mu^2)u\right]$$

$$+ \left[(\Box - \tfrac{1}{4}R - \mu^2)v\right]\ln(\nu^2\,|\sigma|) + (\Box - \tfrac{1}{4}R - \mu^2)w, \quad (7.4.21)$$

where it is understood that the box operator denotes the covariant differentiation of the object on which it acts, e.g. $\Box\sigma = g^{\mu\nu}\nabla_\mu\nabla_\nu\sigma$ and $\Box u = g^{\mu\nu}D_\mu D_\nu u$. The σ^{-2} term gives the following equation for u:

$$\sigma^\lambda u_{;\lambda} + \tfrac{1}{2}(\Box\sigma - 4)u = 0, \quad (7.4.22)$$

which can be solved exactly using Eq. (7.1.37) to link $\Box\sigma - 4$ to the derivative of the Van Vleck-Morette determinant Δ:

$$\sigma^\lambda D_\lambda\left(\Delta^{-\frac{1}{2}}u\right) = 0. \quad (7.4.23)$$

The solution of the above equation is the bi-spinor of parallel transport (2.2.57), given explicitly for the adS space-time in Eq. (7.1.69a). The initial condition Eq. (7.3.34) fixes the integration constant such that u is given by:

$$u(x, x') = \sqrt{\Delta}\Lambda(x, x'), \quad (7.4.24)$$

as presented in Ref. [59].

Next, the coefficient of $\ln(\nu^2\,|\sigma|)$ in Eq. (7.4.21) vanishes when:

$$\left(\Box - \frac{1}{4}R - \mu^2\right)v(x, x') = 0. \quad (7.4.25)$$

If we write $v(x, x') = \alpha_v(s)\Lambda(x, x')$, then α_v is the solution of Eq. (7.3.32) which is regular at the origin, as given in Eq. (7.3.33):

$$v(x, x') = \mathcal{C}_v \cos\tfrac{\omega s}{2}{}_2F_1\left(2 - k, 2 + k; 2; \sin^2\tfrac{\omega s}{2}\right)\Lambda(x, x'). \quad (7.4.26)$$

The integration constant $\mathcal{C}_v$ can be fixed by requiring that the last divergent term in the Dirac equation (7.4.21) vanishes. Hence, the following expression must be of order $O(\sigma)$:

$$\sigma^\lambda v_{;\lambda} + \tfrac{1}{2}(\Box\sigma - 2)v + \tfrac{1}{2}(\Box - \tfrac{1}{4}R - \mu^2)u = O(\sigma). \quad (7.4.27)$$

The first term is of order σ. The second term evaluates to:

$$\Box\sigma - 2 = -1 + 3\omega s \cot\omega s. \quad (7.4.28a)$$

The following intermediate steps are useful for the third term in Eq. (7.4.27):

$$\nabla_\mu \sqrt{\Delta} = \frac{3}{2s}(1 - \omega s \cot \omega s)\sqrt{\Delta}\, n_\mu, \tag{7.4.28b}$$

$$\Box\sqrt{\Delta} = -\frac{3\omega^2}{2}\left[\frac{1}{2(\omega s)^2} - \frac{1}{2\sin^2 \omega s} + \frac{3}{2}\right]\sqrt{\Delta}, \tag{7.4.28c}$$

$$\Box\Lambda = \frac{3\omega^2}{4}\tan^2 \frac{\omega s}{2}\Lambda. \tag{7.4.28d}$$

Hence, the third term evaluates to:

$$\frac{1}{2}\left(\Box - \frac{1}{4}R - \mu^2\right)u = \frac{3\omega^2}{8}\left(-\frac{1}{(\omega s)^2} + \frac{1}{\sin^2 \omega s} + \frac{1}{\cos^2 \frac{\omega s}{2}} - \frac{4k^2}{3}\right)u. \tag{7.4.28e}$$

Since the leading order term in Eq. (7.4.28e) is $\frac{\omega^2}{2}(1-k^2)$ and since $\Box\sigma - 2 = 2 + O(\sigma)$, the integration constant in v must be $C_v = \frac{\omega^2}{2}(k^2 - 1)$, hence:

$$\alpha_H = \frac{\omega k}{8\pi^2}\left\{\frac{\sqrt{\Delta}}{\sigma} + \frac{\omega^2}{2}(k^2 - 1)\cos\frac{\omega s}{2}{}_2F_1(2 - k, 2 + k; 2; \sin^2 \frac{\omega s}{2})\ln(\nu^2 |\sigma|)\right\}. \tag{7.4.29}$$

The expression (7.4.26) for v can be checked by using the method in [59], applicable to generic space-times, where Eq. (7.4.17) does not necessarily hold. On a general space-time, v and w can be written as:

$$v(x, x') = \sum_{n=0}^{\infty} v_n(x, x')\sigma^n, \qquad w(x, x') = \sum_{n=0}^{\infty} w_n(x, x')\sigma^n, \tag{7.4.30}$$

where the bi-spinors v_n and w_n are regular at the coincidence limit and u is given in Eq. (7.4.24). Substituting these expansions in Eq. (7.4.21), the following equations are obtained:

$$\sigma^\mu v_{0;\mu} + \tfrac{1}{2}(\Box\sigma - 2)v_0 + \frac{1}{2}\left(\Box - \tfrac{1}{4}R - \mu^2\right)u = 0, \tag{7.4.31a}$$

$$\sigma^\lambda v_{n+1;\lambda} + \frac{1}{2}(\Box\sigma + 2n)v_{n+1} + \frac{1}{2(n+1)}\left(\Box - \tfrac{1}{4}R - \mu^2\right)v_n = 0, \tag{7.4.31b}$$

$$\sigma^\lambda w_{n+1;\lambda} + \frac{1}{2}(\Box\sigma + 2n)w_{n+1} + \frac{1}{2(n+1)}\left(\Box - \tfrac{1}{4}R - \mu^2\right)w_n$$
$$+\frac{1}{n+1}\sigma^\lambda v_{n+1;\lambda} + \frac{1}{2(n+1)}\left[\Box\sigma + 2(2n+1)\right]v_{n+1} = 0. \tag{7.4.31c}$$

The above equations are in exact agreement with [59]. Factorising $v_0 = f_0 u$ in Eq. (7.4.31a) gives:

$$\partial_{\omega s}(\omega s f_0)u = -\tfrac{1}{2}\left(\Box - \tfrac{1}{4}R - \mu^2\right)u, \tag{7.4.32}$$

which can be integrated using Eq. (7.4.28e) for the RHS:

$$f_0 = \frac{3\omega^2}{8}\left[-\frac{1}{(\omega s)^2} + \frac{\cot\omega s}{\omega s} - \frac{2\tan\frac{\omega s}{2}}{\omega s} + \frac{4k^2}{3}\right]. \tag{7.4.33}$$

Similarly, v_1 can be found from Eq. (7.4.31b) by using an auxiliary function f_1 such that $v_1 = f_1 u$. Using the equation:

$$\tfrac{1}{2}\left(\Box - \tfrac{1}{4}R - \mu^2\right)v_0 = -\frac{\omega}{2s}\partial_{\omega s}\left[\omega s\partial_{\omega s}f_0 + 2f_0 + \tfrac{1}{\omega^2}(\omega s f_0)^2\right], \tag{7.4.34}$$

it is straightforward to find that:

$$\begin{aligned}
f_1 &= \frac{1}{s^2}\left(f_0 - \tfrac{\omega^2}{2}(k^2 - 1)\right) + \frac{\omega}{2s}\partial_{\omega s}f_0 + \frac{1}{2}f_0^2 \\
&= \frac{1}{2}f_0^2 + \frac{\omega^2}{s^2}\left[\frac{3}{16\omega s}\cot\omega s - \frac{3}{16\sin^2\omega s} - \frac{3}{8\omega s}\tan\frac{\omega s}{2} - \frac{3}{16\cos^2\frac{\omega s}{2}} + \frac{1}{2}\right].
\end{aligned} \tag{7.4.35}$$

It is now easy to check that the two approaches presented here give the same small distance behaviour for α_H. The short distance expansion of u and v is:

$$u = \left[1 + \left(\frac{\omega s}{2}\right)^2 + \frac{19}{30}\left(\frac{\omega s}{2}\right)^4 + O(s^6)\right]\Lambda, \tag{7.4.36a}$$

$$v = \tfrac{\omega^2}{2}(k^2 - 1)\left[1 - \tfrac{1}{8}(k^2 - 1)(\omega s)^2 + O(s^4)\right]u \tag{7.4.36b}$$

$$= \tfrac{\omega^2}{2}(k^2 - 1)\left[1 - \tfrac{1}{8}(k^2 - 3)(\omega s)^2 + O(s^4)\right]\Lambda, \tag{7.4.36c}$$

hence, α_H has the following coincidence limit expansion:

$$\alpha_H = \frac{k\omega^3}{16\pi^2}\left[-\frac{4}{(\omega s)^2} - 1 + 2(k^2 - 1)\ln\frac{\nu\,|s|}{\sqrt{2}} + O(s)\right], \tag{7.4.36d}$$

where ν is an arbitrary mass scale. The above expansions match exactly the small distance behaviour of the result in Eq. (7.4.29).

To compute the Hadamard form $S_H(x, x')$ of the Feynman propagator, the function β_H corresponding to α_H in Eq. (7.4.29) can be obtained using the defining equation (7.3.29a):

$$\begin{aligned}
\beta_H = \frac{i\omega^3}{4\pi^2}\Bigg\{ &\frac{\sqrt{\Delta}}{2(\omega s)^3} + \frac{3\sqrt{\Delta}}{2(\omega s)^2\sin\omega s} + \frac{k^2 - 1}{2\omega s}\cos\frac{\omega s}{2}{}_2F_1(2 - k, 2 + k; 2; \sin^2\tfrac{\omega s}{2}) \\
&- \frac{1}{8}k^2(k^2 - 1)\ln(\nu^2\,|\sigma|)\sin\frac{\omega s}{2}{}_2F_1(2 - k, 2 + k; 3; \sin^2\tfrac{\omega s}{2})\Bigg\}.
\end{aligned} \tag{7.4.37}$$

The short distance behaviour of β_H and other functions appearing in Eqs. (7.4.2), relevant for the computation of renormalised expectation values, can readily be

derived:

$$\beta_H = \frac{i}{2\pi^2 s^3} + \frac{i\omega^2(1+2k^2)}{16\pi^2 s} - \frac{i\omega^4 s}{8\pi^2}\left(\frac{1}{60} - \frac{k^2}{4} + \frac{k^4}{16}\right)$$
$$- \frac{i\omega^4 s k^2(k^2-1)}{32\pi^2}\ln\frac{\nu|s|}{\sqrt{2}} + O(s^3),$$

$$4i\frac{\omega}{2}\cot\frac{\omega s}{2}\beta_H = -\frac{2}{\pi^2 s^4} - \frac{\omega^2(1+6k^2)}{12\pi^2 s^2} + \frac{\omega^4}{8\pi^2}\left(\frac{29}{90} - \frac{5k^2}{3} + \frac{k^4}{2}\right)$$
$$+ \frac{\omega^4 k^2(k^2-1)}{8\pi^2}\ln\frac{\nu|s|}{\sqrt{2}} + O(s^2),$$

$$-4i\left(\partial_s - \frac{\omega}{2}\cot\frac{\omega s}{2}\right)\beta_H = -\frac{8}{\pi^2 s^4} - \frac{\omega^2(1+3k^2)}{3\pi^2 s^2} + \frac{\omega^4}{8\pi^2}\left(\frac{17}{90} + \frac{4k^2}{3} - k^4\right) + O(s^2),$$

$$(7.4.38)$$

where, as before, the contributions coming from regular and irregular modes correspond to the $+$ and $-$ signs, respectively.

Finally, by writing the regularised propagator as:

$$S_{\text{reg}}(x, x') = (\alpha_{\text{reg}} + \beta_{\text{reg}}\slashed{n})\Lambda(x, x'), \qquad (7.4.39)$$

the expresions (7.3.26) for α_F and β_F can be regularised by subtracting the corresponding expressions from Eqs. (7.4.38):

$$\alpha_{\text{reg}}^{\pm} \xrightarrow{s\to 0} \frac{\omega^3}{16\pi^2}\left(-k^3 \pm k^2 + \frac{k}{6} \mp 1\right)$$
$$+ \frac{k\omega^3(k^2-1)}{8\pi^2}\left(\ln\frac{\omega}{\nu\sqrt{2}} + \psi(\pm k) + \gamma\right),$$

$$\beta_{\text{reg}}^{\pm} \xrightarrow{s\to 0} 0,$$

$$4i\left(\frac{\omega}{2}\cot\frac{\omega s}{2}\right)\beta_{\text{reg}}^{\pm} \xrightarrow{s\to 0} -\frac{\omega^4}{16\pi^2}\left(\frac{11}{20} \pm k - \frac{19k^2}{6} \mp k^3 + \frac{5k^4}{2}\right)$$
$$+ \frac{\omega^4 k^2(k^2-1)}{8\pi^2}\left[\ln\frac{\omega}{\nu\sqrt{2}} + \psi(\pm k) + \gamma\right],$$

$$-4i\left(\frac{\partial}{\partial s} - \frac{\omega}{2}\cot\frac{\omega s}{2}\right)\beta_{\text{reg}}^{\pm} = 0. \qquad (7.4.40)$$

The renormalised expectation values of the FC and CC follow uneventfully by replacing α_F and β_F with their regularised versions given above in Eqs. (7.4.2a) and (7.4.2b), respectively:

$$\langle\overline{\psi}\psi\rangle_{\text{Had}} = \frac{\omega^3}{4\pi^2}\left[-k^3 \pm k^2 + \frac{k}{6} \mp 1 + 2k(k^2-1)\left(\ln\frac{\omega}{\nu\sqrt{2}} + \psi(\pm k) + \gamma\right)\right],$$

$$(7.4.41a)$$

$$\langle J^\mu\rangle_{\text{Had}} = 0. \qquad (7.4.41b)$$

The calculation of the renormalised expectation value of the SET is, however, not straightforward. Naively applying the same procedure as above to the expression (7.4.2c) for the "canonical" SET gives the following trace $T_{\text{Had}}^{\text{can}}$ of the SET renormalised using the Hadamard method:

$$T_{\text{Had}}^{\text{can}} = -\frac{\omega^4}{4\pi^2}\left(\frac{11}{20} \pm k - \frac{19k^2}{6} \mp k^3 + \frac{5k^4}{2}\right) + \frac{\omega^4 k^2(k^2-1)}{2\pi^2}\left[\ln\frac{\omega}{\nu\sqrt{2}} + \psi(\pm k) + \gamma\right]. \tag{7.4.42}$$

The above expression for the SET exhibits a trace anomaly, but its magnitude is different from the one calculated using the Schwinger-de Witt method (7.4.6).

According to Ref. [27], there is also a problem with the conservation of the regularised SET. These problems stem from the fact that the regularised propagator (7.4.39) does not satisfy the Dirac equation, hence, the SET obtained using the canonical definition (7.4.1c) is no longer divergence-free. The non-conservation of the Hadamard renormalised vacuum stress was also reported in Ref. [17] for photons and the solution proposed was to change the definition of the stress tensor operator with a geometry-dependent term which would effectively cancel the renormalisation-induced divergence. For fermions, Ref. [27] proposes to change the canonical definition of the SET by adding a multiple of the Dirac Lagrangian (2.2.15) multiplied by $g_{\mu\nu}$. Since the Dirac Lagrangian vanishes when solutions of the Dirac equation are considered, this alteration of the definition of the SET does not affect its value in the classical (unrenormalised) case. However, the freedom of having the multiplier of the Dirac Lagrangian as an extra parameter can be used to cancel the non-zero terms in the divergence of the SET, by changing its canonical definition (7.4.1c) to:

$$T_{\mu\nu}^{\text{new}} = T_{\mu\nu}^{\text{can}} - \frac{1}{6}g_{\mu\nu}\left[\frac{i}{2}\overline{\psi}\slashed{D}\psi - \frac{i}{2}\overline{\slashed{D}\psi}\psi - \mu\overline{\psi}\psi\right], \tag{7.4.43}$$

The above redefinition guarantees the conservation of the SET for arbitrary spacetimes. On adS, the renormalised SET is proportional to $g_{\mu\nu}$. Hence, it can be written in terms of its trace as:

$$\langle T_{\mu\nu}\rangle_{\text{Had}}^{\text{new}} = \frac{1}{4}g_{\mu\nu}T_{\text{Had}}^{\text{new}}, \tag{7.4.44}$$

where the trace of the new SET can be written in terms of the old one as:

$$T_{\text{Had}}^{\text{new}} = \frac{1}{3}T_{\text{Had}}^{\text{can}} + \frac{2\omega k}{3}\langle\overline{\psi}\psi\rangle_{\text{Had}}. \tag{7.4.45}$$

The result is:

$$T_{\text{Had}}^{\text{new}} = \frac{\omega^4}{4\pi^2}\left\{-\frac{11}{60} \mp k + \frac{7k^2}{6} \pm k^3 - \frac{3k^4}{2} + 2k^2(k^2-1)\left[\ln\frac{\omega}{\nu\sqrt{2}} + \gamma + \psi(\pm k)\right]\right\}, \tag{7.4.46}$$

where γ is Euler's constant. It is worth quoting the result obtained in Ref. [18] using

zeta-function regularisation for the trace T_ζ of the renormalised vacuum expectation value of the SET:

$$T_\zeta = \frac{\omega^4}{4\pi^2}\left\{-\frac{11}{60} - k + \frac{7k^2}{6} + k^3 - \frac{3k^4}{2} + 2k^2(k^2-1)\left[\ln\frac{\omega}{\nu_\zeta} + \psi(k)\right]\right\}, \quad (7.4.47)$$

where ν_ζ is an arbitrary renormalisation mass scale. Our result Eq. (7.4.46) obtained using Hadamard renormalisation is in excellent agreement with the zeta-function regularisation result above, provided that

$$\nu = \frac{1}{\sqrt{2}}\nu_\zeta e^\gamma. \tag{7.4.48}$$

7.5   Thermal expectation values

In subsections 2.2.5 and 4.3.2, thermal expectation values (t.e.v.s) were calculated using the thermal Hadamard function. In adS, it is convenient to use the closed form expression for the Feynman propagator (7.3.1) to construct its thermal analogue. The advantage of using the Feynman propagator approach, discussed in subsection 7.5.1, is that the expressions obtained for the t.e.v.s of the fermion condensate (FC), charge current (CC) and stress-energy tensor (SET) are simple enough to facilitate physical interpretation. The mode sum approach is presented as an alternative method in subsection 7.5.2 and the results are represented graphically in subsection 7.5.3.

7.5.1   Using the Feynman propagator

The t.e.v.s presented in this section are expressed with respect to the vacuum state and are calculated from the thermal Feynman propagator (2.2.54) after subtracting the $j = 0$ term, corresponding to the vacuum contribution:

$$\Delta S_F^\beta(x, x') = \sum_{j\neq 0}(-1)^j S_F(t + ij\beta, \boldsymbol{x}; t', \boldsymbol{x}'). \tag{7.5.1}$$

The t.e.v.s can be calculated by substituting ΔS_F^β for S_F in Eqs. (7.4.1). Since in this case, the coincidence limit sets the difference along the time coordinate to $\Delta t = ij\beta$ rather than to 0, the following limits of the bi-spinor of parallel transport Λ are required:

$$\Lambda\big\rfloor_{\boldsymbol{x}=\boldsymbol{x}'} = \frac{\cos\frac{\omega\Delta t}{2}}{\cos\frac{\omega s}{2}}, \qquad \slashed{n}\Lambda\big\rfloor_{\boldsymbol{x}=\boldsymbol{x}'} = \frac{\sin\frac{\omega\Delta t}{2}}{\sin\frac{\omega s}{2}\cos\omega r}\gamma^{\hat{t}}. \tag{7.5.2}$$

Thus, the only non-vanishing traces required in Eqs. (7.4.1) are:

$$\text{tr}(\Lambda)_{\boldsymbol{x}=\boldsymbol{x}'} = 4\frac{\cos\frac{\omega\Delta t}{2}}{\cos\frac{\omega s}{2}}, \qquad \text{tr}(\gamma_t\slashed{u}\Lambda)_{\boldsymbol{x}=\boldsymbol{x}'} = -\frac{4\sin\frac{\omega\Delta t}{2}}{\sin\frac{\omega s}{2}\cos^2\omega r}, \tag{7.5.3}$$

leading to the following t.e.v.s:

$$\langle:\overline{\psi}\psi:\rangle_\beta = -\sum_{\substack{j\neq 0 \\ \Delta t=ij\beta}} (-1)^j\text{tr}(\Lambda)\alpha_F(s), \tag{7.5.4a}$$

$$\langle: J^\mu :\rangle_\beta = -\sum_{\substack{j\neq 0 \\ \Delta t=ij\beta}} (-1)^j\text{tr}(\gamma^\mu\slashed{u}\Lambda)\beta_F(s), \tag{7.5.4b}$$

$$\langle: T_{\mu\nu} :\rangle_\beta = \frac{i}{2}\sum_{\substack{j\neq 0 \\ \Delta t=ij\beta}} (-1)^j \lim_{\substack{\boldsymbol{x}\to\boldsymbol{x}' \\ \Delta t=ij\beta}} \left\{ \sin\frac{\omega s}{2}\text{tr}\left(\gamma_{(\mu}\slashed{u}\Lambda\right)[\partial_{\nu)} - \partial_{\nu')}]\left(\frac{\beta_F}{\sin\frac{\omega s}{2}}\right) \right.$$
$$\left. + \omega\cot\frac{\omega s}{2}\text{tr}(\Lambda)g_{\mu\nu}\beta_F \right\}, \tag{7.5.4c}$$

where the coordinates are implicitly given by $\Delta t = ij\beta$ and $\boldsymbol{x} = \boldsymbol{x}'$, such that the geodetic interval s satisfies the following relations:

$$\cos\omega s = \frac{\cos\omega\Delta t}{\cos^2\omega r} - \tan^2\omega r, \qquad \sin^2\frac{\omega s}{2} = \frac{\sin^2\frac{\omega\Delta t}{2}}{\cos\omega r^2}, \qquad \cos^2\frac{\omega s}{2} = 1 - \sin^2\frac{\omega s}{2}. \tag{7.5.5}$$

Putting the traces (7.5.3) in Eqs. (7.5.4) gives the following non-zero components:

$$\langle:\overline{\psi}\psi:\rangle_\beta = -4\sum_{\substack{j\neq 0 \\ \Delta t=ij\beta}} (-1)^j\frac{\cos\frac{\omega\Delta t}{2}}{\cos\frac{\omega s}{2}}\alpha_F(s),$$

$$\langle: J^t :\rangle_\beta = -4\sum_{\substack{j\neq 0 \\ \Delta t=ij\beta}} (-1)^j\frac{\sin\frac{\omega\Delta t}{2}}{\sin\frac{\omega s}{2}}\beta_F(s),$$

$$\langle: T^t_{\ t} :\rangle_\beta = \sum_{j\neq 0} (-1)^j\partial_t\left(\frac{4i\sin\frac{\omega\Delta t}{2}}{\sin\frac{\omega s}{2}}\beta_F\right),$$

$$\langle: T^r_{\ r} :\rangle_\beta = \langle: T^\theta_{\ \theta} :\rangle_\beta = \langle: T^\varphi_{\ \varphi} :\rangle_\beta = \sum_{j\neq 0} (-1)^j\frac{2i\omega\cos\frac{\omega\Delta t}{2}}{\sin\frac{\omega s}{2}}\beta_F. \tag{7.5.6}$$

We see that the thermal distribution of fermions has the same SET as a perfect fluid:

$$\langle: T^\mu_{\ \nu} :\rangle_\beta = \text{diag}(-\rho, p, p, p). \tag{7.5.7}$$

Due to the simplicity of the functions α_F and β_F in the massless case (7.3.27),

the t.e.v.s when $k = 0$ simplify greatly, as follows:

$$\frac{i\omega \cos \frac{\omega \Delta t}{2}}{\sin \frac{\omega s}{2}} \beta_F = -\frac{\omega^4}{8\pi^2} \frac{\cos \frac{\omega \Delta t}{2}}{\left(\sin \frac{\omega s}{2}\right)^4}, \tag{7.5.8}$$

hence, the following expressions are obtained:

$$\frac{i\omega \cos \frac{\omega \Delta t}{2}}{\sin \frac{\omega s}{2}} \beta_F = -\frac{\omega^4}{8\pi^2} \frac{\cosh \frac{j\omega\beta}{2}}{\left(\sinh \frac{j\omega\beta}{2}\right)^4} (\cos \omega r)^4, \tag{7.5.9a}$$

$$\partial_t \left(\frac{4i \sin \frac{\omega \Delta t}{2}}{\sin \frac{\omega s}{2}} \beta_F\right) = \frac{3\omega^4}{4\pi^2} \frac{\cosh \frac{j\omega\beta}{2}}{\left(\sinh \frac{j\omega\beta}{2}\right)^4} (\cos \omega r)^4, \tag{7.5.9b}$$

giving the following formulae for the t.e.v. of the SET:

$$\rho\rfloor_{k=0} = -\frac{3\omega^4}{4\pi^2} (\cos \omega r)^4 \sum_{j=1}^{\infty} (-1)^j \frac{\cosh \frac{j\omega\beta}{2}}{(\sinh \frac{j\omega\beta}{2})^4}, \qquad p\rfloor_{k=0} = \frac{\rho}{3}. \tag{7.5.10}$$

As a consequence of the symmetry with respect to the transformation $j \leftrightarrow -j$ of the summand in $\langle : T^t_{\ t} : \rangle_\beta$, the sum over j now runs only over positive integers. It can be seen that the trace of the SET vanishes when $k = 0$, when the equation of state is $\frac{p}{\rho} = \frac{1}{3}$. It is interesting to note that, in the massless case, the t.e.v. of the SET depends on the coordinates only through a factor of $(\cos \omega r)^4$ (for the upper-lower components).

Two limits can be extracted from Eq. (7.5.10): the small ω and the low temperature (large β) limits. At small ω, the following expansion can be performed:

$$\rho\rfloor_{k=0} = -(\cos \omega r)^4 \sum_{j=1}^{\infty} (-1)^j \left(\frac{12}{j^4 \pi^2 \beta^4} - \frac{\omega^2}{2j^2 \pi^2 \beta^2} + O(\omega^4)\right)$$

$$= (\cos \omega r)^4 \left(\frac{7\pi^2}{60\beta^4} - \frac{\omega^2}{24\beta^2} + O(\omega^4)\right)$$

$$= \frac{7\pi^2}{60\beta^4} - \frac{\omega^2}{24\beta^2} \left(1 + \frac{28\pi^2 r^2}{5\beta^2}\right) + O(\omega^4). \tag{7.5.11}$$

The first term is the Minkowski value of the energy density (8.3.15) of massless fermions at inverse temperature β, showing that if ω is sufficiently small, an observer close enough to $r = 0$ will detect a thermal state very close to the Minkowski state.

For large β (small temperatures), the following expansion can be made:

$$\frac{\cosh \frac{j\omega\beta}{2}}{(\sinh \frac{j\omega\beta}{2})^4} = 8e^{-\frac{3}{2}j\omega\beta} \frac{1 + e^{-j\omega\beta}}{(1 - e^{-j\omega\beta})^4}$$

$$= 8e^{-\frac{3}{2}j\omega\beta} \sum_{n=0}^{\infty} \left(1 + \frac{13n}{6} + \frac{3n^2}{2} + \frac{n^3}{3}\right) e^{-nj\omega\beta}. \tag{7.5.12}$$

A substitution back into Eq. (7.5.10) yields:

$$
\rho\big|_{k=0} = -\frac{6\omega^4}{\pi^2}\frac{(\cos\omega r)^4}{1+e^{\frac{3}{2}\omega\beta}}\sum_{n=0}^{\infty}e^{-n\omega\beta}\left(1+\frac{13n}{6}+\frac{3n^2}{2}+\frac{n^3}{3}\right)\frac{1+e^{-\frac{3}{2}\omega\beta}}{1+e^{-(\frac{3}{2}+n)\omega\beta}}
$$
$$
= -\frac{6\omega^4}{\pi^2}\frac{(\cos\omega r)^4}{1+e^{\frac{3}{2}\omega\beta}}\left(1+5e^{-\omega\beta}+O(e^{-2\omega\beta})\right) \tag{7.5.13}
$$

If k is kept arbitrary, it is more convenient to use the representation (7.3.21) for β. Expressions analogous to Eqs.(7.5.9) can be obtained:

$$
\frac{i\omega\cos\frac{\omega\Delta t}{2}}{\sin\frac{\omega s}{2}}\beta = -\frac{2\omega\cos\frac{\omega\Delta t}{2}}{(\cos\frac{\omega s}{2})^{4+2k}}{}_2F_1\left(1+k,2+k;1+2k;\left(\cos^2\frac{\omega s}{2}\right)^{-1}\right),
$$
$$
\partial_t\left(\frac{4i\sin\frac{\omega\Delta t}{2}}{\sin\frac{\omega s}{2}}\beta\right) = -\frac{2\omega\cos\frac{\omega\Delta t}{2}}{\left(\cos\frac{\omega s}{2}\right)^{4+2k}}\left\{{}_2F_1\left(1+k,2+k;1+2k;\left(\cos^2\frac{\omega s}{2}\right)^{-1}\right)\right.
$$
$$
\left. +\frac{(2+k)\sin^2\frac{\omega\Delta t}{2}}{\cos^2\frac{\omega s}{2}\cos^2\omega r}{}_2F_1\left(1+k,3+k;1+2k;\left(\cos^2\frac{\omega s}{2}\right)^{-1}\right)\right\}. \tag{7.5.14}
$$

The coordinate dependency is non-trivial in this case and the energy density and pressure now take the form:

$$
\rho = -\frac{\omega^4\Gamma(2+k)}{4\pi^{\frac{3}{2}}2^{2k}\Gamma(\frac{1}{2}+k)}(\cos\omega r)^{4+2k}\sum_{j=1}^{\infty}(-1)^j\frac{\cosh\frac{j\omega\beta}{2}}{(\cos^2\omega r+\sinh^2\frac{j\omega\beta}{2})^{2+k}}
$$
$$
\times\left\{\frac{2(2+k)\sinh^2\frac{j\omega\beta}{2}}{\cos^2\omega r+\sinh^2\frac{j\beta\omega}{2}}{}_2F_1\left(1+k,3+k;1+2k;\frac{\cos^2\omega r}{\cos^2\omega r+\sinh^2\frac{j\omega\beta}{2}}\right)\right.
$$
$$
\left. -{}_2F_1\left(1+k,2+k;1+2k;\frac{\cos^2\omega r}{\cos^2\omega r+\sinh^2\frac{j\omega\beta}{2}}\right)\right\}, \tag{7.5.15a}
$$
$$
p = -\frac{\omega^4\Gamma(2+k)}{4\pi^{\frac{3}{2}}2^{2k}\Gamma(\frac{1}{2}+k)}(\cos\omega r)^{4+2k}\sum_{j=1}^{\infty}(-1)^j\frac{\cosh\frac{j\omega\beta}{2}}{(\cos^2\omega r+\sinh^2\frac{j\omega\beta}{2})^{2+k}}
$$
$$
\times{}_2F_1\left(1+k,2+k;1+2k;\frac{\cos^2\omega r}{\cos^2\omega r+\sinh^2\frac{j\omega\beta}{2}}\right), \tag{7.5.15b}
$$

where $N_{\pm k}$ has been substituted according to Eqs. (7.3.21). It can be checked that the massless limit (7.5.10) is exactly recovered. Graphical representations of the above results can be found in subsection 7.5.3, where the bi-spinor of parallel transport approach is validated using the mode sum approach, presented in the following subsection.

7.5.2 Mode sum approach

In the mode sum approach, it is easier to work with the renormalised thermal Hadamard function, which can be written as:

$$\Delta S_\beta^{(1)}(x, x') = -\frac{\omega^2}{4\pi} \frac{(\cos \omega r \cos \omega r')^{\frac{3}{2}}}{\sin \omega r \sin \omega r'} \sum_{n_+, j} \frac{1}{1 + e^{\beta E}} (s^+ - s^-), \qquad (7.5.16)$$

where $s^\pm$ are defined in Eqs. (7.3.3b) and it is understood that the energy E depends on the particular value of κ for each of the terms in s^+ and s^-. The coincidence limit of $\Delta S_\beta^{(1)}(x, x')$ is given by:

$$\Delta S_\beta^{(1)}(x, x') \Big|_{x'=x} = -\frac{\omega^2}{2\pi} \frac{(\cos \omega r)^3}{\sin^2 \omega r} \sum_{n_+, j, \kappa} \frac{j + \frac{1}{2}}{e^{\beta E_\kappa} + 1} \left[(f_{E_\kappa, \kappa}^+)^2 - (f_{E_\kappa, \kappa}^-)^2 \right] \qquad (7.5.17)$$

where the functions $f_{E, \kappa}^\pm$ are given by Eq. (7.2.11c) and E_κ is defined as:

$$E_\kappa = 2n_+ + k + \left| \kappa + \tfrac{1}{2} \right| j + \tfrac{1}{2}. \qquad (7.5.18)$$

It is remarkable that in the coincidence limit, the spinor structure of the Hadamard two-point function is proportional to the identity matrix. Equation (7.5.17) can be expressed in terms of the functions $\hat{f}$ using the definition Eq. (7.2.15):

$$\begin{aligned}
\Delta S_\beta^{(1)}(x, x') \Big|_{x'=x} = -\frac{\omega^2}{2\pi} \frac{(\cos \omega r)^4}{\sin^2 \omega r} \sum_{n_+, j, \kappa} \frac{j + \frac{1}{2}}{e^{\beta E_\kappa} + 1} \\
\times \left[(\hat{f}_{E_\kappa, \kappa}^+)^2 - (\hat{f}_{E_\kappa, \kappa}^-)^2 + 2 \tan \omega r \, \hat{f}_{E_\kappa, \kappa}^+ \hat{f}_{E_\kappa, \kappa}^- \right]. \qquad (7.5.19)
\end{aligned}$$

Starting from the formula for the t.e.v. of the SET:

$$\langle : T_{\hat{\alpha}\hat{\rho}} : \rangle_\beta = \frac{i}{4} \lim_{x' \to x} \mathrm{tr} \left[\gamma_{(\hat{\alpha}} D_{\hat{\rho})} \Delta S_\beta^{(1)}(x, x') - \Delta S_\beta^{(1)}(x, x') \overleftarrow{D_{(\hat{\alpha}'}} \gamma_{\hat{\rho})} \right], \qquad (7.5.20)$$

Using Eqs. (2.2.55a) and (2.2.28), the fermion condensate (FC) can be related to the trace of the SET as follows:

$$\langle : \overline{\psi}\psi : \rangle_\beta = -\frac{1}{\omega k} \langle : T^\mu_{\ \mu} : \rangle_\beta = -\frac{1}{2} \lim_{x' \to x} \mathrm{tr} \Delta S_\beta^{(1)}(x, x'). \qquad (7.5.21)$$

Furthermore, since $\mathrm{tr}(\gamma_{\hat{\alpha}} \Gamma_{\hat{\gamma}}) = 0$, Eq. (2.2.55c) reduces to:

$$\langle : T_{\hat{\alpha}\hat{\rho}} : \rangle_\beta = \frac{i}{4} \lim_{x' \to x} \mathrm{tr} \left\{ \gamma_{(\hat{\alpha}} [\partial_{\hat{\rho})} - \partial_{\hat{\rho}')}] \Delta S_\beta^{(1)}(x, x') \right\}. \qquad (7.5.22)$$

If the points are kept arbitrarily split, the trace of the Feynman propagator multiplied by $\gamma_{\hat{t}}$ (as part of the components $T_{\hat{t}\hat{\alpha}}$ of the SET) is given by:

$$\frac{i}{4}\text{tr}\left[\gamma_{\hat{t}}\Delta S_{\beta}^{(1)}(x,x')\right] = \frac{\omega^2}{2\pi}\frac{(\cos\omega r\cos\omega r')^{\frac{3}{2}}}{\sin\omega r\sin\omega r'}\sum_{n_+,j,\kappa}\frac{(j+\frac{1}{2})\sin E_{\kappa}\Delta t}{e^{\beta E_{\kappa}}+1}$$

$$\times\left[f_{E_{\kappa},\kappa}^{+}f_{E_{\kappa},\kappa}^{+}P_{|\kappa+\frac{1}{2}|-\frac{1}{2}}(\cos\gamma)+f_{E_{\kappa},\kappa}^{-}f_{E_{\kappa},\kappa}^{-}P_{|\kappa-\frac{1}{2}|-\frac{1}{2}}(\cos\gamma)\right]. \quad (7.5.23)$$

The components $\langle: T_{\hat{t}\hat{\ell}}:\rangle_{\beta}$ vanish due to the presence of $\sin E_{\kappa}\Delta t$, while the time-time component of the SET is given by:

$$\langle: T^t{}_t:\rangle_{\beta} = -\frac{\omega^2}{\pi}\frac{(\cos\omega r)^4}{\sin^2\omega r}\sum_{n_+,j}\left\{\frac{E_+(j+\frac{1}{2})}{e^{\beta E_+}+1}\left[(f_+^+)^2+(f_+^-)^2\right]\right.$$

$$\left.+\frac{E_-(j+\frac{1}{2})}{e^{\beta E_-}+1}\left[(f_-^+)^2+(f_-^-)^2\right]\right\}, \quad (7.5.24)$$

where the subscript $\pm$ of the energy and radial functions refers to the sign of κ, i.e. $E_{\pm} = E_{\pm|j+\frac{1}{2}|}$ and $f_{\pm}^+ = f_{E_{\pm},\pm|j+\frac{1}{2}|}^+$.

Next, the trace of $\Delta S_{\beta}^{(1)}$ multiplied by $\gamma_{\hat{\ell}}$ can be safely computed at coincidence along the time axis, since the components $T_{\hat{t}\hat{\ell}}$ have already been shown to vanish:

$$\frac{i}{4}\text{tr}\left[\hat{\boldsymbol{\gamma}}\Delta S_{\beta}^{(1)}(x,x')\right]_{\Delta t=0} = \frac{\omega^2}{2\pi}\frac{(\cos\omega r\cos\omega r')^{\frac{3}{2}}}{\sin\omega r\sin\omega r'}\sum_{n_+,j}\left\{\right.$$

$$\left(\frac{f_-^+f_-^-}{e^{\beta E_-}+1}-\frac{f_+^-f_+^+}{e^{\beta E_+}+1}\right)\left[\frac{\boldsymbol{x}}{r}\left(j+\tfrac{1}{2}\right)P_{j+\frac{1}{2}}(\cos\gamma)+\frac{\boldsymbol{x}\times(\boldsymbol{x}'\times\boldsymbol{x})}{r^2r'}P'_{j+\frac{1}{2}}(\cos\gamma)\right]$$

$$+\left(\frac{f_+^+f_+^-}{e^{\beta E_+}+1}-\frac{f_-^-f_-^+}{e^{\beta E_-}+1}\right)\left[\frac{\boldsymbol{x}}{r}\left(j+\tfrac{1}{2}\right)P_{j-\frac{1}{2}}(\cos\gamma)-\frac{\boldsymbol{x}\times(\boldsymbol{x}'\times\boldsymbol{x})}{r^2r'}P'_{j-\frac{1}{2}}(\cos\gamma)\right]\right\}.$$

$$(7.5.25)$$

The operator $\partial_i-\partial_{i'}$ has a vanishing commutator with functions which are symmetric with respect to $\boldsymbol{x}$ and $\boldsymbol{x}'$, hence:

$$\left[\partial_i-\partial_{i'},\frac{(\cos\omega r\cos\omega r')^{\frac{3}{2}}}{\sin\omega r\sin\omega r'}\right]=0,\quad[\partial_i-\partial_{i'},\cos\gamma]=0,\quad[\partial_i-\partial_{i'},P_l(\cos\gamma)]=0.$$

$$(7.5.26)$$

Thus, $\cos\gamma$ can be replaced by 1 in Eq. (7.5.25) and the Legendre polynomials can be replaced using $P_{\ell}(1) = 1$ and $P'_{\ell}(1) = \frac{1}{2}\ell(\ell+1)$, simplifying the calculations

greatly. The final result is:

$$\langle: T_{ik} :\rangle_\beta = \frac{\omega^3}{\pi} \frac{(\cos \omega r)^2}{\sin^2 \omega r} \sum_{n_+,j} (j + \tfrac{1}{2}) \left\{ \frac{x^i x^k}{r^2} \left[\frac{W_{\omega r}(f_-^-, f_-^+)}{e^{\beta E_-} + 1} + \frac{W_{\omega r}(f_+^-, f_+^+)}{e^{\beta E_+} + 1} \right] \right.$$

$$\left. + \frac{\sin \omega r}{(\omega r)^2} (j + \tfrac{1}{2}) \left(\delta_{ij} - \frac{x^i x^j}{r^2} \right) \left(\frac{f_-^+ f_-^-}{e^{\beta E_-} + 1} - \frac{f_+^+ f_+^-}{e^{\beta E_+} + 1} \right) \right\}, \quad (7.5.27)$$

where the Wronskian $W_{\omega r}(f_\pm^-, f_\pm^+)$ of the functions $f_\pm^-$ and $f_\pm^+$ with respect to ωr can be calculated from the Dirac equation (7.2.11c):

$$W_{\omega r}(f_\pm^-, f_\pm^+) = f_\pm^- \partial_{\omega r} f_\pm^+ - (\partial_{\omega r} f_\pm^-) f_\pm^+$$

$$= \frac{E}{\omega} \left[(f_\pm^+)^2 + (f_\pm^-)^2 \right] \mp \frac{2j+1}{\sin \omega r} f_\pm^+ f_\pm^- - \frac{k}{\cos \omega r} \left[(f_\pm^+)^2 - (f_\pm^-)^2 \right].$$

$$(7.5.28)$$

To switch from Cartesian components (x^1, x^2, x^3) to components with respect to the spherical coordinates (r, θ, φ), the following formulae are useful:

$$\frac{x^i x^j}{r^2} \to \text{diag}(1, 0, 0), \qquad \delta_{ij} \to \text{diag}(1, r^2, r^2 \sin^2 \theta), \qquad (7.5.29)$$

where the (i, j) element on the right of the arrow represent the coordinate component with respect to the basis $(dr, d\theta, d\varphi)$:

$$\frac{x^i x^j}{r^2} dx^i dx^j = dr^2, \qquad \delta_{ij} dx^i dx^j = dr^2 + r^2 d\theta^2 + r^2 \sin^2 \theta d\varphi^2. \qquad (7.5.30)$$

The t.e.v.s of the FC and of the non-vanishing components of the SET are listed below:

$$\langle: \overline{\psi}\psi :\rangle_\beta = \frac{\omega^2}{\pi} \frac{(\cos \omega r)^3}{\sin^2 \omega r} \sum_{n_+,j} (j + \tfrac{1}{2}) \left(\frac{f_+^+ - f_+^-}{e^{\beta E_+} + 1} + \frac{f_-^+ - f_-^-}{e^{\beta E_-} + 1} \right),$$

$$\langle: T^t_{\ t} :\rangle_\beta = -\frac{\omega^2}{\pi} \frac{(\cos \omega r)^4}{\sin^2 \omega r} \sum_{n_+,j} (j + \tfrac{1}{2}) \left\{ \frac{E_+ \left[(f_+^+)^2 + (f_+^-)^2 \right]}{e^{\beta E_+} + 1} + \frac{E_- \left[(f_-^+)^2 + (f_-^-)^2 \right]}{e^{\beta E_-} + 1} \right\},$$

$$\langle: T^r_{\ r} :\rangle_\beta = \frac{\omega^3}{\pi} \frac{(\cos \omega r)^4}{\sin^2 \omega r} \sum_{n_+,j} (j + \tfrac{1}{2}) \left[\frac{W_{\omega r}(f_+^-, f_+^+)}{e^{\beta E_+} + 1} + \frac{W_{\omega r}(f_-^-, f_-^+)}{e^{\beta E_-} + 1} \right],$$

$$\langle: T^\theta_{\ \theta} :\rangle_\beta = \frac{\omega^3}{\pi} \frac{(\cos \omega r)^4}{\sin^3 \omega r} \sum_{n_+,j} (j + \tfrac{1}{2})^2 \left(\frac{f_+^+ f_+^-}{e^{\beta E_+} + 1} - \frac{f_-^+ f_-^-}{e^{\beta E_-} + 1} \right),$$

$$\langle: T^\varphi_{\ \varphi} :\rangle_\beta = \langle: T^\theta_{\ \theta} :\rangle_\beta, \qquad (7.5.31)$$

where the Wronskian has been left in place to keep notation compact. It can be checked that the relation (7.5.21) between the FC and the trace of the SET is satisfied. However, the equality between the spatial components of the SET is

difficult to prove in this setup. Numerical results show that the individual summands (i.e. at fixed n_+ and j) in the radial and angular components are in general not equal, however, the components as a whole approach the same value.

Although the mode sums provide a reliable (numerical) check on the geometric approach of the previous subsection, the massless limit in this formalism is as complicated as the $k \neq 0$ case. Furthermore, in the geometric approach, the asymptotic limits for small ω or large β are easily calculated in the massless case, whereas in the massive case and in the mode sum approach, sending ω to 0 would involve analysing the infinite order limit of hypergeometric functions or Jacobi polynomials, which are not well documented.

The mode sum approach can be used almost in a similar fashion for the analysis of thermal states on the adS space-time rotating at arbitrarily large angular velocities Ω, as discussed in subsection 8.3.1. In contrast, the bi-spinor of parallel transport approach is problematic when Ω is sufficiently large to form a speed of light surface (SOL).

7.5.3 Numerical results

Numerical experiments confirm that the mode sum (7.5.31) and geometric approach (7.5.15) give identical results. In practise, t.e.v.s can be obtained numerically quicker when using mode than when using the geometric approach at small values of β, for all values of k. The geometric approach is slow at $k \neq 0$ as it involves the computation of hypergeometric functions.

Figures 7.2 show the dependence of the FC $\langle : \overline{\psi}\psi : \rangle_\beta$, energy density ρ, pressure p and equation of state $w = \frac{p}{\rho}$ on the radial coordinate. The plots on the left keep $\beta\omega = 1.2$ constant and compare the t.e.v.s corresponding to different masses. The plots on the right compare the t.e.v.s corresponding to $\mu = 0$ and $\mu = 2\omega$ at four values of the temperature.

In the case $k = 0$, Eq. (7.5.10) shows that ρ depends on r through a factor of $\cos^4 \omega r$. Thus its value decreases from a maximum at the origin to 0 on the boundary, where $\omega r = \frac{\pi}{2}$. The same trend is preserved for non-zero values of k, however, the dependence on the radial coordinate is more complicated, as can be seen from the plot of the equation of state $\frac{p}{\rho}$.

Fig. 7.3 shows the dependence of the energy density ρ at the origin on the inverse temperature. Two regimes can be identified: when $\beta\omega$ is small, the field behaves as if it were massless and t.e.v.s approach their Minkowski values (7.5.11). At large $\beta\omega$, the energy density exhibits an exponential decrease, as predicted by Eq. (7.5.13).
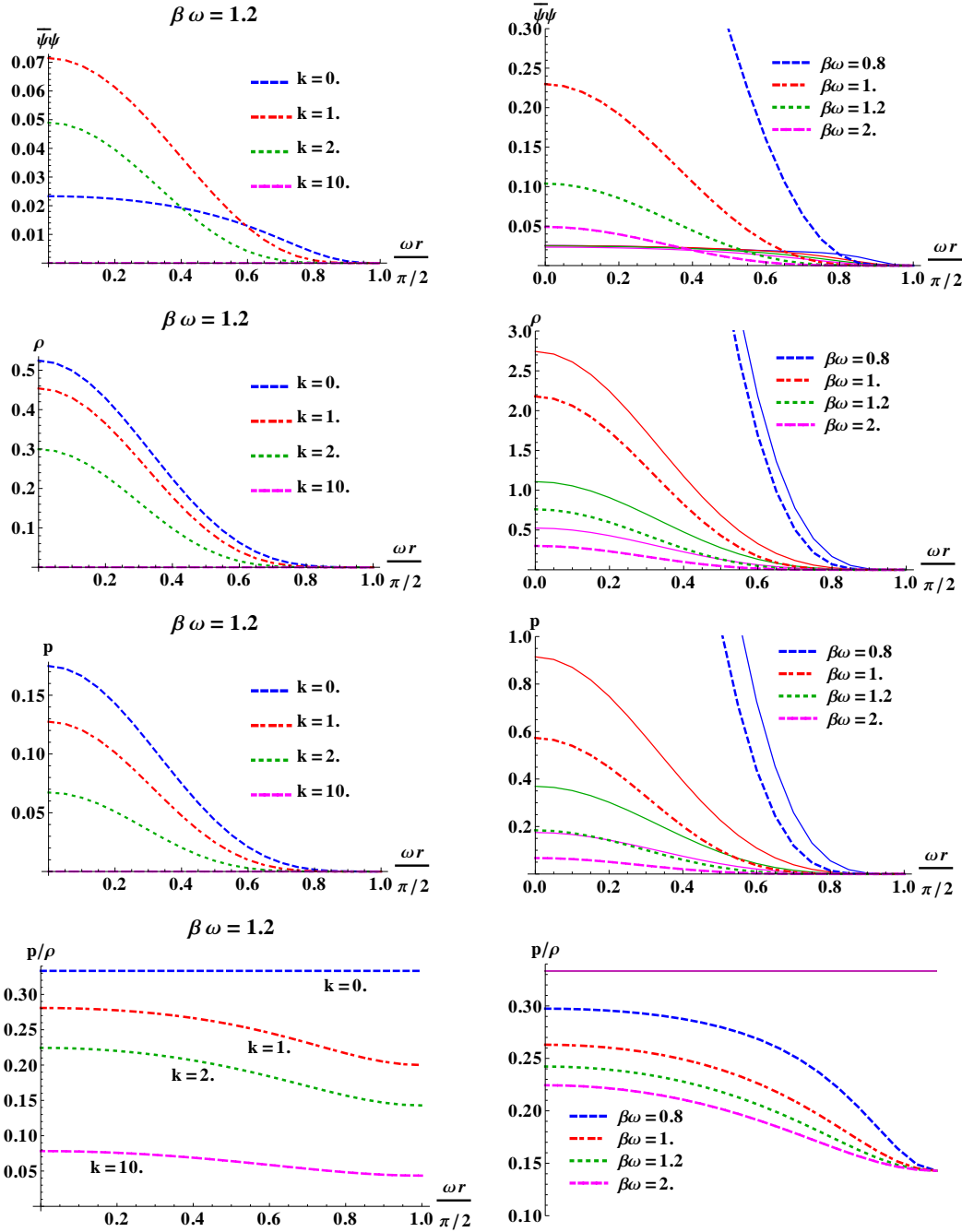
Figure 7.2: Plots showing $\langle : \overline{\psi}\psi : \rangle_\beta$, the energy density ρ, the pressure p and the equation of state $w = \frac{p}{\rho}$ (from top to bottom. The plots on the left show profiles for four masses k at fixed temperature $\beta\omega = 1.2$. The plots on the right show compare the profiles for the same quantities corresponding to massless (thin coloured curves) to those corresponding to fermions of mass $\mu = 2\omega$ (thick dashed coloured curves) at four values of the temperature $\beta\omega$.

7.6 Summary

In this chapter, three main results were presented: the renormalised vacuum expectation values of the fermion condensate (FC) and stress-energy tensor (SET), the closed form expression of the Feynman propagator (including the bi-spinor of parallel transport) and the construction of thermal expectation values (t.e.v.s).

Figure 7.3: The dependence of the energy density at the origin on the inverse temperature β.
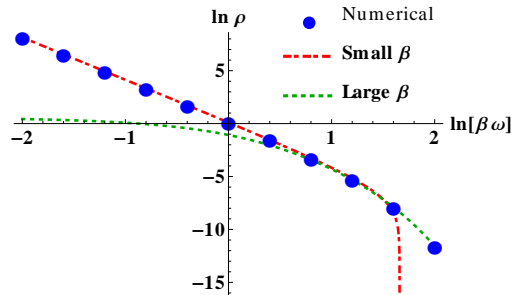
A key ingredient in the construction of the propagator and of thermal states wass the bi-spinor of parallel transport, for which an analytic expression is obtained in subsection 7.1.4 by directly solving the parallel transport equation for the maximally symmetric anti-de Sitter space. The propagator is constructed using two approaches: through the traditional time-ordered product mode sum approach, where it is necessary to set r' at the origin to simplify the calculations. The general form of the propagator can be inferred from the maximally symmetric character of adS, by identifying the bi-spinor of parallel transport and by using the ansatz (7.3.1). The second approach is to find the propagator as a solution of the inhomogeneous Dirac equation, satisfying appropriate boundary conditions. The two approaches are presented separately and the results are compared to confirm the consistency and correctness of the methods.

Renormalisation is performed using two methods: the Schwinger-de Witt method and the Hadamard method. The application of the Schwinger-de Witt method consists in subtracting from the point-split vacuum stress-energy tensor (SET) the counter terms calculated in Ref. [24]. The resulting SET is proportional to the space-time metric $g_{\mu\nu}$ and it matches perfectly the result obtained in Ref. [30] using the Pauli-Villars regularisation method.

For the Hadamard method, the singular part of the propagator is eliminated following [59] in a state-independent fashion, leaving behind a remainder which is no longer a solution of the inhomogeneous Dirac equation. Thus, the SET operator has to be changed to ensure that the renormalised SET is conserved, as discussed in Ref. [27]. The result obtained using Hadamard renormalisation matches perfectly the zeta-function regularisation method presented in Ref. [30].

Thermal states can be constructed either by using mode sums to construct the thermal Hadamard function (the mode sum approach), or by using the closed form expression of the Feynman propagator (the geometric approach). The latter approach exploits the anti-periodicity of the Feynman propagator corresponding to a

thermal state with respect to imaginary time and requires the closed form expression of the bi-spinor of parallel transport. The results obtained using the geometric approach can easily be interpreted physically, showing that the SET of the Dirac field at finite temperature in adS is that of a perfect fluid.

Chapter 8. Rotating fermions on anti-de Sitter space

Just as the construction of rigidly rotating states on Minkowski (flat) space, presented in chapter 4, shares similarities with the construction of vacuum states on the Kerr (rotating black hole) space-time, it is interesting to study quantum states on rigidly rotating anti-de Sitter space-time (adS) for its resemblance to the Kerr-adS space-time. A fundamental difference with respect to the Minkowski space is that adS incorporates a natural boundary, which prevents the speed of light surface (SOL) from forming unless the value of the angular momentum $\Omega = |\boldsymbol{\Omega}|$ of the rotation is large enough.

A study of rigidly rotating states on adS for the scalar field is presented in Ref. [49] and will not be repeated here. Instead, the material of this chapter focuses solely on the investigation of fermion states.

The properties of the space-time are discussed in section 8.1. Section 8.2 presents the Dirac equation, its mode solutions and second quantisation and thermal states are discussed in section 8.3. The full content of this chapter represents original work due for publication in Ref. [9]. A preview of the results is available in Ref. [6].

8.1 Space-time characteristics

By analogy to the rigidly rotating Minkowski space-time, co-rotating coordinates can be obtained from the adS coordinates in Eq. (7.1.4) using the transformation:

$$\varphi = \varphi_{\text{adS}} - \Omega t_{\text{adS}}, \tag{8.1.1}$$

as explained in section 4.1. The metric with respect to the co-rotating coordinates has the form:

$$ds^2 = \frac{1}{\cos^2 \omega r}\left[-\varepsilon_{\text{adS}}\, dt^2 + 2\rho^2\Omega\left(\frac{\sin\omega r}{\omega r}\right)^2 dt d\varphi + dr^2 + \frac{\sin^2\omega r}{\omega^2}(d\theta^2 + \sin^2\theta d\varphi^2)\right], \tag{8.1.2}$$

where $\rho = r\sin\theta$ is the distance from the rotation axis and

$$\varepsilon_{\text{adS}} = 1 - \rho^2\Omega^2\left(\frac{\sin\omega r}{\omega r}\right)^2 \tag{8.1.3}$$
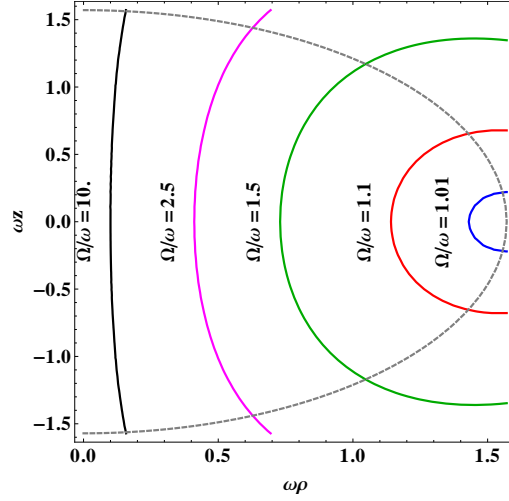
Figure 8.1: The structure of the axi-symmetric SOL, presented at $\varphi = 0$, for various values of the ratio Ω/ω. The horizontal and vertical axes represent distances from and along the rotation axis, respectively. The dotted half-circle centred on $(\rho, z) = (0, 0)$ represents the boundary of adS, given by $r = \sqrt{z^2 + \rho^2} = \frac{\pi}{2\omega}$.

is analogous to $\varepsilon = 1 - \rho^2 \Omega^2$ of the rotating Minkowski space-time, defined in Eq. (4.1.2). This analogy extends to the definition of the speed of light surface (SOL), defined as the surface where $\varepsilon_{\text{adS}} = 0$. Figure 8.1 shows the position of the SOL for various ratios Ω/ω. A suitable tetrad for the adS metric (8.1.2) is:

$$
\begin{aligned}
e_{\hat{t}} &= \cos \omega r \left[\partial_t - \Omega \partial_\varphi \right], \\
e_{\hat{i}} &= \cos \omega r \left[\frac{\omega r}{\sin \omega r} \left(\delta_{ij} - \frac{x^i x^j}{r^2} \right) + \frac{x^i x^j}{r^2} \right] \partial_j,
\end{aligned}
\tag{8.1.4}
$$

having the following associated co-frame one-forms:

$$
\begin{aligned}
\omega^{\hat{t}} &= \frac{dt}{\cos \omega r}, \\
\omega^{\hat{i}} &= \frac{1}{\cos \omega r} \left[\frac{\sin \omega r}{\omega r} \left(\delta_{ij} - \frac{x^i x^j}{r^2} \right) + \frac{x^i x^j}{r^2} \right] dx^j + \frac{\tan \omega r}{\omega r} (\boldsymbol{\Omega} \times \boldsymbol{x})^i dt.
\end{aligned}
\tag{8.1.5}
$$

The Cartan coefficients are the same as in Eq. (7.1.12), with the addition of $c_{\hat{t}\hat{i}}{}^{\hat{j}}$:

$$
c_{\hat{t}\hat{i}}{}^{\hat{t}} = \omega \sin \omega r \frac{x^i}{r}, \qquad c_{\hat{t}\hat{i}}{}^{\hat{j}} = \cos \omega r \, \varepsilon_{ijk} \Omega^k,
$$
$$
c_{\hat{i}\hat{j}}{}^{\hat{k}} = \frac{\omega(1 - \cos \omega r)}{r \sin \omega r} \left(x^j \delta^k{}_i - x^i \delta^k{}_j \right),
\tag{8.1.6}
$$

where Ω^k is the k'th component of $\boldsymbol{\Omega} = (0, 0, \Omega)$. The connection coefficients corresponding to the Cartan coefficients in Eqs. (8.1.6) can be calculated using

Eq. (2.2.19):

$$\Gamma^{\hat{t}}_{\hat{i}\hat{t}} = \omega \sin \omega r \frac{x^i}{r}, \qquad \Gamma^{\hat{i}}_{\hat{j}\hat{t}} = -\frac{1}{2} \cos \omega r \, \varepsilon_{ijk} \Omega^k,$$

$$\Gamma^{\hat{i}}_{\hat{j}\hat{k}} = \frac{\omega(1 - \cos \omega r)}{r \sin \omega r} \left(x^j \delta^i{}_k - x^i \delta_{jk} \right). \tag{8.1.7}$$

As a result, the spin connection changes for the t coordinate:

$$\Gamma_{\hat{t}} = \frac{\omega \sin \omega r}{2r} \gamma^{\hat{t}} (\boldsymbol{x} \cdot \boldsymbol{\gamma}) + \cos \omega r \, (\boldsymbol{\Omega} \cdot \boldsymbol{\Sigma}),$$

$$\Gamma_{\hat{k}} = -\frac{\omega(1 - \cos \omega r)}{2r \sin \omega r} \left[x^k + \gamma^k (\boldsymbol{x} \cdot \boldsymbol{\gamma}) \right]. \tag{8.1.8}$$

8.2 The Dirac equation in rotating coordinates

The co-rotating coordinates can be obtained from the adS coordinates by performing the time-dependent rotation in Eq. (8.1.1). The adS generators of rotation (7.1.105) are the same as on Minkowski space, in particular:

$$J_z = -i\partial_\varphi - iS_z, \tag{8.2.1}$$

where $S_z = \frac{1}{2}\text{diag}(\sigma_3, \sigma_3)$. Hence, the rotation operator for the transformation (8.1.1) takes the form:

$$R_z[-\Omega t] = e^{i\Omega t \partial_\varphi} (\cos \tfrac{\Omega t}{2} + 2i \sin \tfrac{\Omega t}{2} S_z)$$

$$= \text{diag}(e^{\frac{i}{2}\Omega t}, e^{-\frac{i}{2}\Omega t}, e^{\frac{i}{2}\Omega t}, e^{-\frac{i}{2}\Omega t}) e^{i\Omega t \partial_\varphi}. \tag{8.2.2}$$

A solution $\psi(x)$ of the Dirac equation with respect to the co-rotating coordinate frame can be obtained from the non-rotating adS solution ψ_{old} by applying the above rotation operator, as follows:

$$\psi(x) = R_z[-\Omega t]\psi_{\text{old}}(x_{\text{old}}), \tag{8.2.3}$$

where the co-rotating and non-rotating coordinates x and x_{old} are the same except for $\varphi = \varphi_{\text{old}} - \Omega t$. Consequently, the mode solutions of the Dirac equation (7.2.7)

and (7.2.39) have the following expression:

$$U_{E,j,\kappa,m}(x) = \omega r \frac{(\cos \omega r)^{\frac{3}{2}}}{\sin \omega r} \widetilde{U}_{E,j,\kappa,m}(x), \tag{8.2.4a}$$

$$\widetilde{U}_{E,j,\kappa,m}(x) = \frac{1}{r} e^{-i\widetilde{E}t} \left[f_{E,\kappa}^{+}(r)\Phi_{m,\kappa}^{+}(\theta, \varphi) + f_{E,\kappa}^{-}(r)\Phi_{m,\kappa}^{-}(\theta, \varphi) \right], \tag{8.2.4b}$$

$$V_{E,j,m,\kappa} = \omega r \frac{(\cos \omega r)^{\frac{3}{2}}}{\sin \omega r} \widetilde{V}_{E,j,m,\kappa}, \tag{8.2.4c}$$

$$\widetilde{V}_{E,j,m,\kappa} = i(\text{sgn}\kappa)(-1)^{m-\frac{1}{2}} e^{i\widetilde{E}t} \frac{1}{r} \left[f_{E,\kappa}^{+*}(r)\Phi_{-\kappa,-m}^{-}(\theta, \varphi) + f_{E,\kappa}^{-*}(r)\Phi_{-\kappa,-m}^{+}(\theta, \varphi) \right], \tag{8.2.4d}$$

where the angular functions $\Phi_{\kappa,m}^{\pm}(\theta, \varphi)$ are defined in Eq. (7.2.8a) and the radial functions $f_{E,\kappa}^{\pm}(r)$ are related to $\hat{f}_{E,\kappa}^{\pm}(r)$, given in Eq. (7.2.25) through Eq. (7.2.15). The co-rotating frequency $\widetilde{E}$ is related to the adS energy E through:

$$\widetilde{E} = E - \Omega m. \tag{8.2.5}$$

Equation (8.2.5) is actually equivalent to (4.3.3), since m is in both cases the projection of the total angular momentum on the rotation axis. In spherical coordinates, m is an odd half-integer, while in Eq. (4.3.3), m is just an integer.

8.3   Thermal expectation values

The construction of rigidly rotating quantum states on adS and bounded Minkowski space-time share similarities due to adS having a natural boundary. Hence, the co-rotating and non-rotating vacuum states coincide as long as $\widetilde{E}E$ stays positive for all modes. The frequency spectrum of the rotating system is determined by looking at the allowed adS energy, by substituting Eq. (7.2.23) into Eq. (7.2.17):

$$\widetilde{E} = \omega(2n_+ + j + k + 2) - \Omega m = \omega(2n_+ + k + 2) + \omega j - \Omega m. \tag{8.3.1}$$

Since $|m| \leq j$, $\widetilde{E}$ stays positive at arbitrarily large values of j only if $\Omega \leq \omega$, otherwise it can become negative. Hence, if $\Omega \leq \omega$, the rotating vacuum coincides with the adS vacuum. If the vacuum state is the same as in adS, the adS propagator in closed form, discussed in subsection 8.3.2, can be used for the construction thermal states. However, if $\Omega > \omega$, the vacuum state changes and it no longer is described by the adS propagator, in which case mode sums have to be used to construct adequate two-point functions.

The mode sum approach, valid for all values of Ω, is presented in subsection 8.3.1. The geometric approach involving the closed form of the adS propagator, valid for $\Omega \leq \omega$, is considered in subsection 8.3.2.

8.3.1 Mode sums

As in the Minkowski case, there are two choices for the vacuum state: the Vilenkin [72] and the Iyer [47] vacua. The thermal Hadamard Green's function $\Delta S_\beta^{(1)}(x, x')$ with respect to either of these vacuum states can be written as:

$$\Delta S_\beta^{(1)}(x, x') = \omega^2 \frac{(\cos \omega r \cos \omega r')^{\frac{3}{2}}}{\sin \omega r \sin \omega r'} \sum_{n_+=0}^{\infty} \sum_{j,\kappa,m} \left\{ \vphantom{\begin{pmatrix} f \\ f \end{pmatrix}} \right.$$

$$w(\widetilde{E})e^{-i\widetilde{E}\Delta t} \begin{pmatrix} f^+ f^+ \psi_+ \otimes \psi_+^\dagger & -i f^+ f^- \psi_+ \otimes \psi_-^\dagger \\ -i f^- f^+ \psi_- \otimes \psi_+^\dagger & -f^- f^- \psi_- \otimes \psi_-^\dagger \end{pmatrix}$$

$$\left. - w(\overline{E})e^{i\overline{E}\Delta t} \begin{pmatrix} f^- f^- \psi_- \otimes \psi_-^\dagger & -i f^- f^+ \psi_- \otimes \psi_+^\dagger \\ -i f^+ f^- \psi_+ \otimes \psi_-^\dagger & -f^+ f^+ \psi_+ \otimes \psi_+^\dagger \end{pmatrix} \right\}, \quad (8.3.2)$$

where the conventions of subsection 7.5.2 have been used, i.e. $f^\pm \equiv f_{E,\kappa}^\pm$ are the radial functions introduced in Eq. (7.2.7b) and $\psi_\pm \equiv \psi_{j\pm\frac{1}{2}\mathrm{sgn}\kappa}^m$ are two-spinors defined in Eq. (7.2.8b). In the above, $\widetilde{E} = E - \Omega m$, $\overline{E} = E + \Omega m$ and the thermal weight factor $w(z)$ depends on the choice of vacuum as follows:

$$w(z) = \begin{cases} -\dfrac{2}{1 + e^{\beta z}} & \text{for the Vilenkin quantisation,} \\ -\dfrac{2\mathrm{sgn}(z)}{1 + e^{\beta|z|}} & \text{for the Iyer quantisation.} \end{cases} \quad (8.3.3)$$

The weight factor depends implicitly on the sign of $\kappa = \pm(j+\frac{1}{2})$ through the energy:

$$E = \begin{cases} \omega(2n_+ + j + k + 2) & \kappa > 0, \\ \omega(2n_+ + j + k + 1) & \kappa < 0. \end{cases} \quad (8.3.4)$$

From the above expression for E, it follows that in the case when $\Omega \leq \omega$, the Vilenkin and the Iyer vacua coincide, since $\widetilde{E} > 0$:

$$\widetilde{E} = \omega \left[2n_+ + k + \frac{1}{2}(3 + \mathrm{sgn}\kappa) + j - m\frac{\Omega}{\omega} \right]. \quad (8.3.5)$$

The lowest value $\omega \left[k + 1 + j \left(1 - \frac{\Omega}{\omega}\right) \right]$ of $\widetilde{E}$ occurs when $n_+ = 0$, $\kappa < 0$ and $m = j$. It is clear that if $\Omega \leq \omega$, $\widetilde{E} > 0$ for all $E > 0$. However, if $\Omega > \omega$, for any value of n_+, there are combinations of j and m such that $\widetilde{E} < 0$.

Fermion condensate

The fermion condensate (2.2.55a) can be obtained by multiplying the coincidence limit of the trace of Eq. (8.3.2) by $-\frac{1}{2}$:

$$\langle : \overline{\psi}\psi : \rangle_\beta = -\frac{\omega^2(\cos \omega r)^3}{2\sin^2 \omega r} \sum_{n_+,j,m} (\widetilde{w} + \overline{w})[(f_+^{+2} - f_-^{-2})\psi_+^\dagger \psi_+ + (f_-^{+2} - f_+^{-2})\psi_-^\dagger \psi_-],$$

$$(8.3.6)$$

where the radial functions $f_\pm^+$ and $f_\pm^-$, defined in Eq. (7.2.7b), take the argument r, $\widetilde{w} \equiv w(\widetilde{E})$ and $\overline{w} \equiv w(\overline{E})$. In the above, it is understood that the energy in the thermal weight factor multiplying radial functions of positive or negative κ (i.e. their subscript is $+$ of $-$, respectively) also corresponds to positive or negative κ, as follows:

$$(\widetilde{w}+\overline{w})f_+^{\pm 2} \equiv [w(\widetilde{E}_+)+w(\overline{E}_+)]f_+^{\pm 2}, \qquad (\widetilde{w}+\overline{w})f_-^{\pm 2} \equiv [w(\widetilde{E}_-)+w(\overline{E}_-)]f_-^{\pm 2}. \quad (8.3.7)$$

The inner products $\psi_\pm^\dagger \psi_\pm$ in Eq. (8.3.6) can be replaced using Eqs. (C.5.1):

$$\langle : \overline{\psi}\psi : \rangle_\beta = -\frac{\omega^2(\cos \omega r)^3}{4\pi \sin^2 \omega r} \sum_{m=\frac{1}{2}}^{\infty} \sum_{n_+=0}^{\infty} \sum_{j=0}^{\infty} (\widetilde{w} + \overline{w})\frac{(j - m)!}{(j + m)!}$$

$$\{(f_+^{+2} - f_-^{-2})[(j - m + 1)^2 P_+^{-2} + P_+^{+2}] + (f_-^{+2} - f_+^{-2})[(j + m)^2 P_-^{-2} + P_-^{+2}\}, \quad (8.3.8)$$

where $P_\pm^+ \equiv P_{j\pm\frac{1}{2}}^{m+\frac{1}{2}}(\cos \theta)$ and $P_\pm^- \equiv P_{j\pm\frac{1}{2}}^{m-\frac{1}{2}}(\cos \theta)$ are the associated Legendre functions introduced in section C.2.

Charge current

First, let us show that the t.e.v. of the charge current $\langle : J^{\hat{\alpha}} : \rangle_\beta$, given by

$$\langle : J^{\hat{\alpha}} : \rangle_\beta = -\frac{1}{2}\text{tr}\left[\gamma^{\hat{\alpha}} \Delta S_\beta^{(1)}(x' = x)\right], \qquad (8.3.9)$$

vanishes everywhere. Taking the relevant traces on Eq. (8.3.2) gives:

$$\langle : J^{\hat{t}} : \rangle_\beta = -\frac{\omega^2(\cos \omega r)^3}{2\sin^2 \omega r} \sum_{n_+,j,m} (\widetilde{w} - \overline{w})[(f_+^{+2} + f_-^{-2})\psi_+^\dagger \psi_+ + (f_-^{+2} + f_+^{-2})\psi_-^\dagger \psi_-],$$

$$(8.3.10a)$$

$$\langle : J^{\hat{i}} : \rangle_\beta = -\frac{\omega^2(\cos \omega r)^3}{2\sin^2 \omega r} \sum_{n_+,j,m} (\widetilde{w} + \overline{w})(-if_-^- f_+^+ + if_-^- f_-^+)(\psi_+^\dagger \sigma_i \psi_- - \psi_-^\dagger \sigma_i \psi_+).$$

$$(8.3.10b)$$

Equations (C.5.1) show that the $\psi_\pm^\dagger \psi_\pm$ terms are even with respect to $m \to -m$, while $\widetilde{w} - \overline{w}$ is odd. Hence, $\langle : J^{\hat{t}} : \rangle_\beta = 0$. Equations (C.5.9) can be used to show

that the summand in Eq. (8.3.10b) is odd with respect to $m \to -m$, implying that $\langle : J^{\hat{i}} : \rangle_\beta = 0$. Hence, the net charge current vanishes everywhere in the space-time.

Neutrino current

As argued in Ref. [71] and confirmed in subsection 4.3.2, rotating space-times induce a non-vanishing neutrino charge current in thermal states. The charge current for neutrinos $\langle : J^{\hat{\alpha}}_\nu : \rangle_\beta$ can be calculated using:

$$\langle : J^{\hat{\alpha}}_\nu : \rangle_\beta = -\frac{1}{2}\mathrm{tr}\left[\gamma^{\hat{\alpha}}\frac{1}{2}(1-\gamma^5)\Delta S^{(1)}_\beta(x'=x)\right].$$ (8.3.11)

Knowing that the trace of $\gamma^{\hat{\alpha}}\Delta S^{(1)}_\beta$ vanishes, the following expressions can be derived:

$$\langle : J^{\hat{t}}_\nu : \rangle_\beta = -\frac{\omega^2(\cos\omega r)^3}{4\sin^2\omega r}\sum_{n_+,j,m}(\widetilde{w}+\overline{w})(-if^+_+f^-_+ + if^+_-f^-_-)(\psi^\dagger_+\psi_- - \psi^\dagger_-\psi_+),$$
(8.3.12a)

$$\langle : J^{\hat{i}}_\nu : \rangle_\beta = -\frac{\omega^2(\cos\omega r)^3}{4\sin^2\omega r}\sum_{n_+,j,m}(\widetilde{w}-\overline{w})[(f^{+2}_+ + f^{-2}_-)\psi^\dagger_+\sigma_i\psi_+ + (f^{+2}_- + f^{-2}_+)\psi^\dagger_-\sigma_i\psi_-].$$
(8.3.12b)

According to Eqs. (C.5.1), $\psi^\dagger_-\psi_+ = \psi^\dagger_-\psi_+$, since they are the complex conjugates of each other and both are real. Hence, $\langle : J^{\hat{t}}_\nu : \rangle_\beta = 0$, implying that rigidly rotating thermal states contain the same number of neutrinos and anti-neutrinos.

Using Eqs. (C.5.8), the non-zero components of the neutrino charge current can be expressed in cylindrical coordinates:

$$\langle : J^{\hat{\rho}}_\nu : \rangle_\beta = -\frac{\omega^2(\cos\omega r)^3}{4\pi\sin^2\omega r}\sum_{n_+=0}^{\infty}\sum_{m=\frac{1}{2}}^{\infty}\sum_{j=m}^{\infty}(\widetilde{w}-\overline{w})\frac{(j-m)!}{(j+m)!}$$
$$\times\left[(j-m+1)(f^{+2}_+ + f^{-2}_-)P^-_+P^+_+ - (j+m)(f^{+2}_- + f^{-2}_+)P^-_-P^+_-\right],$$
(8.3.13a)

$$\langle : J^{\hat{z}}_\nu : \rangle_\beta = \frac{\omega^2(\cos\omega r)^3}{8\pi\sin^2\omega r}\sum_{n_+=0}^{\infty}\sum_{m=\frac{1}{2}}^{\infty}\sum_{j=m}^{\infty}(\widetilde{w}-\overline{w})\frac{(j-m)!}{(j+m)!}$$
$$\times\{(f^{+2}_+ + f^{-2}_-)[(j-m+1)^2P^{-2}_+ - P^{+2}_+]$$
$$+ (f^{+2}_- + f^{-2}_+)[(j+m)^2P^{-2}_- - P^{+2}_-]\},$$
(8.3.13b)

or, using Eqs. (C.2.7), in spherical coordinates:

$$\langle: J_\nu^{\hat{r}} :\rangle_\beta = \frac{\omega^2(\cos\omega r)^3}{8\pi\sin^2\omega r}\sum_{n_+=0}^{\infty}\sum_{m=\frac{1}{2}}^{\infty}\sum_{j=m}^{\infty}(\widetilde{w}-\overline{w})\frac{(j-m)!}{(j+m)!}$$
$$\times(f_+^{+2}+f_-^{-2}+f_-^{+2}+f_+^{-2})\left[(j+m)(j-m+1)P_-^-P_+^- - P_+^+P_-^+\right],$$
$$(8.3.14\mathrm{a})$$

$$\langle: J_\nu^{\hat{\theta}} :\rangle_\beta = -\frac{\omega^2(\cos\omega r)^3}{8\pi\sin^2\omega r}\sum_{n_+=0}^{\infty}\sum_{m=\frac{1}{2}}^{\infty}\sum_{j=m}^{\infty}(\widetilde{w}-\overline{w})\frac{(j-m)!}{(j+m)!}$$
$$\times(f_+^{+2}+f_-^{-2}-f_-^{+2}-f_+^{-2})\left[(j+m)P_+^+P_-^- + (j-m+1)P_+^-P_-^+\right].$$
$$(8.3.14\mathrm{b})$$

In the above, $P_+^\pm \equiv P_{j+\frac{1}{2}}^{m\pm\frac{1}{2}}(\cos\theta)$ and $P_-^\pm \equiv P_{j-\frac{1}{2}}^{m\pm\frac{1}{2}}(\cos\theta)$ are associated Legendre functions, introduced in section C.2.

Stress-energy tensor

The t.e.v. of the SET is given by the formula:

$$\langle: T_{\hat{\alpha}\hat{\beta}} :\rangle_\beta = \frac{i}{4}\lim_{x'\to x}\mathrm{tr}\left[\gamma_{(\hat{\alpha}}(\partial_{\hat{\beta})}-\partial_{\hat{\beta'})})\Delta S_\beta^{(1)}(x,x') + \left\{\gamma_{(\hat{\alpha}},\Gamma_{\hat{\beta})}\right\}\Delta S_\beta^{(1)}(x,x')\right].$$
$$(8.3.15)$$

For its calculation, the following building blocks are required:

$$\mathrm{tr}\left[\left\{\gamma_{\hat{\alpha}},\Gamma_{\hat{\beta}}\right\}\Delta S_\beta^{(1)}(x,x)\right],\qquad\qquad \lim_{x'\to x}\mathrm{tr}\left[\gamma_{(\hat{\alpha}}\partial_{\hat{\beta})}\Delta S_\beta^{(1)}(x,x')\right].\qquad(8.3.16)$$

It is convenient to keep the part of $\Gamma_{\hat{t}}$ induced by the rotation together with the time derivative, by introducing the following notation:

$$D_{\hat{t}} = \partial_{\hat{t}}^\Omega + \Gamma_{\hat{t}}^0,\qquad(8.3.17)$$

where

$$\partial_{\hat{t}}^\Omega = \cos\omega r\left[\partial_t - \partial_\varphi - (\mathbf{\Omega}\cdot\mathbf{\Sigma})\right],\qquad \Gamma_{\hat{t}}^0 = \frac{\omega\sin\omega r}{2r}\gamma^{\hat{t}}\left(\mathbf{x}\cdot\boldsymbol{\gamma}\right),\qquad(8.3.18)$$

where $\Gamma_{\hat{t}}^0$ is the time component of the spin connection coefficient in the absence of rotation, defined in Eq. (7.1.11), and $\partial_{\hat{t}}^\Omega$ contains the time component of the spin connection coefficient induced by the rotation together with the time derivative with respect to the tetrad, introduced in Eq. (7.1.7). The following relations can be

derived:

$$\left\{\gamma_{\hat{t}}, \Gamma_{\hat{t}}^0\right\} = 0, \tag{8.3.19a}$$

$$\left\{\gamma_{\hat{i}}, \Gamma_{\hat{t}}^0\right\} = \frac{2i\omega}{r} \sin \omega r \, \gamma^{\hat{t}} (\boldsymbol{x} \times \boldsymbol{S})^i, \tag{8.3.19b}$$

$$\left\{\gamma_{\hat{t}}, \Gamma_{\hat{i}}\right\} = -\frac{2i\omega}{r} \frac{1 - \cos \omega r}{\sin \omega r} \gamma^{\hat{t}} (\boldsymbol{x} \times \boldsymbol{S})^i, \tag{8.3.19c}$$

$$\left\{\gamma_{\hat{i}}, \Gamma_{\hat{j}}\right\} = -\frac{\omega(1 - \cos \omega r)}{2r \sin \omega r} \left[4\gamma^{[\hat{i}} x^{j]} + \left[\gamma^{\hat{i}}, \gamma^{\hat{j}}\right] (\boldsymbol{x} \cdot \boldsymbol{\gamma}) \right], \tag{8.3.19d}$$

leading to the following results:

$$\frac{i}{4} \text{tr} \left[\left\{\gamma_{\hat{t}}, \Gamma_{\hat{t}}\right\} \Delta S_\beta^{(1)}(x, x) \right] = 0,$$

$$\frac{i}{4} \text{tr} \left[\left\{\gamma_{(\hat{t}}, \Gamma_{\hat{i})}\right\} \Delta S_\beta^{(1)}(x, x) \right] = -\frac{\omega^3 (\cos \omega r)^4 (1 - \cos \omega r)}{4(\sin \omega r)^3} \sum_{n_+, j, \kappa, m} [w(\widetilde{E}) - w(\overline{E})]$$

$$\times \left[(f^+)^2 \psi_+^\dagger \frac{\boldsymbol{x} \times \boldsymbol{\sigma}}{r} \psi_+ + (f^-)^2 \psi_-^\dagger \frac{\boldsymbol{x} \times \boldsymbol{\sigma}}{r} \psi_- \right],$$

$$\frac{i}{8} \text{tr} \left[\left\{\gamma_{(\hat{i}}, \Gamma_{\hat{j})}\right\} \Delta S_\beta^{(1)}(x, x) \right] = 0. \tag{8.3.20}$$

Next, the derivatives can be evaluated as:

$$\lim_{x' \to x} (\partial_{\hat{t}}^\Omega - \partial_{\hat{t}'}^\Omega) \Delta S_\beta^{(1)}(x, x') = -\frac{2i\omega^2 (\cos \omega r)^4}{\sin^2 \omega r} \sum_{n_+, j, \kappa, m} E \left\{ \right.$$

$$\widetilde{w} \begin{pmatrix} (f^+)^2 \psi_+ \otimes \psi_+^\dagger & -if^- f^+ \psi_+ \otimes \psi_-^\dagger \\ -if^- f^+ \psi_- \otimes \psi_+^\dagger & -(f^-)^2 \psi_- \otimes \psi_-^\dagger \end{pmatrix}$$

$$\left. + \overline{w} \begin{pmatrix} (f^-)^2 \psi_- \otimes \psi_-^\dagger & -if^- f^+ \psi_- \otimes \psi_+^\dagger \\ -if^- f^+ \psi_+ \otimes \psi_-^\dagger & -(f^+)^2 \psi_+ \otimes \psi_+^\dagger \end{pmatrix} \right\}, \tag{8.3.21}$$

$$\lim_{x' \to x} (\partial_{\hat{i}} - \partial_{\hat{i}'}) \Delta S_\beta^{(1)}(x, x') = \frac{\omega^2 (\cos \omega r)^3}{\sin^2 \omega r} e_{\hat{i}}^j \sum_{n_+, j, \kappa, m} \left\{ \right.$$

$$\widetilde{w} \begin{pmatrix} (f^+)^2 (\partial_j - \partial_{j'}) \psi_+ \otimes \psi_+^\dagger & W_- \\ -W_+ & -(f^-)^2 (\partial_j - \partial_{j'}) \psi_- \otimes \psi_-^\dagger \end{pmatrix}$$

$$\left. - \overline{w} \begin{pmatrix} (f^-)^2 (\partial_j - \partial_{j'}) \psi_- \otimes \psi_-^\dagger & -W_+ \\ W_- & -(f^+)^2 (\partial_j - \partial_{j'}) \psi_+ \otimes \psi_+^\dagger \end{pmatrix} \right\}, \tag{8.3.22}$$

where

$$W_\pm = i[\frac{x^j}{r} \omega \, W_{\omega r}(f^+, f^-) \pm f^- f^+ (\partial_j - \partial_{j'})] \psi_\mp \otimes \psi_\pm^\dagger, \tag{8.3.23}$$

The Wronskian $W_{\omega r}(f^+, f^-)$ can be replaced using Eq. (7.5.28).

The following traces can be calculated:

$$\frac{i}{4} \lim_{x' \to x} \text{tr}[\gamma_{\hat{t}}(\widetilde{\partial}_{\hat{t}} - \widetilde{\partial}_{\hat{t}'}) \Delta S_{\beta}^{(1)}(x, x')] = -\frac{\omega^2 (\cos \omega r)^4}{2 \sin^2 \omega r} \sum_{n_+, j, \kappa, m} [w(\widetilde{E}) + w(\overline{E})]$$

$$\times (f^{+2} \psi_+^{\dagger} \psi_+ + f^{-2} \psi_-^{\dagger} \psi_-), \quad (8.3.24a)$$

$$\frac{i}{4} \lim_{x' \to x} \text{tr} \left[\left\{ \gamma_{(\hat{t}}, \Gamma_{\hat{i})} \right\} \Delta S_{\beta}^{(1)}(x, x') \right] = -\frac{\omega^3 (\cos \omega r)^4}{8 \sin^2 \omega r} \tan \frac{\omega r}{2} \sum_{n_+, j, \kappa, m} [w(\widetilde{E}) + w(\overline{E})]$$

$$\times \left[f^{+2} \psi_+^{\dagger} \left(\frac{\boldsymbol{x} \times \boldsymbol{\sigma}}{r} \right)_i \psi_+ + f^{-2} \psi_-^{\dagger} \left(\frac{\boldsymbol{x} \times \boldsymbol{\sigma}}{r} \right)_i \psi_- \right], \quad (8.3.24b)$$

$$\frac{i}{8} \lim_{x' \to x} \text{tr}[\gamma_{\hat{t}}(\partial_{\hat{i}} - \partial_{\hat{i}'}) \Delta S_{\beta}^{(1)}(x, x')] = \frac{i \omega^2 (\cos \omega r)^3}{8 \sin^2 \omega r} \sum_{n_+, j, \kappa, m} [w(\widetilde{E}) + w(\overline{E})]$$

$$\times [(f^+)^2 (\partial_{\hat{i}} - \partial_{\hat{i}'}) \psi_+^{\dagger} \psi_+ + (f^-)^2 (\partial_{\hat{i}} - \partial_{\hat{i}'}) \psi_-^{\dagger} \psi_-], \quad (8.3.24c)$$

$$\frac{i}{8} \lim_{x' \to x} \text{tr}[\gamma_{\hat{i}}(\widetilde{\partial}_{\hat{t}} - \widetilde{\partial}_{\hat{t}'}) \Delta S_{\beta}^{(1)}(x, x')] = \frac{\omega^2 (\cos \omega r)^4}{4 \sin^2 \omega r} \sum_{n_+, j, \kappa, m} [w(\widetilde{E}) + w(\overline{E})]$$

$$\times (-i f^+ f^-)(\psi_+^{\dagger} \sigma^i \psi_- - \psi_-^{\dagger} \sigma^i \psi_+), \quad (8.3.24d)$$

$$\frac{i}{4} \lim_{x' \to x} \text{tr}[\gamma_{\hat{i}}(\partial_{\hat{j}} - \partial_{\hat{j}'}) \Delta S_{\beta}^{(1)}(x, x')] = \frac{\omega^2 (\cos \omega r)^3}{4 \sin^2 \omega r} \sum_{n_+, j, \kappa, m} [w(\widetilde{E}) + w(\overline{E})]$$

$$\times \left[\frac{x^i}{r} \cos \omega r \, W_r(f^+, f^-)(\psi_+^{\dagger} \sigma^j \psi_- + \psi_-^{\dagger} \sigma^j \psi_+) \right.$$

$$\left. + f^- f^+ (\partial_{\hat{i}} - \partial_{\hat{i}'})(\psi_+^{\dagger} \sigma_j \psi_- - \psi_-^{\dagger} \sigma^j \psi_+) \right]. \quad (8.3.24e)$$

The only missing ingredient for the derivation of the components of the SET is a little patience. For $\langle : T_{\hat{t}\hat{t}} : \rangle_{\beta}$, Eqs. (C.5.1) can be used together with Eq. (8.3.24a) to yield:

$$\langle : T_{\hat{t}\hat{t}} : \rangle_{\beta} = -\frac{\omega^2 (\cos \omega r)^3}{4\pi \sin^2 \omega r} \sum_{n_+=0}^{\infty} \sum_{m=\frac{1}{2}}^{\infty} \sum_{j=m}^{\infty} \frac{(j-m)!}{(j+m)!} E[w(\widetilde{E}) + w(\overline{E})] \Big\{$$

$$(f_+^{+2} + f_-^{-2})[(j-m+1)^2 P_+^{-2} + P_+^{+2}] + (f_-^{+2} + f_+^{-2})[(j+m)^2 P_-^{-2} + P_-^{+2}] \Big\}.$$

$$(8.3.25)$$

Just as in the rotating Minkowski space, there is an off-diagonal component mixing time and space. Using Eqs. (C.5.3) in Eq. (8.3.24c), Eqs. (C.5.9) in Eqs. (8.3.24d) and Eqs. (C.5.4) and (C.5.5) in Eq. (8.3.24b), it can be shown that $\langle : T_{\hat{t}\hat{i}} : \rangle_{\beta} \sim$

$(\boldsymbol{x} \times \boldsymbol{\Omega}/\rho\Omega)_i$, which in spherical coordinates translates to $(0, 0, 1)$ for the r, θ, φ components, respectively:

$$
\langle : T_{\hat{t}\varphi} : \rangle_\beta = \frac{\omega^3 (\cos \omega r)^4}{8\pi \sin^2 \omega r} \sum_{n_+=0}^{\infty} \sum_{m=\frac{1}{2}}^{\infty} \sum_{j=m}^{\infty} \frac{(j-m)!}{(j+m)!} [w(\widetilde{E}) + w(\overline{E})] \Bigg\{
$$
$$
\left[\frac{2E}{\omega} (f_-^+ f_-^- - f_+^+ f_+^-) - \frac{1}{2} \tan \frac{\omega r}{2} (f_+^{+2} + f_-^{-2} - f_-^{+2} - f_+^{-2}) \right]
$$
$$
\times [(j-m+1) P_+^- P_-^+ + (j+m) P_-^- P_+^+]
$$
$$
\frac{f_+^{+2} + f_-^{-2}}{\sin\theta \sin \omega r} \left[(m - \tfrac{1}{2})(j-m+1)^2 P_+^{-2} + (m + \tfrac{1}{2}) P_+^{+2} \right]
$$
$$
+ \frac{f_-^{+2} + f_+^{-2}}{\sin\theta \sin \omega r} \left[(m - \tfrac{1}{2})(j+m)^2 P_-^{-2} + (m + \tfrac{1}{2}) P_-^{+2} \right] \Bigg\}. \quad (8.3.26)
$$

The spatial components are determined by Eq. (8.3.24e), where the contractions of the ψ bi-spinors are given by Eqs. (C.5.8d) and (C.5.10e). The terms that appear in these latter two equations have the following (r, θ, φ) tetrad components in spherical coordinates:

$$
\frac{\boldsymbol{\Omega} \times (\boldsymbol{x} \times \boldsymbol{\Omega})}{\rho\Omega^2} = (\sin\theta, \cos\theta, 0), \qquad \frac{\boldsymbol{\Omega}}{\Omega} = (\cos\theta, -\sin\theta, 0), \quad (8.3.27a)
$$

$$
\frac{\boldsymbol{x} \times (\boldsymbol{\Omega} \times \boldsymbol{x})}{\rho\Omega r} = (0, -1, 0), \qquad \frac{\boldsymbol{\Omega} \times \boldsymbol{x}}{\rho\Omega} = (0, 0, 1). \quad (8.3.27b)
$$

The tensors that enter in the expression of $\langle : T_{\hat{i}\hat{j}} : \rangle_\beta$ have the following spherical components:

$$
\frac{x^{(i}}{r} \left[\frac{\boldsymbol{\Omega} \times (\boldsymbol{x} \times \boldsymbol{\Omega})}{\rho\Omega^2} \right]^{j)} = \begin{pmatrix} \sin\theta & \frac{1}{2}\cos\theta & 0 \\ \frac{1}{2}\cos\theta & 0 & 0 \\ 0 & 0 & 0 \end{pmatrix}, \quad (8.3.28a)
$$

$$
\frac{x^{(i}}{r} \frac{\Omega^{j)}}{\Omega} = \begin{pmatrix} \cos\theta & -\frac{1}{2}\sin\theta & 0 \\ -\frac{1}{2}\sin\theta & 0 & 0 \\ 0 & 0 & 0 \end{pmatrix}, \quad (8.3.28b)
$$

$$
\left(\frac{\boldsymbol{\Omega} \times \boldsymbol{x}}{\rho\Omega} \right)_i \left(\frac{\boldsymbol{\Omega} \times \boldsymbol{x}}{\rho\Omega} \right)_j = \begin{pmatrix} 0 & 0 & 0 \\ 0 & 0 & 0 \\ 0 & 0 & 1 \end{pmatrix}, \quad (8.3.28c)
$$

$$
\left(\frac{\boldsymbol{x} \times (\boldsymbol{\Omega} \times \boldsymbol{x})}{\rho^2\Omega} \right)_{(i} \left(\frac{\boldsymbol{\Omega} \times (\boldsymbol{x} \times \boldsymbol{\Omega})}{\rho\Omega^2} \right)_{j)} = \begin{pmatrix} 0 & -\frac{1}{2} & 0 \\ -\frac{1}{2} & -\cot\theta & 0 \\ 0 & 0 & 0 \end{pmatrix}, \quad (8.3.28d)
$$

$$
\left(\frac{\boldsymbol{x} \times (\boldsymbol{\Omega} \times \boldsymbol{x})}{\rho^2\Omega} \right)_{(i} \left(\frac{\boldsymbol{\Omega}}{\Omega} \right)_{j)} = \begin{pmatrix} 0 & -\frac{1}{2}\cot\theta & 0 \\ -\frac{1}{2}\cot\theta & 1 & 0 \\ 0 & 0 & 0 \end{pmatrix}. \quad (8.3.28e)
$$

After changing from $(\partial_i - \partial_{i'})$ to $\partial_{\hat{i}} - \partial_{\hat{i}'}$ in Eq. (C.5.10e), the following expression is found for the $r - r$ component:

$$\langle : T_{\hat{r}\hat{r}} : \rangle_\beta = \frac{\omega^3 (\cos \omega r)^4}{4\pi \sin^2 \omega r} \sum_{n_+=0}^{\infty} \sum_{m=\frac{1}{2}}^{\infty} \sum_{j=m}^{\infty} \frac{(j-m)!}{(j+m)!} [w(\widetilde{E}) + w(\overline{E})]$$
$$\times \left[W_{\omega r}(f_+^+, f_+^-) + W_{\omega r}(f_-^+, f_-^-) \right]$$
$$\times \left\{ \sin\theta \left[(j-m+1)P_+^- P_-^+ - (j+m)P_-^- P_+^+ \right] \right.$$
$$\left. + \cos\theta \left[(j+m)(j-m+1)P_+^- P_-^- + P_+^+ P_-^+ \right] \right\}, \quad (8.3.29)$$

where the Wronskian $W_{\omega r}(f_\pm^+, f_\pm^-)$ can be calculated from Eq. (7.5.28). Equations (C.2.7) can be used to further simplify the above expression:

$$\langle : T_{\hat{r}\hat{r}} : \rangle_\beta = \frac{\omega^3 (\cos \omega r)^4}{4\pi \sin^2 \omega r} \sum_{n_+=0}^{\infty} \sum_{m=\frac{1}{2}}^{\infty} \sum_{j=m}^{\infty} \frac{(j-m)!}{(j+m)!} [w(\widetilde{E}) + w(\overline{E})]$$
$$\times \left[W_{\omega r}(f_+^+, f_+^-) + W_{\omega r}(f_-^+, f_-^-) \right] \left[P_-^{+2} + (j+m)^2 P_-^{-2} \right]. \quad (8.3.30)$$

With a similar application of Eqs. (C.2.7), the $\theta - \theta$ component evaluates to:

$$\langle : T_{\hat{\theta}\hat{\theta}} : \rangle_\beta = \frac{\omega^2 (\cos \omega r)^4 \sin\theta}{4\pi \sin^3 \omega r} \sum_{n_+=0}^{\infty} \sum_{m=\frac{1}{2}}^{\infty} \sum_{j=m}^{\infty} \frac{(j-m)!}{(j+m)!} [w(\widetilde{E}) + w(\overline{E})](f_+^+ f_+^- - f_-^+ f_-^-)$$
$$\left[(j+m) W_{\cos\theta}(P_-^+, P_-^-) + (j-m+1) W_{\cos\theta}(P_+^+, P_+^-) \right], \quad (8.3.31)$$

where $W_{\cos\theta}(P_\pm^+, P_\pm^-)$ are Wronskians of the associated Legendre functions $P_\pm^+$ and $P_\pm^-$ with respect to $\cos\theta$. The explicit form of the associated Legendre functions, defined in section C.2, can be used to obtain the following expressions:

$$W(P_-^+, P_-^-) = \frac{1}{\sin^2\theta} \left[(j-m)P_-^- P_+^+ - (j-m+1)P_-^+ P_+^- \right], \quad (8.3.32a)$$
$$W(P_+^+, P_+^-) = \frac{1}{\sin^2\theta} \left[(j+m)P_-^- P_+^+ - (j+m+1)P_-^+ P_+^- \right], \quad (8.3.32b)$$

Hence, Eq. (8.3.31) can be simplified to:

$$\langle : T_{\hat{\theta}\hat{\theta}} : \rangle_\beta = \frac{\omega^2 (\cos \omega r)^4}{4\pi \sin^3 \omega r \sin\theta} \sum_{n_+=0}^{\infty} \sum_{m=\frac{1}{2}}^{\infty} \sum_{j=m}^{\infty} \frac{(j-m)!}{(j+m)!} [w(\widetilde{E}) + w(\overline{E})](f_+^+ f_+^- - f_-^+ f_-^-)$$
$$\left[(j+m)(2j-2m+1)P_-^- P_+^+ - (j-m+1)(2j+2m+1)P_-^+ P_+^- \right]. \quad (8.3.33)$$

The $\varphi - \varphi$ component follows swiftly:

$$\langle : T_{\hat\varphi\hat\varphi} : \rangle_\beta = \frac{\omega^3(\cos\omega r)^4}{2\pi(\sin\omega r)^3 \sin\theta} \sum_{n_+=0}^{\infty} \sum_{m=\frac{1}{2}}^{\infty} \sum_{j=m}^{\infty} m \frac{(j-m)!}{(j+m)!}[w(\widetilde{E}) + w(\overline{E})](f_+^+ f_+^- - f_-^+ f_-^-)$$

$$\left[(j+m)P_-^- P_+^+ + (j-m+1)P_-^+ P_+^-\right]. \quad (8.3.34)$$

Surprisingly, there appears to be a non-vanishing non-diagonal component in the spatial sector:

$$\langle : T_{\hat r\hat\theta} : \rangle_\beta = \frac{\omega^3(\cos\omega r)^4}{8\pi\sin^2\omega r} \sum_{n_+=0}^{\infty} \sum_{m=\frac{1}{2}}^{\infty} \sum_{j=m}^{\infty} \frac{(j-m)!}{(j+m)!}[w(\widetilde{E}) + w(\overline{E})]$$

$$\times \Bigg\{ \left[W_{\omega r}(f_+^+, f_+^-) + W_{\omega r}(f_-^+, f_-^-)\right]$$

$$\times \left(\cos\theta \left[(j-m+1)P_+^- P_-^+ - (j+m)P_+^+ P_-^-\right]\right.$$

$$\left.- \sin\theta \left[(j+m)(j-m+1)P_+^- P_-^- + P_+^+ P_-^+\right]\right)$$

$$- \frac{\omega r}{\sin\omega r} \sin\theta(f_+^+ f_+^- - f_-^+ f_-^-)$$

$$\times \Big(\sin\theta \left[(j-m+1)W_{\cos\theta}(P_+^-, P_-^+) + (j+m)W_{\cos\theta}(P_-^-, P_+^+)\right]$$

$$+ \cos\theta \left[(j-m+1)(j+m)W_{\cos\theta}(P_+^-, P_-^-) + W_{\cos\theta}(P_+^+, P_-^+)\right]\Big)\Bigg\}. \quad (8.3.35)$$

Eqs. (C.2.7) can be used to show that the first term in the curly brackets (involving the Wronskians of the radial functions) is actually 0, while the second term can be transformed to:

$$\langle : T_{\hat r\hat\theta} : \rangle_\beta = -\frac{\omega^4 r(\cos\omega r)^4 \sin\theta}{8\pi(\sin\omega r)^3} \sum_{n_+=0}^{\infty} \sum_{m=\frac{1}{2}}^{\infty} \sum_{j=m}^{\infty} \frac{(j-m)!}{(j+m)!}[w(\widetilde{E}) + w(\overline{E})](f_+^+ f_+^- - f_-^+ f_-^-)$$

$$\frac{d}{d(\cos\theta)}\left[P_-^{+2} + (j+m)^2 P_-^{-2} - (j-m+1)^2 P_+^{-2} - P_+^{+2}\right]. \quad (8.3.36)$$

Equation (C.2.7) can be applied again to find that:

$$\langle : T_{\hat r\hat\theta} : \rangle_\beta = 0. \quad (8.3.37)$$

8.3.2 The geometric approach

The geometric approach consists in using the ansatz (7.3.1) for the Feynman propagator together with the results in subsection 7.3.2 to compute thermal expectation values. This approach can only be used if the rotating vacuum coincides with the adS vacuum (i.e. when $\Omega \le \omega$). Since one of the fundamental assumptions used in

the construction of the adS propagator is that the space-time is maximally symmetric, if the rotating vacuum is no longer the adS vacuum, it becomes the analogue of the vacuum state considered by Iyer [47] for the rotating Minkowski space-time, discussed in subsection 4.3.1. This vacuum state no longer characterises a state which posseses maximal symmetry, hence, the ansatz (7.3.1) does not hold.

Thermal states are described by the thermal Feynman propagator $S_F^\beta(x, x')$, which can be obtained from the vacuum propagator $S_F(x, x')$ using its anti-periodicity property with respect to imaginary time. In subsection 7.5.1, thermal states on adS were constructed by thermalising with respect to the Hamiltonian $H_{\text{adS}} = i\partial_{t_{\text{adS}}}$. Rigidly rotating thermal states can be obtained by thermalising with respect to the Hamiltonian of the co-rotating system $H = i\partial_t = i\partial_{t_{\text{adS}}} + i\Omega\partial_{\varphi_{\text{adS}}}$, which can be most easily performed by changing to rotating coordinates, as described in subsection 8.3.1. The (adS) Feynman propagator with respect to rotating coordinates can be written as:

$$\Omega S_F(x, x') = R_z(-\Omega t)S_F(x, x')R_{z'}(\Omega t'), \tag{8.3.38}$$

where the rotation operators $R_z(-\Omega t)$ and $R_{z'}(\Omega t')$, defined in Eq. (8.2.2), act on the coordinates x and x' and the the bi-spinor structure.

Thermal states constructed with respect to the adS vacuum are described by the difference $\Delta_\Omega S_F^\beta(x, x')$ between the thermal and vacuum Feynman propagators, as shown in Eq. (7.5.1):

$$\Delta_\Omega S_F^\beta(x, x') = \sum_{j\neq 0}(-1)^j \Delta_\Omega S_F(t + ij\beta, \boldsymbol{x}; t', \boldsymbol{x}'). \tag{8.3.39}$$

Thermal expectation values can now be calculated using Eqs. (7.4.1) by replacing $S_F(x, x')$ with $2\Omega S_F^\beta(x, x')$.

Fermion condensate

The Fermion condensate (FC) can be calculated using Eq. (7.4.1a) by taking the trace of the coincidence limit of $-\Delta_\Omega S_F^\beta(x, x')$. Before giving the result, it is worth noting that scalar product terms of the form $\frac{\boldsymbol{x}\cdot\boldsymbol{\gamma}}{r}$ remain unchanged under the action of the rotation operator $R_z(-\Omega t)$ (but not under $R_{z'}(\Omega t')$), since $R_z(-\Omega t)$ rotates both $\boldsymbol{x}$ and $\boldsymbol{\gamma}$, keeping the angle between them unchanged. Thus, the following traces can be computed:

$$\lim_{\boldsymbol{x}'\to\boldsymbol{x}} \text{tr}[R_z(-\Omega t)\Lambda(x, x')R_{z'}(\Omega t')] = \frac{4\cos\frac{\omega\Delta t}{2}\cos\frac{\Omega\Delta t}{2}}{\cos\omega r\,\cos\frac{\omega s\Omega}{2}},$$

$$\lim_{\boldsymbol{x}'\to\boldsymbol{x}} \text{tr}[R_z(-\Omega t)\slashed{\eta}\Lambda(x, x')R_{z'}(\Omega t')] = 0, \tag{8.3.40}$$

where s_Ω is the geodetic interval defined in Eq. (7.1.25) with $\Delta\varphi$ replaced by $\Delta\varphi - \Omega\Delta t$. The following expression is obtained for the t.e.v. of the FC:

$$\langle : \overline{\psi}\psi : \rangle_\beta = -\sum_{j=1}^{\infty}(-1)^j \frac{8\cosh\frac{\omega j\beta}{2}\cosh\frac{\Omega j\beta}{2}}{\cos\omega r} \left. \frac{\alpha_F(s_\Omega)}{\cos\frac{\omega s_\Omega}{2}}\right|_{\substack{\boldsymbol{x}=\boldsymbol{x}' \\ \Delta t=ij\beta}}. \tag{8.3.41}$$

Equation (7.3.21a) can be used for α_F, while the following expression can be used to eliminate the geodetic interval s_Ω:

$$\left.\sin^2\frac{\omega s}{2}\right|_{\substack{\boldsymbol{x}=\boldsymbol{x}' \\ \Delta t=ij\beta}} = -\frac{1}{\zeta_j}, \tag{8.3.42}$$

where

$$\zeta_j = \cos^2\omega r\left(\sinh^2\frac{\omega j\beta}{2} - \sin^2\omega r\sin^2\theta\sinh^2\frac{\Omega j\beta}{2}\right)^{-1}. \tag{8.3.43}$$

Hence, the t.e.v. of the FC takes the form:

$$\langle : \overline{\psi}\psi : \rangle_\beta = \mp\frac{\omega^3 N_{\pm k}}{2\pi^2}\sum_{j=1}^{\infty}(-1)^j\cosh\frac{\omega j\beta}{2}\cosh\frac{\Omega j\beta}{2}\left(\frac{\zeta_j}{\zeta_j+1}\right)^{2\pm k}$$
$$\times\,_2F_1\left(\pm k, 2\pm k; 1\pm 2k; \frac{\zeta_j}{\zeta_j+1}\right), \tag{8.3.44}$$

where the $+$ and $-$ signs correspond to regular and irregular modes, respectively. It is interesting to note that the sign of the FC changes from positive for regular modes to negative for irregular modes, resembling the effect of ς on the FC (5.3.45) for rigidly rotating thermal states of fermions obeying MIT boundary conditions.

In the massless limit, the t.e.v. of the FC reduces to:

$$\left.\langle : \overline{\psi}\psi : \rangle_\beta\right|_{k=0} = \mp\frac{\omega^3}{2\pi^2}\sum_{j=1}^{\infty}(-1)^j\cosh\frac{\omega j\beta}{2}\cosh\frac{\Omega j\beta}{2}\left(\frac{\zeta_j}{\zeta_j+1}\right)^2. \tag{8.3.45}$$

In the case $\Omega = \omega$ when the speed of light surface (SOL) is just about to form, Eq. (8.3.44) reduces on the equatorial plane ($\theta = \frac{\pi}{2}$) to:

$$\left.\langle : \overline{\psi}\psi : \rangle_\beta\right|_{\substack{\Omega=\omega \\ \theta=\frac{\pi}{2}}} = \mp\frac{\omega^3 N_{\pm k}}{2\pi^2}\sum_{j=1}^{\infty}\frac{(-1)^j}{\cosh^2\frac{\omega j\beta}{2}}\,_2F_1\left(\pm k, 2\pm k; 1\pm 2k; \frac{1}{\cosh^2\frac{\omega j\beta}{2}}\right). \tag{8.3.46}$$

It is remarkable that the FC is constant throughout the equatorial plane ($\theta = \frac{\pi}{2}$) when $\Omega = \omega$. In the massless limit, Eq. (8.3.46) further reduces to:

$$\left.\langle : \overline{\psi}\psi : \rangle_\beta\right|_{\substack{k=0 \\ \Omega=\omega \\ \theta=\frac{\pi}{2}}} = \mp\frac{\omega^3}{2\pi^2}C_2(\beta\omega), \tag{8.3.47}$$

where

$$C_\ell(x) = \sum_{j=1}^{\infty} \frac{(-1)^{j+1}}{(\cosh \frac{jx}{2})^2}. \tag{8.3.48}$$

It is possible to write $C_2(x)$ in closed form by expanding the denominator in a series:

$$C_2(x) = 4 \sum_{j=1}^{\infty} (-1)^{j+1} \sum_{s=0}^{\infty} (-1)^s s\, e^{-jsx}. \tag{8.3.49}$$

The sum over j can be performed as a geometric series, after which $C_2(x)$ can be put in the form:

$$C_2(x) = -4 \frac{d}{dx} \sum_{s=0}^{\infty} (-1)^s \ln(1 + e^{-sx}). \tag{8.3.50}$$

The function $C_2(x)$ can be written in terms of the Q-Pochhammer symbol $(a; q)_n$, defined as:

$$(a; q)_n = \prod_{s=0}^{n} (1 - aq^s), \tag{8.3.51}$$

by splitting the sum over s into sums over even and odd values of s, yielding:

$$C_2(x) = -4 \frac{d}{dx} \left[(-1; e^{-2x})_\infty - (-e^{-x}, e^{-2x})_\infty \right]. \tag{8.3.52}$$

Charge current

The charge current (CC) can be calculated using Eq. (7.4.1b) by replacing $S_F(x, x')$ with $\Delta_\Omega S_F^\beta(x, x')$. Using the following traces:

$$\lim_{\boldsymbol{x}' \to \boldsymbol{x}} \text{tr}[\gamma^{\hat{t}} R_z(-\Omega t) \not\!\Lambda(x, x') R_{z'}(\Omega t')] = \frac{4 \sin \frac{\omega \Delta t}{2} \cos \frac{\Omega \Delta t}{2}}{\cos \omega r \sin \frac{\omega s_\Omega}{2}}, \tag{8.3.53a}$$

$$\lim_{\boldsymbol{x}' \to \boldsymbol{x}} \text{tr}[\gamma^{\hat{\ell}} R_z(-\Omega t) \not\!\Lambda(x, x') R_{z'}(\Omega t')] = -4 \tan \omega r \left(\frac{\boldsymbol{x} \times \boldsymbol{\Omega}}{\Omega r} \right)^\ell \frac{\cos \frac{\omega \Delta t}{2} \sin \frac{\Omega \Delta t}{2}}{\sin \frac{\omega s_\Omega}{2}}, \tag{8.3.53b}$$

it is easy to infer that the charge current vanishes, as the above terms are odd with respect to the transformation $\Delta t \to -\Delta t$ when $\Delta t \to ij\beta$:

$$\langle : J^{\hat{\alpha}} : \rangle_\beta = 0. \tag{8.3.54}$$

Neutrino charge current

The neutrino charge current can be calcualted using Eq. (8.3.11) by replacing $\Delta S_\beta^{(1)}(x, x')$ with $2_\Omega S_F^\beta(x, x')$:

$$\langle : J_\nu^{\hat{\alpha}} : \rangle_\beta = \text{tr}\left[\gamma^{\hat{\alpha}} \frac{1 - \gamma^5}{2} \Delta_\Omega S_F^\beta(x' = x) \right]. \tag{8.3.55}$$

Using the following traces:

$$\lim_{\boldsymbol{x}' \to \boldsymbol{x}} \text{tr}[\gamma^{\hat{t}} \gamma^5 R_z(-\Omega t) \not{n} \Lambda(x, x') R_{z'}(\Omega t')] = 0,$$

$$\lim_{\boldsymbol{x}' \to \boldsymbol{x}} \text{tr}[\gamma^{\hat{\ell}} \gamma^5 R_z(-\Omega t) \not{n} \Lambda(x, x') R_{z'}(\Omega t')] = \left[\cos \omega r \left(\delta_{\ell z} - \frac{x^\ell}{r} \cos \theta \right) + \frac{x^\ell}{r} \cos \theta \right]$$

$$\times \frac{4i \sin \frac{\omega \Delta t}{2} \sin \frac{\Omega \Delta t}{2}}{\cos \omega r \sin \frac{\omega s_\Omega}{2}}, \tag{8.3.56}$$

the only non-vanishing components of the neutrino charge current can be computed:

$$\langle : J_\nu^{\hat{r}} : \rangle_\beta = \frac{\omega^3 N_\pm \cos \theta}{4\pi^2 \cos \omega r} \sum_{j=1}^\infty (-1)^j \sinh \frac{\omega j \beta}{2} \sinh \frac{\Omega j \beta}{2}$$

$$\times \zeta_j^{2 \pm k} {}_2F_1 \left(\pm k, 2 \pm k; 1 \pm 2k; -\zeta_j \right), \tag{8.3.57a}$$

$$\langle : J_\nu^{\hat{\theta}} : \rangle_\beta = -\frac{\omega^3 N_{\pm k} \sin \theta}{4\pi^2} \sum_{j=1}^\infty (-1)^j \sinh \frac{\omega j \beta}{2} \sinh \frac{\Omega j \beta}{2}$$

$$\times \zeta_j^{2 \pm k} {}_2F_1 \left(\pm k, 2 \pm k; 1 \pm 2k; -\zeta_j \right). \tag{8.3.57b}$$

In the massless limit, the neutrino CC simplifies to:

$$\langle : J_\nu^{\hat{r}} : \rangle_\beta \Big|_{k=0} = \frac{\omega^3 (\cos \omega r)^3 \cos \theta}{4\pi^2} \sum_{j=1}^\infty \frac{(-1)^j \sinh \frac{\omega j \beta}{2} \sinh \frac{\Omega j \beta}{2}}{(\sinh^2 \frac{\omega j \beta}{2} - \sin^2 \omega r \sin^2 \theta \sinh^2 \frac{\Omega j \beta}{2})^2},$$

$$\tag{8.3.58a}$$

$$\langle : J_\nu^{\hat{\theta}} : \rangle_\beta \Big|_{k=0} = -\frac{\omega^3 (\cos \omega r)^4 \sin \theta}{4\pi^2} \sum_{j=1}^\infty \frac{(-1)^j \sinh \frac{\omega j \beta}{2} \sinh \frac{\Omega j \beta}{2}}{(\sinh^2 \frac{\omega j \beta}{2} - \sin^2 \omega r \sin^2 \theta \sinh^2 \frac{\Omega j \beta}{2})^2}.$$

$$\tag{8.3.58b}$$

When $\Omega = \omega$, Eqs. (8.3.57) reduce to:

$$
\langle : J_\nu^{\hat{r}} : \rangle_\beta \Big|_{\Omega=\omega} = \frac{\omega^3 N_\pm (\cos \omega r)^{3 \pm 2k} \cos \theta}{4\pi^2 \varepsilon_{\mathrm{adS}}^{2 \pm k}} \sum_{j=1}^{\infty} \frac{(-1)^j}{(\sinh \frac{\omega j \beta}{2})^{2 \pm 2k}}
$$

$$
\times {}_2F_1 \left(\pm k, 2 \pm k; 1 \pm 2k; -\frac{\cos^2 \omega r}{\varepsilon_{\mathrm{adS}} \sinh^2 \frac{\omega j \beta}{2}} \right),
\tag{8.3.59a}
$$

$$
\langle : J_\nu^{\hat{\theta}} : \rangle_\beta \Big|_{\Omega=\omega} = -\frac{\omega^3 N_\pm (\cos \omega r)^{4 \pm 2k} \sin \theta}{4\pi^2 \varepsilon_{\mathrm{adS}}^{2 \pm k}} \sum_{j=1}^{\infty} \frac{(-1)^j}{(\sinh \frac{\omega j \beta}{2})^{2 \pm 2k}}
$$

$$
\times {}_2F_1 \left(\pm k, 2 \pm k; 1 \pm 2k; -\frac{\cos^2 \omega r}{\varepsilon_{\mathrm{adS}} \sinh^2 \frac{\omega j \beta}{2}} \right),
\tag{8.3.59b}
$$

where $\varepsilon_{\mathrm{adS}}$, defined in Eq. (8.1.3), reduces when $\Omega = \omega$ to:

$$
\varepsilon_{\mathrm{adS}} = 1 - \sin^2 \omega r \sin^2 \theta.
\tag{8.3.60}
$$

It can be seen that, in the case when $\Omega = \omega$, $\langle : J_\nu^{\hat{r}} : \rangle_\beta$ vanishes on the equatorial plane, while $\langle : J_\nu^{\hat{\theta}} : \rangle_\beta$ attains a constant value. Setting the mass to 0 reduces Eqs. (8.3.59) to:

$$
\langle : J_\nu^{\hat{r}} : \rangle_\beta \Big|_{\substack{k=0 \\ \Omega=\omega}} = -\frac{\omega^3 (\cos \omega r)^3 \cos \theta}{4\pi^2 \varepsilon_{\mathrm{adS}}^2} S_2(\beta \omega),
\tag{8.3.61a}
$$

$$
\langle : J_\nu^{\hat{\theta}} : \rangle_\beta \Big|_{\substack{k=0 \\ \Omega=\omega}} = \frac{\omega^3 (\cos \omega r)^4 \sin \theta}{4\pi^2 \varepsilon_{\mathrm{adS}}^2} S_2(\beta \omega),
\tag{8.3.61b}
$$

where

$$
S_\ell(x) = \sum_{j=1}^{\infty} \frac{(-1)^{j+1}}{(\sinh \frac{jx}{2})^\ell}.
\tag{8.3.62}
$$

Following the steps leading to Eq. (8.3.52), it is possible to write $S_2(x)$ in a closed form, by expanding the denominator:

$$
S_2(x) = 4 \sum_{j=1}^{\infty} (-1)^{j+1} \sum_{s=0}^{\infty} s\, e^{-jsx}.
\tag{8.3.63}
$$

Since there is no $(-1)^s$ factor in the sum over s, the above equation can be straightforwardly written in terms of the Q-Pochhammer symbol (8.3.51) as:

$$
S_2(x) = -4 \frac{d}{dx} (-1; e^{-x})_\infty.
\tag{8.3.64}
$$

Stress-energy tensor

The formula giving the t.e.v. of the SET can be obtained from Eq. (8.3.15) by replacing $\Delta S_\beta^{(1)}(x, x')$ with $2\Delta_\Omega S_F^\beta(x, x')$. Since $\langle : T_{\hat\alpha\hat\gamma} : \rangle_\beta$ is calculated as the trace of $_\Omega S_F^\beta(x, x')$ multiplied by one gamma matrix $\gamma^{\hat\rho}$, the α_F term in Eq. (7.3.1) does not contribute (the trace of the bi-spinor of parallel transport $\Lambda(x, x')$ multiplied by any odd number of gamma matrices vanishes, as discussed in subsection 7.1.4).

Computation of $\langle : T_{\hat t\hat t} : \rangle_\beta$. The split (8.3.18) for the covariant time derivative into $\partial_{\hat t}^\Omega$ and $\Gamma_{\hat t}^0$ is useful, since:

$$\partial_{\hat t}^\Omega R_z(-\Omega t) = R_z(-\Omega t)\cos\omega r\partial_t. \tag{8.3.65}$$

According to Eq. (8.3.19a), the $\Gamma_{\hat t}^0$ term does not contribute to $\langle : T_{\hat t\hat t} : \rangle_\beta$. Two traces are required for this computation: the first is given in Eq. (8.3.53a) and the second is:

$$\lim_{\boldsymbol{x}'\to\boldsymbol{x}} \operatorname{tr}\left[\gamma_{\hat t}(\partial_{\hat t}^\Omega - \partial_{\hat t'}^\Omega)R_z(-\Omega t)\not\!\!\Lambda(x, x')\sin\tfrac{\omega s}{2} R_{z'}(\Omega t')\right] = -4\cos\frac{\omega\Delta t}{2}\cos\frac{\Omega\Delta t}{2}, \tag{8.3.66}$$

where $\sin\frac{\omega s}{2}$ was added to cancel the $\sin\frac{\omega s}{2}$ factor in the denominator of $\not\!\!\Lambda(x, x')$ (7.1.69b). Also, $\beta_F/\sin\frac{\omega s}{2}$ (7.3.22b) is now a function of $\zeta = -1/\sin^2\frac{\omega s}{2}$. Using the properties:

$$(\partial_t - \partial_{t'})\zeta = \zeta^2\frac{\omega\sin\omega\Delta t}{\cos\omega r\,\cos\omega r'}, \tag{8.3.67a}$$

$$\partial_\zeta\left(\frac{\beta_F(s)}{\sin\frac{\omega s}{2}}\right) = \frac{i\omega^3 N_{\pm k}(2 \pm k)}{16\pi^2}\zeta^{1\pm k}{}_2F_1(\pm k, 3 \pm k; 1 \pm 2k; -\zeta), \tag{8.3.67b}$$

the following result can be obtained:

$$(\partial_t - \partial_{t'})\frac{\beta_F}{\sin\frac{\omega s}{2}} = \frac{i\omega^4 N_\pm(2 \pm k)\sin\omega\Delta t}{16\pi^2\cos\omega r\cos\omega r'}\zeta^{3\pm k}{}_2F_1(\pm k, 3 \pm k; 1 \pm 2k; -\zeta). \tag{8.3.68}$$

Thus, the t.e.v. of the energy density takes the form:

$$\langle : T_{\hat t\hat t} : \rangle_\beta = -\frac{\omega^4 N_{\pm k}}{4\pi^2\cos^2\omega r}\sum_{j=1}^\infty(-1)^j\cosh\frac{\omega j\beta}{2}\cosh\frac{\Omega j\beta}{2}$$
$$\times\left[2(2 \pm k)\sinh^2\frac{\omega j\beta}{2}\,\zeta_j^{3\pm k}{}_2F_1\left(\pm k, 3 \pm k; 1 \pm 2k; -\zeta_j\right)\right.$$
$$\left.-\cos^2\omega r\,\zeta_j^{2\pm k}{}_2F_1\left(\pm k, 2 \pm k; 1 \pm 2k; -\zeta_j\right)\right], \tag{8.3.69}$$

and reduces in the massless limit to:

$$\langle : T_{\hat t\hat t} : \rangle_\beta\Big|_{k=0} = -\frac{\omega^4}{4\pi^2}\sum_{j=1}^\infty(-1)^j\zeta_j^2\cosh\frac{\omega j\beta}{2}\cosh\frac{\Omega j\beta}{2}\left(\frac{4\zeta_j\sinh^2\frac{\omega j\beta}{2}}{\cos^2\omega r} - 1\right). \tag{8.3.70}$$

In the case $\Omega = \omega$, Eq. (8.3.69) reduces to:

$$\langle : T_{\hat{t}\hat{t}} : \rangle_\beta \Big|_{\Omega=\omega} = -\frac{\omega^4 N_{\pm k}(\cos\omega r)^{4\pm 2k}}{4\pi^2 \varepsilon_{\mathrm{adS}}^{3\pm k}} \sum_{j=1}^{\infty} (-1)^j \frac{\cosh^2 \frac{\omega j\beta}{2}}{(\sinh\frac{\omega j\beta}{2})^{4\pm 2k}}$$
$$\times [2(2\pm k)_2 F_1 (\pm k, 3\pm k; 1\pm 2k; -\zeta_j) - \varepsilon_{\mathrm{adS}2}F_1 (\pm k, 2\pm k; 1\pm 2k; -\zeta_j)] , \tag{8.3.71}$$

The presence of $\varepsilon_{\mathrm{adS}}^3$ in the denominator shows that the t.e.v. of the energy density diverges as $\frac{1}{\cos^2\omega r}$ as $\omega r \to \frac{\pi}{2}$. In the massless limit, Eq. (8.3.71) can be written in terms of the functions $S_\ell(\beta\omega)$, defined in Eq. (8.3.62):

$$\langle : T_{\hat{t}\hat{t}} : \rangle_\beta \Big|_{\substack{k=0 \\ \Omega=\omega}} = -\frac{3\omega^4(\cos\omega r)^4}{4\pi^2\varepsilon_{\mathrm{adS}}^3}[S_4(\beta\omega) + S_2(\beta\omega)]. \tag{8.3.72}$$

Unfortunately, the method used to obtain the expression (8.3.64) for $S_2(x)$ in terms of the Q-Pochhammer symbol cannot be applied to $S_4(x)$.

Computation of $\langle : T_{\hat{i}\hat{k}} : \rangle_\beta$. Equation (8.3.19d) shows that the anti-commutator $\{\gamma_{\hat{i}}, \Gamma_{\hat{j}}\}$ is anti-symmetric with respect to $i \rightleftarrows j$, therefore, it does not contribute to $\langle : T_{\hat{i}\hat{k}} : \rangle_\beta$. Since the spatial derivatives ∂_j and $\partial_{j'}$ do not commute with the rotation operators $R_z(-\Omega t)$ and $R_{z'}(\Omega t')$, it is convenient to take them after the rotation is applied. The traces required for this calculation are Eq. (8.3.53b) and:

$$\lim_{\boldsymbol{x'}\to\boldsymbol{x}} \mathrm{tr}\left[\gamma_{\hat{i}}(\partial_{\hat{j}} - \partial_{\hat{j}'})R_z(-\Omega t)\slashed{n}\Lambda(x, x') \sin\tfrac{\omega s}{2} R_{z'}(\Omega t')\right] = 4\cos\frac{\omega\Delta t}{2}\cos\frac{\Omega\Delta t}{2}\delta_{ij}. \tag{8.3.73}$$

The spatial derivative of $\beta_F(s_\Omega) \sin\frac{\omega s_\Omega}{2}$ can be calculated using a chain rule with the intermediate variable

$$\zeta^\Omega = \zeta \Big|_{\substack{r'=r \\ \theta'=\theta \\ \varphi=-\Omega\Delta t}} , \tag{8.3.74}$$

the spatial derivative of which can be calculated as follows:

$$(\partial_{\hat{j}} - \partial_{\hat{j}'})\zeta^\Omega = \zeta_\Omega^2 \tan\omega r \sin\Omega\Delta t \sin\theta \left(\frac{\boldsymbol{x}\times\boldsymbol{\Omega}}{\Omega r}\right)^j. \tag{8.3.75}$$

The spatial derivative of β_F can be calculated by combining Eqs. (8.3.67b) and (8.3.75):

$$(\partial_{\hat{j}} - \partial_{\hat{j}'})\frac{\beta_F(s_\Omega)}{\sin\frac{\omega s_\Omega}{2}} = \frac{i\omega^3 N_\pm(2\pm k)}{16\pi^2}\sin\Omega\Delta t \tan\omega r \left(\frac{\boldsymbol{x}\times\boldsymbol{\Omega}}{r\Omega}\right)^j$$
$$\times \zeta^{3\pm k}{}_2F_1(\pm k, 3\pm k; 1\pm 2k; -\zeta). \tag{8.3.76}$$

Thus, the t.e.v. of the spatial components of the SET can be written as:

$$\langle : T_{\hat{i}\hat{\ell}} : \rangle_\beta = -\frac{\omega^4 N_{\pm k}}{4\pi^2 \cos^2 \omega r} \sum_{j=1}^{\infty} (-1)^j \cosh \frac{\omega j \beta}{2} \cosh \frac{\Omega j \beta}{2}$$

$$\times \left[2(2 \pm k) \sinh^2 \frac{\Omega j \beta}{2} \sin^2 \omega r \left(\frac{\boldsymbol{x} \times \boldsymbol{\Omega}}{r\Omega} \right)^i \left(\frac{\boldsymbol{x} \times \boldsymbol{\Omega}}{r\Omega} \right)^\ell \zeta_j^{3\pm k} {}_2F_1\left(\pm k, 3 \pm k; 1 \pm 2k; -\zeta_j\right) \right.$$

$$\left. + \delta_{ij} \cos^2 \omega r \, \zeta_j^{2\pm k} {}_2F_1\left(\pm k, 2 \pm k; 1 \pm 2k; -\zeta_j\right) \right]. \quad (8.3.77)$$

The first term in the curly brackets only contributes to $\langle : T_{\hat{\varphi}\hat{\varphi}} : \rangle_\beta$, while the second term makes contributions along the diagonal, leading to the following non-zero components:

$$\langle : T_{\hat{r}\hat{r}} : \rangle_\beta = -\frac{\omega^4 N_{\pm k}}{4\pi^2} \sum_{j=1}^{\infty} (-1)^j \cosh \frac{\omega j \beta}{2} \cosh \frac{\Omega j \beta}{2} \zeta_j^{2\pm k} {}_2F_1\left(\pm k, 2 \pm k; 1 \pm 2k; -\zeta_j\right),$$

$$(8.3.78a)$$

$$\langle : T_{\hat{\varphi}\hat{\varphi}} : \rangle_\beta = -\frac{\omega^4 N_{\pm k}}{4\pi^2} \sum_{j=1}^{\infty} (-1)^j \cosh \frac{\omega j \beta}{2} \cosh \frac{\Omega j \beta}{2} \left[\zeta_j^{2\pm k} {}_2F_1\left(\pm k, 2 \pm k; 1 \pm 2k; -\zeta_j\right) \right.$$

$$\left. + 2(2 \pm k) \sinh^2 \frac{\Omega j \beta}{2} \tan^2 \omega r \sin^2 \theta \, \zeta_j^{3\pm k} {}_2F_1\left(\pm k, 3 \pm k; 1 \pm 2k; -\zeta_j\right) \right]$$

$$(8.3.78b)$$

and $\langle : T_{\hat{\theta}\hat{\theta}} : \rangle_\beta = \langle : T_{\hat{r}\hat{r}} : \rangle_\beta$. It is remarkable that while $\langle : T_{\hat{r}\hat{r}} : \rangle_\beta$ and $\langle : T_{\hat{\theta}\hat{\theta}} : \rangle_\beta$ clearly have the same expression in the geometric approach, it was necessary to use numerical calculations to show that their expressions in the mode sum approach give equal t.e.v.s.

In the massless limit, Eqs. (8.3.78a) and (8.3.78b) simplify to:

$$\langle : T_{\hat{r}\hat{r}} : \rangle_\beta \Big|_{k=0} = -\frac{\omega^4}{4\pi^2} \sum_{j=1}^{\infty} (-1)^j \cosh \frac{\omega j \beta}{2} \cosh \frac{\Omega j \beta}{2} \zeta_j^2, \qquad (8.3.79a)$$

$$\langle : T_{\hat{\varphi}\hat{\varphi}} : \rangle_\beta \Big|_{k=0} = -\frac{\omega^4 \Gamma_k}{4\pi^2 \cos^2 \omega r} \sum_{j=1}^{\infty} (-1)^j \cosh \frac{\omega j \beta}{2} \cosh \frac{\Omega j \beta}{2}$$

$$\times \left(\cos^2 \omega r \, \zeta_j^2 + 4 \sinh^2 \frac{\Omega j \beta}{2} \sin^2 \omega r \sin^2 \theta \, \zeta_j^3 \right). \qquad (8.3.79b)$$

In the case when $\Omega = \omega$, the components $\langle : T_{\hat{r}\hat{r}} : \rangle_\beta$ and $\langle : T_{\hat{\varphi}\hat{\varphi}} : \rangle_\beta$ reduce to:

$$\langle : T_{\hat{r}\hat{r}} : \rangle_\beta \bigg|_{\Omega=\omega} = -\frac{\omega^4 N_{\pm k}(\cos\omega r)^{4\pm 2k}}{4\pi^2\varepsilon_{\mathrm{adS}}^{2\pm k}}\sum_{j=1}^{\infty}(-1)^j\frac{\cosh^2\frac{\omega j\beta}{2}}{(\sinh\frac{\omega j\beta}{2})^{4\pm 2k}}$$
$$\times {}_2F_1\left(\pm k, 2\pm k; 1\pm 2k; -\zeta_j\right), \tag{8.3.80a}$$

$$\langle : T_{\hat{\varphi}\hat{\varphi}} : \rangle_\beta \bigg|_{\Omega=\omega} = -\frac{\omega^4 N_{\pm k}(\cos\omega r)^{4\pm 2k}}{4\pi^2\varepsilon_{\mathrm{adS}}^{2\pm k}}\sum_{j=1}^{\infty}(-1)^j\frac{\cosh^2\frac{\omega j\beta}{2}}{(\sinh\frac{\omega j\beta}{2})^{4\pm 2k}}$$
$$\times [2(2\pm k)\varepsilon_{\mathrm{adS}}^{-1}\sin^2\omega r\sin^2\theta\,{}_2F_1(\pm k, 3\pm k; 1\pm 2k; -\zeta_j)$$
$$+ {}_2F_1(\pm k, 2\pm k; 1\pm 2k; -\zeta_j)]. \tag{8.3.80b}$$

While $\langle : T_{\hat{r}\hat{r}} : \rangle_\beta$ (and hence, $\langle : T_{\hat{\theta}\hat{\theta}} : \rangle_\beta$) approach a constant value throughout the equatorial plane, $\langle : T_{\hat{\varphi}\hat{\varphi}} : \rangle_\beta$ diverges as $(\cos\omega r)^{-2}$ as $\omega r \to \frac{\pi}{2}$ in the equatorial plane. The above expressions can be written in terms of the functions $S_\ell(\beta\omega)$ (8.3.62):

$$\langle : T_{\hat{r}\hat{r}} : \rangle_\beta \bigg|_{\substack{k=0 \\ \Omega=\omega}} = -\frac{\omega^4(\cos\omega r)^4}{4\pi^2\varepsilon_{\mathrm{adS}}^2}[S_4(\beta\omega) + S_2(\beta\omega)], \tag{8.3.81a}$$

$$\langle : T_{\hat{\varphi}\hat{\varphi}} : \rangle_\beta \bigg|_{\substack{k=0 \\ \Omega=\omega}} = -\frac{\omega^4(\cos\omega r)^4}{4\pi^2\varepsilon_{\mathrm{adS}}^3}(4\sin^2\omega r\sin^2\theta + \varepsilon_{\mathrm{adS}})[S_4(\beta\omega) + S_2(\beta\omega)]. \tag{8.3.81b}$$

Computation of $\langle : T_{\hat{t}\hat{t}} : \rangle_\beta$.   The following traces are useful for the computation of $\langle : T_{\hat{t}\hat{t}} : \rangle_\beta$:

$$\lim_{\boldsymbol{x}'\to\boldsymbol{x}} \mathrm{tr}\left\{\gamma_{\hat{\ell}}R_z(-\Omega t)[(\partial_{\hat{t}} - \partial_{\hat{t}'})\slashed{n}\Lambda(x, x')\sin\tfrac{\omega s}{2}]R_{z'}(\Omega t')\right\} =$$
$$4\omega\sin\omega r\left(\frac{\boldsymbol{x}\times\boldsymbol{\Omega}}{\Omega r}\right)^\ell\sin\frac{\omega\Delta t}{2}\sin\frac{\Omega\Delta t}{2}, \tag{8.3.82a}$$

$$\lim_{\boldsymbol{x}'\to\boldsymbol{x}} \mathrm{tr}\left\{\gamma_{\hat{t}}R_z(-\Omega t)[(\partial_{\hat{\ell}} - \partial_{\hat{\ell}'})\slashed{n}\Lambda(x, x')\sin\tfrac{\omega s}{2}]R_{z'}(\Omega t')\right\} =$$
$$-4\omega\tan\frac{\omega r}{2}\left(\frac{\boldsymbol{x}\times\boldsymbol{\Omega}}{\Omega r}\right)^\ell\sin\frac{\omega\Delta t}{2}\sin\frac{\Omega\Delta t}{2}, \tag{8.3.82b}$$

$$\lim_{\boldsymbol{x}'\to\boldsymbol{x}} \mathrm{tr}\left[(\{\gamma_{\hat{t}}, \Gamma_{\hat{i}}\} + \{\gamma_{\hat{i}}, \Gamma_{\hat{t}}^0\})R_z(-\Omega t)\slashed{n}\Lambda(x, x')\sin\tfrac{\omega s}{2}R_{z'}(\Omega t')\right] =$$
$$-4\omega\cos\omega r\tan\frac{\omega r}{2}\left(\frac{\boldsymbol{x}\times\boldsymbol{\Omega}}{\Omega r}\right)^\ell\sin\frac{\omega\Delta t}{2}\sin\frac{\Omega\Delta t}{2}, \tag{8.3.82c}$$

where Eqs. (8.3.19b) and (8.3.19c) were used to establish the last equality. Using Eqs. (8.3.68) and (8.3.76) for the derivatives of $\beta_F(s)/\sin\frac{\omega s}{2}$, the following expression

is obtained for $\langle: T_{\hat{i}\hat{t}}:\rangle_\beta$:

$$\langle: T_{\hat{t}\hat{\varphi}}:\rangle_\beta = \frac{\omega^4 N_{\pm k}(2 \pm k)\sin\omega r \sin\theta}{4\pi^2\cos^2\omega r}\sum_{j=1}^\infty (-1)^j \sinh\frac{\omega j\beta}{2}\sinh\frac{\Omega j\beta}{2}$$

$$\times \left(\cosh^2\frac{\omega j\beta}{2} + \cosh^2\frac{\Omega j\beta}{2}\right)\zeta_j^{3+k}{}_2F_1\left(k, 3+k; 1+2k; -\zeta_j\right). \quad (8.3.83)$$

The massless limit is:

$$\langle: T_{\hat{t}\hat{\varphi}}:\rangle_\beta\Big|_{k=0} = \frac{\omega^4\sin\omega r \sin\theta}{2\pi^2\cos^2\omega r}\sum_{j=1}^\infty (-1)^j \sinh\frac{\omega j\beta}{2}\sinh\frac{\Omega j\beta}{2}\zeta_j^3, \quad (8.3.84)$$

while in the $\Omega = \omega$ case, Eq. (8.3.83) reduces to:

$$\langle: T_{\hat{t}\hat{\varphi}}:\rangle_\beta\Big|_{\Omega=\omega} = \frac{\omega^4 N_{\pm k}(2 \pm k)(\cos\omega r)^4}{2\pi^2\varepsilon_{\text{adS}}^{3\pm k}}\sin\omega r \sin\theta \sum_{j=1}^\infty (-1)^j \frac{\cosh^2\frac{\omega j\beta}{2}}{(\sinh\frac{\omega j\beta}{2})^{4\pm 2k}}$$

$$ {}_2F_1\left(k, 3+k; 1+2k; -\zeta_j\right). \quad (8.3.85)$$

Taking the massless limit on the above equation allows $\langle: T_{\hat{t}\hat{\varphi}}:\rangle_\beta$ to be written in terms of the $S_\ell(x)$ functions (8.3.62):

$$\langle: T_{\hat{t}\hat{\varphi}}:\rangle_\beta\Big|_{\substack{k=0\\\Omega=\omega}} = \frac{\omega^4(\cos\omega r)^4}{\pi^2\varepsilon_{\text{adS}}^3}\sin\omega r \sin\theta\, S_4(\omega\beta). \quad (8.3.86)$$

The advantage of the geometric approach is that the resulting expressions can be easily interpreted physically, however, this approach only works when the thermalisation is performed with respect to the maximally symmetric adS vacuum state. The following section presents graphical representations of the t.e.v.s discussed here.

8.4 Numerical results

The plots in this section show the thermal expectation values (t.e.v.s) of the fermion condensate (FC), neutrino charge current (CC) and stress-energy tensor (SET) for massless fermions and for fermions of mass $\mu = 2\omega$ at four values of the inverse temperature $\beta\omega = \{2.0, 1.2, 1.0, 0.8\}$, for various values of the angular momentum $\Omega = |\mathbf{\Omega}|$ of the rotation. All plots presented in this section are in the equatorial plane.
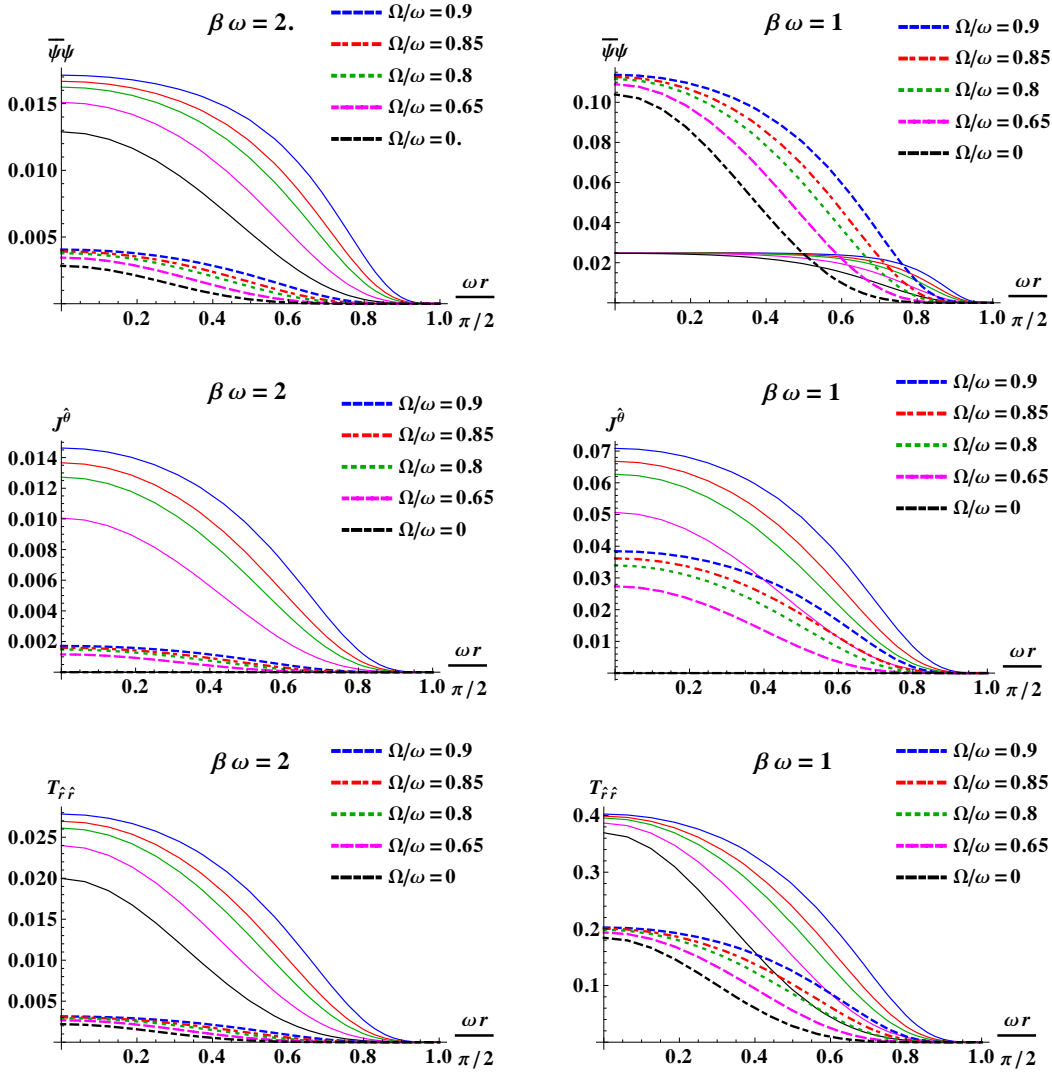
Figure 8.2: Thermal expectation values across the equatorial plane $(\theta = \frac{\pi}{2})$ of the fermion condensate (first line), neutrino charge current (second line) and $T_{\hat{r}\hat{r}} = T_{\hat{\theta}\hat{\theta}}$ (third line) for $\Omega/\omega < 1$ (no speed of light surface present). The thin coloured lines represent results for massless fermions. The mass for the thick dotted lines is $\mu = 2\omega$. The non-rotating case $\Omega = 0$ is also discussed in subsection 7.5.3.
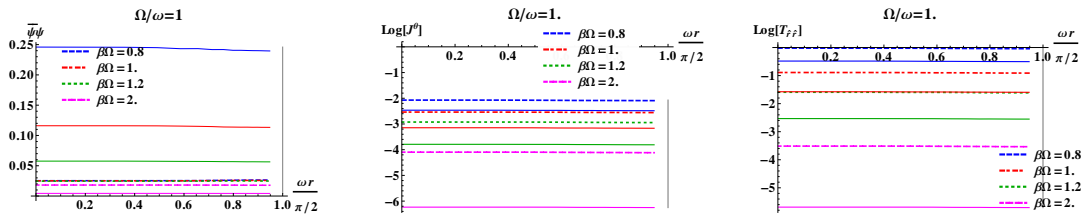
Figure 8.3: Profiles of the fermion condensate (first line), neutrino charge current (second line) and $T_{\hat{r}\hat{r}} = T_{\hat{\theta}\hat{\theta}}$ (from left to right) for $\Omega = \omega$ (speed of light surface just forming at $(r, \theta) = (\frac{\pi}{2\omega}, \frac{\pi}{2})$). The profiles are constant across the equatorial plane. Results for massless fermions (thin coloured lines) are compared to those for fermions of mass $\mu = 2\omega$ (thick dotted lines)

.
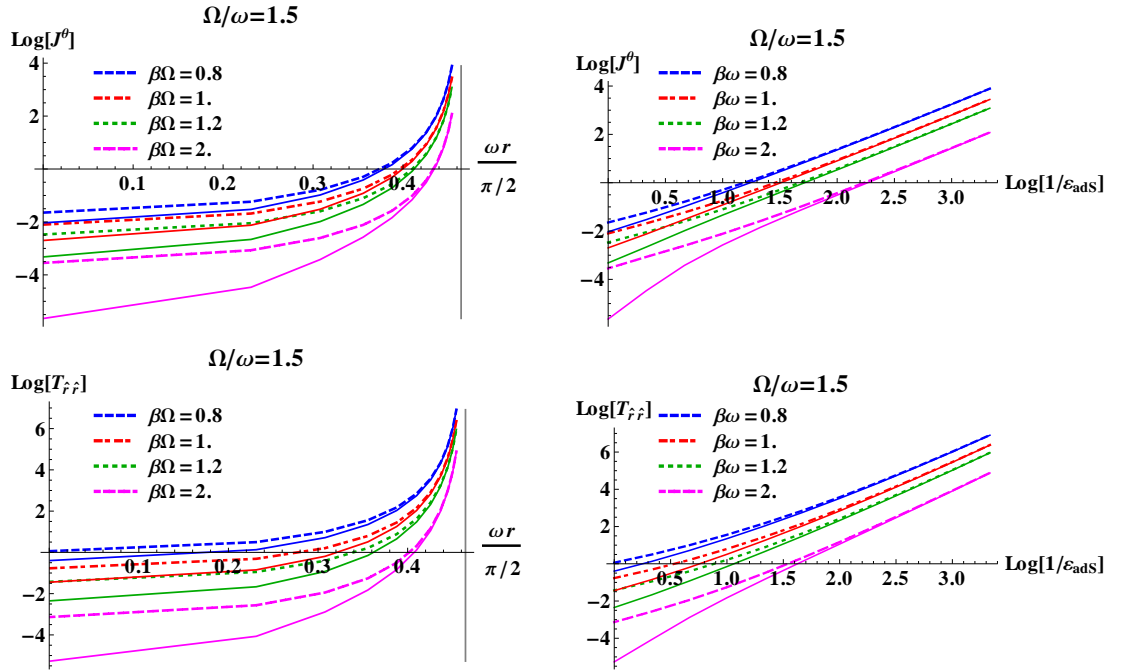
Figure 8.4: Logarithm of neutrino charge current (first line) and $T_{\hat{r}\hat{r}} = T_{\hat{\theta}\hat{\theta}}$ (second line) for $\Omega = 1.5\omega$ across the equatorial plane (the vertical gray line indicates the position of the SOL). The horizontal axis shows the distance from the horizontal axis on the left and the logarithm of the distance to the SOL on the right plot. The plot on the right indicates that the t.e.v.s considered here diverge as inverse powers of the distance to the SOL. Results for massless fermions (thin coloured lines) are compared to those for fermions of mass $\mu = 2\omega$ (thick dotted lines)
.

When $\Omega < \omega$, no speed of light surface (SOL) forms and t.e.v.s stay regular throughout space. In this regime, both the mode sum and the geometric approaches, presented in subsection 8.3.1 and subsection 8.3.2, respectively, can be applied and numerical tests confirm that they yield equivalent results. Plots in this regime of the t.e.v.s of the FC, θ component of the neutrino CC (the r component vanishes in the equatorial plane) and $T_{\hat{r}\hat{r}}$ are given in Figure 8.2 and the plots for $\langle : T_{\hat{t}\hat{t}} :_I \rangle_\beta$, $\langle : T_{\hat{\varphi}\varphi} :_I \rangle_\beta$ and $\langle : T_{\hat{\varphi}\hat{t}} :_I \rangle_\beta$ are given in Figure 8.5. The plots compare the profiles corresponding to various values of the angular velocity of the rotation $\Omega < \omega$ for two values of the temperature: $\beta = \omega^{-1}$ (left column) and $\beta = 2\omega^{-1}$ (right column). At small values of Ω, the profiles corresponding to the rotating states exhibit features close to those of the non-rotating adS space (also discussed in subsection 7.5.3), decreasing from a maximum value on the rotation axis to 0 on the boundary, at $\omega r = \frac{\pi}{2}$. As Ω increases, the maximum value shifts away from the rotation axis increasingly closer to the boundary. Also, the component $T_{\varphi\hat{t}}$ becomes non-zero when $\Omega > 0$.

When $\Omega = \omega$, the SOL just starts to form on the equator of adS, located at $\omega r = \frac{\pi}{2}$ and $\theta = \frac{\pi}{2}$. As in the $\Omega < \omega$ case, both the mode sum and the geometric approaches can be used to compute t.e.v.s. Figure 8.3 shows the t.e.v.s which stay constant throughout the equatorial plane, namely $\langle : \overline{\psi}\psi :_I \rangle_\beta$, $\langle : J_\nu^{\hat{\theta}} :_I \rangle_\beta$ and $\langle : T_{\hat{r}\hat{r}} :_I \rangle_\beta$. The numerical results confirm the analytic predictions of Eqs. (8.3.46), (8.3.59b) and (8.3.80a), obtained using the geometric approach. In Figure 8.6, the t.e.v.s of $T_{\hat{t}\hat{t}}$, $T_{\hat{\varphi}\hat{\varphi}}$ and $T_{\hat{\varphi}\hat{t}}$ are presented. It can be seen that they diverge as the SOL is approached. Our numerical results confirm that the order of the divergence is $O(\varepsilon_{\text{adS}}^{-1})$, as shown using the geometric approach in Eqs. (8.3.71), (8.3.80b) and (8.3.85).

Finally, in the regime $\Omega > \omega$ the geometric approach can no longer be used. In lack of a suitable asymptotic analysis of the mode sum expressions for the t.e.v.s under consideration, an estimate of the order of magnitude of the divergence of t.e.v.s can be made based on numerical results, as follows:

$$\langle : J_\nu^{\hat{\theta}} :_I \rangle_\beta \sim O(\varepsilon_{\text{adS}}^{-2}),$$
$$\langle : T_{\hat{r}\hat{r}} :_I \rangle_\beta = \langle : T_{\hat{\theta}\hat{\theta}} :_I \rangle_\beta \sim O(\varepsilon_{\text{adS}}^{-2.5} \ldots \varepsilon_{\text{adS}}^{-3}),$$
$$\langle : T_{\hat{t}\hat{t}} :_I \rangle_\beta \sim \langle : T_{\hat{\varphi}\hat{\varphi}} :_I \rangle_\beta \sim \langle : T_{\hat{\varphi}\hat{t}} :_I \rangle_\beta \sim O(\varepsilon_{\text{adS}}^{-3.5} \ldots \varepsilon_{\text{adS}}^{-4}), \tag{8.4.1}$$
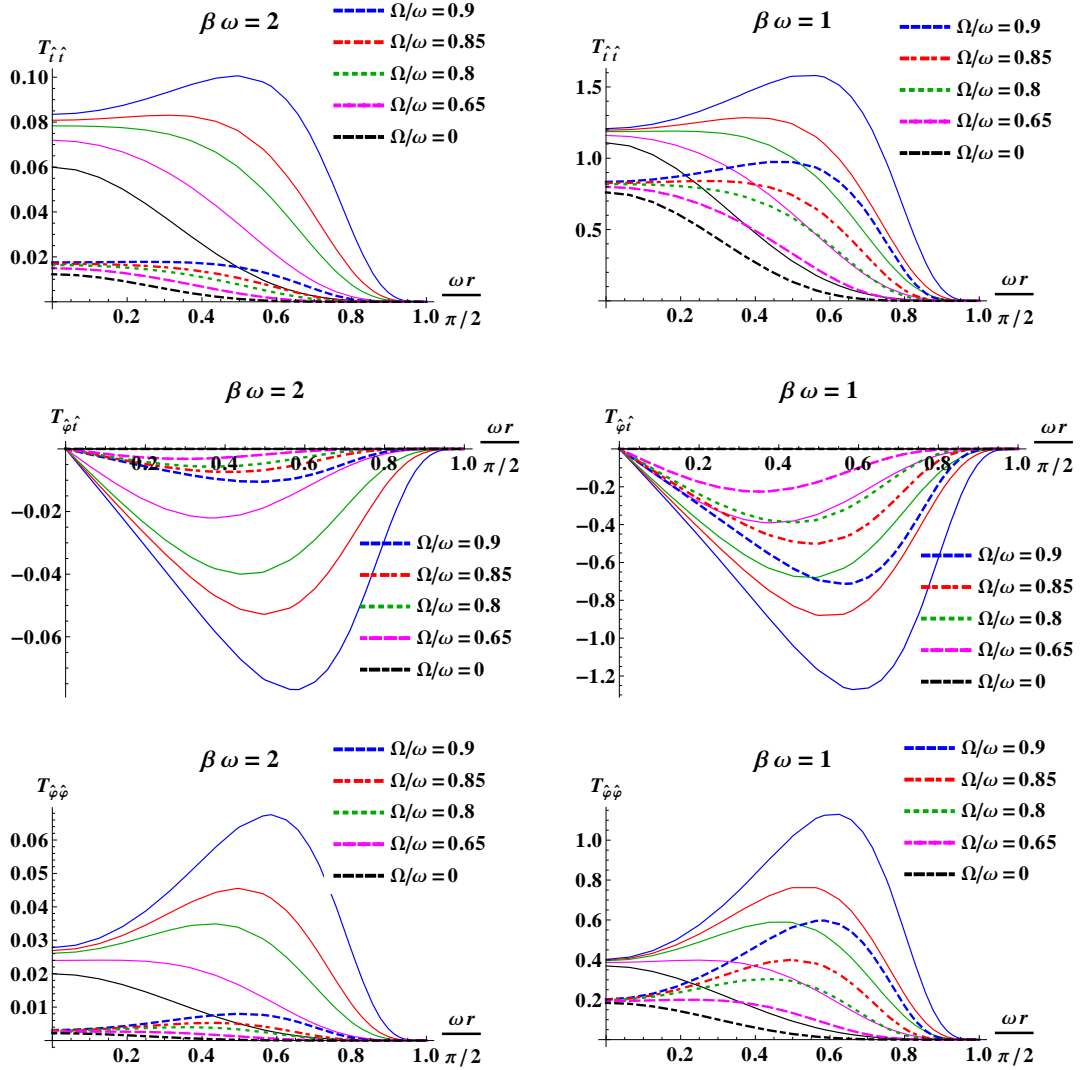
Figure 8.5: Profiles across the equatorial plane $(\theta = \frac{\pi}{2})$ of $\langle : T_{\hat{t}\hat{t}} : \rangle_\beta$, $\langle : T_{\hat{\varphi}\hat{t}} : \rangle_\beta$ and $\langle : T_{\hat{\varphi}\hat{\varphi}} : \rangle_\beta$ (from top to bottom). The thin coloured lines represent results for massless fermions. The mass for the thick dotted lines is $\mu = 2\omega$. The non-rotating case $\Omega = 0$ is also discussed in subsection 7.5.3
.
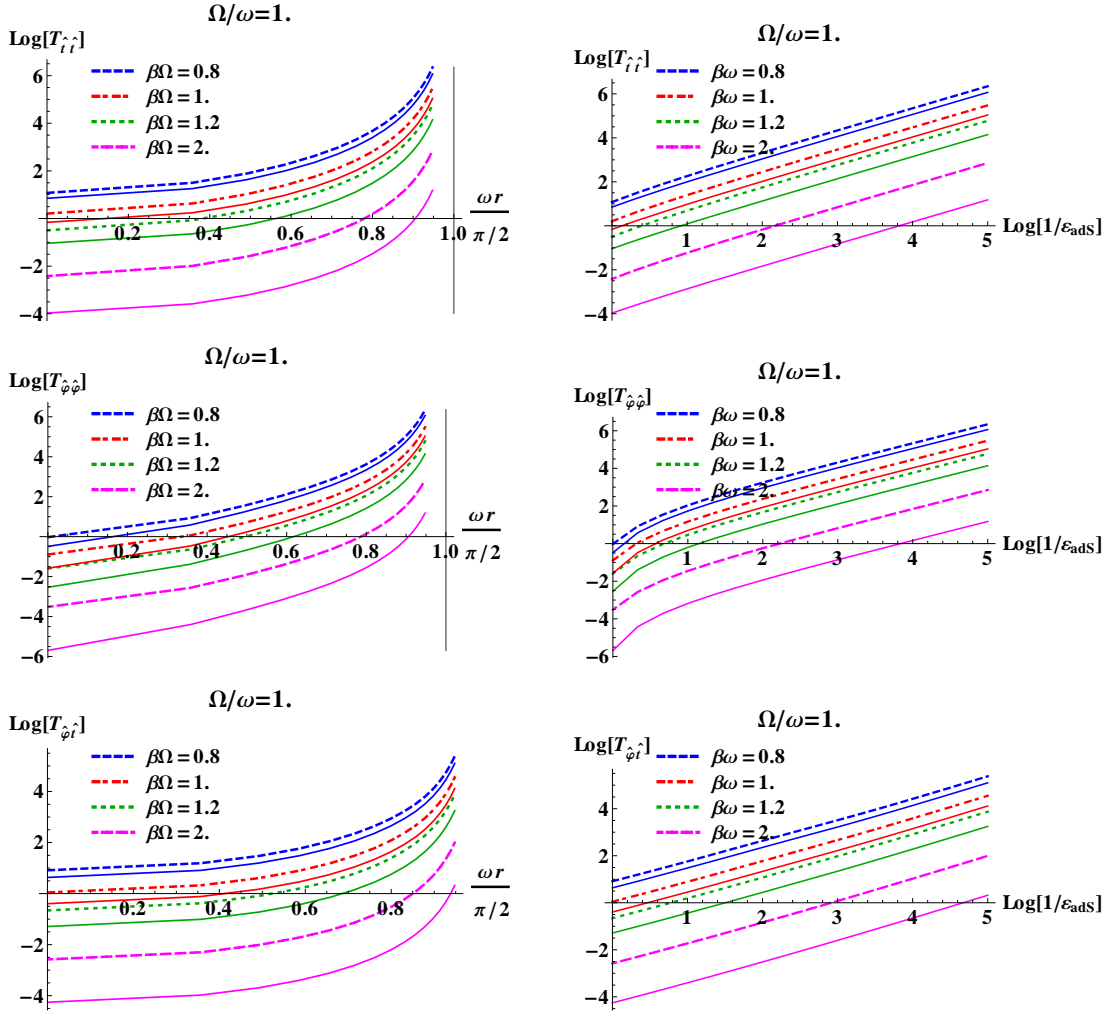
Figure 8.6: Logarithms of $\langle : T_{\hat{t}\hat{t}} : \rangle_\beta$, $\langle : T_{\hat{\varphi}\hat{t}} : \rangle_\beta$ and $\langle : T_{\hat{\varphi}\hat{\varphi}} : \rangle_\beta$ (from top to bottom) at $\Omega = \omega$ (speed of light surface just forming at $(r, \theta) = \left(\frac{\pi}{2\omega}, \frac{\pi}{2}\right)$), plotted against the distance from the rotation axis (left) and logarithm of the distance to the SOL (right). The t.e.v.s here diverge as the SOL is approached. Results for massless fermions (thin coloured lines) are compared to those for fermions of mass $\mu = 2\omega$ (thick dotted lines)
.
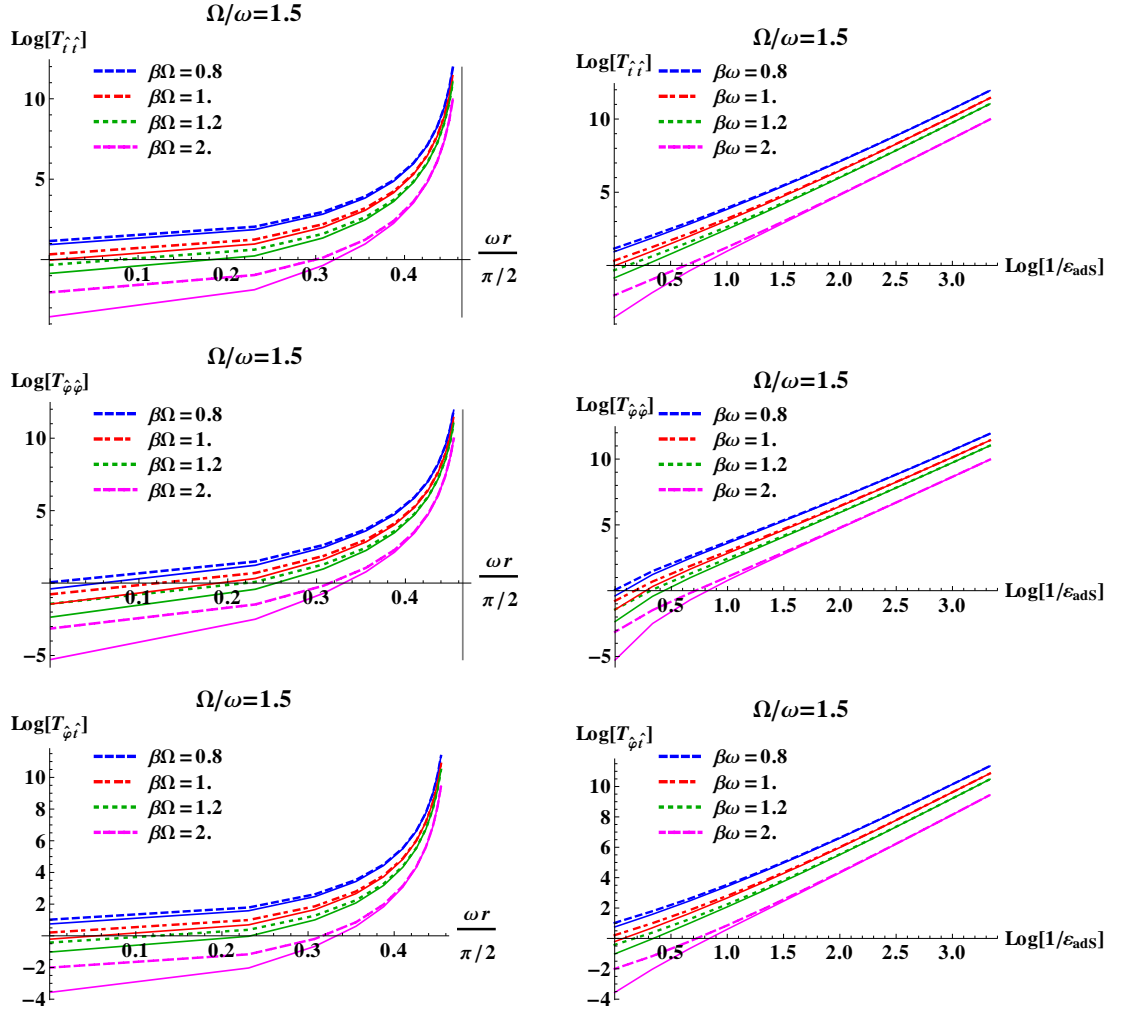
Figure 8.7: Logarithms of $\langle : T_{\hat{t}\hat{t}} : \rangle_\beta$, $\langle : T_{\hat{\varphi}\hat{t}} : \rangle_\beta$ and $\langle : T_{\hat{\varphi}\hat{\varphi}} : \rangle_\beta$ (from top to bottom) across the equatorial plane at $\Omega = 1.5\omega$ (the SOL is shown using a gray vertical line), plotted against the distance from the rotation axis (left) and logarithm of the distance to the SOL (right). These t.e.v.s here diverge as the SOL is approached. Results for massless fermions (thin coloured lines) are compared to those for fermions of mass $\mu = 2\omega$ (thick dotted lines)
.

where the notation $O(\varepsilon^{-3.5} \dots \varepsilon^{-4})$ indicates that for various combinations of Ω and β, out numerical results indicate divergences of orders between $O(\varepsilon_{\mathrm{adS}}^{-3.5})$ and $O(\varepsilon_{\mathrm{adS}}^{-4})$. Unfortunately, the result for $\langle : \overline{\psi}\psi :_I \rangle_\beta$ is currently not available, due to unexpected difficulties in its numerical computation.

After a short digression in section 8.5, the conclusions of this chapter are presented in section 8.6.

8.5 Thermal states using the geometric approach on Minkowski space-time

In section 8.3, rigidly rotating thermal states on anti-de Sitter space-time (adS) were investigated using two approaches: with mode sums and using the explicit form of the Feynman propagator. Since the Feynman propagator calculated in section 7.3 describes the maximally symmetric vacuum state of adS, the latter approach can only be used when the vacuum state of the rotating space-time coincides with the adS vacuum.

The simplicity of the t.e.v.s obtained using the geometric approach makes its limitation to the case $\Omega \leq \omega$ frustrating. In the hope that (maybe in future work) there would be a possibility to extend the geometric method to the case of the non-maximally symmetric rotating vacuum so that it could be used for cases when $\Omega > \omega$, this section is dedicated to answering whether the geometric approach can be used in the case of unbounded rotating Minkowski space, where there is no regime (apart from when $\Omega = 0$) in which the rotating and non-rotating vacua coincide. The answer is neither yes, nor no. The t.e.v.s calculated in subsection 4.3.2, including the temperature-independent spurious terms, can be extracted from the geometric approach expressions, but the method used is a very peculiar regularisation method which unfortunately does not directly generalise to the case of rotating adS.

8.5.1 Minkowski propagator and thermal expectation values

In this subsection, the geometric approach introduced in Ref. [56] and used in subsection 7.3.3 for the anti-de Sitter space-time is used to obtain the Minkowski (non-rotating) propagator and to calculate thermal expectation values.

Minkowski propagator

Given the maximal symmetry of Minkowski space-time, the Feynman propagator can be written using the ansatz (7.3.1):

$$S_F(x, x') = \alpha_M(s) + \beta_M(s)\slashed{n},\qquad(8.5.1)$$

where the bi-spinor of parallel transport is just the identity matrix and the geodetic interval is

$$s^2 = -\eta_{\mu\nu}\Delta x^\mu \Delta x^\nu = (\Delta t)^2 - (\Delta \boldsymbol{x})^2, \tag{8.5.2}$$

where $\eta_{\mu\nu} = \text{diag}(-1, 1, 1, 1)$ is the Minkowski metric and $\Delta x^\mu = (t - t', \boldsymbol{x} - \boldsymbol{x}')$. The tangents to the geodesic can be computed from the geodetic interval (8.5.2):

$$n_\mu = -\frac{\Delta x_\mu}{s}, \tag{8.5.3}$$

The inhomogeneous Dirac equation can be written in the same way as for adS, hence, the resulting equations for α_M and β_M can be obtained from Eqs. (7.3.29) by taking the limit $\omega \to 0$:

$$\beta_M = i\frac{\partial \alpha_M}{\partial(\mu s)}, \tag{8.5.4a}$$

$$i\left[\frac{\partial}{\partial(\mu s)} + \frac{3}{\mu s}\right]\beta_M - \alpha_F = \frac{1}{\mu}\delta^4(x, x'), \tag{8.5.4b}$$

resulting in the following equation for α_M:

$$(\mu s)^2\frac{\partial^2 \alpha_M}{\partial(\mu s)^2} + 3\mu s\frac{\partial \alpha_M}{\partial(\mu s)} + \mu^2 s^2\,\alpha_M = -\mu s^2 \delta^4(x - x'). \tag{8.5.5}$$

The solution of the above equation (ignoring the pole structure induced by the delta function on the right hand side) which is regular at spatial infinity ($s^2 \to -\infty$) is [16, 45]:

$$\alpha_M = -\frac{i\mu^2}{8\pi^2 s}H_1^{(1)}(\mu s), \tag{8.5.6}$$

where $H_1^{(1)}(\mu s)$ is the Hankel function of the first kind (A.1.9) and the overall constant was chosen to match the short-distance behaviour of Eq. (7.3.34) [56]. Substituting Eq. (8.5.6) in (8.5.4a) and using Eq. (A.1.21d), the following result can be obtained:

$$\beta_M = -\frac{\mu^2}{8\pi s}H_2^{(1)}(\mu s). \tag{8.5.7}$$

Thermal expectation values

Using the anti-periodicity of the Feynman propagator with respect to imaginary time [57], the Feynman propagator $\Delta S_F^\beta(x, x')$ for the thermal state (with respect to the Minkowski vacuum) can be written as

$$\Delta S_F^\beta(x, x') = \sum_{j \neq 0}(-1)^j S_F(t + ij\beta, \boldsymbol{x}; t', \boldsymbol{x}'). \tag{8.5.8}$$

The t.e.v.s of the fermion condensate (FC) and stress-energy tensor can be calculated from the above using Eqs. (7.4.1):

$$\langle : \overline{\psi}\psi : \rangle_\beta = -\frac{\mu}{2\pi^2\beta^2} \sum_{j=1}^{\infty} \frac{(-1)^j}{j^2} \left[\frac{i\pi}{s}\mu s H_1^{(1)}(\mu s) \right], \tag{8.5.9}$$

where

$$s^2 = -j^2\beta^2 \tag{8.5.10}$$

was used in the denominator. Due to its imaginary argument $\mu s = ij\beta\mu$, the Hankel function can be replaced with the corresponding modified Bessel function (A.1.16):

$$\langle : \overline{\psi}\psi : \rangle_\beta = -\frac{\mu}{2\pi^2\beta^2} \sum_{j=1}^{\infty} \frac{(-1)^j}{j^2} \left[j\beta\mu K_1(j\beta\mu) \right], \tag{8.5.11}$$

which agrees with Eq. (3.3.74b).

The t.e.v. of the SET can be calculated in a similar fashion:

$$\langle : T_{\hat{t}\hat{t}} : \rangle_\beta = -\frac{i\mu^2}{\pi} \sum_{j=1}^{\infty} \frac{(-1)^j}{s^2} \left[\mu s\, H_1^{(1)}(\mu s) - 3H_2^{(1)} \right], \tag{8.5.12a}$$

$$\langle : T_{\hat{i}\hat{\ell}} : \rangle_\beta = -\frac{i\mu^2}{\pi} \sum_{j=1}^{\infty} \frac{(-1)^j}{s^2} H_2^{(1)}(\mu s)\delta_{i\ell}. \tag{8.5.12b}$$

Applying the connection formula (A.1.16) for the case when $\mu s = ij\beta\mu$ allows the SET to be written using modified Bessel functions:

$$\langle : T_{\hat{t}\hat{t}} : \rangle_\beta = -\frac{2\mu^2}{\pi^2\beta^2} \sum_{j=1}^{\infty} \frac{(-1)^j}{j^2} \left[j\beta\mu\, H_1^{(1)}(j\beta\mu) + 3K_2(j\beta\mu) \right], \tag{8.5.13a}$$

$$\langle : T_{\hat{i}\hat{\ell}} : \rangle_\beta = -\frac{2\mu^2}{\pi\beta^2} \sum_{j=1}^{\infty} \frac{(-1)^j}{j^2} K_2(j\beta\mu)\delta_{i\ell}, \tag{8.5.13b}$$

in perfect agreement with Eqs. (3.3.74).

The above results validate the geometric approach for the construction of thermal states on the maximally symmetric Minkowski space. The next section presents an attempt at applying this method for rotating states.

8.5.2   Rotating thermal states

Let us now switch to co-rotating coordinates. The transformation $\varphi \to \varphi - \Omega t$ (meaning $\varphi_{\text{new}} = \varphi_{\text{old}} - \Omega t_{\text{old}}$) can be written using the generator of rotations about the z axis $J_z = L_z + S_z$. Since the orbital part L_z of J_z commutes with the spin

part S_z, the spin part can be calculated for the transformation in question:

$$R_z(-\Omega t) = e^{-i\Omega t S_z} = \cos\frac{\Omega t}{2} - 2i\sin\frac{\Omega t}{2}S_z = \mathrm{diag}(e^{-\frac{i}{2}\Omega t}, e^{\frac{i}{2}\Omega t}, e^{-\frac{i}{2}\Omega t}, e^{\frac{i}{2}\Omega t}), \quad (8.5.14)$$

hence, the transformed Feynman propagator has the following form:

$$\begin{aligned}
{}_\Omega S_F(x, x') = {}& \left(\alpha_M(s_\Omega) + \frac{\beta_M(s_\Omega)}{s_\Omega}\gamma^{\hat{t}}\Delta t\right)\left(\cos\frac{\Omega\Delta t}{2} - 2iS_z\sin\frac{\Omega\Delta t}{2}\right) \\
& - \frac{\beta_M(s_\Omega)}{s_\Omega}\left[\boldsymbol{\gamma}\cdot\Delta\boldsymbol{x}\cos\frac{\Omega\Delta t}{2} + 2i\sin\frac{\Omega\Delta t}{2}\left(\boldsymbol{\gamma}\cdot\boldsymbol{x}S_z - S_z\boldsymbol{\gamma}\cdot\boldsymbol{x}'\right)\right], \quad (8.5.15)
\end{aligned}$$

where s_Ω is given by Eq. (8.5.2) with $\Delta\varphi$ rotated to $\Delta\varphi - \Omega\Delta t$:

$$s^2 = (\Delta t)^2 - (\Delta\rho)^2 - 4\rho\rho'\cos^2\frac{\Delta\varphi - \Omega\Delta t}{2} - (\Delta z)^2. \quad (8.5.16)$$

The FC is given by the α_M part of Eq. (8.5.15):

$$\begin{aligned}
\langle : \overline{\psi}\psi : \rangle_\beta ={}& -\sum_{j\neq 0}(-1)^j\alpha(s_\Omega) \\
={}& -\frac{\mu\Omega^2}{2\pi^2}\sum_{j=1}^{\infty}\frac{(-1)^j\cosh z_j}{z_j^2 - \rho^2\Omega^2\sinh^2 z_j}\left[-i\mu s K_1(-i\mu s)\right], \quad (8.5.17)
\end{aligned}$$

where

$$z_j = \frac{j\beta\Omega}{2}. \quad (8.5.18)$$

It is interesting that the sum above is actually not equal to $\langle : \overline{\psi}\psi : \rangle_\beta$ (4.3.49). In particular, the SOL is predicted to be at $\rho\Omega = 1$, where Eq. (8.5.17) is still finite. Moreover, there are values of ρ, Ω and β where the denominator vanishes for some value of j, meaning there are irregularity points different from the SOL. However, the insight gained by looking at the analytic result (4.3.49) for the t.e.v. of the FC with respect to the Minkowski (Vilenkin) vacuum suggests that results in the massless case can be obtained by expanding Eq. (8.5.17) in powers of β. Since β only appears in the combination z_j, an expansion in powers of β is equivalent to an expansion in powers of z_j. Since positive powers of j come with positive powers of β, a mechanism is needed to make their coefficients vanish. The problem is that if $j > 0$, the sum over j becomes divergent. In an attempt to eliminate such terms (which shouldn't be making contributions anyway), the sum over j can be regularised by replacing

$(-1)^j$ with $(-\mathfrak{z})^j$, for all $j \geq 0$, for some $0 \leq z < 1$, and using:

$$-\sum_{j=1}^{\infty} \frac{(-1)^j}{j^4} = \frac{7\pi^2}{720}, \tag{8.5.19a}$$

$$-\sum_{j=1}^{\infty} \frac{(-1)^j}{j^2} = \frac{\pi^2}{12}, \tag{8.5.19b}$$

$$-\sum_{j=1}^{\infty} (-\mathfrak{z})^j = \frac{\mathfrak{z}}{1+\mathfrak{z}}, \tag{8.5.19c}$$

$$-\sum_{j=1}^{\infty} (-\mathfrak{z})^j j^{2n} = -Li_{-2n}(-\mathfrak{z}), \tag{8.5.19d}$$

where $Li_s(x)$ is the polylogarithm function [1, 60], defined as:

$$Li_s(x) = \sum_{\ell=1}^{\infty} \frac{x^\ell}{\ell^s}. \tag{8.5.20}$$

The polylogarithm converges for all complex values of s if $|z| < 1$. It also converges for $|z| = 1$ if $\mathfrak{Re}\,s > 1$. In the present case, we seek to extend the polylogarithm by analytic continuation to the ζ function, as follows:

$$Li_{-2n}(-1) = (1 - 2^{1+2n})\zeta(-2n). \tag{8.5.21}$$

According to [60],

$$\zeta(-2n) = 0, \qquad n = 1, 2, 3, \dots, \tag{8.5.22}$$

hence:

$$-\sum_{j=1}^{\infty} (-\mathfrak{z})^j j^{2n} \sim (1 - \mathfrak{z}), \tag{8.5.23}$$

meaning that the above sum vanishes in the limit $z \to 1$. Thus, we justify ignoring terms of higher order than j^0 in the expansion of the t.e.v.s obtained using the geometric approach and find for the t.e.v. of the FC (8.5.17) the familiar result (4.3.49):

$$\langle : \overline{\psi}\psi : \rangle_\beta = \frac{\pi^2}{6\beta^2\varepsilon} + \frac{\Omega^2}{8\varepsilon^2}\left(\tfrac{2}{3} + \tfrac{1}{3}\varepsilon\right), \tag{8.5.24}$$

where $\varepsilon = 1 - \rho^2\Omega^2$ vanishes on the SOL.

For the remainder of this section, the t.e.v. of the SET is be considered only for the case of massless fermions. Unfortunately, we do not have a method to deal with mass terms in a consistent manner (a simple expansion in powers of j of the modified Bessel functions containing the mass dependence would lead to a result polynomial in the mass, which would only hold for very small masses). The massless limit of

the propagator (8.5.15) is:

$$\Omega S_F(x, x') = \frac{i}{2\pi^2 s_\Omega^4} \left[\gamma^{\hat{t}} \Delta t \left(\cos \frac{\Omega \Delta t}{2} - 2i S_z \sin \frac{\Omega \Delta t}{2} \right) \right.$$
$$\left. - \boldsymbol{\gamma} \cdot \Delta \boldsymbol{x} \cos \frac{\Omega \Delta t}{2} - 2i \sin \frac{\Omega \Delta t}{2} (\boldsymbol{\gamma} \cdot \boldsymbol{x} S_z - S_z \boldsymbol{\gamma} \cdot \boldsymbol{x}') \right]. \quad (8.5.25)$$

Noting that:

$$D_{\hat{t}} R_z(-\Omega t) = R_z(-\Omega t) \partial_t, \quad (8.5.26)$$

the trace in the expression for $\langle : T_{\hat{t}\hat{t}} : \rangle_\beta$ selects only the $\gamma^{\hat{t}}$ term:

$$\langle : T_{\hat{t}\hat{t}} : \rangle_\beta = -\frac{\Omega^4}{4\pi^2} \sum_{j=1}^{\infty} (-1)^j \cosh z_j \frac{3z_j^2 + \rho^2 \Omega^2 \sinh^2 z_j}{(z_j^2 - \rho^2 \Omega^2 \sinh^2 z_j)^3}, \quad (8.5.27)$$

where, as before, $z_j = \frac{1}{2} j \beta \Omega$. The terms corresponding to non-positive powers of z_j are:

$$\langle : T_{\hat{t}\hat{t}} : \rangle = \frac{7\pi^2}{60\beta^4} \left(\frac{4}{3} - \frac{\epsilon}{3} \right) + \frac{\Omega^2}{8\beta^2 \epsilon^4} \left(\frac{8}{3} - \frac{16\epsilon}{9} + \frac{\epsilon^2}{9} \right)$$
$$+ \frac{\Omega^4}{64\pi^2 \epsilon^5} \left(\frac{64}{3} - \frac{376\epsilon}{15} + \frac{196\epsilon^2}{45} + \frac{17\epsilon^3}{45} \right). \quad (8.5.28)$$

The above result matches exactly the mode sum result obtained with respect to the Minkowski vacuum (Vilenkin's quantisation), given in Eqs. (4.3.51).

The t.e.v.s of the spatial components of the SET can be evaluated using the following properties:

$$(\nabla - \nabla') s_\Omega \big|_{\boldsymbol{x}=\boldsymbol{x}'} = \frac{4}{s_\Omega} \sin \frac{\Omega \Delta t}{2} \cos \frac{\Omega \Delta t}{2} \left(\frac{\boldsymbol{x} \times \boldsymbol{\Omega}}{\Omega} \right),$$
$$\text{tr} \left(\boldsymbol{\gamma} [\boldsymbol{x} \cdot \boldsymbol{\gamma}, S_z] \right) = - 4i \left(\frac{\boldsymbol{x} \times \boldsymbol{\Omega}}{\Omega} \right), \quad (8.5.29)$$

yielding:

$$\langle : T_{\hat{i}\hat{\ell}} : \rangle_\beta = -\frac{\Omega^4}{4\pi^2} \sum_{j=1}^{\infty} (-1)^j \cosh z_j \left[\frac{\delta_{i\ell}}{(z_j^2 - \rho^2 \Omega^2 \sinh^2 z_j)^2} \right.$$
$$\left. + \frac{4\rho^2 \Omega^2 \sinh^2 z_j}{(z_j^2 - \rho^2 \Omega^2 \sinh^2 z_j)^3} \left(\frac{\boldsymbol{x} \times \boldsymbol{\Omega}}{\rho \Omega} \right)^i \left(\frac{\boldsymbol{x} \times \boldsymbol{\Omega}}{\Omega} \right)^\ell \right]. \quad (8.5.30)$$

The last term above only contributes to $\langle : T_{\hat\varphi\hat\varphi} : \rangle_\beta$:

$$\langle : T_{\hat\rho\hat\rho} : \rangle_\beta = -\frac{\Omega^4}{4\pi^2} \sum_{j=1}^{\infty} \frac{(-1)^j \cosh z_j}{(z_j^2 - \rho^2\Omega^2 \sinh^2 z_j)^2}. \tag{8.5.31a}$$

$$\langle : T_{\hat\varphi\hat\varphi} : \rangle_\beta = -\frac{\Omega^4}{8\pi^2} \sum_{j=1}^{\infty} (-1)^j \cosh z_j \frac{z_j^2 + 3\rho^2\Omega^2 \sinh^2 z_j}{(z_j^2 - \rho^2\Omega^2 \sinh^2 z_j)^3} \tag{8.5.31b}$$

and $\langle : T_{\hat z\hat z} : \rangle_\beta = \langle : T_{\hat\rho\hat\rho} : \rangle$. Employing the summation technique used previously, the following results are obtained:

$$\langle : T_{\hat\rho\hat\rho} : \rangle = \frac{7\pi^2}{180\beta^4\epsilon^2} + \frac{\Omega^2}{24\beta^2\epsilon^3}\left(\frac{4}{3} - \frac{\epsilon}{3}\right) + \frac{\Omega^4}{192\pi^2\epsilon^4}\left(8 - \frac{88\epsilon}{15} - \frac{17\epsilon^2}{15}\right), \tag{8.5.32a}$$

$$\langle : T_{\hat\varphi\hat\varphi} : \rangle_\beta = \frac{7\pi^2}{180\beta^4\epsilon^3}(4 - 3\epsilon) + \frac{\Omega^2}{24\beta^2\epsilon^4}(8 - 8\epsilon + \epsilon^2)$$
$$+ \frac{\Omega^4}{192\pi^2\epsilon^5}\left(64 - \frac{456\epsilon}{5} + \frac{124\epsilon^2}{5} + \frac{17\epsilon^3}{5}\right). \tag{8.5.32b}$$

The only non-vanishing non-diagonal term, $\langle : T_{\hat t\hat\varphi} : \rangle$, can be calculated using:

$$\langle : T_{\hat t\hat\varphi} : \rangle_\beta = \frac{i}{4} \sum_{j\neq 1} (-1)^j \lim_{\substack{\boldsymbol{x}\to\boldsymbol{x}' \\ \Delta t = ij\beta}} \mathrm{tr}\left\{[\gamma_{\hat t}(\partial_\varphi - \partial_{\varphi'})\gamma_{\hat\varphi}(D_{\hat t} - D_{\hat t'})]_\Omega S_F(x, x')\right\}. \tag{8.5.33}$$

Performing the derivatives yields:

$$\langle : T_{\hat t\hat\varphi} : \rangle_\beta = \rho\Omega\frac{\Omega^4}{2\pi} \sum_{j=1}^{\infty} (-1)^j \frac{z_j \sinh z_j(1 + \cosh^2 z_j)}{(z_j^2 - \rho^2\Omega^2 \sinh^2 z_j)^3}$$
$$= -\rho\Omega\left\{\frac{7\pi^2}{45\beta^4\epsilon^3} + \frac{2\Omega^2}{9\beta^2\epsilon^4}\left(\frac{3}{2} - \frac{\epsilon}{2}\right) + \frac{31\Omega^4}{240\pi^2\epsilon^5}\left(\frac{80}{31} - \frac{64\epsilon}{31} + \frac{15\epsilon^2}{31}\right)\right\}. \tag{8.5.34}$$

8.5.3   Summary

In this section, the Feynman propagator corresponding to the fully symmetric Minkowski vacuum was used to construct rotating thermal states. The construction is physically not possible, since the rotating vacuum does not coincide with the Minkowski vacuum and it lacks maximal symmetry. The resulting t.e.v.s do not describe the rotating system, but the information corresponding to rotating thermal states can still be extracted, by employing carefully chosen analytic techniques.

Unfortunately, the massive case requires perhaps a different technique, or maybe a completeley diferent approach. However, given the success of the technique in the present circumstances, it is maybe not that unreasonable to hope that a similar

technique might exist for rotating states on adS which would allow the extension of the domain of applicability of the geometric approach into the case when $\Omega > \omega$ (i.e. when an SOL forms).

8.6 Summary

Two methods are employed in this chapter for the construction of rigidly rotating thermal states: the mode sum method and the geometric method.

In the mode sum method, the Hadamard function for the thermal state is constructed using mode sums, resulting in thermal expectation values (t.e.v.s) written as sums over the main quantum number n_+, total angular momentum j and z-axis projection m of the angular momentum. The resulting expressions are unfortunately too complicated to be interpreted physically, but they are amenable to analysis using numerical methods.

The geometric approach exploits the equivalence of the rotating and adS vacua for the case when the angular velocity Ω of the rotation obeys $\Omega \leq \omega$. In this case, it is possible to obtain the Feynman propagator of the rotating thermal state by rotating and then thermalising the adS vacuum propagator, obtained in section 7.3.

Important features of the t.e.v.s of the fermion condensate (FC), neutrino charge current (CC) and stress-energy tensor (SET) can be inferred using the geometric approach. In the limiting case $\Omega = \omega$, the FC, neutrino CC and $\langle : T_{\hat{r}\hat{r}} :_I \rangle_\beta$ (i.e. the t.e.v. of $T_{\hat{r}\hat{r}}$ with respect to the Iyer vacuum) stay constant throughout the equatorial plane. A more in depth discussion is presented in section 8.4.

At the end of this chapter (in section 8.5), an attempt at extending the geometric approach to the case of rotating thermal states on Minkowski space is made, where the rotating vacuum does not coincide with the Minkowski vacuum for any non-zero value of the angular velocity of the rotation. A knowledge of the analytic formula for t.e.v.s in the rotating Minkowski space time is crucial to devising a technique which extracts the relevant information out of expressions which do not correspond to rotating thermal states on Minkowski space-time. Our hope is to generalise this procedure to the case of the adS space-time, where the geometric approach can be used with such great success in the cases where it is valid, i.e. when $\Omega \leq \omega$.

Chapter 9. Conclusion

Two topics are investigated in this thesis: rotating quantum states on Minkowski and anti-de Sitter space-times and the renormalisation of vacuum expectation values on anti-de Sitter space.

Rigidly rotating thermal states are impossible to construct using scalar particles, while for fermions, our analytic results, presented in subsection 4.3.2, show that thermal expecation values (t.e.v.s) diverge as inverse powers of the distance to the speed of light surface (SOL). Following the discussion of Ref. [47], the spurious temperature-independent terms appearing when the thermal states are constructed with respect to the Minkowski vacuum (as performed by Ref. [72]) are shown to disappear if an appropriate rotating vacuum state is considered, with respect to which no particle mode has negative frequency.

The investigation of rigidly rotating thermal states of fermion particles can prove relevant to the physics of Kerr black holes, where Kay and Wald [48] proved that Israel-Hartle-Hawking (IHH) states are not regular for scalar particles [61]. In 1989, Frolov and Thorne [35] obtained an alternative IHH state which was well defined on the rotation axis by using different thermalisation procedures for normal and super-radiant modes. However, Ottewill and Winstanley [62] showed that Frolov and Thorne's state is ill defined everywhere throughout the rest of the space-time. In 2005, Casals and Ottewill [22] looked at the quantised Maxwell field on a Kerr background space-time, arriving at the same conclusion that the IHH state is not regular. However, the difference in the fundamental nature of fermions and bosons, reflected in their corresponding Fermi-Dirac and Bose-Einstein statistics, respectively, allows fermions to form IHH states [21].

The discussion of rotating quantum states on Minkowski space-time is concluded by enclosing the system inside a boundary. As discussed in Ref. [33], thermal states for scalar fields can now be defined and yield finite t.e.v.s everywhere in the space-time as long as the boundary is inside or on the SOL. In Ref. [34], Frolov and Thorne's [35] suggestion of enclosing the Kerr space-time inside a box before considering the problem of IHH states is implemented by enclosing the space-time inside a cylindrical mirror. The expectation value of the stress-energy tensor in this IHH state is regular everywhere inside the box and thermal close to the horizon.

The boundary is essential for thermal states of rotating fermions as well, due to the divergences occuring as the SOL is approached. The enclosure of the system inside the boundary on which spectral [43] and MIT bag [23] boundary conditions are implemented yields all t.e.v.s finite and well-defined, as long as the boundary

is not outside the SOL. The quasi-Euclidean approach is used in chapter 6 to show that thermal states diverge on the SOL if the boundary is pushed outside the SOL. Similar results are expected for the case of fermion IHH states inside a boundary. The analysis of the Casimir effect shows that the global nature of the spectral boundary conditions makes their corresponding Casimir divergence one order of magnitude worse then for purely local boundary conditions, for which predictions were made in Ref. [31]. The results for the Casimir divergence obtained using the MIT bag boundary conditions are similar to those obtained in Refs. [12, 28, 29] for fermions inside a cylindrical boundary in a $2 + 1$-dimensional space-time obeying MIT bag boundary conditions.

On anti-de Sitter space, the renormalisation of vacuum expectation values with the Schwinger de-Witt and Hadamard methods give vacuum expectation values in perfect agreement with the results obtained using the Pauli-Villars and Zeta-function regularisation techniques, as discussed in subsection 7.4.1 and subsection 7.4.2, respectively. While on adS fermions in thermal states behave as perfect fluids, introducing rotation changes expectation values by the addition of an SOL at values of the angular velocity Ω of the rotation larger than the inverse radius of curvature ω of adS. As in the unbounded Minkowski case, the thermal state is not well defined on and outside the SOL. As Ω is decreased down to ω, the SOL collapses down to the equatorial circle of adS, after which it disappears completely and all t.e.v.s become finite throughout the space-time.

Appendix A: Properties of Bessel functions

This appendix contains some definitions and properties of Bessel functions relevant to the work presented in this thesis. The first section introduces Bessel functions of the first, second and third kind as well as modified Bessel functions. The second section gives asymptotic forms for the Bessel functions for both small and large values of their argument. Some integrals involving Bessel functions over infinite and finite are presented in section A.3, including orthogonality relations. Section A.4 is dedicated to the discussion of infinite sums over the order of products of Bessel functions.a

Most of the properties presented in this appendix are reproduced from standard reference books, e.g., [1, 37, 60, 73].

A.1   Definition

This section covers the definition of Bessel functions of the first, second and third kind as well as of modified Bessel functions and presents some of the recurrence relations they satisfy.

The Bessel functions of the first, second and third kind are solutions to Bessel's equation:

$$\left[z^2 \frac{d^2}{dz^2} + z \frac{d}{dz} + (z^2 - \nu^2) \right] Z_\nu(z) = 0. \tag{A.1.1}$$

The Bessel functions of the first kind of order $\pm\nu$ are the series solutions to (A.1.1) about $z = 0$:

$$J_{\pm\nu}(z) = \left(\frac{z}{2} \right)^{\pm\nu} \sum_{k=0}^{\infty} \frac{(-1)^k}{k!\Gamma(k \pm \nu + 1)} \left(\frac{z}{2} \right)^{2k}. \tag{A.1.2}$$

The Wronskian of Bessel functions of opposite order is given by:

$$W\{J_{-\nu}(z), J_\nu(z)\} = \frac{2 \sin \nu\pi}{\pi z}. \tag{A.1.3}$$

The two solutions of order ν and $-\nu$ are linearly independent for non-integral ν, but for integer order obey the equation:

$$J_{-m}(z) = (-1)^m J_m(z). \tag{A.1.4}$$

A product of two Bessel functions of the first kind can be written as a series about $z = 0$ using the following formula:

$$J_\nu(z) J_\mu(z) = \left(\frac{z}{2}\right)^{\nu+\mu} \sum_{k=0}^{\infty} \frac{(-1)^k}{k! \Gamma(\nu+k+1) \Gamma(\mu+k+1)} \frac{\Gamma(\nu+\mu+2k+1)}{\Gamma(\nu+\mu+k+1)} \left(\frac{z}{2}\right)^{2k}.$$

(A.1.5)

The Bessel functions of the second kind (Neumann functions) can be constructed from $J_{\pm\nu}$:

$$Y_\nu(z) = \frac{J_\nu(z) \cos \nu\pi - J_{-\nu}(z)}{\sin \nu\pi}.$$

(A.1.6)

If the order of the Neumann function is an integer m, the definition (A.1.6) should be understood as the limit $\nu \to m$, in which case $Y_m(z)$ admits the following series representation:

$$Y_m(z) = -\frac{1}{\pi} \left(\frac{z}{2}\right)^{-m} \sum_{k=0}^{m-1} \frac{(m-k-1)!}{k!} \left(\frac{z}{2}\right)^{2k} + \frac{2}{\pi} \ln\left\{\frac{z}{2} J_m(z)\right\}$$
$$- \frac{1}{\pi} \left(\frac{z}{2}\right)^{m} \sum_{k=0}^{\infty} \frac{(-1)^k}{k!(m+k)!} [\psi(k+1) + \psi(m+k+1)] \left(\frac{z}{2}\right)^{2k}, \quad \text{(A.1.7)}$$

valid for $m \geq 0$, with $Y_{-m}(z) = (-1)^m Y_m(z)$. Here, $\psi(z) = \Gamma'(z)/\Gamma(z)$ is the digamma function.

The functions $Y_\nu(z)$ and $J_\nu(z)$ form a linearly independent set, as can be seen from their Wronskian:

$$W\{J_\nu(z), Y_\nu(z)\} = \frac{2}{\pi z}.$$

(A.1.8)

The Bessel functions of the third kind (Hankel functions) are defined by:

$$H_\nu^{(1)}(z) = J_\nu(z) + iY_\nu(z), \qquad H_\nu^{(2)}(z) = J_\nu(z) - iY_\nu(z),$$

(A.1.9)

where $H^{(1)}$ and $H^{(2)}$ are Hankel functions of the first and second kind respectively. A series expansion for the Hankel functions of integer order can be obtained using the series expansions for $J_m(z)$ (A.1.2) and $Y_m(z)$ (A.1.7). The Wronskian of the Hankel function of the first kind and the Hankel function of the second kind is given by:

$$W\{H_\nu^{(1)}(z), H_\nu^{(2)}(z)\} = -\frac{4i}{\pi z},$$

(A.1.10)

and does not vanish, therefore, the two functions are always linearly independent.

Denoting by $\mathcal{C}_\nu$ any of the Bessel functions introduced so far, the following rela-

tions stand:

$$\frac{2\nu}{z}\mathcal{C}_\nu(z) = \mathcal{C}_{\nu-1}(z) + \mathcal{C}_{\nu+1}(z), \tag{A.1.11a}$$

$$2\mathcal{C}'_\nu(z) = \mathcal{C}_{\nu-1}(z) - \mathcal{C}_{\nu+1}(z), \tag{A.1.11b}$$

$$\mathcal{C}'_\nu(z) = \mathcal{C}_{\nu-1}(z) - \frac{\nu}{z}\mathcal{C}_\nu(z), \tag{A.1.11c}$$

$$\mathcal{C}'_\nu(z) = -\mathcal{C}_{\nu+1}(z) + \frac{\nu}{z}\mathcal{C}_\nu(z). \tag{A.1.11d}$$

Let us now turn to the modified Bessel equation, which can be obtained from (A.1.1) by replacing z with iz:

$$\left[z^2\frac{d^2}{dz^2} + z\frac{d}{dz} - (z^2 + \nu^2) \right] \mathcal{Z}_p(z) = 0. \tag{A.1.12}$$

The modified (hyperbolic) Bessel function of order $\pm\nu$ is the series solution to (A.1.12) about $z = 0$:

$$I_{\pm\nu}(z) = \left(\frac{z}{2}\right)^{\pm\nu} \sum_{k=0}^{\infty} \frac{1}{k!\Gamma(k\pm\nu+1)} \left(\frac{z}{2}\right)^{2k} \tag{A.1.13}$$

and is related to the Bessel function of the first kind (A.1.2) through:

$$I_\nu(z) = e^{\mp\frac{1}{2}i\nu\pi} J_\nu(e^{\pm\frac{1}{2}i\pi} z). \tag{A.1.14}$$

The function $I_\nu(z)$ grows exponentially as $z \to \infty$ and is regular at the origin.

Conversely, the modified Bessel function of the second kind (the MacDonald function), defined as

$$K_\nu(z) = \frac{\pi}{2} \frac{I_{-\nu}(z) - I_\nu(z)}{\sin\nu\pi}, \tag{A.1.15}$$

is singular at the origin but decays exponentially at large values of the argument. The functions $K_\nu(z)$ are related to the Hankel function of the first kind (A.1.9) through:

$$K_\nu(z) = \frac{i\pi}{2} \begin{cases} e^{\frac{1}{2}\nu\pi i} H_\nu^{(1)}(e^{\frac{1}{2}i\pi} z), -\pi \le \arg(z) \le \frac{\pi}{2} \\ -e^{-\frac{1}{2}\nu\pi i} H_\nu^{(2)}(e^{-\frac{1}{2}i\pi} z), -\frac{\pi}{2} \le \arg(z) \le \pi \end{cases} \tag{A.1.16}$$

and admit the integral representation:

$$K_\nu(z) = \frac{\sqrt{\pi}}{\Gamma(\nu+1/2)} \left(\frac{z}{2}\right)^\nu \int_1^\infty dz\, e^{-zt}(t^2 - 1)^{\nu/2-1}. \tag{A.1.17}$$

If the order of $K_\nu(z)$ is an integer, the modified Bessel functions of the second kind

admit the following series expansion:

$$
K_m(z) = \frac{1}{2}\left(\frac{z}{2}\right)^{-m}\sum_{k=0}^{m-1}\frac{(m-k-1)!}{k!}(-1)^k\left(\frac{z}{2}\right)^{2k} - \ln\left\{\frac{z}{2}I_m(z)\right\}
$$

$$
+ \frac{(-1)^m}{2}\left(\frac{z}{2}\right)^m\sum_{k=0}^{\infty}\frac{\psi(k+1)+\psi(m+k+1)}{k!(m+k)!}\left(\frac{z}{2}\right)^{2k}. \tag{A.1.18}
$$

Some useful Wronskians are:

$$
W\{I_\nu(z), I_{-\nu}(z)\} = -2\frac{\sin\nu\pi}{\pi z}, \tag{A.1.19a}
$$

$$
W\{K_\nu(z), I_\nu(z)\} = K_{\nu+1}(z)I_\nu(z) + K_\nu(z)I_{\nu+1}(z) = \frac{1}{z}. \tag{A.1.19b}
$$

The modified Bessel functions of opposite orders are related through:

$$
I_{-\nu}(z) = I_\nu(z) + \frac{2}{\pi}K_\nu(z)\sin\pi\nu, \qquad K_{-\nu}(z) = K_\nu(z). \tag{A.1.20}
$$

Denoting by $\mathcal{Z}_\nu$ either $I_\nu(z)$, $e^{\nu\pi i}K_\nu(z)$ or any linear combination of the two, the following recurrence relations hold:

$$
\frac{2\nu}{z}\mathcal{Z}_\nu(z) = \mathcal{Z}_{\nu-1}(z) - \mathcal{Z}_{\nu+1}(z), \tag{A.1.21a}
$$

$$
2\mathcal{Z}'_\nu(z) = \mathcal{Z}_{\nu-1}(z) + \mathcal{Z}_{\nu+1}(z), \tag{A.1.21b}
$$

$$
\mathcal{Z}'_\nu(z) = \mathcal{Z}_{\nu-1}(z) - \frac{\nu}{z}\mathcal{Z}_\nu(z), \tag{A.1.21c}
$$

$$
\mathcal{Z}'_\nu(z) = \mathcal{Z}_{\nu+1}(z) + \frac{\nu}{z}\mathcal{Z}_\nu(z). \tag{A.1.21d}
$$

A.2 Asymptotic forms

At small z but fixed and non-vanishing ν, the Bessel functions of the first, second and third kind admit the following asymptotic expansions:

$$
J_\nu(z) = \frac{1}{\Gamma(\nu+1)}\left(\frac{z}{2}\right)^\nu + O(z^{\nu+2}), \tag{A.2.1a}
$$

$$
Y_\nu(z) = -\frac{\Gamma(\nu)}{\pi}\left(\frac{z}{2}\right)^{-\nu}O(z^{-\nu+2}), \tag{A.2.1b}
$$

$$
H_\nu^{(1)}(z) = \left(\frac{2}{z}\right)^\nu\frac{\Gamma(\nu)}{i\pi} + \left(\frac{z}{2}\right)^\nu\frac{1+i\cot(\pi\nu)}{\Gamma(1+\nu)} + O(z^{2\pm\nu}), \tag{A.2.1c}
$$

$$
H_\nu^{(2)}(z) = -\left(\frac{2}{z}\right)^\nu\frac{\Gamma(\nu)}{i\pi} + \left(\frac{z}{2}\right)^\nu\frac{1-i\cot(\pi\nu)}{\Gamma(1+\nu)} + O(z^{2\pm\nu}). \tag{A.2.1d}
$$

If $\nu = 0$, the Bessel functions have the following leading order behaviour:

$$J_0(z) = 1 + O(z^2), \tag{A.2.2a}$$

$$Y_0(z) = \frac{2}{\pi} \ln\{\tfrac{z}{2} J_0(z)\} + O(z^2), \tag{A.2.2b}$$

$$H_0^{(1)}(z) = \frac{2i}{\pi} \ln\{\tfrac{z}{2} J_0(z)\} + O(z^2), \tag{A.2.2c}$$

$$H_0^{(2)}(z) = -\frac{2i}{\pi} \ln\{\tfrac{z}{2} J_0(z)\} + O(z^2). \tag{A.2.2d}$$

Keeping ν fixed, at large z the functions can be approximated by:

$$J_\nu(z) = \sqrt{\frac{2}{\pi z}} \left[\cos\left(z - \frac{\nu\pi}{2} - \frac{\pi}{4}\right) + O(z^{-1})\right], \tag{A.2.3a}$$

$$N_\nu(z) = \sqrt{\frac{2}{\pi z}} \left[\sin\left(z - \frac{\nu\pi}{2} - \frac{\pi}{4}\right) + O(z^{-1})\right], \tag{A.2.3b}$$

$$H_\nu^{(1)}(z) = \sqrt{\frac{2}{\pi z}} e^{i\left(z - \frac{\nu\pi}{2} - \frac{\pi}{4}\right)} \left[1 + O(z^{-1})\right], \tag{A.2.3c}$$

$$H_\nu^{(2)}(z) = \sqrt{\frac{2}{\pi z}} e^{-i\left(z - \frac{\nu\pi}{2} - \frac{\pi}{4}\right)} \left[1 + O(z^{-1})\right]. \tag{A.2.3d}$$

The asymptotic forms of the modified Bessel functions $I_\nu(z)$, $K_\nu(z)$ for small values of the argument z and non-vanishing ν are:

$$I_\nu(z) = \frac{1}{\Gamma(\nu + 1)} \left(\frac{z}{2}\right)^\nu + O(z^{\nu+2}), \tag{A.2.4a}$$

$$K_\nu(z) = \frac{1}{2}\Gamma(\nu) \left(\frac{z}{2}\right)^{-\nu} + \frac{1}{2}\Gamma(-\nu) \left(\frac{z}{2}\right)^\nu + O(z^{\pm\nu+2}). \tag{A.2.4b}$$

If $\nu = 0$, the leading order term in $K_\nu(z)$ is:

$$K_0(z) = -\ln\left\{\tfrac{z}{2} I_0(z)\right\} + O(z^2). \tag{A.2.4c}$$

At fixed ν and large z, the modified Bessel functions can be approximated by:

$$I_\nu(z) = \frac{e^z}{\sqrt{2\pi z}} \left[1 - \frac{\mu - 1}{8z} + \frac{(\mu - 1)(\mu - 9)}{2!(8z)^2} - \frac{(\mu - 1)(\mu - 9)(\mu - 25)}{3!(8z)^3} + O(z^{-4})\right], \tag{A.2.4d}$$

$$K_\nu(z) = \frac{e^{-z}}{\sqrt{2z/\pi}} \left[1 + \frac{\mu - 1}{8z} + \frac{(\mu - 1)(\mu - 9)}{2!(8z)^2} + \frac{(\mu - 1)(\mu - 9)(\mu - 25)}{3!(8z)^3} + O(z^{-4})\right], \tag{A.2.4e}$$

where $\mu = 4\nu^2$. If both ν and z are allowed to increase, the following approximations

can be used [19, 60]:

$$
I_\nu(\alpha) = \frac{\exp(\sqrt{\nu^2 + \alpha^2} + \nu \ln \frac{\alpha}{\nu + \sqrt{\nu^2 + \alpha^2}})}{\sqrt{2\pi}(\nu^2 + \alpha^2)^{1/4}} \left[1 - \frac{A}{\sqrt{\nu^2 + \alpha^2}} + O((\nu^2 + \alpha^2)^{-1}) \right],
$$

(A.2.5a)

$$
K_\nu(\alpha) = \frac{\exp(-\sqrt{\nu^2 + \alpha^2} - \nu \ln \frac{\alpha}{\nu + \sqrt{\nu^2 + \alpha^2}})}{\sqrt{2/\pi}(\nu^2 + \alpha^2)^{1/4}} \left[1 + \frac{A}{\sqrt{\nu^2 + \alpha^2}} + O((\nu^2 + \alpha^2)^{-1}) \right],
$$

(A.2.5b)

where

$$
A = -\frac{1}{8} + \frac{5\nu^2}{24(\alpha^2 + \nu^2)}.
$$

(A.2.6)

For the analysis of the Casimir divergence for fermions, the asymptotic expansions of the following combinations can be calculated using Eq. (A.2.5a):

$$
I_{\nu-\frac{1}{2}}^2(\alpha) - I_{\nu+\frac{1}{2}}^2(\alpha) = \frac{\nu}{\pi\alpha\sqrt{\nu^2 + \alpha^2}} \exp\left(2\sqrt{\nu^2 + \alpha^2} + 2\nu \ln \frac{\alpha}{\nu + \sqrt{\nu^2 + \alpha^2}} \right)
$$
$$
\times \left[1 + \frac{1}{12\sqrt{\nu^2 + \alpha^2}} \left(1 + \frac{5\alpha^2}{\nu^2 + \alpha^2} \right) + O((\nu^2 + \alpha^2)^{-1}) \right],
$$

(A.2.7a)

$$
2I_{\nu-\frac{1}{2}}(\alpha)I_{\nu+\frac{1}{2}}(\alpha) = \frac{1}{\pi\sqrt{\nu^2 + \alpha^2}} \exp\left(2\sqrt{\nu^2 + \alpha^2} + 2\nu \ln \frac{\alpha}{\nu + \sqrt{\nu^2 + \alpha^2}} \right)
$$
$$
\times \left[1 - \frac{5\nu^2}{12(\nu^2 + \alpha^2)^{\frac{3}{2}}} + O((\nu^2 + \alpha^2)^{-1}) \right],
$$

(A.2.7b)

$$
\frac{K_{\nu-\frac{1}{2}}(\alpha)}{I_{\nu-\frac{1}{2}}(\alpha)} = \frac{\pi x}{\nu + \sqrt{\nu^2 + \alpha^2}} \exp\left(-2\sqrt{\nu^2 + \alpha^2} - 2\nu \ln \frac{\alpha}{\nu + \sqrt{\nu^2 + \alpha^2}} \right)
$$
$$
\times \left[1 + \frac{5}{12(\nu^2 + \alpha^2)^{\frac{3}{2}}} + O((\nu^2 + \alpha^2)^{-1}) \right].
$$

(A.2.7c)

Similarly, the Bessel functions of the first kind admit the following uniform asymptotic expansions:

$$
J_\nu(z > \nu) = \sqrt{\frac{2}{\pi}} \frac{1}{(z^2 - \nu^2)^{\frac{1}{4}}} \left[\cos\left(\sqrt{z^2 - \nu^2} - \nu \text{arcsec} \frac{z}{\nu} - \frac{\pi}{4} \right) + O\left(\frac{1}{z}\right) \right],
$$

(A.2.8a)

$$
J_\nu(z < \nu) = \frac{1}{\sqrt{2\pi}} \frac{1}{(\nu^2 - z^2)^{\frac{1}{4}}} \exp\left\{ \sqrt{\nu^2 - z^2} + \nu \ln \frac{z}{\nu + \sqrt{\nu^2 - z^2}} \right\} \left[1 - O\left(\frac{1}{z}\right) \right].
$$

(A.2.8b)

A.3 Orthogonality relations satisfied by Bessel functions and some integrals

If the range of the argument z is $0..\infty$, the following relation holds:

$$\int_0^\infty dz\, z\, J_\nu(kz) J_\nu(k'z) = \frac{\delta(k-k')}{k}. \tag{A.3.1}$$

It is possible to write down orthogonality relations if z is confined to a finite interval:

$$\int_0^{z_0} z\, dz\, J_\nu\left(\xi_{\nu l}\tfrac{z}{z_0}\right) J_\nu\left(\xi_{\nu m}\tfrac{z}{z_0}\right) = \delta_{\ell m}\tfrac{1}{2}z_0^2 J_{\nu+1}^2(\xi_{\nu m}), \tag{A.3.2}$$

with $\xi_{\nu\ell}$ being the ℓ'th positive zero of $J_\nu(z)$:

$$J_\nu(\xi_{\nu l}) = 0, \quad \xi_{\nu,\ell+1} > \xi_{\nu\ell}. \tag{A.3.3}$$

A similar orthogonality relation for $J_{\nu+1}$ reads:

$$\int_0^{z_0} z\, dz\, J_{\nu+1}(\xi_{\nu\ell}\tfrac{z}{z_0}) J_{\nu+1}(\xi_{\nu m}\tfrac{z}{z_0}) = \delta_{\ell m}\tfrac{1}{2}z_0^2 J_{\nu+1}^2(\xi_{\nu\ell}). \tag{A.3.4}$$

Using the property

$$\rho J_m^2(q\rho) = \frac{d}{d\rho}\left\{\frac{\rho^2}{2}[J_m^2(q\rho) + J_m'^{\,2}(q\rho)] - \frac{m^2}{2q^2}J_m^2(q\rho)\right\}, \tag{A.3.5}$$

which can be proven using the differential equation (A.1.1) satisfied by Bessel functions, the integral of the LHS in (A.3.5) can be written as:

$$\int_0^R \rho\, d\rho\, J_m^2(q\rho) = \frac{R^2}{2}\left[J_m^2(qR) + J_{m\pm1}^2(qR) - \frac{2m}{qR}J_m(qR)J_{m\pm1}(qR)\right]. \tag{A.3.6}$$

Starting from the Bessel equation (A.1.1), the following results can be established:

$$\int_0^R \rho\, d\rho\, J_m(q'\rho)J_m(q\rho) = \pm\frac{R}{q^2-q'^2}\left\{qJ_m(q'R)J_{m\pm1}(qR) - q'J_{m\pm1}(q'R)J_m(qR)\right\}. \tag{A.3.7}$$

A.4 Formulae for summation over order involving a product of two Bessel functions

Using Neumann's Addition Theorem:

$$\mathcal{C}_\nu(u \pm v) = \sum_{k=\pm\infty}^{\infty} \mathcal{C}_{\nu\mp k}(u)\mathcal{C}_k(v), \tag{A.4.1}$$

valid for any Bessel function $\mathcal{C}$, it follows that:

$$\sum_{m=-\infty}^{\infty} J_m(z)J_{m+\ell}(z) = \delta_{l,0}. \tag{A.4.2}$$

Formula (A.4.2) can be used in conjunction with the recursion relations (A.1.11) to further show that:

$$\sum_{m=-\infty}^{\infty} mJ_m(z)J_{m+\ell}(z) = \frac{z}{2}(\delta_{1\ell} + \delta_{-1\ell}), \tag{A.4.3}$$

$$\sum_{m=-\infty}^{\infty} J_m(z)J'_{m+\ell}(z) = \frac{1}{2}(\delta_{1\ell} - \delta_{-1\ell}), \tag{A.4.4}$$

$$\sum_{m=-\infty}^{\infty} mJ'_m(z)J_{m+\ell}(z) = \frac{z}{2}(\delta_{2\ell} - \delta_{-2\ell}), \tag{A.4.5}$$

$$\sum_{m=-\infty}^{\infty} J'_m(z)J'_{m+\ell}(z) = \frac{1}{2}\delta_{0\ell} - \frac{1}{4}(\delta_{2\ell} + \delta_{-2\ell}), \tag{A.4.6}$$

$$\sum_{m=-\infty}^{\infty} m^2 J_m(z)J_{m+\ell}(z) = \frac{z^2}{4}(\delta_{2\ell} + 2\delta_{0\ell} + \delta_{-2\ell}) - \frac{z}{2}(\delta_{1\ell} - \delta_{-1\ell}). \tag{A.4.7}$$

Appendix B: Jacobi Polynomials

This appendix provides properties of Jacobi polynomials relevant to the construction of mode solutions of the Dirac equation on anti-de Sitter space-time, in chapter 7. The following material is provided for completeness, from standard reference books [1, 60].

The Jacobi polynomials are solutions of the Jacobi equation:

$$\left\{(1-z^2)\frac{d^2}{dz^2} + [(\beta-\alpha) - (\alpha+\beta+2)z]\frac{d}{dz} + n(n+\alpha+\beta+1)\right\} P_n^{(\alpha,\beta)}(z) = 0,$$
(B.1)

and are related to the hypergeometric function through the following equation:

$$P_n^{(\alpha,\beta)}(z) = \binom{n+\alpha}{\alpha} {}_2F_1\left(-n, \alpha+\beta+n+1; \alpha+1; \frac{1-z}{2}\right).$$
(B.2)

The Rodriguez representation of the Jacobi polynomial is:

$$P_n^{(\alpha,\beta)}(z) = \frac{(-1)^n}{2^n n!}(1-z)^{-\alpha}(1+z)^{-\beta}\frac{d^n}{dz^n}\left[(1-z)^{\alpha+n}(1+z)^{\beta+n}\right],$$
(B.3)

which is equivalent to the following explicit representations:

$$P_n^{(\alpha,\beta)}(z) = \frac{\Gamma(\alpha+n+1)\Gamma(\beta+n+1)}{n!\Gamma(\alpha+\beta+n+1)}\sum_{m=0}^{n}\binom{n}{m}\binom{\alpha+\beta+n+m}{\alpha+m}(-1)^m\left(\frac{1-z}{2}\right)^m$$
(B.4a)

$$= \frac{\Gamma(\alpha+n+1)\Gamma(\beta+n+1)}{n!\Gamma(\alpha+\beta+n+1)}\sum_{m=0}^{n}\binom{n}{m}\binom{\alpha+\beta+n+m}{\beta+m}(-1)^{n-m}\left(\frac{1+z}{2}\right)^m$$
(B.4b)

$$= \sum_{s=0}^{n}\binom{n+\alpha}{s}\binom{n+\beta}{n-s}\left(\frac{z-1}{2}\right)^{n-s}\left(\frac{z+1}{2}\right)^s.$$
(B.4c)

The Jacobi polynomials obey the following orthogonality relation:

$$\int_{-1}^{1} dz(1-z)^\alpha(1+z)^\beta P_n^{(\alpha,\beta)}(z)P_m^{(\alpha,\beta)}(z)$$

$$= \frac{2^{\alpha+\beta+1}}{2n+\alpha+\beta+1}\frac{\Gamma(n+\alpha+1)\Gamma(n+\beta+1)}{n!\Gamma(n+\alpha+\beta+1)}\delta_{nm}, \quad (B.5)$$

are normalised according to:

$$P_n^{(\alpha,\beta)}(1) = \binom{n+\alpha}{\alpha}$$
(B.6)

and obey the following reflection rule:

$$P_n^{(\alpha,\beta)}(-z) = (-1)^n P_n^{(\beta,\alpha)}(z). \tag{B.7}$$

Using the explicit representation (B.4a), the following identity can be established:

$$\frac{d^k}{dz^k} P_n^{(\alpha,\beta)}(z) = \frac{\Gamma(\alpha+\beta+n+k+1)}{2^k \Gamma(\alpha+\beta+n+1)} P_{n-k}^{(\alpha+k,\beta+k)}(z). \tag{B.8}$$

Eq. (B.4b) can be used to show that:

$$\left[(1+z)\frac{d}{dz} + \beta\right] P_n^{(\alpha,\beta)}(z) = (\beta+n)P_n^{(\alpha+1,\beta-1)}(z), \tag{B.9a}$$

while with the help of Eq. (B.4a), the following identity follows:

$$\left[-(1-z)\frac{d}{dz} + \alpha\right] P_n^{(\alpha,\beta)}(z) = (\alpha+n)P_n^{(\alpha-1,\beta+1)}(z). \tag{B.9b}$$

A formula useful in subsection 7.3.1 for the computation of the Feynman propagator relates a sum over Jacobi polynomials to a hypergeometric function:

$$\sum_{n=0}^{\infty} \frac{\Gamma(\alpha+\beta+n+1)}{\Gamma(\beta+n+1)} t^n P_n^{(\alpha,\beta)}(z) = \frac{\Gamma(\alpha+\beta+1)}{\Gamma(\beta+1)}(1+t)^{-\alpha-\beta-1}$$
$$\times \, _2F_1\left(\frac{\alpha+\beta+1}{2}, \frac{\alpha+\beta+2}{2}; \beta+1; \frac{2t}{(1+t)^2}(1+z)\right). \tag{B.10}$$

Appendix C: Properties of spherical harmonics and applications to the Dirac equation

This appendix contains some standard properties of the spherical harmonics, together with some mathematical details formulae derived for usage in chapters 7 and 8. In particular, the summation formulae in section C.4 are crucial for computing the sum over m in the construction of two-point functions using mode sums on anti-de Sitter space (adS) in subsection 7.3.1 and the contraction formulae in section C.5 are useful when writing t.e.v.s on rotating adS in subsection 8.3.1.

C.1 Properties of Legendre polynomials

The Legendre polynomials are solutions of the Legendre differential equation:

$$\frac{d}{dz}\left[(1-z^2)\frac{d}{dz}P_\ell(z)\right] + \ell(\ell+1)P_\ell(z) = 0, \tag{C.1.1}$$

having the following polynomial form:

$$P_\ell(z) = \frac{1}{2^\ell}\sum_{j=0}^{\lfloor\frac{\ell}{2}\rfloor}\binom{\ell}{j}\binom{2\ell-2j}{\ell}(-1)^j\,z^{\ell-2j}, \tag{C.1.2}$$

which is equivalent to the following Rodriguez representation:

$$P_\ell(z) = \frac{(-1)^\ell}{2^\ell\ell!}\frac{d^\ell}{dz^\ell}(1-z^2)^\ell. \tag{C.1.3}$$

Another way of expressing the Legendre polynomials is through their integral representation:

$$P_\ell(z) = \frac{1}{\pi}\int_0^\pi d\varphi(z + i\sqrt{1-z^2}\cos\varphi)^\ell. \tag{C.1.4}$$

The Legendre polynomials are normalised according to:

$$P_\ell(1) = 1 \tag{C.1.5}$$

and satisfy the following orthogonality relation:

$$\int_{-1}^{1} dx \, P_\ell(x) P_{\ell'}(x) = \frac{2}{2\ell+1} \delta_{\ell\ell'}, \tag{C.1.6}$$

Using the Rodriguez representation (C.1.3) and with the help of the property:

$$x \frac{d^n}{dx^n} f(x) = \frac{d^n}{dx^n} x f - n \frac{d^{n-1}}{dx^{n-1}} f, \tag{C.1.7}$$

the following identities can be established:

$$\left(x \frac{d}{dx} - \ell \right) P_\ell(x) = \frac{d}{dx} P_{\ell-1}(x), \tag{C.1.8a}$$

$$\left(x \frac{d}{dx} + \ell + 1 \right) P_\ell(x) = \frac{d}{dx} P_{\ell+1}(x). \tag{C.1.8b}$$

A useful identity which follows from (C.1.8a) is:

$$\left[\frac{d^2}{dx^2}(1-x^2) + (\ell+m+2)\frac{d}{dx}x - m(\ell+1) \right] P_\ell(x) = (\ell+m)\frac{d}{dx} P_{\ell-1}(x). \tag{C.1.9}$$

The following identities [20, 44] are useful for the the construction of two-point functions on anti-de Sitter space-time, in subsection 7.3.1:

$$\sum_{\ell=0}^{\infty} \frac{2\ell+1}{4\pi} P_\ell(\cos\gamma) = \frac{\delta(1-\cos\gamma)}{2\pi} = \delta(\cos\theta - \cos\theta')\delta(\varphi - \varphi'),$$

$$\sum_{\ell=0}^{\infty} P_\ell(\cos\gamma) = \frac{1}{2\sin\frac{\gamma}{2}} \sim \frac{1}{\gamma} + \frac{\gamma}{24} + \frac{7\gamma^3}{5760} + O(\gamma^5). \tag{C.1.10}$$

C.2 Properties of associated Legendre functions

The associated Legendre functions are generalisations of the Legendre polynomials, satisfying the following differential equation:

$$\left[\frac{d}{dx}(1-x^2)\frac{d}{dx} + \ell(\ell+1) - \frac{m^2}{1-x^2} \right] P_\ell^m(x) = 0. \tag{C.2.1}$$

The associated Legendre functions can be written in terms of the Legendre polynomials:

$$P_\ell^m(x) = (-1)^m (1-x^2)^{\frac{m}{2}} \frac{d^m}{dx^m} P_\ell(x), \tag{C.2.2}$$

or in the Rodriguez representation:

$$P_\ell^m(x) = \frac{(-1)^\ell}{2^\ell \ell!} (1-x^2)^{\frac{m}{2}} \frac{d^{\ell+m}}{dx^{\ell+m}} (1-x^2)^\ell \tag{C.2.3}$$

and satisfy the following orthogonality relation:

$$\int_{-1}^{1} dx\, P_\ell^m(x) P_{\ell'}^m(x) = \frac{2}{2\ell+1}\frac{(\ell+m)!}{(\ell-m)!}\delta_{\ell\ell'}. \tag{C.2.4}$$

Another useful property is the behaviour of P_ℓ^m under the transformation $m \to -m$:

$$P_\ell^{-m}(x) = (-1)^m \frac{(\ell-m)!}{(\ell+m)!} P_\ell^m(x). \tag{C.2.5}$$

The relation (C.2.2) between P_ℓ^m and P_ℓ can be used together with the identity (C.1.9) to establish the following identities:

$$\sqrt{1-x^2}P_\ell^{m+1}(x) - (\ell-m)x\,P_\ell^m(x) = -(\ell+m)P_{\ell-1}^m(x), \tag{C.2.6a}$$
$$(\ell-m)\sqrt{1-x^2}P_\ell^m(x) + xP_\ell^{m+1}(x) = P_{\ell-1}^{m+1}(x), \tag{C.2.6b}$$
$$\sqrt{1-x^2}P_\ell^{m+1}(x) + (\ell+m+1)x\,P_\ell^m(x) = (\ell-m+1)P_{\ell+1}^m(x), \tag{C.2.6c}$$
$$(\ell+m+1)\sqrt{1-x^2}P_\ell^m(x) - xP_\ell^{m+1}(x) = -P_{\ell+1}^{m+1}(x). \tag{C.2.6d}$$

In the language of chapter 8, the above identities can be translated to:

$$\sin\theta\, P_+^+ - (j-m+1)\cos\theta\, P_+^- = -(j+m)P_-^-, \tag{C.2.7a}$$
$$(j-m+1)\sin\theta\, P_+^- + \cos\theta\, P_+^+ = P_-^+, \tag{C.2.7b}$$
$$\sin\theta\, P_-^+ + (j+m)\cos\theta\, P_-^- = (j-m+1)P_+^-, \tag{C.2.7c}$$
$$(j+m)\sin\theta\, P_-^- - \cos\theta\, P_-^+ = -P_+^+, \tag{C.2.7d}$$

where the argument of the generalised Legendre polynomials is $\cos\theta$ and the $+$ and $-$ signs in the superscripts and subscripts control de values of m and j, respectively, i.e. $P_-^+ = P_{j-\frac{1}{2}}^{m+\frac{1}{2}}$.

C.3 Properties of spherical harmonics

The spherical harmonics are solutions of the following eigenvalue equations:

$$L_z Y_{\ell m} = m Y_{\ell m}, \qquad L_z = -i\frac{d}{d\varphi}, \tag{C.3.1a}$$

$$\boldsymbol{L}^2 Y_{\ell m} = \ell(\ell+1)Y_{\ell m}, \qquad \boldsymbol{L}^2 = -\frac{d^2}{d\theta^2} - \cot\theta\frac{d}{d\theta} - \frac{1}{\sin^2\theta}\frac{d^2}{d\varphi^2} \tag{C.3.1b}$$

and are written in terms of the associated Legendre functions $P_\ell^m(\cos\theta)$:

$$Y_{\ell m}(\theta,\varphi) = e^{im\varphi}\sqrt{\frac{2\ell+1}{4\pi}}\sqrt{\frac{(\ell-m)!}{(\ell+m)!}}P_\ell^m(\cos\theta). \tag{C.3.2}$$

The spherical harmonics are normalised according to the following normalisation relation:

$$\int_0^{2\pi} d\varphi \int_{-1}^1 d\cos\theta\, Y^*_{\ell'm'}(\theta,\varphi) Y_{\ell m}(\theta,\varphi) = \delta_{\ell\ell'}\delta_{mm'}, \tag{C.3.3}$$

where the complex conjugate of $Y_{\ell m}$ can be written as:

$$Y^*_{\ell m}(\theta,\varphi) = (-1)^m Y_{\ell,-m}(\theta,\varphi). \tag{C.3.4}$$

A useful property of the spherical harmonics is the addition theorem:

$$\sum_{m=-\ell}^{\ell} Y_\ell^m(\theta,\varphi) Y_\ell^{m*}(\theta',\varphi') = \frac{2\ell+1}{4\pi} P_\ell(\cos\gamma), \tag{C.3.5}$$

in which $\cos\gamma = \sin\theta\sin\theta'\cos(\varphi-\varphi')+\cos\theta\cos\theta'$. In conjunction with Eq. (C.1.10), this can be used to establish the completeness relation:

$$\sum_{\ell=0}^{\infty}\sum_{m=-\ell}^{\ell} Y^*_{\ell m}(\theta',\varphi') Y_{\ell m}(\theta,\varphi) = \delta(\varphi-\varphi')\delta(\cos\theta-\cos\theta'), \tag{C.3.6}$$

The azimuthal number m can be shifted using the standard $\mathfrak{so}(3)$ shifters:

$$L_\pm Y_{\ell m} = \sqrt{(\ell\pm m+1)(\ell\mp m)}\, Y_{\ell,m\pm 1}, \qquad L_\pm = e^{\pm i\varphi}(\pm\partial_\theta + i\cot\theta\,\partial_\varphi). \tag{C.3.7}$$

Explicitly, the action of the shifters is given by:

$$e^{i\varphi}(\partial_\theta + i\cot\theta\,\partial_\varphi)Y_{\ell m} = \sqrt{\ell(\ell+1)-m(m+1)}\, Y_{\ell,m+1}, \tag{C.3.8a}$$

$$e^{-i\varphi}(-\partial_\theta + i\cot\theta\,\partial_\varphi)Y_{\ell m} = \sqrt{\ell(\ell+1)-m(m-1)}\, Y_{\ell,m-1}. \tag{C.3.8b}$$

The relation (C.3.2) between the spherical harmonics and the associated Legendre functions can be used together with the identity (C.2.6a) to prove the following identities:

$$\cos\theta\sqrt{\frac{\ell-m}{\ell+m}}Y_\ell^m(\theta,\varphi) - e^{-i\varphi}\sin\theta\sqrt{\frac{\ell+m+1}{\ell+m}}Y_\ell^{m+1}(\theta,\varphi) = \sqrt{\frac{2\ell+1}{2\ell-1}}Y_{\ell-1}^m(\theta,\varphi), \tag{C.3.9a}$$

$$\cos\theta\sqrt{\frac{\ell+m}{\ell-m}}Y_\ell^m(\theta,\varphi) + e^{i\varphi}\sin\theta\sqrt{\frac{\ell-m+1}{\ell-m}}Y_\ell^{m-1}(\theta,\varphi) = \sqrt{\frac{2\ell+1}{2\ell-1}}Y_{\ell-1,m}(\theta,\varphi). \tag{C.3.9b}$$

The second of the above identities can be obtained by taking the complex conjugate of the first and replacing m with $-m$. Combining the above with the action (C.3.8)

of the shifters $L_\pm$, the above equations can be cast in the form:

$$\sqrt{\frac{2\ell+1}{2\ell-1}}\sqrt{\ell^2-m^2}Y_{\ell-1,m} = (\ell\cos\theta - \sin\theta\partial_\theta)\,Y_{\ell m}, \tag{C.3.10a}$$

$$\sqrt{\frac{2\ell+1}{2\ell+3}}\sqrt{(\ell+1)^2-m^2}Y_{\ell+1,m} = [(\ell+1)\cos\theta + \sin\theta\partial_\theta]\,Y_{\ell m}. \tag{C.3.10b}$$

Finally, Eqs. (C.3.10) can be combined with Eqs. (C.3.8) and the differential equation for the spherical harmonics (C.3.1) to prove the following identities:

$$Y_{\ell+1}^{m-1} = \frac{e^{-i\varphi}}{\sqrt{(\ell-m+1)(\ell-m+2)}}\sqrt{\frac{2l+3}{2\ell+1}}\left[-\cos\theta\partial_\theta + \frac{i\partial_\varphi}{\sin\theta} + (\ell+1)\sin\theta\right]Y_\ell^m,$$

$$\tag{C.3.11a}$$

$$Y_{\ell+1}^{m+1} = \frac{e^{i\varphi}}{\sqrt{(\ell+m+1)(\ell+m+2)}}\sqrt{\frac{2\ell+3}{2\ell+1}}\left[\cos\theta\partial_\theta + \frac{i\partial_\varphi}{\sin\theta} - (\ell+1)\sin\theta\right]Y_\ell^m,$$

$$\tag{C.3.11b}$$

$$Y_{\ell-1}^{m-1} = \frac{e^{-i\varphi}}{\sqrt{(\ell+m-1)(\ell+m)}}\sqrt{\frac{2\ell-1}{2\ell+1}}\left[-\cos\theta\partial_\theta + \frac{i\partial_\varphi}{\sin\theta} - l\sin\theta\right]Y_\ell^m, \tag{C.3.11c}$$

$$Y_{\ell-1}^{m+1} = \frac{e^{i\varphi}}{\sqrt{(\ell-m-1)(\ell-m)}}\sqrt{\frac{2\ell-1}{2\ell+1}}\left[\cos\theta\partial_\theta + \frac{i\partial_\varphi}{\sin\theta} + \ell\sin\theta\right]Y_\ell^m. \tag{C.3.11d}$$

C.4   Useful summation formulae

The aim of this section is to compute sums over m of direct products of the form $\Phi(\theta,\varphi)\otimes\overline{\Phi}(\theta',\varphi')$, where the four-spinors $\Phi_{\kappa,m}^{\pm}$ are the solutions (7.2.8) of the angular eigenvalue problem in a spherically symmetric space-time. The terms of interest are:

$$\psi_{j+\frac{1}{2}}^{m}\otimes\psi_{j+\frac{1}{2}}^{m\dagger} = \frac{1}{2j+2}\begin{pmatrix}(j-m+1)Y_+^-Y_+^{-*} & -\sqrt{(j+1)^2-m^2}Y_+^-Y_+^{+*}\\ -\sqrt{(j+1)^2-m^2}Y_+^+Y_+^{-*} & (j+m+1)Y_+^+Y_+^{+*}\end{pmatrix},$$

$$\psi_{j+\frac{1}{2}}^{m}\otimes\psi_{j-\frac{1}{2}}^{m\dagger} = \frac{1}{\sqrt{2j(2j+2)}}$$
$$\times\begin{pmatrix}\sqrt{(j+m)(j-m+1)}Y_+^-Y_-^{-*} & \sqrt{(j-m+1)(j-m)}Y_+^-Y_-^{+*}\\ -\sqrt{(j+m+1)(j+m)}Y_+^+Y_-^{-*} & -\sqrt{(j+m+1)(j-m)}Y_+^+Y_-^{+*}\end{pmatrix},$$

$$\psi_{j-\frac{1}{2}}^{m}\otimes\psi_{j+\frac{1}{2}}^{m\dagger} = \frac{1}{\sqrt{2j(2j+2)}}$$
$$\times\begin{pmatrix}\sqrt{(j+m)(j-m+1)}Y_-^-Y_+^{-*} & -\sqrt{(j+m+1)(j+m)}Y_-^-Y_+^{+*}\\ \sqrt{(j-m+1)(j-m)}Y_-^+Y_+^{-*} & -\sqrt{(j+m+1)(j-m)}Y_-^+Y_+^{+*}\end{pmatrix},$$

$$\psi_{j-\frac{1}{2}}^{m}\otimes\psi_{j-\frac{1}{2}}^{m\dagger} = \frac{1}{2j}\begin{pmatrix}(j+m)Y_-^-Y_-^{-*} & \sqrt{j^2-m^2}Y_-^-Y_-^{+*}\\ \sqrt{j^2-m^2}Y_-^+Y_-^{-*} & (j-m)Y_-^+Y_-^{+*}\end{pmatrix}. \tag{C.4.1}$$

The convention used in the above expressions is that the first function depends on (θ,φ), while the second one depends on (θ',φ'). The shorthand used for the spherical

harmonics is $Y_{\pm}^{+} = Y_{j\pm\frac{1}{2}}^{m+\frac{1}{2}}$ and $Y_{\pm}^{-} = Y_{j\pm\frac{1}{2}}^{m-\frac{1}{2}}$.

Using the addition theorem (C.3.5) and the identities (C.3.11), the following results follow:

$$\sum_{m=-j}^{j} \psi_{j+\frac{1}{2}}^{m} \otimes \psi_{j-\frac{1}{2}}^{m\dagger} = \frac{1}{4\pi} \left(j + \tfrac{1}{2} - \boldsymbol{\sigma} \cdot \boldsymbol{L} \right) P_{j+\frac{1}{2}}(\cos\gamma),$$

$$\sum_{m=-j}^{j} \psi_{j+\frac{1}{2}}^{m} \otimes \psi_{j-\frac{1}{2}}^{m\dagger} = \frac{\boldsymbol{x} \cdot \boldsymbol{\sigma}}{4\pi r} \left(j + \tfrac{1}{2} + \boldsymbol{\sigma} \cdot \boldsymbol{L} \right) P_{j-\frac{1}{2}}(\cos\gamma),$$

$$\sum_{m=-j}^{j} \psi_{j-\frac{1}{2}}^{m} \otimes \psi_{j+\frac{1}{2}}^{m\dagger} = \frac{\boldsymbol{x} \cdot \boldsymbol{\sigma}}{4\pi r} \left(j + \tfrac{1}{2} - \boldsymbol{\sigma} \cdot \boldsymbol{L} \right) P_{j+\frac{1}{2}}(\cos\gamma),$$

$$\sum_{m=-j}^{j} \psi_{j-\frac{1}{2}}^{m} \otimes \psi_{j-\frac{1}{2}}^{m\dagger} = \frac{1}{4\pi} \left(j + \tfrac{1}{2} + \boldsymbol{\sigma} \cdot \boldsymbol{L} \right) P_{j-\frac{1}{2}}(\cos\gamma). \qquad \text{(C.4.2)}$$

C.5 Contractions of the $\psi_{j\pm\frac{1}{2}}^{m}$ bi-spinors

Due to loss of symmetry, the sums over m cannot be performed in the expressions for t.e.v.s on rotating adS, in subsection 8.3.1. Instead, the contractions of the bi-spinors have to be performed and simplified accordingly.

C.5.1 Contractions of $\psi_{\pm}$

The simplest contractions to perform are those coming up in the t.e.v. of the charge density (8.3.10a) and (8.3.12a) and of the energy density (8.3.24a). Since the derivatives of these contractions are required for $T_{\hat{t}\hat{\varphi}}$, the results below are for arbitrary point splitting:

$$\psi_{+}^{\dagger}\psi_{+} = \frac{1}{4\pi} \frac{(j-m)!}{(j+m)!} \left[e^{i(m-\frac{1}{2})\Delta\varphi}(j-m+1)^2 P_{+}^{-}P_{+}^{-} + e^{i(m+\frac{1}{2})\Delta\varphi} P_{+}^{+}P_{+}^{+} \right], \quad \text{(C.5.1a)}$$

$$\psi_{-}^{\dagger}\psi_{-} = \frac{1}{4\pi} \frac{(j-m)!}{(j+m)!} \left[e^{i(m-\frac{1}{2})\Delta\varphi}(j+m)^2 P_{-}^{-}P_{-}^{-} + e^{i(m+\frac{1}{2})\Delta\varphi} P_{-}^{+}P_{-}^{+} \right], \quad \text{(C.5.1b)}$$

$$\psi_{+}^{\dagger}\psi_{-} = \frac{1}{4\pi} \frac{(j-m)!}{(j+m)!} \left[e^{i(m-\frac{1}{2})\Delta\varphi}(j-m+1)(j+m) P_{-}^{-}P_{+}^{-} + e^{i(m+\frac{1}{2})\Delta\varphi} P_{-}^{+}P_{+}^{+} \right],$$
$$\text{(C.5.1c)}$$

$$\psi_{-}^{\dagger}\psi_{+} = \frac{1}{4\pi} \frac{(j-m)!}{(j+m)!} \left[e^{i(m-\frac{1}{2})\Delta\varphi}(j-m+1)(j+m) P_{+}^{-}P_{-}^{-} + e^{i(m+\frac{1}{2})\Delta\varphi} P_{+}^{+}P_{-}^{+} \right].$$
$$\text{(C.5.1d)}$$

Here, the first and second bi-spinors on the LHS takes arguments (θ', φ') and (θ, φ), respectively. On the RHS, the arguments of the Legendre functions are $\cos\theta$ for the first occurence and $\cos\theta'$ for the second, i.e. $P_{+}^{-}P_{-}^{-} \equiv P_{+}^{-}(\cos\theta)P_{-}^{-}(\cos\theta')$. The

super- and sub-script signs on the Legendre functions change the value of m and j, respectively, by adding or subtracting $\frac{1}{2}$, depending on the sign, i.e.:

$$P_{\pm}^{+} \equiv P_{j\pm\frac{1}{2}}^{m+\frac{1}{2}}, \qquad P_{\pm}^{-} \equiv P_{j\pm\frac{1}{2}}^{m-\frac{1}{2}}. \tag{C.5.2}$$

It can be checked using Eq. (C.2.5) that the above expressions are even with respect to $m \to -m$.

The coincidence limit of the following derivatives can be computed:

$$(\nabla - \nabla')\psi_{+}^{\dagger}\psi_{+}\Big|_{x'=x} = \frac{i(\mathbf{\Omega} \times \boldsymbol{x})}{2\pi\rho^{2}\Omega}\frac{(j-m)!}{(j+m)!}\left[(m-\tfrac{1}{2})(j-m+1)^{2}P_{+}^{-2} + (m+\tfrac{1}{2})P_{+}^{+2}\right], \tag{C.5.3a}$$

$$(\nabla - \nabla')\psi_{-}^{\dagger}\psi_{-}\Big|_{x'=x} = \frac{i(\mathbf{\Omega} \times \boldsymbol{x})}{2\pi\rho^{2}\Omega}\frac{(j-m)!}{(j+m)!}\left[(m-\tfrac{1}{2})(j+m)^{2}P_{-}^{-2} + (m+\tfrac{1}{2})P_{-}^{+2}\right]. \tag{C.5.3b}$$

The above equations are odd with respect to $m \to -m$.

C.5.2   Contractions of $\psi_{\pm}$ sandwiching a σ

The charge current vector and the components of the SET other than $T_{\hat{t}\hat{t}}$ require contractions of ψ's and their derivatives sandwiching a σ matrix.

Let us start with the $\pm, \pm$ combinations, the coincidence limits of which are required for the spatial components of the neutrino charge current (8.3.12b). The $(+,+)$ combinations reduce to:

$$\psi_{+}^{\dagger}\sigma_{1}\psi_{+} = -\frac{\cos\varphi}{2\pi}\frac{(j-m+1)!}{(j+m)!}P_{+}^{-}P_{+}^{+}, \tag{C.5.4a}$$

$$\psi_{+}^{\dagger}\sigma_{2}\psi_{+} = -\frac{\sin\varphi}{2\pi}\frac{(j-m+1)!}{(j+m)!}P_{+}^{-}P_{+}^{+}, \tag{C.5.4b}$$

$$\psi_{+}^{\dagger}\sigma_{3}\psi_{+} = \frac{1}{4\pi}\frac{(j-m)!}{(j+m)!}\left[(j-m+1)^{2}(P_{+}^{-})^{2} - (P_{+}^{+})^{2}\right], \tag{C.5.4c}$$

$$\psi_{+}^{\dagger}\left(\frac{\boldsymbol{x} \times \boldsymbol{\sigma}}{r}\right)\psi_{+} = \frac{\boldsymbol{x} \times \mathbf{\Omega}}{4\pi\rho\Omega}\frac{(j-m)!}{(j+m)!}\left[(j-m+1)P_{+}^{-}P_{-}^{+} + (j+m)P_{+}^{+}P_{-}^{-}\right], \tag{C.5.4d}$$

where Eqs. (C.2.7) were used to obtain the last expression. All the above equations

are odd with respect to $m \to -m$. Similarly, the $-,-$ combinations are given by:

$$\psi^\dagger_- \sigma_1 \psi_- = \frac{\cos\varphi}{2\pi} \frac{(j-m)!}{(j+m-1)!} P^-_- P^+_-, \tag{C.5.5a}$$

$$\psi^\dagger_- \sigma_2 \psi_- = \frac{\sin\varphi}{2\pi} \frac{(j-m)!}{(j+m-1)!} P^-_- P^+_-, \tag{C.5.5b}$$

$$\psi^\dagger_- \sigma_3 \psi_- = \frac{1}{4\pi} \frac{(j-m)!}{(j+m)!} \left[(j+m)^2 (P^-_-)^2 - (P^+_-)^2 \right], \tag{C.5.5c}$$

$$\psi^\dagger_- \left(\frac{\boldsymbol{x} \times \boldsymbol{\sigma}}{r} \right) \psi_- = - \frac{\boldsymbol{x} \times \boldsymbol{\Omega}}{4\pi\rho\Omega} \frac{(j-m)!}{(j+m)!} \left[(j-m+1) P^-_+ P^+_- + (j+m) P^+_+ P^-_- \right]. \tag{C.5.5d}$$

These equations are, again, odd with respect to $m \to -m$.

The $(\pm, \mp)$ combinations are required for the spatial components of the charge current (8.3.10b), $T_{\hat{t}\hat{i}}$ and $T_{\hat{i}\hat{j}}$, the latter also requiring their derivatives. For the $(+, -)$ combinations, the following expressions can be found:

$$\psi^\dagger_+ \sigma_1 \psi_- = \frac{1}{4\pi} \frac{(j-m)!}{(j+m)!} \left[e^{i\varphi + i(m-\frac{1}{2})\Delta\varphi} (j-m+1) P^+_- P^-_+ - e^{-i\varphi + i(m+\frac{1}{2})\Delta\varphi} (j+m) P^-_- P^+_+ \right], \tag{C.5.6a}$$

$$\psi^\dagger_+ \sigma_2 \psi_- = \frac{-i}{4\pi} \frac{(j-m)!}{(j+m)!} \left[e^{i\varphi + i(m-\frac{1}{2})\Delta\varphi} (j-m+1) P^+_- P^-_+ + e^{-i\varphi + i(m+\frac{1}{2})\Delta\varphi} (j+m) P^-_- P^+_+ \right], \tag{C.5.6b}$$

$$\psi^\dagger_+ \sigma_3 \psi_- = \frac{1}{4\pi} \frac{(j-m)!}{(j+m)!} \left[e^{i(m-\frac{1}{2})\Delta\varphi} (j+m)(j-m+1) P^-_- P^-_+ + e^{i(m+\frac{1}{2})\Delta\varphi} P^+_- P^+_+ \right], \tag{C.5.6c}$$

and the combinations $-, +$ follow through complex conjugation and swapping of x and x' in the above:

$$\psi^\dagger_- \sigma_1 \psi_+ = \frac{1}{4\pi} \frac{(j-m)!}{(j+m)!} \left[e^{-i\varphi + i(m+\frac{1}{2})\Delta\varphi} (j-m+1) P^-_+ P^+_- - e^{i\varphi + i(m-\frac{1}{2})\Delta\varphi} (j+m) P^+_+ P^-_- \right], \tag{C.5.7a}$$

$$\psi^\dagger_- \sigma_2 \psi_+ = \frac{i}{4\pi} \frac{(j-m)!}{(j+m)!} \left[e^{-i\varphi + i(m+\frac{1}{2})\Delta\varphi} (j-m+1) P^-_+ P^+_- + e^{i\varphi + i(m-\frac{1}{2})\Delta\varphi} (j+m) P^+_+ P^-_- \right], \tag{C.5.7b}$$

$$\psi^\dagger_- \sigma_3 \psi_+ = \frac{1}{4\pi} \frac{(j-m)!}{(j+m)!} \left[e^{i(m-\frac{1}{2})\Delta\varphi} (j+m)(j-m+1) P^-_+ P^-_- + e^{i(m+\frac{1}{2})\Delta\varphi} P^+_+ P^+_- \right]. \tag{C.5.7c}$$

The coincidence limit of the combinations $(+,-)+(-,+)$ is:

$$\psi_+^\dagger \sigma_1 \psi_- + \psi_-^\dagger \sigma_1 \psi_+ = \frac{\cos\varphi}{2\pi} \frac{(j-m)!}{(j+m)!} \left[(j-m+1)P_+^- P_-^+ - (j+m)P_-^- P_+^+ \right],$$

$$\text{(C.5.8a)}$$

$$\psi_+^\dagger \sigma_2 \psi_- + \psi_-^\dagger \sigma_2 \psi_+ = \frac{\sin\varphi}{2\pi} \frac{(j-m)!}{(j+m)!} \left[(j-m+1)P_+^- P_-^+ - (j+m)P_-^- P_+^+ \right],$$

$$\text{(C.5.8b)}$$

$$\psi_+^\dagger \sigma_3 \psi_- + \psi_-^\dagger \sigma_3 \psi_+ = \frac{1}{2\pi} \frac{(j-m)!}{(j+m)!} \left[(j+m)(j-m+1)P_+^- P_-^- + P_+^+ P_-^+ \right], \quad \text{(C.5.8c)}$$

$$\psi_+^\dagger \boldsymbol{\sigma} \psi_- + \psi_-^\dagger \boldsymbol{\sigma} \psi_+ = \frac{\boldsymbol{\Omega} \times (\boldsymbol{x} \times \boldsymbol{\Omega})}{2\pi\rho\Omega^2} \frac{(j-m)!}{(j+m)!} \left[(j-m+1)P_+^- P_-^+ - (j+m)P_-^- P_+^+ \right]$$
$$+ \frac{\boldsymbol{\Omega}}{2\pi\Omega} \frac{(j-m)!}{(j+m)!} \left[(j+m)(j-m+1)P_+^- P_-^- + P_+^+ P_-^+ \right].$$

$$\text{(C.5.8d)}$$

The coincidence limit of the combinations $(+,-)-(-,+)$ is:

$$\psi_+^\dagger \sigma_1 \psi_- - \psi_-^\dagger \sigma_1 \psi_+ = \frac{i\sin\varphi}{2\pi} \frac{(j-m)!}{(j+m)!} \left[(j-m+1)P_+^- P_-^+ + (j+m)P_-^- P_+^+ \right],$$

$$\text{(C.5.9a)}$$

$$\psi_+^\dagger \sigma_2 \psi_- - \psi_-^\dagger \sigma_2 \psi_+ = \frac{-i\cos\varphi}{2\pi} \frac{(j-m)!}{(j+m)!} \left[(j-m+1)P_+^- P_-^+ + (j+m)P_-^- P_+^+ \right],$$

$$\text{(C.5.9b)}$$

$$\psi_+^\dagger \sigma_3 \psi_- - \psi_-^\dagger \sigma_3 \psi_+ = 0, \quad\quad\quad\quad\quad\quad\quad\quad\quad\quad\quad\quad\quad \text{(C.5.9c)}$$

$$\psi_+^\dagger \boldsymbol{\sigma} \psi_- - \psi_-^\dagger \boldsymbol{\sigma} \psi_+ = \frac{-i\boldsymbol{\Omega} \times \boldsymbol{x}}{2\pi\rho\Omega} \frac{(j-m)!}{(j+m)!} \left[(j-m+1)P_+^- P_-^+ + (j+m)P_-^- P_+^+ \right].$$

$$\text{(C.5.9d)}$$

Finally, the coincidence limit of the derivatives of the above combinations yield:

$$
(\nabla_i - \nabla_{i'})\left(\psi_+^\dagger \sigma_1 \psi_- - \psi_-^\dagger \sigma_1 \psi_+\right) = \frac{1}{2\pi}\frac{(j-m)!}{(j+m)!}\Bigg\{ \tag{C.5.10a}
$$

$$
- 2m \sin\varphi \left(\frac{\boldsymbol{\Omega}\times\boldsymbol{x}}{\rho^2\Omega}\right)^i \left[(j-m+1)P_+^- P_-^+ + (j+m)P_+^+ P_-^-\right]
$$

$$
+ \cos\varphi \left[\frac{\boldsymbol{x}\times(\boldsymbol{\Omega}\times\boldsymbol{x})}{\Omega r^3}\right]^i\left[(j-m+1)W_{\cos\theta}(P_+^-,P_-^+) + (j+m)W_{\cos\theta}(P_-^-,P_+^+)\right]\Bigg\},
$$

$$
(\nabla_i - \nabla_{i'})\left(\psi_+^\dagger \sigma_2 \psi_- - \psi_-^\dagger \sigma_2 \psi_+\right) = \frac{1}{2\pi}\frac{(j-m)!}{(j+m)!}\Bigg\{ \tag{C.5.10b}
$$

$$
2m \cos\varphi \left(\frac{\boldsymbol{\Omega}\times\boldsymbol{x}}{\rho^2\Omega}\right)^i \left[(j-m+1)P_+^- P_-^+ + (j+m)P_+^+ P_-^-\right]
$$

$$
+ \sin\varphi \left[\frac{\boldsymbol{x}\times(\boldsymbol{\Omega}\times\boldsymbol{x})}{\Omega r^3}\right]^i\left[(j-m+1)W_{\cos\theta}(P_+^-,P_-^+) + (j+m)W_{\cos\theta}(P_-^-,P_+^+)\right]\Bigg\},
$$

$$
(\nabla_i - \nabla_{i'})\left(\psi_+^\dagger \sigma_3 \psi_- - \psi_-^\dagger \sigma_3 \psi_+\right) = \left[\frac{\boldsymbol{x}\times(\boldsymbol{\Omega}\times\boldsymbol{x})}{2\pi\Omega r^3}\right]^i\frac{(j-m)!}{(j+m)!}\Big[\tag{C.5.10c}
$$

$$
(j-m+1)(j+m)W_{\cos\theta}(P_+^-,P_-^-) + W_{\cos\theta}(P_+^+,P_-^+)\Big],
$$

$$
(\nabla_i - \nabla_{i'})\left(\psi_+^\dagger \sigma_j \psi_- - \psi_-^\dagger \sigma_j \psi_+\right)\frac{1}{2\pi}\frac{(j-m)!}{(j+m)!} = \Bigg\{ \tag{C.5.10d}
$$

$$
\frac{2m}{\rho}\left(\frac{\boldsymbol{\Omega}\times\boldsymbol{x}}{\rho\Omega}\right)_i\left(\frac{\boldsymbol{\Omega}\times\boldsymbol{x}}{\rho\Omega}\right)_j\left[(j-m+1)P_+^- P_-^+ + (j+m)P_+^+ P_-^-\right]
$$

$$
+ \frac{1}{r}\left[\frac{\boldsymbol{x}\times(\boldsymbol{\Omega}\times\boldsymbol{x})}{\Omega r^2}\right]^i\left[\frac{\boldsymbol{\Omega}\times(\boldsymbol{x}\times\boldsymbol{\Omega})}{\rho\Omega^2}\right]^j
$$

$$
\times \left[(j-m+1)W_{\cos\theta}(P_+^-,P_-^+) + (j+m)W_{\cos\theta}(P_-^-,P_+^+)\right]
$$

$$
+ \frac{1}{r}\left[\frac{\boldsymbol{x}\times(\boldsymbol{\Omega}\times\boldsymbol{x})}{\Omega r^2}\right]^i\left(\frac{\boldsymbol{\Omega}}{\Omega}\right)^j\left[(j-m+1)(j+m)W_{\cos\theta}(P_+^-,P_-^-) + W_{\cos\theta}(P_+^+,P_-^+)\right]\Bigg\},
$$

$$
\tag{C.5.10e}
$$

where $W_{\cos\theta}((P_+^\pm,P_-^\mp))$, $W_{\cos\theta}((P_+^\pm,P_-^\pm))$, etc. are Wronskians of the functions inside the brackets with respect to $\cos\theta$:

$$
W_{\cos\theta}(f,g) = f\frac{\partial g}{\partial(\cos\theta)} - \frac{\partial f}{\partial(\cos\theta)}g. \tag{C.5.11}
$$

Appendix D: Gauss' hypergeometric function

This appendix contains some properties of hypergeometric functions extracted from standard reference books [1, 60], useful throughout chapters 7 and 8.

The hypergeometric functions can be used to construct solutions to Euler's hypergeometric differential equation:

$$z(1-z)\frac{d^2w}{dz^2} + [c - (1 + a + b)z]\frac{dw}{dz} - abw = 0. \tag{D.1}$$

The two linearly independent solutions given as series about $z = 0$ are $_2F_1(a, b; c; z)$ and $z^{1-c}\,_2F_1(1+a-c, 1+b-c; 2-c; z)$, where the hypergeometric series $_2F_1(a, b; c; z)$ is defined as:

$$_2F_1(a, b; c; z) = \frac{\Gamma(c)}{\Gamma(a)\Gamma(b)} \sum_{n=0}^{\infty} \frac{\Gamma(a+n)\Gamma(b+n)}{\Gamma(c+n)} \frac{z^n}{n!}. \tag{D.2}$$

From this explicit series, the following identities can be established [60]:

$$_2F_1(a + 1, b + 1; c + 1; z) = \frac{c}{ab}\frac{d}{dz}\,_2F_1(a, b; c; z), \tag{D.3a}$$

$$_2F_1(a + 1, b; c; z) = \frac{z^{1-a}}{a}\frac{d}{dz}z^a\,_2F_1(a, b; c; z), \tag{D.3b}$$

$$_2F_1(a + 1, b; c + 1; z) = \frac{c}{a(c-b)}\left[a - (1 - z)\frac{d}{dz}\right]\,_2F_1(a, b; c; z), \tag{D.3c}$$

$$_2F_1(1 + k, 2 + k; 1 + 2k; z) = \frac{2}{z}\left[\,_2F_1(k, 2 + k; 2k; z) - \,_2F_1(k, 1 + k; 2k; z)\right], \tag{D.3d}$$

$$_2F_1(k, 2 + k; 1 + 2k; z) = \frac{2}{z}\left[\,_2F_1(k, 1 + k; 2k; z) + (z - 1)\,_2F_1(k, 2 + k; 2k; z)\right]. \tag{D.3e}$$

Abramowitz and Stegun [1] give the following connection formulae:

$$
{}_2F_1\left(a, a + \frac{1}{2}; c; z\right) = (1 + \sqrt{z})^{-2a}{}_2F_1\left(2a, c - \frac{1}{2}; 2c - 1; \frac{2\sqrt{z}}{1 + \sqrt{z}}\right), \tag{D.4a}
$$

$$
{}_2F_1\left(a, b; c; z\right) = (1 - z)^{-a}{}_2F_1\left(a, c - b; c; \frac{z}{z - 1}\right), \tag{D.4b}
$$

$$
\begin{aligned}
{}_2F_1\left(a, a + m; c; z\right) = {} & \frac{\Gamma(c)(-z)^{-a}}{\Gamma(a + m)} \sum_{n=0}^{m-1} \frac{\Gamma(m - n)(a)_n}{\Gamma(c - a - n)} z^{-n} \\
& + \frac{\Gamma(c)(-z)^{-a-m}}{\Gamma(a + m)\Gamma(c - a)} \sum_{n=0}^{\infty} \frac{(a)_{n+m}(1 - c + a)_{n+m}}{n!(n + m)!} z^{-n} \\
\times \, [\ln(-z) & + \psi(1 + m + n) + \psi(1 + n) - \psi(a + m + n) - \psi(c - a - m - n)].
\end{aligned}
$$
$$
\tag{D.4c}
$$

References

[1] M. Abramowitz and I. A. Stegun. *Handbook of mathematical functions with formulas, graphs and mathematical tables.* Dover, New York, 1964.

[2] M. Alcubierre. The warp drive: hyper-fast travel within general relativity. *Class. Quantum Grav.*, 11:L73–L77, 1994.

[3] B. Allen and T. Jacobson. Vector two-point functions in maximally symmetric spaces. *Commun. Math. Phys*, 103:669–692, 1986.

[4] B. Allen and C. A. Lütken. Spinor two-point functions in maximally symmetric spaces. *Commun. Math. Phys*, 106:201–210, 1986.

[5] V. E. Ambruș and E. Winstanley. Bounded rotating fermions. *Phys. Rev. D.* paper in preparation.

[6] V. E. Ambruș and E. Winstanley. Dirac fermions on an anti-de Sitter background. *TIM-2013 conference proceedings.* Paper under revision. Preprint at arXiv:1405.2215 [gr-qc].

[7] V. E. Ambruș and E. Winstanley. Fermions on adS. *Proceedings of First Karl Schwarzschild meeting.* Paper with editors. Preprint at arXiv:1310.7429 [gr-qc].

[8] V. E. Ambruș and E. Winstanley. Rotating fermions. *Marcel Grossman 13 conference proceedings.* Paper under revision. Preprint at arXiv:1302.3791 [gr-qc].

[9] V. E. Ambruș and E. Winstanley. Rotating fermions on anti-de sitter spacetime. *Phys. Rev. D.* paper in preparation.

[10] V. E. Ambruș and E. Winstanley. Rotating quantum states. *Phys. Lett. B*, 734:296–301, 2014.

[11] A. B. Balantekin and A. J. DeWeerd. Second quantization of the Dirac equation in cylindrical coordinates. *unpublished.* http://citeseerx.ist.psu.edu/viewdoc/summary?doi=10.1.1.55.3308.

[12] S. Bellucci, E. R. Bezerra de Mello, and A. A. Saharian. Fermionic condensate in a conical space with a circular boundary and magnetic flux. *Phys. Rev. D*, 83:085017, 2011.

[13] C. G. Beneventano, I. V. Fialkovsky, and E. M. Santangelo. Zeroes of combinations of Bessel functions and mean charge of graphene nanodots. Preprint at arXiv:1407.0615 [math-ph].

[14] I. Bengtsson. Anti-de Sitter space. http://www.physto.se/ ingemar/Kurs.ps, 2009.

[15] M. V. Berry and R. J. Mondragon. Neutrino billiards: time-reversal symmetry-breaking without magnetic fields. *Proc. R. Soc. Lond. A*, 412:53–74, 1987.

[16] N. D. Birrell and P. C. W. Davies. *Quantum fields in curved space.* Cambridge University Press, 1982.

[17] M. R. Brown and A. C. Ottewill. Photon propagators and the definition and approximation of renormalized stress tensors in curved space-time. *Phys. Rev. D*, 34:1776–1786, 1986.

[18] R. Camporesi and A. Higuchi. Stress-energy tensors in anti-de Sitter spacetime. *Phys. Rev. D*, 45:3591–3603, 1992.

[19] P. Candelas and D. Deutsch. On the vacuum stress induced by uniform acceleration or supporting the ether. *Proc. R. Soc. Lond. A*, 354:79–99, 1977.

[20] P. Candelas and K. W. Howard. Vacuum $\langle \phi^2 \rangle$ in Schwarzschild spacetime. *Phys. Rev. D*, 29:1618–1625, 1984.

[21] M. Casals, S. Dolan, B. Nolan, A. C. Ottewill, and E. Winstanley. Quantization of fermions on kerr space-time. *Phys. Rev. D*, 87:064027, 2013.

[22] M. Casals and A. C. Ottewill. Canonical quantization of the electromagnetic field on the Kerr background. *Phys. Rev. D*, 71:124016, 2005.

[23] A. Chodos, R. L. Jaffe, K. Johnson, C. B. Thorn, and V. F. Weisskopf. New extended model of hadrons. *Phys. Rev. D*, 9:3471–3495, 1974.

[24] S. M. Christensen. Regularization, renormalization, and covariant geodesic point separation. *Phys. Rev. D*, 17:946–963, 1978.

[25] I. Cotăescu. External symmetry in general relativity. *J. Phys. A: Math. Gen.*, 33:9177, 2000.

[26] I. Cotăescu. Dirac fermions in de Sitter and anti-de Sitter backgrounds. *Rom. Journ. Phys.*, 52:895–940, 2007.

[27] C. Dappiaggi, T.-P. Hack, and N. Pinamonti. The extended algebra of observables for dirac fields and the trace anomaly of their stress-energy tensor. *Rev. Math. Phys.*, 21:1241–1312, 2009.

[28] E. R. Bezerra de Mello, V. B. Bezerra, A. A. Saharian, and V. M. Bardeghyan. Fermionic current densities induced by magnetic flux in a conical space with a circular boundary. *Phys. Rev. D*, 82:085033, 2010.

[29] E. R. Bezerra de Mello, F. Moraes, and A. A. Saharian. Fermionic Casimir densities in a conical space with a circular boundary and magnetic flux. *Phys. Rev. D*, 85:045016, 2012.

[30] Y. Decanini and A. Folacci. Hadamard renormalization of the stress-energy tensor for a quantized scalar field in a general spacetime of arbitrary dimension. *Phys. Rev. D*, 78:044025, 2008.

[31] D. Deutsch and P. Candelas. Boundary effects in quantum field theory. *Phys. Rev. D*, 20:3063–3080, 1979.

[32] G. Duffy. *Scalar quantum field theory on the Kerr black hole background.* PhD thesis, University College Dublin, Ireland, 2002.

[33] G. Duffy and A. C. Ottewill. Rotating quantum thermal distribution. *Phys. Rev. D*, 67(044002), 2003.

[34] G. Duffy and A. C. Ottewill. Renormalized stress tensor in Kerr space-time: numerical results for the Hartle-Hawking vacuum. *Phys. Rev. D*, 77:024007, 2008.

[35] V. P. Frolov and K. S. Thorne. Renormalized stress-energy tensor near the horizon of a slowly evolving, rotating black hole. *Phys. Rev. D*, 39:2125–2154, 1989.

[36] G. W. Gibbons and S. W. Hawking. Action integrals and partition functions in quantum gravity. *Phys. Rev. D*, 15:2752, 1977.

[37] I. S. Gradshteyn and I. M. Ryzhik. *Table of integrals, series and products.* Elsevier Academic Press, 2007.

[38] P. B. Groves, P. R. Anderson, and E. D. Carlson. Method to compute the stress-energy tensor for the massless spin $1/2$ field in a general static spherically symmetric spacetime. *Phys. Rev. D*, 66:124017, 2002.

[39] S. A. Gundersen and F. Ravndal. The fermionic Casimir effect at finite temperature. *Ann. Phys.*, 182:90–111, 1988.

[40] S. W. Hawking. Black hole explosions? *Nature*, 248:30–31, 1974.

[41] S. W. Hawking. Particle creation by black holes. *Commun. Math. Phys.*, 43:199–220, 1975.

[42] S. Hollands. The Hadamard condition for Dirac fields and adiabatic states on RobertsonWalker spacetimes. *Commun. Math. Phys.*, 216:635–661, 2001.

[43] M. Hortaçsu, K. D. Rothe, and B. Schroer. Zero-energy eigenstates for the Dirac boundary problem. *Nucl. Phys. B*, 171:530–542, 1980.

[44] K. W. Howard. Vacuum $T^{\mu}{}_{\nu}$ in Schwarzschild spacetime. *Phys. Rev. D*, 30:2532–2547, 1984.

[45] K. Huang. *Quantum field theory: from operators to path integrals.* J. Wiley & Sons, New York, 1998.

[46] C. Itzykson and J.-B. Zuber. *Quantum field theory.* Dover Publications, inc., 1980.

[47] B. R. Iyer. Dirac field theory in rotating coordinates. *Phys. Rev. D*, 26:1900–1905, 1982.

[48] B. S. Kay and R. M. Wald. Theorems on the uniqueness and thermal properties of stationary, nonsingular, quasifree states on spacetimes with a bifurcate killing horizon. *Phys. Rep.*, 207:49–136, 1991.

[49] C. Kent. *Quantum scalar field theory on anti-de Sitter space.* PhD thesis, University of Sheffield, UK, 2013.

[50] C. Kent and E. Winstanley. Hadamard renormalized scalar field theory on anti-de Sitter space-time. *in preparation*, 2014. Paper under revision. Preprint at arXiv:1408.6738 [gr-qc].

[51] H. A. Lauwerier. *Asymptotic analysis.* Matematisch Centrum, Amsterdam, 1974.

[52] J. R. Letaw and J. D. Pfautsch. Quantized scalar field in rotating coordinates. *Phys. Rev. D*, 22:1345–1351, 1980.

[53] V. A. De Lorenci and N. F. Svaiter. A rotating quantum vacuum. *Found. Phys.*, 29:1233–1264, 1999.

[54] B. H. J. McKellar, G. J. Jr. Stephenson, and M. J. Thomson. The Dirac equation in Kerr spacetime, spheroidal coordinates and the MIT bag model of hadrons. *J. Phys. A: Math. Gen.*, 26:3649–3657, 1993.

[55] C. W. Misner, K. S. Thorne, and J. A. Wheeler. *Gravitation.* W. H. Freeman and Company, 1973.

[56] W. Mück. Spinor parallel propagator and Green function in maximally symmetric spaces. *J. Phys. A: Math. Gen.*, 33:3021–3026, 2000.

[57] V. F. Mukhanov and S. Winitzki. *Introduction to quantum effects in gravity.* Cambridge University Press, 2010.

[58] A. H. Najmi and A. C. Ottewill. Quantum states and the Hadamard form. i. Energy minimization for scalar fields. *Phys. Rev. D*, D(30):2573–2578, 1984.

[59] A.-H. Najmi and A. C. Ottewill. Quantum states and the Hadamard form. ii. energy minimization for spin-1/2 fields. *Phys. Rev. D*, 30:2573–2578, 1984.

[60] F. W. J. Olver, D. W. Lozier, R. F. Boisvert, and C. W. Clark. *NIST Handbook of Mathematical Functions*. Cambridge University Press, 2010.

[61] A. C. Ottewill and E. Winstanley. Divergence of a quantum thermal state on Kerr space-time. *Phys. Lett. A*, 273:149–152, 2000.

[62] A. C. Ottewill and E. Winstanley. Renormalized stress tensor in Kerr space-time: general results. *Phys. Rev. D*, 62:084018, 2000.

[63] E. Poisson, A. Pound, and I. Vega. The motion of point particles in curved spacetime. *Living Rev. Relativity*, 14, 2011.

[64] A. A. Saharian. The generalized Abel-Plana formula with applications to Bessel functions and Casimir effect. *e-print*, 2006. http://arxiv.org/abs/hep-th/0609093.

[65] K. Stowe. *An introduction to thermodynamics and statistical mechanics*. Cambridge University Press, 2007.

[66] H. Takeno. On relativistic theory of rotating disk. *Prog. Theor. Phys.*, 7:367–376, 1952.

[67] P. Taylor. *Green's functions in axially symmetric space-times with applications in QFT and the self-force*. PhD thesis, University College Dublin, Ireland, 2011.

[68] B. Thaller. *The Dirac equation*. Springer, 2010.

[69] M. G. Trocheries. Electrodynamics in a rotating frame of reference. *Phil. Mag.*, 40:1143–1154, 1949.

[70] W. K. Tung. *Group theory in physics*. World Scientific Publishing Co. Pte. Ltd., 1985.

[71] A. Vilenkin. Parity nonconservation and rotating black holes. *Phys. Rev. Lett.*, 41:1575–1577, 1978.

[72] A. Vilenkin. Quantum field theory at finite temperature in a rotating system. *Phys. Rev. D*, 21:2260–2269, 1980.

[73] G. N. Watson. *A treatise on the theory of Bessel functions*. Cambridge University Press, 1922.